Advances and Technical Standards in Neurosurgery 45
Series Editor: Concezio Di Rocco

Concezio Di Rocco *Editor*

Advances and Technical Standards in Neurosurgery

Volume 45

Springer

Advances and Technical Standards in Neurosurgery

Volume 45

This series, which has earned a reputation over the years and is considered a classic in the neurosurgical field, is now relaunched under the editorship of Professor Concezio Di Rocco, which relies on the collaboration of a renewed editorial board.

Both volumes focused on recent advances in neurosurgery and on technical standards, and monographs devoted to more specific subjects in the neurosurgical field will implement it. Written by key opinion leaders, the series volumes will be useful for young neurosurgeons in their postgraduate training but also for more experienced clinicians.

More information about this series at https://link.springer.com/bookseries/578

Concezio Di Rocco
Editor

Advances and Technical Standards in Neurosurgery

Volume 45

Springer

Editor
Concezio Di Rocco
International Neuroscience Institute
Hannover, Germany

ISSN 0095-4829 ISSN 1869-9189 (electronic)
Advances and Technical Standards in Neurosurgery
ISBN 978-3-030-99165-4 ISBN 978-3-030-99166-1 (eBook)
https://doi.org/10.1007/978-3-030-99166-1

This Springer imprint is published by the registered company Springer Nature Switzerland AG
The registered company address is: Gewerbestrasse 11, 6330 Cham, Switzerland

Preface

Advances and Technical Standards in Neurosurgery (ATSN) represents the successful achievement of the wish of Jean Brihaye, Bernard Pertuised, Fritz Loew and Hugo Krayenbuhl to provide European neurosurgeons in training with a high-level publication to accompany the teaching provided by the European postgraduate course. The project was conceived during the joint meeting of the German and Italian Neurosurgical Societies in Taormina in 1972, and the first volume was published in 1974. The English language was chosen to facilitate the international exchange of information and the circulation of scientific progress. Since then, the ATSN has hosted chapters by eminent European neurosurgeons and has become one of the most renowned educational tools on the continent for both young and experienced neurosurgeons. The successive editorial boards have maintained the ATSN's high scientific quality and ensured a good balance between contributions dealing with advances in neuroscience over the years and detailed descriptions of surgical techniques, as well as analyses of clinical experiences. Additional appeal has been added by the freedom granted by the Editor and Publisher in the length, style and organisation of the published chapters.

The current series aims to preserve the original spirit of the publication and its high-level didactic function but intends to present itself not only as a historic European publication but as a truly international forum for the most advanced clinical research and modern operating standards.

Hannover, Germany — Concezio Di Rocco

Contents

1 International Women in Neurosurgery 1
Silvia Hernández-Durán, Katharine Drummond, Claire Karekezi, Mary Murphy, Farideh Nejat, Nelci Zanon, and Gail Rosseau

2 Functional Approaches to the Surgery of Brain Gliomas 35
Davide Giampiccolo, Sonia Nunes, Luigi Cattaneo, and Francesco Sala

3 Craniopharyngiomas: Surgery and Radiotherapy 97
Sergey Gorelyshev, Alexander N. Savateev, Nadezhda Mazerkina, Olga Medvedeva, and Alexander N. Konovalov

4 Treatment of Cystic Craniopharyngiomas: An Update 139
Federico Bianchi, Alberto Benato, and Luca Massimi

5 Surgical Approach to Thalamic Tumors 177
M. Memet Özek and Baran Bozkurt

6 Convection-Enhanced Delivery in Children: Techniques and Applications 199
K. Aquilina, A. Chakrapani, L. Carr, M. A. Kurian, and D. Hargrave

7 Cortical Spreading Depolarizations in Aneurysmal Subarachnoid Hemorrhage: An Overview of Current Knowledge and Future Perspectives 229
Moncef Berhouma, Omer Faruk Eker, Frederic Dailler, Sylvain Rheims, and Baptiste Balanca

8 State of the Art and Advances in Peripheral Nerve Surgery 245
Javier Robla-Costales, Carlos Rodríguez-Aceves, Fernando Martínez-Benia, and Mariano Socolovsky

9 Disorders of Secondary Neurulation: Suggestion of a New Classification According to Pathoembryogenesis 285
Jeyul Yang, Ji Yeoun Lee, Kyung Hyun Kim, Hee Jin Yang, and Kyu-Chang Wang

10 The Management of Idiopathic and Refractory Syringomyelia 317
Pasquale Gallo and Chandrasekaran Kaliaperumal

11 Evolution of Complex Spine Surgery in Neurosurgery: From Big to Minimally Invasive Surgery for the Treatment of Spinal Deformity 339
Mohamed Macki and Frank La Marca

12 Thoracoscopic Microdiscectomy with Preservation of Rib and Costovertebral Joint 359
E. M. J. Cornips and E. A. M. Beuls

13 Efficacy of Selective Dorsal Rhizotomy and Intrathecal Baclofen Pump in the Management of Spasticity 379
Pramath Kakodkar, Hidy Girgis, Perla Nabhan, Sharini Sam Chee, and Albert Tu

Chapter 1
International Women in Neurosurgery

Silvia Hernández-Durán, Katharine Drummond, Claire Karekezi, Mary Murphy, Farideh Nejat, Nelci Zanon, and Gail Rosseau

1.1 Introduction

Neurosurgery has recently celebrated its first century as a specialty, and the increasing role of women neurosurgeons is a major theme. This article documents the early women pioneers in neurosurgery from around the world. Table 1.1 lists the first

S. Hernández-Durán (✉)
Department of Neurological Surgery, Universitätsmedizin Göttingen, Göttingen, Germany

European Association of Neurosurgical Societies, Diversity Task Force, Brussels, Belgium
e-mail: silvia.hernandez@med.uni-goettingen.de

K. Drummond
Department of Neurosurgery, The Royal Melbourne Hospital, Parkville, VIC, Australia

Department of Surgery, Faculty of Medicine, Dentistry and Health Sciences, University of Melbourne, Parkville, VIC, Australia
e-mail: kate.drummond@mh.org.au

C. Karekezi
Neurosurgery Unit, Department of Surgery, Rwanda Military Hospital, Kigali, Rwanda

M. Murphy
Victor Horsley Department of Neurosurgery, National Hospital for Neurology and Neurosurgery, London, UK
e-mail: marymurphy2@nhs.net

F. Nejat
Tehran University of Medical Science, Children's Medical Center, Tehran, Iran
e-mail: nejat@sina.tums.ac.ir

N. Zanon
Department of Neurology and Neurosurgery, Federal University of São Paulo, São Paulo, Brazil

CENEPE Centro de Neurocirurgia pediátrica (Pediatric Neurosurgical Center), São Paulo, Brazil

G. Rosseau
Department of Neurosurgery, George Washington University School of Medicine and Health Sciences, Washington, DC, USA

C. Di Rocco (ed.), *Advances and Technical Standards in Neurosurgery*, Advances and Technical Standards in Neurosurgery 45,
https://doi.org/10.1007/978-3-030-99166-1_1

women in neurosurgery in every country in the world. The contributions of these trailblazers to the origins, academics, and international professional organizations of neurosurgery are highlighted. The formation of Women in Neurosurgery (WINS) in 1989 in the United States was an important inflection point. This organization has played a significant role, by inspiring the creation of other similar organizations worldwide and introducing and promoting talented women in the profession. Contributions of women neurosurgeons to academic medicine and society as a

Table 1.1 Chronology of women in neurosurgery around the world

Country	Year of training begin or completion	Name of first WIN	Current % of WIN
Germany	1924	Alice Rosenstein	13
Russia	1929	Serafima Semyonova Bryusova	2
United Kingdom	1939	Diana Beck	12
Romania	1945	Sophia Ionescu	23
Poland	1947	Halina Koźniewska	9
Belarus	1948	Marfa Pavlovets	7
Estonia	1950	Ruth Paimre	10
Kazakhstan	1950s	Evgenija Azarova	2
Mexico	1951	María García-Sancho y Álvarez-Tostado	N/A
Uruguay	1954	María Teresa Sande de García Guelfi	N/A
Bulgaria	1959	Nadezda Smilkova	11
Latvia	1959	Ludmila Trusle	20
Turkey	1959	Aysima Altinok	5
Hungary	1960s	Róza Gombi	5
Israel	1960	Yafa Doron	8
Lithuania	1960s	Jadvyga Subaciute	7
United States of America	1961	Ruth Kerr Jakoby	N/A
Cuba	1965	Irene Zamalea Bess	N/A
Slovakia	1965	Veronika Krafcova	8
India	1968	Thanjavur Santhanakrishna Kanaka	3
Canada	1968	Marina Kyriazidou	N/A
Brazil	1969	Noya Rocha da Silva Chavez	N/A
France	1969	Aimée Redondo	14
Sweden	1969		17
Australia	1970	Elizabeth Lewis	15
El Salvador	1970s	María Castillo Rodas and Dania Trinidad Arévalo	N/A
Georgia	1970s	Larisa Tskrialashvili	N/A
Peru	1970	Blanca Neira	N/A
Slovenia	1970s	Milena Jezernik	14

Table 1.1 (continued)

Country	Year of training begin or completion	Name of first WIN	Current % of WIN
Mongolia	1971	Dorj Javzmaa	25
Italy	1973	Milena Auretta Rosso	36
Argentina	1974	Martha Villafañe	N/A
Dominican Republic	1974	Sonia Corona Ferín Víctor de Sánchez	N/A
Spain	1975	Josefa Ramiro Hernandez and Balbina Ferreras	24
Iran	1978	Zahra Taati Asl	6
Venezuela	1978	Rosario Medina de Lissot	N/A
Belgium	1980s	Vera van Velthoven	13
Czechia (Czech Republic)	1980s	Eva Urbánková	9
Denmark	1980s	Birgit Mosdal, Benedicte Dahlerup and Elizabeth Hoppe-Hirsch	3
Guatemala	1980	Graciela Mannucci	N/A
Morocco	1980s	Najia El Abbadi	17
Netherlands	1980s	Saskia Bakker-Niezen	15
Philippines	1980	Camellia Josefina Nierras Posoncuy	10
Serbia	1980	Mirjana Nagulic	16
China	1981	Pu Peiyu	2
Algeria	1982	Faiza Lalam	N/A
Chile	1983	Lucía Zamorano	N/A
South Korea	1983	Hyo-Sook Chung	2
Japan	1985	Yoko Kato	6
Costa Rica	1986	Silvia Urbina Ortega	N/A
Palestine state	1986	Georgette Kidess	4
Colombia	1987	Martha Pulido	N/A
Greece	1988	Maria Varela-Stavrinou	10
Saudi Arabia	1990s	Samia Maimani	3
Singapore	1990s	Tan Tze Ching	4
Tunisia	1990s	Faten Abid	16
Bolivia	1992	Karin Urresti Destre	N/A
Thailand	1992	Kritssanee Karnjanapanch	9
Vietnam	1993	Lien Ngoc Ly	1
Norway	1994	Sissel Reinlie	14
South Africa	1994	Minette du Preez	7
Zimbabwe	1994	Nozipho Maraire	< 1
Ecuador	1995	Patricia Guzmán	N/A
Finland	1996	Leena Kivipelto	28
Honduras	1996	Ena Miller Molina	N/A
Indonesia	1996	Jeanne PMR Winaktu	5

(continued)

Table 1.1 (continued)

Country	Year of training begin or completion	Name of first WIN	Current % of WIN
New Zealand	1997	Suzanne Jackson	25
Egypt	2000s	Djamila Kafoufi Benderbous	< 1
Pakistan	2000s	Aneela Darbar	9
Senegal	2000s	Mame Salimata diene	2
Armenia	2001	Anna Galstyan	7
Bosnia and Herzegovina	2001	Selma Jakupović	10
Bangladesh	2006	Rezina (Rose) Hamid	4
Côte d'Ivoire	2006	Espérance Maman You Broalet	< 1
Iceland	2006	Hulda Magnadottir	0
Ireland	2006	Mary Murphy	0
Nicaragua	2006	Carolina Cantarero	N/A
Panama	2007	Alina Pupo	N/A
Cameroon	2008	Mirelle Moumi	2
Malaysia	2008	Sharon Casilda Theophilus	16
Nepal	2009	Maya Bhattachan	6
Kuwait	2010	Alya Hasan	N/A
Luxembourg	2010s	Dagmar Broeker	10
Sri Lanka	2010s	Maheshi Wijerathne	5
Uganda	2010s	Juliet Sekabunga	10
Yemen	2010	Asmaa Almasoudi	< 1
Iraq	2011	Qadamkhear Hama	3
North Macedonia	2011	Aleksandra Dimovska-Gavrilovska	4
Albania	2015	Ejona Lilamani and Jetmira Kërxhaliu	20
Ethiopia	2015	Yordanos Ashagre	8
Jamaica	2015	Charmaine Munthra	N/A
Kenya	2015	Susan Karanja and Sylvia Shitsama	27
Myanmar (formerly Burma)	2015	Thilda Hlaing	4
Paraguay	2015	Thamara Portillo Cino	N/A
Croatia	2016	Nikolina Sesar	7
Rwanda	2016	Claire Karekezi	50*
Lebanon	2018	Hiba Sharafeldeen	12
Democratic Republic of the Congo	2019	Sarah Mutomb	< 1
Nigeria	2019	Salamat Ahuoiza Aliu-Ibrahim	2
Jordan	2020	Redab Al Khataybeh	< 1
Cyprus	2021	Maria Karampouga	0

Table 1.1 (continued)

Country	Year of training begin or completion	Name of first WIN	Current % of WIN
United Arab Emirates	2021	UK All current practicing WIN foreigners	4
Montenegro	2022 est	Ivana Jovanovic	0
Papua New Guinea	2022	Esther Apuahe	0
Austria	Unknown		19
Cabo Verde	Unknown		< 1
Gabon	Unknown		1
Gambia	Unknown		< 1
Guinea	Unknown		< 1
Madagascar	Unknown		17
Niger	Unknown		< 1
Portugal	Unknown		22
Qatar	Unknown		31
Sudan	Unknown		29
Switzerland	Unknown		14
Tanzania	Unknown		50*
Ukraine	Unknown		7
Dominica	N/A		N/A
Grenada	N/A		N/A
Guyana	N/A		N/A
North Korea	N/A		N/A
Suriname	N/A		N/A
Syria	N/A		N/A
Trinidad and Tobago	N/A		N/A
Afghanistan	No WIN		0
Andorra	No WIN		0
Angola	No WIN		0
Antigua and Barbuda	No WIN		0
Azerbaijan	No WIN		0
Bahamas	No WIN		0
Bahrain	No WIN		0
Barbados	No WIN		0
Belize	No WIN		0
Benin	No WIN		0
Bhutan	No WIN		0
Botswana	No WIN		0
Brunei	No WIN		0
Burkina Faso	No WIN		0
Burundi	No WIN		

(continued)

Table 1.1 (continued)

Country	Year of training begin or completion	Name of first WIN	Current % of WIN
Cambodia	No WIN		0
Canada	No WIN		
Central African Republic	No WIN		0
Chad	No WIN		0
Comoros	No WIN		0
Congo (Congo-Brazzaville)	No WIN		0
Djibouti	No WIN		0
Equatorial Guinea	No WIN		0
Eritrea	No WIN		0
Eswatini (fmr. "Swaziland")	No WIN		0
Fiji	No WIN		0
Ghana	No WIN		0
Guinea-Bissau	No WIN		0
Haiti	No WIN		0
Kiribati	No WIN		0
Kyrgyzstan	No WIN		0
Laos	No WIN		0
Lesotho	No WIN		0
Liberia	No WIN		0
Libya	No WIN		0
Liechtenstein	No WIN		0
Malawi	No WIN		0
Maldives	No WIN		0
Mali	No WIN		0
Malta	No WIN		0
Marshall Islands	No WIN		0
Mauritania	No WIN		0
Mauritius	No WIN		0
Micronesia	No WIN		0
Moldova	No WIN		0
Monaco	No WIN		0
Mozambique	No WIN		0
Namibia	No WIN		0
Nauru	No WIN		0
Oman	No WIN		0
Palau	No WIN		0
Saint Kitts and Nevis	No WIN		0
Saint Lucia	No WIN		0

Table 1.1 (continued)

Country	Year of training begin or completion	Name of first WIN	Current % of WIN
Saint Vincent and the Grenadines	No WIN		0
Samoa	No WIN		0
San Marino	No WIN		0
Sao Tome and Principe	No WIN		0
Seychelles	No WIN		0
Sierra Leone	No WIN		0
Solomon Islands	No WIN		0
Somalia	No WIN		0
South Sudan	No WIN		0
Tajikistan	No WIN		0
Timor-Leste	No WIN		0
Togo	No WIN		0
Tonga	No WIN		0
Turkmenistan	No WIN		0
Tuvalu	No WIN		0
Uzbekistan	No WIN		0
Vanuatu	No WIN		0
Zambia	No WIN		0

N/A information not available
*Denotes countries in which the total neurosurgical workforce is ten or less

whole are briefly described. Contemporary efforts and initiatives indicate future directions in which women may lead neurosurgery in its second century.

1.2 Europe

Traditionally considered the cradle of Western civilization, Europe can also be considered the cradle of women in neurosurgery, as it was Europeans who were the first women to pursue a career in the specialty in the world [1]. At present, one European country also boasts the highest percentage of women in neurosurgery worldwide, with 36% of the Italian neurosurgical workforce being female [2–4]. Despite advances in recruitment into the specialty, underrepresentation in leadership positions prevails, with only 6% of the leaders in European national neurosurgical societies being women [5]. International efforts are underway to increase participation of women in organized neurosurgery in Europe, for example, through the creation of the Diversity Task Force within the European Association of Neurosurgical Societies [6].

1.2.1 The Beginnings

The first woman to perform surgery on peripheral nerves in Europe was probably Latvian Anna Bormane (1896–1990). After studying in Russia and the Ukraine, she graduated from the University of Latvia in 1923 and was the first woman in Latvia to obtain an academic degree in medicine [7]. After the Soviet reoccupation of Latvia in 1944 during World War II, she fled to Germany, interrupting her surgical career. She then returned to her homeland in 1947 and worked as a surgeon until her 85th birthday, performing peripheral nerve and other neurosurgical procedures [8].

The first woman to perform cranial neurosurgery in the world was probably Alice Rosenstein (1898–1991). She was born in Breslau, modern-day Wroclaw, Poland, to a renowned Jewish gynecologist and his American wife. After obtaining her medical license in 1923, Rosenstein embarked on a vast training journey, gaining clinical experience in both ophthalmology and neurology, while also obtaining her academic degree for her dissertation on acromegaly and syphilis [9]. In 1924, Rosenstein began her formal training under Otfrid Foerster, father of German neurosurgery, in neurology, psychiatry, and neurosurgery [10]. Foerster's Breslau was, at the time, a world-renowned center for neurosurgical training; Wilder Penfield, Percival Bailey, and Paul Bucy all visited the German hospital to expand their knowledge [11]. It was here that Rosenstein performed her first neurosurgical procedures, and she developed the technique to show the foramen of Monro on pneumoencephalography [12]. In 1929, Rosenstein moved to Frankfurt to inaugurate a new operating room exclusively for neurological patients. Here, she performed ventriculographies, brain tumor resections, and cordectomies. However, she was forced to leave her post in Frankfurt and emigrate to the United States in 1934 due to her Jewish background and the rise of the Nazi party in Germany. Thanks to her American family ties, she was able to escape the Holocaust, but she did not continue to practice neurosurgery in her exile [13].

Five years after Rosenstein's exile to the United States, in 1939, England's Diana Beck (1902–1956) began her neurosurgical career in Oxford. She trained under one of Harvey Cushing's pupils, the father of British neurosurgery, Sir Hugh Cairns [14]. Thanks to her surgical dexterity, Beck received a consultant's position at the Royal Free Hospital in 1943, but during World War II she was called upon to serve in the Emergency Medical Service. In 1947, Beck was appointed consultant at The Middlesex Hospital in London, where she quickly earned the respect of her male colleagues and founded the neurosurgical service [15]. She also carried out numerous research projects on idiopathic intracranial hypertension, cranioplasty, and surgical treatment of intracerebral hemorrhage [1, 16]. The latter earned her notoriety in both Europe and North America. Beck's career was brought to an abrupt and unfortunate halt in 1956, when she succumbed to a pulmonary embolism after suffering a myasthenic crisis and undergoing a thymectomy [15].

Romania's Sofia Ionescu (1920–2008) was acknowledged as the first female neurosurgeon during the 13th World Federation of Neurosurgical Societies (WFNS) Congress in 2005 [17]. Ionescu enrolled in medical school in 1939, at the beginning of World War II. By the end of her studies in 1944, the war had reached Romania

and casualties abounded. When Ionescu had to evacuate an epidural hematoma from a young boy, she became enthralled with neurosurgery and her illustrious career began [18]. After becoming a consultant in 1954, Ionescu published over 120 scientific papers, developed a minimally invasive technique to evacuate intracranial hemorrhages, and described the packing of carotid dissections with muscle flaps [19]. Due to the Cold War, however, her work remained largely unknown to her contemporaries in the Western world [20]. In her passion for work, Ionescu would travel all over the country to provide care to patients, and she even lived in the hospital during the 1960s for 7 years to ensure continuous, uninterrupted neurosurgical coverage. Because of her unrelenting dedication, Ionescu received honors from the Romanian Academy of Medical Sciences and the National Confederation of Women in Romania, among many others [18, 19].

1.2.2 The Soviet Pioneers

One of the most fascinating yet obscure chapters in the history of women in neurosurgery and neurosurgery at large lies behind the former Iron Curtain, where female leaders contributed to the establishment of the specialty throughout the entire Soviet Union. However, much of their legacy remains unknown to the Western world.

At the end of the nineteenth century, brain tumors were already being excised in Imperial Russia, and new instruments for cranial surgery were being developed. In 1897, a new department for neurological conditions was opened at the Imperial Military Medical Academy in St. Petersburg, where the first neurosurgical procedures were carried out by invited surgeons, with the assistance of trained neurologists. By 1910, Vladimir Mikhailovich Bekhterev (1857–1927) had already established the Empire's first neurosurgical unit, and his pupil, Ludwig Martynovich Pussep (1875–1942) was carrying out surgeries as complex as the resection of vestibular schwannomas [21].

However, these developments were brought to an abrupt halt by World War I and the Soviet Revolution of 1917. During these events, the recently established dedicated neurosurgical units were repurposed as military hospitals. At the same time, a profound change was taking place in terms of gender equality. To mobilize the population and maximize the workforce, women were given the right to vote and encouraged to participate not only in the frontlines of the revolution, but also in all other aspects of society and the economy as part of the new Bolshevik ideology [22]. Thus, many of them fought alongside men during World War I and served as field nurses [23]. This key political, ideological, and social shift set the stage for extraordinary women to become neurosurgeons and advance the field in the region.

The first woman to become a neurosurgeon in Russia was the Muscovite Serafima Semyonovna Bryusova (1894–1958). Originally trained as a philologist and historian, Bryusova served as a nurse at the frontlines of World War I. Assisting in the surgical treatment of soldiers with traumatic head injury changed her life dramatically, and she began studying medicine at the II Moscow Institute for Medicine in 1917. Upon completion of her studies, she began working as a surgery resident. In

1929, she became one of the closest and only female associates of Nikolay Burdenko (Fig. 1.1), the recognized father of Russian neurosurgery [24]. Under Burdenko, Bryusova benefitted from training in the entire spectrum of neurosurgery. Because of her background as a philologist and her multilingual talents, she translated many seminal neurosurgical works into Russian, thus creating a bridge between the advances being made in the West and her home country [25].

Another remarkable woman and trailblazer in Soviet neurosurgery was Ksenia Ivanovna Kharitonova (1916–1993). Like many of her contemporaries, her formative years as a physician were marked by war. When she graduated from the Novosibirsk Institute of Medicine in 1939, World War II erupted, and she ended up serving as a military surgeon. During this experience, she treated soldiers with traumatic brain injuries and gunshot trauma to peripheral nerves, which shaped her future clinical career and research interests [26]. In 1946, Kharitonova moved to the newly established Institute of Reconstructive Surgery (VOJITO) in Novosibirsk, later renamed the Research Institute of Traumatology and Orthopedics. Four years later, in 1950, she founded a neurosurgical clinic here, despite many adversaries who did not want neurosurgery to become a separate specialty. She led this department for the next 35 years [27]. From this new neurosurgical unit, she directed experimental work and developed new methods for the prevention and treatment of infectious intracranial complications in penetrating traumatic brain injury.

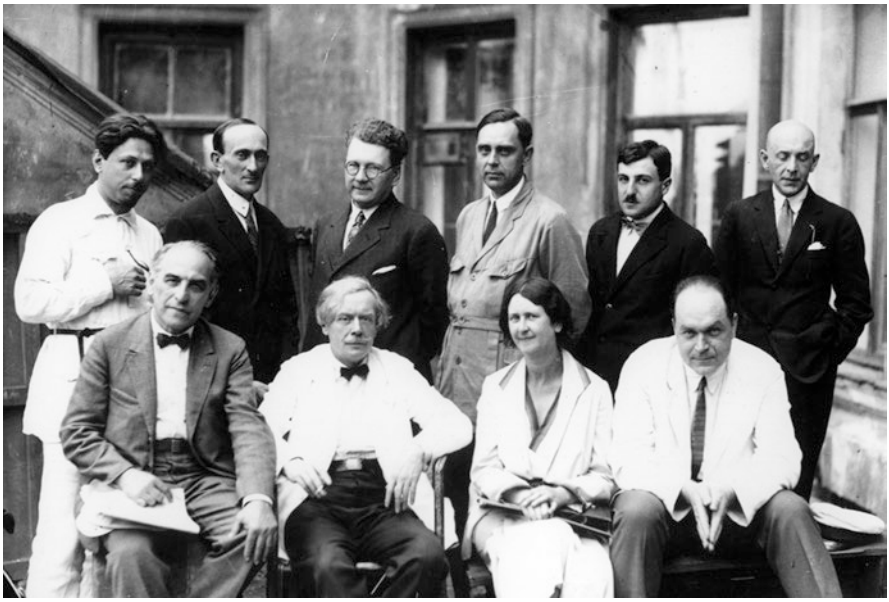

Fig. 1.1 Serafima Semyonovna Bryusova in Nikolay Burdenko's team. Upper row, left to right: E. M. Rossels, S. M. Berg, A. S. Chernyshov, A. A. Arendt, K. G. Terian, M. U. Rapoport and lower row, left to right: G. S. Cimmerman, V. V. Kramer, S. S. Bryusova, B. G. Egorov ca. 1930. Picture rights: B. Liktherman and G. Danilov. (Reproduced with permission from *Journal of Clinical Neuroscience*)

Furthermore, she launched other neurosurgical departments in many Siberian cities, such as Krasnoyarsk, Kemerovo, Prokopievsk, Barnaul, and Tomsk. Thus, she is considered the mother of Siberian neurosurgery [28].

Beyond Russia, other women in the Soviet Union also introduced the neurosurgical specialty into their regions. Evgenija Azarova (1913–1996) founded the Department for Neurosurgery at the Alma Ata Military Hospital and established the first training program for neurosurgeons in Kazakhstan. Like other pioneering women in neurosurgery, Azarova drew her inspiration from patients with traumatic brain injury, whom she treated as a military surgeon. Through her efforts, the outcome of patients with traumatic brain injury greatly improved [29]. Alexandra Chirkova Illarionovna and Rufina Zhukova Nikolaevna followed her footsteps and led the neurosurgical department at Alma Ata in the 1970s. However, neighboring Kyrgyzstan, Tajikistan, Turkmenistan, and Uzbekistan still await their first woman neurosurgeon [2].

Women were not only responsible for introducing neurosurgery into multiple parts of the Soviet Union, but also for launching neurosurgical subspecialties in the region. Belarussian Marfa Vasilievna Pavlovets (1916–2007) is highly recognized for her military achievements and participation in the Great Patriotic War, and also for being one of the driving forces behind the establishment of vascular neurosurgery in the Soviet Union [30]. Similarly, Azerbaijani Anna "Neta" Artaryan (1922–2020) is considered the mother of academic pediatric neurosurgery in the region, and possibly even the world's first dedicated pediatric neurosurgeon. After serving as an army physician during World War II, Artaryan began her neurosurgical training in Moscow. From 1969 on, she taught pediatric neurosurgery to neurosurgeons, general surgeons, and neurologists all over the Soviet Union, developing her own curriculum. She passionately believed that pediatric neurosurgery should be its own subspecialty, for children's anatomy and physiology greatly differ from those of adults. Thirteen years later, in 1982, the first chair of pediatric neurosurgery was created at the Central Institute for Advanced Medical Education, and Artaryan held this position for over 30 years [31].

In the field of pediatric neurosurgery, other Soviet women also made great contributions. Alexandra Georgievna Zemskaya (1920–2010) trained with Wilder Penfield at the Montreal Neurological Institute in Canada and introduced the surgical treatment of epilepsy in children and adults to the Soviet Union. Wanda Iosifovna Rostovskaya (1919–2003) also made pediatric contributions, developing the surgical treatment for children with spina bifida in Moscow [32].

Poland's first woman in neurosurgery, Halina Koźniewska, started practice in 1945 and founded the neurosurgical department in Lublin, whereas Bulgaria's first woman in neurosurgery, Nadezda Smilkova, founded the first neurosurgical department at the Multidisciplinary University Hospital in Ruse in 1963, the largest and oldest regional hospital in north-eastern Bulgaria [2].

Despite a vast number of women pioneers, the current neurosurgical workforce in Russia includes just 2% of women. In former Soviet countries, the proportion is not significantly higher, with the Ukraine being the highest at 6% [33]. This downward trend merits further research, so that future generations can follow in the footsteps of these trailblazers.

1.2.3 Past, Present, and Future

European women have not only been the first neurosurgeons in the world, they have also advanced the field in their countries. Welsh-Brazilian Carys Bannister specialized in spina bifida. She set up a fetal management unit as a tertiary referral center for neurodevelopmental defects in Manchester in the 1980s, which she ran for her entire career [34]. Armenian Anna Galstyan became her country's first woman in neurosurgery in 2001 and, in 2017, she cofounded the first pediatric neurosurgical department [2]. Austrian Monika Killer-Oberpfalzer, one of very few dual-trained neurosurgeons/neurointerventionalists, cofounded the Paracelsus Medizinische Privatuniversität in Salzburg in 2001 and leads one of the few centers in Central Europe for endovascular training in neurosurgery [35].

Scientifically, European women have made great contributions to neurosurgery. Belgian Veerle Visser-Vanderwalle is a pioneer in deep brain stimulation. She was the first neurosurgeon to treat Tourette's syndrome in 1999 [36] and was appointed professor in both The Netherlands and Germany. Portugal's Claudia Faria coinvented Alsterpaullone, a novel small molecule to target group 3 medulloblastoma and founded Lisbon's brain tumor biobank [37, 38]. Meanwhile, Switzerland's Kathleen Seidel codeveloped a dynamic aspirator for intracavitary stimulation and intraoperative neuromonitoring during tumor surgery. Seidel has also launched projects to bring neuromonitoring to low-income countries [2].

Global neurosurgery and social equity have been major concerns for women in neurosurgery in Europe. In France, Francoise Lapierre and Évelyne Émery have launched neurosurgical collaborations with Vietnam and Western Africa, respectively, thus contributing to the development of the neurosurgical infrastructure and care in these areas [6] (Fig. 1.2). Spain's Ana Pastor Zapata leads a teaching

Fig. 1.2 Prof. Emery hosting a neurosurgical course in the Ivory Coast. (Picture reproduced with permission from Prof. E. Emery)

collaboration with Niger's Nemay Hospital [39]. In Serbia, Danica Grujicic founded the organization "Together for Youths", which supports young and talented students [6], while Ljiljana Vujotic launched the ''Voice of Heart" organization to improve the quality of life of elderly people, refugees, and minorities. She is also a plastic surgeon, endocrinologist, and introduced endoscopic surgery to Serbia [40].

1.3 Latin America

Neurosurgery is one of the most important medical legacies from Pre-Columbian cultures in Latin America. Early practitioners performed cranial trephination, intentional cranial deformation, and head shrinking well before neurosurgery was established as a separate specialty. In terms of gender parity in neurosurgery, Latin America is second only to Europe in the emergence of women in neurosurgery. As early as 1951, Mexican María García-Sancho y Álvarez-Tostado became the first female neurosurgeon in Latin America [4]. García-Sancho was trained in Chile and, upon returning to her home country, cofounded the Mexican Society of Neurosurgery, served as professor at the renowned Universidad Nacional Autónoma de México, and was the leader of the First National Congress of Mexican Women Doctors. Thanks to her dedication, a new generation of neurosurgeons could be trained in Mexico, whereas before her time they had to travel abroad to obtain their neurosurgical qualifications [41].

A decade later, the Caribbean saw its first woman in neurosurgery, Irene Zamalea Bess (1939–2006), who would also be a pioneer in global neurosurgery. Bess worked in Angola, Tanzania, and Nicaragua on traumatic brain injury and collaborated on the landmark study on the use of antifibrinolytic agents in traumatic hemorrhage (CRASH-2 trial) [42]. Efforts to improve patient care have also been made by other women trailblazers in Latin America. In Honduras, Ena Miller Molina, the country's first woman in neurosurgery, has launched a nationwide advocacy program for the prevention of traumatic brain and spinal cord injury called "Piensa Primero (Think First), Honduras", which is currently taught in schools. She has been a passionate advocate for intercultural exchange for the improvement of neurosurgical care in low- and middle-income countries [43].

In Peru, two women advanced neurosurgery by introducing subspecialties to the country. Azucena Dávila is the mother of endovascular procedures, while Alicia Becerra founded the Epilepsy Unit for both adults and children at the Hospital Nacional Edgardo Rebagliati Martins in Lima, where she chairs the Functional and Interventional Department of Neurosurgery [4]. Other Latin American women have also made outstanding contributions to functional neurosurgery. Chilean Lucia Zamorano, both an engineer and a neurosurgeon, developed the Zamorano-Duchovny stereotactic frame and currently practices in the United States, after having undergone extensive training in her home country, Germany, and the United States [44]. Alessandra Gorgullo is the founder and president of the Brazilian Society of Radiosurgery. Soon after the introduction of awake craniotomies

worldwide, Alicia Becerra in Peru, Gabriela Moguilner in Paraguay, and Tatiana Vilasboas in Brazil started to perform these in their home countries [4].

The pursuit of improved patient care can also be seen in pediatric neurosurgery in Latin America. Graciela Mannucci, the first woman to practice neurosurgery in Guatemala, founded and currently directs the San Juan de Dios Spina Bifida Multidisciplinary Clinic, a large referral center in the country. She is a tireless advocate for early surgery in spinal dysraphism and a respected expert in the field [45]. In Ecuador, Victoria Ronquillo was the first woman to become a pediatric neurosurgeon and was elected vice-president of the Ecuadorian Society of Neurosurgery [4]. In Mexico, Ana Siordia Karam cofounded the Pediatrics Neurosurgery Department at Hospital Infantil Universitario in Ciudad de Torreón, Coahuila, to improve care of pediatric neurosurgical patients in the region [46]. Since appropriate patient care begins with proper training, Giselle Coelho, from Brazil, developed a simulator for hydrocephalus and craniosynostosis to aid residents in developing their surgical skills. This project earned her the Young Neurosurgeons Award from the World Federation of Neurosurgical Societies (WFNS) [47]. Zulma Tovar Spinoza, from Venezuela, trained neurosurgery in Israel and pediatric neurosurgery in Toronto. In 2009, she assumed her appointment as Director of Pediatric Neurosurgery at SUNY Upstate Medical University in Syracuse, USA. Now an associate professor, she has been elected the AANS/CANS pediatric liaison to the ISPN.

Women are also involved in shaping healthcare policies in Latin America. Marise Audi, a neurosurgeon from Sao Paulo, has been a political candidate in her country [48], while Maria Castillo ran for president of El Salvador and was widely recognized as “Hija Meritisima de El Salvador,” an honorary distinction conferred by the legislative assembly upon an individual for their significant contributions to their country. Elizabeth Hinostroza was the first woman neurosurgeon to be appointed as General of the National Police of Peru. In addition, she served as the Minister of Health of Peru from 2019 to 2020. Nelci Zanon was recently elected as a member of the Academy of Medicine of Sao Paulo, Brazil, and President Elect of the Brazilian Medical Women Association (ABMM), affiliated to the Medical Women International Association (MWIA) [4]. Her dedicated efforts to link women neurosurgeons throughout Latin America are leading to increased academic activity throughout the region.

1.4 Middle East

A diverse region where civilizations have converged since Antiquity, the Middle East has fostered several acclaimed women neurosurgeons. At the same time, several countries in the region still institutionalize traditional gender roles, making career progression for women in general, and women in neurosurgery specifically more challenging. Additionally, poverty, frail infrastructures, and political instability make practicing the specialty in the region difficult. Women neurosurgeons are advocating for better medical services for their patients, designing better education

for themselves and for younger doctors and enriching medical practice through their scientific endeavors [49].

Aysima Altınok became the first woman neurosurgeon in Turkey and the Middle East upon completing her training in 1959 at Haydarpaşa Numune Hospital. From 1968 to 1992, she was chief of neurosurgery at Bakirköy Mental and Psychological Health Hospital. Here, she improved the hospital's infrastructure to provide better care to patients and enable both clinical and laboratory researches. In 1968, Altınok cofounded the Turkish Neurosurgical Society. Her notable contributions to Turkish medicine earned her the "Medical Doctor of the Year in Turkey" Award in 1990 [50]. Nurperi Gazioğlu cofounded the Istanbul University Pituitary Center in Turkey in 2015. Since 2017, she has chaired the neurosurgical department at the Demiroglu Bilim University in Istanbul [51].

Altinok was an exception in the region, for even though the history of neurosurgery in the Middle East dates to prehistoric times, with documented trephinations in Iran, until recently, there were no established residency programs in most countries in the Middle East. Young medical graduates had to travel abroad, posing a major obstacle for Middle Eastern women from traditional backgrounds, who may not have been allowed to travel independently [52].

An outstanding example is Georgette Kidess (Fig. 1.3), the first and only woman neurosurgeon in Palestine. Kidess emigrated to Germany as a medical student and went on to train in neurosurgery at the University of Kiel in Northern Germany, where she was not only one of the few women, but also one of the few trainees of immigrant background. Upon completion of her training, she returned to Palestine in 1986 and started working at the Hadassah Ein Karem Hospital in Jerusalem. Later, she moved to the Ramallah Governmental Hospital, Ramallah, West Bank, where she established the first neurosurgical department in Palestine. She faced many obstacles from gender bias and lack of resources in a politically tumultuous area. Thanks to her efforts, the Palestinian Neurosurgical Society was founded in 2014, in cooperation with Jordanian neurosurgeons, and she has trained a whole generation of Palestinian neurosurgeons. The achievements of this trailblazer become even more impressive when one considers the ongoing conflicts in the region and the challenges that posed to the advancement of healthcare and education [53].

Political conflicts have marked the lives of other Middle Eastern women neurosurgeons. Israel's first female neurosurgeon fled the holocaust and her Polish home in 1934. Her name was Yafa Doron. After training in Switzerland, the United States, and Jerusalem, she became a board-certified neurosurgeon in Israel in 1960. However, in the 1970s, she abandoned neurosurgery to become a neuropathologist [2].

The academic training of neurosurgery in Iran was started by Nosratollah Ameli in the 1950s. Zahra Taati Asl became the first woman neurosurgeon in Iran. In the 1980s, she was part of the neurosurgery team who treated military patients during the Iran–Iraq war [49]. In spite of setbacks, women have greatly contributed to the establishment of neurosurgical subspecialties in the region. In Iran, Farideh Nejat established the first fellowship program in pediatric neurosurgery at Tehran University of Medical Sciences (TUMS) in 2015. She also runs a prolific research laboratory [54] and founded the Iranian Pediatric Neurosurgery Committee, in

Fig. 1.3 Georgette Kidess, the first woman neurosurgeon in Palestine. Upper: Kidess at her high school graduation in 1971. Lower: Kidess performing surgery under the microscope at the Ramallah Hospital in Palestine, 1992. (Reproduced with permission from *Journal of Clinical Neuroscience*)

association with the Neurosurgical Society of Iran (Fig. 1.4). Similarly, Alya Hasan, Kuwait's first board-certified woman neurosurgeon, established a pediatric neurosurgery unit in Ibn Sina hospital in 2014 [49].

Women have also advanced vascular neurosurgery in the Middle East. Samira Zabihyan was the first woman neurosurgeon in the Great Khorasan province of Iran. After completing a fellowship in vascular neurosurgery at Barrow Neurological Institute with Robert Spetzler, she created an academic neurovascular training program at Mashhad University of Medical Sciences (MUMS) and is currently the Residency Program Director and Vice Chair of the neurosurgery department here. Samia Maimani, the first Saudi woman in neurosurgery, was the inventor of the Maimani aneurysm clip applier and remover for use with neuroendoscopy and stereotactic systems [55]. Another Saudi woman to advance neurosurgery in her country is Tahreed Alsiani, who currently holds the position of head of the neurosurgery department in King Fahad Hospital. She also founded a neuroendoscopy course in Western Saudi Arabia in 2019, where trainees can hone their endoscopic and transnasal skills. She is also the regional

Fig. 1.4 Several Iranian women in neurosurgery. Picture taken during the annual meeting of the Iranian Society of Neurosurgery in 2014. From left to right: Mahvash Amini, Zahra Taati (first Iranian woman in neurosurgery), Mina Izadi (third Iranian woman in neurosurgery), Nahid Nasri, Zohreh Habibi, and Farideh Nejat. (Reproduced with permission from Farideh Nejat)

healthcare coordinator, a governmental position [49]. One woman who was able to complete training abroad and return to her native Middle Eastern country of Saudi Arabia was Ikhlas Altweijry. After completing her neurosurgical residency at University of Ottawa in 2009, she completed a pediatric neurosurgery fellowship in Canada. Upon her return, she started working at the King Khalid University Hospital as a pediatric neurosurgeon. She is also part of a team of leading surgeons who successfully performed the first auditory brainstem implant in Saudi Arabia [49].

Thanks to the arduous work of these trailblazers, the future of women in neurosurgery in the Middle East looks bright. In Turkey, there are currently 93 board-certified female neurosurgeons; eight are full professors and 14 are associate professors, one of the highest proportions of women in academic neurosurgery worldwide [6]. Furthermore, in countries such as the United Arab Emirates, Kuwait, and Saudi Arabia, almost half of all neurosurgery residents are women, thus posing an imminent change in the gender distribution and representation in neurosurgery in the region.

1.5 North America

Many women have played key roles in the progress of neurological surgery, but no account of North American neurosurgical origins would be complete without consideration of Louise Eisenhardt. If Harvey Cushing is regarded as the founder of modern neurosurgery, Louise Eisenhardt was his right hand. Their collaboration began in 1915, when she worked as his editorial assistant, and continued while she pursued her medical degree at Tufts University School of Medicine. While not a neurosurgeon, she was the first woman to become a neuropathologist and was Cushing's surgery associate from 1928–1934, making on-the-spot diagnoses of tumors as they were being removed by Cushing [56]. While actively pursuing this busy clinical practice, she kept a cumulative case log, made exhaustive efforts to obtain follow-up on patients to provide accurate outcome data, coauthored landmark papers with Cushing, and taught neuropathology at Tufts. She became the first editor of the *Journal of Neurosurgery* and held this position from 1944 to 1965, continually elevating the standards of academic literature. She also served as the first President of the American Association of Neurological Surgeons (AANS), known at that time as the Harvey Cushing Society [57].

It was a number of years, however, until women in the United States became neurosurgeons. The first was Ruth Kerr Jakoby, who completed a neurosurgical residency in 1959 at George Washington University, where Hugo V. Rizzoli was Chairman. In 1961, she became the first female Diplomat of the American Board of Neurological Surgery (ABNS). She was elected President of the Washington Academy of Neurosurgery in 1972, planning and overseeing continuing neurosurgical education opportunities for fellow neurosurgeons in the nation's capital [58].

Joan Venes, the first female neurosurgery resident at Yale University and the third diplomat of the ABNS in 1974, was the first woman to be awarded the Van Wagenen Fellowship. Venes was a pioneer who helped develop pediatric neurosurgery as a subspecialty. She was one of the founding members of the American Society of

Pediatric Neurosurgery (ASPN) and the first chairwoman of the Pediatric Section of the AANS. In 1990, she was the first woman to be appointed Professor of Neurosurgery, at the University of Michigan [56].

In 1977, Frances Conley, after having completed residency training at Stanford, became the fifth woman to become board-certified in neurosurgery. In 1988, she was appointed Professor of Neurosurgery at the Stanford School of Medicine and became the first tenured female professor in neurosurgery. Conley was also the first woman Division Chief of Neurosurgery at the Palo Alto Veterans Affairs Hospital [59]. Conley famously resigned her tenured position at Stanford University in protest of sexism in her department, chronicling the events in her 1998 memoir, "Walking out on the Boys." [60].

Neurosurgery celebrated a historic milestone in 1981 when Alexa Canady became the first African American female neurosurgeon. She received her M.D. cum laude from the University of Michigan in 1975 and was elected into the Alpha Omega Alpha Medical Honor Society. She then completed her neurosurgical residency training at the University of Minnesota [5]. Canady continued a productive career as a pediatric neurosurgeon, excelling in research, leadership, and mentorship. Her accomplishments particularly inspired many women and people of color toward neurosurgery careers [61].

In 1989, a group of eight American women met at a neurosurgery meeting in Atlanta, all noting that this was the first time they had seen other women at a professional meeting. Their conversations that day led to the creation of the organization, Women in Neurosurgery (WINS). WINS was established with the mission to "educate, inspire, and encourage women neurosurgeons to realize their professional and personal goals, and to serve neurosurgery in addressing the issues inherent to training and maintaining a diverse and balanced workforce [62]." In the early years of WINS, there were so few women in the field that the exhibit floor at national meetings featured a map with the names and locations of every woman in neurosurgery in the U.S. WINS joined other affiliated neurosurgical groups by becoming a Joint Section of the AANS and Congress of Neurological Surgeons (CNS) in 2016 (Fig. 1.5). Many other outstanding, trailblazing women followed as leaders of the organization, adding incorporation, governance structure, outreach, communication, and scholarship: all elements that strengthened and expanded the organization (Fig. 1.6). For 30 years, WINS has been providing valuable leadership training for individuals and groups of women neurosurgeons, from which all of neurosurgery has benefited [63].

North American women have celebrated many noteworthy achievements. In 1991, Carole Miller was the first woman elected President of the Neurosurgical Society of America. She spoke for many women in the profession when she said, "It never occurred to me I couldn't be a neurosurgeon" [64]. In 2014, Deborah Benzil became the first woman to chair the Council of State Neurosurgical Societies. Gail Rosseau was the first woman elected to the Board of Directors of the AANS and became the first officer when she served as Vice President in 2015–2016. Linda Sternau was the first woman to serve on the CNS Executive Board. Jamie Ullman served the CNS as Vice President and was honored with their Distinguished Service Award in 2018. There are notable women leaders at the forefront of advancing the field of neurosurgery in new and creative directions: Edie Zusman is a nationally

Fig. 1.5 WINS Leadership with Sally Ride, first American woman astronaut, on the occasion of the first AANS Louise Eisenhardt Lecture, celebrating women's accomplishments, 2007. (Reproduced with permission from Deborah Benzil, MD)

Fig. 1.6 WINS Leadership with Celia Sandys, granddaughter of Winston Churchill, on the occasion of her lecture on leadership at the CNS Annual Meeting in Chicago, 2006. (Reproduced with permission from Deborah Benzil, MD)

recognized expert on health systems and has devised new models for healthcare; Isabella Germano is an expert in cutting-edge technological innovations for brain tumor surgery. In April 2018, Shelly Timmons broke through a glass ceiling and was elected as the first female neurosurgeon to become President of the AANS [56]. Anne Stroink is soon to be President-Elect.

Since the specialty began, women have been integral to the progress of neurosurgical leadership and education. In 2005, Karin Muraszko, a pediatric neurosurgeon at the University of Michigan, was the first woman to be appointed chair of a U.S. Department of Neurosurgery and, several years later, was the first woman to be elected to the American Academy of Neurological Surgeons [65]. Additional women department chairs have recently been appointed. Linda Liau, in 2017, became the chair of the neurosurgery department at the David Geffen School of Medicine at University of California Los Angeles. In 2018, Aviva Abosch was appointed chair of the Department of Neurosurgery at the University of Nebraska Medical Center College of Medicine, and in 2019, Shelly Timmons was appointed chair of the Department of Neurosurgery at Indiana University [56].

In 2018, Linda Liau's contributions to healthcare and science were cited when she was named to the National Academy of Medicine. A number of other women have represented neurosurgery well by serving other medical organizations: Maya Babu served on the Board of Trustees of the American Medical Association (AMA) [66], Crystal Tomei received the AMA Excellence in Medicine Award, and Gail Rosseau chairs the Liaison Committee of the WFNS to the World Health Organization (WHO) [67]. Additional North American women neurosurgeons have published books for the general public about their experiences in neurosurgery. Katrina Firlik described her experience as a neurosurgery resident at the University of Pittsburgh in her 2006 book, "Another Day in the Frontal Lobe." [68].

Currently, women students outnumber men enrolled in American medical schools. Yet women make up only 16.3% of neurosurgical residents and 6.1% of board-certified neurosurgeons [69]. New studies have been conducted with a gender-based focus to track career paths of women in neurosurgery. Renfrow et al. [70, 71] demonstrate that over a quarter of women pursued fellowship training and the majority ended up in private practice clinical settings. Additionally, women are severely underrepresented in leadership positions. Slowly but surely, the field of neurosurgery in the U.S. is changing; there is a growing recognition of the systemic barriers that exist for professional women in neurosurgery, fuelling collective movements to address the glass ceiling and the leaky pipelines.

In Canada, 5 years after neurosurgery emerged, Kenneth G. McKenzie became the first Canadian neurological surgeon in 1924. Canadian neurosurgery remained dominated by men until the late 1960s when the early female pioneers immigrated from Europe. Quebec was the province that welcomed the trailblazers. Marina Kyriazidou from Greece trained in Quebec City, becoming the first trained and licensed female neurosurgeon in the country in 1968. Originally from France, Colette Luneau completed her training at Sherbrooke University in 1978. The same year, Elaine Joy Arpin obtained her neurosurgery certification at McGill, and eventually practiced in the U.S. Overcoming numerous obstacles was required for

Elizabeth MacRae, the first Canadian-born and trained female neurosurgeon to complete her specialization at the University of Toronto in 1981. She dedicated her career to train and inspire future generations of women in the field as a mentor and role model at the University of Calgary Cumming School of Medicine and carried a busy clinical practice at Foothills Medical Center in Calgary.

MacRae encouraged and paved the way for future generations of women who blossomed to become the first subspecialized female neurosurgeons: Liliana Goumnerova (pediatrics), Line Jacques (peripheral nerve), Shirley Stiver (vascular), Geneviève Milot (vascular and endovascular), Judith Marcoux (neurotrauma), Zelma Kiss (stereotactic and functional), Lilyana Angelov (neuro-oncology), and Sagun Tuli and Sarah Woodrow (spine). With significant effort, these women acquired important roles in neurosurgical academia. Jacques became the first woman in neurosurgery to be appointed Residency Program Director at McGill, in 2002. Milot was the first to serve as Chief Medical Examiner of the Royal College Boards of Neurosurgery. Mojgan Hodaie was the first woman to be appointed Professor of Neurosurgery in Toronto (2016). In 2020, Gelareh Zadeh became the first female to be appointed Chair of the Division of Neurosurgery at the University of Toronto and holds the Wilkins Family Chair in Neurosurgical Brain Tumor Research.

Canadian women in neurosurgery (Fig. 1.7) are also recognized for their international involvement. Hodaie is a world leader in trigeminal neuralgia research and a

Fig. 1.7 Canadian women in neurosurgery (left to right) Sarah Woodrow, Eve Tsai and Ann Parr at the Great Wall of China, during the 2019 WFNS Congress. (Reproduced with permission from Sarah Woodrow, MD)

pioneer in international neurosurgical education. With the goals of improving spine training and surgical care globally, Angelov serves as Vice-President of the World Spinal Column Society and Sarah Woodrow leads spine surgery missions in Ethiopia. Marie Long founded and is cochairperson of Global Nutrition Empowerment, a nonprofit organization dedicated to improving women's nutrition and preventing neural tube birth defects in Nepal.

Several other women serve in various leadership positions outside organized neurosurgery. Susan Brien is a physician leader and health authority with roles as CEO of Cancer Care Ontario for the Windsor Region, Director of Operations for the Canadian Patient Safety Institute and Director of Practice and System Innovation at the Royal College of Physicians and Surgeons of Canada. Sheila Singh from McMaster University has explored the frontiers of health innovation as a scientist-entrepreneur, founding and serving as CEO of Empirica Therapeutics, a company targeting glioblastoma immunotherapies.

All these women are examples of resilience and determination. After overcoming multiple challenges in a male-dominated field, they have emerged as leaders in their subspecialties and are now recognized worldwide. Nonetheless, the representation of women in Canadian neurosurgery lags behind their male counterparts, both for trainees and practicing neurosurgeons. In the years to come, the promotion of awareness of gender inequality in the field, the introduction of programs supportive of maternity and childcare, and mentorship programs will likely encourage more women to join neurosurgery and to succeed in becoming experts and innovators in their subspecialties.

1.6 Asia and Australasia

The region of Asia and Australasia is possibly the most culturally, politically, and socially diverse worldwide, encompassing countries as small as the island states in the Pacific and as geographically vast and populous as China and India. This diversity is also reflected in the disparity in neurosurgical care: in some of the island nations, there are no neurosurgeons and most rely on basic neurosurgical services provided by local general surgeons or nearby neighbors. In Timor Leste, an Australian general surgeon, Katherine Edyvane, provided trauma neurosurgical services until 2015 [72]. On the other hand, Japan has the highest number of neurosurgeons per capita in the world [73], showcasing the great heterogeneity that characterizes this region. The representation of women in Asian and Australasian neurosurgery is just as diverse: while 30% of Mongolia's neurosurgical workforce are women, many countries such as the Kingdoms of Bhutan and Cambodia still await their first woman in neurosurgery [3].

The first woman neurosurgeon in Asia was India's Thanjavur Santhanakrishna Kanaka (1932–2018), who completed her training in 1968 after many struggles to prove her worth and be taken seriously by her male superiors as a woman in neurosurgery [74] (Fig. 1.8). Kanaka pioneered stereotactic surgery in Madras in the 1960s, and her team was the first to perform stereotactic surgical procedures in

Fig. 1.8 China Forum of Women in Neurosurgery, attended by Asia's first woman in neurosurgery, T. S. Kanaka from India (insert), accompanied by other pioneers in Asian neurosurgery to her right: Ling Feng from China Yoko Kato from Japan. (Reproduced with permission from *Journal of Clinical Neuroscience*)

India, treating movement disorders, psychiatric conditions, and epilepsy. Thanks to her efforts, Madras became a world-renowned center for stereotactic neurosurgery [75]. She also carried out research in spinal cord stimulation for paraplegia. Kanaka was an extraordinarily dedicated physician, recognized for her selfless service, hard work, and rigor. She volunteered in 1962–1963 during the Indo-China War as a war doctor to treat military casualties. After her retirement in 1990, she used her savings to set up the prestigious Sri Santhanakrishna Padmavathi Health Care and Research Foundation, which offers free treatment to the poor [74].

The struggle of women to receive medical and surgical training in the region is further exemplified in Australia. Here, the Queen Victoria Medical Centre (QVMC) was founded in Melbourne in 1896 by five women doctors who could not gain employment elsewhere. They established a "shilling fund", whereby every woman in the state would give one shilling to establish the hospital. It was a hospital run by women for women, where Elizabeth Lewis, Australia's first woman in neurosurgery, began her general surgery training. She went on to become a pediatric neurosurgeon, trained both in the United Kingdom and Australia. She is revered as a tough and tenacious role model [76].

Most women in Australasia and Asia had to travel abroad to obtain neurosurgical training. Mongolia's first woman in neurosurgery, Dorj Javzmaa was trained in Russia [77]. In the Philippines, Camellia Josefina Nierras Posoncuy pursued a fellowship at the Hadassah University Hospital, Jerusalem. Her placement, however,

was abruptly interrupted by the Yom Kippur War in 1973, and she ventured to Switzerland, where she completed her neurosurgery residency under Professor Gazi Yasargil. She returned to the newly formed University of the Philippines-Philippine General Hospital Neurosurgery Program in the 1980s, where she has served as a role model for fellow women in neurosurgery in the country.

Similarly, Suzanne Jackson underwent training in Germany and the United Kingdom, first in general surgery and then neurosurgery, before returning to her native New Zealand to complete the Australasian neurosurgery training program. She became her country's first woman in neurosurgery in 1997 [3]. Nicole Keong Chwee Har was trained in the United Kingdom and emigrated to Singapore in 2013, while Maheshi Wijerathne was also trained in the United Kingdom and is the sole female neurosurgeon in Sri Lanka [78].

Women neurosurgeons in the region have also been involved in humanitarian causes and have contributed to the expansion of neurosurgical care in their respective countries and beyond. Nantaka Tepaamondej provided neurosurgical care for 18 years to civilians living in a war zone in Southern Thailand [3]. Similarly, Indonesia's Jeanne PMR Winaktu (Fig. 1.9) joined her country's navy and devoted her life to neurosurgery, disaster management, and military health research [79]. China's Ling Feng has worked to establish orphanage schools in her country, as well as WFNS Neurosurgery Training Programs in Africa. Furthermore, she introduced the endovascular treatment of arteriovenous malformations to her country. Taiwan's Wen-Lin Chen leads a company that provides services to medical workers in challenging environments, while India's Asha Bakshi works to bring affordable

Fig. 1.9 Jeanne PMR Winaktu, Indonesia's first woman in neurosurgery. (Reproduced with permission from *Journal of Clinical Neuroscience*)

neurosurgical care to parts of India, Kashmir, Kabul, and Tajikistan [3]. Australia's Kate Drummond is committed to delivering surgical multidisciplinary education in low- and middle-income countries through Pangea Global Health Education [80]. At the pinnacle of societal achievement, Australian neurosurgeon Ruth Mitchell jointly launched the International Campaign to Abolish Nuclear Weapons (ICAN), which led to negotiations for a treaty to ban nuclear weapons at the United Nations in 2017, and to a Nobel Peace Prize for the organization [81].

Asian and Australasian women in neurosurgery have also made great contributions to academic neurosurgery. China's first woman in neurosurgery, Pu Peiyu, completed a research fellowship at the Sloan Kettering Cancer Institute in the United States in the 1980s. Upon her return to China, she founded her own neuro-oncology laboratory and is currently recognized as a pioneer in the treatment of gliomas [82]. Pakistan's Aneela Darbar completed her residency training at the State University of New York, Syracuse in the U.S., and is currently the medical director and head of neurosciences at the Mukhtar A. Sheikh Hospital, Multan. In addition to authoring multiple chapters in books and publications, she also provides free treatment to children in Zanzibar through a nongovernmental organization [83].

Japan's Yoko Kato was not only the country's first woman in neurosurgery, but she is also globally recognized as a leader in vascular neurosurgery. Her research on aneurysm morphology and flow dynamics has greatly contributed to the advancement of the field [84]. In addition to her prolific academic career, she has been a fervent advocate of women in neurosurgery, founding the Asian Women in Neurosurgery Chapter in 1996. She is also deeply committed to training young neurosurgeons and is a champion of global neurosurgery. Her foundation regularly purchases medical equipment for neurosurgeons in low- to middle-income countries [85].

While much remains to be done to break the glass ceiling for women in Asian and Australasian neurosurgery, their contributions to the field exemplify how much can be achieved by a diverse neurosurgical workforce.

1.7 Africa

In most African countries, the number of women within the neurosurgical field is still low. According to Karekezi et al. [86], the estimated total number of African Women in Neurosurgery (AWIN) as of November, 2020, is roughly 243 (female residents/trainees excluded). Northern Africa accounts for 187, which is approximately 77% of all AWIN. Algeria has the highest number of women neurosurgeons and leads with more than half of the continent's WIN ($n = 135$ [87]).

The history of women in neurosurgery in Africa began in 1977 in Algeria, with Professor Faiza Lalam. She completed certification in 1982, beginning to work at the surgical department of Tizi Ouzou University Hospital, where in 2011, she was appointed professor and department chair [88]. In 2014, Professor Souad Bakhti became the first woman President of a national neurosurgical society in Africa. In

2017, she was appointed Department Chair at the Specialized Hospital Ali Ait Idir in Algiers. Morocco follows this listing, with 25 women neurosurgeons. In 1994, Moroccan Professor Najia El Abbadi became the first African female professor of neurosurgery. In 2018, she became the first female President of the Pan Arab Neurosurgical Society [89].

Sudan has 13 women neurosurgeons, led by Sawsan Aldeaf, a prominent researcher on the molecular genetics of meningiomas. Egypt has the highest number of male neurosurgeons, currently over 500, yet only 3 women neurosurgeons. The rest of Africa is still underrepresented; some countries are without a single practicing neurosurgeon, male or female [87]. It is encouraging, however, to see that numbers are rising.

Nigerian E. Latunde Odeku was trained in the U.S., then relocated to the University of Ibadan [90]. Over 50 years later, Nigeria had its first female neurosurgeon: Salamat Ahuoiza Aliu-Ibrahim, who was admitted as a fellow in neurosurgery of the West African College of Surgeons in 2015. She completed her residency training at the National Hospital in Abuja and set the path for female neurosurgeons in her country. Nigeria has 80 registered neurosurgeons at last count; only 5 (6.2%) are female.

In 2006, Espérance Maman You Broalet became the first woman in neurosurgery in West Africa. She practiced at the Yopougon University Hospital in Abidjan, Ivory Coast until 2015, after which she relocated to the Université de Bouaké. In October 2019, she set up the St. Joseph Moscati Catholic Hospital in Yamoussoukro, where she is currently the department chair. Broalet is an academic and philanthropic leader within the field of neurosurgery: in 2013, she founded "Espérance's Hope," which is an Ivorian association that aims to combat hydrocephalus and neural tube defects in the region [91].

Senegal has trained the highest number of female neurosurgeons within the West African region, a total of ten women qualified, not only from Senegal but also Cameroon, Gabon, Democratic Republic of the Congo (DRC), and Niger. To date, Senegal counts four female Senegalese-certified neurosurgeons, and 13 of 37 neurosurgical trainees are women.

The region of Central Africa has nine countries with a population of 180.4 million, but within this region, several countries do not have a single practicing neurosurgeon to date. These countries include Central African Republic, Equatorial Guinea, and São Tomé and Príncipe. The DRC is the largest country within the region and has a population of 84.07 million; it is served by only 11 qualified neurosurgeons. Sarah Mutomb, who was trained in Senegal and qualified in 2019, is the first and currently only female neurosurgeon in the DRC. Cameroon has the highest number of female neurosurgeons in Central Africa, with a total of five. Mirelle Moumi was the first female graduate, after completing training in Dakar, Senegal in 2008.

The Eastern African region comprises 15 countries with a population of 537.9 million. Countries such as Comoros, Djibouti, Eritrea, and Seychelles do not have a single practicing neurosurgeon. In addition, Burundi, Djibouti, Malawi, and Somalia do not have a female neurosurgeon. Kenya leads the region with six female

neurosurgeons. Sylvia Shitsama and Susan Karanja both graduated in 2015 from the University of Nairobi and KwaZulu-Natal, respectively, and became pioneers in Kenya. Tanzania follows with four female neurosurgeons. Aingaya Kaale and Happiness Rabiel graduated as neurosurgeons in 2018, followed by two additional female neurosurgeons in 2020 [92].

Ethiopia has two qualified women neurosurgeons, the first being Yordanos Ashagre (2015). Juliet Sekabunga is the first female neurosurgeon to graduate from Uganda, and she continued her studies and completed her pediatric fellowship at Toronto's Hospital for Sick Children. Claire Karekezi graduated from the WFNS Rabat Training Center, Morocco, in 2016 and became the first female neurosurgeon in Rwanda. She completed a neuro-oncology and skull-base surgery fellowship at the University of Toronto, Toronto Western Hospital. In June 2018, she established a new neurosurgical unit at the Rwanda Military Hospital, in the capital city Kigali [93].

Southern Africa is located on the southernmost tip of the continent. It comprises the following eight countries: Botswana, Lesotho, Mozambique, Namibia, Republic of South Africa (RSA), Swaziland, Zambia, and Zimbabwe. The history of female neurosurgeons within this region started in the early 1990s. The first female neurosurgeon to qualify in this region was Minette du Preez, who trained at the University of the Free State. Her Zimbabwean-born colleague, Nozipho Maraire, was trained as a neurosurgeon at the Yale University School of Medicine in the U.S. These women laid a solid foundation for the next generation of Southern Africa's women to thrive in this discipline and continue their legacy. RSA ranks third in female representation in neurosurgery in the continent with 18 female neurosurgeons. Five women surgeons in RSA are full-time academic staff; three are at the University of Cape Town. Regarding leadership positions, Coceka Mfundisi became the first woman to qualify as a neurosurgeon in RSA, from the University of Pretoria in its 100-year history [94].

The male-dominated culture in many parts of Africa remains a major barrier faced by women choosing any medical field. Yet women now make up more than 50% of medical school graduates on the continent. In Africa, only 3% of women neurosurgeons are full professors and all are found within Northern Africa [87, 95, 96].

1.8 Conclusion

Women in other surgical specialties have joined forces to create organizations with goals similar to those of WINS. In Asia, Yoko Kato founded the Asian Women's Neurosurgical Association in 1996. In Europe, the Diversity Task Force was created in 2019 to tackle gender diversity issues. While there are some national WINS in Latin America, the Federation of Latin American Neurosurgical Societies was to launch a WINS chapter for the entire region in 2020, but due to the global pandemic, the initiative was postponed. Similar efforts are underway in Africa. Since 1981, the

Association of Women Surgeons has advocated for women throughout their careers in surgery. Recently, the Gender Equity Initiative in Global Surgery (GEIGS) at the Harvard Program for Global Surgery and Social Change (PGSSC) was formed to reduce gender disparities in the surgical workforce and empower women surgeons worldwide through research, advocacy, and mentorship. These and other organizations are stimulating the much-needed policy changes to bring about gender equity in the surgical workforce.

Breaking new ground, international women neurosurgeons of the profession's first century have persisted, succeeded, and made their marks in this male-dominated field. These pioneers have recruited and encouraged younger women to join the field. Thanks to these trailblazing leaders, other bright women have gained entry and have excelled in the profession, advancing the field of neurosurgery in a multitude of directions over the past century. The past 30 years, in particular, have been a period of increasing involvement and responsibility for women in neurosurgery. We must now focus on continual system improvements that will promote a diverse and talented workforce, building a welcoming environment for all aspiring neurosurgeons, in order to advance the specialty in the service of neurosurgical patients.

Acknowledgements Amal Abou-Hamden, Salamat Ahuoiza Aliu-Ibrahim, Hissah K. Al Abdulsalam, Redab A.M. Alkhataybeh, Zarina Ali Shabhay, Noora Al-Shehhi, Roqia Al-Azzani, Talivaldis Apinis, Esther Apuahe, Nada Ayedh HadiSouad Bakhti, Alicia Becerra Zegarra, Hajar Bechri, Mouna Bougrine, Espérance Maman You Broalet, Marike Broekman, Jebet Beverly Cheserem, Jacquelyn Corley, Aneela Darbar, Mania de Praeter, Annie Dubuisson, Najia El Abbadi, Évelyne Emery, Ulrike Eisenberg, Roxanna M. Garcia, Debora Garozzo Nurperi Gazioglu, Rachel Grossman, Zohreh Habibi, Alya Hasan, Tijana Ilic, Daniela Ivan, Insa Katrin Janssen, Maria Karampouga, Shweta Kedia, Lika Khorbaladze, Eliana Kim, Meng-Fai Kuo, Xanthoula Lambrianou, Elizabeth Lewis, Boleslav Liktherman, Laura Lippa, Lynne Lourdes N. Lucena, Hulda Magnadottir, Wirginia Maixner, Maguette Mbaye, Stiliana Mihaylova, Ena I. Miller Molina, Su Myat Mok, Thana Namer, Milagros Niquen-Jimenez, Sarah Olson, Ermira Pajaj, Ann Parr, Chris Phillips, Woralux Phusoongnernm, Hama Quadamkhear, Dunia Patricia Quiroga, Katrin Rabiei, Alma Griselda Ramírez-Reyes, Ana Rodríguez-Hernández, Aseel Sbeih, Resha Shrestha, Martina Stippler, Jennifer Sweet, Anastasia Tasiou, Nqobile Thango, Nabila Tighilt, Nujerling Vargas Santana, Pia Vayssiere, Lin Yan, Samira Zabihyan.

References

1. Hernández-Durán S, Kim E, Ivan D, et al. Four Athenas—Europe's first female neurosurgeons. J Clin Neurosci. 2021;86:332–6. https://doi.org/10.1016/j.jocn.2021.01.033.
2. Hernández-Durán S, Murphy M, Kim E, et al. European women in neurosurgery: I—a chronology of trailblazers. J Clin Neurosci. 2021;86:316–23. https://doi.org/10.1016/j.jocn.2021.01.026.
3. Drummond KJ, Kim EE, Apuahe E, et al. Progress in neurosurgery: contributions of women neurosurgeons in Asia and Australasia. J Clin Neurosci. 2021;86:357–65. https://doi.org/10.1016/j.jocn.2021.02.002.
4. Zanon N, Niquen-Jimenez M, Kim EE, et al. Progress in neurosurgery: contributions of women neurosurgeons in Latin America. J Clin Neurosci. 2021;86:347–56. https://doi.org/10.1016/j.jocn.2021.01.054.

5. Wolfert C, Rohde V, Mielke D, Hernández-Durán S. Female neurosurgeons in Europe—on a prevailing glass ceiling. World Neurosurg. 2019;129:460–6. https://doi.org/10.1016/j.wneu.2019.05.137.
6. Murphy M, Hernández-Durán S, Kim E, et al. European women in neurosurgery: II—historical characters and living legends. J Clin Neurosci. 2021;86:324–31. https://doi.org/10.1016/j.jocn.2021.01.024.
7. Bormane A. https://timenote.info/lv/Anna-Bormane-03.04.1896. Accessed 26 May 2021.
8. University of Latvia. History of Sciences and Museology. University of Latvia. 2004. http://inis.iaea.org/search/search.aspx?orig_q=RN:36084093.
9. Rosenstein A. Uber Akromegalie und cerebrale Lues. Z Für Gesamte Neurol Psychiatr. 1923;88(1):420–33. https://doi.org/10.1007/BF02906633.
10. Ga R, Gagel O, Professur B, et al. Sein Lebenswerk im. Rahmen der Wissenschaft; 1943.
11. Sarikcioglu L. Otfrid Foerster (1873–1941): one of the distinguished neuroscientists of his time. J Neurol Neurosurg Psychiatry. 2007;78:650. https://doi.org/10.1136/jnnp.2006.112680.
12. Rosenstein A. Die Darstellung des Foramen Monroi im encephalographischen Bilde. Zeitschrift für die gesamte Neurologie und Psychiatrie. 1926;102:420–4. https://doi.org/10.1007/BF02962290.
13. Eisenberg U, Collmann H, Dubinski D. Execrated–expatriated–eradicated: the lives and works of German neurosurgeons persecuted after 1933. Berlin: Hentrich und Hentrich Verlag; 2019.
14. Jefferson G. Memories of Hugh Cairns. J Neurol Neurosurg Psychiatry. 1959;22:155–66. https://doi.org/10.1136/jnnp.22.3.155.
15. Gilkes C. An account of the life and achievements of Miss Diana Beck, neurosurgeron (1902–1956). Neurosurgery. 2008;62:738–42. https://doi.org/10.1227/01.NEU.0000297112.95496.68.
16. Beck DJK, Russell DS, Small JM, Graham MP. Implantation of acrylic-resin discs in rabbits' skulls. Br J Surg. 1945;33:83–6. https://doi.org/10.1002/bjs.18003312913.
17. Ogrezeanu I. Women in neurosurgery: Romania. In: The 13th WFNS Congress. Oral presentation mentioned in the abstract book of the Congress. 2005.
18. Idu A-A, Mohan A-G, Saceleanu M-V, Ciurea A-V. Historical vignette. Romanian Neurosurg. 2020;34(2):209–12. https://doi.org/10.33962/roneuro-2020-032.
19. Ciurea AV, Moisa HA, Mohan D. Sofia ionescu, the first woman neurosurgeon in the world. World Neurosurg. 2013;80:650–3. https://doi.org/10.1016/j.wneu.2013.02.031.
20. Hitchins K. Romania. Am Hist Rev. 1992;97(4):1064–83. https://doi.org/10.2307/216549321.
21. Lichterman B. Emergence and early development of Russian neurosurgery (1890s–1930s). J Hist Neurosci. 2007;16:123–37. https://doi.org/10.1080/09647040600700245.
22. Engel BA. Women in Russia and the Soviet Union. Signs J Women Cult Soc. 1987;12:781–96. https://doi.org/10.1086/494366.
23. Sowers S. Women combatants in world war I: a Russian case study. Carlisle: Army War College; 2003. https://apps.dtic.mil/dtic/tr/fulltext/u2/a414547.pdf.
24. Kisteneva O, Vovk J, Linnik M, Kistenev V. Nikolay Nilovic Burdenko (the 140th anniversary of birth). Int Sci Rev. 2016. https://amosov.org.ua/index.php/naukovi-materiali/mikola-nilovich-burdenko-do-140-richchja-vid-dnja.
25. Likhterman LB. In memories of Serafima Semenovna Bryusova (on occasion of the 125th birthday). Burdenkos J Neurosurg. 2019;83(6):135–6. https://doi.org/10.17116/neiro201983061135.
26. Likhterman LB. Female face of neurosurgery (to the 100th birthday anniversary of K.I. Kharitonova). Russ J Neurosurg. 2016;4:14–6.
27. [Unknown]. Prominent spine specialists. Kseniya Ivanovna Kharitonova Hirurgiâ pozvonočnika. Spine Surg. 2006;1:098–9.
28. Monument to Ksenia Kharitonova | Library of Siberian Local Lore. http://bsk.nios.ru/content/pamyatnik-ksenii-haritonovoy. Accessed 26 May 2021.
29. Department of Neurosurgery KazMUNO. To the 100th anniversary of Evgenia Andreevna Azarova. Neurosurg Neurol Kazakhstan. 2014;2(35):38–9.

30. Khalimov A. Development of Neurotraumatology in Almaty on the example of the neurosurgical Department of the City Clinical Hospital no.7. Neurosurg Neurol Kazakhstan. 2011;3(24):9–10.
31. Lichterman B. Anna A Artaryan: paediatric neurosurgeon who created the first chair in the specialty. Br Med J. 2020;269:m2298. https://doi.org/10.1136/bmj.m2298.
32. Rostotskaya WI. Spina bifida and its surgical treatment (Russian). Acad Honey Sciences; 1954.
33. Steklacova A, Bradac O, de Lacy P, Benes V. E-WIN project 2016: evaluating the current gender situation in neurosurgery across Europe—an interactive, multiple-level survey. World Neurosurg. 2017;104:48–60. https://doi.org/10.1016/j.wneu.2017.04.094.
34. Miyan J. Carys Margaret Bannister. Br Med J. 2010;341:c7238. https://doi.org/10.1136/bmj.c7238.
35. Trinka E. Internationaler Preis für Wissenschaft und Forschung. Amsterdam: Elsevier; 2009.
36. Ackermans L, Temel Y, Visser-Vandewalle V. Deep brain stimulation in Tourette's syndrome. Neurotherapeutics. 2008;5:339–44. https://doi.org/10.1016/j.nurt.2008.01.009.
37. Faria CC, Agnihotri S, Mack SC, et al. Identification of alsterpaullone as a novel small molecule inhibitor to target group 3 medulloblastoma. Oncotarget. 2015;6:21718–29. https://doi.org/10.18632/oncotarget.4304.
38. de Faria CMC. Bio | Diverse Leaders in Neurosurgery. https://www.eans.org/page/ClaudiaMariaCoelhodeFaria-Bio. Accessed 22 Jun 2021.
39. Pastor A, del CHUO, rumbo a Níger para formar a médicos. https://www.laregion.es/articulo/ourense/ana-pastor-chuo-rumbo-niger-formar-medicos/20191007072042898173.html. Accessed 22 Jun 2021.
40. Vujotic L. Bio | Diverse Leaders in Neurosurgery. https://www.eans.org/page/LjiljanaVujotic-Bio. Accessed 22 Jun 2021.
41. López GC, de Romo ACR. María Cristina García-Sancho y Álvarez-Tostado: Primera neurocirujana en Latinoamérica. Salud Mental. 2010;33:111–21.
42. Goyenechea Gutiérrez F. Historia de la Neurocirugía en Cuba. RCNN. 2013;3:39–47.
43. Miller EI, De la Riva R, Ortega JE, et al. Current situation of neurosurgery in Central America: an analysis and suggestions for improvement. World Neurosurg. 2013;80(5):e53–7.
44. About Dr. Zamorano—Zamorano L, MD, PLC. https://www.luciazamorano.com/about-dr-zamorano/. Accessed 8 Jun 2021.
45. Manucci G, von Quednow E. Como lo hago yo: anomalías del tubo neural en Guatemala—Mielomeningocele unidad de espina bífida e hidrocefalia. Surg Neurol Int. 2014;5:S13. https://doi.org/10.4103/2152-7806.128463.
46. Mejía-Pérez SI, Cervera-Martínez C, Sánchez-Correa TE, Corona-Vázquez T. La mujer en neurocirugía en el Instituto Nacional de Neurología y Neurocirugía (INNN). Gaceta Medica de Mexico. 2017;153:279–82.
47. Coelho G, Zymberg S, Lyra M, et al. New anatomical simulator for pediatric neuroendoscopic practice. Childs Nerv Syst. 2015;31:213–9. https://doi.org/10.1007/s00381-014-2538-9.
48. Eleições 2018 | Dra. Marise Audi Deputado Federal 3060 | Estadão. https://politica.estadao.com.br/eleicoes/2018/candidatos/sp/deputado-federal/dra-marise-audi,3060. Accessed 9 Jun 2021.
49. Habibi Z, Hadi NA, Kim EE, et al. Progress in neurosurgery: contributions of women neurosurgeons in the Middle East. J Clin Neurosci. 2021;86:337–46. https://doi.org/10.1016/j.jocn.2021.01.055.
50. Balak N, Elmaci I. A pioneering female neurosurgeon: Dr. Aysima Altinok. Acta Neurochir. 2007;149:943–8. https://doi.org/10.1007/s00701-007-1252-8.
51. Gazioğlu N. Bio|Diverse Leaders in Neurosurgery. https://www.eans.org/page/NurperiGaziolu-Bio. Accessed 10 Jun 2021.
52. Saudi Arabia allows women to travel without male guardian's approval | Saudi Arabia | The Guardian. https://www.theguardian.com/world/2019/aug/01/saudi-women-can-now-travel-without-a-male-guardian-reports-say. Accessed 12 Jun 2021.

53. Darwazeh R, Darwazeh M, Kato Y, et al. Georgette Kidess, the first female neurosurgeon in Palestine. World Neurosurg. 2019;124:414–22. https://doi.org/10.1016/j.wneu.2018.12.163.
54. Alimi M, Taslimi S, Ghodsi SM, Rahimi-Movaghar V. Quality and quantity of research publications by Iranian neurosurgeons: signs of scientific progress over the past decades. Surg Neurol Int. 2013;4:38. https://doi.org/10.4103/2152-7806.109651.
55. Maimani S. Maimani aneurysm clip applier and remover for use with neuroendoscopes and stereotactic systems. 1997. https://europepmc.org/article/PAT/WO9918840. Accessed 30 Oct 2020.
56. Corley J, Kim E, Philips CA, et al. One hundred years of neurosurgery: contributions of American women. J Neurosurg. 2020;134(2):337–42. https://doi.org/10.3171/2019.12.JNS192878.
57. Davey LM. Louise Eisenhardt, MD: first editor of the Journal of Neurosurgery (1944–1965). J Neurosurg. 1994;80:342–6. https://doi.org/10.3171/jns.1994.80.2.0342.
58. Jakoby RK, MD|Women In Neurosurgery (WINS). http://www.neurosurgerywins.org/doctor/dr-ruth-jakoby. Accessed 1 Jul 2021.
59. Conley FK, MD|Women In Neurosurgery (WINS). http://www.neurosurgerywins.org/doctor/dr-frances-conley. Accessed 1 Jul 2021.
60. Conley FK. Walking out on the boys. New York: Farrar, Straus and Giroux; 1998.
61. Changing the Face of Medicine|Alexa Irene Canady. https://cfmedicine.nlm.nih.gov/physicians/biography_53.html. Accessed 1 Jul 2021.
62. Benzil DL, Abosch A, Germano I, et al. The future of neurosurgery: a white paper on the recruitment and retention of women in neurosurgery. J Neurosurg. 2008;109:378–86. https://doi.org/10.3171/JNS/2008/109/9/0378.
63. Renfrow JJ, Rodriguez A, Wilson TA, et al. Tracking career paths of women in neurosurgery. Clin Neurosurg. 2018;82:576–81. https://doi.org/10.1093/neuros/nyx251.
64. Biography—Miller C, MD (Ohio). https://wayback.archive-it.org/org-350/20190508153456/https://www.nlm.nih.gov/exhibition/locallegends/Biographies/Miller_Carole.html. Accessed 1 Jul 2021.
65. Paving the Way: Dr. Karin Muraszko reshapes the medical field as the first (and only) female chair of neurosurgery. https://www.michigandaily.com/uncategorized/muraszko/. Accessed 1 Jul 2021.
66. Maya A. Babu Biography—cns.org. https://www.cns.org/maya-a-babu-biography. Accessed 1 Jul 2021.
67. Rosseau G. The G4 Alliance. http://www.theg4alliance.org/gail-rosseau. Accessed 1 Jul 2021.
68. Firlik K. Another day in the frontal lobe: a brain surgeon exposes life on the inside. New York: Random House; 2007.
69. Corley J, Williamson T. Women in neurosurgery: final frontier of career women's movement. World Neurosurg. 2018;111:130–1. https://doi.org/10.1016/j.wneu.2017.12.086.
70. Renfrow JJ, Rodriguez A, Wilson TA, et al. Tracking career paths of women in neurosurgery. Neurosurgery. 2018;82:576–82. https://doi.org/10.1093/neuros/nyx251.
71. Renfrow JJ, Rodriguez A, Liu A, et al. Positive trends in neurosurgery enrollment and attrition: analysis of the 2000–2009 female neurosurgery resident cohort. J Neurosurg. 2016;124:834–9. https://doi.org/10.3171/2015.3.JNS142313.
72. Edyvane K|RACS. https://www.surgeons.org/about-racs/about-the-college-of-surgeons/in-memoriam/obituaries/katherine-edyvane. Accessed 13 Jun 2021.
73. Mukhopadhyay S, Punchak M, Rattani A, et al. The global neurosurgical workforce: a mixed-methods assessment of density and growth. J Neurosurg JNS. 2019;130:1142–8. https://doi.org/10.3171/2018.10.JNS171723.
74. Satyarthee GD, Jagdevan A. TS Kanaka: first Asian woman neurosurgeon, who pioneered stereotactic, functional and cerebral electrode implant surgery and developed separate neurosurgical speciality in India early 1970. Asian J Neurosurg. 2019;14:1050. https://doi.org/10.4103/ajns.AJNS_287_18.

75. Balasubramaniam V, Kanaka TS. Stereotaxic surgery in developing countries—a review. Zentralblatt fur Neurochirurgie. 1981;42:69–74.
76. Lewis EA|Women's Museum of Australia. https://wmoa.com.au/collection/herstory-archive/lewis-1. Accessed 14 Jun 2021.
77. Dulam E, Khairulla J, Batchuluun B, et al. The history of neurosurgery in Mongolia. Multidisciplinary brain science, vol. 1. Paris: IBRO; 2017.
78. Dr. Maheshi elected NASL President—News Features|Daily Mirror. https://www.dailymirror.lk/139928/Dr-Maheshi-elected-NASL-President-. Accessed 14 Jun 2021.
79. (No Title). https://www.wfns.org/WFNSData/Uploads/files/INS-Obituary-Dr-Jeanne.pdf. Accessed 14 Jun 2021.
80. Pangea Global Health Education. https://www.pangeaghe.org/. Accessed 14 Jun 2021.
81. A pub in Carlton: the story of Australia's first Nobel Peace Prize|InSight+. https://insightplus.mja.com.au/2017/48/a-pub-in-carlton-the-story-of-australias-first-nobel-peace-prize/. Accessed 14 Jun 2021.
82. Zhang Z, Zhou J, Zhang J, et al. Downregulation of lncRNA-HOXA11-AS modulates proliferation and stemness in glioma cells. Chin Neurosurg J. 2017;3:25. https://doi.org/10.1186/s41016-017-0091-6.
83. Darbar A. Profile—Practicing neurosurgery as a woman in Pakistan—cns.org. https://www.cns.org/publications/congress-quarterly/congress-quarterly-detail/aneela-darbar-profile-practicing-neurosurgery-as-w. Accessed 14 Jun 2021.
84. Shah A. Yoko Kato: the silent warrior of neurosurgery. Neurosurg Focus. 2021;50:E17. https://doi.org/10.3171/2020.12.FOCUS20899.
85. Donation from Professor Yoko Kato in 2016|WFNS. https://www.wfns.org/news/8/. Accessed 14 Jun 2021.
86. Karekezi C, Thango N, Aliu-Ibrahim SA, et al. History of African women in neurosurgery. Neurosurg Focus. 2021;50:1–9. https://doi.org/10.3171/2020.12.FOCUS20905.
87. Sadler SJ, Yuki Ip HK, Kim E, et al. Investing in the future: a call for strategies to empower and expand representation of women in neurosurgery worldwide. Neurosurg Focus. 2021;50:E8. https://doi.org/10.3171/2020.12.FOCUS20963.
88. Chair's Report: WIN–WFNS in Global Neurosurgery|WFNS. https://www.wfns.org/newsletter/225. Accessed 1 Jul 2021.
89. El Abbadi N. Chairman of Neurosurgery in Rabat, Rabat-Sale-Kenitra, MoroccoleMedEvents. https://www.emedevents.com/speaker-profile/najia-el-abbadi. Accessed 1 Jul 2021.
90. McClelland S 3rd, Harris KS. E. Latunde Odeku: the first African-American neurosurgeon trained in the United States. Neurosurgery. 2007;60:769–72. discussion 772. https://doi.org/10.1227/01.NEU.0000255410.69022.E8.
91. L'Ivoirienne Espérance Broalet, première femme agrégée en anatomie et neurochirurgie du CAMES (PORTRAIT)—Abidjan.net. https://news.abidjan.net/h/670144.html. Accessed 1 Jul 2021.
92. 10 Remarkable African Women Breaking Barriers in Health Care. https://www.globalcitizen.org/en/content/african-women-in-heath-medicine-doctors/?template=next. Accessed 1 Jul 2021.
93. Karekezi C. Profile—Practicing neurosurgery in Sub-Saharan Africa—cns.org. https://www.cns.org/publications/congress-quarterly/congress-quarterly-detail/claire-karekezi-profile-practicing-neurosurgery-in. Accessed 1 Jul 2021.
94. Meet Dr. Mfundisi C. Who was one of the first black women to qualify as a neurosurgeon in SA|W24. https://www.news24.com/w24/work/jobs/meet-dr-coceka-mfundisi-who-was-one-of-the-first-black-women-to-qualify-as-a-neurosurgeon-in-sa-20210308. Accessed 1 Jul 2021.
95. Dada OE, Karekezi C, Mbangtang CB, et al. State of neurosurgical education in Africa: a narrative review. World Neurosurg. 2021;151:172–81. https://doi.org/10.1016/j.wneu.2021.05.086.
96. Balasubramanian SC, Palanisamy D, Bakhti S, et al. Women in neurosurgery (WIN): barriers to progress, world WIN directory and the way forward. Asian J Neurosurg. 2020;15:828–32. https://doi.org/10.4103/ajns.AJNS_108_20.

Chapter 2
Functional Approaches to the Surgery of Brain Gliomas

Davide Giampiccolo, Sonia Nunes, Luigi Cattaneo, and Francesco Sala

2.1 Introduction

2.1.1 Early 2000 and a Role for Extent of Resection in Overall Survival

Every year, ~100,000 people worldwide are diagnosed as having diffuse gliomas [1]. Although it comprises <1% of all newly diagnosed cancers, diffuse glioma is associated with substantial mortality and morbidity [1]. Glioblastoma, the highest grade glioma, accounts for 70–75% of all diffuse glioma diagnoses and has a median overall survival of 14–17 months in the adult population, with a similar life expectancy in children despite different driving mutations and different location.

D. Giampiccolo
Section of Neurosurgery, Department of Neurosciences, Biomedicine and Movement Sciences, University Hospital, University of Verona, Verona, Italy

Department of Clinical and Experimental Epilepsy, UCL Queen Square Institute of Neurology, University College London, London, UK

Victor Horsley Department of Neurosurgery, National Hospital for Neurology and Neurosurgery, Queen Square, London, UK

Institute of Neurosciences, Cleveland Clinic London, London, UK
e-mail: d.giampiccolo@ucl.ac.uk

S. Nunes · F. Sala (✉)
Section of Neurosurgery, Department of Neurosciences, Biomedicine and Movement Sciences, University Hospital, University of Verona, Verona, Italy
e-mail: soniaelizabeth.queiroznunes@univr.it; francesco.sala@univr.it

L. Cattaneo
Center for Mind and Brain Sciences (CIMeC) and Center for Medical Sciences (CISMed), University of Trento, Trento, Italy

C. Di Rocco (ed.), *Advances and Technical Standards in Neurosurgery*, Advances and Technical Standards in Neurosurgery 45,
https://doi.org/10.1007/978-3-030-99166-1_2

The previously classified lower grade "diffuse gliomas" have a slower progression, but inevitably progress into glioblastomas. While in the past low grade gliomas (LGG) showed an overall survival of 6 years, they currently have a median overall survival of 13 years, with deterioration due to an inevitable malignant transformation [2, 3]. Since the seminal classification of Percival Bailey and Harvey in the early twentieth century [4], the diagnosis has been histological with the prognosis being highly variable. Already at that time, there were concern that these tumours may underlie high heterogeneity possibly suggesting the limit of a classification based only on tumour morphology [4]. However, stemming initially from 16 different histotypes [4], a classification based only on histomorphological distinction resisted until 2016. Arguing on the high variability in survival, the adjuvant role of radiotherapy, and the burden of neurological deficits, the value of surgery outside debulking and histological diagnosis was questioned for glioblastoma, as "little scientifically credible evidence is available to support the assertion that aggressive surgical resection prolongs survival" [5], particularly when resection was combined with post-operative radiotherapy [6]. Surgery had moreover to be counterbalanced by a high risk for neurological deficits, up to a fourth of cases (25.7%) [7]. Similarly, for adult LGGs, often watchful waiting was proposed considering that the benefits of resection early in the course of the disease had not been proven in terms of survival [8], with possibly a poorer prognosis in terms of cognition and quality of life [9].

The beginning of the new millennium signed a major change for surgical indication to gliomas. For glioblastoma, Lacroix et al. [10] showed compelling evidence that extent of resection was significantly associated with survival in glioblastoma, particularly in cases the resection was over 98%, and showing little benefits if extent of resection was inferior to 89%. This was also replicated by other groups [11] and it has since been demonstrated that even partial resection compared to biopsy can enhance survival in the elderly [12]. Similarly, Jakola compared two centres to show that early resection of LGG was associated with a more favourable outcome (9.7 years, median not reached at the time of the study) compared to watchful waiting (5.6 years) [3]. Importantly, also malignant transformation was delayed following early resection [2]. In the meanwhile, an incredible progression in the genetics of gliomas paved the way to more clear indication to surgery. On one side, the development of genetics provided evidence that glioblastomas would derive from central nervous stem cells instead of differentiated astrocytoma, possibly along the periventricular zone [13, 14]. On the other side, molecular diagnostics caused a Copernican revolution in adult glioma classification, which is currently divided following IDH-mutation and 1p19q codeletion, with now five much better defined tumour groups with accurately delineated ages at diagnosis and prognosis [15]. Patients with glioblastoma, IDH-wild type have, on average, the highest age at diagnosis (median 59 years) and the worst prognosis (median overall survival 1.2 years). Patients with glioblastoma, IDH-mutant tend to be younger (median age at diagnosis 38 years) and have a better prognosis (median overall survival 3.6 years) than those with glioblastoma, IDH-wild type. Patients with astrocytoma, IDH-wild type, regardless of grade II or grade III histology, have a median age at diagnosis of

52 years; their median overall survival (only 1.9 years) is closer to that of patients with glioblastoma, IDH-wild type than to that of patients with glioblastoma, IDH-mutant. By contrast, patients with astrocytoma, IDH-mutant have a median age at diagnosis of 36 years and median overall survival of 9.3 years [1]. Patients with oligodendroglioma, IDH-mutant and 1p19q co-deleted are also relatively young at diagnosis (median age 44 years) and have the longest median overall survival (17.5 years) [1].

It is now not debated anymore that gliomas should be resected, since for all types this has proven now to be a major determinant of overall survival. Extent of resection is important since up to 0.1 cm^2 of residual tumour strongly decreases overall survival [16]. A resection deemed to be beyond tumour border (supratotal) has also been proposed [17]. The rationale for this, especially for LGGs, is that tumour cells can be found up to 20 mm around MR imaging abnormalities [18], and therefore could be unseen by borders delineated by MR imaging. This has profound clinical implications, as life expectancy in patients with LGG can now reach 17 years thanks to combined reoperation and multistaged approached [19, 20].

Surgery can extend life expectancy, but resection of essential anatomy impairs brain function. Neurological deficits occur, traditionally in 5–25% of operated patients [21]. On this perspective, indication to resection has always to be balanced with the risk of neurological deficits. This has been termed onco-functional balance [22]. The onco-functional balance differs for LGGs and HGGs, as life expectancy for HGGs is months compared to years in LGGs. Accordingly, both maximizing extent of resection, as no reoperation is normally envisioned, and avoiding both permanent and temporary deficits, since these will strongly decrease quality and limit life expectancy, are more critical in HGGs.

However, these aspects are not of secondary importance for LGGs. When resection is extensive enough, other measures such as chemo- or radiotherapy can be delayed without harming the patient [23]. Similarly, supra-total resections extend life expectancy and strongly delay malignant transformation [2, 20]. Nevertheless, it must be remembered that surgical excision, no matter how extensive, cannot prevent relapse. In this scenario, we believe there is no benefit in an extensive resection when burdened by neurological deficit. This is particularly crucial considering that independently from the resection, the lesion will regrow with a rate of 3–4 mm/year and will have higher chances of malignant transformation when tumour volume is beyond 10 cc [19, 24]. In this scenario, the objective should not be to offer total or supratotal resection at all costs, but to delay malignant transformation thus enhancing life expectancy without losing quality of life. In a way, LGGs can be envisioned as a chronic disease. In this scenario, multistaged, repeated treatment with temozolomide and/or vincristine can be adopted to reduce/stabilize tumour volume to/under 15 cc and repeated surgeries should be already planned after the first surgery, particularly in case malignant transformation occurs [19]. Radiotherapy can be also a valuable tool, but is associated to cognitive decline [25]. For this reason, it may be delayed up to when the lesion infiltrates essential connectivity that cannot be resected and therefore surgery is no more an option [23]. Similarly, decision on

reoperation following molecular classification should be considered case per case for LGGs. There is evidence that LGGs with foci of malignant transformation have life expectancy similar to LGGs if the foci are resected [23]. This is the case also for IDH-wt LGG, with general overall survival of 77.27% at 5 years [26]. In this scenario, radiological patterns, particularly in case of bulky tumours that are not infiltrating essential white matter anatomy [27], may also be considered in planning the extent of resection, since resectability is nowadays an important factor to predict overall survival.

2.1.2 Preservation of Function in Glioma Surgery: From Phrenology to Connectomics

While the first interest in cortical anatomy had its foundation in phrenology [28], the theoretical underpinnings for cortical localizationism developed from paradigmatic cases coming from brain injury and stroke, such as those of Phineas Gage and Broca's patients Lelong and Leborgne. Produced in the Berlin laboratory of Oskar and Cecile Vogt, Korbinian Brodmann's first cortical cytoarchitectonic map [29] was based on the assumption that differences in structure match differences in function ("Sie gingen dabei yon der heuristischen Idee aus, dab sich funktionelle Verschiedenheiten in Strukturdifferenzen") [30]. In the same time, Otfried Foester, a pupil of Carl Wernicke [31], produced the first brain carthography from direct stimulation of the cortex in awake patients. This was performed on the strong belief that anatomy was insufficient to localize ambiguous epileptic foci and therefore stimulation inducing patient's aura must have been performed. Importantly, to highlight the awareness for a need for anatomo-functional correspondence, Foerster constructed his map overlaid onto Brodmann's cytoarchitectonic subdivision.

Brain mapping techniques since then were mostly applied to epilepsy surgery. As function was reputed to lie in eloquent cortices, it should be of no surprise that cortical stimulation started in the field of epilepsy surgery, as seizures are a cortical phenomenon which should resolve after cortical ablation. In this vein, it may be equally unsurprising that brain mapping was not performed subcortically. This was supported by brain models which postulated that higher-order brain function would reside in the cortex, which has been largely supported until very recently—and still represent a bias in conceiving cortico-cortical connections.

In the following years, while procedures for mapping continued almost unchanged, the role for awake surgery declined. This happened already during Penfield's time, as it is reported that he progressively stopped mapping after functional maps were acquired and more and more of his fellows were operating in asleep fashion according to those maps. This occurred also for epilepsy surgery, as the introduction of surface and depth electrodes for a better understanding of the epileptogenic zone [32] could be used to target resection in asleep fashion. Until the early 2000, indications to awake surgery were mostly confined to surgery in language areas.

From the early 1990s, however, retrospective reports from the neurosurgical literature showed a benefit for glioma resection independently by grading. Nevertheless, extent of resection had to be maximized avoiding neurological deficit in a disease that is conceived as a white matter disease. Indeed, neurological deficits for surgery in eloquent areas were high [33].

The development of the field of neuroimaging in neuroscience, which allowed a more thorough comparison of the amount of tumour resection, and particularly the description of tractography in 1994 by LeBihan and Pierpaoli [34], first reinvigorated a space for subcortical anatomy in brain function, paving the way for a conceptual shift from cortical localization to hodology [35, 36]. Within neurosurgery, the independent development of routine subcortical mapping during awake surgery by Berger and Duffau provided clear evidence of the primacy of subcortical anatomy in preventing neurological deficits and maximizing extent of resection in glioma surgery [37, 38].

2.1.3 Asleep Mapping

As much as cortical and subcortical mapping during awake surgery are well-established as a standard method when it comes to the localization and preservation of cognitive functions, not all patients are possible candidates for awake surgery as conditions of poor compliance, such as anxiety or pediatric age, do not allow for reliable evaluation. This may also vary during the operation, with task performance decaying as the resection proceeds. The same holds for preoperative deficits, which would impair intraoperative task-testing. In this settings, other functional techniques need to be offered, as otherwise the patient would undergo surgery with no intraoperative functional data at all. Some forms of mapping, especially motor mapping, were developed in asleep fashion. However, the classical Penfield's technique (50–60 Hz, bipolar stimulation) was not very efficient in evoking movement in an asleep patient, with intraoperative seizures being particularly high [39, 40].

Intraoperative neurophysiological monitoring (IONM) was applied initially to spinal surgery [41], with the use of somatosensory-evoked potentials (SEPs) to evaluate injury to the spinal cord during scoliosis or intramedullary surgery in the anesthetized patient. However, it was through motor-evoked potentials that IONM grew in importance in the neurosurgical field. As an alternative to Penfield's technique, the so-called "short train of stimuli technique", normally performed with five stimuli (To5), was introduced by the group of Schramm in 1993 in Bonn [40]. This stimulation had a number of benefits compared to the one previously performed. First, the To5 is more efficient in eliciting muscle contraction than the classical 50 Hz stimulation in both the adult and pediatric population [39], and it can be used as both a *mapping* and *monitoring* technique. Second, by evaluating MEP amplitude coupled with electromyography allows for a quantitative information about the proportion of damage to the motor pathways and potentially leave space for timely

corrective measures (such as papaverine irrigation for ischemic insult). Third, the risk of inducing intraoperative seizures is much lower than with Penfield's technique [39, 42].

However, despite being successful in mapping some aspects of motor function, IONM until very recently had no techniques to map and monitor connectivity underlying wider brain function, such as language, during asleep surgery. This still represents a limitation to its use beyond preservation of the corticospinal tract. At current, two novel stimulation techniques for asleep cognitive mapping have been described, cortico-cortical-evoked potentials (CCEPs) [43] and dual strip MEP-conditioning [44], which will be described in the next paragraphs.

2.2 Preoperative Mapping

The history of preoperative mapping techniques is strongly intertwined with that of neuroimaging. The first non-invasive mapping technique, positron emission tomography (PET), was developed in 1975 only a few years after the development of the first computer tomography (CT) scanner. By using brain metabolism, PET provided initial localization of brain function allowing good reproducibility among subjects. But it is with the development of magnetic resonance imaging (MRI) in 1977 and particularly with the adoption of functional MRI (fMRI) in 1990 that brain mapping became available with unparalleled resolution. Subsequently, preoperative mapping was implemented by two other techniques which recently gained relevance in the field. The first is tractography, which provides in vivo information on subcortical white matter pathway [34]. The second is navigated transcranial magnetic stimulation (nTMS), which allows for cortical functional information with millimetrical resolution [45].

2.2.1 fMRI

Functional magnetic resonance image (fMRI) was introduced in the early 1990s [46]. Initially adopted for scientific research, fMRI has been progressively adopted as a preoperative method to localize brain function ([47–49]).

fMRI utilizes blood oxygen level-dependent (BOLD) signal changes during the performance of a particular task (task-based fMRI) or at rest (resting-state fMRI) ([47–50]; Cirillo et al. 2019). fMRI signals are dependent on the coupling of neuronal activity to regional increases in cerebral blood flow leading to synaptic activity, which produces local changes in oxyhemoglobin and deoxyhemoglobin levels [50]. The BOLD signal does not directly evaluate the neural activity, but rather the complex interaction between the neural, vascular, and metabolic systems [51]. Neuronal activation triggers changes in cerebral blood flow, cerebral metabolic rate, and

cerebral blood volume. These factors regulate the deoxyhemoglobin (dHb) content of the brain microvasculature affecting the magnetic field within and around the blood vessels, altering the magnetic resonance signal [51]. The BOLD signal is sensitive to changes in the concentration of paramagnetic deoxygenated hemoglobin. Although these responses are robust, they require a rigorous methodology to analyse data [51]. Moreover, there is a number of caveats that are specific to tumour surgery and that should be considered when using fMRI for oncological presurgical planning. The most crucial is that fMRI may result to be unreliable when vascular changes develop in the region of the tumour resulting in neurovascular uncoupling instead of regular coupling [48, 52]. This can lead to false-negative fMRI results which may cause misinterpretation of eloquent tissue as non-eloquent and theoretically lead to resection of essential tissue.

In task-based fMRI, external sensory stimuli (i.e. visual or acoustic) or actions (naming, finger tapping) are used to induce modification in ongoing brain activity which is recorded through BOLD signal variation [47]. Task-based fMRI has been initially validated for the motor system: motor tasks include finger tapping, lip pouting, flexion, and extension of the toes, with primary as well as secondary motor areas (supplementary motor area and premotor areas) also being activated and showing good correlation with direct electrical stimulation [47]. Beyond motor function, several studies over the past 20 years have proposed task-based fMRI for preoperative evaluation of language areas [47]. While reports of its efficacy have been published [47], concerns for sensitivity and specificity of the technique have been raised. Both Weng and colleagues and Metwali and colleagues compared fMRI findings with DES (direct electrical stimulation) and found that the fMRI showed little correlation to DES when mapping speech areas [53, 54]. While these discrepancies between language fMRI activation sites and DES may be related to a difference between the preoperative tasks and intraoperative tasks administered during surgery [55], this is a critical concern that should be considered, especially as recent meta-analysis has shown that sensitivity of task-based fMRI for DES may not be higher than 59% [56].

Resting fMRI (rs-fMRI) represents spontaneous brain activity in the absence of any specific stimuli or tasks, where widespread functional networks are expected to communicate by firing in the same time-scale [57–59]. Various functional connectivity networks have been delineated such as motor, sensorimotor, language, visual, auditory, and attention. Adoption of rs-fMRI is at its infancy in preoperative planning for surgical resection and there are currently few reports on its use for presurgical planning, particularly for language function [60]. However, it may be particularly beneficial for patients with preoperative deficits, as involved language networks could be tested preoperatively without a task. Preliminary results from Vakamudi and colleagues showed that distance between DES and rs-fMRI connectivity in motor cortex, Broca's, and Wernicke's areas was within 1 cm, suggesting rs-fMRI may be a valuable tool for presurgical mapping. However, they also reported discordant rs-fMRI and DES localization for Wernicke's area in one patient due to possible cortical reorganization and/or altered neurovascular coupling, which suggest these results should still be interpreted with caution [60].

2.2.2 Tractography

The study of subcortical white matter pathways dates back to the pioneeristic studies of Johan Reil and Burdach in the early nineteenth century, which were performed ex vivo. While a relevance for connectivism was theorized during the century by Von Monakow and supported by the work of Wernicke and Lichtheim, this fell out of favour during the twentieth century following the evidence for cortical function provided by the work of Sherrington in animal and by Penfield in human studies. When diffusion tensor imaging was first described by Basser and LeBihan in 1994 [34], this had only limited resonance in the neurosurgical field. Water does not diffuse homogenously across the body, as membranes can oppose to its movement. Accordingly, because of existing barriers such a myelin sheets in the axon, water diffusion differs if the magnetic field is administered in different directions (i.e. along the main axonal direction or towards the myelin sheet). In diffusion tensor imaging tractography, the main direction of water molecules can therefore be used to infer fiber orientation voxel per voxel and reconstruct streamlines representing white matter bundles. This became relevant in the early 2000 as white matter pathways using tractography were made accessible by Catani et al. [61]. In this seminal paper, white matter pathways that had been until then described with blunt dissection but were difficult to visualize, such as the arcuate fasciculus, the inferior fronto-occipital fasciculus, the inferior longitudinal fasciculus, the uncinate fasciculus, and the corticospinal tract, become clearly delineated [61]. This theoretically complemented the dissatisfaction for neurological deficit avoidance predicted by using cortical localization alone [62]. Also, it provided evidence of subcortical responses not predicted by cortical localization, as phonemic paraphasia in the parietal lobe for subcortical arcuate fasciculus stimulation [38], facilitating the initial paradigm shift from cortical localization to connectomics [63]. Since then, a first atlas of white matter connections was provided which could be used to aid surgery by recognizing projections of relevant white matter tracts in healthy subjects as a guide for sparing these tracts during surgery [64].

Despite this major development, tractography suffers from major limitations and a role for tractography in tailoring surgical resection is debated [65]. Tractography reconstruction is prone to artefacts. The most common type of artefacts, false-positive results [66], can bias reconstruction connecting areas that should not be connected. However, this can be solved by using automated filtering (i.e. COMMIT2 [67]) or by manually filtering the streamlines, even if this is up to individual anatomical knowledge. On the other hand, tractography also suffers from false-negative results, which means that it may not display existing tracts [61]. This represents a critical issue, as it suggests surgery may be safe in territories in which it is not. Notably, this can only be partially solved by using advanced methods for tractography reconstruction [i.e. high angular resolution diffusion tensor imaging (HARDI)], which allow visualization of crossing fibers (occurring in more than 80% voxels in the brain when operating with clinical 2 mm voxel resolution [68]), as for example, between the corticospinal tract and the corpus callosum. When combined with neuronavigation, tractography suffers also from limitations of the neuronavigation systems, such as

brain shift phenomena occurring after dura opening due to liquid loss, or parenchymal shift because of positioning or debulking. Nimsky and colleagues systematically investigated these shifts using neuronavigation and intraoperative magnetic resonance, showing a mean of 8.4 mm for the cortex and 4.4 mm for deep tumour margin [69]. Accordingly, tractography should not be used alone for targeting resection [55]. Brain stimulation should be preferred to other techniques correcting for brain shift phenomena (intraoperative MRI, ultrasound, stereovision) since it has been shown that tractography corresponds with subcortical stimulation [70, 71].

Besides a role for presurgical mapping, tractography can also be used for risk stratification. Damage to the arcuate is associated with permanent post-operative deficits [72], while tractography combined with navigated transcranial magnetic stimulation can be used to stratify surgical risk in both motor and language domains [73–75].

2.2.3 Navigated Transcranial Magnetic Stimulation (nTMS)

Transcranial magnetic stimulation was developed in 1985 [76] as an alternative to the painful transcranial electric stimulation (TES) in the awake subject. Since its discovery, similarities and differences between TES and TMS have been established and TMS has been particularly valuable to measure motor ability and wider motor behaviour in normal subjects [76, 77], but also in neurologically injured patients [78]. Stimulation during behavioural tasks was first introduced in 1998 for language evaluation [79]. TMS can provide causal information compared with other mapping methods, such as fMRI, which rely on correlation. In neurosurgery, however, the first clinical series was introduced more than 20 years later [80]. This may seem surprising considering the theoretical advantage when compared with other preoperative mapping techniques. However, this derived from a limited reproducibility of stimulation in non-neuronavigated systems, affecting accuracy of neurophysiologic responses. Briefly, TMS generates a rapid magnetic field which is supposed to cause an electric depolarization at the level of axons bending in the gray–white matter boundaries. However, it is sensitive to a number of variables: coil shape (round- or butterfly-shaped), stimulation field direction, coil distance and perpendicularity to the brain cortex, stimulation intensity, and type of stimulation (single for motor mapping, repetitive for language/cognitive mapping). Under this premise, any movement between two stimulations strongly biases reproducibility. The implementation of a reliable neuronavigation system, which combines the patient's head with their MRI and online presentation of coil position, offers a solution to these physical issues. Accordingly, while focality for single stimulus stimulation has been shown to be around 2 mm [45], stimulation accuracy is circa 5 mm [81].

Picht et al. [82] provided the first comparison for motor mapping with direct cortical stimulation for neurosurgical planning, describing a motor mapping aimed at maximally reducing the intensity of stimulation in order to increase stimulation focality, which is now standard for presurgical planning [83]. Currently, correspondence between DCS and nTMS ranges from 2.1 to 5 mm [82, 84], with nTMS being superior to MEG and fMRI [85]. Notably, the combination of nTMS for motor

mapping and direct cortical stimulation (DCS) has shown to increase resection safety in glioblastomas [74]. On the other hand, nTMS-tractography for the corticospinal tract can be used to assess risk stratification for motor damage counting on impaired excitability measured with resting motor threshold of stimulation (RMT), distance inferior to 7 mm to the corticospinal tract, and drop in fractional anisotropy [74, 86].

nTMS is also performed for preoperative language mapping [84, 87, 88]. While it shows a rather high negative predictive value (83.4–99%) [84, 88], correspondence between nTMS- and DCS-induced errors was low (positive predictive value of 35.6–69%). It is unclear why there is such a high discrepancy between these two techniques. This is specific for language mapping, as reproducibility for motor mapping is higher. Indeed, there are fundamental differences in stimulation parameters: while language mapping is commonly performed using a 50/60 Hz stimulation lasting for 3 or 4 s, nTMS language mapping normally involves 5 pulse stimuli at 5 Hz or 7 pulse stimuli at 7 Hz [89, 83] (Fig. 2.1). This is to prevent the risk of inducing seizures [90].

Fig. 2.1 Illustrative case no. 1, on cortical and subcortical mapping. 63 years old man, left-hand dominance, presenting with generalized seizures. T2-weighted FLAIR MRI disclosed a right non-enhancing lesion bordering the lower part of the precentral gyrus (Berger zone 3). Clinical examination showed no deficits. (**a**–**c**) Pre-operative MRI. The pre-operative axial (**a**), coronal (**b**) and sagittal (**c**) T2-weighted FLAIR images show a non-enhancing precentral lesion. (**d**) Navigated transcranial magnetic stimulation (nTMS) mapping of language showing cortical spots evoking semantic paraphasia (blue dots), speech arrest (white dots), anomia (yellow dots), and hesitation (green dots). (**e**) The same eloquent cortical areas are overlapped to the advanced tractography reconstruction using high angular resolution diffusion imaging (HARDI), showing clusters of speech arrest at cortical terminations of the frontal aslant tract in the ventral premotor cortex. (**f**) nTMS motor mapping of hand showed responses clustering anterosuperior to the lesion. Grey dots: no response. Red dots: motor responses between 50–500 μV. Yellow dots: motor responses between 500–1000 μV. (**g**) TMS motor mapping of facial muscles with responses clustering anteroinferior to the lesion. Grey dots: no response. Red dots: motor responses between 50–500 μV. (**h**) Spherical deconvolution (HARDI)-tractography showing the corticobulbar tract (lower) and the corticospinal tract (higher), suggesting the lesion lies between hand and orofacial projections. (**i**, **j**) Comparison between 3D reconstruction of neuronavigation with nTMS motor responses (blue) and microscopic view after dura opening. (**k**–**m**) Microscopic (**k**) and neuronavigation (**l**) view of DCS stimulation eliciting response from hand muscles (*APB* abductor pollicis brevis; green dot). The APB muscle responses (blue traces in panel **m**) were induced at 10 mA of intensity (train of five stimuli of 0.5 ms duration each). *OOM* orbicularis oris, *Bic* biceps brachii, *APB* abductor pollicis brevis, *EXT* extensor digitorum communis, *Qua* quadriceps femoris, *TA* tibialis anterior; tongue. Arcuate fasciculus (red) and corticospinal tract (blue) are indicated. (**n**–**p**) Microscopic (**n**) and neuronavigation (**o**) view of subcortical stimulation eliciting response from face muscles (*Orb Oris* orbicularis oris; tongue; green dot). The facial and tongue muscle responses (respectively orange and white traces in panel **p**) were induced at 4 mA of intensity (train of 5 stimuli of 0.5 ms duration each). *OOM* orbicularis oris, *Bic* biceps brachii, *APB* abductor pollicis brevis, *EXT* extensor digitorum communis, *Qua* quadriceps femoris, *TA* tibialis anterior; tongue. Arcuate fasciculus (red) and corticospinal tract (blue) are indicated. (**q**) Microscopic view after resection. (**r**–**t**) Postoperative MRI showing complete resection of the lesion. (**u**, **v**) Postoperative nTMS stimulation showing preserved MEPs in hand muscles (**u**) and face muscles (**v**). Grey dots: no response. Red dots: motor responses between 50–500 μV. Yellow dots: motor responses between 500–1000 μV

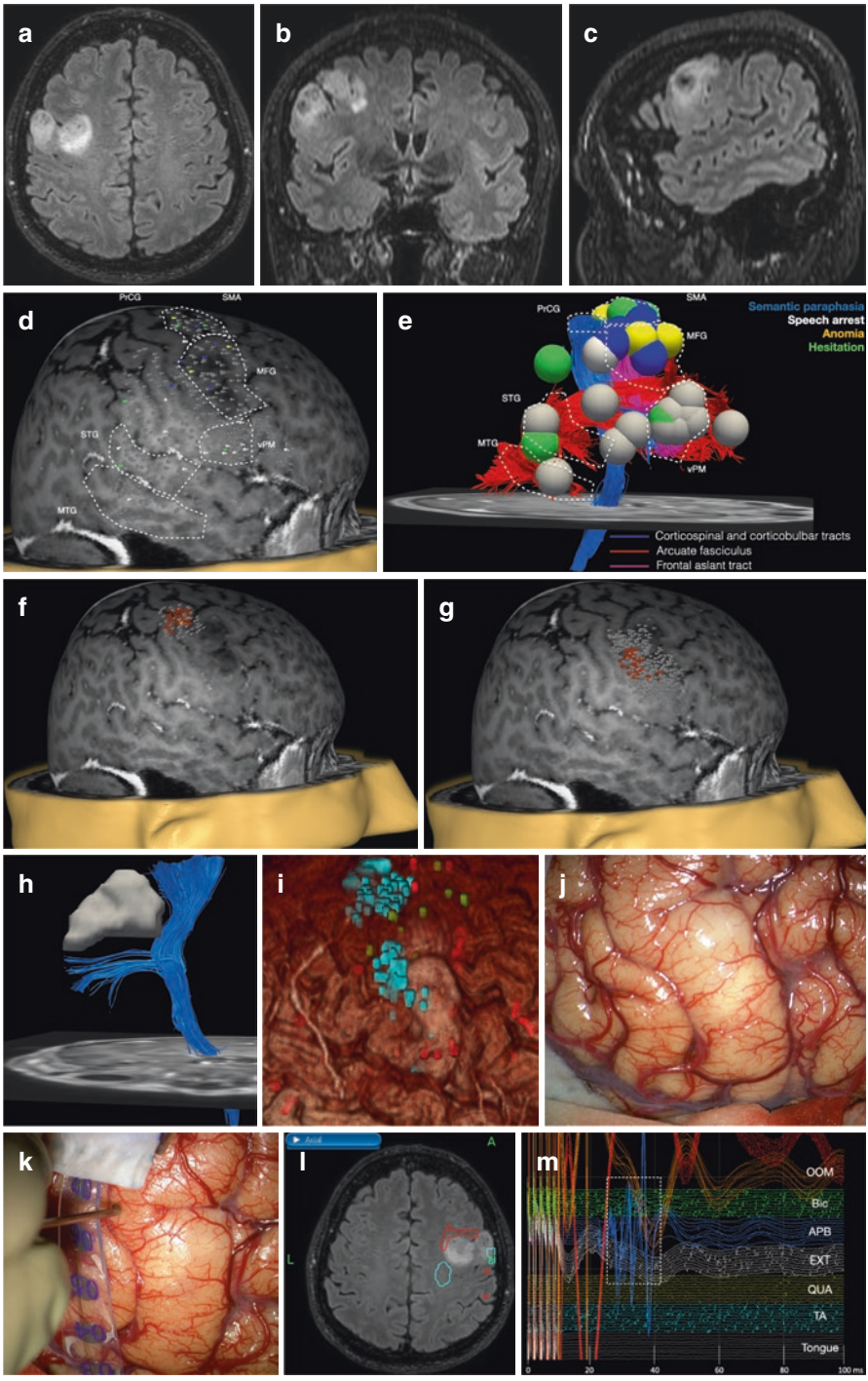
a
b
c
d
PrCG
SMA
MFG
STG
vPM
MTG
e
PrCG
SMA
MFG
STG
MTG
vPM
Semantic paraphasia
Speech arrest
Anomia
Hesitation
Corticospinal and corticobulbar tracts
Arcuate fasciculus
Frontal aslant tract
f
g
h
i
j
k
l
A
L
m
OOM
Bic
APB
EXT
QUA
TA
Tongue
0
20
40
60
80
100 ms

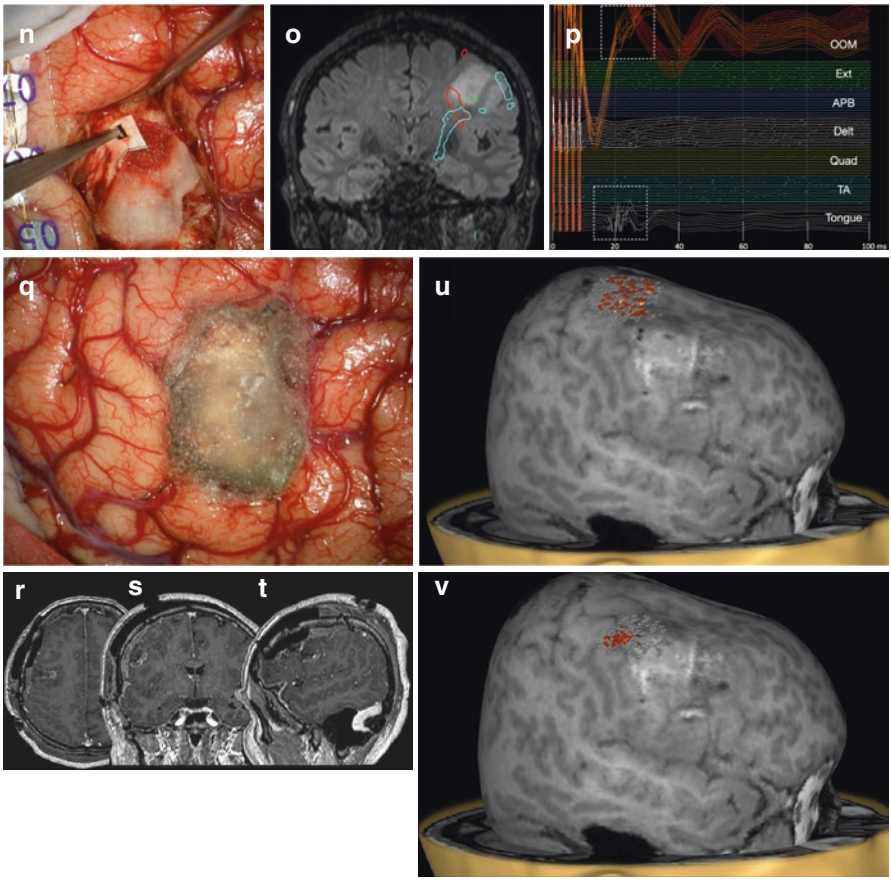

Fig. 2.1 (continued)

It is worth noting that language nTMS seems to be more effective for speech and articulation than semantics [88]. This is evident for stimulation of Broca's area, where positive predictive value increases [88], but also for regions involved in speech articulation, such as the supramarginal gyrus/Geschwind's territory [91]. Considering the high negative predictive value, language nTMS is more reliable for negative mapping—which is predicting non-responsive cortices during DCS. Nevertheless, it should be always combined with awake surgery when possible. Some data suggest that awake surgery with preoperative nTMS language mapping improves patient's outcome when compared to DCS alone [75]. Few studies exist for surgery using nTMS without awake surgery for tumours in language areas. While these showed good results and nTMS was planned as a rescue method [92], we underlie that nTMS language must be combined with awake surgery whenever feasible. Even if results for negative mapping are promising, the lack of

positive predictive value is a limitation for language mapping. Indeed, negative mapping is no more accepted as a means for safe mapping paradigm during intraoperative DES [93]. Evidence has since illustrated that insufficient current intensity and inadequate stimulation parameters can lead to false-negative mapping in intraoperative cortical and subcortical stimulation in up to a third of cases [94]. Hence, a more reliable positive nTMS language mapping is needed. On this perspective, integration of nTMS with subcortical structural information obtained from tractography has recently been proposed [95], particularly for preservation of the arcuate fasciculus. The combination of nTMS and tractography has accordingly allowed to promote models of risk stratification for tumour patients with lesions in the perisylvian area [96], benefitting from improved tractography seeding from nTMS positive stimulations [95, 97]. However, the tractography used in these studies involves commercial diffusion tensor techniques which cannot solve fiber crossing and do not offer adequate pre-processing and head-movement correction, which may bias these tractography results [75, 97]. Interestingly, a recent study has evaluated correspondence for whole brain deterministic HARDI tractography for cortical terminations of the three segments of the arcuate fasciculus and nTMS language positive errors in tumour patients. It showed that the arcuate fasciculus is an optimal predictor for language errors also in case of distorted anatomy. In this perspective, selection of nTMS language errors on the cortical termination of white matter tracts can be used to increase positive predictive value of nTMS language mapping [98].

2.3 Neuropsychological Assessment

A comprehensive, perioperative neuropsychological evaluation is mandatory to evaluate patient's outcome. Surprisingly, relatively few neuro-oncological centres have dedicated neuropsychologists. There is a general assumption that neuropsychologist should be involved only in cases of awake surgery to be performed. For this reason, neuropsychological evaluation on patient's outcome generally relates to language function. However, we believe that perioperative and follow-up neuropsychological evaluation for brain tumour and epilepsy surgery should be always performed in the awake as well as in the asleep setting whenever this is feasible. A recent survey reviewed neuropsychological assessments of 21 centres in 11 countries in Europe, showing that neuropsychological evaluation is progressively growing of importance in surgical neuro-oncology [99]. This survey suggested a core battery consisting of language tests—phonological and semantic verbal fluency tasks, object naming task, and semantic association task [generally the Pyramids and Palm Trees Test (PPTT)]. It also included attention and working memory evaluation using the Forward and Backward Digit Span, Rey–Osterrieth Complex Figure Test, and Executive functions (i.e. cognitive control, attention, response inhibition)—Trail Making Test and the Stroop Test [100].

While these tests can be administrated preoperatively and post-operatively, intraoperative testing time is constrained [101]. Intraoperatively, the most common tests used are counting, visual object naming, the PPTT, line bisection, online repetitive movement for upper and lower limbs, and the mind behind the eyes test. Specific task-based tests are commonly performed with rhythmic movement as a double task [58]. To conclude, neuropsychological assessment is commonly administered to those patients in whom awake surgery would be indicated as a way to decide candidability for awake surgery. However, we remark that neuropsychological assessment should not be used only for awake surgery screening, but for surgical indication, considering that patients who are not able to perform tasks are at higher risk of neurological deficits, and to allow the best post-operative rehabilitation possible considering postsurgical decrement of preoperative task performance.

2.4 Intraoperative Mapping

2.4.1 Principles of Brain Mapping: Stimulation Parameters, Probes, and Risk of Intraoperative Seizures

Brain stimulation techniques date from the first reports on awake dogs from Fritz and Hitzig [102], but have been included into clinical practice by the work of Penfield. The stimulation paradigm and the stimulation probe first adopted have since then become the standard in awake surgery and continue to be used in this manner without substantial modification. These involve a bipolar stimulating probe delivering biphasic pulses every 20 ms (50 Hz) for a stimulation duration up to 3–4, which would correspond to 150/200 stimuli. However, it should not be assumed that mapping has to be performed with a bipolar probe or with a 50 Hz stimulation, as other stimulation paradigms and probes exist. In the 1930s, 50 Hz was the maximum frequency of stimulation achievable and therefore it may be unsurprising that higher frequency stimulation (such as 250 Hz stimulation) has been included in clinical practice more recently. A bipolar probe has been historically more commonly used, having the benefit of higher focality and a more comfortable setup, since it has both cathode and anode on the probe and thus avoids adding a second electrode on the scalp. It should nevertheless be emphasized that *bipolar* and *monopolar* refer exclusively to the kind of probe used to deliver the stimulus, the first delivering a more focal electrical field, not to the parameters of stimulation.

Together with the development of more powerful stimulators reaching frequencies up to 1000 Hz, in 1993 Taniguchi and colleagues tested systematically multipulse stimulation (up to 5 stimuli) with a frequency ranging from 200 to 800 Hz over the primary motor cortex with the aim to generate motor-evoked potentials (MEPs) under general anaesthesia. They demonstrated that a train of five stimuli every 4 ms (250 Hz) evoked MEPs reliably and with the lowest current intensity and used a monopolar probe with reference on the scalp at Fpz. As previously

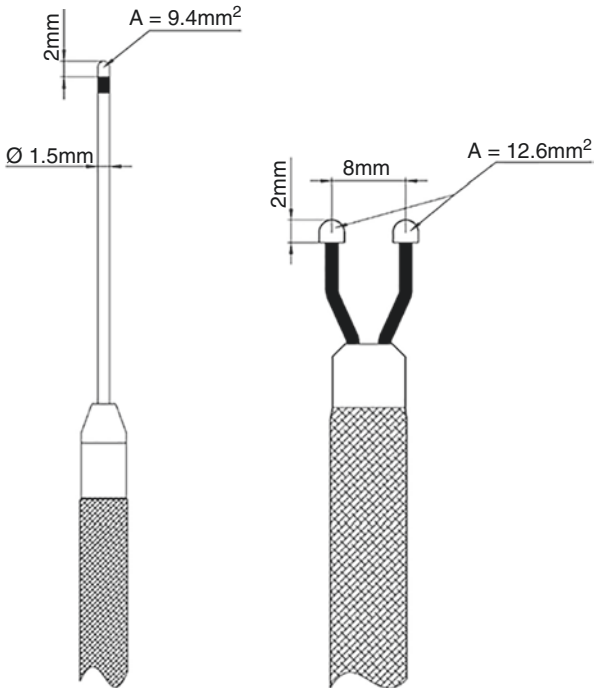

Fig. 2.2 A comparison between monopolar and bipolar stimulation probes. On the left, monopolar probe. On the right, bipolar probe. (Reprinted with consent from [39])

mentioned, this is still commonly used at present, although the probe can be switched to bipolar or even concentric bipolar in conditions in which higher focality is needed [103] (Fig. 2.2).

Cortical stimulation provides access to brain function, but it also can cause seizures. This has to be taken into account when performing functional neurosurgery since epilepsy can hinder further stimulation. While direct cortical stimulation always carries the risk of inducing a seizure, stimulation paradigms have different epileptogeneicity, which may be related to the administered charge density [104]. Szelenyi and colleagues investigated this systematically, demonstrating that the epileptogenicity for 50 Hz stimulation is higher (6.8–20%) than 250 Hz stimulation (1.2–4.4%) [42]. Notably, the number of stimulation-related seizures may be underappreciated, especially among neurosurgeons using the 50 Hz stimulation technique, if electrocorticography (ECoG) is not used. Historically, surgery performed awake does not use ECoG, and therefore seizures are normally evaluated only clinically [105] . In this scenario, intraoperative seizures may be underappreciated, and therefore may be more than those clinically described. Moreover, besides charge density, pulse frequency, and type of stimulation probe, pause length (the time the probe is not touching the cortex) between two stimulations may also have a role. It may be expected that rapid repetition of stimulations with only a short pause between repeating cortical stimulation may have a role in seizurogeneity. However, we are not aware of any paper evaluating this aspect of cortical stimulation (Table 2.1).

Table 2.1 Comparison of probes, stimulation paradigms, and epileptogeneicity generally used in asleep and awake settings

	Probe	Type of task	Type of stimulation	Type of mapping	Intensity	Monitoring	Frequency	ISI	Number of stimuli (pulses)	Duration	Epilepsy rate
Asleep	Monopolar	Motor (language)	Monophasic	Cortical/ subcortical	5–25 mA	Yes, from cortical strip electrode (cortical MEPs)	250/400 Hz	2–4 ms	5 (but also from 2 to 7)	0.5 ms	1.2–4.4%
Awake	Bipolar	Cognitive/ language (motor)	Biphasic	Cortical/ subcortical	1–8 mA	Yes, using a continuous motor or cognitive task	50–60 Hz	20 ms	200 (in 4 s)	1 ms	6.8–20%

With regard to subcortical stimulation, a comparison among probes and stimulation paradigms has been performed for motor and language networks [39, 106]. For motor networks, 250 Hz stimulation is more effective in eliciting MEPs than 50 Hz stimulation regardless of the type of probe used, while the monopolar probe was more effective in eliciting MEPs compared to the bipolar probe independent of the stimulation technique performed [39]. For language networks, Riva and colleagues provided evidence that 250 Hz monopolar stimulation is also effective in generating language disturbances, with induced errors akin to those induced with Penfield' stimulation as soon as the repetition rate of 250 Hz stimulation is increased from 1 (every second) to 3 Hz (circa every 300 ms) [106]. Notably, these were not due to motor responses from the vocal tract, as highlighted by silent EMG recordings. However, while there was no statistical difference in the number of responses evoked, 50 Hz bipolar stimulation was slightly more successful.

2.4.2 Intraoperative Cortical and Subcortical Mapping and Monitoring of Brain Function

We have discussed the various types of probes and stimulation paradigms, as we strongly believe that understanding this is crucial for every surgeon who approaches neuro-oncological resection with the aim of preserving brain function. The tools available are numerous, and as the right microsurgical instruments are expected to be appropriately requested by the surgeon under the microscope, similarly stimulation probes and paradigms represent the necessary armamentarium of the functional neurosurgeon. In the next section, we will describe how these stimulation protocols can be used to perform the two aspects of intraoperative stimulation: localization of function, *mapping*, and online surveillance that a function is intact, *monitoring*.

Stimulation and anesthesia protocols largely diverge according to the network needed to be preserved. However, even if protocols may differ, we would like to suggest a three-step approach when performing surgery in deemed essential areas as follows.

First, once the dura is opened and the cortex is exposed, we apply direct electrical stimulation over the cortex to identify eloquent areas and distinguish them to the ones that are not functional or carrying other functions. In this step, cortical mapping is performed to ensure a safe "entry zone" avoiding "eloquent zones". In a second step, once functional cortices are detected, one strip (motor-evoked potentials) is positioned over the brain surface and tumour resection commences. Very recently, we investigated the possibility to use two strip electrodes to monitor cortico-cortical-evoked potentials [44, 107], as a potential method for future clinical application.

While surgery proceeds, continuous stimulation is performed to monitor cortico-cortical or cortico-subcortical integrity, and as the operation continues, increasing attention is given to subcortical functional borders. In this step, monitoring is used to safely approach resection margins. In the third and last step, subcortical mapping and monitoring are performed together to localize essential subcortical anatomy in order to maximize surgical resection while avoiding permanent neurological deficits. In this step, subcortical mapping is used to evaluate distance to subcortical borders and perform a careful resection in the closest proximity of functional margins.

In this part, we will purposefully focus on motor and language mapping as these functions are the most mapped in neurosurgery. We want to stress, however, that this is far from comprehensive and that other functions in both left and right hemisphere are pivotal to behaviour and should be mapped. Moreover, in the individual patients, a need for brain mapping is dictated by plasticity. As this latter can reshape brain networks differently individual from individual [108], intraoperative mapping is mandatory as preoperative measures to predict it are at current insufficient.

2.4.2.1 Motor

Primary Motor Cortex

Cortical Mapping

The primary motor cortex has been classically considered inoperable, with Penfield himself stating: “in the therapeutic approach, it should be pointed out that only very rarely has the Rolandic area been included in any excision and never has this region of the brain been touched unless a lesion was present that could be demonstrated grossly by operative inspection. This digression is made in the hope of discouraging surgical removal of normal brain from the Rolandic area, or elsewhere, whatever may have been the pattern of epileptic seizure.” [109]. For many decades, this has been a dogma in epilepsy and glioma surgery, corroborated by a localizationistic perspective. When performing cortical motor stimulation, both 50 and 250 Hz stimulation paradigms can be applied. In Penfield’s technique a single cortical biphasic stimulus of 0.5-ms duration with a frequency of 50–60 Hz lasting from 1–4 s is applied over the cortex with a bipolar probe. If no responses are recorded with an intensity up to 25 mA, following a 2 mA stepwise increment, that part of the cortex is considered not functional. However, before labelling a cortical area as non-eloquent or non-functional, it is advisable to repeat the stimulation for consistency and to exclude possible technical problems. A stimulation study that is entirely negative may well be unreliable unless a severe or even complete preoperative deficit existed.

While Penfield's technique is still considered a prime method for performing cognitive mapping, it has some disadvantages for mapping the primary motor cortex and the corticospinal tract. First, its reliability is highly dependent on the anaesthesia protocol, with stimulation in asleep technique requiring much higher currents and possibly leading to false-negative mapping. Second, it may not provide reliable negative mapping in patients with an extensive history of seizures, patients undergoing reoperation, or in the presence of diffuse tumours, such as glioblastomas [94]. Third, Penfield's technique has a very low success rate in eliciting motor responses in the paediatric cohort and may not be effective at all when performed in children under the age of 6 years [110]. Fourth, the incidence of intraoperative seizures is high and can occur up to a fifth of patients [42]. As an alternative to Penfield's technique, the so-called "short train of stimuli technique", normally performed with five stimuli (To5), was introduced by Taniguchi et al. [40] and, since then, it has progressively replaced Penfield's technique for motor mapping, in both asleep and awake fashion. It is important that this type of stimulation is generally monopolar, and as the reference is distant (generally on the scalp), one has to pay attention for stimulation to be anodic when stimulating the cortex, cathodic when stimulating subcortically. This type of stimulation is closer to the physiological firing from the primary motor cortex, which generates a direct potential for the corticospinal tract, called D-wave, with an optimal refractory period of circa 3.5 ms (285 Hz) [111]. It also better explains responses in the precentral gyrus, which can be considered as divided in an anterior premotor region and a posterior primary motor region [112, 113], with the anterior portion possibly representing M1-striatal fibers and the posterior corticospinal (motoneuronal) projections to the spinal cord. Accordingly, only stimulation of the posterior part of the precentral gyrus causes MEPs when stimulating at threshold [113], while stimulation of anterior parts of the precentral gyrus causes motor inhibition [112, 113]. Similarly, subcortical stimulation of projecting fibers from the anterior precentral gyrus causes motor inhibition [114], supporting also a subcortical anterior/posterior distinction [103, 113].

To conclude, the To5 is less epileptogenic and more effective in eliciting motor-evoked potentials (MEPs) in both adults and children [39, 42, 115].

Monitoring

Another advantage of Taniguchi's method compared to Penfield's technique is that it allows for continuous monitoring of cortico-subcortical pathways. In the monitoring of motor function, a multi-contact strip electrode is placed under the dura overlapping the precentral gyrus; this gyrus can be directly or indirectly identified; directly with cortical stimulation and the aid of the neuronavigation; indirectly using a phase-reversal technique to localize the central sulcus [116], or using the stimulation points of the preoperative nTMS motor mapping, which can also allow for a better understanding of M1 somatotopy. It is our practice to select the stimulation point which evoked MEPs with the lowest current, in order to minimize

possible electrical spread: this is highly facilitated if the nTMS stimulation points are uploaded colour-coded for amplitude. The electrode with the lowest stimulation threshold in eliciting a contralateral muscle response is chosen for continuous MEP monitoring [117].

One of the main advantages of MEP monitoring is that it enables the monitoring of the functional integrity of the corticospinal tract along the whole pathway from the cortex to the muscles. In fact, MEP changes may occur not only due to a mechanical injury to the corticospinal tracts following coagulation, traction, or tissue damage, but also as a result of an ischaemic injury in the case of vessel occlusion or vasospasm. These vascular derangements can be identified and possibly prevented using only MEP monitoring, and not through cortical or subcortical mapping techniques.

During surgery, once the strip is placed and MEP monitoring is initiated, careful attention is required to ensure stable MEPs throughout the surgery, as it is well-established that MEP deterioration predicts motor deficits [117–119]. Therefore, warning criteria for MEP monitoring have been developed, with significant reduction being associated with permanent motor deficit [117, 118]. Overall, warning thresholds between 50–80% of amplitude reduction have been proposed in the literature, the 50% criterion being less specific and the 80% being less sensitive [117–119]. MEP monitoring is particularly valuable in case of vascular insults, since it allows to enact corrective measures before ischemia causes permanent damage. Rapid cessation of the surgery, warm irrigation, hypertension, and papaverine administration can reverse vascular ischemia in a third of cases, therefore preventing hemiplegia [119].

To ensure the best surgical outcome, MEP monitoring should be combined with subcortical stimulation. When subcortical stimulation is performed without MEP monitoring, the corticospinal tract may be mechanically disconnected and this may go unnoticed by the surgeon. This may happen for CST stimulation caudal to the disconnection, since stimulation here can still provide MEPs. This phenomenon is prevented by MEP monitoring, since direct damage to the CST is revealed by reduction in MEP amplitude as the CST is evaluated in its full extension from the cortex. Conversely, MEP monitoring without subcortical mapping cannot provide the distance from the corticospinal tract, and therefore MEP reduction could occur with the corticospinal tract already been irreparably disconnected/damaged. In this regard, it is worth describing a phenomenon which could provide similar information to subcortical mapping: MEP fluctuations monitoring. When surgical resection approximates the corticospinal tract (<5 mm distance), often MEPs from the cortical strip may become unstable, with a normal amplitude MEP followed by a reduced one. As in our experience this suggests that the corticospinal tract is within 3–5 mm distance (unpublished data), we advise to perform subcortical mapping every time cortical MEP fluctuations are individuated intraoperatively.

MEP changes may give false-positive and false-negative results, with the interpretation being not always straightforward as it can be complicated by the large variability of MEP amplitude, even under physiological conditions. Anaesthesia,

body temperature, blood pressure, and parameters of stimulation may all affect the reproducibility of MEPs: expertise is required to interpret these signals. However, there are cases in which false-positive and false-negative results in MEP monitoring are not due to technical or interpretative issue, but from theoretical misconceptions.

One of such cases applies to surgical series combining direct cortical and transcranial MEP monitoring. As the type of stimulation and the stimulation paradigm are the same, it could be assumed that they have the same predictive value [120]. However, it must be emphasized that the predictive value of MEP monitoring is obtained from direct cortical stimulation. In transcranial electrical stimulation, the international 10–20 EEG montage with a C1–C2 or a C3–C4 montage is used to evaluate the integrity of the corticospinal tract stimulating directly from the scalp using needle or cork-screw electrodes [121]. We want to stress that transcranial MEP monitoring has limitations with respect to direct cortical MEP monitoring and cannot substitute it. The first obstacle to overcome is the electrode placement. This is necessarily suboptimal, as ideal electrode position is modified to fit the surgical flap, thus decreasing focality. The second obstacle is faced once the dura is opened, as brain shift due to positioning, CSF drainage, and tumour resection can modify the relative position of the primary motor cortex with respect to the placed electrodes, further decreasing focality. Decreased focality and associated increased stimulation intensity, often associated to a shift to larger dipoles (C3/C4 compared to C1/C2), activate the corticospinal tract deeper and more distant from the cortex, potentially at thalamic level or lower [121]. This means that the CST closest to the lesion may be bypassed, thus preventing from effective MEP monitoring: in this case disconnection of the CST at a level superior to the thalamus will be unnoticed. This means that for a perirolandic tumour, tcMEP and dcMEP may be discordant: one could lose dcMEP with preserved tcMEP. In this case, tcMEP are 'falsely' preserved: the CST has been in fact disconnected before the level of the thalamus. Indeed, tcMEP (as opposed to dcMEP) cannot signal this because tcMEP are monitoring the CST from the thalamus downstream to the muscles, while it is the warning from dcMEP providing 'true' monitoring signal. Thus, even if tcMEP monitoring combined with dcMEP monitoring can be valuable in excluding technical issues, we advise against the use of tcMEP monitoring alone when performing supratentorial resection as it may oversee vascular or mechanical CST damage for cortically located tumours.

To conclude, another case in which MEP monitoring may provide false-negative results is for resection of SMA lesions [122], and more broadly, for circuits of motor control (e.g. anterior M1, inferior parietal cortex). We want to stress that MEPs represent a neurophysiological marker for motor execution, specifically for the corticospinal tract [118, 123], and do not provide information regarding preservation of other white matter anatomy involved in motor control. Under these premises, the cases should not be considered false-negative as other mapping techniques should be adopted to prevent them [44, 103]. The issue of using MEP monitoring for surgery in areas of motor control and how to monitor these white matter structures will be addressed specifically in the next paragraphs.

Subcortical Mapping

While at the cortical level, mapping aims to guide the surgeon on "where to enter" to obtain access to subcortical lesions, at the subcortical level the main goal is to decide "when to stop" the removal of a brain tumour. It is important to remember that, overall, two thirds of the cortex may be buried within the sulci and therefore negative cortical stimulation may not exclude function subcortically.

This is of particular importance in surgical operations since subcortical tracts are extremely compact (millimeters to few centimeters in diameter) and the distance from safe margin is minimal. This would hold true for thalamic tumours close to the internal capsule or insular tumours: as MEP monitoring alone may be insufficient to ensure safe resection, subcortical mapping can be used to characterize the proximity of essential white matter anatomy.

As with motor mapping, the CST can be localized at a subcortical level using the same techniques used for cortical stimulation. It is our preference to use the To5 technique using a monopolar probe rather than Penfield's technique, for both cortical and subcortical mapping. Leaving aside that the To5 is less epileptogenic and more successful in eliciting MEPs, it has the advantage of determining the distance between the resection and the corticospinal tract [124].

Nevertheless, we would like to emphasize that, regardless of the technique, the most important variable for successful mapping is the individual experience of the team (neurosurgeon and neurophysiologist/neuropsychologist).

In the recent past, there has been a great interest in the relationship between the threshold current necessary to elicit a subcortical motor response (subcortical threshold) and the distance between the stimulation site and the corticospinal tract itself. Evidence suggests that a subcortical threshold current of 1 mA correlates with a 1 mm distance between stimulation site and the CST [71, 125]. However, this "rule of thumb" depends on the parameters of stimulation. Shiban and colleagues found that this correlation is more proximal to the 1:1 when the pulse duration ranges from 0.5 to 0.7 ms and cathodal rather than anodal stimulation is used [126]. Hence, with these parameters, one can expect that a stimulation with a subcortical motor threshold of 10, 5, and 1 mA corresponds to a distance from the CST of 10, 5 and 1 mm, respectively. These criteria must be applied carefully to the non-adult/paediatric population, as the myelination of the CST differs across infancy and adolescence and the related threshold may vary accordingly [127].

A matter of great interest is the correlation between subcortical mapping thresholds and the risk of post-operative deficits. Most of the data available in the literature are related to motor function. It is intuitive that the lower the threshold capable of eliciting a motor response, the higher the risk of incurring a post-operative deficit (because of the proximity to the motor pathways). So, for example, if the threshold is lower than 3–4 mA, there is a significant risk of damage as the CST would be generally expected to be only 3–4 mm away from the dissection. In general, while thresholds above 5 mA can be considered safe, a threshold of 2–3 mA is reported to be significantly related to higher risk of post-operative paresis—at least transient [128] (Fig. 2.3).

It is important to point out that subcortical mapping strategies differ according to stimulation paradigm. Penfield' stimulation is currently used with a stable intensity of stimulation: once cortical intensity of stimulation causing transient deficit (usually speech arrest) is identified, this is kept constant through the surgery, in both cortical and subcortical mapping [129]. As previously discussed, this does not apply to 250 Hz stimulation: subcortical stimulation here reflects distance to the corticospinal tract, and therefore it is adjusted according to its proximity. This difference is particularly critical during awake surgery with a Penfield' stimulation. During perirolandic surgery with this type of stimulation paradigm, intraoperative subcortical stimulation inducing movement has been shown to be associated with CST disconnection [130]. This means that every time the stimulation was inducing movement, there was a higher chance of causing permanent deficit by transecting the CST and therefore bipolar stimulation may not be efficient enough to map the CST before it is disconnected [120]. In this scenario, we believe that switching the probe and stimulation parameters to a To5 paradigm in order to more efficiently map the CST should be the first choice [94].

Recently, technological innovation has significantly aided subcortical mapping. Thus, suction devices and ultrasonic aspirators have been combined with stimulating probes, allowing the surgeon to perform continuous or sub-continuous subcortical mapping without the need to periodically alternate tissue removal with stimulation [131]. It is likely that, apart from the instance of vascular injuries, irreversible MEP changes during tissue removal at apparently safe subcortical mapping threshold (above 3–5 mA) may be due to inappropriate temporal and spatial coupling of the surgical field, with transection of the CST occurring between the two consecutive subcortical stimulations. With the technical adjustments offered by these new tools, it has been suggested that subcortical thresholds as low as 1–2 mA can be tolerated, resulting in only transient deficits [125, 132]. We would caution that such outstanding results also reflect robust and well-established experience in both intraoperative neurophysiology and brain tumour surgery as much as the subcortical mapping. While subcortical mapping will be pushed forward in coming years, at the current state of the art, we would regard as critical any threshold below 3–5 mA and would not recommend tissue removal below this level to avoid any permanent injury to CST (Fig. 2.4).

Surgery for Intrarolandic Tumours

Although the first evidence for resecting lesions surrounding the precentral gyrus started in the 1980s [33, 133], the first systematic series on gliomas were described in the early 2000 [38, 134, 135]. Keles and colleagues described a retrospective series of 294 glioma patients operated with Penfield' stimulation both in awake and in asleep technique, showing that resection of perirolandic areas was feasible—and despite 20.4% of patients suffering from post-operative motor deficits, only 4.8% were permanent [134]. Interestingly, while they were able to recruit motor activity from the cortex in 260 patients, in only 132 patients the

corticospinal tract could also be elicited subcortically. Subcortical stimulation of the corticospinal tract was significantly associated with a worse outcome, with a risk of permanent motor deficits increasing from 2 to 7.6%. This has been confirmed more recently in a larger series by the same group, with 703 perirolandic gliomas [130]. In this series, they described a higher rate of deficits, with 30% of patients showing post-operative motor deficits and 6.9% of patients suffering from long-term deficits. The corticospinal tract could be found subcortically in less than half of patients (43%). Again, patients in whom the CST was elicited subcortically had a significantly higher risk for permanent motor deficits of 12% compared to 3.2%. In a series of 591 gliomas using the 250 Hz stimulation, Bello and colleagues showed 63.9% of post-operative deficits, but only 3% of permanent motor deficits. Importantly, they compared this technique with the Penfield' stimulation, showing up to 60% of false-negative mapping using Penfield's technique [94].

This is even more critical when considering intrarolandic surgery. In the past, the precentral gyrus was deemed inoperable [109] and also currently resection within this area is largely debated [136]. A surgery within the precentral gyrus questions a system where the motoneuronal corticospinal output makes up the whole fiber population of the precentral gyrus, as there would be no entry zone. However, the precentral gyrus represents also a cortical hub where cortico-cortical and subcortico-cortical association and projection fibers converge before cortical motor output, and as such, it comprises also of intragyral, short-range and long-range association fibers, and fronto-striatal projections [114, 137, 138]. As these fibers may have more plastic potentials than cortico-motoneuronal projections to

Fig. 2.3 Illustrative case no. 2, on subcortical mapping and tractography. A 8-year old right handed boy presented with a left hemiparesis (3/5). (**a**–**c**) Contrast-enhanced, T1-weighted MRI showed a lesion occupying the right thalamus and displacing anteriorly the internal capsule. (**d**–**f**) Optimised HARDI-tractography revealed the corticospinal tract (in light blue) displaced anteriorly and laterally to the tumour. (**g**) 3D reconstruction of subcortical stimulation sites described in "**i**". (**h**) During surgery, TES evoked MEP from the left abductor pollicis brevis (APB) and the left tibialis anterior (TA) were elicited at 120 mA and 200 mA respectively, while no MEPs were obtained following DCS up to 35 mA after cortical stimulation (not shown). (**i**) Response from the left APB, extensor digitorum communis (EXT) and TA were recorded following subcortical stimulation at 10 mA as showed in the stimulation point A. Approaching the core of the lesion, response from the left APB, EXT and TA was recorded at stimulation intensity of 3 mA in point B. Towards the end of tumour resection, subcortical mapping at stimulation point C showed responses from the left APB, EXT and TA at 2 mA, when stimulating the anterior inferior margin of the tumour. At this point, surgery was abandoned. Noteworthy, from a single spot multiple muscle response are elicited due to the convergence of corticospinal tract fibers in the proximity of the internal capsule. Pathology revealed a pylomixoid astrocytoma (WHO II). On post-operative day one, the child developed a hematoma in the surgical cavity, which required surgical removal. Clinically, he woke up with a severe hemiparesis (2/5), which incompletely recovered at the 3 month follow-up (4/5). (**j**–**l**) The 3-month post-operative T1-weighted MRI with gadolinium displays a subtotal resection. *L OOM* left orbicularis oris, *L EXT* left extensor digitorum communis, *L Bic* left biceps brachii, *L APB* left abductor pollicis brevis, *L TIB ANT* left tibialis anterior

the spine, these may be therefore amenable to surgery [139]. Indeed, cytoarchitectonic maps [140], intraoperative stimulation [113, 141], and non-human primate models [142] suggest a distinction within the so-called primary motor cortex in the precentral gyrus, interpreted in the form of a motor/premotor distinction [112] or

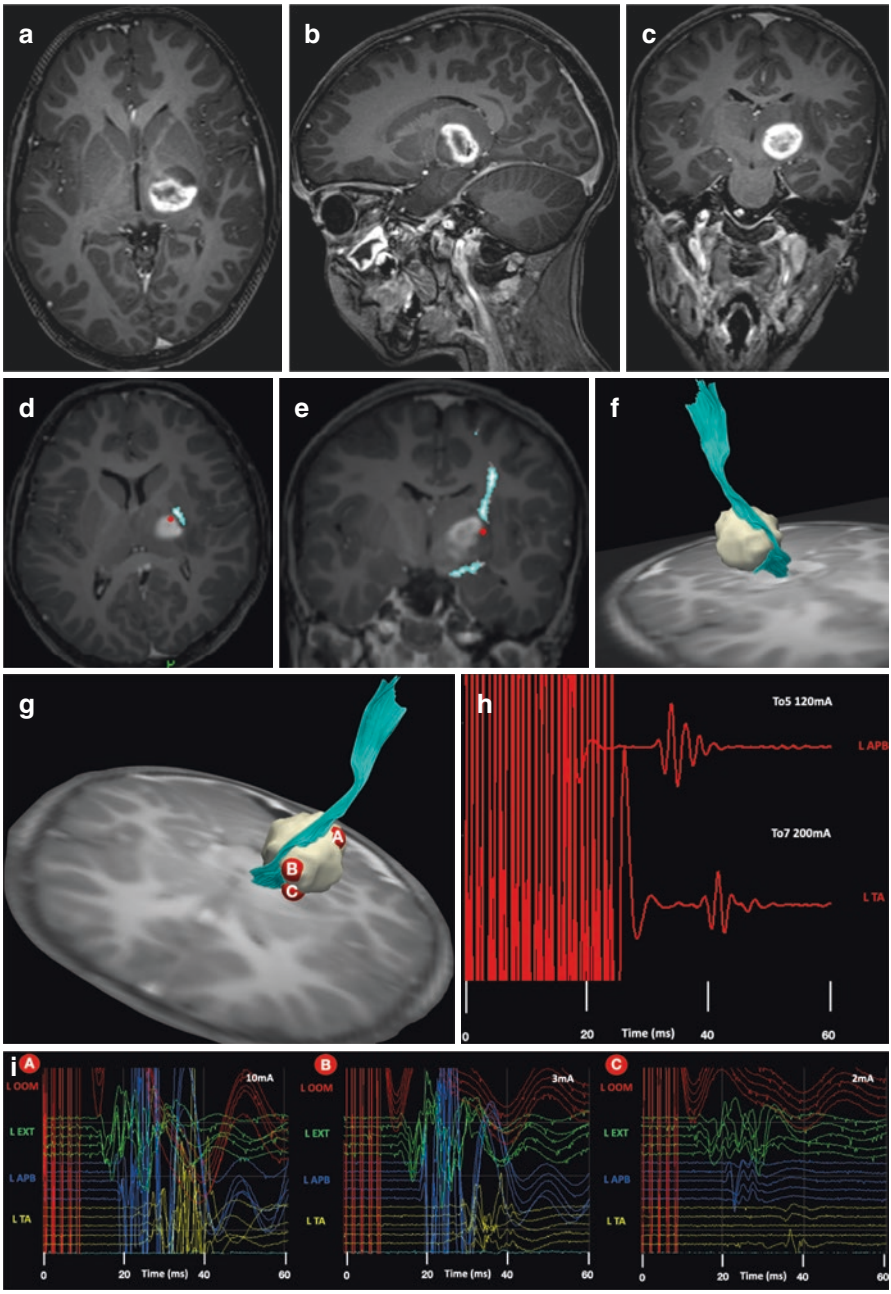

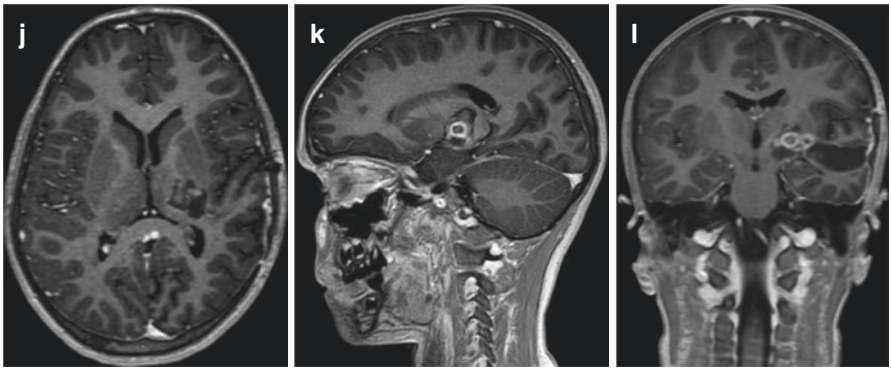

Fig. 2.3 (continued)

as an older M1 in the anterior precentral gyrus and a newer M1 in the posterior precentral gyrus and in the depth of the central sulcus [142]. This was already described in Brodmann (1909); [30], which termed the anterior areas in the precentral gyrus as 6a and 6b, with the primary motor cortex area 4 lying more posterior. Indeed, intrarolandic surgery has been shown without incurring hemiplegia [103, 139, 143]. Accordingly, gliomas, and particularly LGG, are currently being resected also within this area.

A first series is that of Magill [143], for which 49 patients underwent intrarolandic surgery using a Penfield's stimulation. While extent of resection was optimal (91%), a third of patient incurred long-term hemiparesis. A more recent series is the one of Rossi [103], showing intrarolandic resection in 102 patients using a modified To5 technique with decreased or increased number of pulses (from To2 to To9).

Fig. 2.4 Illustrative case no. 3, on tractography and subcortical mapping for re-operation of thalamic tumor recurrence. After 4 years, the same patient was admitted to the ER for nausea and headache. Clinical examination at admission showed 4/5 right hemiparesis on the upper and lower limb. (**a–c**) Contrast-enhanced, T1-weighted images showed a recurrence of the tumor occupying the right thalamus and displacing anteriorly and laterally the internal capsule (**a–c**). (**d–f**) Optimised HARDI-tractography revealed the corticospinal tract (in light blue) displaced anteriorly and laterally to the tumour. (**g**) Optimised HARDI-tractography of the corticospinal tract is shown and location of subcortical stimulation sites is shown (red spheres: A; B). (**h**) At surgery, MEPs from the left abductor pollicis brevis (APB) and the left tibialis anterior (TA) were elicited at 200 mA using transcranial electrical stimulation (TES). (**i**) Subcortical stimulation. MEPs from the left OOM were evoked at 20 mA (A). At the end of tumour resection, subcortical mapping B responses from the left OOM, EXT and APB at 15 mA (B), when stimulating the anterior margin of the tumour. (**j–l**) Postoperative T1-weighted MRI with gadolinium. At discharge, the clinical examination showed unchanged motor status, with the pre-existing right arm and leg hemiparesis (4/5). *APB* abductor pollicis brevis, *L APB* left abductor pollicis brevis, *L Bic* left biceps brachii, *L EXT* left extensor digitorum communis, *L OOM* left orbicularis oris, *L TIB ANT* left tibialis anterior, *TA* tibialis anterior, *TES* transcranial electrical stimulation

While extent of resection was similar (85.3%), long-term neurological morbidity was lower (2%). Interestingly, none of the LGG operated showed permanent deficits, suggesting that in case of LGGs the surgery within the precentral gyrus may be pushed to the corticospinal tract also considering sacrificing cortico-cortical association and corticofugal (striatal) white matter projection tracts involved in wider motor behaviour [139] (Fig. 2.5).

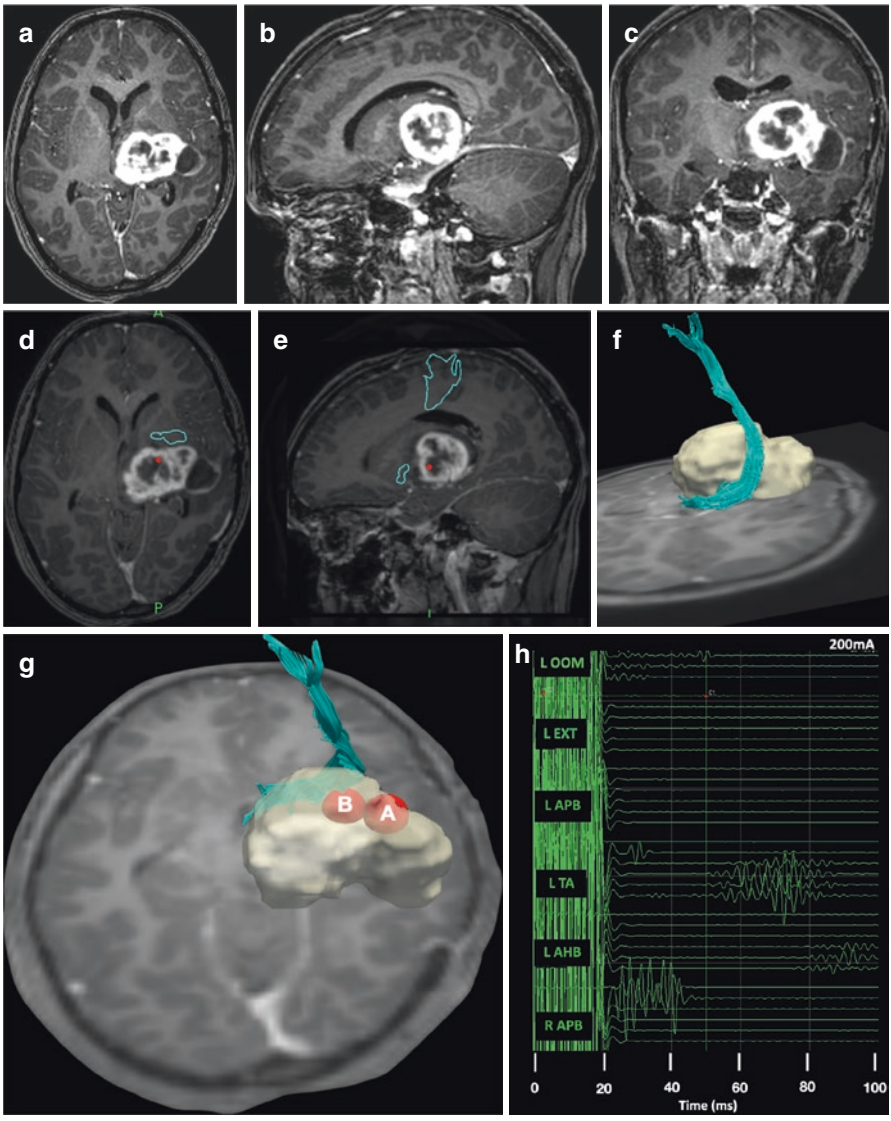

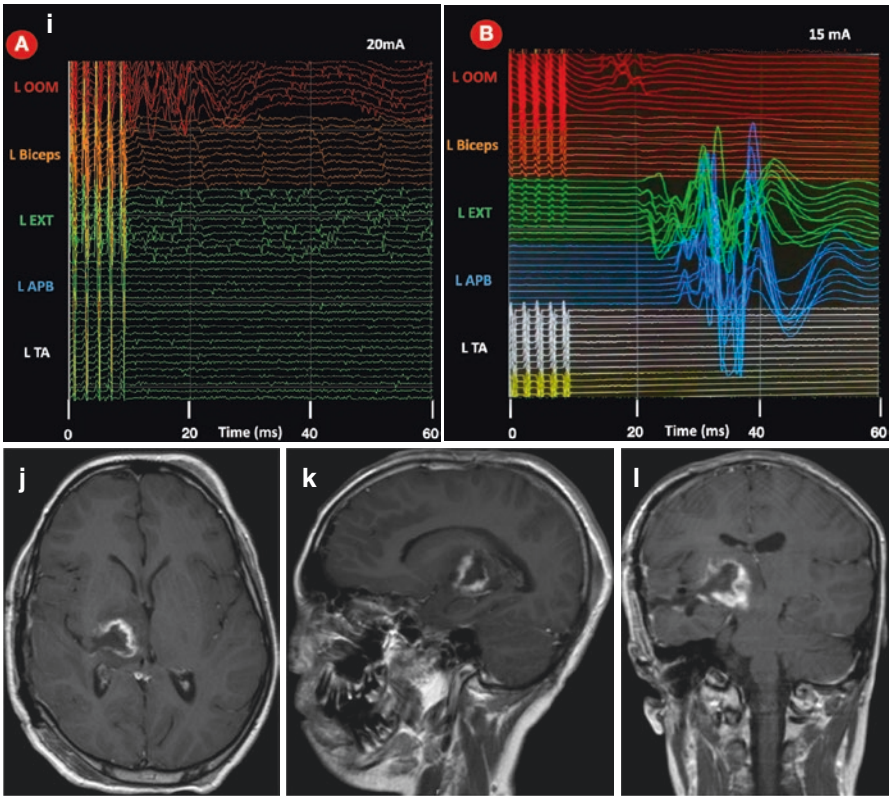

Fig. 2.4 (continued)

Secondary Motor Areas

Surgery outside the primary motor areas is generally considered to be safe, as permanent motor strength deficits are assumed to arise only from corticospinal tract damage. In this perspective, MEP monitoring combined with cortical and subcortical mapping should be sufficient to prevent every permanent deficits, since MEPs are a neurophysiological marker of the integrity of the corticospinal tract [111]. However, if loss of MEPs predicts long-term motor deficit [118, 144], preservation of MEPs at the end of the procedure does not ensure preserved motor ability [118]. This has been historically shown for resections within the superior frontal gyrus. Resection of the SMA/preSMA complex causes a striking contralateral hemiplegia/hemiakinesia (accompanied by aphasia on the dominant side) despite preserved intraoperative MEPs [122]. This is not due to MEP loss after strip electrodes removal: post-operative TMS [123, 145] shows that MEPs in these patients are preserved despite inability to move. Recently, we investigated this phenomenon in a cohort of 125 patients undergoing surgery with IONM for perirolandic tumours [118]. We divided patients' deficits according to MEP monitoring variations using a

50% drop threshold, as generally used [119, 144], and evaluated motor deficits in three periods, at 2 and 5 days after surgery and at least 3 months follow-up. The post-operative results indicated that motor deficits other than corticospinal tract damage are more common than debated: of 63 patients with post-operative deficits, two thirds occurred despite no MEP reduction. Notably, SMA damage corresponded only to half of these post-operative deficits, leaving place for a large system of motor control in both the frontal and the parietal lobe also to make up for motor deficits. More importantly, we observed cases in which long-term deficits occurred for resections outside of the corticospinal tracts: of 22 patients, 12 suffered from permanent deficits despite no MEP variation, although the vast majority of the deficits were mild to moderate. Analysis of resection cavities showed that these deficits do not represent false-negative results of MEP monitoring, but instead represent a form of permanent SMA-syndrome. In fact, long-term deficits despite no MEP reduction specifically occurred for resections of the SMA/preSMA complex including also the anterior cingulate cortex, including Brodmann area 32, and the dorsal premotor cortex at the level of the anterior precentral gyrus, possibly underlying a system where both internally driven and externally driven goal-directed actions are damaged [146]. While on a clinical perspective this advocates to re-evaluate other motor mapping techniques, especially during awake surgery [147], novel stimulation modalities [44] may allow to perform this also in the asleep patient.

These results question a surgery on motor areas centered exclusively on the corticospinal tract. First, they show that motor strength deficits may originate not only for disorders of motor execution, but also for disturbances of motor control, similar to what can happen in other motor disorders, such as Parkinson's disease. Second, they pinpoint to all those higher-order motor syndromes that do not involve motor execution but impact wider motor behaviour. These syndromes, such as apraxia, abulia, athymorrmia, and amimia, could be as impairing as hemiplegia. In this perspective, dual strip stimulation techniques, which involved MEP modulation to unravel cortico-cortical connectivity converging on the primary motor cortex, may allow for unprecedented monitoring possibilities and could be an avenue to a novel system of mapping behaviour in the asleep patient. Outside supratentorial surgery, this is the case for cerebello-motor stimulation [107], where direct cerebellar stimulation is combined with transcranial MEPs and MEP modulation underlies the cerebello-dento-thalamocortical pathway, therefore representing a way to possibly prevent a behavioural disorder most common in pediatric posterior fossa surgery, akinetic mutism [148].

In summary, while complete disappearance of MEPs predicts permanent loss of motor function, preservation of MEP does *not* ensure motor ability. Rather than considering it a false-negative result, motor deficit with preserved MEP may reflect a condition in which adequate motor ability necessitates a wider frontal and parietal, cortico-cortical, but also cortico-striatal/−brainstem network involving motor programming and control rather than sole motor execution [146, 149, 150]. In this scenario, monitoring of MEPs provides an essential but incomplete information, as it specifically focuses on the integrity of the corticospinal tract (CST) [111], while

Fig. 2.5 Illustrative case no. 4, on cortical and subcortical mapping. A 57-year-old right-handed woman with a history of high grade serous ovarian carcinoma (FIGO grade IVB) presented to the ER with sudden severe right hemiparesis (MRC scale 2), which rapidly deteriorated into hemiplegia (MRC scale 0) in 2 days. Right-sided hyperreflexia and positive Babinski's sign were noted. (**a**) Contrast-enhanced, T1-weighted MRI showing two left Rolandic lesions with conspicuous perilesional oedema. (**b**) Preoperative HARDI tractography of the corticospinal tract (CST, in yellow). The two lesions (in red) were located between and anterior to the CST, that appeared to be displaced posteriorly. (**c**) Cortical stimulation showing MEPs at 15 mA for the ABP and EXT. *APB* abductor pollicis brevis, *EXT* extensor digitorum communis; (**d**) Intraoperative site for cortical MEP (APB) as disclosed by the neuronavigation (green dot). *APB* abductor pollicis brevis. (**e**) MEP monitoring throughout surgical resection showing preserved MEPs at 23 mA (train of five stimuli, each of 0.5 ms duration) for the upper limb. Note that MEP for the lower limb were not monitored due to strip placement. (**f**) Intraoperative picture showing sites for cortical (green dot, like in picture "**d**") and subcortical stimulations (yellow asterisk). (**g**) Subcortical stimulation showing preserved MEPs at 15 mA for the ABP. *APB* abductor pollicis brevis. (**h**) After 3 months MRI revealed complete resection of the lesions in the precentral gyrus. (**i**) The postoperative HARDI-optimised tractography at 3 month showed cortico-subcortical integrity for the corticospinal tract (yellow). (**j**) After 1 year nTMS showed bilateral MEP persistence for upper (APB; FDI) and lower limb muscles (TA; AH). Grey dots: no response. Red dots: motor responses between 50–500 μV. Yellow dots: motor responses between 500–1000 μV. White dots: motor responses over 1000 μV. *APB* abductor pollicis brevis, *FDI* first dorsal interosseous, *TA* tibialis anterior, *AH* abductor hallucis. Early postoperatively, the patient remained hemiplegic (MRC scale 0), but after 1 month she reported voluntary movement of the formerly paralyzed contralateral hand, and after 2 months, movement of the contralateral leg during sleep. At 3 months, the patient walked with spastic gait when supported, with mild paresis in right upper and lower extremities (MRC scale 4) and right foot dorsiflexion (MRC scale 3). After 1 year, complete motor recovery for both right upper and lower extremities was reported (MRC scale 5), except from a mild foot dorsiflexion deficit (MRC scale 4). Therefore, preserved intraoperative MEPs in a clinical hemiplegic patient were predictive of motor recovery. (Reprinted with consent from [98])

other methods may need to be developed for extensive assessment of motor kinematics. On the other hand, besides the adoption of awake procedures, techniques pioneering MEP modulation could potentially represent systems to preserve cortico-cortical connections involved in higher-order motor syndromes, and therefore motor cognition.

2.4.2.2 Language

Traditional and Current Cortical Localization of Function

The mapping of language function started with the introduction of task-based mapping. This was introduced in the operating theatre by Penfield and Roberts using a naming task [151]. At that time, classical cortical localizationism relied on a strict segregation between a language production cortex, Broca's area, in the inferior frontal gyrus, and an (auditory) perception cortex, Wernicke's area in the superior temporal gyrus [152]. This was strongly supported by clinical data from aphasiology, where large strokes involving either the frontal or the temporal lobe were

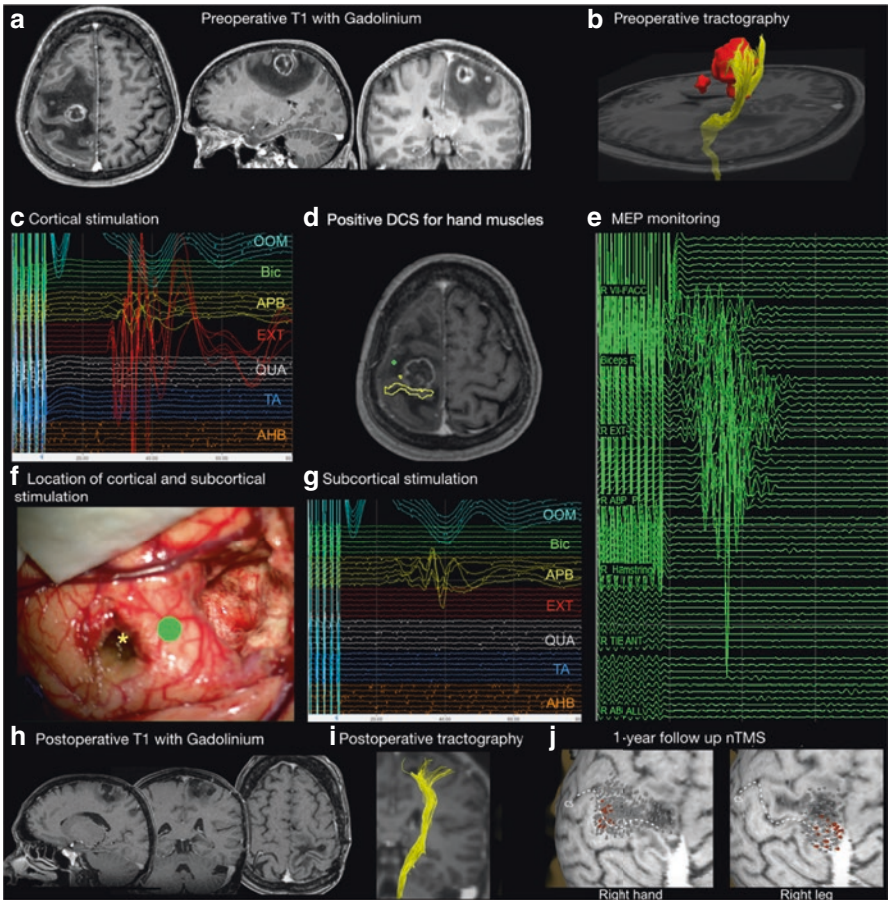

known to cause respectively production or comprehension deficits. From a conceptual point of view, this division survives until nowadays in the dual stream model of Hickok and Poeppel [153], where ventral cortices map sound to meaning and dorsal sound to action. However, already early on clinical experience showed that resection of language-unrelated areas, such as the parietal lobe, could incur language deficits [62] which could not be fully explained by these models. On this aspect, the advent of tractography [61] but most of all the beginning of subcortical awake mapping [38] revolutionized surgical practice, allowing to increase surgical extent of resection preventing language deficits [21, 38]. This allowed also to attribute function specific to subcortical structures, especially phonological encoding to the arcuate fasciculus [38], semantics to the inferior fronto-occipital fasciculus (IFOF) [154], and articulation to the third branch of the superior longitudinal fasciculus (SLF-III) [155]. Moreover, this allowed to constrain to subcortical anatomy the two streams in a ventral stream mapping language to meaning subserved by IFOF and

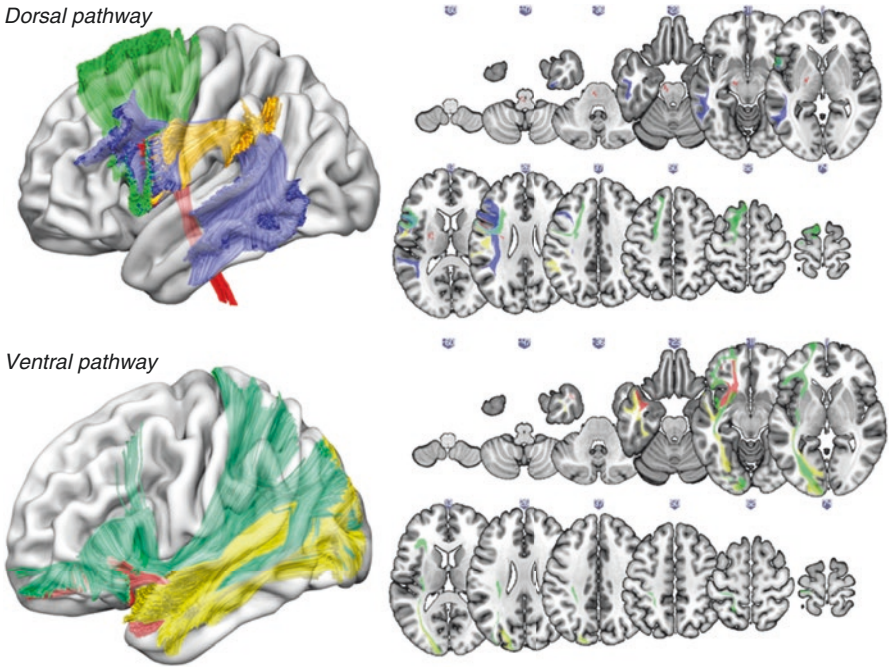

Fig. 2.6 Dorsal and ventral pathways involved in language function

ILF [156] and a dorsal stream mapping language to speech output subserved by AF/SLF-III [58, 129]. It is noteworthy that both the role of the pars opercularis in Broca's area and the posterior temporal gyrus in Wernicke's area have been recently reappraised. First, it is now widely accepted that the pars opercularis is not the primary motor area for speech [157, 158], while this is represented by the end of the precentral gyrus, the ventral premotor cortex [155]. Similarly, the posterior superior temporal gyrus reliably causes speech arrest and as such is involved in production, clashing with the tradition for which it is involved in Wernicke's aphasia [159].

Subcortical Anatomy of Language Function

As previously mentioned, current models of language function rely on a dorso-ventral cortical distinction [153] (Fig. 2.6). Cortically, this is at odds with anatomical [160, 161], neuroimaging [162, 163], and stimulation evidence [158] that these systems are adjacent and/or even overlapping in both deemed dorsal and ventral cortices. On a subcortical level, however, an articulatory/phonological (dorsal) and lexico/semantic (ventral) distinction within the language system is well-established [58, 129].

Within the dorsal phonological stream, the AF runs deeper than the SLF-III and provides connections between the posterior and middle temporal structures (superior, middle, and inferior temporal and fusiform gyri) and the posterior frontal gyrus

(ventral premotor cortex, pars opercularis, and triangularis), but also the most ventral and posterior part of the dorsolateral prefrontal cortex (posterior middle frontal gyrus). The SLF-III is more superficial and is instead dedicated to articulation/phono-motor conversion. It is important to stress that this tract links both the supramarginal gyrus and the posterior part of the superior temporal gyrus (area Spt) [159] with the ventral premotor cortex, but also the inferior frontal gyrus. As such, stimulation of the posterior STG that cause articulation deficits reflects stimulation of the SLF-III and not of the AF [164]. In this view, the AF provides phonological/phonetic data to be translated into articulatory motor programs within the ventral premotor cortex conveyed by the SLF-III. Notably, this subcircuit also supports the conversion of auditory inputs, which are processed in the verbal working memory system, into phonological/articulatory representations in the ventral premotor cortex [165]. At the level of the ventral premotor cortex, the vocal tract motor area can convey the appropriate motor command thanks to the corticobulbar tract that is connected to vocal tract nuclei within the rhomboid fossa in the brainstem [166, 167]. It is important to stress that the area involved in motor execution for the vocal tract lies in both the precentral and postcentral gyrus [168], with a somatotopic cranio-caudal distribution—except for duplication of the larynx area [169] which seems to be specific to human [170, 171]. This is a critical aspect, as speech is performed with vocal tract modulation during expiration [167] and therefore airflow through the larynx has to occur before any other phonatory modulation justifying why this second larynx area is at the most dorsal end of this somatotopic cranio-caudal distribution of the vocal tract [169].

Of note, the frontal aslant tract (FAT) is also involved in speech initiation as well as in speech control in the dominant hemisphere [172].

The ventral route, which has a more bilateral distribution [153], is composed of a direct white matter pathway, the IFOF, and indirect subpathways supported by both the anterior ILF and the UF [156]. It is generally accepted that the IFOF connects the occipital lobe, middle/superior temporal, and fusiform gyri with frontal regions, including the pars triangularis, the orbitofrontal cortex [164, 173]. More recent investigations as well as evidence from intraoperative stimulation would moreover include IFOF components in the superior parietal lobule, precuneus, and dorsolateral prefrontal cortex [174, 175]. As the main pathway of the ventral language system, the IFOF should play a pivotal role in verbal and non-verbal semantic processing. Indeed, electrostimulation of this circuit generates semantic paraphasias in left hemisphere or non-verbal semantic impairments in both the left and right hemispheres [176]. The indirect pathway is formed by the ILF that links occipito-temporal junction at the level of the posterior fusiform gyrus with the anterior temporal pole (ATL). The latter area constitutes a conceptual node enabling multimodal integration of the multiple invariant semantic-related signals originating from the sensory systems [177]. Accordingly, the ILF has been associated with lexical access [178].

We will describe language function using picture naming, as this is the most common paradigm used during awake surgery. We want however to stress that

during picture naming visual access is used instead of acoustic input, which differs from conversation.

First, visual input is conveyed from the eyes to V1 in the occipital lobe through the optic pathways allowing visual perception. Then, the ILF may carry the visual information from V1 to the inferior-ventral temporo-occipital junction, either in the visual word form area (VWFA) [179] in the left hemisphere if the perceived object is a letter or a word, or in the object word form area in other cases [180]. Stimulation at this level causes pure alexia [181]. From this ventral epicenter, the language network diverges into streams that process information in parallel: a dorsal phonological stream supported by the SLF-III/AF and a ventral semantic stream supported by the IFOF/ILF/UF.

Surgery in the Left Temporal Lobe

Surgery in the temporal lobe is generally deemed at risk because of the proximity with the so-called Wernicke's area [182, 183]. However, some caveats have to be considered. The first is that cortical mapping in the temporal lobe is highly variable [184] and often negative [185], to the point that one could erroneously assume that no function is present at that level because no positive mapping could be evoked. However, it has to be noted that inferior temporal regions are often covered by the bone and cannot be tested, while it has been shown that these induce transient language deficits [186]. Therefore, negative mapping in the temporal lobe may often reflect undersampling of the cortical surface in the inferior and fusiform temporal gyri. These aspects stress the importance of individual subcortical mapping.

The second caveat is that the type of deficit arising clinically after temporal damage is often more subtle than that in the frontal lobe: except for disconnection of the SLF-III component branching to area Spt in the posterior superior temporal lobe, aphasias for surgery in the temporal lobe are fluent. These deficits, as for anomia, conduction aphasia, or Wernicke's aphasia, may be less striking than non-fluent aphasia, often need neuropsychological evaluation to be unmasked, and are nevertheless overwhelming for the patient. Accordingly, neuropsychological evaluation must always be performed perioperatively and during rehabilitation, also in those cases that cannot undergo awake surgery.

Cortical Mapping

When mapping the temporal lobe, cortical mapping should be performed first. The most common cortical error is anomia [159, 184]. Chang and colleagues reported that the posterior superior temporal gyrus has both the highest probability and also the highest variability for showing anomia. However, anomia has also been generally shown when stimulating the middle superior temporal gyrus, which has been confirmed in a recent atlas of cortical and subcortical stimulation during awake surgery [164]. This location corresponds to the end of transverse/Heschl's gyrus and has been recently shown to be specifically involved in encoding of phonetic features

[187, 188]. It is important to stress that this area covers the middle superior temporal gyrus, and not the posterior, which is commonly an area for speech arrest [159].

Literature on mapping the temporal lobe generally focuses on the importance of the (posterior) superior temporal gyrus. On one hand, we believe it is important to stress that both the posterior and the middle superior temporal may be equally important, as an antero-posterior gradient in the human superior temporal gyrus has been debated [187, 189] whereby more anterior regions may be devoted to perception (acoustic feature recognition [187, 188]) and more posterior areas to action [auditory-motor processing/articulation and spatial hearing [190 159]. On the other hand, we want to stress that the ventral tem-poral lobe represents another critical cortical language area [186]. This has been clearly shown by Lüders, who first demonstrated using grid electrodes that a large basal lateral temporal area from 3 to 7 cm behind the tip of the temporal lobe causes a striking anomia when stimulating [186]. As previously mentioned, this strongly points out that negative mapping may reflect a limitation in cortical exposure where inferior temporal and fusiform gyri are not accessible. We believe this latter aspect is critical when targeting surgery in the temporal lobe, because the cortical function of the ventral temporal lobe is not as well-acknowledged as it has been historically less investigated during awake surgery. Notably, this area not only includes the visual word form area (VWFA) at the occipito-temporal junction whose resection has been associated with long-term alexia [181], but also the ventral lateral anterior temporal lobe (vATL), which has been independently associated with permanent anomia in epilepsy [191] and glioma surgery [136].

Subcortical Mapping

From an anatomical point of view, a critical subcortical structure that is often forgotten is the stratum sagittale [192, 193]. Initially described by Dejerine, the stratum sagittale is a multilayered structure crossing longitudinally the temporal lobe over the temporal horn and atrium of the ventricle. This densely myelinated structure carries the majority of white matter pathways in this area, which means that damage to this can cause almost complete disconnection of the temporal lobe [192]. The superficial layer carries the IFOF and the ILF, while the deeper layer carries thalamic projections to the temporal and the occipital cortex, namely the optic and acoustic radiation. It is also an important anatomical landmark, since just over it runs the arcuate fasciculus [193, 194].

As a matter of surgical practice, numerous white matter fascicles are involved in language function in the left temporal lobe. These include the arcuate fasciculus and the SLF-III for the dorsal pathway and the IFOF, the ILF, and possibly the UF.

Stimulation of the arcuate fasciculus reliably causes phonological paraphasia. Accordingly, surgical resection should stop whenever causing phonological paraphasia, as it has been shown that disconnection of the arcuate fasciculus is associated with permanent aphasia [72]. It is important to note that in a recent cortical and subcortical white matter atlas, phonological paraphasias associated to the arcuate fasciculus largely exceeded the generally accepted cortical terminations of this tract

within the classical Wernicke's area in the superior temporal gyrus to include extra-Wernicke cortical terminations in more ventral anterior (anterior/middle ITG; middle fusiform gyrus) as well as posterior (posterior ITG; VWFA) cortices. This points at a wider system for phonology supported by the arcuate fasciculus as normally acknowledged and that should be taken into account when targeting posterior temporal lobe resection. As suggested by Carl Wernicke, a damage to the arcuate fasciculus is supposed to cause conduction aphasia [183], a phonological encoding disorder where speech is fluent but with frequent phonological paraphasias, repetition disturbances, and impossibility to repeat or read pseudowords. This is opposed to non-fluent aphasia, characterized by the articulation disorders and forms of apraxia of speech, which is associated with the SLF-III [195]. As mentioned, the SLF-III has components reaching the temporal lobe, particularly the posterior superior temporal gyrus. This area is continuous to the posterior supramarginal gyrus (anterior to the sulcus of Jensen where the parietal continues into the temporal lobe) and overlaps with area Spt. Indeed, stimulation of the SLF-III in both the frontal and also in the temporal lobe causes articulation disorders to the extent of speech arrest [159, 164], representing also in the temporal lobe a pattern of "Broca's aphasia".

It is generally acknowledged, even though non-unanimously [196], that the IFOF provides semantic information [129]. This has been clearly shown for the first time using awake surgery [154] and then confirmed using fMRI-tractography [197]. Indeed, semantic paraphasias after IFOF stimulation are well-established. In the temporal lobe, this occurs at the level of the superior layer of the stratum sagittale, over the atrium and temporal horn of the ventricle. For this reason, preservation of the IFOF posteriorly allows to protect also the optic radiation, which at this level lies on a deeper layer [173]. Progressing toward the temporal stem, the IFOF dissociate from the ILF which posteriorly runs lower to the IFOF. At this level, the IFOF enters the temporal stem and then the external capsule to progress to the frontal lobe, while the ILF projections inferiorly to the ventral anterior temporal lobe. Damage to the ILF can cause lasting disorders of lexical retrieval and its stimulation causes anomia [136].

To sum up, for surgeries in the temporal lobe and once cortical mapping is performed, the arcuate fasciculus together with the SLF-III can theoretically represent the posterior anterior and postero-inferior subcortical border, the IFOF the medial border, and the ILF the inferior medial and inferior border. Pragmatically, considering the huge plastic potential of some of these structures (especially IFOF and ILF), mapping must guide resection to ensure the most suitable borders [108, 136].

Surgery in the Left Frontal Lobe

Cortical Mapping

Since Paul Broca, the pars opercularis has been considered a critical area in speech production, and for this reason, awake mapping has been advocated when operating the frontal lobe. However, surgical [198, 199] as well as stroke evidence [157] has

shown that this area is not necessarily associated to permanent language deficits. In the contemporary view, the critical area for speech production is located at the end of the precentral gyrus [112, 158]. This area corresponds to area 6b in Brodmann's original maps [200, 201] and arguably area 6v/43 in the Glasser parcellation [202]. Its stimulation can cause both hand and face movement inhibition [112], and for this it is generally considered homologous of the ventral premotor cortex in non-human primate [141, 203]. Therefore, when considering a primary area for speech output, it has to be stressed that this is represented by the ventral premotor cortex and not the pars opercularis. Indeed, comparing lesions in the pars opercularis against those in the ventral premotor cortex, Bizzi and colleagues showed that gliomas involving the ventral PMC were fivefold more likely to cause aphasia compared to gliomas involving the inferior frontal gyrus [204]. Currently, the pars opercularis is instead considered as an optimal route for the transcortical approach to the insula [199] and its resection is therefore advocated. This is normally a safe entry point in LGGs; however, cortical mapping is always of primary importance. When discussing primary articulatory areas, it is important to stress that a second output area has been identified dorsally to the ventral premotor cortex [169], possibly corresponding with area 55b in the Glasser parcellation [202]. This also can cause speech arrest when stimulated [112, 159] as well as vocalization [109].

When stimulating the ventral premotor cortex during a double task (naming and arm movement) [58], as a *rule of thumb*, if speech arrest is combined with movement inhibition, this may be reputed to reflect transitory disconnection of the frontal aslant tract (FAT), while speech arrest/articulation disorders in isolation may be attributed to the SLF-III. However, recent data from Viganò and Howells [205] show that EMG patterns are critical to distinguish these motor phenomena, and therefore quantitative studies on MEP pattern variations during awake surgery are needed to assert possible neurophysiological features of these cortico-subcortical structures. Moreover, speech arrest occurring when stimulating the pre-SMA may represent both cortico-cortical (FAT) and fronto-striatal connections (FST) involved in action initiation [206] (Fig. 2.7).

Another critical structure for preservation in the frontal lobe is the posterior middle frontal gyrus, also referred to as the dorso-lateral prefrontal cortex (DLPFC) in the surgical literature [174]. Indeed, stimulation of this area, during both naming and pyramid and palm tree test (PPTT), induces semantic disturbances [154] and represents a newly described critical semantic hub [174], which may be non-specific for language. Conversely, semantic paraphasias evoked on the inferior frontal gyrus, particularly in the pars triangularis, may reflect verbal semantics. Both verbal and non-verbal semantic disturbances at this level may be due to stimulation of cortical terminations of the IFOF [173].

Subcortical Mapping

As for the temporal lobe, there are a number of subcortical structures that are considered critical for language in the frontal lobe. Together with frontal terminations of the arcuate fasciculus, the SLF-III and the IFOF, other white matter tracts that are

of prime importance are the corticobulbar tract, fronto-striatal projections (from both vPM and the pre-SMA), and the FAT. It is important to remember the location of the arcuate fasciculus and the SLF-III in the coronal plane: as the arcuate runs deeper, it runs medial to the SLF-III. One could use the circular sulcus of the insula as an imaginary plane to divide the two tracts on the coronal plane: the AF runs medial while instead the SLF-III runs lateral to this sulcus. This is critical when targeting insular gliomas through a transcortical approach, since once in the insula the arcuate and the SLF-III represent the superior border, one more medial and the other more lateral.

Progressing anteriorly from the temporal lobe, the IFOF enters the temporal stem and then covering the anterior perforating substance within the external capsule projects superiorly to the DLPFC and anteriorly to the pars triangularis, opercularis, and the lower orbitofrontal gyrus. As there are no Sylvian perforating arteries at the level of the temporal stem, this area can be well addressed with subpial dissection also when approaching it from the temporal lobe. As discussed, when resecting the insula through a transcortical approach, language function can be encountered superiorly (SLF-III) or within the posterior insula, since the IFOF enters at this level the stratum sagittale from the parietal lobe [175]. However, resection within the insula during awake surgery deals medially with fronto-lenticular [207] projections from

Fig. 2.7 Illustrative case no. 5, on cortical and subcortical mapping. A 29-year-old woman with right hand dominance was admitted for focal motor (orofacial) seizures, secondarily generalized. The neurological examination showed no deficits. (**a**–**c**) The pre-operative axial (**a**), coronal (**b**) and sagittal (**c**) T2-weighted gradient-echo MR images disclosed a left infero-frontal lesion with contrast enhancement compatible with a cavernoma. (**d**) Pre-operative high angular resolution tractography (HARDI) showing that the lesion lies in proximity of the arcuate fasciculus (in red) but far from the corticospinal and corticobulbar tracts (in yellow). (**e**) Pre-operative language mapping using navigated transcranial magnetic stimulation (nTMS). During stimulation language errors clustered at the level of the superior temporal gyrus and precentral gyrus. Yellow spheres: semantic paraphasia; green sphere: hesitations; tracts: arcuate fasciculus (red); corticospinal tract (blue). (**f**) Pre-operative high angular resolution tractography (HARDI) combined with nTMS results. Yellow spheres: semantic paraphasia; green sphere: hesitations; blue sphere: anomia; tracts: arcuate fasciculus (red); corticospinal tract (yellow). (**g**–**i**) Direct cortical stimulation (DCS) of the middle superior temporal gyrus (Wernicke's area). Anomia was elicited (Letter "A"). Electrocorticography (ECoG) from the strip electrode was used to detect afterdischarges and prevent DCS-induced seizures. Panels (**h**) and (**i**) show the location of anomia in the neuronavigation system, in 3D reconstruction and axial view respectively. Arcuate fasciculus (red) and corticospinal tract (blue) are indicated. (**j**–**l**) Direct cortical stimulation (DCS) over the ventral premotor cortex evoking speech arrest (Letter "M"). Electrocorticography (ECoG) from the strip electrode was used to detect afterdischarges and prevent DCS-induced seizures. Panels (**k**) and (**l**) show the location of speech arrest in the neuronavigation system, in 3D reconstruction and axial view respectively. (**m**–**o**) The site of subcortical stimulation evoking semantic paraphasia is indicated by the tip of the probe (green dot) in the intraoperative navigation system (projections of the inferior fronto-occipital fascicle are not shown). (**p**) Illustration of DCS responses on HARDI tractography. HARDI tractography reconstruction illustrating the location of semantic paraphasia during subcortical stimulation (in yellow). (**q**–**s**) Post-operative CT scan showing complete resection of the lesion

motor areas, and only posteriorly with the posterior part of the internal capsule carrying the corticospinal tract but also sensory thalamocortical projections to the parietal lobe. In asleep fashion, this surgery may be performed using MEP monitoring and taking advantage of the 1 mA:1 mm rule setting the minimum current intensity at 3 mA. In this way, since the internal capsule becomes more lateral at the end of the insular cortex and 'opposes' the access to the atrium of the ventricle [208], using an MEP amplitude of at least 3 mm can allow to spare both corticospinal and thalamocortical projections when accepting possible residuals in the posterior insula.

When considering tumours confined to the frontal lobe, subcortical borders may differ. Despite a high inter-individual variability and the necessity for mapping, one could have the ventral premotor component of the FAT causing both speech arrest

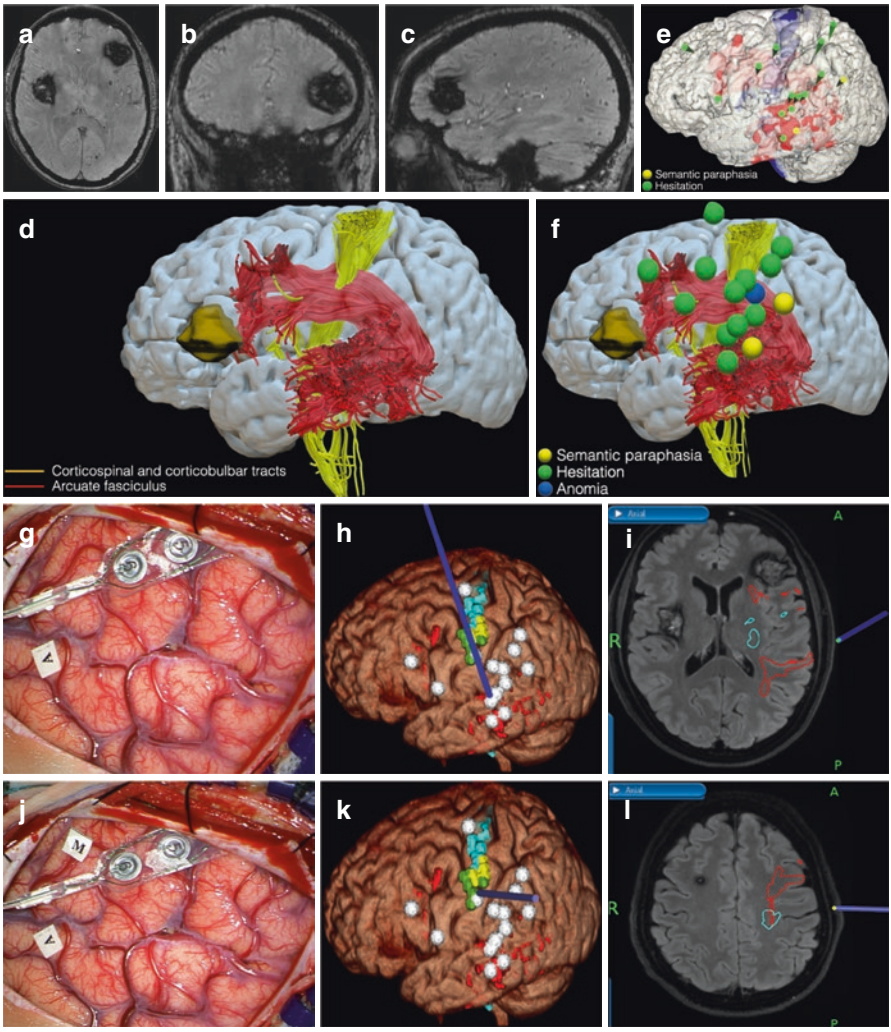

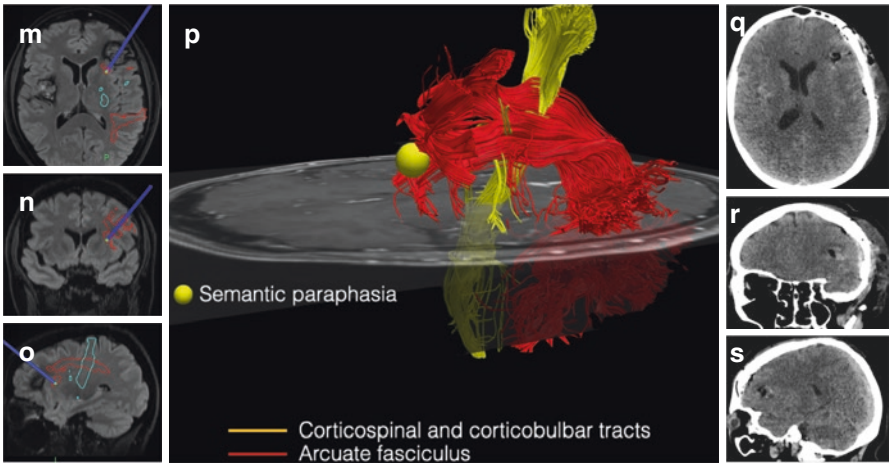

Fig. 2.7 (continued)

and movement arrest as a posterior border, together with speech arrest in isolation caused by SLF-III stimulation. More superiorly, the arcuate fasciculus and the IFOF run in close proximity underneath the middle frontal gyrus, and stimulation can cause anomia, or either phonological paraphasia for the arcuate fasciculus as opposed to perseverations [209] or semantic paraphasia when stimulating the IFOF. Perseveration are most common when approximating the caudate nucleus [209].

Damage to the ventral premotor cortex causes Broca's aphasia, a non-fluent type of aphasia with agrammatism and difficulty in articulating and repeating words [195]. This is largely contributed by multiple disconnection of the SLF-III [155, 195], but also the corticobulbar tract, the arcuate fasciculus, and possibly also FAT/FST components. Conditions with disorders of speech initiation resulting in aphasia, but transient, should reflect instead disconnection of the FAT/FST.

Surgery in the Left Parietal Lobe

While surgeries in the left frontal or temporal lobe are deemed to be at higher risk of language deficits, because of past cortical localizationism it was commonly assumed for surgery in the parietal lobe to be safer. At current, it is well-established that surgery in the parietal lobe (particularly at the level of the supramarginal gyrus or Geschwind's area) is at a very high risk of language deficit. Together with a risk of cortically damaging the parietal portion of the SLF-III and therefore causing non-fluent/Broca's aphasia, the main issue is the disconnection of all components of the AF and the SLF-III subcortically, with devastating consequences for the patient. Moreover, superior parietal/precuneal components of the IFOF project in the depth medially to the arcuate fasciculus to reach the external capsule causing often non-verbal semantic disturbances at this level [175, 210].

Cortical Mapping

Cortical mapping at the level of the posterior supramarginal gyrus, anterior to Jensen' sulcus, until the posterior superior temporal gyrus can result in articulation disturbances, until speech arrest [155, 159]. Superior cortical terminations of the IFOF are rarely investigated and it is uncertain whether they would correspond with the superior parietal, the dorsal posterior postcentral gyrus continuing into the cingulate gyrus, or even the precuneal cortex [175].

Subcortical Mapping

The critical structures that must be preserved at this level are the SLF-III/AF complex and, more medially, the IFOF. Anatomically, the SLF-III runs more superficial than the AF and turns to the posterior superior temporal gyrus already at the level of the anterior supramarginal gyrus, possibly together with some fibers from the superior temporal and middle temporal component of the arcuate fasciculus [211, 212]. Conversely, a more dorsal component of the AF (dorsal arcuate) runs more deeper and turns under angular gyrus [212]. As discussed, on a coronal plane, the SLF-III runs ventral and lateral, the AF dorsal and medial. When approaching this region, it is important to remember that during subcortical mapping, after having evoked articulation disorders, deeper resection will encounter the arcuate fasciculus, as the SLF-III covers it only ventrally and superficially [155]. For resections in the depth, medial to the arcuate fasciculus, the IFOF can cause semantic disturbances, possibly associated with awareness disorders [175]. Therefore, when targeting resection in the parietal lobe, thalamocortical projections to S1 may represent the anterior border, together with subcortical components of the arcuate fasciculus (deeper and dorsal) and of the SLF-III (superficial and medial). It is moreover important that at the level of the angular gyrus, it is still possible to disconnect the arcuate fasciculus for deep resection. To conclude, more superior and deeper semantic disturbances may be elicited for stimulation parietal projections of the IFOF [213].

Clinically, white matter damage at this level generally causes non-fluent aphasia for disconnection of the SLF-III. Conversely, damage to the arcuate fasciculus in isolation (approached from the posterior supramarginal gyrus or angular gyrus) may cause instead conduction aphasia.

Asleep Language Mapping

In the precedent sections, we specifically referred to patients operated awake. Of course, since language evaluation is task-based, there is potentially no system that can map or monitor this function during asleep surgery. Indeed, even if awake mapping should be always advocated, there are cases in which this is not feasible. Patients suffering preoperative language deficits or having an inappropriate psychological profile are generally not candidates. This is critical for paediatric neurosurgery, since no awake operation is indicated below the age of 10 years [214], and

even after indication awake surgery is disputed [110]. For these patients, being operated under general anaesthesia without mapping means undergoing surgery without methods to online preserve functional anatomy. With the understanding of the cortico-subcortical structures subserving language, however, an attempt can be made in preserving part of language function by preserving specific connections. We want to stress that conceptually, this may not differ from monitoring the corticospinal tract using MEP to preserve motor function instead of having the patient performing a repertoire of motor gestures.

In awake surgery, cortico-cortical-evoked potentials (CCEPs) have been initially described by Matsumoto and colleagues as a mean to evaluate language connectivity represented by the arcuate fasciculus in perisylvian but also extra-sylvian cortices [43]. In CCEPs, one of two cortical terminations of a white matter tract is stimulated electrically, and cortical-evoked activity is recorded at the other cortical termination in form of evoked potentials. Twenty to 120 raw traces are conventionally averaged, similarly to cortically recorded somatosensory-evoked potentials. Initially, CCEPs were described having two components, an N1 between 20 and 30 ms [43, 215], and a second, later component peaking at 100–150 ms [43], though some authors claim this later component could represent epileptogenic activity instead [216]. More recently, earlier positive components have also been described, such as P1 [217] or P0 [218, 219]. During awake surgery, modification of N1 amplitude has been shown to correspond with language outcome [220, 221]. However, even if some potentials have been recorded in the awake patient also during the asleep phase [220], clinical use of these specifically in a fully asleep patient has been lacking until very recently [222, 223] and therefore monitoring of the N1 component has to be validated in this cohort of patients.

The recording of CCEPs is generally limited to awake patients, on one side because of the suppression of neural activity due to anesthesia [224], on the other side by chance to identify location for strip electrodes' placement using functional mapping [43, 225]. In a recent work in a cohort of nine patients with tumours in the left perisylvian area who could not undergo awake surgery, we recorded CCEPs of the arcuate fascicle undergoing asleep tumour resection [222]. Results indicated that reliable potentials of small amplitude (of the order of 20–200 μV) could be obtained from the arcuate fasciculus also under anesthesia and that strip electrode placement can be made more effective by combining tractographic MR information and presurgical neuronavigated TMS (nTMS). Results in the asleep setting resembled those in the awake setting: an N1 potential with a latency of 21 ms was shown, together with an earlier positive potential peaking at 12 ms (P1). This is well in line with the results of Suzuki and colleagues showing that anaesthesia impacts CCEPs' amplitude more than latency [224] and our results have been recently replicated in other two studies [223, 226]. In our preliminary results, evoked potentials clustered in the middle temporal gyrus while stimulation mainly covered the ventral premotor cortex. However, inferior temporal gyrus components of the arcuate fasciculus have not been extensively investigated in this study, which must be taken into account as previous work showed CCEPs also being recorded in basal temporal areas [43]. Moreover, no data on language outcome could be provided.

To sum up, there is a growing interest in mapping language function also in the asleep patient. While these preliminary results are encouraging, a rigorous investigation of how they impact functional language outcome has not been performed. Indeed, the arcuate fasciculus cannot be used as the only tract to be monitored as its preservation is insufficient to preserve language function and therefore outcome just based on arcuate/N1 component preservation is biased. Nevertheless, it is expected for this field to grow in the following years as cortico-subcortical structures and their network involvement will be unraveled.

2.5 Future Perspectives

Since the early 2000, glioma surgery experienced an unprecedented improvement in both overall survival and quality of life offered to the patient. This was accompanied by formulation of important theoretical concepts, such as that of onco-functional balance [22], and direct evidence for the existence of neuroplasticity [227].

This has offered novel possibility to increase extent of resection and preservation/restoration of function. Nevertheless, current evidence has posed new challenges. Crucially, it has highlighted that the right hemisphere is far from being "silent" [58]. Under this premise, mapping and understanding better the right hemisphere represents an impending issue for neurooncological surgery [228].

2.5.1 Neuroplasticity, Prediction, and "Prehabilitation"

Evidence for brain plasticity after damage was initially documented in stroke [229]. This clashed with a static idea of brain function towards an integrated systems of connection in which function can re-adapt dynamically [58, 227, 230].

Hence, a "meta-networking theory" of brain function has been proposed [58]. In this system, input from the periphery (such as: visual pathways, ascending sensory pathway) and output to the periphery (efferent motor pathways) should have very low plastic potential [231], while more integrated networks, such as those involved in goal-directed and context-based action, but also emotion, would have higher plasticity [58]. This anchors subcortically the cortical gradients hierarchically ordered in primary and unimodal cortices with sensory and motor functions to higher-order, transmodal association cortices first proposed by Mesulam [232] and currently established to be rooted in structure [233], evolution [234], neurodevelopment [235], and function [236]. In this view, higher plasticity of transmodal association cortices is also reflected in higher plasticity of the white matter tracts that connect them. Notably, while previous models [136, 231] proposed a cortex/white matter duality with the cortex being more plastic that the white matter, this model rebalances models of plasticity according to network integration. In this view, networks such as the IFOF, which widely integrates (transmodal association) frontal,

parietal, temporal, and occipital cortices, can reorganize after damage. This has been shown in a recent atlas of plasticity [178], but also considering reorganization after surgery [237]. Similarly, frontal cortical terminations of the arcuate fasciculus in pars opercularis, pars triangularis and the middle frontal gyrus can have potential for neuroplasticity, and therefore can be resected during surgery without causing permanent language deficits [198, 199]. In this scenario, damage to cortico-subcortical network, but not complete disconnection, can support reorganization and plasticity for restoration of function [58]. This has important surgical implications, particularly when considering reoperation, as commonly occurs for LGGs [11, 238]. Reoperation should be always considered whenever the tumour volume grows over 10–15 cc, as the risk of malignant transformation is higher [19, 24]. However, it is the second operation which may be critical, as neuroplasticity and reorganization occurring after the first surgery may allow more extensive resection during the second surgery, as functions may migrate [237, 239].

The first implication of a dynamic model of brain function is that intraoperative mapping is always necessary. In this perspective, the function of a network cannot be inferred from the anatomy in the single patient except for input and output systems (primary and unimodal cortices with sensory and motor functions) [235]. This means that while function for the corticospinal or visual pathways may be assumed also from the anatomy, the other networks have to be mapped in the individual patient. The reason for this is that, on one side, complete disconnection of a functional subcortical network will cause long-term loss of function, on the other side, sparing non-functional subcortical networks based on imaging can reduce extent of resection, thus diminishing the individual patient's life expectancy without justifications when total or possibly supratotal resection could be achieved. It is important to note that overall survival in LGGs is strongly enhanced despite molecular biology when performing supratotal resection, whenever the tumour is IDH-mut and co-deleted, only IDH-mut or even IDH-wild-type [20, 23, 26].

It is important to stress that reorganization of function is not just based on patterns of cortices being connected, but it is supported and allowed by the white matter on a network level. For example, the IFOF and the AF share a similar pattern of connectivity in the middle temporal gyrus and pars triangularis. However, the IFOF does not vicariate phonological encoding if the AF is damaged and, conversely, the AF does not vicariate semantics if the IFOF is damaged. This supports a vision in streams, as for dual [240] and three-way [241] streams, where function diverges in subcortical pathways in a parallel and segregated way while it integrates in cortical hubs [58]. Similarly, a network should be specifically involved in a group of functions, but not others (i.e. phonology for the AF and semantics for the IFOF), and mapping will be used to test whether a predicted function is present or absent for that specific connection. Neuroplasticity as migration of function from previously responsive cortices is now a well-established phenomenon, which has been shown with both DES [242] and nTMS [243]. In neurosurgery, this may be the case of SMA-syndromes: recovery of movement, also for motor dexterity, can occur with extensive movement rehabilitation whenever resection of motor–premotor

connections is not complete [118]. This is particularly apparent in LGGs. Of course, in LGG the tumour itself pushes brain plasticity [237]. Its slow growth, around 3 mm/year, allows for reorganization and it's the foundation why patients with LGGs are normally asymptomatic (except for seizures), despite such voluminous tumours [11]. Indeed, seizure may represent the limit of plasticity and a sign that the brain is/can no more compensate the tumour mass [244].

In LGGs, initial evidence of specific pattern of reorganization has been provided. Herbet et al. [108] showed that stimulation of the ILF systematically induces pure anomia only when the temporal pole is not infiltrated by the tumour, showing that the information conveyed by this tract can be rerouted to alternative pathways when the temporal pole is widely lesioned and abandons its function. Importantly, in the patient in whom the tract was functional and was disconnected, aphasia was permanent, suggesting that reorganization needs at least partial white matter preservation. Moreover, also the wider cortex of the temporal lobe is remapped, showing plasticity to underlie whole networks reorganization.

A second reason to propose systematic mapping is that studies on cortical and subcortical function are mostly coming from mapping in LGGs. Therefore, the assumption that areas, such as Broca's area, are surgically amenable [199], maps regarding plasticity [136], and atlases of white matter function [164] is based on a patient population where it is known that plasticity is particularly developed [227]. There is strong evidence to suggest that neuroplasticity does not take place in HGG as in LGG as the tumour growth in the first group of patient is faster [20]. This implies a need for developing maps that are specific to a "native" brain, a brain which has not already reorganized allowing for enhanced resections more typical of LGG. This is a critical aspect, as patients with HGGs not only have a lower life expectancy, but may also have a higher risk of neurological deficit, as it has been recently shown [20]. From this point of view, while maps developed from LGGs can provide information of neuroplasticity, particularly for cases with a second surgery, still maps of function should be performed in other groups of patients, where HGGs, cavernomas, and epilepsy patients may represent more appropriate patient to provide a "native brain" map.

As previously mentioned, a system of meta-networks suggests a hierarchical reorganization of brain function. Evidence from non-invasive stimulation in stroke [245] and also in aphasic patients [246] suggests that this network can be pushed to reorganize, and therefore plasticity can be externally targeted and enhanced, allowing for behavioural improvement to complete restitution of function. This issue has been recently addressed by Duffau [230], suggesting that non-invasive stimulation should be performed post-operatively in areas that were found functional during the surgery to further increase behavioural rehabilition and the reoperation. Notably, preliminary studies using invasive plasticity stimulated before reoperation to enhance resection have been carried out successfully [247]. We believe this proposal should be further enhanced. Indeed, preoperative TMS, as well as resting-state fMRI, can provide information of cortical function, thus enhancing cortical mapping during surgery. In this scenario, it may also be used to approximate cortical areas deemed to

be functional before the first surgery. Under this premise, preoperative techniques such as nTMS can potentially first inform the state of brain function through a task-based mapping. Then nTMS mapping-positive sites can be used for targeted repetitive stimulation to push reorganization before surgery (or "prehabilitation"). To conclude, surgery could be performed increasing the extent of resection without neurological deficit. We believe this may be particularly critical for those patients, such as those suffering from HGGs, where there is less space for reoperation.

2.5.2 A Need for Mapping the Right Hemisphere and a Reappraisal of Psychosurgery

Awake surgery is generally indicated for left hemispheric tumour in regions deemed to be associated with language function, with the right hemisphere considered as non-dominant and mapping for this hemisphere as not necessary beyond preservation of the corticospinal tract and the visual pathways. This is highlighted by the fact that very few centres operate right hemisphere tumours awake and no specific mapping for right-lateralized function in the asleep setting has been developed. Similarly, a comparison for surgery in the right hemisphere comparing asleep and awake setting is also lacking.

While the right hemisphere is generally reputed to be less noble (at least surgically), evidence from neuropsychological analyses challenges this surgical dogma [228]. Indeed, there is evidence that patients with right hemispheric tumour report poorer quality of life compared with those with left hemispheric tumours, particularly for tumours involving the frontal lobe [248]. This is surprising, considering that language deficits strongly impact life quality [249] and this function is strongly left-lateralized. Attention [250], cognitive control [251], and emotional processing [252, 253] are considered predominantly right-lateralized functions, with the right hemisphere supposed to have dominance in social cognition [254]. Indeed, both attention and cognitive control are impaired in patients operated in the right hemisphere [255].

Since the paradigm shift in the early 2000 from cortical localizationism to connections, there has been progressively more interest in white matter anatomy. However, possibly driven by language, a system that is most recent evolutionarily [256], the main focus has been on association tracts (cortico-cortical connections), with surpassed cortical localizationism seemingly becoming cortico-cortical localizationism. There is both theoretical [257] and clinical evidence [258, 259] that this conception should be revised. Indeed, breakthrough discoveries in deep brain stimulation (DBS) [260] are those that most strikingly advocate for a revision of cortico-cortical models. The recent unification of DBS targets for obsessive compulsive disorder in a white matter tract connecting the brainstem to the middle frontal gyrus and the preSMA [259, 260] is a prime example of this. During awake surgery, fronto-caudate connections have been those addressed by a larger number of studies [100, 261, 262]. Indeed, fronto-striatal connections are crucial and should be further

elucidated [147]. However, connections from the anterior internal capsule—and generally connections from DBS targets in psychiatric diseases—should be integrated also in tumour surgery as their disconnection may be burdened by personality or mood disorders also in resective surgery. Together with the anterior cingulate for negative emotions [263], projections from the anterior internal capsule have been demonstrated to be pivotal in mood regulation [264]. This is unsurprising, as bilateral disconnection of the anterior internal capsule represents the first target in the history of psychosurgery in the form of prefrontal leucotomy, or lobotomy, pioneered by Moniz [265].

To sum up, we strongly believe that mapping the right hemisphere is crucial and should be considered a priority. A recent study on 1333 stroke patient recently investigated function of white matter using existing task-related fMRI meta-analysis and the 7 T diffusion dataset of the HCP project. This study clearly showed that much less is known about the white matter function of the right hemisphere in comparison with the left [228], urging a reappraisal. We believe this is particularly important in resective surgery as it is in stroke literature, and we firmly believe that adequate mapping, functional identification, and preservation of essential anatomy also in the right hemisphere is crucial to preserve patient's higher-order behaviour, and thus, identity.

2.6 Conclusions

Tumour surgery has experienced dramatic progress in the last 20 years, thanks to a better understanding of subcortical anatomy and the adoption of subcortical mapping. Advances in clinical practice resulting from this paradigm shift have allowed to confront lesions previously regarded as inoperable, but also to preserve essential cortico-subcortical anatomy, thus extending life expectancy and enhancing quality of life.

We have described well-established stimulation techniques and the warning criteria for cortical and subcortical resection in the motor and the language system. As mapping has become crucial in resective surgery, we stress that adequate knowledge of stimulation paradigms and functional anatomy is mandatory whenever performing this type of surgery. We would caution that the surgeon should always remember that a number of variables can affect the results of mapping: pulse duration, current intensity, number of pulses, train duration, frequency of stimulation, and stimulating probe (bipolar vs. monopolar). In addition, it should be kept in mind that subcortical mapping only localizes subcortical structures, while it is monitoring that can provide continuous feedback regarding their functional integrity. When surgery is performed in proximity of motor areas, the role of MEPs is invaluable and we believe that MEP monitoring combined with cortical and subcortical mapping using a To5 techniques should be preferred, as it is more effective than the more common Penfield's stimulation paradigm. While we are of the opinion that awake surgery should be performed whenever feasible, we are aware that this is not always possible. In this

scenario, even if MEP monitoring combined with cortical and subcortical mapping is sufficient to assess the corticospinal tract's integrity, we must stress that motor behaviour largely exceeds motor execution [146] and therefore more sophisticated forms of mapping should be introduced. On this aspect, we believe that in asleep patients MEP-conditioning paradigms [44, 266] or cortico-cortical-evoked potentials [222, 266] may be valuable options, although results using these techniques are only preliminary. When considering language function, current evidence suggests revision of a fronto-temporal production/comprehension duality. Speech production is evidenced in both the so-called Broca's and Wernicke's areas, and Lüders' basal temporal areas [186] advocated existence of language cortices outside Wernicke's area in the temporal lobe. Moreover, contemporary language models imply a wider system to be mapped, way beyond the preservation of the sole arcuate fasciculus as it is often advocated. In this scenario, not only the arcuate fasciculus, but also the SLF-III, the IFOF, the FAT, and the ILF (among other tracts) should be systematically preserved using brain mapping whenever functional. Whenever surgery in these areas has to be performed asleep, novel monitoring technique such as CCEPs should be considered, but still needs clinical validation.

Glioma patients can, and particularly LGGs should, be reoperated. In this scenario, it is our opinion that also temporary deficits (i.e. SMA syndrome) should be avoided during the first surgery as function often is migrated in the second surgery, thus allowing for larger resections with optimal quality of life. In case of incidental gliomas, "preventive" surgery should be considered as supratotal resection is likely [267], thus increasing patients' life expectancy [20]. Under this premise, we believe that forms of targeted plasticity, both invasive [247] and non-invasive [230, 246], may represent the future of the discipline, enhancing both functional preservation and extent of resection.

To conclude, there is increasing evidence for the importance of mapping the right hemisphere. While only few centres are currently operating the right hemisphere using functional mapping, we believe this represents a pressing issue. This is particularly crucial considering the ample evidence that this hemisphere is specialized in social behaviour. As a role of the right hemisphere and the frontal lobe in general can be dated back to the dawn of psychosurgery [265], we believe that current evidence from DBS must be appraised also in resective surgery of these areas [268, 269], since mapping and preservation of these structures represent our current ethical responsibility to truly preserve not only patient's cognition, but personality and identity.

References

1. Molinaro AM, Taylor JW, Wiencke JK, Wrensch MR. Genetic and molecular epidemiology of adult diffuse glioma. Nat Rev Neurol. 2019;15(7):405–17. https://doi.org/10.1038/s41582-019-0220-2.
2. Duffau H. Long-term outcomes after supratotal resection of diffuse low-grade gliomas: a consecutive series with 11-year follow-up. Acta Neurochir. 2016;158(1):51–8. https://doi.org/10.1007/s00701-015-2621-3.

3. Jakola AS, Myrmel KS, Kloster R, et al. Comparison of a strategy favoring early surgical resection vs a strategy favoring watchful waiting in low-grade gliomas. JAMA J Am Med Assoc. 2012;308(18):1881–8. https://doi.org/10.1001/jama.2012.12807.
4. Bailey P, Cushing H. A classification of the tumors of the glioma group on a histogenetic basis with a correlated study of prognosis. Baltimore: Lippincott; 1926.
5. Wong ET, Hess KR, Gleason MJ, et al. Outcomes and prognostic factors in recurrent glioma patients enrolled onto phase II clinical trials. J Clin Oncol. 1999;17(8):2572.
6. Nazzaro JM, Neuwelt EA. The role of surgery in the management of supratentorial intermediate and high-grade astrocytomas in adults. J Neurosurg. 1990;73(3):331–44. https://doi.org/10.3171/jns.1990.73.3.0331.
7. Gulati S, Jakola AS, Nerland US, Weber C, Solheim O. The risk of getting worse: surgically acquired deficits, perioperative complications, and functional outcomes after primary resection of glioblastoma. World Neurosurg. 2011;76(6):572–9. https://doi.org/10.1016/j.wneu.2011.06.014.
8. Recht LD, Lew R, Smith TW. Suspected low-grade glioma: is deferring treatment safe? Ann Neurol. 1992;31(4):431–6. https://doi.org/10.1002/ana.410310413.
9. Reijneveld JC, Sitskoorn MM, Klein M, Nuyen J, Taphoorn MJB. Cognitive status and quality of life in patients with suspected versus proven low-grade gliomas. Neurology. 2001;56(5):618–23. https://doi.org/10.1212/WNL.56.5.618.
10. Lacroix M, Abi-Said D, Fourney DR, et al. A multivariate analysis of 416 patients with glioblastoma multiforme: prognosis, extent of resection, and survival. J Neurosurg. 2001;95(2):190–8. https://doi.org/10.3171/jns.2001.95.2.0190.
11. Capelle L, Fontaine D, Mandonnet E, et al. Spontaneous and therapeutic prognostic factors in adult hemispheric World Health Organization grade II gliomas: a series of 1097 cases. J Neurosurg. 2013a;118(6):1157–68. https://doi.org/10.3171/2013.1.JNS121.
12. Sanai N, Polley M-Y, McDermott MW, Parsa AT, Berger MS. An extent of resection threshold for newly diagnosed glioblastomas. J Neurosurg. 2011;115(1):3–8. https://doi.org/10.3171/2011.2.JNS10998.
13. Alcantara Llaguno S, Sun D, Pedraza AM, et al. Cell-of-origin susceptibility to glioblastoma formation declines with neural lineage restriction. Nat Neurosci. 2019;22(4):545–55. https://doi.org/10.1038/s41593-018-0333-8.
14. Sanai N, Alvarez-Buylla A, Berger MS. Neural stem cells and the origin of gliomas. N Engl J Med. 2005;353(8):811–22. https://doi.org/10.1056/nejmra043666.
15. Louis DN, Perry A, Reifenberger G, et al. The 2016 World Health Organization classification of tumors of the central nervous system: a summary. Acta Neuropathol. 2016;131(6):803–20. https://doi.org/10.1007/s00401-016-1545-1.
16. Wijnenga MMJ, French PJ, Dubbink HJ, et al. The impact of surgery in molecularly defined low-grade glioma: an integrated clinical, radiological, and molecular analysis. Neuro Oncol. 2018;20(1):103–12. https://doi.org/10.1093/neuonc/nox176.
17. Yordanova YN, Moritz-Gasser S, Duffau H. Awake surgery for WHO grade II gliomas within "noneloquent" areas in the left dominant hemisphere: toward a "supratotal" resection. J Neurosurg. 2011;115(2):232–9. https://doi.org/10.3171/2011.3.jns101333.
18. Pallud J, Varlet P, Devaux B, et al. Diffuse low-grade oligodendrogliomas extend beyond MRI-defined abnormalities. Neurology. 2010;74(21):1724–31. https://doi.org/10.1212/WNL.0b013e3181e04264.
19. Duffau H, Taillandier L. New concepts in the management of diffuse low-grade glioma: proposal of a multistage and individualized therapeutic approach. Neuro Oncol. 2015;17(3):332–42. https://doi.org/10.1093/neuonc/nou153.
20. Rossi M, Gay L, Ambrogi F, et al. Association of supratotal resection with progression-free survival, malignant transformation, and overall survival in lower-grade gliomas. Neuro Oncol. 2020;10:1–15. https://doi.org/10.1093/neuonc/noaa225.
21. De Witt Hamer PC, Robles SG, Zwinderman AH, Duffau H, Berger MS. Impact of intraoperative stimulation brain mapping on glioma surgery outcome: a meta-analysis. J Clin Oncol. 2012;30(20):2559–65. https://doi.org/10.1200/JCO.2011.38.4818.

22. Duffau H, Mandonnet E. The "onco-functional balance" in surgery for diffuse low-grade glioma: integrating the extent of resection with quality of life. Acta Neurochir. 2013;155(6):951–7. https://doi.org/10.1007/s00701-013-1653-9.
23. Darlix A, Rigau V, Fraisse J, Gozé C, Fabbro M, Duffau H. Postoperative follow-up for selected diffuse low-grade gliomas with WHO grade III/IV foci. Neurology. 2020;94(8):e830–41. https://doi.org/10.1212/WNL.0000000000008877.
24. Capelle L, Fontaine D, Mandonnet E, et al. Spontaneous and therapeutic prognostic factors in adult hemispheric World Health Organization grade II gliomas: a series of 1097 cases. J Neurosurg. 2013b;118(6):1157–68. https://doi.org/10.3171/2013.1.JNS121.
25. Attia A, Page BR, Lesser GJ, Chan M. Treatment of radiation-induced cognitive decline. Curr Treat Options Oncol. 2014;15(4):539–50. https://doi.org/10.1007/s11864-014-0307-3.
26. Poulen G, Gozé C, Rigau V, Duffau H. Huge heterogeneity in survival in a subset of adult patients with resected, wild-type isocitrate dehydrogenase status, WHO grade II astrocytomas. J Neurosurg. 2019;130(4):1289–98. https://doi.org/10.3171/2017.10.JNS171825.
27. Ferracci FX, Michaud K, Duffau H. The landscape of postsurgical recurrence patterns in diffuse low-grade gliomas. Crit Rev Oncol Hematol. 2019;138:148–55. https://doi.org/10.1016/j.critrevonc.2019.04.009.
28. Gall FJ, Spurzheim JC. Anatomie et physiologie, vol. 226. London: Wellcome Library; 1810.
29. Brodmann K. Feinere anatomie des Großhirns. In: Lewandowsky M, editor. Handbuch der neurologie. Erster Band. Allgemeine neurologie. Berlin: Springer; 1910.
30. Vogt C, Vogt O. Felderung der groghirnrinde unter beriicksichtigung den menschlichen. 1926.
31. Foerster O, Penfield W. The structural basis of traumatic epilepsy and results of radical operation. Brain. 1930;53(2):99–119. https://doi.org/10.1093/brain/53.2.99.
32. Talairach J, Bancaud J. The cingulate gyrus and human behaviour. Electroencephalogr Clin Neurophysiol. 1973;34(1):45–52.
33. Ebeling U, Schmid UD, Reulen HJ. Tumour-surgery within the central motor strip: surgical results with the aid of electrical motor cortex stimulation. Acta Neurochir. 1989;101(3–4):100–7. https://doi.org/10.1007/BF01410522.
34. Basser PJ, Mattiello J, LeBihan D. MR diffusion tensor spectroscopy and imaging. Biophys J. 1994;66(1):259–67. https://doi.org/10.1016/S0006-3495(94)80775-1.
35. Catani M. From hodology to function. Brain. 2007;130(3):602–5. https://doi.org/10.1093/brain/awm008.
36. De Benedictis A, Duffau H. Brain hodotopy: from esoteric concept to practical surgical applications. Neurosurgery. 2011;68(6):1709–23. https://doi.org/10.1227/NEU.0b013e3182124690.
37. Keles, G. Evren, Kathleen R. Lamborn, and Mitchel S. Berger. "Low-grade hemispheric gliomas in adults: a critical review of extent of resection as a factor influencing outcome." Journal of neurosurgery 95.5 (2001):735–45.
38. Duffau H, Capelle L, Denvil D, et al. Functional recovery after surgical resection of low grade gliomas in eloquent brain: hypothesis of brain compensation. J Neurol Neurosurg Psychiatry. 2003;74(7):901–7. https://doi.org/10.1136/jnnp.74.7.901.
39. Szelényi A, Senft C, Jardan M, et al. Intra-operative subcortical electrical stimulation: a comparison of two methods. Clin Neurophysiol. 2011;122(7):1470–5. https://doi.org/10.1016/j.clinph.2010.12.055.
40. Taniguchi M, Cedzich C, Schramm J. Modification of cortical stimulation for motor evoked potentials under general anesthesia: technical description. Neurosurgery. 1993;32(2):219–26. https://doi.org/10.1227/00006123-199302000-00011.
41. Tamaki T, Yamashita T, Kobayashi H, Hiryama H. Spinal cord evoked potential after stimulation to the spinal cord (SCEP). Spinal cord monitoring—basic data obtained from animal experimental studies (abstract in Japanese). Nouha to Kindennzu (Jpn J Electroenceph Electromyogr) 1972;1:196.
42. Szelényi A, Joksimovič B, Seifert V. Intraoperative risk of seizures associated with transient direct cortical stimulation in patients with symptomatic epilepsy. J Clin Neurophysiol. 2007;24(1):39–43. https://doi.org/10.1097/01.wnp.0000237073.70314.f7.

43. Matsumoto R, Nair DR, LaPresto E, et al. Functional connectivity in the human language system: a cortico-cortical evoked potential study. Brain. 2004;127(10):2316–30. https://doi.org/10.1093/brain/awh246.
44. Cattaneo L, Giampiccolo D, Meneghelli P, Tramontano V, Sala F. Cortico-cortical connectivity between the superior and inferior parietal lobules and the motor cortex assessed by intraoperative dual cortical stimulation. Brain Stimul. 2020;13(3):819–31. https://doi.org/10.1016/j.brs.2020.02.023.
45. Romero MC, Davare M, Armendariz M, Janssen P. Neural effects of transcranial magnetic stimulation at the single-cell level. Nat Commun. 2019;10(1):1–11. https://doi.org/10.1038/s41467-019-10638-7.
46. Ogawa S, Lee T-M, Kay AR, Tank DW. Brain magnetic resonance imaging with contrast dependent on blood oxygenation. Proc Natl Acad Sci. 1990;87(24):9868–72.
47. Castellano A, Cirillo S, Bello L, Riva M, Falini A. Functional MRI for surgery of gliomas. Curr Treat Options Neurol. 2017;19(10):1–23.
48. Silva MA, See AP, Essayed WI, Golby AJ, Tie Y. Challenges and techniques for presurgical brain mapping with functional MRI. NeuroImage Clin. 2018;17:794–803. https://doi.org/10.1016/j.nicl.2017.12.008.
49. Rigolo L, Essayed WI, TieY, Norton I, Mukundan Jr S, Golby A. Intraoperative use of functional MRI for surgical decision making after limited or infeasible electrocortical stimulation mapping. Journal of Neuroimaging. 2020;30(2):184–91.
50. Krueger G, Granziera C. The history and role of long duration stimulation in fMRI. Neuroimage. 2012;62(2):1051–5.
51. Liu TT. Neurovascular factors in resting-state functional MRI. Neuroimage. 2013;80:339–48.
52. Orringer DA, Golby A, Jolesz F. Neuronavigation in the surgical management of brain tumors: current and future trends. Expert Rev Med Devices. 2012;9(5):491–500.
53. Metwali H, Raemaekers M, Kniese K, Kardavani B, Fahlbusch R, Samii A. Reliability of functional magnetic resonance imaging in patients with brain tumors: a critical review and meta-analysis. World Neurosurg. 2019;125:183–90. https://doi.org/10.1016/j.wneu.2019.01.194.
54. Weng J-C, Chou Y-S, Huang G-J, Tyan Y-S, Ho M-C. Mapping brain functional alterations in betel-quid chewers using resting-state fMRI and network analysis. Psychopharmacology (Berl). 2018;235(4):1257–71.
55. Azad TD, Duffau H. Limitations of functional neuroimaging for patient selection and surgical planning in glioma surgery. Neurosurg Focus. 2020a;48(2):E12.
56. Giussani C, Roux FE, Ojemann J, Sganzerla EP, Pirillo D, Papagno C. Is preoperative functional magnetic resonance imaging reliable for language areas mapping in brain tumor surgery? Review of language functional magnetic resonance imaging and direct cortical stimulation correlation studies. Neurosurgery. 2010;66(1):113–20. https://doi.org/10.1227/01.NEU.0000360392.15450.C9.
57. Ghinda DC, Wu JS, Duncan NW, Northoff G. How much is enough—can resting state fMRI provide a demarcation for neurosurgical resection in glioma? Neurosci Biobehav Rev. 2018;84:245–61. https://doi.org/10.1016/j.neubiorev.2017.11.019.
58. Herbet G, Duffau H. Revisiting the functional anatomy of the human brain: toward a meta-networking theory of cerebral functions. Physiol Rev. 2020;100(3):1181–228. https://doi.org/10.1152/physrev.00033.2019.
59. Logothetis NK. What we can do and what we cannot do with fMRI. Nature. 2008;453(7197):869–78. https://doi.org/10.1038/nature06976.
60. Vakamudi K, Posse S, Jung R, Cushnyr B, Chohan MO. Real-time presurgical resting-state fMRI in patients with brain tumors: quality control and comparison with task-fMRI and intraoperative mapping. Hum Brain Mapp. 2020;41(3):797–814.
61. Catani M, Howard RJ, Pajevic S, Jones DK. Virtual in vivo interactive dissection of white matter fasciculi in the human brain. Neuroimage. 2002;17(1):77–94. https://doi.org/10.1006/nimg.2002.1136.
62. Sawaya R, Hammoud M, Schoppa D, et al. Neurosurgical outcomes in a modern series of 400 craniotomies for treatment of parenchymal tumors. Neurosurgery. 1998;42(5):1044–55.

63. Catani M, Mesulam M. The arcuate fasciculus and the disconnection theme in language and aphasia: history and current state. Cortex. 2008;44(8):953–61. https://doi.org/10.1016/j.cortex.2008.04.002.
64. Catani M, de Schotten T. Atlas of human brain connections. Oxford: Oxford University Press; 2012.
65. Azad TD, Duffau H. Limitations of functional neuroimaging for patient selection and surgical planning in glioma surgery. Neurosurg Focus. 2020b;48(2):E12. https://doi.org/10.3171/2019.11.FOCUS19769.
66. Maier-Hein KH, Neher PF, Houde JC, et al. The challenge of mapping the human connectome based on diffusion tractography. Nat Commun. 2017;8(1):1349. https://doi.org/10.1038/s41467-017-01285-x.
67. Schiavi S, Ocampo-Pineda M, Barakovic M, et al. A new method for accurate in vivo mapping of human brain connections using microstructural and anatomical information. Sci Adv. 2020;6(31):aba8245. https://doi.org/10.1126/sciadv.aba8245.
68. Jeurissen B, Leemans A, Tournier JD, Jones DK, Sijbers J. Investigating the prevalence of complex fiber configurations in white matter tissue with diffusion magnetic resonance imaging. Hum Brain Mapp. 2013;34(11):2747–66. https://doi.org/10.1002/hbm.22099.
69. Nimsky C, Ganslandt O, Cerny S, Hastreiter P, Greiner G, Fahlbusch R. Quantification of, visualization of, and compensation for brain shift using intraoperative magnetic resonance imaging. Neurosurgery. 2000;47(5):1070–80. https://doi.org/10.1097/00006123-200011000-00008.
70. Bello L, Gambini A, Castellano A, et al. Motor and language DTI fiber tracking combined with intraoperative subcortical mapping for surgical removal of gliomas. Neuroimage. 2008;39(1):369–82. https://doi.org/10.1016/j.neuroimage.2007.08.031.
71. Nossek E, Korn A, Shahar T, et al. Intraoperative mapping and monitoring of the corticospinal tracts with neurophysiological assessment and 3-dimensional ultrasonography-based navigation. J Neurosurg. 2011a;114(3):738–46. https://doi.org/10.3171/2010.8.JNS10639.
72. Caverzasi E, Hervey-Jumper SL, Jordan KM, et al. Identifying preoperative language tracts and predicting postoperative functional recovery using HARDI q-ball fiber tractography in patients with gliomas. J Neurosurg. 2016;125(1):33–45. https://doi.org/10.3171/2015.6.JNS142203.
73. Ille S, Sollmann N, Hauck T, et al. Combined noninvasive language mapping by navigated transcranial magnetic stimulation and functional MRI and its comparison with direct cortical stimulation. J Neurosurg. 2015;123(1):212–25. https://doi.org/10.3171/2014.9.JNS14929.
74. Rosenstock T, Giampiccolo D, Schneider H, et al. Specific DTI seeding and diffusivity-analysis improve the quality and prognostic value of TMS-based deterministic DTI of the pyramidal tract. NeuroImage Clin. 2017a;16:276–85. https://doi.org/10.1016/j.nicl.2017.08.010.
75. Sollmann N, Giglhuber K, Tussis L, Meyer B, Ringel F, Krieg SM. NTMS-based DTI fiber tracking for language pathways correlates with language function and aphasia—a case report. Clin Neurol Neurosurg. 2015a;136:25–8. https://doi.org/10.1016/j.clineuro.2015.05.023.
76. Barker AT, Jalinous R, Freeston IL. Non-invasive magnetic stimulation of human motor cortex. Lancet. 1985;1(8437):1106–7. https://doi.org/10.1016/s0140-6736(85)92413-4.
77. Day B, Dressler D, Maertens de Noorhout A, et al. Electric and magnetic stimulation of human motor. J Physiol. 1989;412:449–73. https://doi.org/10.1113/jphysiol.1989.sp017626.
78. Lefaucheur JP, Picht T. The value of preoperative functional cortical mapping using navigated TMS. Neurophysiol Clin. 2016;46(2):125–33. https://doi.org/10.1016/j.neucli.2016.05.001.
79. Epstein CM. Transcranial magnetic stimulation: language function. J Clin Neurophysiol. 1998;15(4):325–32.
80. Picht T, Mularski S, Kuehn B, Vajkoczy P, Kombos T, Suess O. Navigated transcranial magnetic stimulation for preoperative functional diagnostics in brain tumor surgery. Neurosurgery. 2009;65(6 Suppl. 1):93–8; discussion 98–9. https://doi.org/10.1227/01.NEU.0000348009.22750.59.
81. Ruohonen J, Karhu J. Navigated transcranial magnetic stimulation. Neurophysiol Clin/Clin Neurophysiol. 2010;40(1):7–17. https://doi.org/10.1016/j.neucli.2010.01.006.

82. Picht T, Schmidt S, Brandt S, et al. Preoperative functional mapping for rolandic brain tumor surgery: comparison of navigated transcranial magnetic stimulation to direct cortical stimulation. Neurosurgery. 2011;69(3):581–8. https://doi.org/10.1227/NEU.0b013e3182181b89.
83. Krieg SM, Lioumis P, Mäkelä JP, et al. Protocol for motor and language mapping by navigated TMS in patients and healthy volunteers; workshop report. Acta Neurochir. 2017;159(7):1187–95. https://doi.org/10.1007/s00701-017-3187-z.
84. Tarapore PE, Findlay AM, Honma SM, et al. Language mapping with navigated repetitive TMS: proof of technique and validation. Neuroimage. 2013;82:260–72. https://doi.org/10.1016/j.neuroimage.2013.05.018.
85. Weiss C, Nettekoven C, Rehme AK, et al. Mapping the hand, foot and face representations in the primary motor cortex—retest reliability of neuronavigated TMS versus functional MRI. Neuroimage. 2013;66:531–42. https://doi.org/10.1016/j.neuroimage.2012.10.046.
86. Rosenstock T, Grittner U, Acker G, Schwarzer V, Kulchytska N, Vajkoczy P, Picht T. Risk stratification in motor area-related glioma surgery based on navigated transcranial magnetic stimulation data. J Neurosurg. 2017b;126(4):1227–37.
87. Krieg SM, Sollmann N, Hauck T, Ille S, Meyer B, Ringel F. Repeated mapping of cortical language sites by preoperative navigated transcranial magnetic stimulation compared to repeated intraoperative DCS mapping in awake craniotomy. BMC Neurosci. 2014a;15:1. https://doi.org/10.1186/1471-2202-15-20.
88. Picht T, Krieg SM, Sollmann N, et al. A comparison of language mapping by preoperative navigated transcranial magnetic stimulation and direct cortical stimulation during awake surgery. Neurosurgery. 2013;72(5):808–19. https://doi.org/10.1227/NEU.0b013e3182889e01.
89. Epstein CM, Lah JJ, Meador K, Weissman JD, Gaitan LE, Dihenia B. Optimum stimulus parameters for lateralized suppression of speech with magnetic brain stimulation. Neurology. 1996;47(6):1590–93.
90. Wassermann EM. Risk and safety of repetitive transcranial magnetic stimulation: report and suggested guidelines from the International Workshop on the Safety of Repetitive Transcranial Magnetic Stimulation, June 5–7, 1996. Electroencephalogr Clin Neurophysiol. 1978;108:1–16. https://doi.org/10.1016/0306-4522(79)90146-5.
91. Giampiccolo D, Cattaneo L, Basaldella F, et al. Intraoperative neuromonitoring predicts motor recovery in a long-term hemiplegic patient with a Rolandic metastasis. Clin Neurophysiol. 2020a;131(9):2276–8.
92. Ille S, Sollmann N, Butenschoen VM, Meyer B, Ringel F, Krieg SM. Resection of highly language-eloquent brain lesions based purely on rTMS language mapping without awake surgery. Acta Neurochir. 2016;158(12):2265–75. https://doi.org/10.1007/s00701-016-2968-0.
93. Sanai N, Berger MS. Mapping the horizon: techniques to optimize tumor resection before and during surgery. Clin Neurosurg. 2008;55:14–9.
94. Bello L, Riva M, Fava E, et al. Tailoring neurophysiological strategies with clinical context enhances resection and safety and expands indications in gliomas involving motor pathways. Neuro Oncol. 2014;16(8):1110–28. https://doi.org/10.1093/neuonc/not327.
95. Raffa G, Bährend I, Schneider H, et al. A novel technique for region and linguistic specific nTMS-based DTI fiber tracking of language pathways in brain tumor patients. Front Neurosci. 2016;10:1–17. https://doi.org/10.3389/fnins.2016.00552.
96. Sollmann N, Ille S, Hauck T, et al. The impact of preoperative language mapping by repetitive navigated transcranial magnetic stimulation on the clinical course of brain tumor patients. BMC Cancer. 2015b;15(1):1–8. https://doi.org/10.1186/s12885-015-1299-5.
97. Negwer C, Sollmann N, Ille S, et al. Language pathway tracking: comparing nTMS-based DTI fiber tracking with a cubic ROIs-based protocol. J Neurosurg. 2017;126(3):1006–14. https://doi.org/10.3171/2016.2.JNS152382.
98. Giampiccolo D, Howells H, Bährend I, et al. Preoperative transcranial magnetic stimulation for picture naming is reliable in mapping segments of the arcuate fasciculus. Brain Commun. 2020b;2(2):1–15. https://doi.org/10.1093/braincomms/fcaa158.

99. Rofes A, Mandonnet E, Godden J, et al. Survey on current cognitive practices within the European low-grade glioma network: towards a European assessment protocol. Acta Neurochir. 2017;159(7):1167–78. https://doi.org/10.1007/s00701-017-3192-2.
100. Puglisi G, Howells H, Sciortino T, et al. Frontal pathways in cognitive control: direct evidence from intraoperative stimulation and diffusion tractography. Brain. 2019;142(8):2451–65. https://doi.org/10.1093/brain/awz178.
101. Mandonnet E, Sarubbo S, Duffau H. Proposal of an optimized strategy for intraoperative testing of speech and language during awake mapping. Neurosurg Rev. 2017;40(1):29–35. https://doi.org/10.1007/s10143-016-0723-x.
102. Hitzig E. Untersuchungen über das gehirn: abhandlungen physiologischen und pathologischen inhalts. Braunlage: A Hirschwald; 1874.
103. Rossi M, Conti Nibali M, Viganò L, et al. Resection of tumors within the primary motor cortex using high-frequency stimulation: oncological and functional efficiency of this versatile approach based on clinical conditions. J Neurosurg. 2019;133:642–54. https://doi.org/10.3171/2019.5.jns19453.
104. Agnew WF, McCreery DB. Considerations for safety in the use of extracranial stimulation for motor evoked potentials. Neurosurgery. 1987;20(1):143–7.
105. Boetto J, Bertram L, Moulinié G, Herbet G, Moritz-Gasser S, Duffau H. Electrocorticography is not necessary during awake brain surgery for gliomas. World Neurosurg. 2016;91:656–7. https://doi.org/10.1016/j.wneu.2016.03.030.
106. Riva M, Fava E, Gallucci M, et al. Monopolar high-frequency language mapping: can it help in the surgical management of gliomas? A comparative clinical study. J Neurosurg. 2016;124(5):1479–89. https://doi.org/10.3171/2015.4.JNS14333.
107. Giampiccolo D, Basaldella F, Badari A, Squintani GM, Cattaneo L, Sala F. Feasibility of cerebello–cortical stimulation for intraoperative neurophysiological monitoring of cerebellar mutism. Childs Nerv Syst. 2021a;37(5):1505–14.
108. Herbet G, Moritz-Gasser S, Lemaitre AL, Almairac F, Duffau H. Functional compensation of the left inferior longitudinal fasciculus for picture naming. Cogn Neuropsychol. 2019;36(3–4):140–57. https://doi.org/10.1080/02643294.2018.1477749.
109. Penfield W, Boldrey E. Somatic motor and sensory representation in the cerebral cortex of man as studied by electrical stimulation. Brain. 1937;60(4):389–443. https://doi.org/10.1093/brain/60.4.389.
110. Lohkamp LN, Mottolese C, Szathmari A, et al. Awake brain surgery in children—review of the literature and state-of-the-art. Childs Nerv Syst. 2019;35(11):2071–7. https://doi.org/10.1007/s00381-019-04279-w.
111. Deletis V, Rodi Z, Amassian VE. Neurophysiological mechanisms underlying motor evoked potentials in anesthetized humans. Part 2. Relationship between epidurally and muscle recorded MEPs in man. Clin Neurophysiol. 2001;112(3):445–52. https://doi.org/10.1016/S1388-2457(00)00557-5.
112. Rech F, Herbet G, Gaudeau Y, et al. A probabilistic map of negative motor areas of the upper limb and face: a brain stimulation study. Brain J Neurol. 2019;142(4):952–65. https://doi.org/10.1093/brain/awz021.
113. Viganò L, Fornia L, Rossi M, et al. Anatomo-functional characterisation of the human "hand-knob": a direct electrophysiological study. Cortex. 2018;113:239–54. https://doi.org/10.1016/j.cortex.2018.12.011.
114. Rech F, Herbet G, Moritz-Gasser S, Duffau H. Somatotopic organization of the white matter tracts underpinning motor control in humans: an electrical stimulation study. Brain Struct Funct. 2016;221(7):3743–53. https://doi.org/10.1007/s00429-015-1129-1.
115. Roth J, Korn A, Sala F, et al. Intraoperative neurophysiology in pediatric supratentorial surgery: experience with 57 cases. Childs Nerv Syst. 2020;36(2):315–24.
116. Cedzich C, Taniguchi M, Schäfer S, Schramm J. Somatosensory evoked potential phase reversal and direct motor cortex stimulation during surgery in and around the central region. Neurosurgery. 1996;38(5):962–70. https://doi.org/10.1097/00006123-199605000-00023.

117. Krieg SM, Schäffner M, Shiban E, et al. Reliability of intraoperative neurophysiological monitoring using motor evoked potentials during resection of metastases in motor-eloquent brain regions. J Neurosurg. 2013;118(6):1269–78. https://doi.org/10.3171/2013.2.JNS121752.
118. Giampiccolo D, Parisi C, Meneghelli P, et al. Long-term motor deficit in brain tumor surgery with preserved intraoperative motor evoked potentials. Brain Commun. 2021c;3:fcaa226. https://doi.org/10.1093/braincomms/fcaa226.
119. Neuloh G, Pechstein U, Schramm J. Motor tract monitoring during insular glioma surgery. J Neurosurg. 2007;106(4):582–92.
120. Gogos AJ, Young JS, Morshed RA, et al. Triple motor mapping: transcranial, bipolar, and monopolar mapping for supratentorial glioma resection adjacent to motor pathways. J Neurosurg. 2020;134:1728–37. https://doi.org/10.3171/2020.3.jns193434.
121. Deletis V, Camargo A. Transcranial electrical motor evoked potential monitoring for brain tumor resection. Neurosurgery. 2001;49(6):1488–9.
122. Zentner J, Hufnagel A, Pechstein U, Wolf HK, Schramm J. Functional results after resective procedures involving the supplementary motor area. J Neurosurg. 1996;85(4):542–9. https://doi.org/10.3171/jns.1996.85.4.0542.
123. Seidel K, Häni L, Lutz K, et al. Postoperative navigated transcranial magnetic stimulation to predict motor recovery after surgery of tumors located in motor eloquent areas. Neurosurgery. 2018;65(CN_suppl_1):124. https://doi.org/10.1093/neuros/nyy303.306.
124. Nossek E, Korn A, Shahar T, et al. Intraoperative mapping and monitoring of the corticospinal tracts with neurophysiological assessment and 3-dimensional ultrasonography-based navigation. J Neurosurg. 2011b;114(3):738–46. https://doi.org/10.3171/2010.8.jns10639.
125. Shiban E, Krieg SM, Haller B, et al. Intraoperative subcortical motor evoked potential stimulation: how close is the corticospinal tract? J Neurosurg. 2015b;123(3):711–20. https://doi.org/10.3171/2014.10.JNS141289.
126. Shiban E, Krieg SM, Obermueller T, Wostrack M, Meyer B, Ringel F. Continuous subcortical motor evoked potential stimulation using the tip of an ultrasonic aspirator for the resection of motor eloquent lesions. J Neurosurg. 2015a;123(2):301–6. https://doi.org/10.3171/2014.11.JNS141555.
127. Sala F, Manganotti P, Grossauer S, Tramontanto V, Mazza C, Gerosa M. Intraoperative neurophysiology of the motor system in children: a tailored approach. Childs Nerv Syst. 2010;26(4):473–90. https://doi.org/10.1007/s00381-009-1081-6.
128. Seidel K, Beck J, Stieglitz L, Schucht P, Raabe A. The warning-sign hierarchy between quantitative subcortical motor mapping and continuous motor evoked potential monitoring during resection of supratentorial brain tumors. J Neurosurg. 2013;118(2):287–96. https://doi.org/10.3171/2012.10.JNS12895.
129. Duffau H. Stimulation mapping of white matter tracts to study brain functional connectivity. Nat Rev Neurol. 2015;11(5):255–65.
130. Han SJ, Morshed RA, Troncon I, et al. Subcortical stimulation mapping of descending motor pathways for perirolandic gliomas: assessment of morbidity and functional outcome in 702 cases. J Neurosurg. 2018;131:201–8. https://doi.org/10.3171/2018.3.JNS172494.
131. Raabe A, Beck J, Schucht P, Seidel K. Continuous dynamic mapping of the corticospinal tract during surgery of motor eloquent brain tumors: evaluation of a new method. J Neurosurg. 2014;120(5):1015–24. https://doi.org/10.3171/2014.1.JNS13909.
132. Seidel K, Schucht P, Beck J, Raabe A. Continuous dynamic mapping to identify the corticospinal tract in motor eloquent brain tumors: an update. J Neurol Surg Pt A Cent Eur Neurosurg. 2020;81(02):105–10. https://doi.org/10.1055/s-0039-1698384.
133. Black PM, Ronner SF. Cortical mapping for defining the limits of tumor resection. Neurosurgery. 1987;20(6):914–9.
134. Keles GE, Lundin DA, Lamborn KR, Chang EF, Ojemann G, Berger MS. Intraoperative subcortical stimulation mapping for hemispheric perirolandic gliomas located within or adjacent to the descending motor pathways: evaluation of morbidity and assessment of functional outcome in 294 patients. J Neurosurg. 2004;100(3):369–75.

135. Sala F, Lanteri P. Brain surgery in motor areas: the invaluable assistance of intraoperative neurophysiological monitoring. J Neurosurg Sci. 2003;47(2):79–88.
136. Herbet G, Moritz-Gasser S, Boiseau M, Duvaux S, Cochereau J, Duffau H. Converging evidence for a cortico-subcortical network mediating lexical retrieval. Brain. 2016a;139(11):3007–21. https://doi.org/10.1093/brain/aww220.
137. Catani M, Dell'Acqua F, Vergani F, et al. Short frontal lobe connections of the human brain. Cortex. 2012;48(2):273–91. https://doi.org/10.1016/j.cortex.2011.12.001.
138. Magro E, Moreau T, Seizeur R, Gibaud B, Morandi X. Characterization of short white matter fiber bundles in the central area from diffusion tensor MRI. Neuroradiology. 2012;54(11):1275–85. https://doi.org/10.1007/s00234-012-1073-1.
139. Rossi M, Viganò L, Puglisi G, et al. Targeting primary motor cortex (M1) functional components in M1 gliomas enhances safe resection and reveals M1 plasticity potentials. Cancer. 2021;13(15):3808. https://doi.org/10.3390/cancers13153808.
140. Geyer S, Ledberg A, Schleicher A, et al. Two different areas within the primary motor cortex of man. Nature. 1996;382(6594):805–7. https://doi.org/10.1038/382805a0.
141. Fornia L, Rossi M, Rabuffetti M, et al. Direct electrical stimulation of premotor areas: different effects on hand muscle activity during object manipulation. Cereb Cortex. 2019;30(1):391–405. https://doi.org/10.1093/cercor/bhz139.
142. Rathelot J-A, Strick PL. Subdivisions of primary motor cortex based on cortico-motoneuronal cells. Proc Natl Acad Sci. 2009;106(3):918–23. https://doi.org/10.1073/pnas.0808362106.
143. Magill ST, Han SJ, Li J, Berger MS. Resection of primary motor cortex tumors: feasibility and surgical outcomes. J Neurosurg. 2018;129:61–972. https://doi.org/10.1097/SLA.0000000000001729.
144. Neuloh G, Pechstein U, Cedzich C, et al. Motor evoked potential monitoring with supratentorial surgery. Neurosurgery. 2004;54(5):1061–72. https://doi.org/10.1227/01.NEU.0000119326.15032.00.
145. Sala F, Krzan MJ, Jallo G, Epstein FJ, Deletis V. Prognostic value of motor evoked potentials elicited by multipulse magnetic stimulation in a surgically induced transitory lesion of the supplementary motor area: a case report. J Neurol Neurosurg Psychiatry. 2000;69(6):828–31. https://doi.org/10.1136/jnnp.69.6.828.
146. Cisek P, Kalaska JF. Neural mechanisms for interacting with a world full of action choices. Annu Rev Neurosci. 2010;33:269–98. https://doi.org/10.1146/annurev.neuro.051508.135409.
147. Rech F, Wassermann D, Duffau H. New insights into the neural foundations mediating movement/language interactions gained from intrasurgical direct electrostimulations. Brain Cogn. 2020;142:105583. https://doi.org/10.1016/j.bandc.2020.105583.
148. Jabarkheel R, Amayiri N, Yecies D, et al. Molecular correlates of cerebellar mutism syndrome in medulloblastoma. Neuro Oncol. 2020;22(2):290–7. https://doi.org/10.1093/neuonc/noz158.
149. Cisek P, Kalaska JF. Neural correlates of reaching decisions in dorsal premotor cortex: specification of multiple direction choices and final selection of action. Neuron. 2005;45(5):801–14. https://doi.org/10.1016/j.neuron.2005.01.027.
150. Thura D, Cisek P. Microstimulation of dorsal premotor and primary motor cortex delays the volitional commitment to an action choice. J Neurophysiol. 2020;123(3):927–35. https://doi.org/10.1152/jn.00682.2019.
151. Penfield W, Roberts L. The evidence from cortical mapping. In: Speech and brain mechanisms. Princeton: Princeton University Press; 1959.
152. Dick AS, Bernal B, Tremblay P. The language connectome: new pathways, new concepts. Neuroscientist. 2014;20(5):453–67. https://doi.org/10.1177/1073858413513502.
153. Hickok G, Poeppel D. The cortical organization of speech processing. Nat Rev Neurosci. 2007;8(5):393–402. https://doi.org/10.1038/nrn2113.
154. Duffau H, Gatignol P, Mandonnet E, Peruzzi P, Tzourio-Mazoyer N, Capelle L. New insights into the anatomo-functional connectivity of the semantic system: a study using cortico-subcortical electrostimulations. Brain. 2005;128(4):797–810. https://doi.org/10.1093/brain/awh423.

155. van Geemen K, Herbet G, Moritz-Gasser S, Duffau H. Limited plastic potential of the left ventral premotor cortex in speech articulation: evidence from intraoperative awake mapping in glioma patients. Hum Brain Mapp. 2014;35(4):1587–96. https://doi.org/10.1002/hbm.22275.
156. Duffau H, Moritz-Gasser S, Mandonnet E. A re-examination of neural basis of language processing: proposal of a dynamic hodotopical model from data provided by brain stimulation mapping during picture naming. Brain Lang. 2014;131:1–10. https://doi.org/10.1016/j.bandl.2013.05.011.
157. Gajardo-Vidal A, Lorca-Puls DL, Team P, et al. Damage to Broca's area does not contribute to long-term speech production outcome after stroke. Brain. 2021;144(3):817–32. https://doi.org/10.1093/brain/awaa460.
158. Tate MC, Herbet G, Moritz-Gasser S, Tate JE, Duffau H. Probabilistic map of critical functional regions of the human cerebral cortex: Broca's area revisited. Brain. 2014;137(10):2773–82. https://doi.org/10.1093/brain/awu168.
159. Lu J, Zhao Z, Zhang J, et al. Functional maps of direct electrical stimulation-induced speech arrest and anomia: a multicentre retrospective study. Brain. 2021;144(8):2541–53. https://doi.org/10.1093/brain/awab125.
160. Panesar SS, Yeh FC, Deibert CP, et al. A diffusion spectrum imaging-based tractographic study into the anatomical subdivision and cortical connectivity of the ventral external capsule: uncinate and inferior fronto-occipital fascicles. Neuroradiology. 2017;59(10):971–87. https://doi.org/10.1007/s00234-017-1874-3.
161. Sarubbo S, De Benedictis A, Merler S, et al. Structural and functional integration between dorsal and ventral language streams as revealed by blunt dissection and direct electrical stimulation. Hum Brain Mapp. 2016;37(11):3858–72. https://doi.org/10.1002/hbm.23281.
162. Vigneau M, Beaucousin V, Hervé PY, et al. Meta-analyzing left hemisphere language areas: phonology, semantics, and sentence processing. Neuroimage. 2006;30(4):1414–32. https://doi.org/10.1016/j.neuroimage.2005.11.002.
163. Yarkoni T, Poldrack RA, Nichols TE, Van Essen DC, Wager TD. Large-scale automated synthesis of human functional neuroimaging data. Nat Methods. 2011;8(8):665–70. https://doi.org/10.1038/nmeth.1635.
164. Sarubbo S, Tate M, de Benedictis A, Merler S, Herbet G, Duffau H. Mapping critical cortical hubs and white matter pathways by direct electrical stimulation: an original functional atlas of the human brain. Neuroimage. 2019;205:116237. https://doi.org/10.1016/j.neuroimage.2019.116237.
165. Moritz-Gasser S, Duffau H. The anatomo-functional connectivity of word repetition: insights provided by awake brain tumor surgery. Front Hum Neurosci. 2013;7:1–4. https://doi.org/10.3389/fnhum.2013.00405.
166. Simonyan K, Ackermann H, Chang EF, Greenlee JD. New developments in understanding the complexity of human speech production. J Neurosci. 2016;36(45):11440–8. https://doi.org/10.1523/JNEUROSCI.2424-16.2016.
167. Simonyan K, Horwitz B. Laryngeal motor cortex and control of speech in humans. Neuroscientist. 2011;17(2):197–208. https://doi.org/10.1177/1073858410386727.
168. Breshears JD, Molinaro AM, Chang EF. A probabilistic map of the human ventral sensorimotor cortex using electrical stimulation. J Neurosurg. 2015;123(2):340–9.
169. Bouchard KE, Mesgarani N, Johnson K, Chang EF. Functional organization of human sensorimotor cortex for speech articulation. Nature. 2013;495(7441):327–32. https://doi.org/10.1038/nature11911.
170. Jürgens U. Neural pathways underlying vocal control. Neurosci Biobehav Rev. 2002;26(2):235–58. https://doi.org/10.1016/S0149-7634(01)00068-9.
171. Kumar V, Croxson PL, Simonyan K. Structural organization of the laryngeal motor cortical network and its implication for evolution of speech production. J Neurosci. 2016;36(15):4170–81. https://doi.org/10.1523/JNEUROSCI.3914-15.2016.
172. Fontaine D, Capelle L, Duffau H. Somatotopy of the supplementary motor area: evidence from correlation of the extent of surgical resection with the clinical patterns of deficit. Neurosurgery. 2002;50(2):297–305.

173. Sarubbo S, de Benedictis A, Maldonado IL, Basso G, Duffau H. Frontal terminations for the inferior fronto-occipital fascicle: anatomical dissection, DTI study and functional considerations on a multi-component bundle. Brain Struct Funct. 2013;218(1):21–37. https://doi.org/10.1007/s00429-011-0372-3.
174. Herbet G, Moritz-Gasser S, Duffau H. Electrical stimulation of the dorsolateral prefrontal cortex impairs semantic cognition. Neurology. 2018;90(12):e1077–84. https://doi.org/10.1212/WNL.0000000000005174.
175. Roux A, Lemaitre AL, Deverdun J, Ng S, Duffau H, Herbet G. Combining electrostimulation with fiber tracking to stratify the inferior fronto-occipital fasciculus. Front Neurosci. 2021;15:683348. https://doi.org/10.3389/fnins.2021.683348.
176. Moritz-Gasser S, Herbet G, Duffau H. Mapping the connectivity underlying multimodal (verbal and non-verbal) semantic processing: a brain electrostimulation study. Neuropsychologia. 2013;51(10):1814–22. https://doi.org/10.1016/j.neuropsychologia.2013.06.007.
177. Lambon Ralph M, Jefferies E, Patterson K, Rogers TT. The neural and computational bases of semantic cognition. Nat Rev Neurosci. 2016;18(1):42–55. https://doi.org/10.1038/nrn.2016.150.
178. Herbet G, Maheu M, Costi E, Lafargue G, Duffau H. Mapping neuroplastic potential in brain-damaged patients. Brain. 2016b;139(3):829–44. https://doi.org/10.1093/brain/awv394.
179. Epelbaum S, Pinel P, Gaillard R, et al. Pure alexia as a disconnection syndrome: new diffusion imaging evidence for an old concept. Cortex. 2008;44(8):962–74. https://doi.org/10.1016/j.cortex.2008.05.003.
180. Cohen L, Lehéricy S, Chochon F, Lemer C, Rivaud S, Dehaene S. Language-specific tuning of visual cortex? Functional properties of the visual word form area. Brain. 2002;125(5):1054–69. https://doi.org/10.1093/brain/awf094.
181. Zemmoura I, Herbet G, Moritz-Gasser S, Duffau H. New insights into the neural network mediating reading processes provided by cortico-subcortical electrical mapping. Hum Brain Mapp. 2015;36(6):2215–30. https://doi.org/10.1002/hbm.22766.
182. Mesulam MM, Thompson CK, Weintraub S, Rogalski EJ. The Wernicke conundrum and the anatomy of language comprehension in primary progressive aphasia. Brain. 2015;138(8):2423–37. https://doi.org/10.1093/brain/awv154.
183. Wernicke C. Der Aphasische Symptomen complex. Eine Psychologische Studie Auf Anatomischer Basis. [The aphasia symptom complex. A psychological study on an anatomical basis]. Arch Neurol. 1874;22(3):280–2.
184. Chang EF, Breshears JD, Raygor KP, Lau D, Molinaro AM, Berger MS. Stereotactic probability and variability of speech arrest and anomia sites during stimulation mapping of the language dominant hemisphere. J Neurosurg. 2017;126(1):114–21.
185. Sanai N, Mirzadeh Z, Berger MS. Functional outcome after language mapping for glioma resection. N Engl J Med. 2008;358(1):18–27. https://doi.org/10.1056/nejmoa067819.
186. Lüders H, Lesser RP, Hahn J, et al. Basal temporal language area. Brain. 1991;114(2):743–54. https://doi.org/10.1093/brain/114.2.743.
187. Hamilton LS, Oganian Y, Chang EF. Topography of speech-related acoustic and phonological feature encoding throughout the human core and parabelt auditory cortex. bioRxiv. 2020. https://doi.org/10.1101/2020.06.08.121624.
188. Mesgarani N, Cheung C, Johnson K, Chang EF. Phonetic feature encoding in human superior temporal gyrus. Science. 2014;343(6174):1006–10. https://doi.org/10.1126/science.1245994.
189. Scott SK. From speech and talkers to the social world: the neural processing of human spoken language. Science. 2019;366(6461):58–62. https://doi.org/10.1126/science.aax0288.
190. Kyle J, Lima CF, Scott SK. "Understanding rostral–caudal auditory cortex contributions to auditory perception." Nature Reviews Neuroscience. 2019;20.7:425–34.
191. Binder JR, Tong JQ, Pillay SB, et al. Temporal lobe regions essential for preserved picture naming after left temporal epilepsy surgery. Epilepsia. 2020;61(9):1939–48. https://doi.org/10.1111/epi.16643.
192. Dejerine J, Dejerine J, Dejerine-Klumpke A. Anatomie des centres nerveux, vol. 1. Paris: Rueff; 1895.

193. Di Carlo DT, Benedetto N, Duffau H, et al. Microsurgical anatomy of the sagittal stratum. Acta Neurochir. 2019;161(11):2319–27. https://doi.org/10.1007/s00701-019-04019-8.
194. Berro DH, Herbet G, Duffau H. New insights into the anatomo-functional architecture of the right sagittal stratum and its surrounding pathways: an axonal electrostimulation mapping study. Brain Struct Funct. 2021;226(2):425–41. https://doi.org/10.1007/s00429-020-02186-4.
195. Fridriksson J, Guo D, Fillmore P, Holland A, Rorden C. Damage to the anterior arcuate fasciculus predicts non-fluent speech production in aphasia. Brain. 2013;136(11):3451–60. https://doi.org/10.1093/brain/awt267.
196. Hula WD, Panesar S, Gravier ML, et al. Structural white matter connectometry of word production in aphasia: an observational study. Brain. 2020;143(8):2532–44. https://doi.org/10.1093/brain/awaa193.
197. Saur D, Kreher BW, Schnell S, et al. Ventral and dorsal pathways for language. Proc Natl Acad Sci. 2008;105(46):18035–40. https://doi.org/10.1073/pnas.0805234105.
198. Benzagmout M, Gatignol P, Duffau H. Resection of World Health Organization grade II glioma involving Broca's area: methodological and functional considerations. Neurosurgery. 2007;61(4):741–53. https://doi.org/10.1227/01.NEU.0000280069.13468.B2.
199. Duffau H. The error of Broca: from the traditional localizationist concept to a connectomal anatomy of human brain. J Chem Neuroanat. 2018;89:73–81. https://doi.org/10.1016/j.jchemneu.2017.04.003.
200. Brodmann K. Vergleichende Lokalisationslehre der Grosshirnrinde in ihren Prinzipien dargestellt auf Grund des Zellenbaues. Barth. 1909.
201. Amunts K, Zilles K. Architectonic mapping of the human brain beyond Brodmann. Neuron. 2015;88(6):1086–107.
202. Glasser MF, Coalson TS, Robinson EC, et al. A multi-modal parcellation of human cerebral cortex. Nature. 2016;536(7615):171–8. https://doi.org/10.1038/nature18933.
203. Borra E, Gerbella M, Rozzi S, Luppino G. The macaque lateral grasping network: a neural substrate for generating purposeful hand actions. Neurosci Biobehav Rev. 2017;75:65–90. https://doi.org/10.1016/j.neubiorev.2017.01.017.
204. Bizzi A, Nava S, Ferrè F, et al. Aphasia induced by gliomas growing in the ventrolateral frontal region: assessment with diffusion MR tractography, functional MR imaging and neuropsychology. Cortex. 2012;48(2):255–72. https://doi.org/10.1016/j.cortex.2011.11.015.
205. Viganò L, Howells H, Fornia L, et al. Negative motor responses to direct electrical stimulation: behavioral assessment hides different effects on muscles. Cortex. 2021;137:194–204. https://doi.org/10.1016/j.cortex.2021.01.005.
206. Aron AR, Behrens TE, Smith S, Frank MJ, Poldrack RA. Triangulating a cognitive control network using diffusion-weighted magnetic resonance imaging (MRI) and functional MRI. J Neurosci. 2007;27(14):3743–52. https://doi.org/10.1523/JNEUROSCI.0519-07.2007.
207. Borra E, Rizzo M, Gerbella M, Rozzi S, Luppino G. Laminar origin of corticostriatal projections to the motor putamen in the macaque brain. J Neurosci. 2021;41(7):1455–69. https://doi.org/10.1523/JNEUROSCI.1475-20.2020.
208. Petersen MV, Mlakar J, Haber SN, et al. Holographic reconstruction of axonal pathways in the human brain. Neuron. 2019;104(6):1056–64. https://doi.org/10.1016/j.neuron.2019.09.030.
209. Mandonnet E, Herbet G, Moritz-Gasser S, Poisson I, Rheault F, Duffau H. Electrically induced verbal perseveration: a striatal deafferentation model. Neurology. 2019;92(6):e613–21. https://doi.org/10.1212/WNL.0000000000006880.
210. Herbet G, Moritz-Gasser S, Duffau H. Direct evidence for the contributive role of the right inferior fronto-occipital fasciculus in non-verbal semantic cognition. Brain Struct Funct. 2017;222(4):1597–610. https://doi.org/10.1007/s00429-016-1294-x.
211. De Benedictis A, Duffau H, Paradiso B, et al. Anatomo-functional study of the temporo-parieto-occipital region: dissection, tractographic and brain mapping evidence from a neurosurgical perspective. J Anat. 2014;225(2):132–51. https://doi.org/10.1111/joa.12204.

212. Yagmurlu K, Middlebrooks EH, Tanriover N, Rhoton AL. Fiber tracts of the dorsal language stream in the human brain. J Neurosurg. 2016;124(5):1396–405. https://doi.org/10.3171/2015.5.JNS15455.
213. Martino J, Brogna C, Robles SG, Vergani F, Duffau H. Anatomic dissection of the inferior fronto-occipital fasciculus revisited in the lights of brain stimulation data. Cortex. 2010;46(5):691–9. https://doi.org/10.1016/j.cortex.2009.07.015.
214. Gallentine WB, Mikati MA. Intraoperative electrocorticography and cortical stimulation in children. J Clin Neurophysiol. 2009;26(2):95–108. https://doi.org/10.1097/WNP.0b013e3181a0339d.
215. Keller CJ, Bickel S, Entz L, et al. Intrinsic functional architecture predicts electrically evoked responses in the human brain. Proc Natl Acad Sci U S A. 2011;108(25):10308–13. https://doi.org/10.1073/pnas.1019750108.
216. Valentin A. Responses to single pulse electrical stimulation identify epileptogenesis in the human brain in vivo. Brain. 2002;125(8):1709–18. https://doi.org/10.1093/brain/awf187.
217. Kunieda T, Yamao Y, Kikuchi T, Matsumoto R. New approach for exploring cerebral functional connectivity: review of cortico-cortical evoked potential. Neurol Med Chir. 2015;55(5):374–82. https://doi.org/10.2176/nmc.ra.2014-0388.
218. Boyer A, Duffau H, Mandonnet E, et al. Attenuation and delay of remote potentials evoked by direct electrical stimulation during brain surgery. Brain Topogr. 2020;33(1):143–8. https://doi.org/10.1007/s10548-019-00732-w.
219. Vincent MA, Bonnetblanc F, Mandonnet E, Boyer A, Duffau H, Guiraud D. Measuring the electrophysiological effects of direct electrical stimulation after awake brain surgery. J Neural Eng. 2020;17(1):1–37. https://doi.org/10.1088/1741-2552/ab5cdd.
220. Yamao Y, Matsumoto R, Kunieda T, et al. Intraoperative dorsal language network mapping by using single-pulse electrical stimulation. Hum Brain Mapp. 2014;35(9):4345–61. https://doi.org/10.1002/hbm.22479.
221. Yamao Y, Suzuki K, Kunieda T, et al. Clinical impact of intraoperative CCEP monitoring in evaluating the dorsal language white matter pathway. Hum Brain Mapp. 2017;38(4):1977–91. https://doi.org/10.1002/hbm.23498.
222. Giampiccolo D, Parmigiani S, Basaldella F, et al. Recording cortico-cortical evoked potentials of the human arcuate fasciculus under general anaesthesia. Clin Neurophysiol. 2021b;132:1966–73. https://doi.org/10.1016/j.clinph.2021.03.044.
223. Mariani V, Sartori I, Revay M, et al. Intraoperative corticocortical evoked potentials for language monitoring in epilepsy surgery. World Neurosurg. 2021;151:e109–21.
224. Suzuki Y, Enatsu R, Kanno A, et al. The influence of anesthesia on corticocortical evoked potential monitoring network between frontal and temporoparietal cortices. World Neurosurg. 2019;123:e685–92. https://doi.org/10.1016/j.wneu.2018.11.253.
225. Saito T, Tamura M, Muragaki Y, et al. Intraoperative cortico-cortical evoked potentials for the evaluation of language function during brain tumor resection: initial experience with 13 cases. J Neurosurg. 2014;121(4):827–38. https://doi.org/10.3171/2014.4.JNS131195.
226. Yamao Y, Matsumoto R, Kunieda T, et al. Effects of propofol on cortico-cortical evoked potentials in the dorsal language white matter pathway. Clin Neurophysiol. 2021;132(8):1919–26. https://doi.org/10.1016/j.clinph.2021.04.021.
227. Duffau H. Lessons from brain mapping in surgery for low-grade glioma: insights into associations between tumour and brain plasticity. Lancet Neurol. 2005;4(8):476–86. https://doi.org/10.1016/S1474-4422(05)70140-X.
228. Thiebaut de Schotten M, Foulon C, Nachev P. Brain disconnections link structural connectivity with function and behaviour. Nat Commun. 2020;11(1):1. https://doi.org/10.1038/s41467-020-18920-9.
229. Nudo RJ, Wise BM, SiFuentes F, Milliken GW. Neural substrates for the effect of rehabilitative training on motor recovery after ischaemic stroke. Science. 1996;21(5269):1791–4.
230. Duffau H. Can non-invasive brain stimulation be considered to facilitate reoperation for low-grade glioma relapse by eliciting neuroplasticity? Front Neurol. 2020;11:1–5. https://doi.org/10.3389/fneur.2020.582489.

231. Duffau H. A two-level model of interindividual anatomo-functional variability of the brain and its implications for neurosurgery. Cortex. 2017;86:303–13. https://doi.org/10.1016/j.cortex.2015.12.009.
232. Mesulam MM. From sensation to cognition. Brain. 1998;121(6):1013–52.
233. Burt JB, Demirtaş M, Eckner WJ, et al. Hierarchy of transcriptomic specialization across human cortex captured by structural neuroimaging topography. Nat Neurosci. 2018;21(9):1251–9.
234. Xu T, Nenning K-H, Schwartz E, et al. Cross-species functional alignment reveals evolutionary hierarchy within the connectome. Neuroimage. 2020;223:117346.
235. Sydnor VJ, Larsen B, Bassett DS, et al. Neurodevelopment of the association cortices: patterns, mechanisms, and implications for psychopathology. Neuron. 2021;109(18):2820–46.
236. Margulies DS, Ghosh SS, Goulas A, et al. Situating the default-mode network along a principal gradient of macroscale cortical organization. Proc Natl Acad Sci. 2016;113(44):12574–9.
237. Picart T, Herbet G, Moritz-Gasser S, Duffau H. Iterative surgical resections of diffuse glioma with awake mapping: how to deal with cortical plasticity and connectomal constraints? Clin Neurosurg. 2019;85(1):105–16.
238. Martino J, Taillandier L, Moritz-Gasser S, Gatignol P, Duffau H. Re-operation is a safe and effective therapeutic strategy in recurrent WHO grade II gliomas within eloquent areas. Acta Neurochir. 2009;151(5):427–36. https://doi.org/10.1007/s00701-009-0232-6.
239. Krieg SM, Tarapore PE, Picht T, et al. Optimal timing of pulse onset for language mapping with navigated repetitive transcranial magnetic stimulation. Neuroimage. 2014b;100:219–36. https://doi.org/10.1016/j.neuroimage.2014.06.016.
240. Mishkin M, Ungerleider LG, Macko KA. Object vision and spatial vision: two cortical pathways. Trends Neurosci. 1983;6(C):414–7. https://doi.org/10.1016/0166-2236(83)90190-X.
241. Pitcher D, Ungerleider LG. Evidence for a third visual pathway specialized for social perception. Trends Cogn Sci. 2021;25(2):100–10. https://doi.org/10.1016/j.tics.2020.11.006.
242. Southwell DG, Hervey-Jumper SL, Perry DW, Berger MS. Intraoperative mapping during repeat awake craniotomy reveals the functional plasticity of adult cortex. J Neurosurg. 2016;124(5):1460–9. https://doi.org/10.3171/2015.5.JNS142833.
243. Krieg SM, Shiban E, Droese D, et al. Predictive value and safety of intraoperative neurophysiological monitoring with motor evoked potentials in glioma surgery. Neurosurgery. 2012;70(5):1060–70. https://doi.org/10.1227/NEU.0b013e31823f5ade.
244. Szalisznyo K, Silverstein DN, Duffau H, Smits A. Pathological neural attractor dynamics in slowly growing gliomas supports an optimal time frame for white matter plasticity. PLoS One. 2013;8(7):e69798. https://doi.org/10.1371/journal.pone.0069798.
245. Rossi S, Rossini PM. TMS in cognitive plasticity and the potential for rehabilitation. Trends Cogn Sci. 2004;8(6):273–9. https://doi.org/10.1016/j.tics.2004.04.012.
246. Jung J, Lambon Ralph MA. Braunlage enhancing vs inhibiting semantic performance with transcranial magnetic stimulation over the anterior temporal lobe: frequency- and task-specific effects. Neuroimage. 2021;234:117959. https://doi.org/10.1016/j.neuroimage.2021.117959.
247. Rivera-Rivera PA, Rios-Lago M, Sanchez-Casarrubios S, et al. Cortical plasticity catalyzed by prehabilitation enables extensive resection of brain tumors in eloquent areas. J Neurosurg. 2017;126(4):1323–33. https://doi.org/10.3171/2016.2.JNS152485.
248. Salo J, Niemelä A, Joukamaa M, Koivukangas J. Effect of brain tumour laterality on patients' perceived quality of life. J Neurol Neurosurg Psychiatry. 2002;72(3):373–7. https://doi.org/10.1136/jnnp.72.3.373.
249. Osoba D, Aaronson NK, Muller M, et al. The development and psychometric validation of a brain cancer quality-of-life questionnaire for use in combination with general cancer-specific questionnaires. Qual Life Res. 1996;5(1):139–50. https://doi.org/10.1007/BF00435979.
250. Corbetta M, Shulman GL. Control of goal-directed and stimulus-driven attention in the brain. Nat Rev Neurosci. 2002;3(3):201–15. https://doi.org/10.1038/nrn755.
251. Aron AR. The neural basis of inhibition in cognitive control. Neuroscientist. 2007;13(3):214–28. https://doi.org/10.1177/1073858407299288.
252. Etkin A, Egner T, Kalisch R. Emotional processing in anterior cingulate and medial prefrontal cortex. Trends Cogn Sci. 2011;15(2):85–93. https://doi.org/10.1016/j.tics.2010.11.004.

253. Puce A, Perrett D. Electrophysiology and brain imaging of biological motion. Philos Trans R Soc B Biol Sci. 2003;358(1431):435–45. https://doi.org/10.1098/rstb.2002.1221.
254. Adolphs R. The neurobiology of social cognition. Curr Opin Neurobiol. 2001;11(2):231–9.
255. Hendriks EJ, Habets EJJ, Taphoorn MJB, et al. Linking late cognitive outcome with glioma surgery location using resection cavity maps. Hum Brain Mapp. 2018;39(5):2064–74. https://doi.org/10.1002/hbm.23986.
256. Cisek P. Resynthesizing behavior through phylogenetic refinement. Atten Percept Psychophys. 2019;81(7):2265–87. https://doi.org/10.3758/s13414-019-01760-1.
257. Shine JM. The thalamus integrates the macrosystems of the brain to facilitate complex, adaptive brain network dynamics. Prog Neurobiol. 2021;199:101951. https://doi.org/10.1016/j.pneurobio.2020.101951.
258. Cochereau J, Lemaitre AL, Wager M, Moritz-Gasser S, Duffau H, Herbet G. Network-behavior mapping of lasting executive impairments after low-grade glioma surgery. Brain Struct Funct. 2020;225(8):2415–29. https://doi.org/10.1007/s00429-020-02131-5.
259. Li N, Baldermann JC, Kibleur A, et al. Stimulation in obsessive–compulsive disorder. Nat Commun. 2020; https://doi.org/10.1038/s41467-020-16734-3.
260. Baldermann JC, Schüller T, Kohl S, et al. Connectomic deep brain stimulation for obsessive–compulsive disorder. Biol Psychiatry. 2021;90(10):678–88.
261. Duffau H, Capelle L, Sichez N, et al. Intraoperative mapping of the subcortical language pathways using direct stimulations. An anatomo-functional study. Brain. 2002;125(1):199–214. https://doi.org/10.1093/brain/awf016.
262. Robles SG, Gatignol P, Capelle L, Mitchell MC, Duffau H. The role of dominant striatum in language: a study using intraoperative electrical stimulations. J Neurol Neurosurg Psychiatry. 2005;76(7):940–6. https://doi.org/10.1136/jnnp.2004.045948.
263. Mayberg HS, Lozano AM, Voon V, et al. Deep brain stimulation for treatment-resistant depression. Neuron. 2005;45(5):651–60. https://doi.org/10.1016/j.neuron.2005.02.014.
264. Schlaepfer TE, Bewernick BH, Kayser S, Hurlemann R, Coenen VA. Deep brain stimulation of the human reward system for major depression—rationale, outcomes and outlook. Neuropsychopharmacology. 2014;39(6):1303–14. https://doi.org/10.1038/npp.2014.28.
265. Moniz E. Prefrontal leucotomy in the treatment of mental disorders. Am J Psychiatry. 1937;93(6):1379–85.
266. Sala F, Giampiccolo D, Cattaneo L. Novel asleep techniques for intraoperative assessment of brain connectivity. Frontiers in Neurology. 2021;12.
267. Boetto J, Ng S, Duffau H. Predictive evolution factors of incidentally discovered suspected low-grade gliomas: results from a consecutive series of 101 patients. Neurosurgery. 2020;88(4):1–7. https://doi.org/10.1093/neuros/nyaa532.
268. Haber SN, Yendiki A, Jbabdi S. Four deep brain stimulation targets for obsessive–compulsive disorder: are they different? Biol Psychiatry. 2020;90:667. https://doi.org/10.1016/j.biopsych.2020.06.031.
269. Lemaitre A-L, Herbet G, Duffau H, Lafargue G. Personality and behavioral changes after brain tumor resection: a lesion mapping study. Acta Neurochir. 2021;163(5):1257–67. https://doi.org/10.1007/s00701-021-04756-9.

Chapter 3
Craniopharyngiomas: Surgery and Radiotherapy

Sergey Gorelyshev, Alexander N. Savateev, Nadezhda Mazerkina, Olga Medvedeva, and Alexander N. Konovalov

Cranipharyngiomas offer the most baffling problem which confronts the neurosurgeon (H. Cushing, 1932)

Craniopharyngioma still remains a frustrating and disappointing lesion because of its inaccessibility (D. Matson, 1969)

To this day the surgical management of craniopharyngiomas remains a challenging experience to every neurologic surgeon (R. Rand, 1985)

There is perhaps no other primary brain tumor that evokes more passion, emotion, and, as a result, controversy than does the craniopharyngioma (James T. Ruthka, 2002)

Current treatment strategies are debated, ranging from radical surgical strategies … to limited surgical approaches … focused on quality of life (Stephanie Puget, 2019)

Ninety years have passed, but the craniopharyngioma is still an unsolved problem…

3.1 Introduction

Craniopharyngiomas are rare histologically benign embryonic neoplasms of the sellar/parasellar region that represent 0.5–2.5 cases per one million, that is, 2–5% of all primary brain tumors in adults [1] and 5.6–13% in children [2]. Most often,

S. Gorelyshev (✉) · N. Mazerkina · O. Medvedeva · A. N. Konovalov
Federal State Autonomous Institution (N. N. Burdenko National Medical Research Center of Neurosurgery) of the Ministry of Health of the Russian Federation, Moscow, Russia
e-mail: SGorel@nsi.ru

A. N. Savateev
Moscow Gamma-Knife Center, Moscow, Russia

C. Di Rocco (ed.), *Advances and Technical Standards in Neurosurgery*, Advances and Technical Standards in Neurosurgery 45,
https://doi.org/10.1007/978-3-030-99166-1_3

craniopharyngiomas appear in the age groups of 5–14 years and 50–74 years [3]. These tumors form the largest group of non-glial tumors in children. CP contribute to up to 56% all tumors of the chiasmo-sellar region in children [2]. In 2011, Nielsen et al. performed a meta-analysis of 15 epidemiological studies of CP (with total of 1232 patients). According to these data, the incidence was 1.34 (1.24–1.46) per one million people and 1.44 (1.33–1.56) per one million children [4].

3.2 Our Experience

During last 40 years, more than 2000 patients with craniopharyngiomas were operated in the National Burdenko Neurosurgical Center (Moscow).

Since 2005 till 2015, more than 350 children (0–18 years) with craniopharyngiomas were operated and more than 200 patients have been treated in the Department of Radiotherapy and Radiosurgery. From April 2009 to January 2015, 68 patients were irradiated with the CyberKnife.

For the comparative analysis of the treatment results of surgery and radiotherapy, 155 patients with known follow-up (mediana = 7.1 years), endocrinological, ophthalmological, quality of life investigations performed before and after surgery, MRI before, after treatment, and during follow-up were analyzed. Two hundred and ten surgical procedures including transcranial microsurgery (135), endonasal endoscopy (65), and Ommaya reservoir (10) were done. Radiotherapy was performed in 75 patients in this group.

The majority of transcranial surgery was performed by the first author.

3.3 Embriology

CPs develop from the embryonic remnants of the craniopharyngeal duct (Rathke's pouch), connecting primary digestive tract and hypophysis during the process of pituitary gland formation. Stem cells deposited along its migratory path play a crucial role in CP formation [5].

3.4 Biology

There are two histological types of CP: adamantinomatous and papillary. Adamantinomatous CP are diagnosed both in children and adults (with two peaks 4–14 years and 40–65 years), while papillary CP are found only in adult age (50–60 years old).

Papillary craniopharyngiomas. Papillary CP usually harbor somatic BRAF V600E mutations. These tumors are composed of solid sheets of well-differentiated

squamous epithelial cells interrupted by cores of fibro-vascular stroma. Keratinization and calcification are usually absent. Tumors are generally encapsulated and separated from surrounding brain tissue and are typically solid.

Adamantinomatous craniopharyngiomas. Adamantinomatous CP are driven by somatic mutations in CTNNB1 (which encodes β-catenin) and drastically improve β-catenin stability (Fig. 3.1b). Tumors consist of epithelial lobules. Cells at the periphery are palisaded, whereas internally situated cells are loosely textured ("stellate" reticulum). Extensive keratinization and calcification are common. Tumors are locally invasive with glial "pseudocapsule" and are predominantly cystic.

Recently, we performed whole exome sequencing (WES) in two half-sisters with adamantinomatous craniopharyngioma-produced evidence for the APC gene dysfunction as a novel tumorigenic driver in adamantinomatous CP (Fig. 3.1c). CTNNB1 remained intact, while the disruption of both APC alleles in the tumor strongly suggested the role of a second hit event [6].

Glial capsule of craniopharyngioma. Tumor cells may penetrate into surrounding brain tissue of thalamus and hypothalamus. Gliotic reactive tissue at the tumor boarder may facilitate the resection, but on the other hand provide false impression of a gross total removal (Fig. 3.2).

High expression of GHR (growth hormone receptor) is associated with shorter duration of postoperative stable disease in patients with craniopharyngioma. If high GHR expression is found in the surgical specimens of craniopharyngiomas, GH supplementation should be introduced more carefully [7].

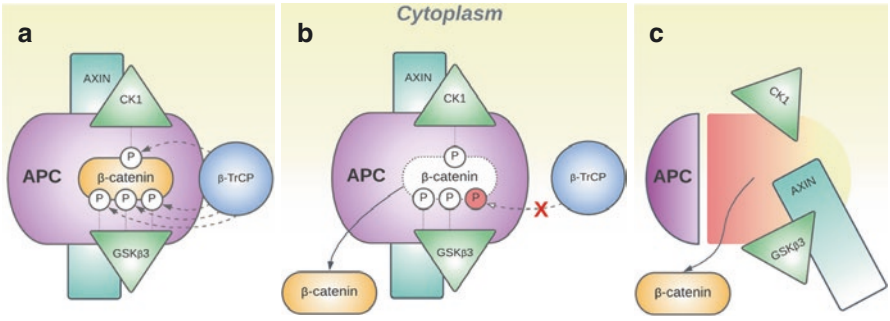

Fig. 3.1 β-Catenin destruction complex under normal conditions (**a**), with a CTNNB1 exon 3 missense mutation (**b**), and with an APC truncation (**c**). Normally, β-catenin destruction complex enables a β-TrCP ubiquitin ligase to mark β-catenin for proteasome-mediated degradation. This relies upon β-catenin being phosphorylated by specific amino acid residues encoded in exon 3 (**a**, blue circles). This mechanism fails if a missense mutation is introduced to or adjacent to these sites (**b**). Alternatively, a truncating mutation may render APC incapable of stabilizing the destruction complex, which allows cytoplasmic β-catenin to escape even when the exon 3 is intact (**c**). In both scenarios, β-catenin becomes free to reach the nucleus and induce the expression of its target genes. S33, S38, T41, and S45 denote amino acid residues and their position in the protein sequence (S for serine and T for threonine). *APC* adenomatous polyposis coli, *AXIN* axin1, *CK1* casein kinase 1 alpha 1, *CTNNB1* catenin beta 1, *GSK-3β* glycogen synthase kinase 3 beta, *βTrCP* beta-transducin repeat containing E3 ubiquitin protein ligase

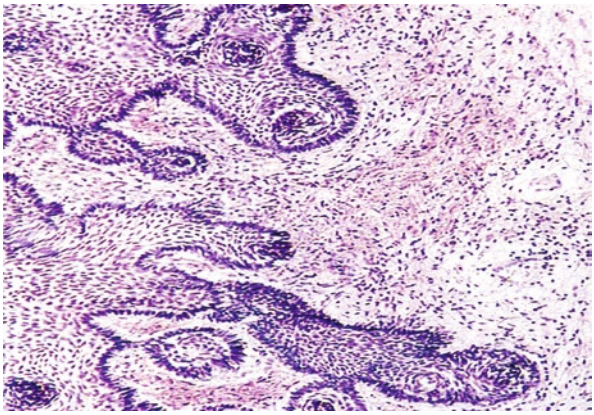

Fig. 3.2 Tumor digitations into the brain tissue. Gliotic reactive tissue at the tumor boarder may facilitate the resection, but on the other hand provide false impression of a gross total removal

3.5 Classification

Many classifications were proposed to reflect the biological peculiarities of CP and to facilitate the surgical planning.

Choux, Raybaud (1991) proposed the classification of these tumors based on their relation to the sellar, pituitary stalk, and third ventricle: intracellar, infundibular, intraventricular, and global.

Kassam et al. [8] in his classification based on the anatomical relation of tumor to infundibulum define the preinfundibular craniopharyngiomas (Type I), transinfundibular (Type II), and retroinfundibular (Type IIIa, b) [8].

Puget et al. [9] advocated classification based on the functional relation of the tumor to hypothalamus. Thus, she outlines the tumors with no hypothalamic involvement and thus no possible surgical hypothalamic damage (Grade 0); cases where hypothalamus is displaced by the tumor and minimal hypothalamic damage is possible (Grade 1)—and with hypothalamic involvement and severe possible hypothalamic damage (Grade 2) [9].

In the Burdenko National Neurosurgical Center, the classification based on the embriological origin is used. Thus, the following groups are distinguished: endosuprasellar, pituitary stalk, and intraextraventricular (Fig. 3.3).

Endosuprasellar craniopharyngiomas (Fig. 3.4) take their origin in the embryonic remnants of the craniopharyngeal duct in the anterior hypophysis. Thus, it primarily grows in the sella, destroys the hypophysis, and may expand to the suprasellar region. Diaphragm may be distended and become an external layer of a tumor capsule or may be penetrated when tumor grows along the stalk. Hypothalamus is displaced but not destroyed. These tumors usually manifest with the signs of hormone pituitary deficiency followed by visual disturbances.

Pituitary stalk craniopharyngiomas (Fig. 3.5) have an origin in the pituitary stalk and primarily destroy it. They grow above the diaphragm and beneath the third ventricle floor and minimally invade the hypothalamus. Tumor capsule is separated from the brain tissue by pia mater and from vessels—by arachnoidea. The major part of these tumors are cystic and may grow anteriorly under the frontal lobe

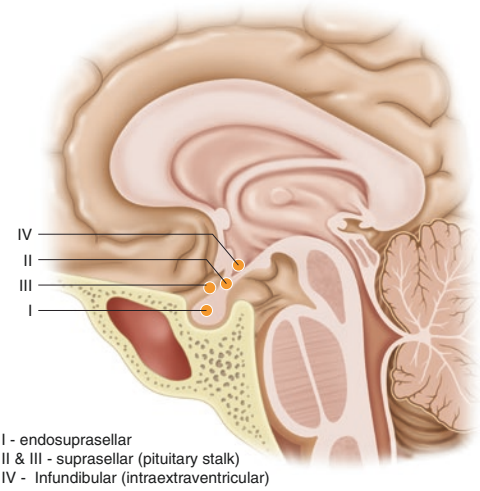

Fig. 3.3 National Burdenko Neurosurgical Center classification: I—endosuprasellar CP, II—Suprasellar (pituitary stalk) CP, III—Infundibular (intraextraventricular) CP

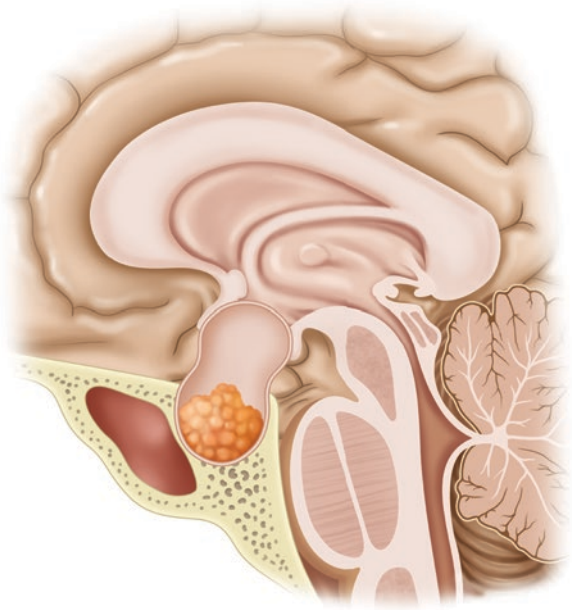

Fig. 3.4 Endosuprasellar craniopharyngiomas have their origin in the cellar

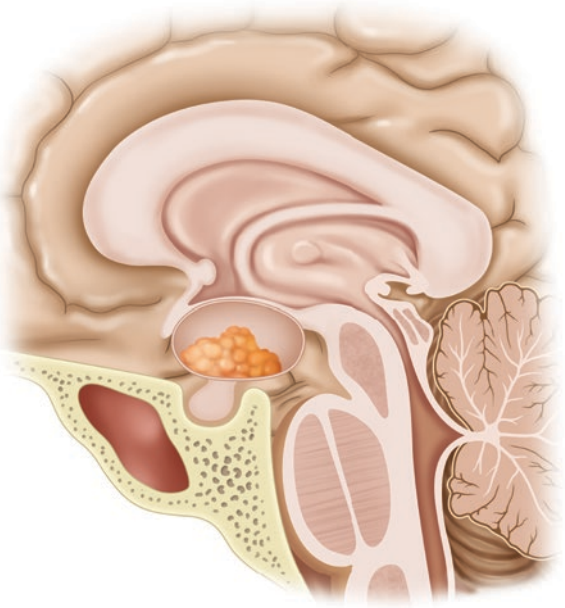

Fig. 3.5 Suprasellar-extraventricalar CP originate in the pituitary stalk

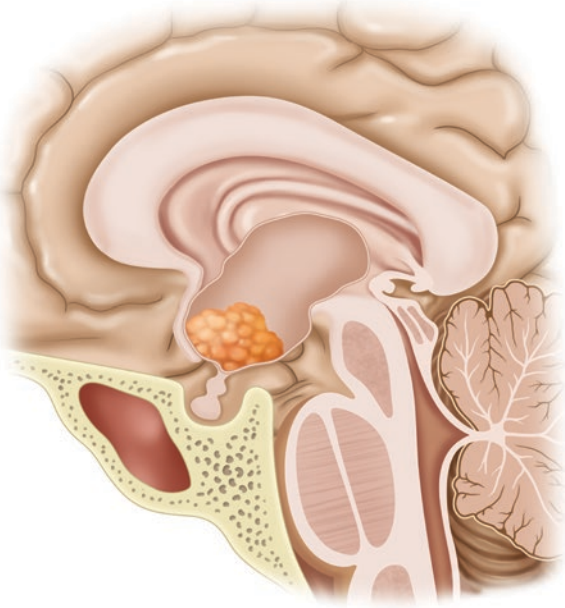

Fig. 3.6 Intraextraventricular CP originate in the infundibulum

(antesellar growth), posteriorly (retrosellar growth) into the prepontine cystern, and laterally to the middle fossa. The first sign is usually visual loss.

Intraextraventricular craniopharyngiomas (*third ventricle CP*) (Fig. 3.6) originate in the floor of the III ventricle and severely destroy the hypothalamus. This type of CP typically manifests with the signs of raised intracranial pressure.

3.6 Surgery

Surgery is still the first step in almost all the cases [10–18]. But today the surgical challenge is not only the visual function, not only the tumor control, not yet the endocrine function, but prevention of hypothalamic disturbances and restauration of an acceptable quality of life [19–22].

The main task of a surgeon, and at the same time the main challenge, is the identification of hypothalamus during surgery and assessment of the degree of its involvement in order to prevent its damage. It is much easier to totally remove CP than to perform subtotal removal and to leave a small fragment of a tumor capsula specially near the hypothalamic area. Unfortunately, we cannot monitor the hypothalamus!

Because of the unacceptably high complications rate and the lack of 100% prevention of recurrence following radical tumor resection, there has been a growing advocacy for less-invasive tumor resection with adjuvant therapy [9, 23].

We outline 3 grades of radicality of tumor removal: total—when there are no visible remnants on MRI (performed 24–48 h after surgery); subtotal—with flat remnants of capsula less than 0.5 cm^2 (volume can't be estimated precisely); and partial with volumetric 3D part of the tumor.

In our series, the gross total removal (GTR) was achieved in 40% of patients, subtotal (STR)—in 26%, partial (PR)—in 19%, endonasal endoscopic evacuation—in 11%, and aspiration via Ommaya reservoir—in 4% of patients.

Primary surgery has significantly better survival rate (due to more radical removal) than secondary one: 43% 5-PFS, vs. 19% 5-PFS (Gehan's Wilcoxon: $p = 0.03$; Log-Rank: $p = 0.05$).

Localization of a tumor has no influence on recurrent free survival. There was no significant difference between groups of patients according to surgical approach; nevertheless, for the endosuprasellar tumors, recurrence free survival with transcranial approach is worse; may be due to worse visualization of the endosellar region.

Location of tumor remnants has minor influence on recurrence free survival rates. Despite the absence of significant difference, we see more rapid relapses in cases with endosellar remnants (medium RFS is 7.2 months vs. other localizations—15.0 months, Mann–Whitney; $p = 0.0053$). Thorough follow-up or immediate adjuvant radiotherapy should be kept in mind.

3.6.1 Endosuprasellar Craniopharyngiomas

The best option for the removal of endosuprasellar craniopharyngiomas is the endoscopic transnasal (transsphenoidal) approach (Figs. 3.4, 3.7 and 3.8). If the tumor has an anterior extension and trancranial approach is impossible (due to short optic nerves), the anterior extended transsphenoidal approach may be used (Figs. 3.9 and 3.10). If the transnasal approach is impossible (in young children, absence of sinus

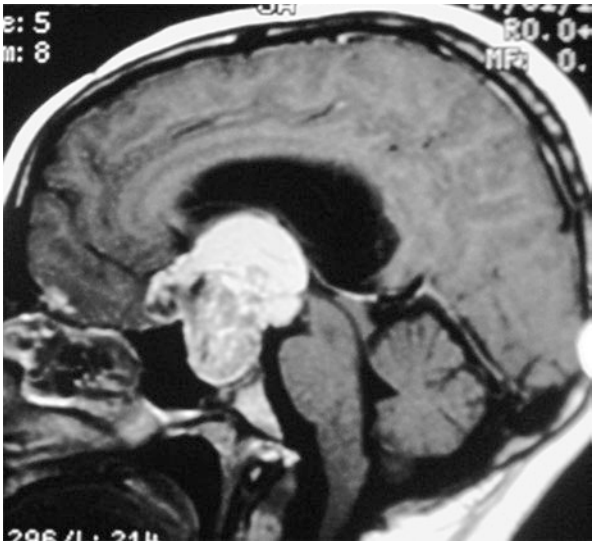

Fig. 3.7 MRI T1 CE. Endosuprasellar CP before surgery

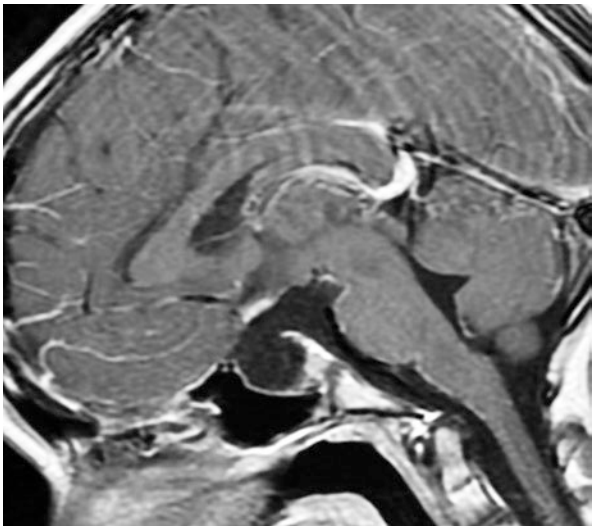

Fig. 3.8 MRI T1 CE. Endosuprasellar CP after radical surgery

sphenoidalis), the transcranial subfrontal approach is indicated with endoscopic assistance, which gives the possibility to view, and manipulated in the sella with angled optics and instruments (Fig. 3.11).

Hypothalamus is usually far from the operating field and remains intact. The visual nerves in the majority of cases are long (which makes possible the removal of a tumor via subchiasmal approach).

The origin of a tumor is inside the sella, thus remnants of pituitary stalk may be seen on the upper pole of the tumor.

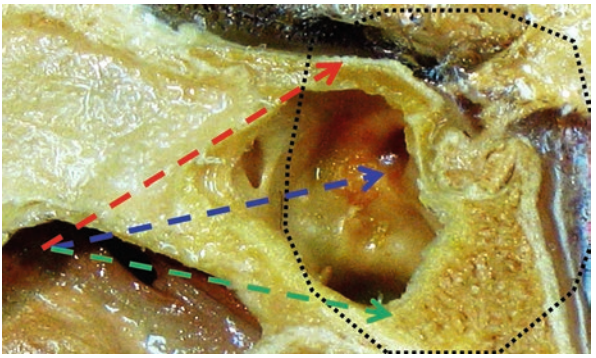

Fig. 3.9 Transnasal approaches: blue arrow—straight approach, red arrow—anterior extended, green arrow—posterior extended

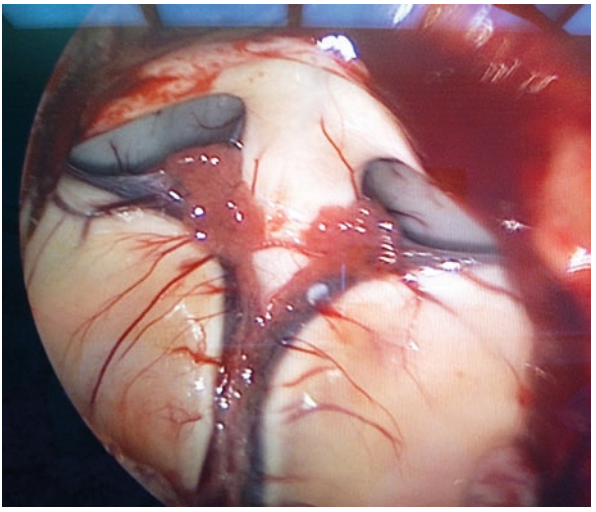

Fig. 3.10 Transnasal endoscopic approach. The view on the roof of the III ventricle. Both foramen Monro, fornix, choroid plexus, and internal veins are seen

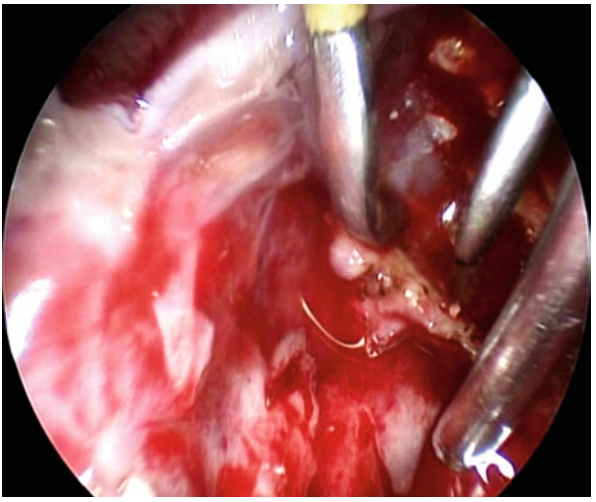

Fig. 3.11 Microsurgical endoscope-assisted approach. The view to the sella cavity, radical removal. Coagulation of the CP remnants by angled forceps

3.6.2 *Pituitary Stalk Craniopharyngiomas (Suprasellar-Extraventricular)*

The whole set of approaches were proposed for the removal of suprasellar and intraventricular tumors (Fig. 3.12).

Usually suprasellar-extraventricular CP has large cysts which facilitate surgical actions. In cases of anterior extension, a tumor is clearly seen just below the frontal lobes (Figs. 3.13 and 3.14). The ACA and AcoA are on the posterior pole of the tumor. The subfrontal approach is indicated in such cases. Visual nerves may be rather long what makes possible to remove a tumor subchiasmatically (Fig. 3.15).

In cases of suprasellar-lateral growth, pterional approach may be used. The position of the bifurcation of ICA which may be disclocated, compressed, or covered by the tumor should be kept in mind (It is extremely dangerous to manipulate above the ACA even if the tumor capsula is clearly seen as it is possible to damage the tiny perforating arteries that go across it (Figs. 3.16 and 3.17).

The most difficult situation occurs in CPs with retrosellar growth (Fig. 3.18). In these cases, the combination of subfrontal and retrosygmoid approach may be useful for the removal of both parts of the tumor.

Infundibulum is usually stretched and displaced upwards and located on the upper pole of the tumor. Capsula of suprasellar CP due to its origin is covered by the arachnoidea and even though there may be tight adhesions, it is usually feasible to find the cleavage between the capsula and infundibulum and remove tumor with minimal damage to hypothalamus.

Visual nerves and a chiasm are usually tightly attached to the tumor capsula and here is the second place where the remnants of a capsula may be left in order to preserve visual functions.

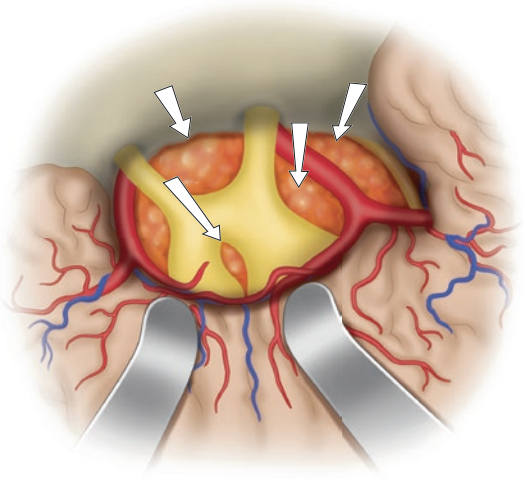

Fig. 3.12 Approaches to the retrochiasmal space and III ventricle

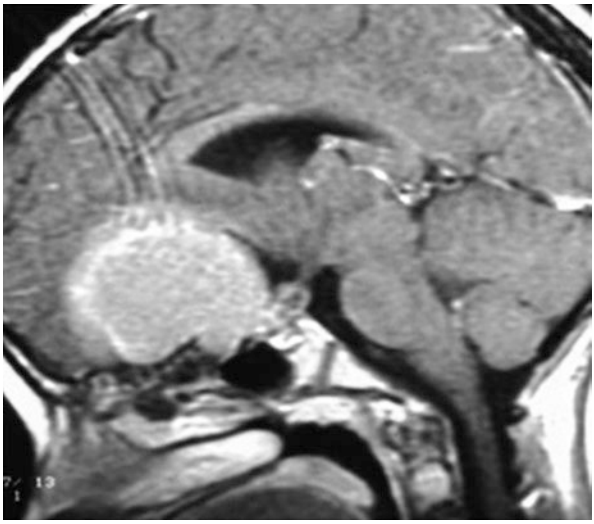

Fig. 3.13 MRI T1 CE. Suprasellar-extraventricalar CP with anterior extention before surgery

Fig. 3.14 MRI T1 CE. Suprasellar-extraventricalar CP with anterior extention after surgery. The preserved hypothalamus is seen

The origin of a tumor is at the pituitary stalk but above the sella, thus its remnants may be seen on the inferior (basal) surface of the tumor. In the very rare cases, it is feasible to maintain its anatomical integrity, but function is unfortunately lost.

There are three pathological components in the tumor: solid, liquid, and calcified. The latter can be represented as a huge coral-like structure which is impossible to divide into parts. It can be a source of relapse and such patients need irradiation.

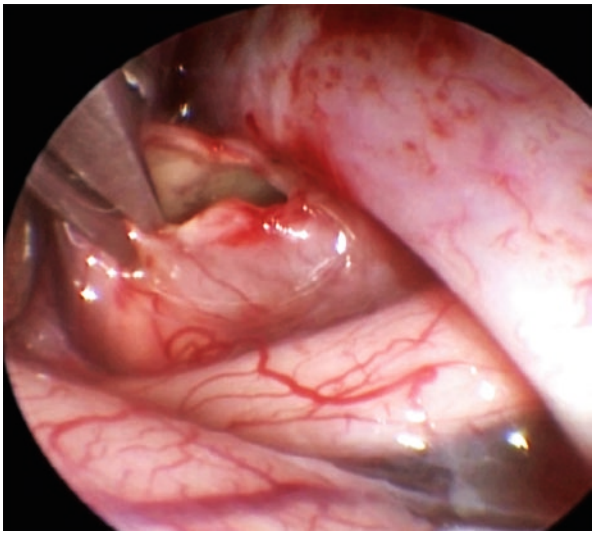

Fig. 3.15 Microsurgery with endoscope assistance. Removal of a tumor capsula with the subfrontal subchiasmal approach

Fig. 3.16 MRI T1 CE. Suprasellar-extraventricalar CP with retrosellar growth after surgery. Small remnants of capsula near the big vessels

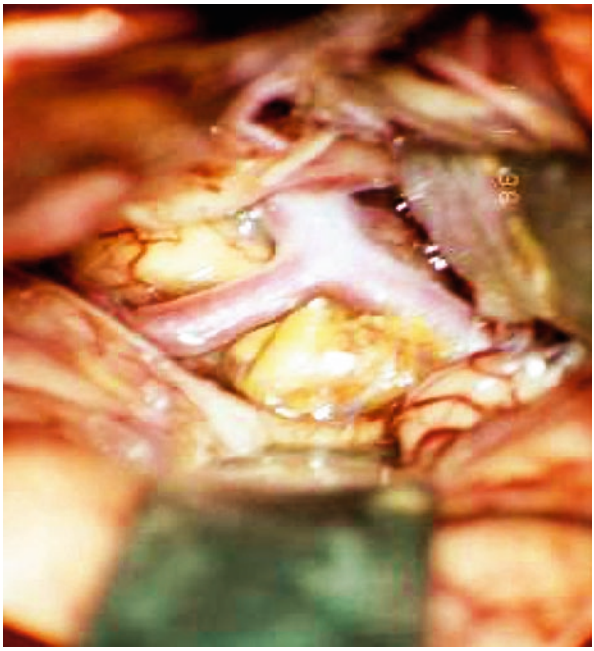

Fig. 3.17 Microscopic view on the suprasellar CP. Bifurcation of ICA compressed by suprasellar tumor

Fig. 3.18 MRI T1 CE. Suprasellar-extraventricalar CP with retrosellar growth before surgery

3.6.3 Intraextraventricular (III Ventricle) Craniopharyngiomas

Intraextraventricular CP are located both on the scull base predominantly behind the chiasm and in the III ventricle (Figs. 3.6, 3.19 and 3.20).

The variety of basal approaches may be used for the removal of the inferior part of the tumor (Fig. 3.12).

Subchiasmal approach is the least useful as the chiasm usually shifted anteriorly and pressed to the scull base.

Translaminaterminalis approach may be used for the removal of the anterior intraventricular part of the tumor, but it is rather narrow as the distance between the chiasm and ACoA may be very small [24]. In addition, it requires the large traction of the frontal lobes (Fig. 3.21). There is a variant of this approach above the AcoA up to anterior commissure [18].

An approach through the optico-carotid triangle allows to remove the retrochiasmal part of a tumor, but it is limited by the chiasm, ICA and ACoA (Fig. 3.22). Despite the narrow space, an approach may be enlarged by gentle shift of the chiasm and ICA; an arterial spasm which often seen during surgery has no clinical significance and need no treatment.

All manipulations lateral to ICA should be very carefully done in order not to damage the a. choroidea ant. and III nerve.

Trancallosal approach (Fig. 3.23) is possible in patients with hydrocephalus. There are three ways to reach the cavity of the III ventricle: through foramen Monro, subchoroideal, and transfornical.

An access via the enlarged *foramen Monro* (Fig. 3.24) allows to view the whole cavity of the III ventricle except the most anterior part. Ventricle roof, aqueductus Sylvii, midbrain, basilar artery, and Lilienkvist membrane are easily seen after the gross total removal of a craniopharyngioma. The dorsum sella is the most anterior

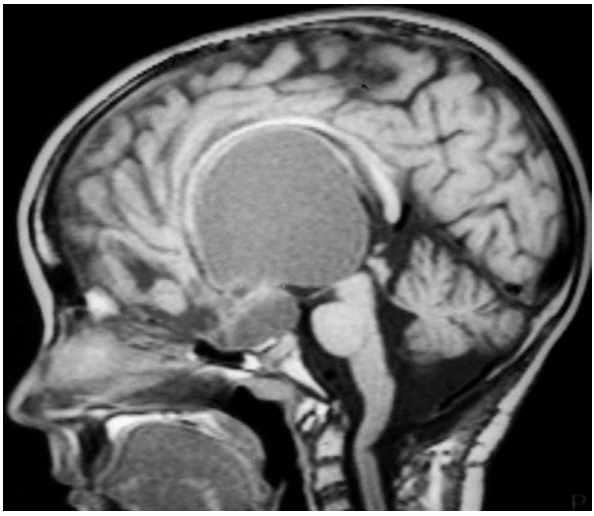

Fig. 3.19 MRI T1. Intraextraventricular CP occupying the whole cavity of the III ventricle

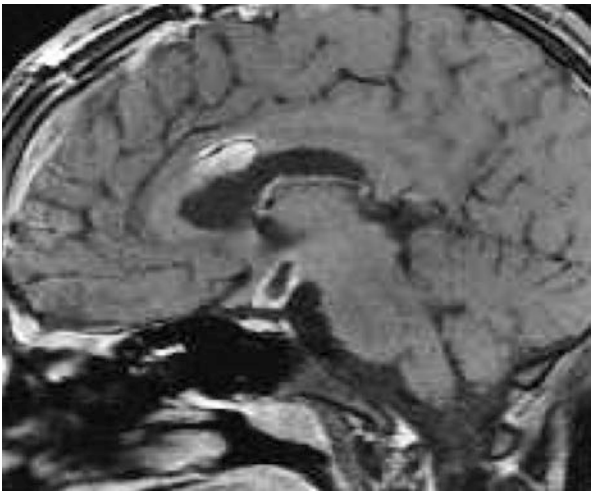

Fig. 3.20 MRI T1 CE. Small remnants of the tumor capsula in the hypothalamic region

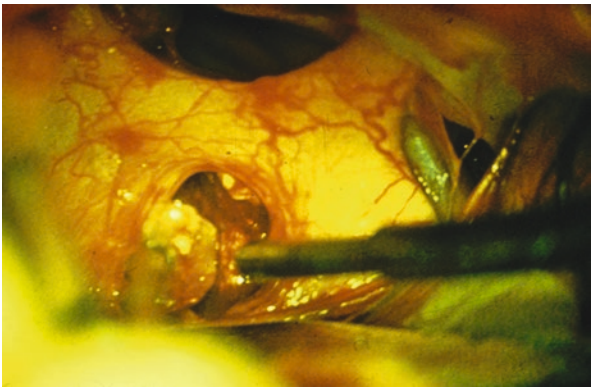

Fig. 3.21 Approach to the III ventricle via lamina terminalis

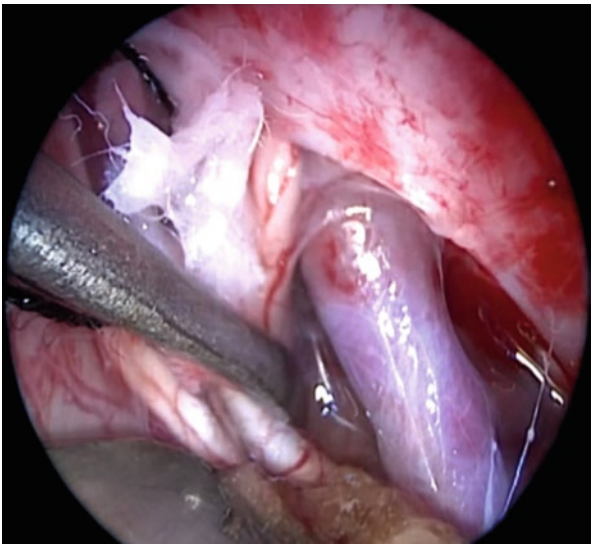

Fig. 3.22 Microsurgery with endoscope assistance. Removal of a tumor using an approach through the optico-carotid triangle

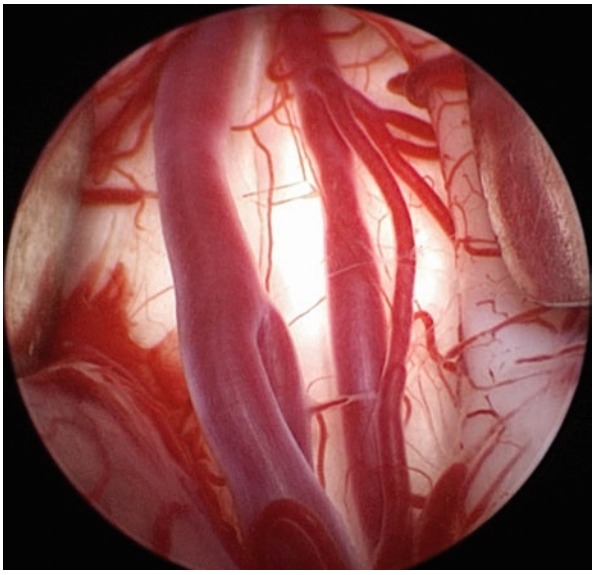

Fig. 3.23 Transcallosal approach. The view to the pericallosal and callosomarginal arteries, lying on the corpus callosum (white matter)

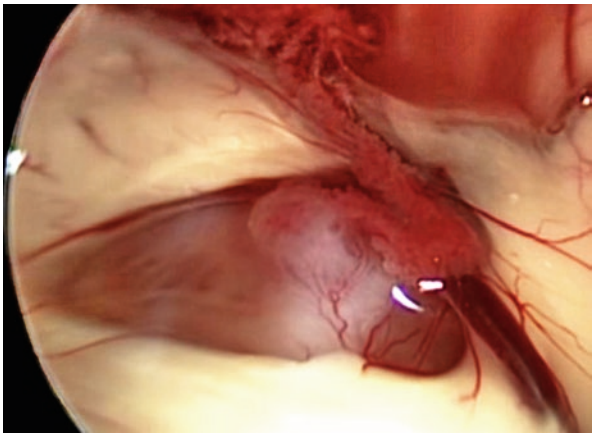

Fig. 3.24 Transcallosal approach. View on foramen Monro obstructed by CP in the III ventricle

structure seen in the operating field. The anterior view is limited because of risk of columna fornicis damage which leads to fixation amnesia (Fig. 3.25). Nevertheless, transcallosal approach is the method of choice for the resection of large tumors occupying the III ventricle.

Subchoroideal access lays through the fissure between thalamus and tela choroidea and permits view of the most posterior part of the III ventricle up to the pineal region.

Transfornical approach performed by the longitudinal splitting of fornix could provide an ideal access to all parts of the III ventricle, but it is feasible only in cases of huge tumors pushing apart the bodies of the fornix. Otherwise, we have a great risk to damage it.

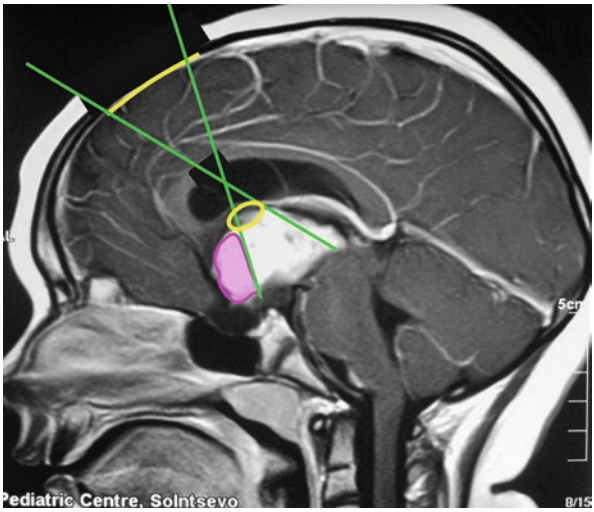

Fig. 3.25 The "geometry" of transcallosal approach. The "blind area" in the anterior part of the III ventricle

Transcortical approach is much easier than transcallosal one, but it is more "lateral" and cannot provide an adequate view of the ipsilateral part of the III ventricle.

In order to reach both basal and intraventricle part of the tumor, it is useful to combine basal and transcallosal approaches.

Hypothalamus is located on both sides of a tumor as an "equator" and can be hardly differentiated from tumor capsule. As this type of CP arises in the III ventricle floor, it doesn't separate from the brain tissue by arachnoidea and thus may have digitations into hypothalamus (Fig. 3.2). That's why, it is better to leave some remnants in this area in order to preserve the diencephalic functions.

3.7 Endoscopy-Assisted Microsurgery

Endoscope assistance during microsurgical removal of craniopharyngiomas may be performed for initial inspection of operating field, especially its deepest part and areas "around the corner". During removal of the tumor, it provides better illumination of the operating field, additional magnification, and manipulations beyond the microscope view. In the end of the surgery, it allows to find the remnants of the tumor, to look for, and stop the possible hemorrhage in remote places.

Endoscope assistance may be performed in air or water environment.

In air environment, endoscope-assisted microsurgery is performed with a special assistant endoscope, microscope, and conventional microinstruments. For the keyhole neurosurgery, an assistant endoscope with special "para"endoscopic instruments or traditional endoscope with two working canals and endoscopic instruments may be used.

In water environment, the routine one or two working canals endoscope with endoscopic instruments may be useful.

In cases of craniopharyngioma surgery (Figs. 3.15, 3.22, 3.26 and 3.27), an endoscope allows to view the suprasellar area under the frontal lobes, the retrochiasmal space, the endosellar area, to easily identify the pituitary stalk, ACA and ACoA hidden behind the tumor, remove the endosellar part of a tumor via the subfrontal approach, and even reach the retrosellar part. The special application of this method is in the course of transcallosal approach where it

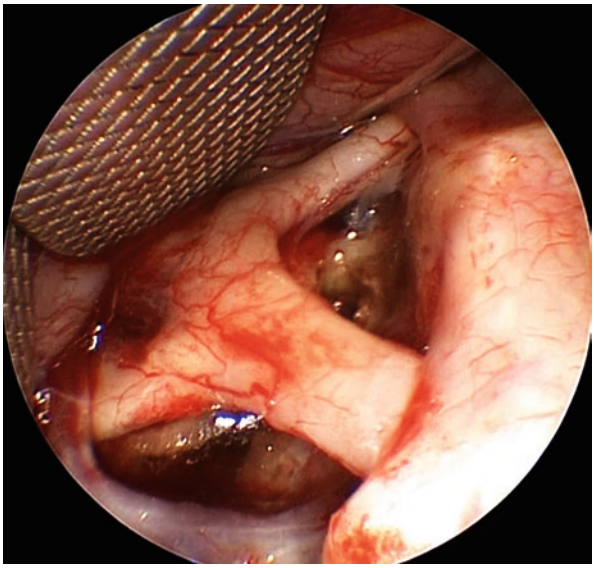

Fig. 3.26 Endoscope assistance. View to chiasma. 0^0 optics. The OCT is enlarged

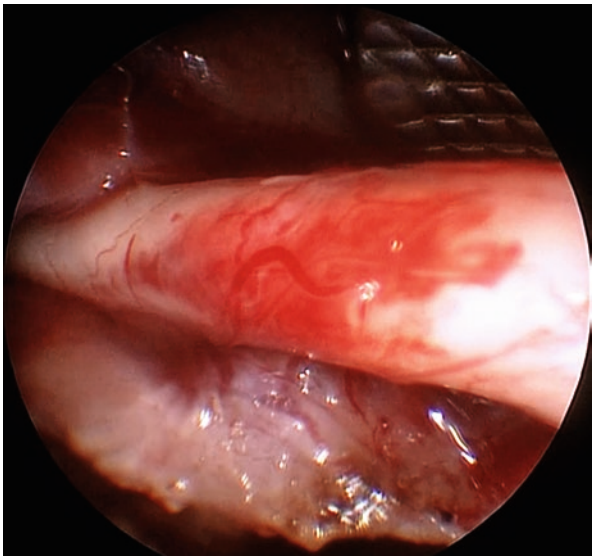

Fig. 3.27 Endoscope assistance. View under chiasma with 30^0 optics through the enlarged OCT. Capsula attached to chiasma is clearly seen

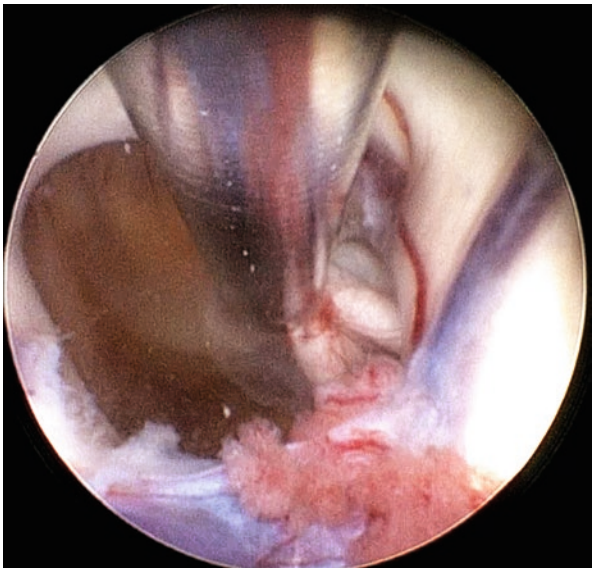

Fig. 3.28 Endoscopic ultrasound aspiration of CP. v.thalamostriata (on the right), choroid plexus (in the bottom), CP capsula being removed by US-aspirator is seen in f. Monro

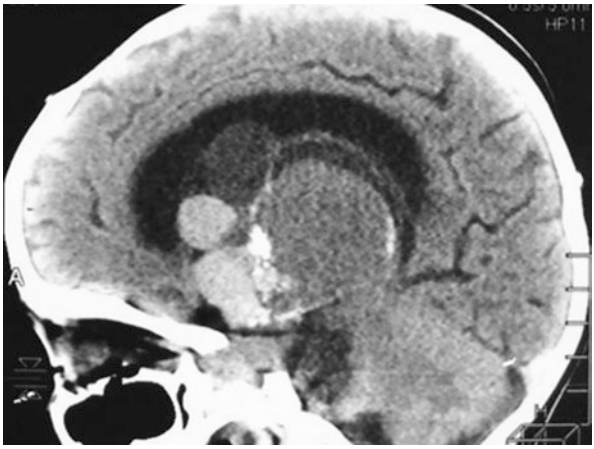

Fig. 3.29 MRI T1 CE. Giant policystic CP

makes possible the removal of the tumor anterior to foramen Monro (columna fornicis).

For endoscopic ultrasound aspiration, the Gaab endoscope, Söring endoscopic US-aspirator, water pump, bipolar endoscopic coagulation, and holding arm are necessary. For the safety of this procedure, it is necessary to maintain the balance of irrigation and suction. Irrigation is performed with the water pump through the canal of endoscope and suction—through US-aspirator. As a result, we have the clear view even in a case of bleeding! (Fig. 3.28).

In cases of cystic CP (especially polycystic ones), endoscopy may be used for fenestration of all cysts and installation of only one catheter for intracavitary treatment or controlling the cysts volume during radiotherapy (Figs. 3.29 and 3.30).

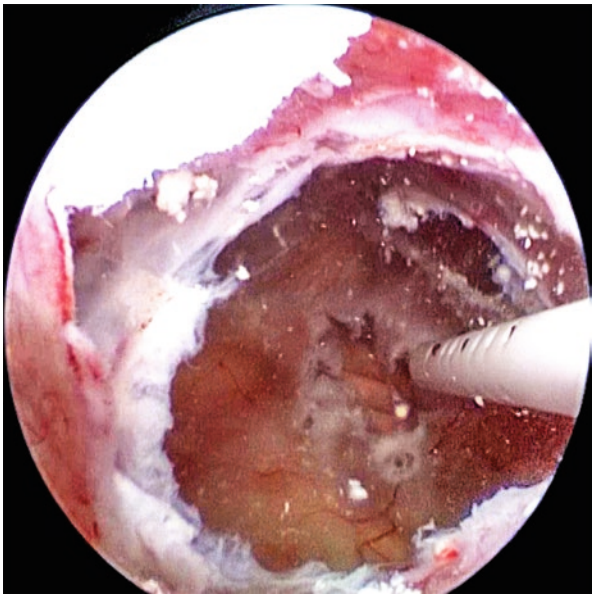

Fig. 3.30 All cavities are fenestrated with endoscope and connected with one catheter

3.8 Radiation Therapy

3.8.1 Historical Note

Attempts to use radiotherapy (RT) for the treatment of CP have been undertaken since the beginning of the twentieth century. The first results of irradiation of patients with CP, published by Carpenter in 1937, were unsatisfactory and the authors concluded that "tumors of the pituitary stalk can be resistant to radiation exposure" [25].

However, in 1950, Love et al. got good results of irradiation after partial removal of the tumor [26]. Subsequently, conventional fractionated RT has begun to be used more often in patients with CP.

Kramer published the first report of RT for pediatric CP in the Royal Marsden Hospital in 1961. Between March 1952 and March 1954, six children and four adults underwent stereotactic aspiration of cyst with subsequent conventional radiotherapy. The tumor dose delivered by radiotherapy varied from 5000 R in 37 days to 6550 R in 57 days in the children, and from 5580 R in 51 days to 6950 R in 39 days in the adults. One adult patient died in 2 years of intercurrent disease, but all six children were alive and free from tumor relapse over 6.5–7 years [27].

In 1993, Rajan et al. published their results: 77 patients after non-radical surgical removal underwent a course of radiation therapy to a total dose of about 56 Gy in 1950–1986. 5-year and 10-year PFS was 83% and 79%, respectively [28].

Later with the development of technology stereotactic irradiation techniques appeared. The use of radiation therapy with incomplete removal of CP allowed to increase a progression-free survival up to 75–90% [28–32].

Currently, only stereotactic irradiation techniques should be used in CP, including stereotactic radiosurgery (SRS), standard fractionated, and hypofractionated RT [33].

3.8.2 Single-Fraction Radiosurgery

For the treatment of small residual tumor or relapses of CP, a stereotactic radiosurgery (SRS) can be used with a relatively high dose of radiation during a single fraction. Through this radiation technique, the dose outside the target decreases sharply without substantial damage to healthy brain tissue [34].

It was shown that PFS after radiosurgery with CP is equivalent to survival after fractionated stereotactic RT. The 5-year PFS of patients who received SRS immediately after surgery or for recurrence of craniopharyngioma was 56.7–91.6%, while the 5- and 10-year OS were 86–97% and 88–91%, respectively [35–38]. The weighted average value of the 5-year PFS, estimates on the data from several studies (231 patients) [35, 37–39], was 67%. It should be noted that most relapses occur outside the volume of radiosurgical irradiation.

No significant differences in the efficacy of SRS and fractionated RT were disclosed by Jeon et al. after an analysis of 50 observations [39]. The volume of tumor smaller than 1.6 cm^3 and the dose more than 14.5 Gy [35] were found out by Xu et al. [35] as prognostic factors for better tumor control. The authors considered the absence of a cystic component of the tumor and the minimum number of surgical procedures before radiation as additional factors associated with a good response of CP to SRS [35].

3.8.3 Image-Guided Radiosurgery and Hypofractionated Radiotherapy

Stereotactic navigation during radiosurgery can be performed with a frame (Gamma Knife, Novalis, etc.) or using frameless navigation (CyberKnife). There may be difficulties with fixing the frame in young children, patients after surgery, especially after large bifrontal approaches, while CyberKnife has no such disadvantage. Besides that, frameless navigation provides the possibility of multiple uniform positioning of the patient, which allows to perform the hypofractional irradiation. The doses used by CyberKnife are similar to those using the Gamma Knife [40, 41] and the geometric accuracy is higher than 0.5 mm [42–44].

During last 20 years, the hypofractionation mode in the treatment of brain tumors was actively introduced into practice. This process was facilitated by the usage of robotic linear accelerator for the frameless stereotaxis as CyberKnife, in which modes of radiosurgery or hypofractionated radiotherapy may be carried out.

Hypofractionated radiation therapy which is performed in 2–10 fractions has a set of advantages in comparison with the standard course of radiotherapy and radiosurgery. First, unlike radiosurgical treatment, it is feasible to irradiate patients with relatively large tumors located close to or inside vital structures such as visual pathways, brainstem, pituitary gland, and hypothalamus. On the other hand, according to the biology of the tumor, the hypofractionation is similar to radiosurgery. Second, in the treatment of patients with cystic CP, fast fractionation mode which takes from 3 to 5 days allows to avoid an increase in the tumor cyst during radiotherapy and, thus not to lose the tumor borders beyond the limits of the radiation volume, which can happen with the standard course of radiotherapy (6-week duration). Third, from the radiobiological point of view, hypofractionation mode let us target the hypoxic cells.

The hypofractionation regimen uses a single dose (SD) more than 3 Gy. Irradiation in this mode can be carried out at many linear electron accelerators. However, in the majority of publications devoted to hypofractionated RT, the CyberKnife was used.

In the situation of compression of the optic chiasm by the tumor, Lee et al. reported no complications and a 90% tumor control with preservation of visual functions in 11 patients with craniopharyngiomas after treatment with CyberKnife (total dose was 20–25 Gy in 3–5 fractions) [41].

Iwata et al. analyzed results of hypofractionated radiotherapy (2–5 fractions with marginal dose of 13–25 Gy) by CyberKnife in 40 patients with craniopharyngiomas and reported the 85% PFS with a median follow-up of 3 years (tumor volume was 0.09–20.8 $cm^{3,}$ the hypofractionation regimens 8 Gy × 2 fractions, 7 Gy × 3 fractions, and 5 Gy × 5 fractions were used). The author noted a temporary increase of cystic component after treatment in nine patients, but no serious complications were reported [40].

Presently, the dose of 25–27.5 Gy with hypofractionated irradiation is considered to be optimal for craniopharyngiomas, as tolerant doses to critical structures [33].

We recommend to include both solid and cystic components of the tumor in the GTV when planning radiation therapy. Any tumor capsula fragments in the operative field as well as cyst walls and all calcifications visible on high resolution MRI and CT scans should be incorporated in GTV.

It is helpful to use a preoperative MR and CT scan in addition to MRI and CT studies at the time of radiation therapy, taking into consideration the data of the surgical protocol. It is recommended to use CTV equal to GTV, and PTV is formed as CTV plus 1–2 mm margin for SRS or hypofractionated SRT.

For cases with a small GTV when the position of a tumor border allows to exclude optic chiasm and the hypothalamus from the PTV, single-fraction SRS is recommended. Hypofractionated SRT can be used even in cases where critical structures are inside the tumor.

3.8.4 Standard Fractionated Radiotherapy

For standard fractionated radiotherapy, dose per fraction is less than 2.2 Gy (for WBRT—up to 3.0 Gy). Stereotactic technology of irradiation provides full coverage of tumor and minimal dose to healthy tissue and vessels. It allows to reduce risk of side effects [45–49].

5-year PFS after SRT for CP with total dose 50–54 Gy exceeds 73% [50]. Regime after analysis of 56 patients with 17 years median follow-up after SRT demonstrated that recurrence risk increased to 44% with dose less than 54 Gy in contrast with 16% with dose more than 54 Gy [51]. Currently, total dose for standard fractionates stereotactic radiotherapy is usually 54 Gy, delivered in 30 fractions.

According to the experience of the National Burdenko Neurosurgical Center, 5-year PFS after SRT with total dose 54 Gy for partial resected CP or it's relapse is 83.6%. It is recommended to include in CTV all solid and cystic parts of tumor and tumor bed which may contain small residual fragments of tumor.

3.9 Results of Surgical Treatment and Irradiation

As it was mentioned above, the main task of a craniopharyngioma treatment is the avoidance of recurrence on one hand and prevention of hypothalamic disturbances on the other hand. That's why it is so important to compare two main methods of treatment: radical surgery and subtotal surgery with irradiation.

3.9.1 Recurrence-Free Survival

Conservative surgery is associated with higher recurrence rates with an average rate of 75%. Limited surgery and RT have demonstrated results equivalent to radical surgery alone. Recent studies report at least 90% disease control with 5-year follow-up [52].

Radiotherapy dramatically increases the survival rate in non-total surgery (Fig. 3.31). The degree of radicality does not matter, but almost all non-totally removed CP (partial and subtotal) recover sooner or later! We obtained the exactly equal results of GTR and non-GTR + radiotherapy (Fig. 3.32).

Another important question is the time when to start radiotherapy in cases of small remnants: either to start immediately after surgery or to wait for the first signs of recurrence. The timing of post-surgery RT remains controversial [53]. Several

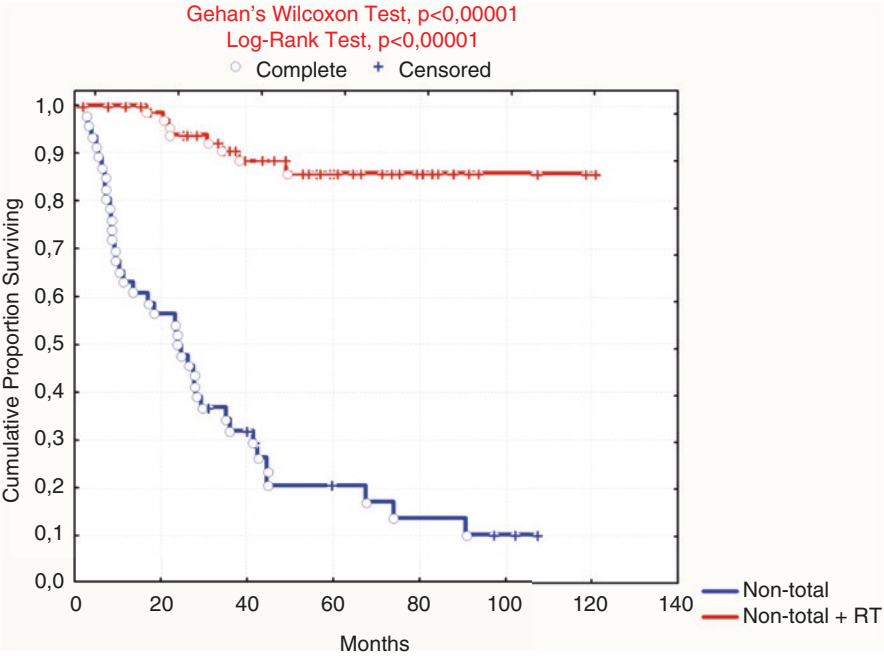

Fig. 3.31 Radiotherapy dramatically increase the survival rate in non-total surgery

studies demonstrated no significant difference in progression-free survival after early postoperative versus late radiotherapy for tumor regrowth [54]. In contrast, others found fewer craniopharyngioma relapse with early radiotherapy given as initial therapy when compared with those received late radiotherapy for recurrence [55]. Our investigation shows that PFS rates after adjuvant and salvage radiotherapy are equal (Fig. 3.33).

From April 2009 to January 2020, more than 200 patients were irradiated. All of them had previous surgery, 2/3 of them—by transcranial and 1/3—by transnasal approaches.

Radiosurgery was performed in patients with small tumors (<5 cm^3) and sufficient distance to optic pathways, or for tumors in contact with the optic nerve on the side of the blind eye. Median dose was 16 Gy. Median target volume—1.7 cm^3 (0.07–5.1). 5-year PFS was 85%.

Patients with larger tumors (>5 cm^3) and/or with a tumor adjacent to critical structures were irradiated with hypofractionated regimen. The following regimens were used: 3 fr. × 7 Gy (total dose 21 Gy), 5 fr. × 5 Gy (total dose 25 Gy), and 5 fr. × 5.5 Gy (total dose 27.5 Gy). Median tumor volume was 3.1 cm^3 (0.25–15.3). After hypofractionated SRT for CP, 5-year PFS was 91%. After irradiation with a dose of 27.5 Gy for 5 fractions, PFS was higher and reached 96%.

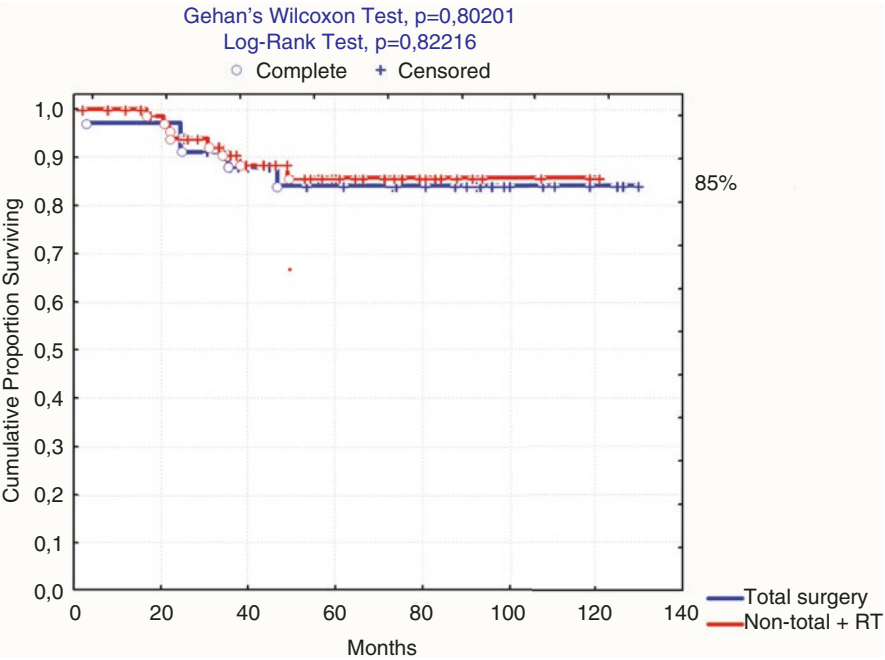

Fig. 3.32 The RFS rates of GTR and non-total + radiotherapy are equal

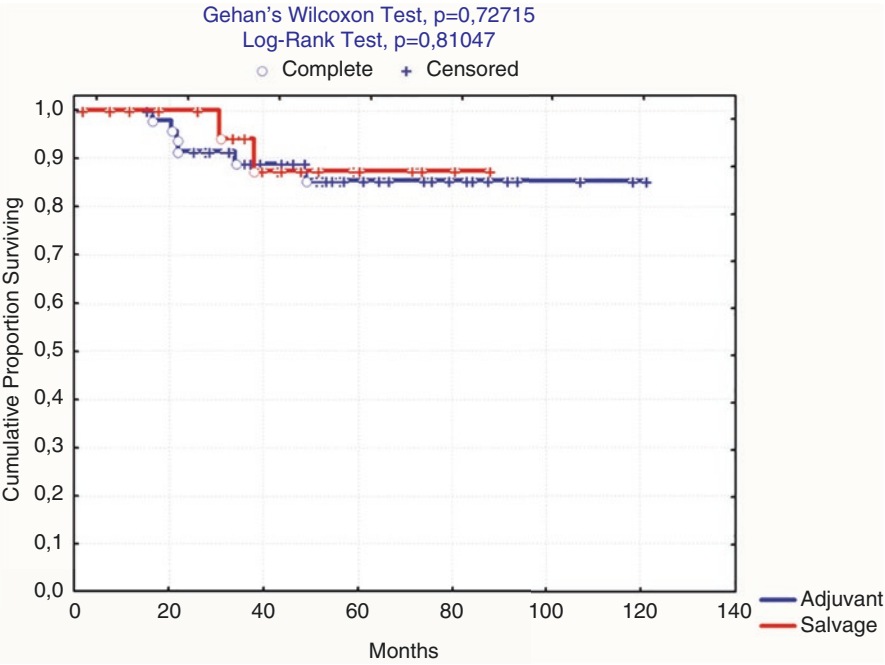

Fig. 3.33 The RFS rates of adjuvant and salvage radiotherapy are equal

Standard fractionated SRT was performed for patients with the largest tumors, with infiltration of the optic nerves and in the presence of multiple small fragments of the capsule along the tumor bed after surgery. Median dose was 54 Gy. 10-year PFS reached 82%.

The median follow-up was 48.4 months (1.4–95.1 months). Progression of cystic component was observed in 4.4% patients (which required aspiration of the cyst or its surgical removal). Progression of the solid component of the tumor was absent. Average 5-year PFS after all types of SRT and SRS (86%) was higher than after partial or subtotal removal of CP without subsequent irradiation (19%), $p < 0.00001$, and equivalent to 5-year PFS after total removal of the tumor (79%), $p = 0.4$.

3.9.2 Surgical and Radiation Morbidity

Although RT now is more commonly used in the management of childhood onset CP, it may carry considerable morbidity and mortality. Endocrinopathies, vasculopathies, visual deterioration, neurocognitive impairment, and second malignancies (1.9% at 10 years) are registered following RT for these tumors [52]. However, the vast majority of studies of side effects of radiation treatment reflect the risks associated with the use of conventional RT—a method which is currently no longer used in CP. Stereotactic irradiation methods provide much lower doses on critical structures minimizing complications.

Thus, with surgery and stereotactic radiation therapy, only visual, endocrine, and cognitive complications should be monitored.

3.9.3 Visual Deficits

In the majority of patients (80%) after surgery, visual functions remain stable or improve (Fig. 3.34). Only in 20% of patients, vision deterioration was detected. These cases are related to situations where capsule was firmly attached to the visual pathways, or to an attempt to resect a solid calcification behind the chiasm. The main risk factor for visual deterioration is the low vision before surgery. The worse the vision was before surgery, the greater was the risk of its further decline.

It is believed that the maximal tolerance single dose to the visual pathways is 10–12 Gy [29, 56]. The risk of radiation damage to the visual pathways is associated with fraction dose and total dose. According to the published data, radiation injury to the optic nerves is observed in 1–2% of patients who received a dose of 50 Gy or more with conventional irradiation and more often is observed in patients who had previously shown visual disturbances [28, 57].

Among patients who received 50–55 Gy with 1.8 Gy per fraction, the risk of visual deficit is less than 2.5% [58–60]. However, the frequency of this complication significantly increases at doses of 55–60 Gy [51, 61]. After stereotactic

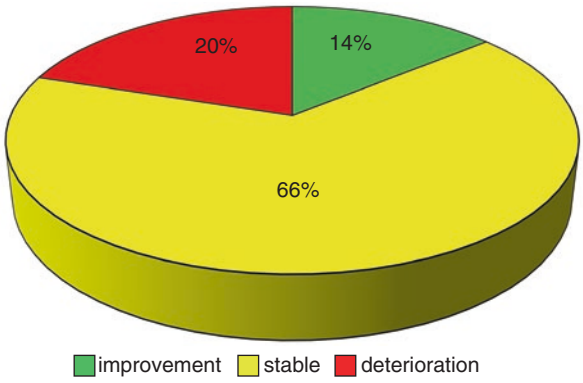

Fig. 3.34 Visual functions in the follow-up period after surgery

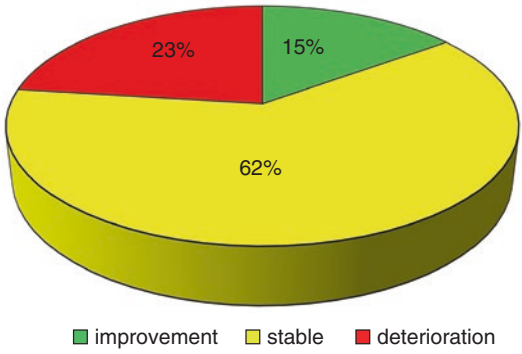

Fig. 3.35 Visual functions in the follow-up period after surgery + RT

radiosurgery and hypofractionated RT, damage to the optic nerves was noted only in a few cases [41, 62].

The same results were supported in our investigations (Fig. 3.35).

3.9.4 Endocrinological Dysfunctions

To estimate an influence of surgery and radiotherapy on endocrine functions, it is necessary to compare the state of endocrinological functions before and after treatment in the long-term follow-up period.

3.9.4.1 Endocrine Disorders at the Time of Diagnosis

Tumor embryogenesis determines its close approximation to hypothalamus–pituitary complex and high incidence of endocrine disorders in CP patients. Inflammation could be an additional factor in the formation of hypopituitarism, particularly GH deficiency through IL-1α-induced pituitary fibrosis [63].

The first clinical symptoms of CP include headache, vomiting, visual loss, and endocrine disorders: growth retardation, delayed puberty in elder children, excessive thirst and polyuria, weight gain, and fatigue.

According to analysis of 411 pediatric patients [64], the most frequent symptom before diagnosis was headache—50%; the combination of headache and growth failure was most frequent (18%). The median time between appearance of first sign of disease until diagnosis was 12 months, with a range of 0.01–96 months. Stunt growth and weight gain were the symptoms observed with the longest duration of history. A combination of headache, visual impairment, decreased growth velocity, weight gain, and polydipsia and/or polyuria is highly specific for childhood CP and should lead to further investigation [65].

Endocrine disorders include anterior pituitary deficiencies, diabetes insipidus, and weight gain/obesity. At the time of CP diagnosis, at least one endocrine deficit is presented in 40–87% of patients [66–68].

GH deficiency is the most common deficit in children occurring in up to 75% of patients at the time of diagnosis [69]. The main symptom is decreased growth velocity (less than 4 cm/year), resulting in short stature. Other signs include decreased muscle mass and strength, increased subcutaneous and visceral fat mass, and dyslipidemia.

Gonadotropin deficiency (LH and FSH) is the most common deficit in adolescents occurring in up to 50–70% of patients resulting in arrested puberty in younger children, amenorrhea, or erectile dysfunction in elder adolescents.

Secondary hypothyroidism (TSH deficiency) is present in 21–42% of cases. Symptoms include weight gain, dry skin, dry and brittle hair, fatigue, cold intolerance, and bradycardia.

Secondary adrenal insufficiency (ACTH deficiency) occurs in 20–25% of patients at the time of diagnosis and can present with fatigue, myalgias, arthralgias, weakness, and hypoglycemia and hyponatremia due to glucocorticoid deficiency.

Diabetes insipidus (ADH deficiency) occurs in 17–28% of patients and may present with polydipsia and polyuria with low urine osmolality.

Obesity/weight gain is the third most common clinical endocrine abnormality associated with CP. Hypothyroidism, GH deficiency, and direct hypothalamic injury can contribute to obesity and weight gain. Obesity and weight gain are reported in about 20% of presenting patients.

Hypopituitarism can be easily diagnosed using basal hormone levels except GH and ACTH deficiency, which may require the stimulation tests. Preoperative assessment includes detecting of basal levels of TSH/T4, cortisol, LH/FSH, sex steroids, cortisol, IGF-1 levels, urinary output, and osmolality. Obtained test results allow for perioperative hormone replacement as necessary and may be helpful in CP topography detection.

Some studies have reported about higher incidence of pituitary dysfunction at the diagnosis in childhood onset CP, than in adult onset [66–68].

According to our data of 155 CP pediatric patients, endocrine deficit depends on the tumor location. Patients with endosellar CP had more prominent pituitary deficiency before surgery (20% panhypopituitarism) than patients with suprasellar CP

(5% panhypopituitarism). In patients with endosellar CP, the incidence of GH deficiency before surgery was 98%, TSH deficiency 74.5%, ACTH deficiency 67.4%, gonadotropin deficiency 86.7%, diabetes insipidus 25.9%, and 20% had panhypopituitarism. In patients with suprasellar CP, the incidence of GH deficiency before surgery was 81.5%, TSH deficiency 18.2%, ACTH deficiency 14.9%, gonadotropin deficiency 88.5%, diabetes insipidus 10.5%, and 5% had panhypopituitarism [70]. Preoperative assessment of endocrine function can be useful in the detection of CP location and surgery planning.

3.9.4.2 Endocrine Disorders After Surgery and Radiotherapy

Hypothalamic–pituitary dysfunction may result from the tumor itself or its surgical or radiation treatment; however, additional dysfunction may develop in the months to years following initial treatment.

Pituitary Insufficiency

Majority of clinical studies provide data on the deterioration of endocrine function upon treatment at the follow-up up to 95–100% of pediatric onset CP. Patients have at least one endocrine deficiency and about 50% children are obese [66–68, 70, 71].

According to our data, 80% patients after surgery had panhypopituitarism and diabetes insipidus [70]. Therefore, RT as a risk factor for endocrine deficiency is important only in 20% of patients with partially preserved endocrine functions.

Nevertheless, hormone deficit before and after surgery depends on the localization of a tumor. It increases nearly to the same extent in all types of tumors, but the initial state is much worse in endosuprasellar tumors (Fig. 3.36a–c).

The majority of studies showed that the incidence of anterior pituitary insufficiency is similar in patients treated with surgery alone compared to those who had surgery and RT [68]. The dynamics of endocrine functions after combined treatment in our series were estimated only in patients with partial hormone deficit after surgery before irradiation. There was a minor deterioration of hormone state after radiation therapy due only to the increased ACTH deficiency [70] (Fig. 3.36d).

It was shown that an average single dose of 15 Gy or less to adenohypophysis does not cause hypothyroidism and hypogonadism, and a single dose of 18 Gy or less does not cause hypocortisolism [72].

The rate of radio-induced endocrinopathies is a dose-dependent parameter. With conventional irradiation with a dose of more than 60 Gy, the new endocrine deficiency was detected in more than 80% of patients and with dose of 54–60 Gy—in 36% [73]. Now the doses greater than 60 Gy are not used in RT.

Xu et al. showed that SRS in patients with endosellar pituitary adenoma causes pituitary deficiency up to 30% of irradiated patients within 3 years, developing in

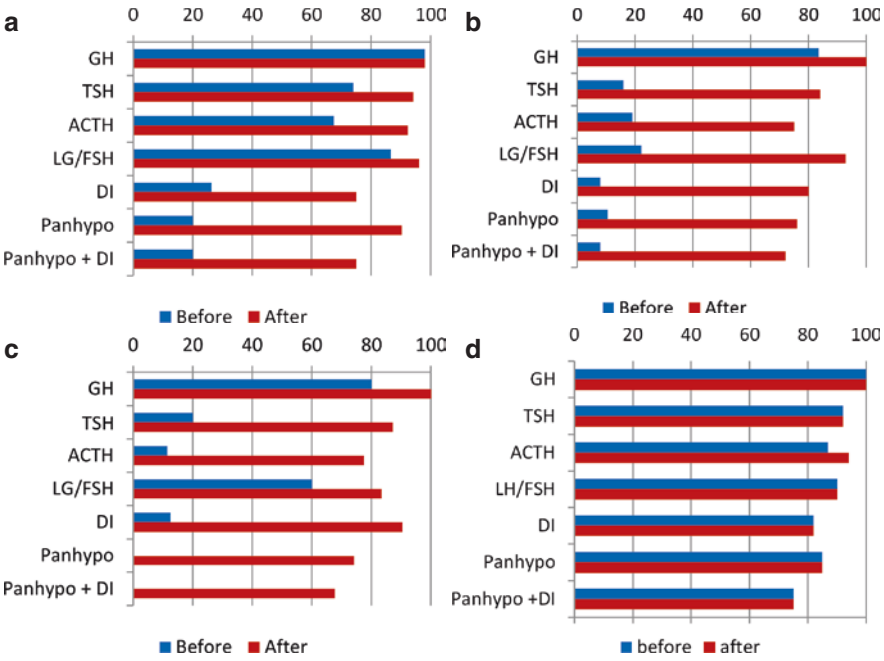

Fig. 3.36 Dinamics of endocrine functions before and after surgery in patients with endosellar (**a**), suprasellar (**b**) and intraextraventricular (**c**) CP. Dinamics of endocrine function before and after radiation treatment (**d**)

the majority of cases somatotropic insufficiency and hypothyroidism, less often hypogonadism, and even less often hypocorticism.

Diabetes insipidus is not typical for RT/SRS and appears in the majority of cases due to tumor regrowth, rather than to radiation damage [52].

Hormonal Substitutional Therapy

Adequate hormonal substitutional therapy can restore normal pituitary physiology. The impact of hypopituitarism on the QoL is low [74], so preservation of pituitary function isn't the goal of the surgery.

Substitutional therapy includes GH therapy in GH deficiency, L-thyroxine in hypothyroidism, hydrocortisone in adrenal insufficiency, and desmopressin in diabetes insipidus. As ACTH deficiency can be life-threatening, substitution should be initiated as soon as a deficit is confirmed. Hypogonadism is usually compensated by sex steroids replacement in both sexes; LH, FSH analogs, or pulsatile gonadotropin-releasing hormone may be recommended in fertility induction.

Despite GH deficiency, some CP patients after tumor resection have normal or accelerated growth. Insulin and leptin presumably play a leading role in this phenomenon.

Patients with pituitary insufficiency have higher rates of cardiovascular complications and mortality in comparison to the general population [75], so follow-up and proper hormonal replacement therapy in CP patients are crucially important. GH substitution is safe in terms of its possible effect on the risk of tumor recurrence [76] and may have a positive effect on body composition and lipid profile. Compensation of hypogonadism with low-dose estrogens instead of contraceptives in female and avoiding of glucocorticoid overreplacement may decrease cardiovascular morbidity and mortality.

Hypothalamic Dysfunction and Obesity

Another factor worsening quality of life and increasing the risks of metabolic syndrome, cardiovascular disease, and contributing to early mortality is weight gain/obesity.

In 1996, De Vile et al. for the first time have shown that hypothalamic lesions positively correlated with weight gain after tumor resection [77].

Hypothalamic area is a relatively small structure of 100 mm^3 volume, containing several nuclei and tracts which have highly diverse molecular, functional, and structural organization, providing important functions which can be summarized to maintain homeostasis. It includes regulation of endocrine, metabolic, autonomic, emotional, and behavioral functions, including neurohormonal control of the pituitary gland, hemodynamic, water and electrolyte metabolism, energy supply, body weight and eating behavior, sexual/reproduction functions, sleep cycles, body temperature regulation, and cognitive and memory function .

The symptoms of hypothalamic dysfunction may include rapid weight gain/obesity (in rare cases cachexia), emotional and behavioral changes, disturbed circadian rhythm (daytime sleepiness), body temperature disturbances (hyper/hypothermia), imbalances in regulation of thirst, hemodynamic homeostasis (heart rate, and/or blood pressure), memory and cognitive impairment, and in rare cases urinary/fecal incontinence.

At the time of CP diagnosis, signs of hypothalamic dysfunction may present in about 20–35% of childhood patients, but its incidence dramatically increases following surgical treatment up to 50–70% [69].

Obesity. Patients usually rapidly have increased weight within the first year after surgery due to impairment of satiety regulation and hyperphagia. In contrast to ordinary obesity, caloric restriction and lifestyle modification have usually low effect to prevent or treat the hypothalamic obesity due to their multifactorial origin.

The pathogenesis of hypothalamic obesity involves the inability of adequate transduction of afferent hormonal signals of adiposity, in effect mimicking a

state of CNS starvation [78]. It is associated with several endocrine dysfunctions, such as hyperleptinemia, hyperinsulinemia, decreased metabolic rate due to suppression of sympathetic nervous system activity, impaired 11β-hydroxysteroid dehydrogenase-1 activity, and dysregulation of melatonin and oxytocin secretion. Furthermore, increased daytime sleepiness, reduced physical activity, chronic apathy, and psychosocial problems may also contribute to the obesity development.

Despite theoretical understanding in mechanisms of hypothalamic obesity, effective medical treatment has not yet been developed.

In our investigations, it was shown that radicality of tumor removal and its location plays a crucial role in deterioration of hypothalamic dysfunction. Body mass index (BMI) as a marker of a diencephalic damage is much higher in patients with total surgery (Kolmogorov–Smirnov = 0.25, 160, $p < 0.01$) (Table 3.1) BMI also correlates with tumor location: it is significantly higher in patients with III ventricle craniopharyngiomas ($p = 0.0252$) (Table 3.2).

The role of radicality of tumor removal and the importance of preservation of hypothalamic area may be illustrated on two very similar cases of intraextraventricular craniopharyngiomas. In the first case (Fig. 3.37), the CP was removed totally with unavoidable hypothalamic damage which resulted in panhypopituitarism, diabetes insipidus, obesity, body temperature disturbances, memory and cognitive impairment, and limited socialization. In another case, the tumor was resected subtotally and a small piece of capsula was intentionally left at infundibulum which allowed to avoid hypothalamic disturbances. Stereotactic irradiation prevented recurrence without further deterioration of endocrine functions (Fig. 3.38).

Table 3.1 Correlation between radicality of a tumor removal and BMI (as a marker of a diencephalic damage)

Radicality	Mediana Δ SDS BMI (before and after surgery)
Total	0.80 (−1.51 to 7)
Non-total	0.30 (−3.04 to 4.4)
– Subtotal	0.47 (−3.04 to 2.5)
– Partial	0.28 (−0.73 to 4.44)
– Aspiration	0.11 (−1.73 to 3.6)

Table 3.2 Correlation between localization of a tumor and BMI

Localization	Mediana Δ SDS BMI (before and after surgery)
Endosuprasellar	0.11 (−3.0 to 4.4)
Suprasellar	0.63 (−1.1 to 3.6)
III ventricle	0.80 (−0.7 to 7.0)

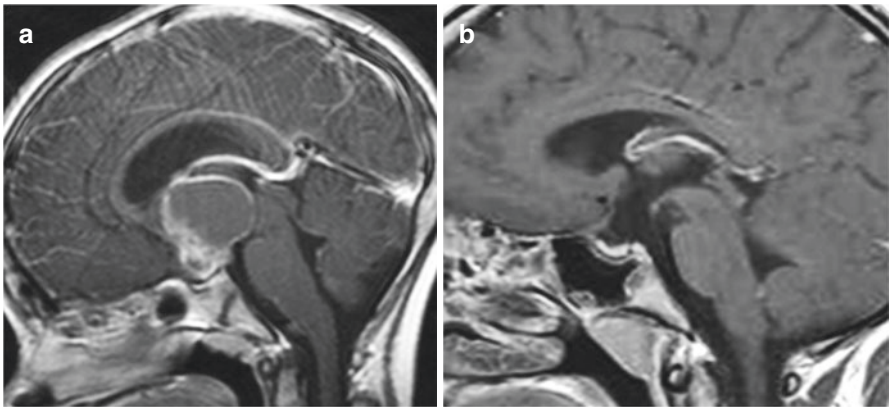

Fig. 3.37 A case of radical excision of intraextraventricular craniopharyngioma. (**a**) MRI T1 CE before surgery; (**b**) MRI T1 CE shows radical removal of the tumor hypothalamic area is damaged

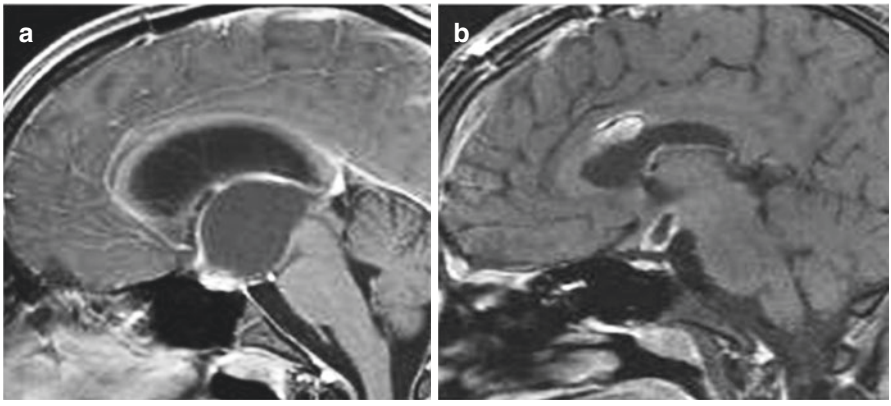

Fig. 3.38 A case of radical excision of intraextraventricular craniopharyngioma (nearly the same picture as the previous one). (**a**) MRI T1 CE before surgery; (**b**) MRI T1 CE after surgery. The small remnant of a CP capsula near the infundibulum dramatically changes the endocrinological outcome

Quality of Life

Hypothalamic obesity is the major factor, negatively influencing QoL in CP patients. In the multinational KRANIOPHARYNGEOM 2007 trial, CP patients treated with gross total resection resulting in hypothalamic lesions presented with significantly lower self- and parent-assessed QoL during the follow-up of 3 years after surgery than patients treated with incomplete resection with or without radiotherapy [79].

Since the main factor determining the decline in the quality of life in CP patients is hypothalamus dysfunction over the last two decades, the morbidity associated

with hypothalamic function has become the focus of CP outcome. Planning of surgery strategy and avoiding irreversible hypothalamic damage became key goals in the treatment and have led to a trend towards more conservative surgery, aiming to preserve hypothalamic structures, with a greater reliance on postoperative radiation treatment [80].

Recent studies demonstrate that gross total resection associates with higher morbidity and mortality compared to subtotal resection and RT [81].

Despite the trend towards hypothalamus-sparing surgery in patients with initial hypothalamic tumor involvement and as a result, decrease of the frequency of hypothalamic obesity, about half of the patients are morbidly obese [82].

In our study on 155 CP pediatric patients in cases of endosellar CP, the degree of tumor resection didn't influence QoL. In patients with suprasellar CP, QoL score was significantly higher after partial resection/Omaya followed by RT, than after gross total resection (Fig. 3.39).

3.9.5 Cognitive and Neuropsychological Dysfunction

After radiation treatment of tumors of sellar and parasellar localization, cognitive deficiency was observed in the 1990s [83, 84]. The correlation between cognitive impairment and exposure of large area of the brain in conventional RT is well known. The invention of stereotactic RT and SRS decreased the frequency and severity of cognitive disturbances [28, 51, 85–88].

Merchant (2006) analyzed IQ in 27 patients with craniopharyngiomas before and after stereotactic RT. Follow-up during 48 months showed a significant difference in the IQ between patients younger and older than the age of 7.4 at the time of RT. Moreover, the intelligence level of children younger than 7.4 years after RT decreased linearly over time, while in older patients it remained almost stable [86].

Kiehna together with Merchant analyzed in 2010 32 articles concerning RT in children with craniopharyngiomas and noted that IQ remains stable during 5 years after conformal RT with a possible subsequent decrease [52]. The following negative prognostic factors for cognitive functions were found: an age less than 7 years old at the time of RT, female gender, presence of hydrocephalus, large cystic component, traumatic surgery, and diabetes insipidus before surgery [52].

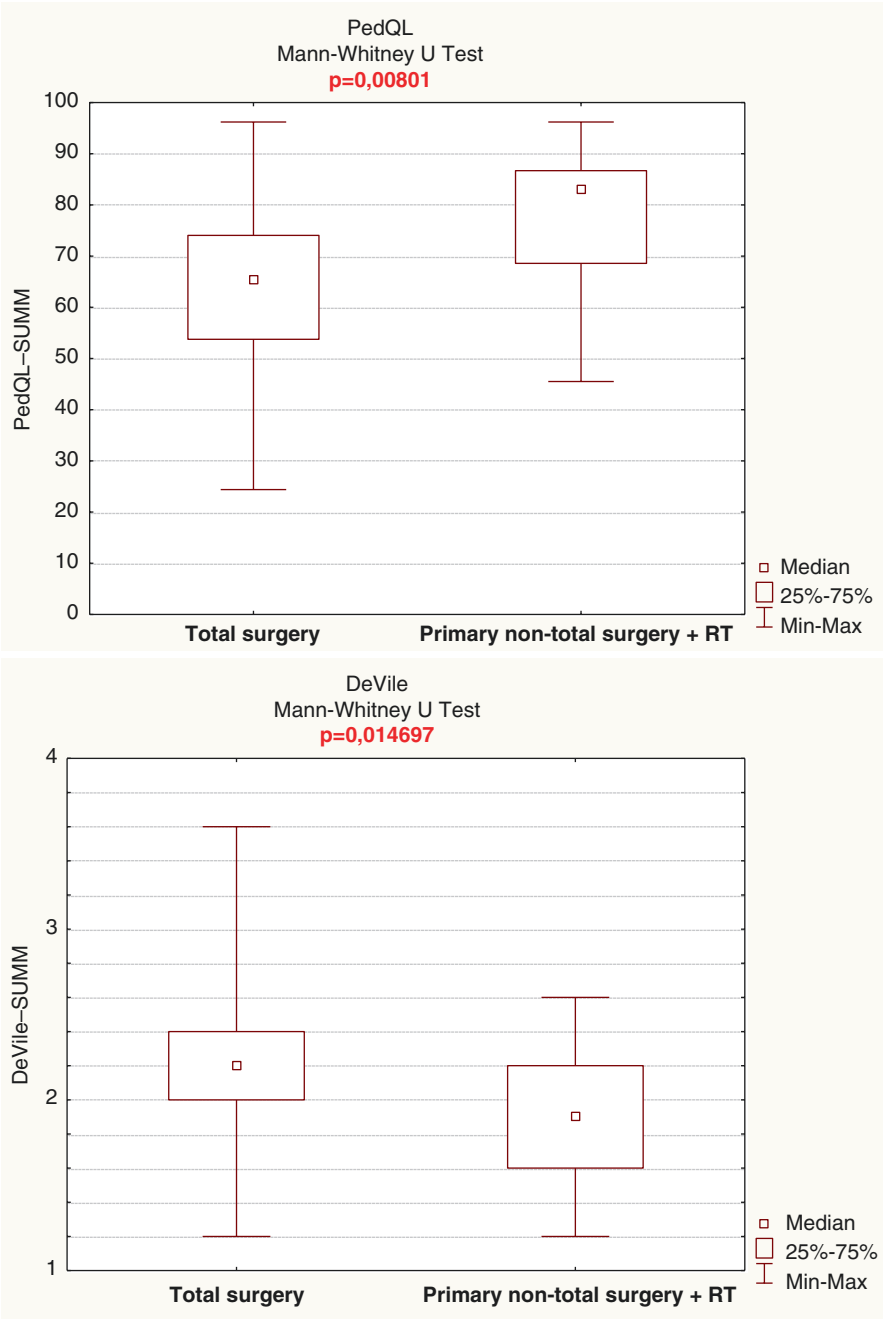

Fig. 3.39 PedQl and DeVile scales show better quality of life in patients after primary non-total surgery + RT than after primary total removal

3.10 Conclusions

We advocate the treatment of CrPh according to the degree of hypothalamic involvement estimated by localization of tumor and confirmed at surgery (Fig. 3.40).

To the low-risk group, we refer the patients with endosupresellar and suprasellar extraventricular tumors. There is no hydrocephalus in such patients as there are no CSF occlusion in the III ventricle area. Due to their origin, these tumors don't infiltrate the hypothalamus and the safe gross total removal may be performed.

In the high-risk group, there are patients with third ventricle craniopharyngiomas (intraextraventricular) with related hydrocephalus and hypothalamic syndrome. These tumors usually invade the hypothalamic area and cannot be totally removed without its damage.

Despite the MRI data, the precise relation of CP to hypothalamus may be revealed only during surgery.

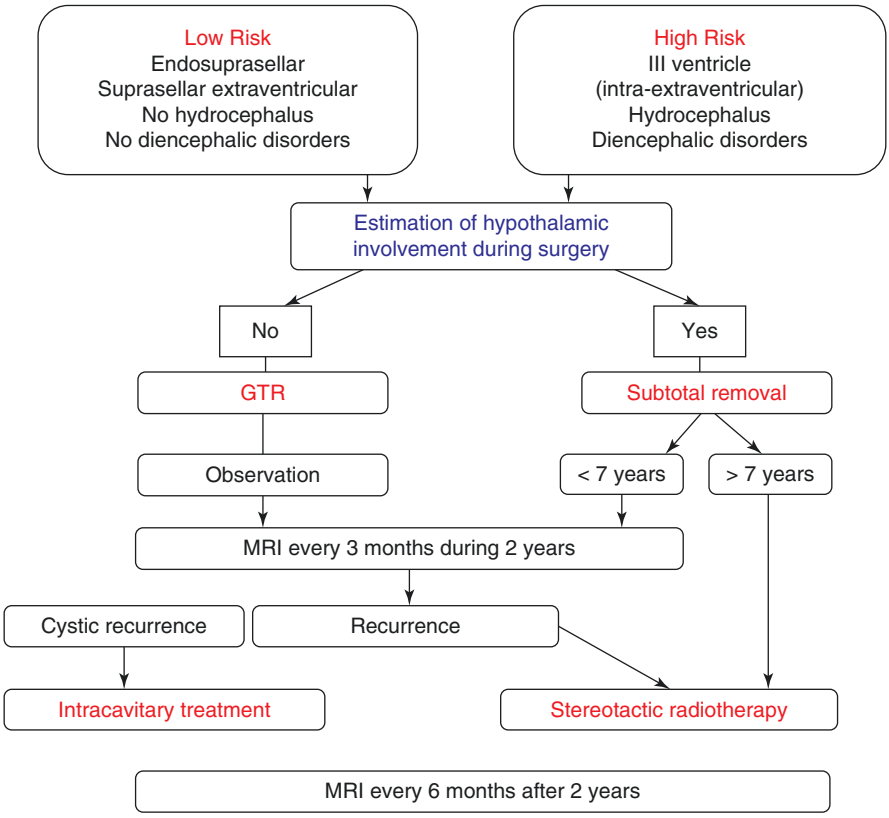

Fig. 3.40 Our strategy in pediatric craniopharyngioma treatment

In cases of GTR, we recommend observation with MRI investigations every 6 months at least during 2 years, then once a year. In patients older than 7 years with subtotal removal, the stereotactic radiotherapy is indicated.

If the purely cystic recurrence is diagnosed, the intracavitary treatment may be performed.

The use of stereotactic radiotherapy or radiosurgery in a setting of presence of a residual tumor, tumor relapse, or progression of craniopharyngioma significantly increases the disease-free survival after non-radical surgery to a level similar to that obtained after total resection of the tumor. SRT and SRS after non-radical surgery are safer for visual function preservation than total removal of the craniopharyngioma.

Stereotactic irradiation in patients with CP rarely exacerbates hormonal deficiency (6.7% of cases). Hypofractionated SRT and SRS do not lead to a worsening of the diencephalic disorders. In patients with CP that infiltrates the third ventricle, the quality of life is higher after non-radical operations followed by stereotactic radiation than after total or subtotal removal of the tumor.

References

1. Samii M, Tatagiba M. Craniopharyngioma. In: Kaye AH, Laws Jr ER, editors. Brain tumors: an encyclopedic approach. New York: Churcill Livingstone; 1995. p. 873–94.
2. Rickert CH, Paulus W. Epidemiology of central nervous system tumors in childhood and adolescence based on the new WHO classification. Childs Nerv Syst. 2001;17(9):503–11.
3. Bunin GR, Surawicz TS, Witman PA, Preston-Martin S, Davis F, Bruner JM. The descriptive epidemiology of craniopharyngioma. J Neurosurg. 1998;89(4):547–51.
4. Nielsen EH, Feldt-Rasmussen U, Poulsgaard L, Kristensen LO, Astrup J, Jorgensen JO, et al. Incidence of craniopharyngioma in Denmark (n = 189) and estimated world incidence of craniopharyngioma in children and adults. J Neurooncol. 2011;104(3):755–63.
5. Martinez-Barbera JP, Andoniadou CL. Concise review: paracrine role of stem cells in pituitary tumors: a focus on adamantinomatous craniopharyngioma. Stem Cells. 2016;34(2):268–76.
6. Gorelyshev A, Mazerkina N, Medvedeva O, Vasilyev E, Petrov V, Ryzhova M, et al. Second-hit APC mutation in a familial adamantinomatous craniopharyngioma. Neuro Oncol. 2020;22(6):889–91.
7. Ogawa Y, Watanabe M, Tominaga T. Prognostic factors of craniopharyngioma with special reference to autocrine/paracrine signaling: underestimated implication of growth hormone receptor. Acta Neurochir. 2015;157(10):1731–40.
8. Kassam AB, Gardner PA, Snyderman CH, Carrau RL, Mintz AH, Prevedello DM. Expanded endonasal approach, a fully endoscopic transnasal approach for the resection of midline suprasellar craniopharyngiomas: a new classification based on the infundibulum. J Neurosurg. 2008;108(4):715–28.
9. Puget S, Garnett M, Wray A, Grill J, Habrand JL, Bodaert N, et al. Pediatric craniopharyngiomas: classification and treatment according to the degree of hypothalamic involvement. J Neurosurg. 2007;106(1 Suppl):3–12.
10. Elliott RE, Wisoff JH. Surgical management of giant pediatric craniopharyngiomas. J Neurosurg Pediatr. 2010;6(5):403–16.
11. Gorelyshev S. Surgical treatment of craniopharyngiomas of the III ventricle in children. The dissertation for the degree of candidate of medicine doctor. Moscow: USSR Academy of Medical Sciences; 1989.

12. Konovalov AN, Gorelyshev SK. Surgical treatment of anterior third ventricle tumours. Acta Neurochir. 1992;118(1–2):33–9.
13. Hoffman HJ, De Silva M, Humphreys RP, Drake JM, Smith ML, Blaser SI. Aggressive surgical management of craniopharyngiomas in children. J Neurosurg. 1992;76(1):47–52.
14. Konovalov AN, Vikhert TM, Korshunov AG, Gorelyshev SK. Evaluation of the radicalness of the removal of craniopharyngioma of the 3d ventricle in children and the possible sources of their continued growth and recurrence. Zh Vopr Neirokhir Im N N Burdenko. 1988;6:7–12.
15. Elliott RE, Jane JA Jr, Wisoff JH. Surgical management of craniopharyngiomas in children: meta-analysis and comparison of transcranial and transsphenoidal approaches. Neurosurgery. 2011;69(3):630–43; discussion 43.
16. Fahlbusch R, Honegger J, Paulus W, Huk W, Buchfelder M. Surgical treatment of craniopharyngiomas: experience with 168 patients. J Neurosurg. 1999;90(2):237–50.
17. Zuccaro G. Radical resection of craniopharyngioma. Childs Nerv Syst. 2005;21(8–9):679–90.
18. Shi XE, Wu B, Fan T, Zhou ZQ, Zhang YL. Craniopharyngioma: surgical experience of 309 cases in China. Clin Neurol Neurosurg. 2008;110(2):151–9.
19. Barajas MA, Ramirez-Guzman G, Rodriguez-Vazquez C, Toledo-Buenrostro V, Velasquez-Santana H, del Robles RV, et al. Multimodal management of craniopharyngiomas: neuroendoscopy, microsurgery, and radiosurgery. J Neurosurg. 2002;97(5 Suppl):607–9.
20. Albright AL, Hadjipanayis CG, Lunsford LD, Kondziolka D, Pollack IF, Adelson PD. Individualized treatment of pediatric craniopharyngiomas. Childs Nerv Syst. 2005;21(8–9):649–54.
21. Schoenfeld A, Pekmezci M, Barnes MJ, Tihan T, Gupta N, Lamborn KR, et al. The superiority of conservative resection and adjuvant radiation for craniopharyngiomas. J Neurooncol. 2012;108(1):133–9.
22. Muller HL, Merchant TE, Warmuth-Metz M, Martinez-Barbera JP, Puget S. Craniopharyngioma. Nat Rev Dis Primers. 2019;5(1):75.
23. Tomita T, Bowman RM. Craniopharyngiomas in children: surgical experience at children's memorial hospital. Childs Nerv Syst. 2005;21(8–9):729–46.
24. Rhoton AL Jr, Yamamoto I, Peace DA. Microsurgery of the third ventricle: part 2: operative approaches. Neurosurgery. 1981;8(3):357–73.
25. Carpenter RC, Chamberlin GW, Frazier CH. The treatment of hypophyseal stalk tumors by evacuation and irradiation. Am J Roentgenol. 1937;38:162–77.
26. Love JG, Marshall TM. Craniopharyngiomas. Surg Gynecol Obstet. 1950;90(5):591–601.
27. Kramer S, McKissock W, Concannon JP. Craniopharyngiomas: treatment by combined surgery and radiation therapy. J Neurosurg. 1961;18:217–26.
28. Rajan B, Ashley S, Gorman C, Jose CC, Horwich A, Bloom HJ, et al. Craniopharyngioma—a long-term results following limited surgery and radiotherapy. Radiother Oncol. 1993;26(1):1–10.
29. Aggarwal A, Fersht N, Brada M. Radiotherapy for craniopharyngioma. Pituitary. 2013;16(1):26–33.
30. Hetelekidis S, Barnes PD, Tao ML, Fischer EG, Schneider L, Scott RM, et al. 20-year experience in childhood craniopharyngioma. Int J Radiat Oncol Biol Phys. 1993;27(2):189–95.
31. Habrand JL, Ganry O, Couanet D, Rouxel V, Levy-Piedbois C, Pierre-Kahn A, et al. The role of radiation therapy in the management of craniopharyngioma: a 25-year experience and review of the literature. Int J Radiat Oncol Biol Phys. 1999;44(2):255–63.
32. Van Effenterre R, Boch AL. Craniopharyngioma in adults and children: a study of 122 surgical cases. J Neurosurg. 2002;97(1):3–11.
33. Golanov AV, Savateev AN, Trunin YY, Antipina NA, Nikitin KV, Konovalov AN. Craniopharyngiomas. In: Conti A, Romanelli P, Pantelis E, Soltys SG, Cho YH, Lim M, editors. CyberKnife NeuroRadiosurgery. Cham: Springer; 2020.
34. Leksell L. The stereotaxic method and radiosurgery of the brain. Acta Chir Scand. 1951;102(4):316–9.

35. Xu Z, Yen CP, Schlesinger D, Sheehan J. Outcomes of gamma knife surgery for craniopharyngiomas. J Neurooncol. 2011;104(1):305–13.
36. Hasegawa T, Kobayashi T, Kida Y. Tolerance of the optic apparatus in single-fraction irradiation using stereotactic radiosurgery: evaluation in 100 patients with craniopharyngioma. Neurosurgery. 2010;66(4):688–94; discussion 94–5.
37. Niranjan A, Kano H, Mathieu D, Kondziolka D, Flickinger JC, Lunsford LD. Radiosurgery for craniopharyngioma. Int J Radiat Oncol Biol Phys. 2010;78(1):64–71.
38. Kobayashi T, Kida Y, Mori Y, Hasegawa T. Long-term results of gamma knife surgery for the treatment of craniopharyngioma in 98 consecutive cases. J Neurosurg. 2005;103(6 Suppl):482–8.
39. Jeon C, Kim S, Shin HJ, Nam DH, Lee JI, Park K, et al. The therapeutic efficacy of fractionated radiotherapy and gamma-knife radiosurgery for craniopharyngiomas. J Clin Neurosci. 2011;18(12):1621–5.
40. Iwata H, Tatewaki K, Inoue M, Yokota N, Baba Y, Nomura R, et al. Single and hypofractionated stereotactic radiotherapy with CyberKnife for craniopharyngioma. J Neurooncol. 2012;106(3):571–7.
41. Lee M, Kalani MY, Cheshier S, Gibbs IC, Adler JR, Chang SD. Radiation therapy and CyberKnife radiosurgery in the management of craniopharyngiomas. Neurosurg Focus. 2008;24(5):E4.
42. Iwata H, Sato K, Tatewaki K, Yokota N, Inoue M, Baba Y, et al. Hypofractionated stereotactic radiotherapy with CyberKnife for nonfunctioning pituitary adenoma: high local control with low toxicity. Neuro Oncol. 2011;13(8):916–22.
43. Chang SD, Main W, Martin DP, Gibbs IC, Heilbrun MP. An analysis of the accuracy of the CyberKnife: a robotic frameless stereotactic radiosurgical system. Neurosurgery. 2003;52(1):140–6. discussion 6–7
44. Antypas C, Pantelis E. Performance evaluation of a CyberKnife G4 image-guided robotic stereotactic radiosurgery system. Phys Med Biol. 2008;53(17):4697–718.
45. Cocchi U. Radiotherapy of brain tumors; therapeutic results and complications. Strahlentherapie. 1957;15(Sonderbd. 37):317–55.
46. Fike JR, Cann CE, Turowski K, Higgins RJ, Chan AS, Phillips TL, et al. Radiation dose response of normal brain. Int J Radiat Oncol Biol Phys. 1988;14(1):63–70.
47. Delattre JY, Poisson M. Neurologic complications of brain radiotherapy: contribution of experimental studies. Bull Cancer. 1990;77(7):715–24.
48. Abayomi OK. Pathogenesis of irradiation-induced cognitive dysfunction. Acta Oncol. 1996;35(6):659–63.
49. Amaral F. Current knowledge on major complications after whole brain radiotherapy or radiosurgery. Acta Med Port. 2010;23(1):85–94.
50. Clark AJ, Cage TA, Aranda D, Parsa AT, Sun PP, Auguste KI, et al. A systematic review of the results of surgery and radiotherapy on tumor control for pediatric craniopharyngioma. Childs Nerv Syst. 2013;29(2):231–8.
51. Regine WF, Mohiuddin M, Kramer S. Long-term results of pediatric and adult craniopharyngiomas treated with combined surgery and radiation. Radiother Oncol. 1993;27(1):13–21.
52. Kiehna EN, Merchant TE. Radiation therapy for pediatric craniopharyngioma. Neurosurg Focus. 2010;28(4):E10.
53. Kortmann RD. Different approaches in radiation therapy of craniopharyngioma. Front Endocrinol (Lausanne). 2011;2:100.
54. Stripp DC, Maity A, Janss AJ, Belasco JB, Tochner ZA, Goldwein JW, et al. Surgery with or without radiation therapy in the management of craniopharyngiomas in children and young adults. Int J Radiat Oncol Biol Phys. 2004;58(3):714–20.
55. Lin LL, El Naqa I Leonard JR, Park TS, Hollander AS, Michalski JM, , et al. Long-term outcome in children treated for craniopharyngioma with and without radiotherapy. J Neurosurg Pediatr 2008;1(2):126–130.

56. Leber KA, Bergloff J, Pendl G. Dose-response tolerance of the visual pathways and cranial nerves of the cavernous sinus to stereotactic radiosurgery. J Neurosurg. 1998;88(1):43–50.
57. Brada M, Thomas DG. Craniopharyngioma revisited. Int J Radiat Oncol Biol Phys. 1993;27(2):471–5.
58. Combs SE, Thilmann C, Huber PE, Hoess A, Debus J, Schulz-Ertner D. Achievement of long-term local control in patients with craniopharyngiomas using high precision stereotactic radiotherapy. Cancer. 2007;109(11):2308–14.
59. Merchant TE. Craniopharyngioma radiotherapy: endocrine and cognitive effects. J Pediatr Endocrinol Metab. 2006;19(Suppl 1):439–46.
60. Minniti G, Saran F, Traish D, Soomal R, Sardell S, Gonsalves A, et al. Fractionated stereotactic conformal radiotherapy following conservative surgery in the control of craniopharyngiomas. Radiother Oncol. 2007;82(1):90–5.
61. Varlotto JM, Flickinger JC, Kondziolka D, Lunsford LD, Deutsch M. External beam irradiation of craniopharyngiomas: long-term analysis of tumor control and morbidity. Int J Radiat Oncol Biol Phys. 2002;54(2):492–9.
62. Chiou SM, Lunsford LD, Niranjan A, Kondziolka D, Flickinger JC. Stereotactic radiosurgery of residual or recurrent craniopharyngioma, after surgery, with or without radiation therapy. Neuro Oncol. 2001;3(3):159–66.
63. Mao J, Qiu B, Mei F, Liu F, Feng Z, Fan J, et al. Interleukin-1alpha leads to growth hormone deficiency in adamantinomatous craniopharyngioma by targeting pericytes: implication in pituitary fibrosis. Metabolism. 2019;101:153998.
64. Hoffmann A, Boekhoff S, Gebhardt U, Sterkenburg AS, Daubenbuchel AM, Eveslage M, et al. History before diagnosis in childhood craniopharyngioma: associations with initial presentation and long-term prognosis. Eur J Endocrinol. 2015;173(6):853–62.
65. Muller HL. The diagnosis and treatment of craniopharyngioma. Neuroendocrinology. 2020;110(9–10):753–66.
66. Wijnen M, van den Heuvel-Eibrink MM, Janssen JA, Catsman-Berrevoets CE, Michiels EM, van Veelen-Vincent MC, et al. Very long-term sequelae of craniopharyngioma. Eur J Endocrinol. 2017;176(6):755–67.
67. Jazbinsek S, Kolenc D, Bosnjak R, Faganel KB, Zadravec ZL, Jenko BB, et al. Prevalence of endocrine and metabolic comorbidities in a national cohort of patients with craniopharyngioma. Horm Res Paediatr. 2020;93(1):46–57.
68. Hussein Z, Glynn N, Martin N, Alkrekshi A, Mendoza N, Nair R, et al. Temporal trends in craniopharyngioma management and long-term endocrine outcomes: a multicentre cross-sectional study. Clin Endocrinol (Oxf). 2021;94(2):242–9.
69. Muller HL. Craniopharyngioma. Endocr Rev. 2014;35(3):513–43.
70. Mazerkina NA, Konovalov AN, Gorelyshev SK, Semenova ZB, Krasnova TS, Tenedieva VD. Endocrine disorders in craniopharyngiomas in children: dependence on the site of a tumor. Zh Vopr Neirokhir Im N N Burdenko. 2008;1:23–9.
71. Tiulpakov AN, Mazerkina NA, Brook CG, Hindmarsh PC, Peterkova VA, Gorelyshev SK. Growth in children with craniopharyngioma following surgery. Clin Endocrinol (Oxf). 1998;49(6):733–8.
72. Xu Z, Lee Vance M, Schlesinger D, Sheehan JP. Hypopituitarism after stereotactic radiosurgery for pituitary adenomas. Neurosurgery. 2013;72(4):630–7.
73. Regine WF, Kramer S. Pediatric craniopharyngiomas: long term results of combined treatment with surgery and radiation. Int J Radiat Oncol Biol Phys. 1992;24(4):611–7.
74. Tang B, Xie S, Huang G, Wang Z, Yang L, Yang X, et al. Clinical features and operative technique of transinfundibular craniopharyngioma. J Neurosurg. 2019;133(1):119–28.
75. Bulow B, Hagmar L, Eskilsson J, Erfurth EM. Hypopituitary females have a high incidence of cardiovascular morbidity and an increased prevalence of cardiovascular risk factors. J Clin Endocrinol Metab. 2000;85(2):574–84.
76. Alotaibi NM, Noormohamed N, Cote DJ, Alharthi S, Doucette J, Zaidi HA, et al. Physiologic growth hormone-replacement therapy and craniopharyngioma recurrence in pediatric patients: a meta-analysis. World Neurosurg. 2018;109:487–96.

77. De Vile CJ, Grant DB, Kendall BE, Neville BG, Stanhope R, Watkins KE, et al. Management of childhood craniopharyngioma: can the morbidity of radical surgery be predicted? J Neurosurg. 1996;85(1):73–81.
78. Lustig RH. Hypothalamic obesity after craniopharyngioma: mechanisms, diagnosis, and treatment. Front Endocrinol (Lausanne). 2011;2:60.
79. Hoffmann A, Warmth-Metz M, Gebhardt U, Pietsch T, Pohl F, Kortmann RD, et al. Childhood craniopharyngioma—changes of treatment strategies in the trials KRANIOPHARYNGEOM 2000/2007. Klin Padiatr. 2014;226(3):161–8.
80. Cossu G, Jouanneau E, Cavallo LM, Elbabaa SK, Giammattei L, Starnoni D, et al. Surgical management of craniopharyngiomas in adult patients: a systematic review and consensus statement on behalf of the EANS skull base section. Acta Neurochir. 2020;162(5):1159–77.
81. Marcus HJ, Rasul FT, Hussein Z, Baldeweg SE, Spoudeas HA, Hayward R, et al. Craniopharyngioma in children: trends from a third consecutive single-center cohort study. J Neurosurg Pediatr. 2019;25(3):242–50.
82. van Iersel L, Meijneke RW, Schouten-van Meeteren AY, Reneman L, de Win MM, van Trotsenburg AP, et al. The development of hypothalamic obesity in craniopharyngioma patients: a risk factor analysis in a well-defined cohort. Pediatr Blood Cancer. 2018;65(5):e26911.
83. Grattan-Smith PJ, Morris JG, Shores EA, Batchelor J, Sparks RS. Neuropsychological abnormalities in patients with pituitary tumours. Acta Neurol Scand. 1992;86(6):626–31.
84. Peace KA, Orme SM, Sebastian JP, Thompson AR, Barnes S, Ellis A, et al. The effect of treatment variables on mood and social adjustment in adult patients with pituitary disease. Clin Endocrinol (Oxf). 1997;46(4):445–50.
85. Merchant TE, Kiehna EN, Sanford RA, Mulhern RK, Thompson SJ, Wilson MW, et al. Craniopharyngioma: the St. Jude Children's Research Hospital experience 1984–2001. Int J Radiat Oncol Biol Phys. 2002;53(3):533–42.
86. Merchant TE, Kiehna EN, Kun LE, Mulhern RK, Li C, Xiong X, et al. Phase II trial of conformal radiation therapy for pediatric patients with craniopharyngioma and correlation of surgical factors and radiation dosimetry with change in cognitive function. J Neurosurg. 2006;104(2 Suppl):94–102.
87. Pemberton LS, Dougal M, Magee B, Gattamaneni HR. Experience of external beam radiotherapy given adjuvantly or at relapse following surgery for craniopharyngioma. Radiother Oncol. 2005;77(1):99–104.
88. Savateev AN, Trunin YY, Mazerkina NA. Radiotherapy and radiosurgery in treatment of craniopharyngiomas. Zh Vopr Neirokhir Im N N Burdenko. 2017;81(3):94–106.

Chapter 4
Treatment of Cystic Craniopharyngiomas: An Update

Federico Bianchi, Alberto Benato, and Luca Massimi

4.1 Introduction

Adamantinomatous craniopharyngioma (AC) is a rare brain tumor arising from remnants of the craniopharyngeal duct epithelium. It accounts for 1.53–2.92/100,000 cases/year in children under 15 years and for 5–10% of sellar tumors in the pediatric population [1, 2]. AC is largely most common than the papillary variant in children and, in about 90% of the cases, it shows a cystic or multicystic component with a variable size [3].

Since the first experience with this tumor by Harvey Cushing [4], AP still continues to represent a significant challenge for the clinicians for several reasons:

1. The cystic components may reach a huge volume, determining acute hydrocephalus as well as causing compression even in intracranial districts far from the site of origin (Figs. 4.1 and 4.2). Cases of gigantic AC even reaching the posterior fossa and the cerebello-pontine angle are not rare in the clinical practice [5];
2. The site of origin together with the progressive growth in the cisternal spaces accounts for both the frequent encasement of eloquent or vital structures (optic pathways, pituitary gland and stalk, hypothalamus, Willis' circle) and the possible endocrinological, visual, and neurological deficits at diagnosis and after the treatment (Figs. 4.1 and 4.2);

F. Bianchi · A. Benato
Pediatric Neurosurgery, Fondazione Policlinico Universitario A. Gemelli IRCCS, Rome, Italy

L. Massimi (✉)
Pediatric Neurosurgery, Fondazione Policlinico Universitario A. Gemelli IRCCS, Rome, Italy

Università Cattolica del Sacro Cuore-Rome, Rome, Italy

C. Di Rocco (ed.), *Advances and Technical Standards in Neurosurgery*,
Advances and Technical Standards in Neurosurgery 45,
https://doi.org/10.1007/978-3-030-99166-1_4

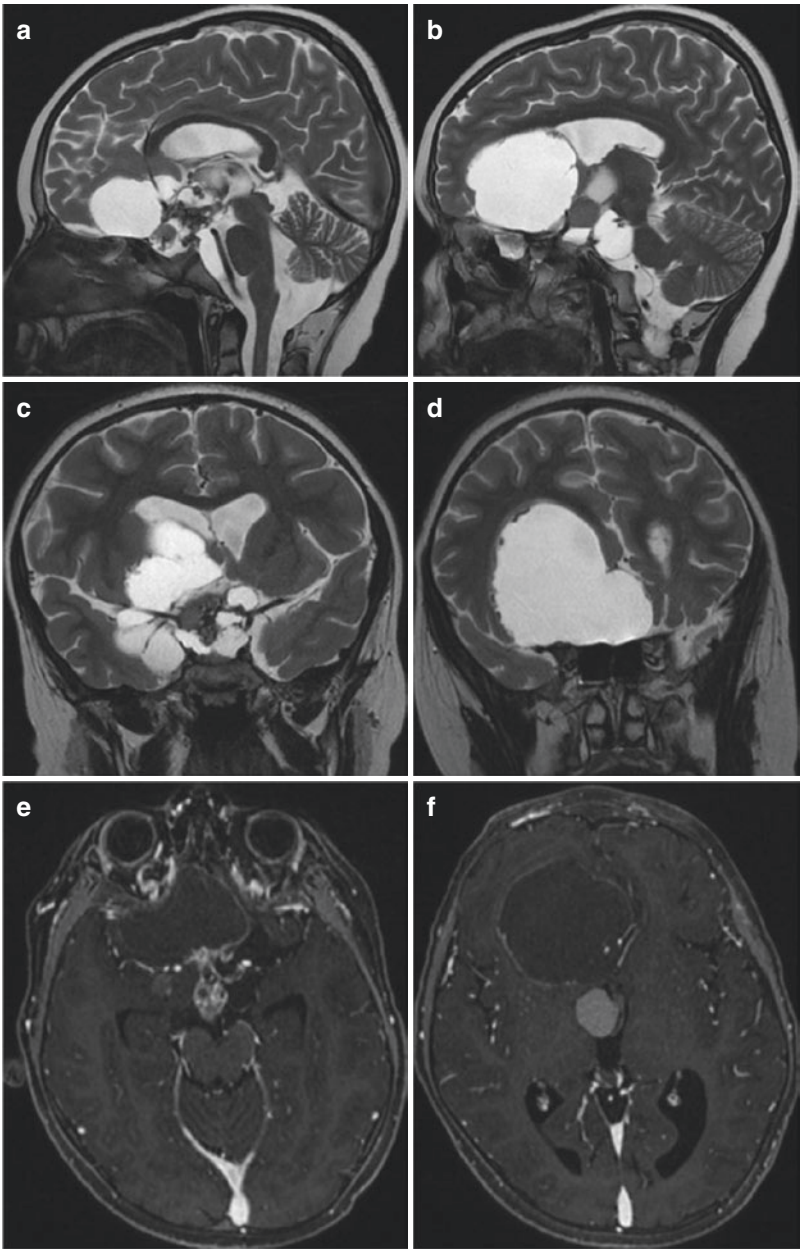

Fig. 4.1 Typical MRI appearance of AC in a 9-year-old boy. Note the large, multiple, and not homogeneous cysts (**a**–**f**), invading also the retroclival space of the posterior fossa (**b**). The solid portion is extended from the sellar/suprasellar region to the third ventricle, making the hypothalamus not recognizable (**a**) and the third ventricle visible only in its posterior part (**f**). An encasement of the Willis' circle is present (**c**). After gadolinium administration, an irregular enhancement of the solid portion and a thin enhancement of the wall of the major cyst can be appreciated (**e**, **f**). Because of the mass effect, especially due to the greater cyst (**d**), a biventricular hydrocephalus results (**b**, **c**)

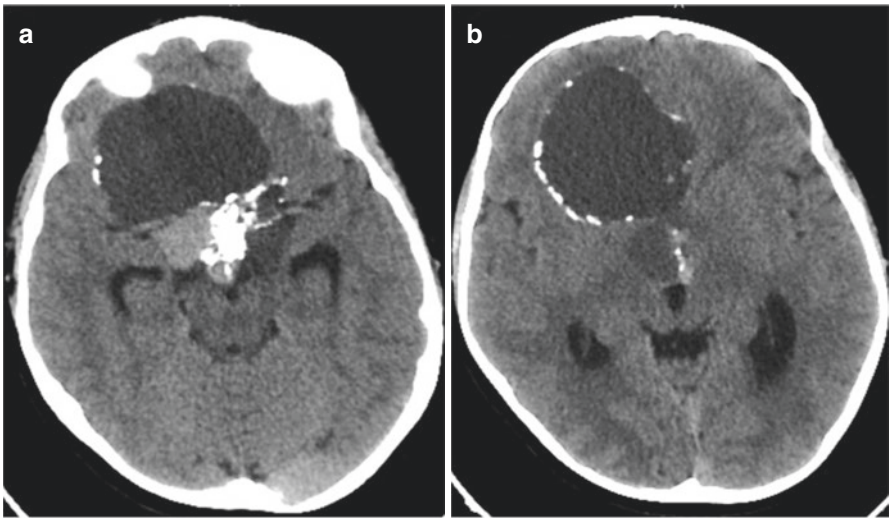

Fig. 4.2 CT scan of the same case in Fig. 4.1. Note the irregular appearance of the cysts and the gross calcifications in the solid portion (**a**) and along the wall of the major cyst (**b**)

3. The aforementioned aspects make the surgical management of AC challenging. The gross total resection (GTR) of this tumor, which is still the most effective treatment option whenever possible to ensure the longest disease and progression free survival, is hard to be obtained [3, 6];
4. In spite of the apparently benign biological behavior, the risk of tumor recurrence is high even after GTR [3]. Moreover, AC can show an aggressive course with recurrence even after an appropriate surgical and adjuvant (radiation therapy) management [7];
5. A solid multidisciplinary team is needed for a proper management of the patients affected by AC, either in childhood and adulthood, namely because of the possibly permanent posttreatment deficits, which range from the hormonal to the visual, neurological, and cognitive ones. Moreover, successful surgery can be complicated also by unusual events, such as vasospasm in case of huge cyst removal [8].

In this chapter, the latest advances in the knowledge and the management of cystic AC are addressed, focusing onto the pertinent literature as well as on the authors' experience. The first part of the article is dedicated to the most important new insights from the base research. Actually, to improve the knowledge of such a complex tumor is mandatory to enhance its treatment, looking also for possible target therapies. Under a biologically and molecular point of view, indeed, AC is a surprisingly rich tumor. The second part encompasses the progresses in the management strategies.

4.2 Basic Research

4.2.1 CTNNB1-WNT–β-Catenin

The dysregulation of WNT/β-catenin pathway is typical of AC, being observed in 57–96% of cases [9]. The WNT pathway is necessary for the organ formation during the embryogenesis and for maintaining the stem cells in adulthood, while the β-catenin is a key protein among the WNT pathway encoded by CTNNB1 gene [10, 11]. More in details, β-catenin is a cytoplasmic protein whose role is to control gene transcription and cell adhesion and migration. Somatic mutations in exon3 of CTNNB1 gene are hallmarks leading to lack of regulatory residues of the β-catenin protein stability. Following such modifications, β-catenin tends to accumulate inside the cells as a result of lacking β-catenin destruction complex formation (via alterations of serine and threonine residues at phosphorylation sites of GSK-3β) [12, 13]. Cytoplasmatic increase in β-catenin levels leads to its translocation into the nucleus where interaction with transcription factors, as lymphoid enhancer–binding factor 1/T-cell-specific transcription factor, takes place. Those interactions stimulate cell proliferation and migration through the expression of the actin bundling protein fascin-1 and activation of WNT pathway [9]. Such a condition leads to a growth factor signaling disruption and eventually to an increased expression in epidermal growth factor receptor (EGFR), vascular endothelial growth factor (VEGF), fibroblast growth factor (FGF), growth hormone (GH) receptor, and insulin-like growth factor (IGF)-1 receptor (IGF-1R), thus explaining the invasion properties of AC cells [14, 15].

The β-catenin accumulation has been shown also by immunohistochemical studies demonstrating how, though tumor cells show normal membranous expression of β-catenin (despite carrying CTNNB1 mutations), not all tumoral cells but, rather, only clusters of them present the β-catenin accumulation [3, 13, 15–17]. Only this small population of cells would be responsible for AC growth and proliferation [18].

Animal studies depicted the role of β-catenin-accumulating cell clusters as a control tower for AC cells. In these experiments on murine models, a degradation-resistant (activated) form of β-catenin is expressed in either Rathke's pouch derivatives (Hesx1Cre/+/Ctnnb1lox(ex3)/+ mouse line; AC embryonic model) or Sox2-expressing adult pituitary stem cells (Sox2CreERT2/+/Ctnnb1lox(ex3)/+ mouse line; AC inducible model) [19]. Clusters of this β-catenin would act in a paracrine manner by secreting promoting factors or inflammatory modulators as SHH, FGFs, BMPs, TGFB1, IL1, IL6, and other chemokines. The described paracrine tumorigenesis mechanism is believed to be determined by β-catenin cluster cells' positivity for cellular senescence markers, such as viable but nonproliferative expression of cell-cycle inhibitors, increased lysosomal compartment, presence of DNA damage, and activation of a DNA damage response [3, 20]. These cluster cells are, thus, able to promote proliferation and invasion of the nearer AC cells improving at the same time their pro-tumorigenic microenvironment. Further corroboration of the importance of senescence in AC came from the upcoming evidence of efficacy of 'senolytics' drugs in reducing tumorigenic potential [3, 21].

Despite the centrality of the WNT/β-catenin signaling in AC development, no current targeted treatment options are available yet. In adults, non-CNS tumors' inhibition via reagents such as XNW7201, CGX1321, and RXC004 is reported in ongoing trials, but there are no data on children yet also because of the concerns on the possible off-target effects [9]. However, the CTNNB1 mutation remains an important prognostic factor, pointing a higher risk of recurrence [22]. The recent study by Zhu et al. actually confirmed that the cyst components in AC with CCTNB1 mutation show more aggressive radiological characteristics than in the wild type [23]. These radiological characteristics are: presence of multiple cysts (vs. single cyst), irregular shape of the cyst (vs. regular shape), hypointense signal of the interior cyst on T1-MRI (vs. hyperintense), enhancement of the cyst wall after gadolinium (vs. missing enhancement), and adherence to the optic chiasm (vs. no compression on the optic chiasm).

4.2.2 Inflammatory Mediators

Differently from the WNT/β-catenin pathway, which is crucial to understand the ontogenesis of AC but still with a limited role for its treatment, the inflammatory response that AC can generate plays a promising role not only to explain the tumor development and progression but also to find possible therapeutic targets. Both AC cystic and solid components, indeed, express various cytokines, chemokines, and inflammatory mediators, which can be involved in various cancer cells activities [24]. Therefore, the link between immune response and AC raises a great interest in the scientific community just because of the potentially wide field of therapeutic options that it opens [9, 14, 19, 25].

According to immunohistochemical and proteomic studies, the composition of cystic fluid appears to be characterized by a rich spectrum of well-known cytokines. Actually, some studies highlighted the presence of high levels of cyst fluid IL-6, IL-8, CXCL1, and IL-10, while other studies reported on high levels of tumor necrosis factor as well as inflammasome-like patterns triggered by the cholesterol crystals typically present in AC [19, 26]. The aforementioned studies also pointed out an overexpression of immunosuppressive factors (IL-10, indoleamine-pyrrole 2,3-dioxygenase and galectin-1) as well as programmed death ligand 1 (PD-L1) [14, 15, 19, 21, 26, 27].

The proteomic analysis, performed onto AC cystic fluid with high-performance liquid chromatography and mass spectrometry, usually shows high levels of inflammatory proteins [28]. In the authors' group experience, α-defensins 1–3 were the first of such proteins to be detected [29]. Human α-defensins are contained in the azurophilic granules of neutrophils, working as antibacterial and antiviral factors. Increased levels can be observed in the saliva of patients with oral squamous cells carcinoma and in the plasma of patients with sepsis. The high levels observed in AC cystic fluid would suggest no blood barrier disruption for the cyst formation, since

the serum levels of defensins are very low. The preoperative high levels of α-defensins we found would therefore indicate a role of inflammation in stimulating the secretion of cyst fluid by the epithelial cells of the cyst wall, while the decrease of defensins in the postoperative period would account for the reduced fluid production and the cyst shrinkage [29]. As further support to this hypothesis, the same study demonstrated that a treatment with interferon-α (an antiviral protein produced by peripheral leukocytes) is able to reduce the defensins levels through an antitumoral effect on the squamous epithelial cells, an immunomodulatory action on the recruitment of inflammatory cells, and an antiangiogenic activity. Moreover, Jokonoya et al. reported on the antibacterial properties of AC cyst fluid mediated by α-defensins [30]. Their study started from the evidence of a low rate of infection in exposed Ommaya reservoir after skin breakdown in patients with AC. The α-defensins' immune response of AC cyst fluid was demonstrated against Gram positives, but not against Gram negatives. A possible explanation for this discrepancy is that some components of the cystic fluid, like magnesium, alkaline phosphatase, blood urea nitrogen, glucose, urea, and creatinine, are more likely to interfere with Gram-positive bacteria than Gram-negative ones. Finally, other studies depicted how interferon-α treatment leads to a decrease not only in the cyst fluid concentrations of α-defensins, but also in the cyst volume (tumor shrinkage). Such a fluid volume reduction appears to be mediated by the activation of the Fas apoptotic pathway [31, 32].

The extensive proteomic analysis on AC cystic fluid, obtained by integrating bottom-up and the top-down approach, allowed us to find several other inflammatory or similar proteins, thus leading to the hypothesis that AC is an "inflammatory" tumor [28, 33–35]. The most important among them are: (1) Apolipoproteins, possibly involved in the cyst fluid formation and characterization. Apolipoprotein C-I (synthetized in the liver and secreted in the plasma but expressed also in the brain) is actually necessary for the cholesterol and triglycerides' removal from the tissues. Apolipoprotein A-I, on the other hand, is involved in the inverse cholesterol transport and cholesterol esterification and is characterized by anti-inflammatory and antioxidant properties; (2) α1-antichymotrypsin, possibly involved in the production of the cyst fluid. Secreted glycoprotein of the serpin family, this protein acts as inhibitor of chymotrypsin-like serine proteases and mast cell chymasesm, thus having a role in inducing the acute phase of inflammation (it is upregulated in CSF of patients with glioblastoma); (3) α2-HS-glycoprotein (or fetuin A), possibly involved in the cyst fluid formation and characterization. It is a serum glycosylated heterodimer involved in the tissue mineralization and in the processes of pathological mineralization. By binding of small clusters of calcium and phosphate, it can act as pro-inflammatory, pro-calcification, and signaling protein; (4) β-thymosins, possibly involved in the progression of AC. β-Thymosins are a family of 16 peptides first isolated from the calf thymus. The isoform β4 and β10 are abundant in extracellular fluid because of a cell damage or a secretory process. In cystic AC, the isoform β4 (Tβ4) is 10 times more expressed than β10. Tβ4 is a major G-actin-sequestering molecule in mammals, regulating the organization of the cytoskeleton and thus influencing the cell differentiation, migration, and morphogenesis. In

addition, it promotes angiogenesis, tissue repair, and tumor growth. The upregulation of Tβ4 would be able to promote the motility and invasion of AC cells by activating the matrix metalloproteinase 7 and by activating the WNT/β-catenin pathway [36, 37].

The key role of inflammation in the genesis/progression of AC has been confirmed by several other studies demonstrating an overexpression of inflammatory mediators both in the solid and in the cystic component [19, 25–27, 38–41]. In summary, these studies show that: (1) The cyst fluid has a high concentration of cytokines and chemokines (namely, IL-6, IL-8, IL-10, CXCL1) that correspond to the transcriptomic analysis of the solid counterpart; (2) IL-6, in particular, seems involved in inducing the inflammatory reaction surrounding the tumor. AC is able to produce IL-6 and its receptor (IL-6R) and glycoprotein 130 which are useful also for the AC cells migration; the block of IL-6 with monoclonal antibody (tocilizumab) significantly decreases AC cells migration; (3) The transcriptomic analysis, on the other hand, demonstrates high levels of several inflammatory factors (FGF, TGFB, and BMP families) as evidenced by immunostaining against the phosphorylated proteins pERK1/2, pSMAD3, and pSMAD1/5/9. The inhibition of the MAPK/ERK pathway with trametinib (a MEK inhibitor) reduces the proliferation and increases the apoptosis in AC cultures; (4) On these grounds, given this inflammatory role in AC genesis and progression, several targets for inflammation blockade are under investigation. As mentioned, one of the more interesting targets is IL-6, whose blockage was proven efficient in systemic illnesses such as juvenile idiopathic arthritis, multicentric Castleman disease, and CAR (chimeric antigen receptor) T-cell-induced cytokine release syndrome. Tocilizumab and siltuximab are indeed human monoclonal antibodies binding both IL-6 receptor and IL-6, thus hindering IL-6 from exerting its proinflammatory effects. In addition, antagonists of pro-inflammatory cytokines such as IL-8 and CXCL1 have also shown therapeutic potential in preclinical human cancer models. Among the potential drugs, BX-IL8, an antibody that inhibits IL-8 function, is supposed to be useful in countering tumor growth in various preclinical studies, even though no definite data are available yet, thus preventing clinical application at the moment [42, 43].

4.2.3 Other Factors and Pathways

4.2.3.1 Programmed Cell Death Protein 1/Programmed Death-Ligand 1 (PD-1/PD-L1)

AC has been demonstrated to show tumor cell-intrinsic PD-1 expression in whorled epithelial cells with nuclear-localized β-catenin and to express PD-L1 by tumor cells comprising the cyst lining [44]. PD-1 and PD-L1 could be potential targets since the epithelial cells exhibit elevated target for rapamycin (mTOR) and mitogen-activated protein kinase (MAPK) signaling.

4.2.3.2 Sonic Hedgehog Pathways (SHH)

SHH was considered a promising source for target therapy because it plays a role in the regulation of cell differentiation and proliferation, and because it is involved in the development of the Rathke's pouch [45]. Actually, an upregulation of SHH signaling has been found in AC [46]. Nevertheless, the studies on animal models discourage the use of SHH inhibitors for the treatment of AC. Indeed, visomodegib, a SHH pathway inhibitor, produces a significant reduction of the median survival in murine models and increases the tumor cells proliferation in AC human cultures [47].

4.2.3.3 BRAF

BRAF mutations, although peculiar of papillary craniopharyngioma (PC), can be encountered also in AC. BRAF gene encodes for B-Raf, a cytosolic kinase in the mitogen-activated protein kinase (MAPK) pathway. The mutation on V600E point raises great interest about the possible therapeutic implications. Indeed, in tumors like melanoma, targeted therapies against this variant of mutated BRAF showed a significant efficacy, modifying completely the prognosis and the treatment protocols [3, 15]. An interesting report on BRAF role in AC has been provided by Petralia et al. who made a thorough proteomic analysis [48]. Accordingly, even though the BRAFV600E mutation is rare in AC in comparison with PC, the proteomic changes in non-mutated AC still resemble those of BRAFV600E low grade glioma tumors. Such a finding would suggest a hypothetical benefit of chemotherapy against BRAF mutation, despite the presence of the gene alteration.

4.2.3.4 Retinoic Acid Receptors (RARs)

As confirmation of the relatively high number of molecular alterations that it can show, AC also presents immunoreactivity to RARs, namely RARa, RARb, and RARg, the RARg/RARb immunoreactivity ratio being strictly related to the AC recurrence risk. RARs' role is to drive cell maturation and differentiation; therefore, alterations in their pathways might result in tumorigenesis. RAR isotypes' expression seems to be associated with a higher recurrence rate. Such a finding was related to the expression of specific cathepsins, which are proteases necessary for cell turnover. Cathepsins D, B, and K seem to be most important cathepsins involved, which are already known to have a role in neurodegenerative diseases [14, 15, 49–51].

4.2.3.5 BMP and MMPs

Bone morphogenetic protein (BMP) and matrix metalloproteinases (MMPs) pathways are involved in the aforementioned paracrine growth-related signaling [15, 18]. Those proteins are downstream effectors of the WNT/β-catenin-mediated transcription, thus being abnormal in function in CTNNB1 mutations. AC cells highly

express both BMP2 and BMP4, which result in the formation of the intracystic calcic components. Alterations in MMPs encoding, on the other hand, lead to a modification in the extracellular environment resulting in an enhanced tumor invasive capacity.

4.2.3.6 VEGF and HIF-1α

Vascular endothelial growth factor (VEGF) is a key regulator in angiogenesis being involved in many tumor growths, while hypoxia inducible factor 1α (HIF1α) is a transcription factor often altered affected in cancer cells where the cellular response to hypoxia is downregulated. With regard to AC, there are conflicting results about the role these factors could play in the tumor recurrence. Actually, Liu et al. documented their high levels in recurrent AC, while Xu and colleagues did not experience this phenomenon [52, 53].

4.2.3.7 Survivin

Survivin, which is an antiapoptotic protein, seems to be involved in AC tumorigenesis. In fact, this protein was found to be selectively increased in AC compared to normal brain [54]. In addition, survivin is present in higher levels in recurrent ACs compared with nonrecurrent ones [14].

4.2.3.8 Ep-CAM

Epithelial cell adhesion molecule (Ep-CAM) is a cell-to-cell adhesion molecule whose altered expression can be found in several various systemic tumors as well as in the AC stellate reticulum cells and whorl-like arrays. This finding is considered to be associated with higher risk of AC recurrence [14, 55].

4.2.3.9 Osteonectin

Osteonectin is a protein that can be seldom involved in metastatic cancers. Some studies suggested its role in organizing the stromal tissue surrounding AC cells facilitating their diffusion [14, 56].

4.2.3.10 P53 Protein

p53 is a well-known cell-cycle regulatory protein and tumor suppressor most often involved in tumorigenesis [57]. Its role in AC was largely debated, being initially denied and, afterwards, reconsidered based on new evidences that seem to correlate p53 level increase with the AC recurrence risk: the higher the p53 levels, the higher the chance to have a more aggressive AC [14, 58].

4.2.3.11 Ki-67

Ki-67 is a nuclear protein commonly used as a proliferation marker [59]. Similarly, to what happen with p53, increased Ki-67 expression appears to be common in aggressive AC. Prieto et al. suggested that high Ki-67 expression can be considered as a reliable marker in predicting aggressive behavior and recurrence risk of AC [14, 60].

4.3 Treatment Options

4.3.1 Evolution of the Surgical Management

Being deep-seated tumors, embracing vital neural and vascular structures, AC has been representing one of the major challenges for neurosurgery over the last century. Nonetheless, progress and diffusion of microsurgical techniques made these lesions increasingly approachable, leading to a progressive adoption of aggressive resective strategies. This was motivated by the traditional belief that the "benign" histology of craniopharyngioma made it a curable disease, so that it was worth taking the risks of radical excision. This trend, culminating in the 1990s, was reinforced by the increased availability of hormonal substitutes, which permitted to balance the postoperative endocrinological and electrolyte disturbances that were one of the dreaded consequences of aggressive surgical approaches [61, 62]. On the other hand, however, thanks to the accumulating evidence gathered through large follow-up series, the long-term outcome of aggressively treated patients (especially those with hypothalamic involvement) was often showed to be disappointing because of the relatively high rate of recurrence (in at least 17.6% of patients after microsurgical gross total resection) and the inveterate consequences of multihormone imbalances (with up to 70% of patients developing diabetes insipidus and 30% obesity or hyperphagia) [61, 63–65]. Therapeutic approaches thus started to shift towards the experimentation of less invasive strategies that could provide a good balance between disease control and perioperative and long-term morbidity.

Owing to its peculiar characteristics, AC has especially benefited from this trend, with the introduction of dedicated treatment options that promise to reach such a balance [61, 62, 66, 67]. Indeed, the search for an equilibrium is favored, on one hand, by high recurrence rates of AC (up to 47%) and, on the other hand, by the significant decompression that can be obtained with less efforts by employing treatment strategies that are less invasive and well-tolerated [66, 68]. The second phase in the history of AC treatment has thus seen the diffusion of a less radical surgical philosophy, with the affirmation of maximal safe resection followed by adjuvant radiosurgery; in parallel, tumors with predominant cystic components started to be treated with minimally invasive catheter drainage (with or without the intracystic administration of therapeutic substances), eventually followed by irradiation of the remaining solid tumor components.

In the last years, the accumulating data on long-term outcome of patients treated with minimally invasive strategies, and especially on the long-term consequence of radiation treatment in children [69], have promoted a resurgence of interest towards surgery, with a special look towards novel approaches that could allow for the benefits of substantial/complete resection in face of lower complication rates when compared to traditional microsurgical approaches.

In the next paragraphs, an outline of the different treatment options, which have been developed or enhanced in the last years to offer new strategies to deal with this complex disease, is provided. An important limit of the literature concerning AC is the difficulty in making comparisons among the different studies. First of all, the definition of disease progression varies widely, with different authors attributing different meanings to cyst regrowth [70]. A second bias is related to the fact that the data are mainly referred to patients treated in an elective setting, even if also after an emergent treatment (e.g., AC associated with acute hydrocephalus) there is room for planning the surgical steps in order to obtain a good balance between immediate treatment efficacy and long-term outcome. A further limitation is generated by the still existing discussion about the use of microsurgical (craniotomic) versus endoscopic (transsphenoidal) approaches. Microsurgery offers a wider exposure of the surgical field and a large space for the surgical maneuvers, while endoscopy grants a minimally invasive approach with a better visualization of hidden angles. Therefore, it is about two different techniques to be used for different types of patients. Since the goal of the present chapter is the management of cystic AC, the advances in the endoscopic approaches are reported because they have resulted particularly useful in this subset of patients also due to the double option provided by the transsphenoidal and the transventricular option.

4.3.2 Endoscopic Approaches

Compared with microsurgery, whose evolution started much earlier, the endoscopic approaches have showed huge progresses in the last two decades and are gaining more and more consensus in the management of AC [71]. The success of endoscopic techniques is favored by the possibility to obtain a significant shrinkage of the (often huge) cystic component of the tumor with a poorly invasive approach, which is easily used even in emergency. Should tumor remnants be left behind or the tumor regrowth, the treatment can be completed with adjuvant therapies. Indeed, endoscopic techniques can be used alone and in combination with each other or with other treatment modalities. A recent development of endoscopic surgery, designed to decrease complications and enhance effectiveness, is represented just by the combination of endonasal and transventricular endoscopy for the management of very large AC. Deopujari et al. reported on 18 cases (16 children and 2 young adults) out of a series of 125 cases who were treated first with a transventricular endoscopic procedure to decompress the cystic component, followed by EES 2–6 days later [72]. This strategy allowed the patients to improve after the cyst

decompression (often also because of relief of hydrocephalus) and to undergo the remaining tumor removal in an optimal setting. GTR was actually obtained in 84% of these patients, with only two cases of permanent diabetes insipidus and no cases of morbid obesity.

4.3.2.1 Endonasal Transsphenoidal Surgery

The use of endonasal endoscopic surgery (EES) in the pediatric population has significantly expanded over the last decade, as documented by the parallel increase in the number of published data on this technique; more than one third of the papers including the keywords "transsphenoidal" and "children" have been published in the last 5 years. This growing interest has also been reflected in the field of craniopharyngioma treatment, motivated, on one side, by the resurgence of surgery (as opposed to conservative treatments) and, on the other, by the need to find alternative approaches to the traditional microsurgical treatment.

Some peculiarities of pediatric patients were traditionally deemed as potential obstacles to EES (i.e., small nostrils and nasal cavities, insufficient pneumatization of the sphenoid bone); through the accumulation of experience (and thanks to the refinement in endoscopic instrumentation), it has been shown that these drawbacks can be easily overcome [71, 73]. In fact, endonasal endoscopic approaches have been shown to be a feasible and safe alternative for the treatment of pediatric craniopharyngiomas. In 2011, Elliott and colleagues published a systematic review comparing EES and traditional trans-frontal surgery (TFS), gathering data on 2773 microsurgically treated patients vs. 373 EES cases, with a special focus on pediatric patients [63]. In spite of the obvious limitations of such a study (retrospective analysis, inherent selection bias), the evidence showed that EES was associated with good postoperative outcome and lower rates of complications with respect to traditional surgical approaches. Indeed, a 72.1% vs. 60.9% GTR, 8.0% vs. 17.6% recurrence after GTR, 85.5% vs. 47.7% vision improvement, 2.3% vs. 13% vision deterioration, 3.1% vs. 9.4% neurological morbidity, and 23.9% vs. 69.1% postoperative diabetes insipidus were reported; the rate of postoperative obesity/hyperphagia was the same for both types of treatment (32%). These observations have been confirmed by other large-scale studies, as the national retrospective series published by Lin and colleagues in 2017, outlining the outcome of the 314 craniopharyngioma patients treated in the USA in 2003, 2006, and 2009 [74]. When compared to TFS, EES was associated with lower rates of diabetes insipidus (38% vs. 69%), lower rates of panhypopituitarism (5% vs. 8%), cranial nerve deficits (1% vs. 6%), postoperative stroke (2% vs. 5%), seizures (0 vs. 12%), and death (0% vs. 1%). As expected, there was a statistically significant association between EES and shorter hospital length-of-stay (LOS), EES patients having a 6.6-days mean LOS (median 4 days), while TFS patients a 12.3-days mean LOS (median 10 days). However, cerebrospinal fluid (CSF) leak affected 19% EES versus 4% TFS resections, thus confirming this complication as the weakest aspect of this kind of surgery.

The view offered by EES is advantageous over TFS especially when dealing with AC with sellar extension and/or origin from the pituitary stalk (as often seen in children), allowing a good direct visualization of pituitary gland and stalk, optic pathways, and related feeding vessels. For this reason, EES was originally reserved to predominantly intrasellar craniopharyngiomas. In recent years, however, the alternative viewpoint on suprasellar structures (and hypothalamus itself) provided by EES has been increasingly exploited to approach lesions with suprasellar extension or even purely extrasellar location [72, 75–79] and recurrent tumors [78]. Reported outcomes of these more extensive approaches are generally good, and even if they appear less optimal when compared to the mentioned general data on EES, they still compare favorably with TFS. GTR rates actually range from 45 to 85% (similar to TFS) [78, 79], and complication rates as follows: new onset diabetes insipidus from 31 to 63%, new anterior pituitary dysfunction between 40% and 80%, visual deterioration between 0 and 26%, and new onset neurologic deficits between 0 and 10% [75, 78, 79]. The number of published cases is still limited, and the heterogeneity of data suggests that there is still room for improvement with increasing expertise. Indeed, the complication rates are still too high in these instances. It is interesting to note that, according to the blind post-hoc survey performed by Jeswani and colleagues among the series of extensive EES approaches, all their EES and TFS cases could have been approached by both routes according to the preference of the different surgeons, somewhat attenuating the selection bias but also suggesting the surgeons' preference and expertise as a way to reduce complications [79].

If the transcranial microsurgical route still maintains a remarkable value in the AC management, the microsurgical sublabial access (SA) is almost abandoned in favor of EES. Especially in children, the authors' personal experience on 51 children (34 undergoing EES and 17 undergoing SA) demonstrated several statistically significant advantages of EES over SA that can be summarized as follows [73, 80]: (1) shorter mean LOS (4 vs. 5 days); (2) lower transfusion rate (20% vs. 60%); (3) lower need of nasal packing (20% vs. 100%); (4) better quality of the early postoperative course as measured by a 0–8 pain scale (2.7 vs. 4.2 mean value). The 2 nostrils-4 hands technique provided also a significantly better intraoperative view other than a poorer mucosal trauma and, in particular, a minor disruption of nasofacial bone structures that is important for the facial growth in children.

4.3.2.2 Transventricular Endoscopy (TE)

In approaching AC extending to the third ventricle, Hollon and colleagues developed a score to help in selecting patients who are candidates to transventricular endoscopic treatment [81]. According to their algorithm, lesions without hypothalamic involvement are candidate to surgical resection (EES or TFS), aiming at radicality whenever possible; lesions with hypothalamic involvement are treated with TE if predominantly cystic in nature or in absence of chiasmopathy. If chiasmopathy is present, lesions with hypothalamic involvement are preferably candidate to

surgical debulking. Aside from the predominantly cystic nature of tumors, the main criterion dictating the choice of an endoscopic versus open microsurgical approach was hypothalamic involvement, due to the high risk of endocrine disruption associated with open resection in these cases [64]. According to the TE technique, the tumor cyst lesion is approached and fenestrated superiorly through the foramen of Monro and then inferiorly (at the level of the floor of the third ventricle) by "passing through" the cyst and creating a third-ventriculostomy. The authors report good postoperative outcomes, with good cyst volume reduction and no patients developing postoperative hormonal imbalances or acute visual deficits; residual disease was managed with stereotactic radiosurgery (unfortunately, data on long-term follow-up are limited). Takano and colleagues have reported good long-term results in terms of disease control and endocrinologic function with TE cyst fenestration followed by radiosurgery for residual tumor tissue: the reported 5-year recurrence rate for the 9 treated patients was 14.6%; no endocrinologic or visual complications were observed [68].

One of the main risks of endoscopic cyst fenestration is represented by potential spillover of cystic fluid in the ventricular system, resulting in aseptic meningitis, even if it is difficult to quantify the real impact of this phenomenon on surgical practice [68, 82–84]. It is worth noting that the spillage of the fluid outside the cyst did not produce any ill effects both in the personal series and in that of other authors [85]. However, to drain the cyst content through an endoscopically guided catheter before fenestrating the cyst has been proposed as an easy and effective way to prevent this event [83].

As mentioned, TE can also be indicated as a first approach in patients developing symptomatic hydrocephalus due to third ventricular involvement. An endoscopic procedure, while less immediately available than the placement of an external CSF drainage, allows for both a rapid and reliable treatment of hydrocephalus while easing the way for an elective surgical step [68, 72].

4.3.2.3 Keyhole Endoscopic-Assisted Surgical Approaches

Strategies to deal with giant cystic craniopharyngiomas, which pose significant challenges to surgeons, have been repeatedly described in the literature [5, 86–88]. In such cases, an intracystic endoscopic approach can provide significant advantages, allowing to safely access impervious anatomical locations by "navigating through" the cyst. After strategical placement of an expanded burr hole (or minicraniotomy), the dura is opened, surgical route is explored and prepared microsurgically, and then an endoscope is introduced to access the lesion. There are reports of huge cases that have been successfully managed with an endoscopic approach alone by entering the cyst and promoting its collapse while removing its solid components [86]. It is interesting to compare such reports with almost identical cases managed through complex skull base approaches, e.g., trans-petrous route, with good results [5]. Both endoscopic-assisted and craniotomic experiences on such complex cases, however, are often based on case reports with missing data on long-term follow-up.

In cases that cannot be managed satisfactorily through endoscopic approaches alone, endoscopy can anyway be helpful in decompressing the cyst and allowing for a safer and easier microsurgical resection [87]. Moreover, as described below, transventricular endoscopy can be useful to optimally guide the positioning of an intracystic catheter, in order to obtain a good communication between the cyst cavity and the ventricular system and thus promoting both cyst collapse and continuous washout by CSF circulation. This can be followed by other treatments (such as radiosurgery).

4.3.3 Radiation Therapy (RT)

As previously mentioned, there is a solid experience with the use of RT for the adjuvant treatment of AC. The progressive adoption of radiosurgical techniques to treat tumor residue (or recurrence) has paralleled the trend towards a less aggressive surgical philosophy, encouraged by data supporting the non-inferiority of subtotal resection plus adjuvant radiation treatment versus gross total resection in terms of disease control [89–91]. In particular, according to the systematic review published by Yang and colleagues in 2010, the long-term outcome of GTR and STR + RT did not differ significantly, the 5-year PFS being 67% after GTR and 69% after STR + SR; and the 10-year OS being 98% after GTR and 95% after STR + RT [92]. Both groups had comparable mean tumor sizes and epidemiological data. The benefits of adjuvant radiation treatment after complete or incomplete surgical resection have also been confirmed by later reviews, which emphasized the low rates of postoperative endocrinological and visual complications [90]. Complication rate appears to be lower for patients treated by an adjuvant setting than in those treated for recurrence [89]. Table 4.1 summarizes the main case series published to date covering different radiation treatments [89, 93–97].

With respect to older radiosurgical techniques, which allowed for the targeting of spherical volumes (e.g., gamma knife), more recent techniques (such as proton beam therapy, or intensity-modulated radiation treatment) are able to precisely mold the irradiation target on tumor conformation, potentially allowing for an even lower rate of normal tissue injury (with reported visual morbidity rate 0–6% for cyber knife) [70, 90]. At the same time, the progressive adoption of frameless technologies has allowed for a better flexibility in dose fractionation [7, 89, 90]. A well-known limit of these treatments is the restricted accessibility due to high costs and the complex technological apparatuses required. Moreover, no significant differences on PFS have been demonstrated with different radiosurgical techniques [70]. For example, in the comparative case series dealing with proton beam therapy vs. intensity-modulated radiation treatment published by Bishop and colleagues, no significant differences between groups were identified in 3-year overall survival rate, cyst progression, and nodular progression [89]. It is worth noting, however, that the follow-up period was too short to formulate definitive comparisons.

Table 4.1 Summary of the main case series dealing with radiation treatment of craniopharyngiomas

Source (year)	N. of patients	Mean/ median age	Type (modality)	Mean/median follow-up (years)	Disease control at 10 years	Disease control at 20 years	RT-related morbidity (%)	Overall survival rate (years)
Rajan et al. (1993)	173	19	EBRT (adjuvant or primary)	12	83% (PFS)	79% (PFS)	Endocrine (50%); no new visual deficits	77% (10), 66% (20)
Kobayashi et al. (2005)	98	33.6 (mean)	GKS (adjuvant)	5	60.8% (PFS)	NR	Endocrine or visual (6%)	91% (10)
Tsugawa et al. (2020)	242	41 (mean)	GKS (adjuvant)	5	42.6% (PFS)	NR	Visual (2%), endocrine (4%), hypothalamic (0.4%); global 6%	82% (10)
Iwata et al. (2011)	43	44	CKS (adjuvant)	3	NR	NR	Endocrine (2%); no new visual or other neurologic disturbances	100% (3)
Harrabi et al. (2014)	55	37 (median)	FSRT (adjuvant)	10	92%	88%	No new endocrine, visual, or other neurologic disturbances after RT	83.3% (10), 67.8% (20)
Bishop et al. (2014) (a)	21	9 (median)	PBT (adjuvant)	2.75	NR	NR	Endocrine (76%), visual (5%), vascular (10%), hypothalamic (19%)	94.1% (3)
Bishop et al. (2014) (b)	31	8.8 (median)	IMRT (adjuvant)	8.8	67.8% (cyst control)	NR	Endocrine (77%), visual (13%), vascular (10%), hypothalamic (29%)	96.8% (3)

CKS cyber knife surgery, *EBRT* external beam radiation therapy, *FSRT* fractionated stereotactic radiation treatment, *GKS* gamma knife surgery, *IMRT* intensity modulated radiation treatment, *NR* not reported, *PBT* proton beam therapy, *PFS* progression free survival, *RT* radiation treatment

In spite of these technological advances, AC continues to represent a special challenge also when dealing with RT. In contrast with solid craniopharyngiomas, cystic tumors show an unpredictable response to RT, and the behavior of the solid and cystic components of mixed tumors during treatment appears to be independent from each other [7, 91, 98]. Indeed, the shrinkage of the solid part can often be accompanied by stability or increase of the cyst volume (in up to 40% of patients) [89, 99–101]. This causes both a modification of target conformation over the course of treatment and an increase in the radiation dose required to cover the cyst volume, which besides is relatively insensitive to radiation [89]. The integrated management of the cyst by means of a catheter with reservoir (see below) would be then useful to make radiation treatment more effective by reducing the volume of the cystic component [99, 101]. There could be also room for the development of protocols combining RT and intracystic therapies. This would allow to effectively target all components of the tumor.

The management of patients showing recurrence after RT is complex. Considering the potential number of surgical procedures that patients may undergo after the first recurrence, it has been proposed that, at least in this context, GTR should remain a goal [102]. This supports the reemerging tendency towards radical surgical approaches in selected cases, as described above. Additional treatment strategies with subcutaneously administered interferon have also been proposed to slow the course of the disease in these patients, in order to delay the surgical intervention (see below).

4.3.4 Specific Management Options for the Cyst

4.3.4.1 Intracystic Catheter

One of the major changes in the treatment of AC has been the larger use of approaches specifically focused on the management of the cystic component. The most direct among them is the cyst drainage through an intracystic catheter connected to a subcutaneous reservoir (Rickham or, more frequently, Ommaya reservoir). This simple tool allows a rapid cyst decompression with symptom relief and repeated percutaneous cyst aspirations in case of intracystic fluid re-accumulation. Such an approach is considered as a transient measure in (quickly) growing AC or in patients in poorly clinical condition to gain time for a more “radical” treatment. However, quite surprisingly, good results in purely cystic AC have been reported after the stereotactic placement of the catheter alone. More in details, up to 70% of patients did not require further treatments after a follow-up longer than 7 years [103] and the progression free survival did not differ significantly from that of microsurgically treated patients [66]. Two thirds of the patients in the series by Moussa and colleagues were younger than 16 years, thus pointing out the need for even longer observation to confirm the good published results [103], while the patients treated stereotactically in the series by Rachinger and colleagues were

considerably older (median age: 54 years) [66]. Similar results have been obtained also with different approaches to implant the catheter for the cyst aspiration, e.g., with endoscopic guidance [104].

A proper placement of the catheter is mandatory to achieve good results. A key point is represented by the position of the catheter holes, which should span across the cyst wall, thus ensuring a continuous drainage of cystic fluid into CSF spaces (cisterns and/or ventricles). To enhance this effect, some authors proposed to modify the catheter by placing additional holes [105] and to pierce through the cyst from wall to wall, creating a double communication with both the ventricular system and the basal cisterns [66].

When dealing with mixed or anatomically complex AC, the "catheter plus reservoir" option can be utilized as part of a more elaborate surgical strategy. For example, preoperative stereotactic reservoir system placement and staged cyst aspiration have been used in patients with mixed lesions candidate to microsurgical resection, facilitating surgery and reportedly obtaining lower rates of postoperative hormonal and electrolyte imbalances with respect to microsurgical resection alone [88]. Placement of reservoir systems has also been presented as a valuable adjunct to radiosurgical treatment [99, 101]. As mentioned, cystic tumors are challenging radiosurgical targets, partly due to the inhomogeneous radiation sensitivity of their components and partly because of the often-huge size reached by the tumor. Therefore, preemptive stereotactic cyst drainage facilitates radiosurgery and allows an optimization of conformational and dosimetric parameters by removing the least radiosensitive part of the mass and by reducing the irradiation field [101]. On the contrary, catheter drainage for cyst recurrence after radiosurgery has shown disappointing results, with most patients eventually requiring further treatments [102].

Catheters can be also left in place after transventricular endoscopic resection of lesions abutting the ventricular system [105, 106]. With respect to stereotactic guidance (neuronavigation), catheter placement under direct visualization provides the theoretical advantage of a tailored targeting, thus offering a more effective and persistent drainage of the cyst fluid [104, 106–108]. This approach would be especially useful for granting an optimal communication of the catheter with both the cyst and ventricular system, as already mentioned. For this reason, it has also been proposed for tumors without direct involvement of the third ventricle or without associated hydrocephalus [109]. Recently, robotic guidance of stereotactic procedures has been used as another means to improve targeting accuracy compared with standard neuronavigation [99, 101]. In these reports, frameless navigation with laser-assisted registration of anatomical landmarks provided guidance to a robotic instrument holder that was precisely brought to the desired trajectory.

On the other hand, at least according to past studies, a significant difference in terms of complication rates among the different techniques for catheter placement has not been observed [110]. In fact, a rate of complications (misplacement or contrast leakage) of 16.3% has been reported regardless the surgical modality. Such a result was explained considering variations in resistance and elasticity of the cyst wall as the decisive factor affecting the surgical outcome. Independently from the

surgical technique, actually, the increased resistance of the cyst wall could determine the sliding of the catheter over the cyst rather than its actual perforation [110].

4.3.4.2 Beta-Emitting Radionuclides

Intracystic injection with β-emitting sources (such as Yttrium^{90}, Rhenium^{186}, Aurum^{198}, or Phosphorous^{32}) has been used as another means to directly target neoplastic tissue with sparing of the surrounding neural and vascular structures. The 3–4 mm penetration width of beta-radiation makes it especially effective in damaging the cyst wall, while solid tumor nodules are less affected. Their use still raises some controversies because of the feared side effects and, in particular, the safety principles required for their transport, handle and disposal, and the poor availability of the radioisotopes, which reduce their application.

Phosphorous^{32} (P32) is generally preferred over Yttrium^{90} and other radionuclides due to its longer half-life, lower required dose, and lower half-value tissue penetrance (0.8–1.1 mm vs. 1.1–2.2 mm) [111, 112]. Brachytherapy with intracystic injection of P32 has been proposed as a relatively safe means of providing selective radiation damage to tumoral tissue. When used alone, however, this treatment has shown a partial effectiveness, with short-term induction of cyst shrinkage in 70–80% of patients but significant rates of recurrence, especially due to the limited efficacy of P32 on the solid part of the tumor and on the collateral cysts [113–115]. Also, case series reported good results (75% rate of disease control), but mainly after a short follow-up period (mean follow-up: 48.6 months) [116].

The observed endocrinological and visual sequelae after intracystic irradiation vary widely, even if the global incidence of side effects appears to be generally as low as <5% [85, 114–116]. Long-term collateral radiation damage to vascular and neural structures cannot be excluded [85, 111]. According to Kickingereder et al., who reported on one of the largest series (53 patients), a permanent neurological side effect was observed in 3.9% of cases, while the rate of deterioration in hormonal functions was 2% [112]. Therefore, the complication risk seems to be competitive with other treatments.

With regard to another feared risk of radioactive drugs, which is represented by the spillover of the radioactive agent itself into the cerebrospinal fluid, it is difficult to quantify the incidence of this phenomenon (which anyway appears to be anecdotical) and to evaluate its real toxic impact [117]. In order to improve the management of the treated patients, some authors have presented experimental biochemical and physical means of monitoring radioactivity diffusion through the evaluation of radioactivity in biological patient samples and the use of gamma cameras [117, 118].

The future in this field could be represented by the identification of the responders to radionuclides, in order to propose such a limited resource only to the best candidates. This way has been followed by Hu et al. who recently reported on an interesting study on P32 interstitial therapy for recurrent craniopharyngiomas (both AC e PC) [119]. In details, the authors investigated 32 patients with recurrent craniopharyngioma treated by P32 colloid interstitial radiotherapy. The tumor imaging features of the

patients were classified into 4 types according to the thickness of the cyst wall: I-purely cystic with thin wall; II-mainly cystic (solid part <25%) with one or more cyst, thin wall; III-as above but with thick wall; IV-partially cystic, multiple cysts, thick wall. The expression of vascular endothelial growth factor (VEGF)/vascular endothelial growth factor receptor-2 (VEGFR-2) was evaluated with immunohistochemistry before radiotherapy. Only VEGFR-2 expression was associated with the imaging features of tumors. As a final result, craniopharyngiomas with thin cysts (type I and II) and expression of VEGFR-2 (clues of high radiosensitivity) showed a good response to P32 treatment, while types III and IV (no VEGFR-2 expression) did not.

A further means to improve the control of the disease and to limit the radiation exposure is to identify other therapeutic substances for intracystic injection. The crucial point advancing the search for nonsurgical and non-radiating therapeutic methods is the need, namely in younger children, to delay the time of surgical and/or radiation treatment and the related potential adverse effects on growth, hormonal and electrolyte balance, and neurologic function. The main experience has been accumulated around bleomycin and, more recently, around interferon-alpha.

4.3.4.3 Bleomycin

After the studies conducted in vitro by Kubo and colleagues in 1974 [120], who demonstrated the toxicity of bleomycin on craniopharyngioma cell cultures, several authors have presented the results of in vivo intracystic injection of this drug. In spite of the long experience with this treatment and the relative abundance of gathered data, the available evidence is highly heterogeneous. Actually, even three sequential Cochrane reviews failed in providing any recommendation about intracystic bleomycin use in the clinical practice, suggesting the need of randomized trials conducted on larger and more homogeneous patient samples [121–123]. However, the missing randomized trials, justified by the rarity of AC and the small niche represented by the intracystic treatments, do not cancel the impact of a 30-year experience and about 300 articles on the use of bleomycin [124].

Bleomycin is a glycopeptide antibiotic secreted by Streptomyces verticillus acting on inhibition of DNA and RNA synthesis. It is very effective in squamous cell carcinomas and, for this reason, it has been used also in AC (with presently the same epithelial characteristics). Bleomycin is instilled in the tumor cyst through an Ommaya reservoir. The dose varies according to the Center and the size of the cyst (usually 2–5 mg for each administration; 3 doses per week (daily administration in some Centers); meanly for 5 weeks).

Generally, good immediate or early results on the cyst volume reduction are reported in the literature, with a variable but significant percentage of patients achieving a > 90% cyst reduction, compared with disappointing data on long-term disease control [85, 125]. A single randomized controlled trial, conducted on a small patient sample (7 patients; mean age 9.6 years), compared intracystic bleomycin, intracystic P32, and the combination of both [126]. The results suggested that combination treatment (bleomycin+P32) is more effective than the different treatments alone; nevertheless, two patients in this series (22%) reported severe adverse

events (bilateral thalamic infarction). Indeed, more than the short-term effect, the main limit of intracystic bleomycin therapy seems to be the adverse reactions associated with the treatment and the possible extracystic drug diffusion. Commonly, patients experience fever (up to 70% of cases), headache, and nausea just after bleomycin administration; moreover, some patients show delayed toxic effects due to documented damage to nearby neural and vascular structures [122, 127]. These range from steroid-responsive neurological deficits, to severe manifestations such as ischemic vasculopathy, irreversible optic pathway damage, hypothalamic damage, and diabetes insipidus [127–130]. Unfortunately, a negative leakage test does not eliminate the risk of such reactions [128, 129].

For these reasons, the use of bleomycin as an intracystic agent is progressively falling out of favor, while research has been directed towards the experimentation of less toxic agents, such as interferon alpha and, more recently, target therapies [125].

4.3.4.4 Interferon Alpha

Interferon-α (IA) is a cytokine produced by leucocytes belonging to the family of interferons (natural signaling proteins with antiviral activities) together with interferon-β (fibroblasts) and interferon-γ (lymphocytes) [131, 132]. IA is secreted by macrophages and lymphocytes as response to viral infection or tumor progression. It is codified by 15 genes of the chromosome 9. Its antitumoral activity is realized through three different mechanisms: (1) differentiation of T-lymphocytes into T-helper 1 lymphocytes (response against a specific target) and inhibition of other lymphocytes; (2) stimulation of the proliferation on natural killer cells and macrophages, and stimulation of their production interleukine-1 and IA itself; (3) increased identification of the tumor cells through the expression of the major histocompatibility complex class 1 and expression of surface antigens.

The rationale for the use of IA for the treatment of AC originates from the experience with skin tumors sharing the same embryological origin (i.e., squamous and basal cell carcinomas), where subcutaneously administered IA has a well-documented efficacy [133]. This rationale was further supported by the favorable combination between the characteristics of AC cyst (inflammatory genesis) and the immunomodulatory, proapoptotic, and antimicrobial effects of IA that can effectively act against the cyst reaccumulation or growth [9, 30, 32, 35, 41]. In the late 199's, Jakacki and colleagues conducted the first exploratory phase II trial by administering subcutaneous IA to patients with craniopharyngioma, demonstrating a significant radiologic response in 25% of treated subjects [133]. On this basis, other groups started to investigate the use of intra-tumoral interferon injection, with the potential advantages of having both less systemic side effects and higher local drug activity and persistence. Cavalheiro and colleagues realized the first clinical studies on the IA intracystic injection and reported a complete response in about two thirds of patients with cystic tumors in the short term (mean follow-up: 1.7 years), with only mild adverse events (mainly self-limiting headaches, fever, fatigue) [31]. Therefore, the authors prepared an administration protocol, which is shared by all the Centers using IA (with small variants), emphasizing the possibility

to repeat the treatment several times and the absence of treatment discontinuation [6]. The dose scheme for IA intracystic administration is three million International Units (IU) of interferon-α-2a every other day for a total of 12 administrations per cycle (36 million IU). The cycle can be repeated 1 month after the end of the previous one for 3 or more times. IA is administered through an Ommaya reservoir and an intracystic catheter, previously placed by a microsurgical approach (almost abandoned), by neuronavigation alone, or by neuroendoscopic control (especially if hydrocephalus has to be managed at the same time).

The results on the clinical studies with IA published so far have been summarized on Table 4.2. Such a cumulative experience shows a response of AC cyst in the majority of cases, with a complete cyst effacement in about a half of the patients (as a result both cysts collapse due to the aspiration and effects of IA) and a partial response or cyst/stabilization in the remaining cases (Fig. 4.3). Such a result is variably maintained during the follow-up (meanly lower than 5-years), about one third of cases requiring further treatments during this period. The largest study published to date is an international multicenter cooperative study provided in 2017 by Kilday and colleagues [136]. Overall, 56 children affected by AC received intracystic IA according to the Toronto protocol (borrowed from the original Cavalheiro et al. one), that is: (1) permeability study, conducted at least 2 weeks after catheter implantation; (2) aspiration of cystic fluid and instillation of three million IU every other day for 12 days (totaling 36 million IU); (3) cycle repeated if deemed appropriate and tolerated. All patients were under 18 years of age (median age: 6.3 years): 23% received intracystic IA as a first treatment, while the others had previously received other treatments. Median follow-up was of 5.1 years (median follow-up after IA administration: 2.7 years). Seventy-five percent of patients showed clinical or radiological progression during observation, but 33% of them did not require treatment for this progression at last follow-up. The mean time to surgery or radiotherapy for progression was of 5.8 years. Forty-one percent of patients in the cohort did not experience any adverse event; the most common side effects of treatment were influenza-like malaise (29%), headaches (18%), fatigue (13%), transient hyponatremia (2%), appetite loss (2%), and weight loss (2%). None of these symptoms were severe (maximum grade II). However, there were two cases of brain toxicity (optic pathway damage with radiologic evidence of edema and brain atrophy with hydrocephalus) due to suspected extravasation of IA in CSF spaces.

A possible advantage of IA over other intracystic drugs is its safety. Indeed, IA was generally believed to show a low potential for toxicity in case of extracystic diffusion [6, 31, 134, 135]. Also in the personal experience, based on only one case of brain IA diffusion, this event did not produce any symptoms. However, along with the progressive accumulation of clinical data, there have been reports of suspected IA neurotoxicity [136, 138, 139]. Although, in some instances, the toxicity shows a spontaneous resolution, this event raises the problem of reliable leak tests before administration (Fig. 4.4).

Aside from studies about intracystic IA, there has been some continuing interest around subcutaneously administered pegylated IA (PIA), which has been used by Yeung and colleagues [135], who treated recurrent AC with 1–3 μg/kg/week of PIA for 2 years, and recently by Goldman and colleagues [137], who treated recurrent or

Table 4.2 Review of the literature on interferon alpha use in the treatment of cystic craniopharyngioma

	N. of patients	Mean age (years)	Modality (duration)	Previous treatments (%)	Response	% of patients requiring further treatment during follow-up	Median time to further treatment (mo)	Mean/ median follow-up (mo)	Complications	Severe adverse events
Jakacki et al. [133]	15	11.5	Subcutaneous IFN-alpha (1 year)	RT (40%), intracystic P32 (13%)	6% complete, 6% partial, 6% minor	80%	24	31	Fever, liver toxicity	Hypoadrenal shock
Cavalheiro et al. [31]	10	10.0	Intracystic IFN-alpha (30 days cycles)	None	70% complete, 20% partial	0%	–	20	Fever, fatigue; depression (1 patient)	None
Ierardi et al. [32]	21	10.0	Intracystic IFN-alpha (30 days cycles)	None	52% complete, 33% partial, 14% minor	10%	NR	27	NR	NR
Cavalheiro et al. [134]	60	11.0	Intracystic IFN-alpha2a (30 days cycles)	None	78% partial or more	22%	NR	44	Fever, headache, chronic fatigue syndrome	None
Dastoli et al. [6]	19	11.0	Intracystic IFN-alpha (30 days cycles)	None	58% complete, 42% partial	0%	–	36	Headache, fatigue, depression, erythema	None
Bartels et al. (2012)	6	10.8	Intracystic IFN-alpha2b (30 days cycles)	None	25% complete, 50% partial, 1 stable	NR	NR	17	Headache, nausea	None

(continued)

Table 4.2 (continued)

	N. of patients	Mean age (years)	Modality (duration)	Previous treatments (%)	Response	% of patients requiring further treatment during follow-up	Median time to further treatment (mo)	Mean/ median follow-up (mo)	Complications	Severe adverse events
Yeung et al. [135]	5	13.0	Subcutaneous peg-IFN-alpha2b	Surgery (100%), RT (20%)	40% complete, 40% partial	20%	12	43	Fever, fatigue, nausea, mild liver toxicity	Grade 2 hematologic toxicity
Kilday et al. [136]	56	6.3	Intracystic IFN-alpha (30 days cycles)	Surgery (52%), RT (30%)	25% complete 75% partial	57%	70	61	Fever, headache, fatigue,	Suspected neurotoxicity (2 cases)
Goldman et al. [137]	18	13.1	Subcutaneous peg-IFN-alpha2b	Surgery (100%), RT (60%)	69% stable disease at 1 year	NR	NR	8	Fever, grade 1–2 liver or hematologic toxicity	Grade 3 hematologic toxicity (11%); grade 3 liver toxicity (5%)
Personal series	16	8.8	Intracystic IFN-alpha (30 days cycles)	Surgery (25%)	43.5% complete, 37.5% partial, 12.5% stable, 6.5% progression	18.5%	36	49	Fever, headache	None

The entity of resection is intended as follows: complete resection: >90%; partial: between 90 and 50%; minor: less than 50%. *RT* radiation treatment

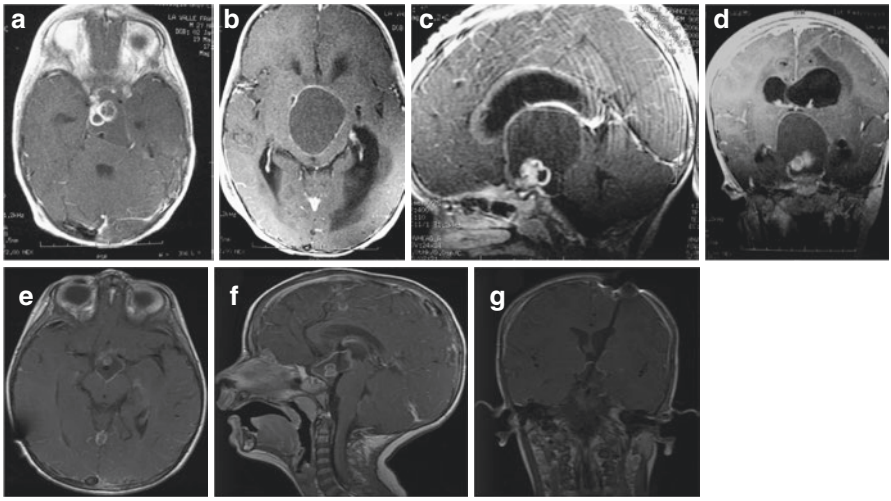

Fig. 4.3 Pretreatment MRI of a large AC in a 5-year-old girl: axial (**a**, **b**), sagittal (**c**), and coronal views (**d**) after gadolinium show a small suprasellar solid component and a large suprasellar cyst, effacing the third ventricle and causing biventricular hydrocephalus. MRI of the same case performed 8 months later (after endoscopic insertion of intracystic catheter, intraoperative cyst reduction by aspiration and one cycle of IA): note the significant reduction of the cyst and the re-expansion of the third ventricle with resolution of the hydrocephalus (**e**–**g**). The solid portion of AC is roughly unchanged

unresectable AC in children and young adults with or up to 18 courses (108 weeks) of PIA (Table 4.2). In spite of the limited number of patients (overall: 23 cases) and the short follow-up in both series, these studies provide some promising data in terms of disease stabilization. Yeung et al. actually had all their 5 patients stabilized or better after a 43-month mean follow-up [135]. According to Goldman et al., no significant radiological response was evident (especially in patients who previously received RT), but an improvement of the median PFS was detected (19.5 months) [137]. As foreseeable, systemic toxicities were more frequent and severe than those reported with intracystic therapy alone. However, only grade 2 and 3 hematologic toxicities occurred (no grade 4 or 5). Further studies are needed to better assess this treatment modality.

In summary, therapy with intracystic IA offers a favorable risk/benefit ratio and a safe and relatively easy means to control disease progression. However, it has to be considered mainly as a transient option to delay more aggressive treatments. Due to the relative rarity of AC, it is hard to evaluate its implications in a randomized setting and on homogeneous patient samples. Further studies shall better explore the implications of its usage in clinical practice, both alone and in combination with other treatments.

4.3.4.5 Future Directions

In the era of target therapies, the results of the aforementioned basic researches are expected to allow for the development of therapeutic agents (both intracystic and systemic) acting on the molecular pathways guiding tumor growth and cyst

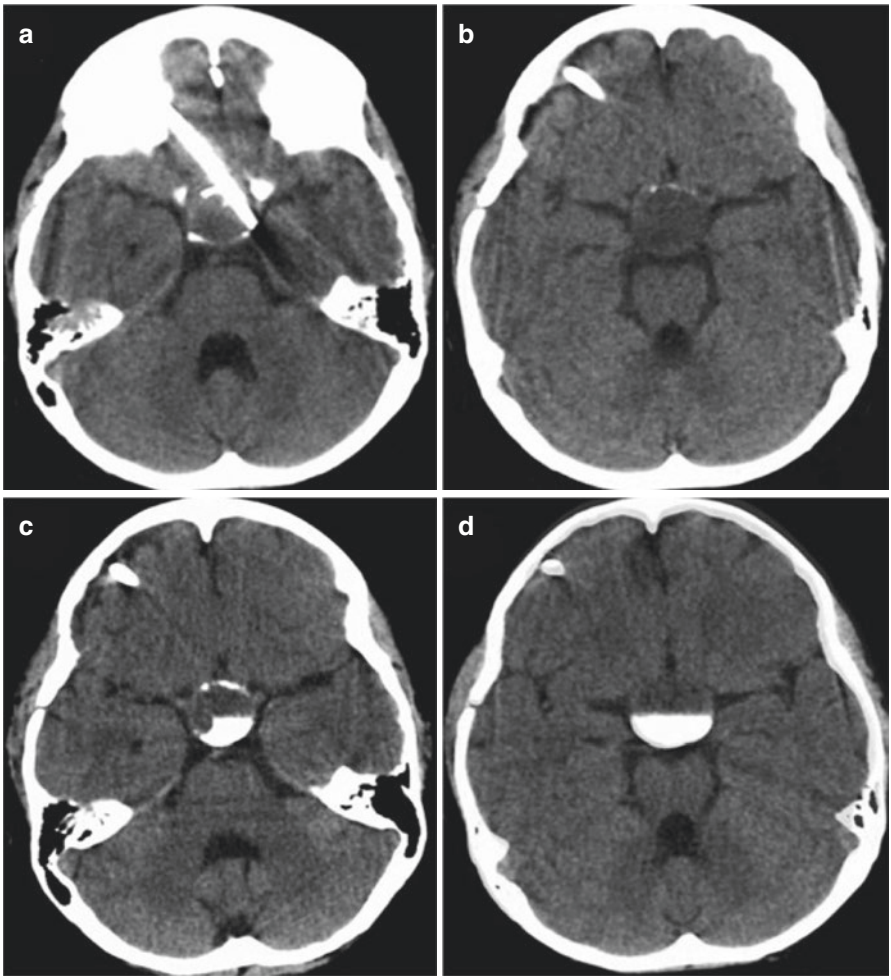

Fig. 4.4 CT-scan-based leak test. First, a basal CT scan is performed to verify the correct placement of the catheter and size and volume of the cyst (**a**, **b**). Afterwards, the iodate contrast medium is injected into the cyst through the subcutaneous reservoir looking for a possible spillage of the contrast. The quantity of contrast medium to be administered is calculated according to the quantity of cyst fluid taken out before the injection. The test is negative if the cyst is «designed» by the contrast medium without its diffusion into the brain (**c**–**f**)

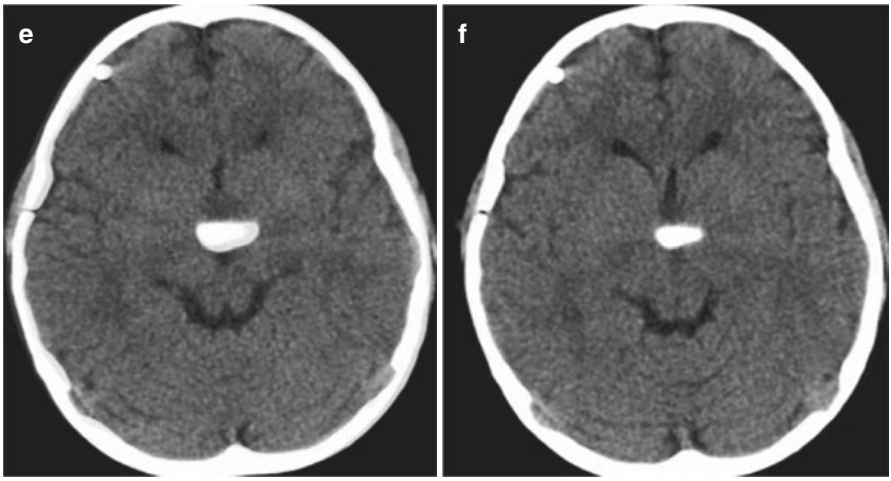

Fig. 4.4 (continued)

accumulation and maintenance [15, 41]. One example is the IL-6 pathway, for which target drugs are already available and have been tried in craniopharyngioma patients with initial but promising data [25]. Tocilizumab (an anti-IL6 monoclonal antibody) was systemically administered to two patients as a compassionate treatment after recurrence. The first patient (age: 7 years) was treated for recurrence after catheter cyst drainage and radiosurgery; he completed a 7-month cycle obtaining tumor volume reduction (and stability during subsequent follow-up) and no side effects. Another patient (age: 3 years) had the first cycle interrupted after 8 months due to disease progression; therapy was then started again with a combination of tocilizumab and bevacizumab (an antiangiogenetic, anti-VEGF monoclonal antibody) obtaining disease control. During this second cycle with combination therapy, the patient developed transient grade 3 neutropenia [25].

Application of similar treatments for intracystic administration could allow for a greater local effect with less adverse events. This could allow for a long-lasting tumor (and symptoms) control, both as a means to delay surgery and/or RT, to make them less invasive and to prevent recurrence afterwards.

4.4 Placement of Intracystic Catheter

The Ommaya placement is a crucial option in the current management of AC, either to perform cyst aspiration and to deliver selected drugs into the cyst, being intracystic chemotherapy one of the major advances in AC treatment. Some authors use a direct microsurgical placement via subfrontal craniotomic approach (mainly in the past) [31, 140], while others utilize a stereotactic navigated or robotized insertion [104, 141]. Although both the previous options maintain their effectiveness, the placement of the intracystic catheter by a navigated endoscopic transventricular approach is the most commonly used technique in the current clinical practice. This

type of approach, indeed, conjugates the mini-invasiveness of neuroendoscopy with the reliability of neuronavigation and offers the possibility of a direct visual control of the position of the catheter across the cyst and the opportunity to perform additional surgical maneuvers, if needed (e.g., tumor biopsy, cyst aspiration, third ventriculostomy, septostomy). As expected, several differences can be observed among the different authors with regard to technical details, as head positioning, instrumentation, number of burr holes, width in the opening of the cyst wall, and so on. On the other hand, there is quite a general agreement in considering neuronavigation as a key feature in performing this kind of surgery.

Head position: As a basic principle of neuroendoscopy, the patient's head is placed in neutral position with a degree of flexion sufficient to have the burr hole in the higher point of the surgical field to minimize CSF leak and bubbles formation. Many authors, namely pediatric neurosurgeons, do not utilize head holders in this procedure [104–109]. On the other hand, authors mainly dealing with adults reported the use of the Mayfield head holder as a key feature of their ventriculoscopic technique [81].

Instrumentation: The choice of the ventriculoscope represents the main difference alongside the reported technical notes, as result of the experience and the resources of the different centers. The endoscopes most commonly used were: (1) 7-mm rigid endoscope with a 30° optic and associated trocar (Karl Storz, Tuttlingen, Germany) [105, 108]; (2) 4 mm rigid endoscope with a 0° optic and associated trocar (Karl Storz, Tuttlingen, Germany) [81, 104]; (3) Oi-Samii neuroendoscopic system (Oi-Samii Handi Pro; Karl Storz, Germany) introduced through a 14-F peel-away sheath [107]; (3) videoscope (Olympus Corporation, Tokyo, Japan) passed by an endoscopic sheath (NeuroportTM; Olympus Corp., Tokyo, Japan) [109]; (4) Gaab with 0° optic telescope (Karl Storz, Tuttlingen, Germany) with its trocar [106].

Number of burr holes: The number of burr holes also varies according to the author's experience. All papers report the pre-coronal area as the chosen location for the burr hole(s). Some authors suggest to use a single burr hole to insert both the endoscope and the catheter [81, 104–106, 109], while other authors prefer to use two accesses to optimize control of the instruments [107]. In our institution, we prefer to adapt this choice tailoring it on the patient's characteristics, selecting the one-hole approach in cases with large ventricles and the two-hole approach in case of small ventricles. Such a strategy represents the evolution of the technique reported in 2009 [108].

Width in the opening of the cyst wall: A further difference found in the literature is the size of cyst wall opening. In fact, some authors suggest to make a small opening in the cyst wall to avoid excessive leakage of the intracystic fluid as well as to reduce the chance of dislocation of the catheter [107, 108], while other authors propose to widely open the cyst to aspirate the fluid and to shrink the cyst before inserting the catheter [81, 104–106, 109].

Further steps: The most commonly reported extra procedures are ETV [109] and tumor biopsy [106]. A general agreement exists on to carefully reconstruct the galea and to suture the skin in multiple layers to reduce CSF leak and to adequately protect the subcutaneous reservoir.

Figures 4.5 and 4.6 summarize the personal procedure for intracystic catheter placement.

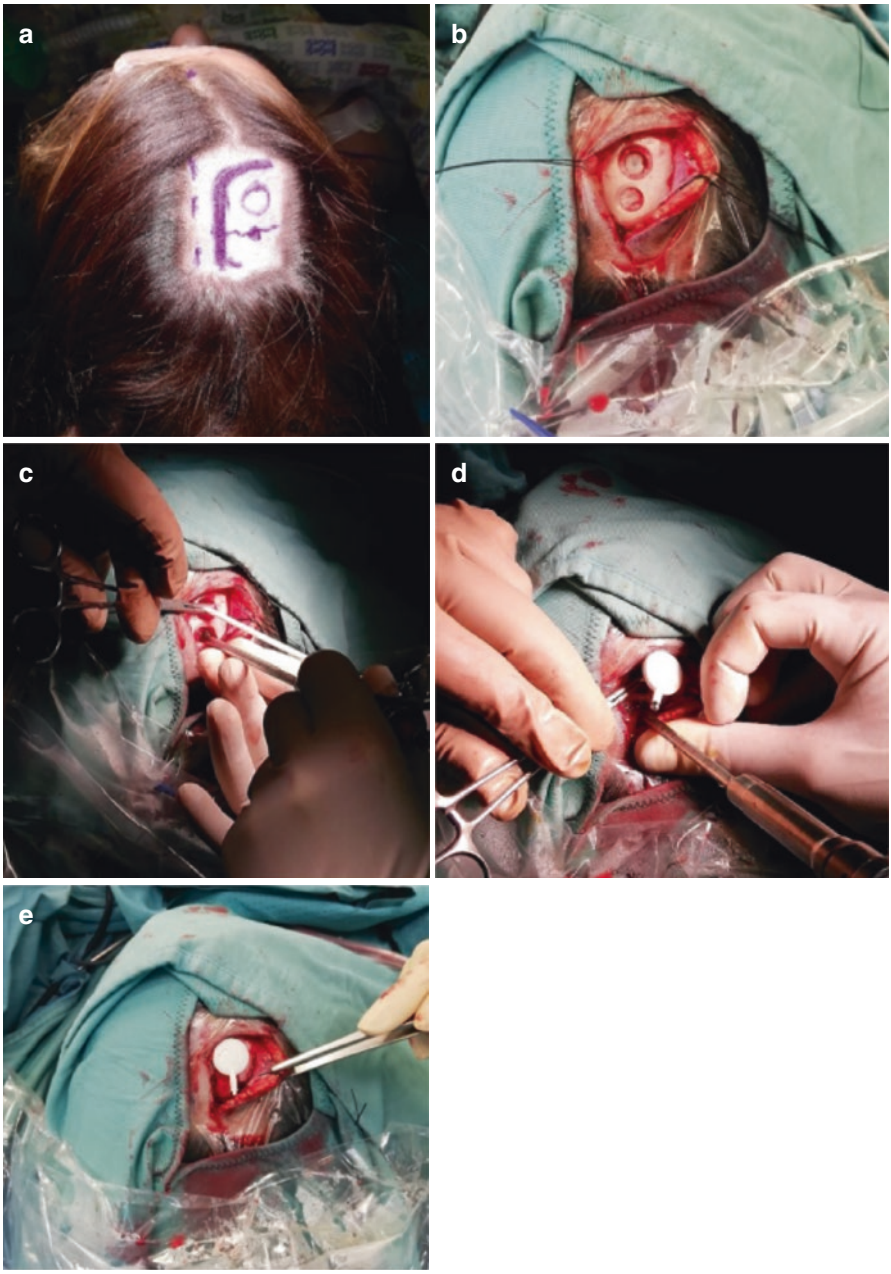

Fig. 4.5 The patient is supine with the head slightly flexed. A L-shaped skin flap is planned according to the trajectory selected by navigation (**a**). Two pre-coronal burr holes are then placed: the posterior one is used to introduce the endoscope, while the anterior one is utilized to introduce the catheter under both navigation and endoscopic views (**b**, **c**). The endoscope is kept in place until the end of the procedure (in particular, once the subcutaneous reservoir is connected) to rule out possible displacement of the catheter (**d**). Finally, the skin is sutured (**e**)

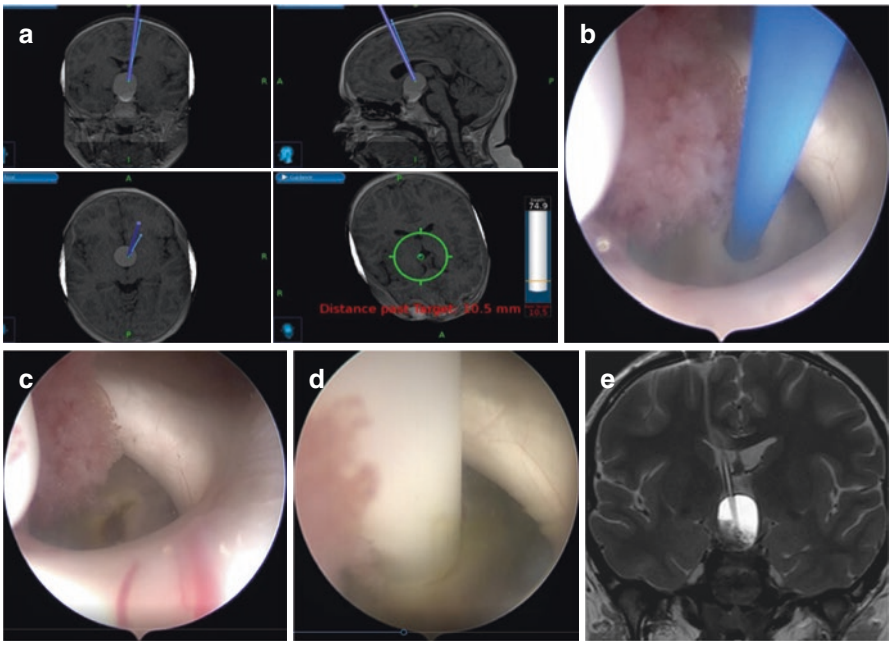

Fig. 4.6 Intraoperative endoscopic view of the case in Fig. 4.5. The procedure is performed under neuronavigation, either because of the small ventricles and because of the need to follow the right trajectory (**a**). The AC cyst is approached through the right foramen of Monroe and fenestrated by Thulium-laser (**b**). The catheter is ready to be inserted into the cyst (asterisk) (**b**). A small fenestration is done to ensure a quick closure of the cyst wall around the catheter and to avoid possible dislocation of the catheter rather than to limit the spillage of the cyst fluid (**c**). Finally, the catheter is introduced into the cyst for the length previously calculated according to the MRI (**d**). Postoperative MRI showing the correct position of the catheter (**e**)

References

1. Prabhu VC, Brown HG. The pathogenesis of craniopharyngiomas. Childs Nerv Syst. 2005;21(8–9):622–7.
2. Wang K-C, Hong SH, Kim S-K, Cho B-K. Origin of craniopharyngiomas: implication on the growth pattern. Childs Nerv Syst. 2005;21(8–9):628–34.
3. Müller HL, Merchant TE, Warmuth-Metz M, Martinez-Barbera J-P, Puget S. Craniopharyngioma. Nat Rev Dis Primers. 2019;5(1):75.
4. Cushing H. Intracranial tumours. J Nerv Ment Dis. 1932;76(5):539.
5. Kiran NAS, Suri A, Kasliwal MK, Garg A, Ahmad FU, Mahapatra AK. Gross total excision of pediatric giant cystic craniopharyngioma with huge retroclival extension to the level of foramen magnum by anterior trans petrous approach: report of two cases and review of literature. Childs Nerv Syst. 2008;24(3):385–91.
6. Dastoli PA, Nicácio JM, Silva NS, Capellano AM, Toledo SRC, Ierardi D, Cavalheiro S. Cystic craniopharyngioma: intratumoral chemotherapy with alpha interferon. Arq Neuropsiquiatr. 2011;69(1):50–5.
7. Moorthy RK, Backianathan S, Rebekah G, Rajshekhar V. Utility of interval imaging during focused radiation therapy for residual cystic craniopharyngiomas. World Neurosurg. 2020;141:e615–24.

8. Yu Y, Dong Z, Chen D, Chen F. Pediatric giant craniopharyngioma: surgical field soak in diluted nimodipine solution reduces cerebral vasospasm. World Neurosurg. 2020;141:113.
9. Hengartner AC, Prince E, Vijmasi T, Hankinson TC. Adamantinomatous craniopharyngioma: moving toward targeted therapies. Neurosurg Focus. 2020;48(1):E7.
10. Cani CMG, Matushita H, Carvalho LRS, Soares IC, Brito LP, Almeida MQ, Mendonça BB. PROP1 and CTNNB1 expression in adamantinomatous craniopharyngiomas with or without β-catenin mutations. Clinics (Sao Paulo). 2011;66(11):1849–54.
11. Hölsken A, Stache C, Schlaffer SM, Flitsch J, Fahlbusch R, Buchfelder M, Buslei R. Adamantinomatous craniopharyngiomas express tumor stem cell markers in cells with activated Wnt signaling: further evidence for the existence of a tumor stem cell niche? Pituitary. 2014;17(6):546–56.
12. Kato K, Nakatani Y, Kanno H, et al. Possible linkage between specific histological structures and aberrant reactivation of the Wnt pathway in adamantinomatous craniopharyngioma. J Pathol. 2004;203(3):814–21.
13. Sekine S, Shibata T, Kokubu A, Morishita Y, Noguchi M, Nakanishi Y, Sakamoto M, Hirohashi S. Craniopharyngiomas of adamantinomatous type harbor beta-catenin gene mutations. Am J Pathol. 2002;161(6):1997–2001.
14. Coury JR, Davis BN, Koumas CP, Manzano GS, Dehdashti AR. Histopathological and molecular predictors of growth patterns and recurrence in craniopharyngiomas: a systematic review. Neurosurg Rev. 2020;43(1):41–8.
15. Gupta S, Bi WL, Giantini Larsen A, Al-Abdulmohsen S, Abedalthagafi M, Dunn IF. Craniopharyngioma: a roadmap for scientific translation. Neurosurg Focus. 2018;44(6):E12.
16. Buslei R, Hölsken A, Hofmann B, Kreutzer J, Siebzehnrubl F, Hans V, Oppel F, Buchfelder M, Fahlbusch R, Blümcke I. Nuclear beta-catenin accumulation associates with epithelial morphogenesis in craniopharyngiomas. Acta Neuropathol (Berl). 2007;113(5):585–90.
17. Gaston-Massuet C, Andoniadou CL, Signore M, et al. Increased wingless (Wnt) signaling in pituitary progenitor/stem cells gives rise to pituitary tumors in mice and humans. Proc Natl Acad Sci U S A. 2011;108(28):11482–7.
18. Wang C-H, Qi S-T, Fan J, Pan J, Peng J-X, Nie J, Bao Y, Liu Y-W, Zhang X, Liu Y. Identification of tumor stem-like cells in admanatimomatous craniopharyngioma and determination of these cells' pathological significance. J Neurosurg. 2019;133(3):664–74.
19. Apps JR, Carreno G, Gonzalez-Meljem JM, et al. Tumour compartment transcriptomics demonstrates the activation of inflammatory and odontogenic programmes in human adamantinomatous craniopharyngioma and identifies the MAPK/ERK pathway as a novel therapeutic target. Acta Neuropathol (Berl). 2018;135(5):757–77.
20. Gonzalez-Meljem JM, Martinez-Barbera JP. Senescence drives non-cell autonomous tumorigenesis in the pituitary gland. Mol Cell Oncol. 2018;5(3):e1435180.
21. Zhu Y, Tchkonia T, Pirtskhalava T, et al. The Achilles' heel of senescent cells: from transcriptome to senolytic drugs. Aging Cell. 2015;14(4):644–58.
22. Hara T, Akutsu H, Takano S, et al. Clinical and biological significance of adamantinomatous craniopharyngioma with CTNNB1 mutation. J Neurosurg. 2018;131(1):217–26.
23. Zhu W, Tang T, Yuan S, Chang B, Li S, Chen M. Prediction of CTNNB1 mutation status in pediatric cystic adamantinomatous craniopharyngioma by using preoperative magnetic resonance imaging manifestation. Clin Neurol Neurosurg. 2021;200:106347.
24. Martelli C, Serra R, Inserra I, et al. Investigating the protein signature of adamantinomatous craniopharyngioma pediatric brain tumor tissue: towards the comprehension of its aggressive behavior. Dis Markers. 2019;2019:3609789.
25. Grob S, Mirsky DM, Donson AM, Dahl N, Foreman NK, Hoffman LM, Hankinson TC, Mulcahy Levy JM. Targeting IL-6 is a potential treatment for primary cystic craniopharyngioma. Front Oncol. 2019;9:791.
26. Donson AM, Apps J, Griesinger AM, et al. Molecular analyses reveal inflammatory mediators in the solid component and cyst fluid of human adamantinomatous craniopharyngioma. J Neuropathol Exp Neurol. 2017;76(9):779–88.

27. Whelan R, Prince E, Gilani A, Hankinson T. The inflammatory milieu of adamantinomatous craniopharyngioma and its implications for treatment. J Clin Med. 2020;9(2):519. https://doi.org/10.3390/jcm9020519.
28. Martelli C, Iavarone F, Vincenzoni F, et al. Proteomic characterization of pediatric craniopharyngioma intracystic fluid by LC-MS top-down/bottom-up integrated approaches. Electrophoresis. 2014;35(15):2172–83.
29. Pettorini BL, Inzitari R, Massimi L, Tamburrini G, Caldarelli M, Fanali C, Cabras T, Messana I, Castagnola M, Di Rocco C. The role of inflammation in the genesis of the cystic component of craniopharyngiomas. Childs Nerv Syst. 2010;26(12):1779–84.
30. Jokonya L, Reid T, Kasambala M, Mduluza-Jokonya TL, Fieggen G, Mduluza T, Kalangu KKN, Naicker T. Antimicrobial effects of craniopharyngioma cystic fluid. Childs Nerv Syst. 2020;36(11):2641–6.
31. Cavalheiro S, Dastoli PA, Silva NS, Toledo S, Lederman H, da Silva MC. Use of interferon alpha in intratumoral chemotherapy for cystic craniopharyngioma. Childs Nerv Syst. 2005;21(8–9):719–24.
32. Ierardi DF, Fernandes MJS, Silva IR, Thomazini-Gouveia J, Silva NS, Dastoli P, Toledo SRC, Cavalheiro S. Apoptosis in alpha interferon (IFN-alpha) intratumoral chemotherapy for cystic craniopharyngiomas. Childs Nerv Syst. 2007;23(9):1041–6.
33. Desiderio C, Martelli C, Rossetti DV, et al. Identification of thymosins β4 and β10 in paediatric craniopharyngioma cystic fluid. Childs Nerv Syst. 2013;29(6):951–60.
34. Desiderio C, Rossetti DV, Castagnola M, Massimi L, Tamburrini G. Adamantinomatous craniopharyngioma: advances in proteomic research. Childs Nerv Syst. 2021;37(3):789–97.
35. Massimi L, Martelli C, Caldarelli M, Castagnola M, Desiderio C. Proteomics in pediatric cystic craniopharyngioma. Brain Pathol. 2017;27(3):370–6.
36. Andoniadou CL, Gaston-Massuet C, Reddy R, Schneider RP, Blasco MA, Le Tissier P, Jacques TS, Pevny LH, Dattani MT, Martinez-Barbera JP. Identification of novel pathways involved in the pathogenesis of human adamantinomatous craniopharyngioma. Acta Neuropathol (Berl). 2012;124(2):259–71.
37. Nemolato S, Restivo A, Cabras T, et al. Thymosin β4 in colorectal cancer is localized predominantly at the invasion front in tumor cells undergoing epithelial mesenchymal transition. Cancer Biol Ther. 2012;13(4):191–7.
38. Jones G, Sebba A, Gu J, et al. Comparison of tocilizumab monotherapy versus methotrexate monotherapy in patients with moderate to severe rheumatoid arthritis: the AMBITION study. Ann Rheum Dis. 2010;69(1):88–96.
39. Markham A, Patel T. Siltuximab: first global approval. Drugs. 2014;74(10):1147–52.
40. Todd CM, Salter BM, Murphy DM, Watson RM, Howie KJ, Milot J, Sadeh J, Boulet L-P, O'Byrne PM, Gauvreau GM. The effects of a CXCR1/CXCR2 antagonist on neutrophil migration in mild atopic asthmatic subjects. Pulm Pharmacol Ther. 2016;41:34–9.
41. Zhou J, Zhang C, Pan J, Chen L, Qi S-T. Interleukin-6 induces an epithelial-mesenchymal transition phenotype in human adamantinomatous craniopharyngioma cells and promotes tumor cell migration. Mol Med Rep. 2017;15(6):4123–31.
42. Huang S, Mills L, Mian B, Tellez C, McCarty M, Yang X-D, Gudas JM, Bar-Eli M. Fully humanized neutralizing antibodies to interleukin-8 (ABX-IL8) inhibit angiogenesis, tumor growth, and metastasis of human melanoma. Am J Pathol. 2002;161(1):125–34.
43. Mian BM, Dinney CPN, Bermejo CE, Sweeney P, Tellez C, Yang XD, Gudas JM, McConkey DJ, Bar-Eli M. Fully human anti-interleukin 8 antibody inhibits tumor growth in orthotopic bladder cancer xenografts via down-regulation of matrix metalloproteases and nuclear factor-kappaB. Clin Cancer Res. 2003;9(8):3167–75.
44. Coy S, Rashid R, Lin J-R, et al. Multiplexed immunofluorescence reveals potential PD-1/PD-L1 pathway vulnerabilities in craniopharyngioma. Neuro-Oncol. 2018;20(8):1101–12.
45. Rimkus TK, Carpenter RL, Qasem S, Chan M, Lo H-W. Targeting the sonic hedgehog signaling pathway: review of smoothened and GLI inhibitors. Cancer. 2016;8(2):22. https://doi.org/10.3390/cancers8020022.

46. Gump JM, Donson AM, Birks DK, et al. Identification of targets for rational pharmacological therapy in childhood craniopharyngioma. Acta Neuropathol Commun. 2015;3:30.
47. Carreno G, Boult JKR, Apps J, et al. SHH pathway inhibition is protumourigenic in adamantinomatous craniopharyngioma. Endocr Relat Cancer. 2019;26(3):355–66.
48. Petralia F, Tignor N, Reva B, et al. Integrated proteogenomic characterization across major histological types of pediatric brain cancer. Cell. 2020;183(7):1962–85.
49. Cermak S, Kosicek M, Mladenovic-Djordjevic A, Smiljanic K, Kanazir S, Hecimovic S. Loss of cathepsin B and L leads to lysosomal dysfunction, NPC-like cholesterol sequestration and accumulation of the key Alzheimer's proteins. PLoS One. 2016;11(11):e0167428.
50. Lefranc F, Chevalier C, Vinchon M, et al. Characterization of the levels of expression of retinoic acid receptors, galectin-3, macrophage migration inhibiting factor, and p53 in 51 adamantinomatous craniopharyngiomas. J Neurosurg. 2003;98(1):145–53.
51. Lubansu A, Ruchoux M-M, Brotchi J, Salmon I, Kiss R, Lefranc F. Cathepsin B, D and K expression in adamantinomatous craniopharyngiomas relates to their levels of differentiation as determined by the patterns of retinoic acid receptor expression. Histopathology. 2003;43(6):563–72.
52. Liu H, Liu Z, Li J, Li Q, You C, Xu J. Relative quantitative expression of hypoxia-inducible factor 1α messenger ribonucleic acid in recurrent craniopharyngiomas. Neurol India. 2014;62(1):53–6.
53. Xu J, Zhang S, You C, Wang X, Zhou Q. Microvascular density and vascular endothelial growth factor have little correlation with prognosis of craniopharyngioma. Surg Neurol. 2006;66(Suppl 1):S30–4.
54. Zhu J, You C. Craniopharyngioma: survivin expression and ultrastructure. Oncol Lett. 2015;9(1):75–80.
55. Tena-Suck ML, Ortiz-Plata A, Galán F, Sánchez A. Expression of epithelial cell adhesion molecule and pituitary tumor transforming gene in adamantinomatous craniopharyngioma and its correlation with recurrence of the tumor. Ann Diagn Pathol. 2009;13(2):82–8.
56. Ebrahimi A, Honegger J, Schluesener H, Schittenhelm J. Osteonectin expression in surrounding stroma of craniopharyngiomas: association with recurrence rate and brain infiltration. Int J Surg Pathol. 2013;21(6):591–8.
57. Kim S, An SSA. Role of p53 isoforms and aggregations in cancer. Medicine (Baltimore). 2016;95(26):e3993.
58. Tena-Suck ML, Salinas-Lara C, Arce-Arellano RI, Rembao-Bojórquez D, Morales-Espinosa D, Sotelo J, Arrieta O. Clinico-pathological and immunohistochemical characteristics associated to recurrence/regrowth of craniopharyngiomas. Clin Neurol Neurosurg. 2006;108(7):661–9.
59. Scholzen T, Gerdes J. The Ki-67 protein: from the known and the unknown. J Cell Physiol. 2000;182(3):311–22.
60. Prieto R, Pascual JM, Subhi-Issa I, Jorquera M, Yus M, Martínez R. Predictive factors for craniopharyngioma recurrence: a systematic review and illustrative case report of a rapid recurrence. World Neurosurg. 2013;79(5–6):733–49.
61. Flitsch J, Aberle J, Burkhardt T. Surgery for pediatric craniopharyngiomas: is less more? J Pediatr Endocrinol Metab. 2015;28(1–2):27–33.
62. Sainte-Rose C, Puget S, Wray A, Zerah M, Grill J, Brauner R, Boddaert N, Pierre-Kahn A. Craniopharyngioma: the pendulum of surgical management. Childs Nerv Syst. 2005;21(8–9):691–5.
63. Elliott RE, Jane JA, Wisoff JH. Surgical management of craniopharyngiomas in children: meta-analysis and comparison of transcranial and transsphenoidal approaches. Neurosurgery. 2011;69(3):630–43.
64. Enayet AER, Atteya MME, Taha H, Zaghloul MS, Refaat A, Maher E, Abdelaziz A, El Beltagy MA. Management of pediatric craniopharyngioma: 10-year experience from high-flow center. Childs Nerv Syst. 2021;37(2):391–401.
65. Puget S, Garnett M, Wray A, et al. Pediatric craniopharyngiomas: classification and treatment according to the degree of hypothalamic involvement. J Neurosurg. 2007;106(1 Suppl):3–12.

66. Rachinger W, Oehlschlaegel F, Kunz M, Fuetsch M, Schichor C, Thurau S, Schopohl J, Seelos K, Tonn J-C, Kreth F-W. Cystic craniopharyngiomas: microsurgical or stereotactic treatment? Neurosurgery. 2017;80(5):733–43.
67. Schubert T, Trippel M, Tacke U, van Velthoven V, Gumpp V, Bartelt S, Ostertag C, Nikkhah G. Neurosurgical treatment strategies in childhood craniopharyngiomas: is less more? Childs Nerv Syst. 2009;25(11):1419–27.
68. Takano S, Akutsu H, Mizumoto M, Yamamoto T, Tsuboi K, Matsumura A. Neuroendoscopy followed by radiotherapy in cystic craniopharyngiomas—a long-term follow-up. World Neurosurg. 2015;84(5):1305–15.
69. Burman P, van Beek AP, Biller BMK, Camacho-Hübner C, Mattsson AF. Radiotherapy, especially at young age, increases the risk for de novo brain tumors in patients treated for pituitary/sellar lesions. J Clin Endocrinol Metab. 2017;102(3):1051–8.
70. Greenfield BJ, Okcu MF, Baxter PA, Chintagumpala M, Teh BS, Dauser RC, Su J, Desai SS, Paulino AC. Long-term disease control and toxicity outcomes following surgery and intensity modulated radiation therapy (IMRT) in pediatric craniopharyngioma. Radiother Oncol. 2015;114(2):224–9.
71. Locatelli D, Massimi L, Rigante M, Custodi V, Paludetti G, Castelnuovo P, Di Rocco C. Endoscopic endonasal transsphenoidal surgery for sellar tumors in children. Int J Pediatr Otorhinolaryngol. 2010;74(11):1298–302.
72. Deopujari CE, Karmarkar VS, Shah N, Vashu R, Patil R, Mohanty C, Shaikh S. Combined endoscopic approach in the management of suprasellar craniopharyngioma. Childs Nerv Syst. 2018;34(5):871–6.
73. Massimi L, Rigante M, D'Angelo L, Paternoster G, Leonardi P, Paludetti G, Di Rocco C. Quality of postoperative course in children: endoscopic endonasal surgery versus sublabial microsurgery. Acta Neurochir. 2011;153(4):843–9.
74. Lin Y, Hansen D, Sayama CM, Pan I-W, Lam S. Transfrontal and transsphenoidal approaches to pediatric craniopharyngioma: a national perspective. Pediatr Neurosurg. 2017;52(3):155–60.
75. Alalade AF, Ogando-Rivas E, Boatey J, Souweidane MM, Anand VK, Greenfield JP, Schwartz TH. Suprasellar and recurrent pediatric craniopharyngiomas: expanding indications for the extended endoscopic transsphenoidal approach. J Neurosurg Pediatr. 2018;21(1):72–80.
76. Ali ZS, Lang S-S, Kamat AR, Adappa ND, Palmer JN, Storm PB, Lee JYK. Suprasellar pediatric craniopharyngioma resection via endonasal endoscopic approach. Childs Nerv Syst. 2013;29(11):2065–70.
77. Almeida JP, Suppiah S, Karekezi C, Marigil-Sanchez M, Wong JS, Vescan A, Gentili F, Zadeh G. Extended endoscopic approach for resection of craniopharyngiomas. J Neurol Surg Part B Skull Base. 2018;79(2):S201–2.
78. Bal E, Öge K, Berker M. Endoscopic endonasal transsphenoidal surgery, a reliable method for treating primary and recurrent/residual craniopharyngiomas: nine years of experience. World Neurosurg. 2016;94:375–85.
79. Jeswani S, Nuño M, Wu A, Bonert V, Carmichael JD, Black KL, Chu R, King W, Mamelak AN. Comparative analysis of outcomes following craniotomy and expanded endoscopic endonasal transsphenoidal resection of craniopharyngioma and related tumors: a single-institution study. J Neurosurg. 2016;124(3):627–38.
80. Rigante M, Massimi L, Parrilla C, Galli J, Caldarelli M, Di Rocco C, Paludetti G. Endoscopic transsphenoidal approach versus microscopic approach in children. Int J Pediatr Otorhinolaryngol. 2011;75(9):1132–6.
81. Hollon TC, Savastano LE, Altshuler D, Barkan AL, Sullivan SE. Ventriculoscopic surgery for cystic retrochiasmatic craniopharyngiomas: indications, surgical technique, and short-term patient outcomes. Oper Neurosurg. 2018;15(2):109–19.
82. Chen JX, Alkire BC, Lam AC, Curry WT, Holbrook EH. Aseptic meningitis with craniopharyngioma resection: consideration after endoscopic surgery. J Neurol Surg Rep. 2016;77(4):e151–5.

83. Halliday J, Cudlip S. A new technique of endoscopic decompression of suprasellar craniopharyngioma cyst. Acta Neurochir. 2019;161(11):2285–8.
84. Satoh H, Uozumi T, Arita K, Kurisu K, Hotta T, Kiya K, Ikawa F, Goishi J, Sogabe T. Spontaneous rupture of craniopharyngioma cysts. A report of five cases and review of the literature. Surg Neurol. 1993;40(5):414–9.
85. Steinbok P, Hukin J. Intracystic treatments for craniopharyngioma. Neurosurg Focus. 2010;28(4):E13.
86. Chen A, Zhou R, Yao X, Ai M, Sun T. Neuroendoscopic treatment of giant cystic craniopharyngioma in the foramen magnum: report of two cases. Childs Nerv Syst. 2020;37(7):2387–90. https://doi.org/10.1007/s00381-020-04965-0.
87. Gangemi M, Seneca V, Mariniello G, Colella G, Magro F. Combined endoscopic and microsurgical removal of a giant cystic craniopharyngioma in a six-year-old boy. Clin Neurol Neurosurg. 2009;111(5):472–6.
88. Zhu W, Li X, He J, Sun T, Li C, Gong J. A reformed surgical treatment modality for children with giant cystic craniopharyngioma. Childs Nerv Syst. 2017;33(9):1491–500.
89. Bishop AJ, Greenfield B, Mahajan A, et al. Proton beam therapy versus conformal photon radiation therapy for childhood craniopharyngioma: multi-institutional analysis of outcomes, cyst dynamics, and toxicity. Int J Radiat Oncol Biol Phys. 2014;90(2):354–61.
90. Conti A, Pontoriero A, Ghetti I, Senger C, Vajkoczy P, Pergolizzi S, Germanò A. Benefits of image-guided stereotactic hypofractionated radiation therapy as adjuvant treatment of craniopharyngiomas. A review. Childs Nerv Syst. 2019;35(1):53–61.
91. Lee C-C, Yang H-C, Chen C-J, Hung Y-C, Wu H-M, Shiau C-Y, Guo W-Y, Pan DH-C, Chung W-Y, Liu K-D. Gamma knife surgery for craniopharyngioma: report on a 20-year experience. J Neurosurg. 2014;121(Suppl):167–78.
92. Yang I, Sughrue ME, Rutkowski MJ, Kaur R, Ivan ME, Aranda D, Barani IJ, Parsa AT. Craniopharyngioma: a comparison of tumor control with various treatment strategies. Neurosurg Focus. 2010;28(4):E5.
93. Harrabi SB, Adeberg S, Welzel T, Rieken S, Habermehl D, Debus J, Combs SE. Long term results after fractionated stereotactic radiotherapy (FSRT) in patients with craniopharyngioma: maximal tumor control with minimal side effects. Radiat Oncol Lond Engl. 2014;9:203.
94. Iwata H, Tatewaki K, Inoue M, Yokota N, Baba Y, Nomura R, Shibamoto Y, Sato K. Single and hypofractionated stereotactic radiotherapy with CyberKnife for craniopharyngioma. J Neurooncol. 2012;106(3):571–7.
95. Kobayashi T, Kida Y, Mori Y, Hasegawa T. Long-term results of gamma knife surgery for the treatment of craniopharyngioma in 98 consecutive cases. J Neurosurg. 2005;103(6 Suppl):482–8.
96. Rajan B, Ashley S, Gorman C, Jose CC, Horwich A, Bloom HJ, Marsh H, Brada M. Craniopharyngioma—a long-term results following limited surgery and radiotherapy. Radiother Oncol. 1993;26(1):1–10.
97. Tsugawa T, Kobayashi T, Hasegawa T, et al. Gamma knife surgery for residual or recurrent craniopharyngioma after surgical resection: a multi-institutional retrospective study in Japan. Cureus. 2020;12(2):e6973.
98. Niranjan A, Lunsford LD. The role of Leksell radiosurgery in the management of craniopharyngiomas. Prog Neurol Surg. 2019;34:166–72.
99. Jarebi M, Coutte A, Bartier F, Khormi Y, Peltier J, Lefranc M. A novel, hybrid, stereotactic approach (radiosurgery and dual Ommaya reservoirs) for the treatment of mixed (polycystic and solid) craniopharyngioma. Stereotact Funct Neurosurg. 2019;97(4):266–71.
100. Lamiman K, Wong KK, Tamrazi B, Nosrati JD, Olch A, Chang EL, Kiehna EN. A quantitative analysis of craniopharyngioma cyst expansion during and after radiation therapy and surgical implications. Neurosurg Focus. 2016;41(6):E15.
101. Laville A, Coutte A, Capel C, Maroote J, Lefranc M. Dosimetric and volumetric outcomes of combining cyst puncture through an Ommaya reservoir with index-optimized hypofrac-

tionated stereotactic radiotherapy in the treatment of craniopharyngioma. Clin Transl Radiat Oncol. 2020;23:66–71.
102. Klimo P, Venable GT, Boop FA, Merchant TE. Recurrent craniopharyngioma after conformal radiation in children and the burden of treatment. J Neurosurg Pediatr. 2015;15(5):499–505.
103. Moussa AH, Kerasha AA, Mahmoud ME. Surprising outcome of Ommaya reservoir in treating cystic craniopharyngioma: a retrospective study. Br J Neurosurg. 2013;27(3):370–3.
104. Frio F, Solari D, Cavallo LM, Cappabianca P, Raverot G, Jouanneau E. Ommaya reservoir system for the treatment of cystic craniopharyngiomas: surgical results in a series of 11 adult patients and review of the literature. World Neurosurg. 2019;132:e869–77.
105. Lauretti L, Legninda Sop FY, Pallini R, Fernandez E, D'Alessandris QG. Neuroendoscopic treatment of cystic craniopharyngiomas: a case series with systematic review of the literature. World Neurosurg. 2018;110:e367–73.
106. Shukla D. Transcortical transventricular endoscopic approach and Ommaya reservoir placement for cystic craniopharyngioma. Pediatr Neurosurg. 2015;50(5):291–4.
107. Joki T, Oi S, Babapour B, Kaito N, Ohashi K, Ebara M, Kato M, Abe T. Neuroendoscopic placement of Ommaya reservoir into a cystic craniopharyngioma. Childs Nerv Syst. 2002;18(11):629–33.
108. Pettorini BL, Tamburrini G, Massimi L, Caldarelli M, Di Rocco C. Endoscopic transventricular positioning of intracystic catheter for treatment of craniopharyngioma. J Neurosurg Pediatr. 2009;4(3):245–8.
109. Ndukuba K, Ogiwara T, Nakamura T, Abe D, Ichinose S, Horiuchi T, Ohaegbulam S, Hongo K. Cyst fenestration and Ommaya reservoir placement in endoscopic transcortical transventricular approach for recurrent suprasellar cystic craniopharyngioma without ventriculomegaly. J Clin Neurosci. 2020;72:425–8.
110. Zanon N, Cavalheiro S, da Silva MC. Does the choice of surgical approach to insert an intratumoral catheter influence the results of intratumoral cystic treatment? Surg Neurol. 2008;70(1):66–9.
111. Julow JV. Intracystic irradiation for craniopharyngiomas. Pituitary. 2013;16(1):34–45.
112. Kickingereder P, Maarouf M, El Majdoub F, et al. Intracavitary brachytherapy using stereotactically applied phosphorus-32 colloid for treatment of cystic craniopharyngiomas in 53 patients. J Neurooncol. 2012;109(2):365–74.
113. Ansari SF, Moore RJ, Boaz JC, Fulkerson DH. Efficacy of phosphorus-32 brachytherapy without external-beam radiation for long-term tumor control in patients with craniopharyngioma. J Neurosurg Pediatr. 2016;17(4):439–45.
114. Barriger RB, Chang A, Lo SS, Timmerman RD, DesRosiers C, Boaz JC, Fakiris AJ. Phosphorus-32 therapy for cystic craniopharyngiomas. Radiother Oncol J Eur Soc Ther Radiol Oncol. 2011;98(2):207–12.
115. Maarouf M, El Majdoub F, Fuetsch M, Hoevels M, Lehrke R, Berthold F, Voges J, Sturm V. Stereotactic intracavitary brachytherapy with P-32 for cystic craniopharyngiomas in children. Strahlenther Onkol Organ Dtsch Rontgengesellschaft Al. 2016;192(3):157–65.
116. Yu X, Zhang J, Liu R, Wang Y, Wang H, Wang P, Chen J, Liu S. Interstitial radiotherapy using phosphorus-32 for giant posterior fossa cystic craniopharyngiomas. J Neurosurg Pediatr. 2015;15(5):510–8.
117. Chang H, Zhang J, Cao W, Wang Y, Zhao H, Liu R, Guo S. Drug distribution and clinical safety in treating cystic craniopharyngiomas using intracavitary radiotherapy with phosphorus-32 colloid. Oncol Lett. 2018;15(4):4997–5003.
118. Babaei M, Ghahramani-Asl R, Sadoughi H-R, Sardari D, Shahzadi S. Evaluation of bremsstrahlung radiation dose in stereotactically radiocolloid therapy of cystic craniopharyngioma tumors with 32P radio-colloid. Australas Phys Eng Sci Med. 2018;41(3):697–711.
119. Hu C, Chen J, Meng Y, Zhang J, Wang Y, Liu R, Yu X. Phosphorus-32 interstitial radiotherapy for recurrent craniopharyngioma: expressions of vascular endothelial growth factor and its receptor-2 and imaging features of tumors are associated with tumor radiosensitivity. Medicine (Baltimore). 2018;97(26):e11136.

120. Kubo O, Takakura K, Miki Y, Okino T, Kitamura K. Intracystic therapy of bleomycin for craniopharyngioma—effect of bleomycin for cultured craniopharyngioma cells and intracystic concentration of bleomycin (author's transl). No Shinkei Geka. 1974;2(10):683–8.
121. Liu W, Fang Y, Cai B, Xu J, You C, Zhang H. Intracystic bleomycin for cystic craniopharyngiomas in children (abridged republication of cochrane systematic review). Neurosurgery. 2012;71(5):909–15.
122. Zhang S, Fang Y, Cai BW, Xu JG, You C. Intracystic bleomycin for cystic craniopharyngiomas in children. Cochrane Database Syst Rev. 2016;7:CD008890.
123. Zheng J, Fang Y, Cai BW, Zhang H, Liu W, Wu B, Xu JG, You C. Intracystic bleomycin for cystic craniopharyngiomas in children. Cochrane Database Syst Rev. 2014;9:CD008890.
124. Wisoff JH. Commentary: Intracystic bleomycin for cystic craniopharyngiomas in children (abridged republication of Cochrane systematic review). Neurosurgery. 2012;71(5):E1063–4.
125. Mrowczynski OD, Langan ST, Rizk EB. Craniopharyngiomas: a systematic review and evaluation of the current intratumoral treatment landscape. Clin Neurol Neurosurg. 2018;166:124–30.
126. Jiang R, Liu Z, Zhu C. Preliminary exploration of the clinical effect of bleomycin on craniopharyngiomas. Stereotact Funct Neurosurg. 2002;78(2):84–94.
127. Lafay-Cousin L, Bartels U, Raybaud C, Kulkarni AV, Guger S, Huang A, Bouffet E. Neuroradiological findings of bleomycin leakage in cystic craniopharyngioma: report of three cases. J Neurosurg. 2007;107(4 Suppl):318–23.
128. Belen D, Er U, Yigitkanli K, Bolay H. Delayed neurotoxic complication of intracavitary bleomycin therapy for craniopharyngioma in a child who had previously undergone radiosurgery: case report. J Neurosurg. 2007;106(5 Suppl):391–3.
129. Cho W-S, Kim S-K, Wang K-C, Phi JH, Cho B-K. Vasculopathy after intracystic bleomycin administration for a recurrent cystic craniopharyngioma: case report. J Neurosurg Pediatr. 2012;9(4):394–9.
130. Hukin J, Steinbok P, Lafay-Cousin L, Hendson G, Strother D, Mercier C, Samson Y, Howes W, Bouffet E. Intracystic bleomycin therapy for craniopharyngioma in children: the Canadian experience. Cancer. 2007;109(10):2124–31.
131. Jonasch E, Haluska FG. Interferon in oncological practice: review of interferon biology, clinical applications, and toxicities. Oncologist. 2001;6(1):34–55.
132. Taniguchi T, Ogasawara K, Takaoka A, Tanaka N. IRF family of transcription factors as regulators of host defense. Annu Rev Immunol. 2001;19:623–55.
133. Jakacki RI, Cohen BH, Jamison C, et al. Phase II evaluation of interferon-alpha-2a for progressive or recurrent craniopharyngiomas. J Neurosurg. 2000;92(2):255–60.
134. Cavalheiro S, Di Rocco C, Valenzuela S, et al. Craniopharyngiomas: intratumoral chemotherapy with interferon-alpha: a multicenter preliminary study with 60 cases. Neurosurg Focus. 2010;28(4):E12.
135. Yeung JT, Pollack IF, Panigrahy A, Jakacki RI. Pegylated interferon-α-2b for children with recurrent craniopharyngioma. J Neurosurg Pediatr. 2012;10(6):498–503.
136. Kilday J-P, Caldarelli M, Massimi L, et al. Intracystic interferon-alpha in pediatric craniopharyngioma patients: an international multicenter assessment on behalf of SIOPE and ISPN. Neuro-Oncol. 2017;19(10):1398–407.
137. Goldman S, Pollack IF, Jakacki RI, et al. Phase II study of peginterferon alpha-2b for patients with unresectable or recurrent craniopharyngiomas: a pediatric brain tumor consortium report. Neuro-Oncol. 2020;22(11):1696–704.
138. Sharma J, Bonfield CM, Singhal A, Hukin J, Steinbok P. Intracystic interferon-α treatment leads to neurotoxicity in craniopharyngioma: case report. J Neurosurg Pediatr. 2015;16(3):301–4.
139. Tiedemann LM, Manley P, Smith ER, Dagi LR. Visual field loss in a case of recurrent cystic craniopharyngioma during concomitant treatment with pegylated interferon α-2b. J Pediatr Hematol Oncol. 2016;38(1):e26–8.

140. Cavalheiro S, Sparapani FV, Franco JO, da Silva MC, Braga FM. Use of bleomycin in intratumoral chemotherapy for cystic craniopharyngioma: case report. J Neurosurg. 1996;84(1):124–6.
141. Alén JF, Boto GR, Lagares A, de la Lama A, Gómez PA, Lobato RD. Intratumoural bleomycin as a treatment for recurrent cystic craniopharyngioma. Case report and review of the literature. Neurocir Astur Spain. 2002;13(6):479–85; discussion 485.

Chapter 5
Surgical Approach to Thalamic Tumors

M. Memet Özek and Baran Bozkurt

5.1 Introduction

Thalamic tumors comprise 1–5% of all brain tumors [1–3]. They can occur in all age groups; however, a preponderance of children and adolescents has been reported by several authors [2, 4–6]. Presenting signs and symptoms are increased intracranial pressure, hydrocephalus, focal motor and sensory findings, tremor, visual problems, neuropsychological symptoms, and occasionally seizures [2, 3, 5–8].

Thalamic lesions, historically, have been inoperable due to complex architectural organization of vital thalamic nuclei and the proximity to critically important structures such as the internal capsule, subthalamus, and basal ganglia. Therefore, the outcome of children with thalamic gliomas has been poor [6]. Still some authors tend to be conservative in their surgical approach to these lesions, since the resection of thalamic tumors has been associated with an unacceptably high rate of morbidity and mortality [7, 9].

However, recent improvements and developments in pre- and intraoperative technologies have allowed a more accurate approach to these lesions, and a reduction in morbidity and mortality [5, 10, 11]. These refinements have centered on improving the neurosurgical technique of tumor resection. Therefore, perioperative mortality has dropped from as high as 40% to as low as 0–1% [1, 5, 6, 11, 12].

M. M. Özek (✉)
Department of Neurosurgery, Division of Pediatric Neurosurgery, Acıbadem University, School of Medicine, Istanbul, Turkey

B. Bozkurt
Neuroanatomy Laboratory at Department of Neurosurgery, Acıbadem University, School of Medicine, Istanbul, Turkey

C. Di Rocco (ed.), *Advances and Technical Standards in Neurosurgery*, Advances and Technical Standards in Neurosurgery 45,
https://doi.org/10.1007/978-3-030-99166-1_5

In some studies, histologic verification has been found useful, both for planning a treatment protocol and for judging the effectiveness of the treatment. Therefore, most neurosurgeons nowadays believe that all thalamic tumors should be verified histologically, and radical removal of the tumor must be the goal of the treatment, especially in patients with low-grade tumors [1, 2, 5, 6, 11, 13, 14]. These studies have demonstrated improved outcomes with aggressive surgical resection. Resection of thalamic tumors needs specific anatomical knowledge and surgical experience since the surrounding structures may limit a radical resection.

5.2 Territories of Thalamus and Their Arterial Blood Supply

Thalamus is often represented as a tetrahedron with three free surfaces exposed to ventricular system and one surface in contact with critical neural structures [15]. Composed of multiple nuclear grouping, the thalamus is a large mass of gray matter. The nuclear groups have their own pattern of afferent and efferent connections. It is bounded ventrally by the hypothalamic sulcus. Its caudal limit is at the level of the posterior commissure and aqueduct, its rostral limit is at the interventricular foramen, and superiorly it is related to the stria medullaris and the roof of the third ventricle. The lateral and caudal parts of the thalamus are enlarged and overlie the midbrain structures [1, 12].

The arterial and venous vascularization of the thalamus is well described in the literature and the thalamus is supplied by anterolateral (PCoA), lateral (AChoA), posterolateral (thalamogeniculate arteries), medial (diencephalic interpeduncular branches), and dorsal (P2) arterial systems [1, 16] (Fig. 5.1). These main arteries supply different nuclei in different parts of the thalamus through their terminal branches. Accordingly, seven different vascular thalamic territories have been defined [16].

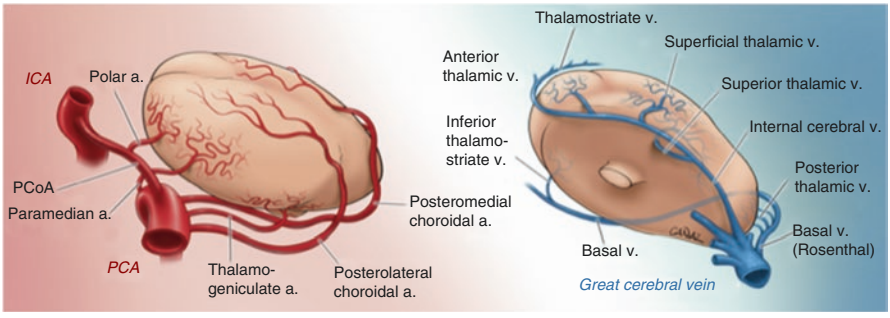

Fig. 5.1 Arterial blood supply and venous drainage of thalamus

5.2.1 Anterior Territory

The anterior territory includes parts of the anterior, ventral, and intralaminar regions of the thalamus and this part is supplied by the tuberothalamic artery [17]. It is absent in about a third of the normal population; in this case the anterior thalamic region is supplied by the paramedian artery or, more generally, the percheron artery [18]. The percheron artery is a rare variant of the posterior cerebral circulation, characterized by a solitary trunk and supplies bilaterally to the paramedian thalami and rostral midbrain [19]. The psychiatric syndrome of anterior thalamic infarction is unique. In the early stages of anterior thalamic infarction, patients may show shifting states of consciousness and may become withdrawn. In the later course of the disorder, recurrent personality changes are seen, which include disorientation of time and place, euphoria, loss of understanding, apathy, and lack of spontaneity [20–22].

5.2.2 Inferolateral Territory

The inferolateral territory includes the medial geniculate nucleus, the ventral posterior, and ventral lateral nuclei and the pulvinar nuclei [17, 23]. The inferolateral arteries are composed of 5–10 arteries also known as the thalamogeniculate or inferior external optic arteries that arise from the P2 or ambient segment of the posterior cerebral artery [24]. There are three main groups: the medial geniculate, principal inferolateral, and inferolateral pulvinar arteries. The medial geniculate nucleus supplied by the medial branches occupies the inferolateral region, the ventral posterior and ventral lateral nuclei supplied by the major inferolateral branches, and the pulvinar nuclei supplied by the inferolateral pulvinar branches [17, 20, 23, 25].

Inferolateral artery infarction presents with the thalamic syndrome which includes sensory loss to a variable extent, with impaired extremity movement, sometimes with postlesion pain. The most prominent characteristic of this condition is the extreme pain that analgesics cannot alleviate, which can be associated with isolation of the thalamus from cortical inhibition [26, 27].

5.2.3 Paramedian Territory

The paramedian territory includes parts of the anterior, medial, and ventral thalamus. The intralaminar zone is also included in this territory [17].

The Paramedian Thalamic Territory is supplied by the paramedian arteries which are the posterior thalamosubthalamic paramedian arteries, posterior thalamoperforate arteries, or mesencephalic arteries. They arise from the P1 segment of the posterior cerebral artery, also known as mesencephalic artery [23, 24, 28].

Sections of the anterior, posterior, and ventral thalamus as well as parts of the intralaminar region form the paramedian territory which comprises of reticular, limbic, effector, associative, unique sensory, and intralaminar from the nuclear classes supplied by the paramedian arteries [16].

Infarction or injury of the paramedian arteries group may result in some complex clinical conditions such as vision disturbance, hemiparesis, memory disturbances, and akinetic mutism [29, 30].

5.2.4 Posterior Territory

The posterior territory includes mainly the geniculate nuclei, parts of the intralaminar region, and the pulvinar [16]. It is supplied by the posterior choroidal arteries. The posterior choroidal arteries are derived from the distal P1 or proximal P2 portion of the posterior cerebral artery. The medial branches pass to the choroid plexus under the corpus callosum and supply the choroid plexus in the roof of the third ventricle and a portion of that in the body of the lateral ventricle. The lateral branches pass to the cerebral peduncles, thalamus, and supply a portion of the choroid plexus in the atrium and posterior part of the temporal horn and body [31]. Most frequent symptom in patients with posterior choroidal artery infarction is homonymous quadrantanopia. A lateral posterior choroidal artery infarction may be presented with hemisensory failure. There can also be transcortical aphasia and memory disruptions [32].

5.2.5 Variant Thalamic Territories

5.2.5.1 Anteromedian Territory

As suggested by the term, the anteromedian territory is created by merging the conventional anterior and paramedian territories. Specifically, the posterior part of the anterior territory and the anterior part of the paramedian territory are merged [33]. Serious neuropsychological conditions, which are more severe where the infarctions are bilateral, are the prevalent trait of anteromedian territorial infarcts. A typical characteristic of anteromedian territorial infarcts is extreme anterograde amnesia [16].

5.2.5.2 Central Territory

The central thalamic territory consists of the four traditional thalamic territories' central intersection. While infarctions affecting this area alone are exceedingly rare, symptoms of cognitive decline, vertical gaze paresis, arousal loss, and ataxia are likely to show in patients [24, 33].

5.2.5.3 Posterolateral Territory

The posterolateral territory consists of the fusion of the posterior part of the inferolateral territory with the posterior part of the posterior territory and the posterior segment of the vascular inferolateral territory [32]. Aphasia, ataxia, and lack of higher executive function are associated with infarction in this area. The signs of aphasia, ataxia, and lack of executive functions are well accompanied by a loss of associative nuclei activity due to infarction of the pulvinar and ventral region, which can be thought to offend this territory [16, 33].

5.3 Thalamic Venous Drainage

The thalamus is drained by deep cortical veins such as the thalamostriate and lateral thalamic veins [34] (Fig. 5.1). These drain into the internal cerebral veins with the caudate portion drained particularly by the Rosenthal basal vein and then enter Galen vein except for invariant instances [34]. It is important to remember that there are variable clinical manifestations of venous infarctions and neoplasms since they do not affect individual arterial regions. As predicted, there are greatly differing clinical effects ranging from headache to death (hemiplegia, mutism, drowsiness, hemorrhagic infarction of the basal ganglia) in case reports of patients with thalamic insults related to cerebral venous thrombosis [35].

5.4 Thalamic Peduncles

Thalamic peduncles or radiations are large projection fiber bundles that connect the thalamus and the cortex. It has been well described in both human and monkey brains and these bundles consist of both afferent and efferent fibers [36]. Based on cortical projections, five main fiber bundles have been defined: The *anterior, superior, lateral, posterior, and inferior peduncles* [1, 37]. These peduncles represent the staging areas of fibers originating from the cerebral cortex before passing through the reticular nucleus to enter the thalamic nuclei [16]. The functions of the thalamic peduncles can be inferred from the corresponding cortical areas where the fibers are projected. And lots of clinical information and evolving experimental evidence indicate that the various thalamic nuclei have different intended roles [17, 20].

5.4.1 Superior Thalamic Peduncle

The superior thalamic peduncle is bounded laterally by the internal capsule and runs through the most medial portion of the internal capsule-posterior limb [36, 37]. Anatomically, it is located superior to the caudate nucleus and ventral to the

thalamus [38]. The superior thalamic radiations connect the ventral nuclear group of the thalamus with the precentral, postcentral gyrus, the caudal part of the cingulate gyrus, the parahippocampal gyrus, and the prefrontal cortex through the superior thalamic peduncle and the posterior limb of the internal capsule [36, 37].

In voxel-based morphometry studies, it has been shown that the superior thalamic peduncle shows significant fractional anisotropy in patients with bipolar disorder. Therefore, it is thought that anisotropy in the superior thalamic peduncle may be considered as a risk factor in bipolar disorder [39].

5.4.2 Posterior Thalamic Peduncle

The posterior thalamic peduncle is a bundle of projection fibers, including optic radiation, that run through the posterior limb of the internal capsule providing the connection between the pulvinar and lateral geniculate nuclei of the thalamus and the posterior parietal and occipital cortex. This fiber bundle also includes optical radiation and is involved in visual and motor integration [40, 41]. Additionally, anomalies in the posterior thalamic radiation and left mediodorsal thalamic nucleus may result in anorexia nervosa. It has been claimed that the disorder of these white matter pathways may lead to impairment in the visual perception of the body and therefore may play a role in anorexia nervosa [42]. Recent studies have focused on the role of the posterior thalamic fiber bundle in high cognitive functions. In the DTI study conducted in 4400 subjects without a history of strokes, where the effect of microstructural changes of white matter pathways on cognitive performance was investigated, it has been reported that the lowest cognitive and grasping performance may be mostly related to microstructural changes in the posterior thalamic projection fiber bundle relative to other white matter pathways [43].

5.4.3 Anterior Thalamic Peduncle

The anterior thalamic peduncle passes through the anterior limb of the internal capsule and enters the most rostral part of the thalamus, and these fiber bundles form a reciprocal connection between the prefrontal and orbitofrontal part of the cortex and the cingulate gyrus. It also includes the fiber bundles between the supplementary motor area and the thalamus.

The anterior limb of the internal capsule contains anterior thalamic peduncle and frontopontine fibers and has been associated with the ability to dynamically shift focus and attention to various environmental stimuli. This feature is an indicator of cognitive flexibility [44, 45]. Also, it has been reported that there is a relationship between anterior thalamic radiation abnormalities and negative symptoms and cognitive abnormalities in schizophrenia [46]. Accordingly, a significant correlation was observed between the integrity of the anterior limb of the right internal capsule

and cognitive functions (administrative function, working memory) in patients with schizophrenia, and it was reported that structural changes in the anterior limb of the right internal capsule may cause cognitive dysfunction in schizophrenia [46].

5.4.4 Inferior Thalamic Peduncle

The inferior thalamic peduncle passes medial to the posterior limb of the internal capsule and reaches the ventromedial side of the thalamus. These fiber bundles connect the thalamus with the orbitofrontal, insular, and temporal cortex and the amygdala [47, 48]. The inferior thalamic peduncle was first described by Velasco as a potential stimulation site for resistant depression [49]. In patients diagnosed with major depression, the inferior thalamic peduncle was thought to be metabolically abnormal, and this theory was confirmed by functional imaging and PET studies [50]. These studies also showed that hyperactive adverse interaction with pharmacological treatment was also possible, and it has been claimed that metabolic hypoactivity is improved in this area by DBS [50–52]. In subsequent studies, in addition to major depressive disorder, significant remission results were obtained in other psychiatric conditions such as obsessive–compulsive disorder, resistant anxiety, and mood disorder [53, 54].

5.4.5 Lateral Thalamic Peduncle

The lateral thalamic peduncle is located between the proper thalamus and the reticular nucleus, and it is adjacent to the posterior limb of the internal capsule. This peduncle contains fibers from the upper and lower parietal lobules, superior temporal gyrus and sulcus, cingulate gyrus, and motor cortex [37]. It was named with the term "extracapsular thalamic peduncle" in another study and anatomically it was defined as fibers originating from the surface of the third ventricle of the thalamus and joining under the anterior commissure with the ansa peduncularis to reach the amygdala and temporal cortex. These peduncle fibers run outside the internal capsule opposed to the fibers of the anterior, superior, posterior, and inferior peduncles [12].

5.5 Surgical Approaches

Yaşargil described three different growth patterns of thalamic tumors [14]. Those with local expansion, which distort as well as displace the surrounding structures. The second group is those tumors with an expansion into the lateral ventricular cavity without ependymal penetration. The third group of tumors may expand laterally and superiorly into the white matter of an adjoining gyrus.

To reach thalamic region surgically, various surgical approaches have been described [10]. The popular ones are transcortical transventricular approach [5, 55], anterior interhemispheric transcallosal approach [10, 11], contralateral infratentorial supracerebellar approach [13], posterior interhemispheric parasplenial approach [14], and transsylvian–transinsular approach [1, 15]. Each of these approaches has its own indications and risk of complications.

5.5.1 Transcortical Transventricular Approach

Various transcortical transventricular approaches have been described for thalamic tumor resection, such as a frontal transventricular approach [4, 7] for superior anteriorly located tumors, occipital or parieto-occipital transventricular approaches [7, 13] for posteriorly located tumors, and a transcortical transtemporal approach between T1 and T2 [1, 5, 55] for ventral posteriorly located tumors. For removal of more marked lateral expansion of the tumor, often in proximity to the temporal horn, a transcortical transtemporal approach is recommended because the risk of injuring important vessels is lower [5] (Figs. 5.2, 5.3 and 5.4).

The patient is placed in a supine position with the head rotated opposite to the lesion fixed in a head holder. A question mark or C-shaped incision is made to include above the posterior part of the zygomatic arc extending above the tragus and auricle. Alternatively, a straight skin incision can also be used. After the temporalis muscle is retracted anteriorly, craniectomy is performed above the middle temporal gyrus projection. Corticotomy parallel to the middle temporal gyrus is performed. Depending on the lesion location, the temporal horn of the lateral ventricle can be exposed to provide wider exposure. Arcuate fascicule fibers are situated underneath the cortex with the optic radiation below and the tapedial fibers on the posterior. The temporal horn can be accessed after going through the ependyma. Body of

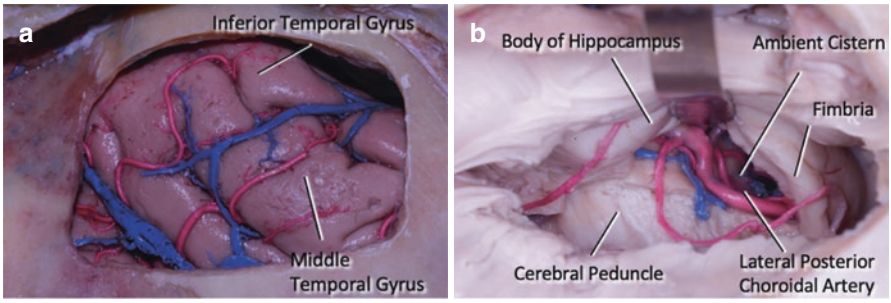

Fig. 5.2 Transtemporal–transventricular approach. (**a**) Temporal craniotomy is performed. (**b**) Body of hippocampus can be visualized and atrium of the lateral ventricle can be accessed posteriorly. Dissection of the choroid fissure provides access to the ambient cistern. Posterior cerebral artery can be identified at this point. The fimbria of the fornix, the lateral posterior choroidal artery is exposed. The cerebral peduncle access is possible for inferiorly located lesions

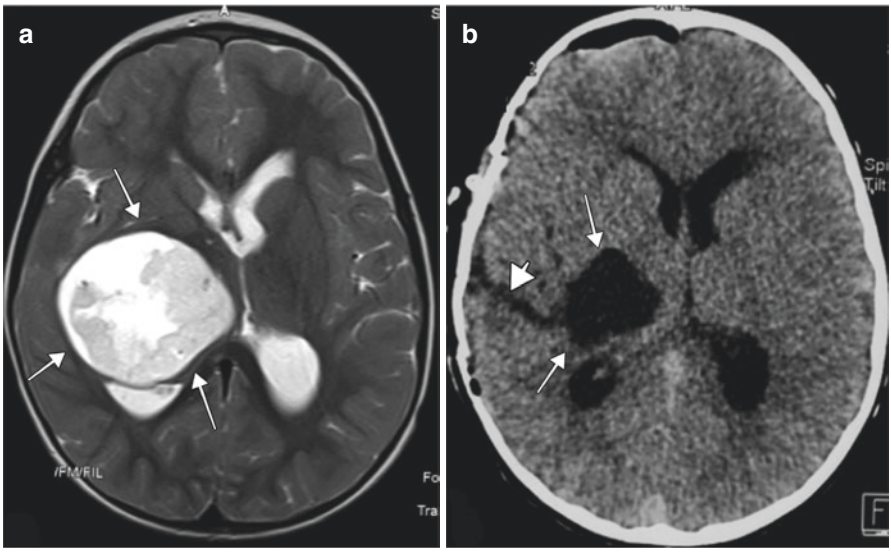

Fig. 5.3 5 years old patient presented with mild hemiparesis. (**a**) T2-weighted MR imaging demonstrated cystic large lesion in the right thalamic region. (**b**) Early postoperative CT demonstrates complete removed using transcortical-temporal approach

hippocampus can be visualized, with the collateral eminence inferolaterally and the choroid plexus superiorly. Atrium of the lateral ventricle can be accessed posteriorly and the calcar avis can be visualized at the deep end of the exposure. Dissection of the choroid fissure provides access to the ambient cistern. Posterior cerebral artery can be identified at this point (Fig. 5.2). The cerebral peduncle access is possible for inferiorly located lesions. Superiorly, the optic tract is located anteriorly, and the lateral geniculate nucleus is located posteriorly. Cinalli reported that when tumor cysts were present, usually the surgical corridor was dictated by the location of the cyst that contributed to significant displacement of the corticospinal tract [5].

5.5.2 Anterior Interhemispheric Approach

Most neurosurgeons prefer an anterior interhemispheric transcallosal approach in patients with a paramedian tumor with significant intraventricular component or located immediately below the ependyma in proximity to the choroid plexus attachment—superior–anterior thalamic tumors [1, 5, 7, 9, 14]. With this approach, there is great flexibility for exploring the lateral ventricle with no disruption of hemisphere tissue, no cortical incision. This approach can be utilized for gaining exposure of the medial thalamus. Another advantage of this approach is the possibility of an endoscope usage. For this approach, the head is positioned either in supine with 20° flexion or laterally with the lesion side below for the ipsilateral approach. Lesion

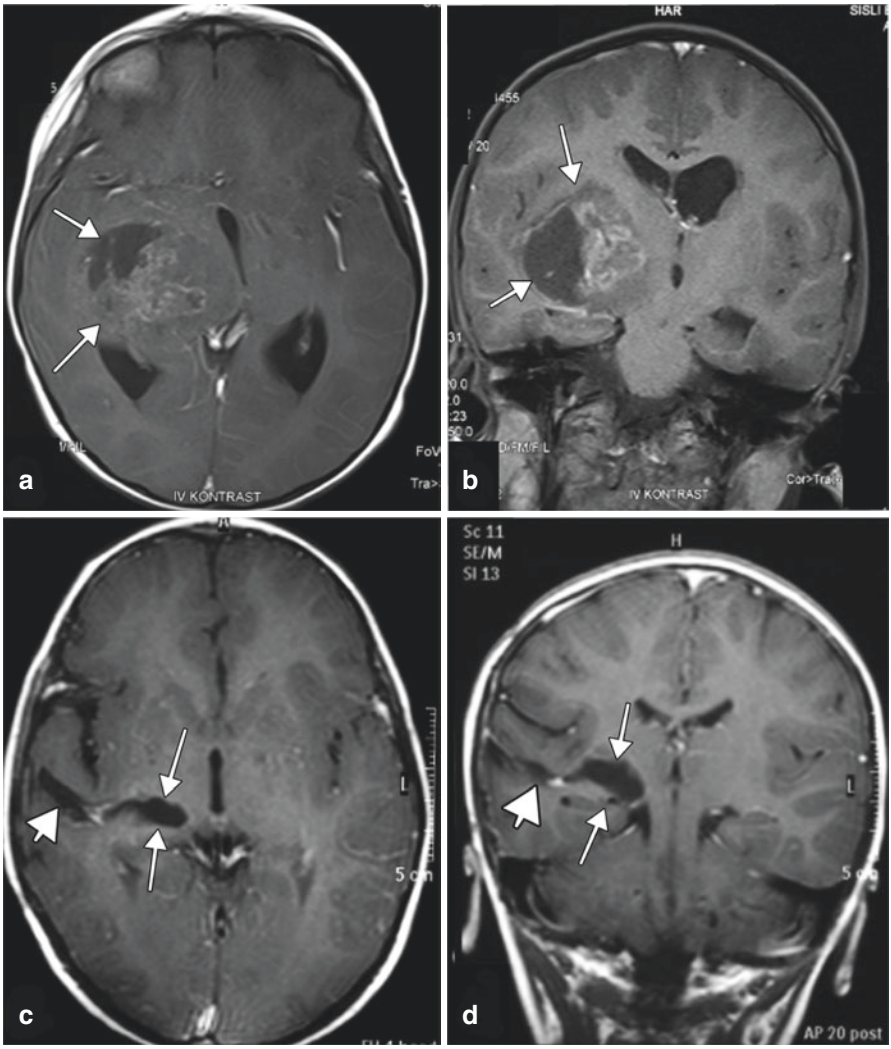

Fig. 5.4 (**a**, **b**) Preoperative contrast T1 axial and coronal cuts of the same patient demonstrate heterogeneous contrast enhancement of the large right thalamic tumor. (**c**, **d**) Postoperative MR 3 months later does not present any contrast enhancement. Histopathology: pilocytic astrocytoma

side should be placed superiorly if a contralateral interhemispheric approach is planned. After craniotomy, the dura is incised in C shape and folded over the superior sagittal sinus. The interhemispheric bridging veins are dissected and preserved. After dissecting the interhemispheric adhesions, the cingulate gyrus can be visualized. Callosomarginal artery can be traversing along the cingulate gyrus and can be seen at this point. After progressing through the interhemispheric space, pericallosal arteries and body of the corpus callosum can be seen. Callosotomy is performed toward the targeted ventricle at this point. The thalamostriate vein, anterior septal vein, and choroid plexus can serve as landmarks after the lateral ventricle is

penetrated. When the lateral ventricle exposure is achieved, caudate nucleus, medial thalamus, choroidal fissure, and fornix can be seen.

Lesion located in the superior part of the thalamus can be accessed without further dissection into the third ventricle. If necessary, entry into the third ventricle can be achieved by splitting the choroid plexus from the choroid fissure or from the foramen of Monroe. If the choroid fissure is dissected from the medial side, care should be given not to damage the fornix as this may lead to memory deficits. Internal cerebral veins can be seen after entry as the extent of the thalamostriate vein. Meticulous hemostasis is required as in all ventricular approaches to prevent an obstruction in the aqueduct of Sylvius. Serra et al. recommend continuously flushing for at least 30 min after lesion resection [11] (Figs. 5.5 and 5.6).

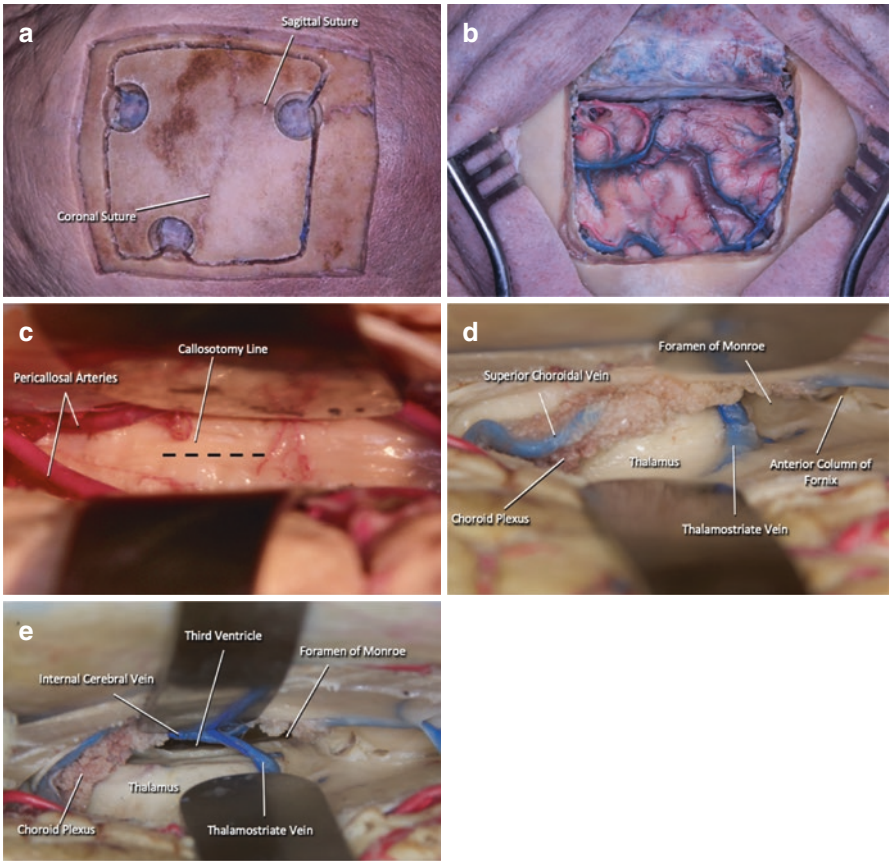

Fig. 5.5 Anterior interhemispheric approach. (**a**) The craniotomy flap is turned by crossing the midline and two thirds of the craniotomy is made on the anterior side of the coronal suture and one thirds on the posteior side. (**b**) after craniotomy, the dura is incised in C shape and folded over the superior sagittal sinus. (**c**) Exposure of the corpus callosum after dissecting the interhemispheric adhesions. The corpus callosum is incised in a vertical direction. (**d**) The thalamostriate vein, anterior septal vein, and choroid plexus can serve as landmarks after the lateral ventricle is penetrated. (**e**) Access to the third ventricle can be achieved by splitting the choroid plexus from the choroid fissure or from the foramen of Monroe

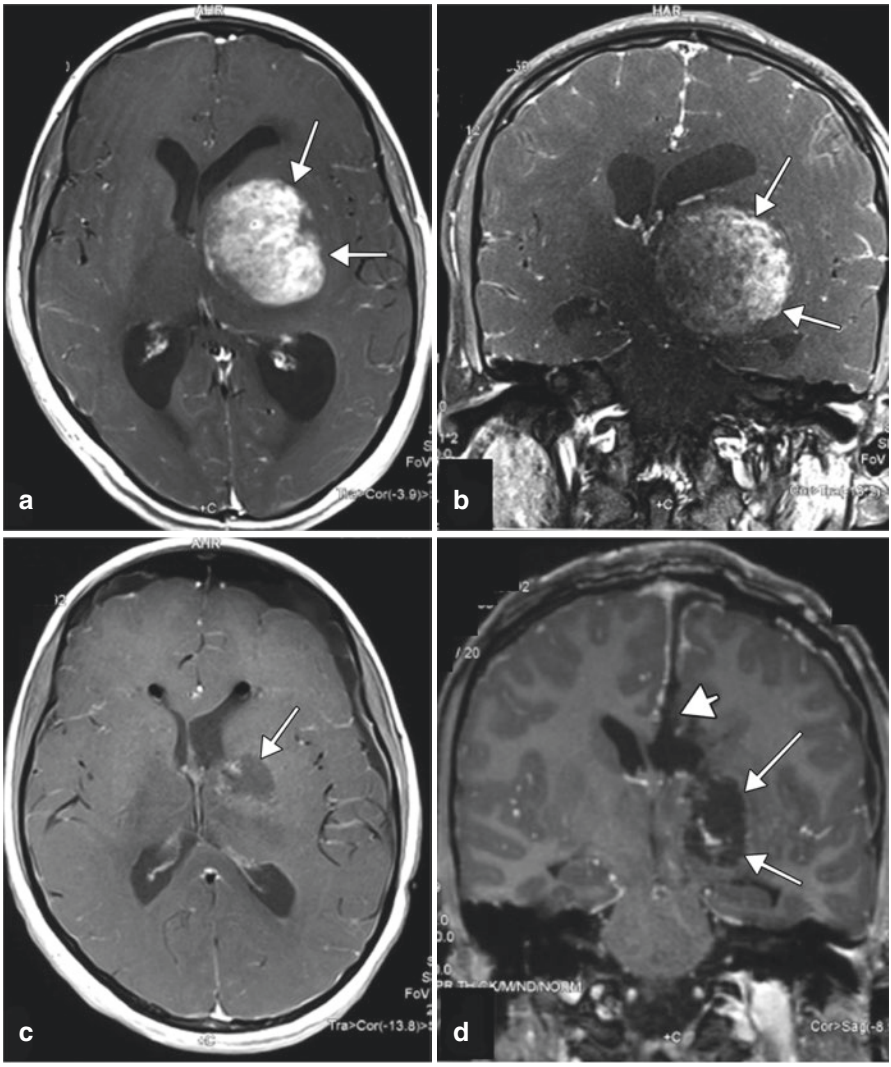

Fig. 5.6 (**a**, **b**) Axial and coronal preoperative T1-weighted MR imaging with contrast shows large well-circumscrabed lesion in the left thalamic region. It has shifted the lateral ventricle to the cranial direction. (**c**, **d**) After radical removal of the tumor using an anterior interhemispheric approach. Histology: pilocytic astrocytoma

5.5.3 Posterior Interhemispheric Approach

Posterior thalamic-pulvinar lesions can be reached using a posterior interhemispheric approach easily. With this approach, a large section of the parasplenial area can be explored. Subsplenially, the pineal and parapineal areas as well as the pulvinar thalami are exposed [11, 14]. For the posterior interhemispheric approach, the

patient is positioned either prone or laterally with the lesion side falling inferiorly. The craniotomy is performed to include the sagittal suture and lambdoid suture (Fig. 5.7). The angle of approach depends on the location of the lesion as well as the density of the bridging veins. It is very important to preserve the bridging veins of this area. Although the gravity helps with the retraction of the ipsilateral hemisphere, a retractor may be needed. It is important to avoid placing the retractor over the calcarine sulcus as this may cause hemianopsia and, coupled with the splenium resection, may lead to disconnection syndromes. After dissecting the interhemispheric adhesions, splenium of the carpus callosum is visualized. Falcotentorial junction can be seen posterior to the splenium. Anterior calcarine vein, also known

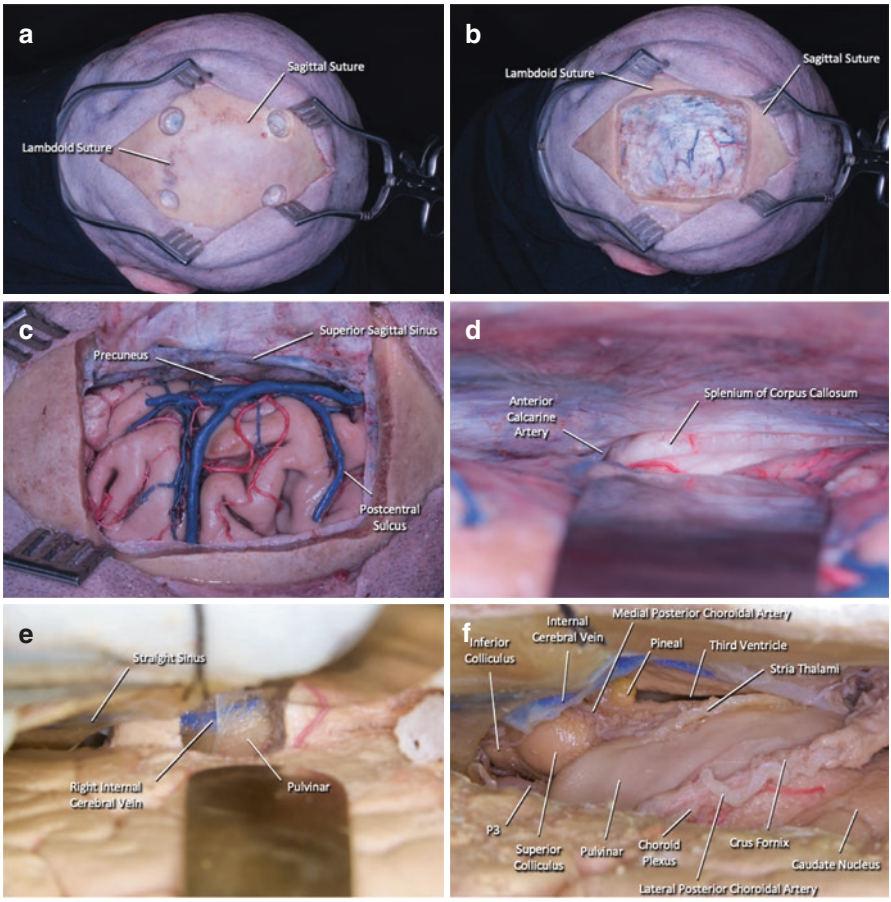

Fig. 5.7 Posterior interhemispheric approach. (**a**, **b**) Right paramedian occipital craniotomy is performed to include the sagittal suture and lambdoid suture. (**c**, **d**) After dissecting the interhemispheric adhesions splenium of the carpus callosum is visualized. (**e**) The splenial resection will provide wide exposure of the pineal gland internal cerebral veins and the pulvinar. (**f**) Exposure of posterior thalamic region after a more lateral incision and extend of callosotomy

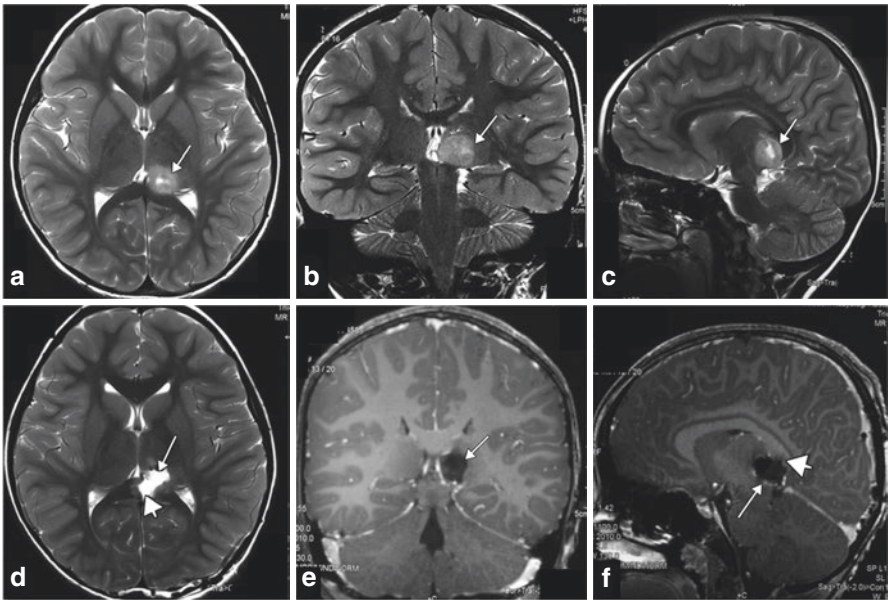

Fig. 5.8 7 years old boy was admitted to the hospital with visual disturbances. (**a–c**) T2-weighted images demonstrated a left medial pulvinar thalami lesion. A posterior interhemispheric approach with splenial dissection was performed with total excision of the lesion (**d–f**). Histology: pilomyxoid astrocytoma

as the internal occipital vein, can be seen crossing from the occipital lobe to below the falcotentorial junction. Although small, this vein should be preserved as failure may cause venous congestion and infarcts on the medial occipital region which will cause visual deficits. The splenial resection will provide wide exposure of the pineal gland internal cerebral veins and the pulvinar (Fig. 5.8). An incision in the precuneal region to preserve the integrity of the optic radiation enables entry into the atrium to resect bigger tumors extending into the atrium. But more aggressive retraction may be necessary for this approach (Fig. 5.9).

5.5.4 Supracerebellar Infratentorial Approach

Supracerebellar infratentorial approach has also been recommended for patients with pulvinar tumors, especially located in the medial posteroinferior aspect of the thalamus [5, 7, 13]. For this approach, the patient can be positioned in the sitting position or Concorde position. The craniotomy is done in the midline including the torcula. The dura is opened and suspended over the torcula. The cerebellar bridging veins will be encountered and required to be ligated. There are four main groups of bridging veins at the superior aspect of the cerebellum; the superior and inferior vermian bridging veins are situated at the midline, while the superior and inferior

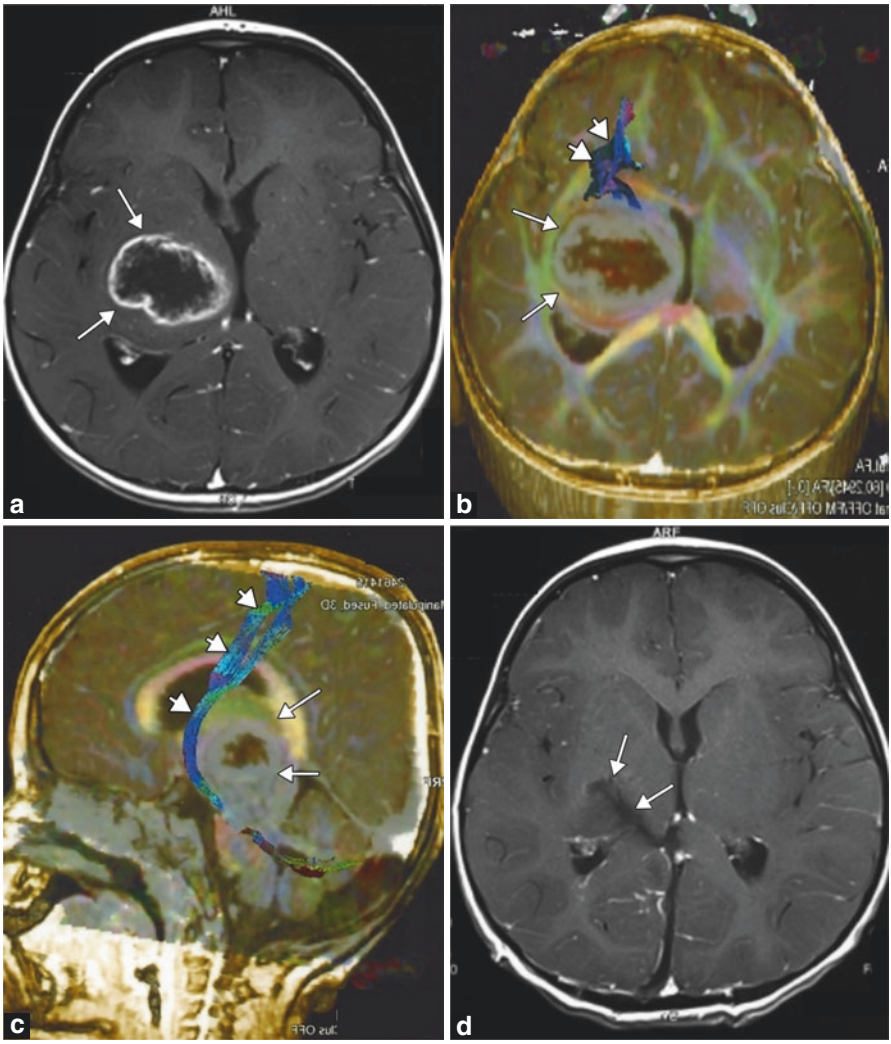

Fig. 5.9 9 years old girl presented with hemiparesis. (**a**) T1-weighted contrast study presented a big thalamic lesion. (**b**, **c**) DTI demonstrated clearly that the corticospinal tract was shifted anteriorly. Therefore, a posterior interhemispheric precuneal approach was used. (**d**) The surgical tract to the lesion is presented with arrows. Total excision of the lesion is achieved. Histology: pilocytic astrocytoma

hemispheric veins are situated more lateral. The tentorial angle will be limiting factor of the extent of this approach. The steep pitch of the tentorium on either will also be limiting for the lateral exposure. The deep venous system can be seen after advancing along the midline. The superior vermian veins can be joined by the basal veins of Rosenthal to form the vein of Galen which will constitute the roof of the exposure. The internal cerebral veins also drain into the Galen which are situated

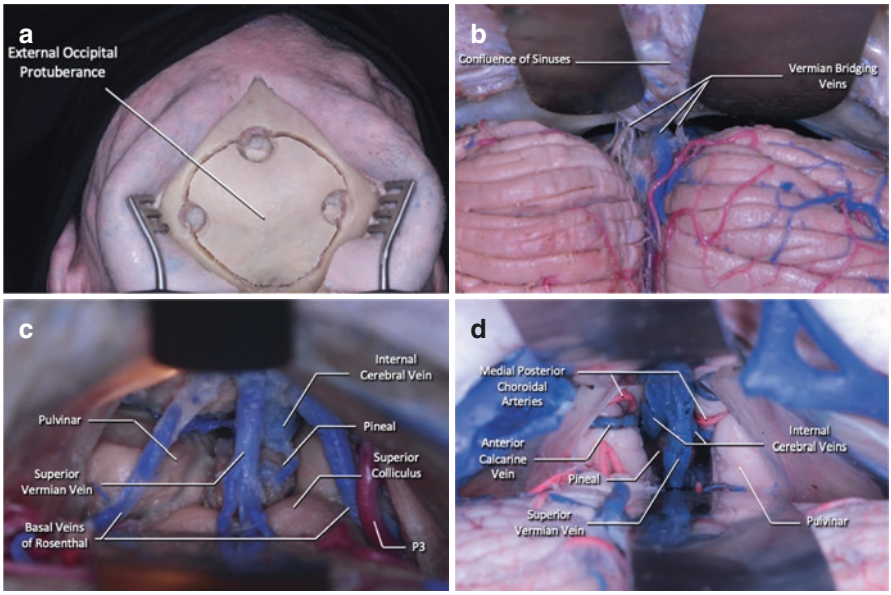

Fig. 5.10 Supracerebellar infratentorial approach. (**a**) Median suboccipital craniotomy is performed. (**b**) Supracerebellar infratentorial space is dissected. (**c**) Exposure of quadrigeminal cistern. (**d**) Pulvinar exposure after dissection of quadrigeminal cistern

opposite of this approach. The pineal gland can be exposed after dissecting the thick arachnoid. Superior colliculi are situated inferiorly. The medial aspects of both pulvinar can be exposed through this approach. The infratentorial way is completely extra-axial and less invasive. But the window between the two basal veins of Rosenthal is limited, and processes with a lateral extent of more than approximately 1 cm from the midline cannot be removed by using this route. Therefore, this approach can only be used for small tumors originating in the medial aspect of the pulvinar thalami (Fig. 5.10). An important advantage of this approach is that no white matter pathway is disrupted for gaining exposure.

5.6 Paramedian Variation

The paramedian variation of the SCIT approach can be chosen over the midline approach when one-sided approach to the pulvinar is needed. This variation is ideal for lesions of the lateral posteroinferior thalamus. Less retraction is required on the cerebellum because of the angled structure of its superior surface. The craniotomy is performed extending laterally. After the dural opening and suspension of the dural flap, the superior and inferior hemispheric bridging veins can be encountered and may be required to be ligated. Further advancing will show the free edge of the tentorium and pulvinar on the medial. It is possible that the parahypocampal gyrus

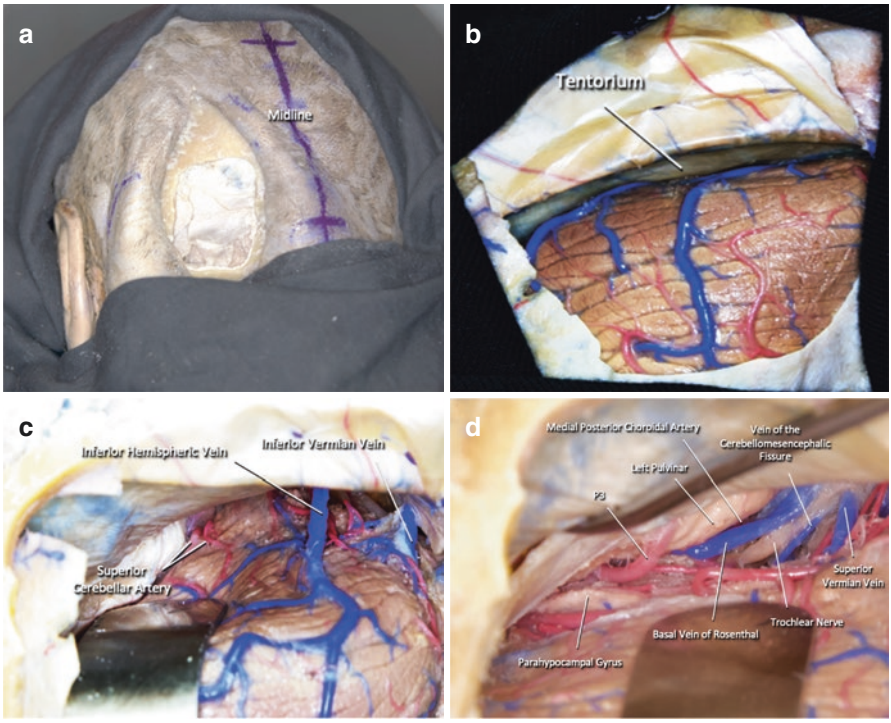

Fig. 5.11 Paramedian supracerebellar infratentorial approach. (**a**) The craniotomy is performed extending laterally (left side). (**b**) After the dural opening and suspension of the dural flap, the superior and inferior hemispheric bridging veins can be encountered. (**c**) Supracerebellar infratentorial space is dissected. (**d**) Exposure of the free edge of the tentorium and left pulvinar on the medial

may obstruct the pulvinar access along with the tentorium. The tentorium in that case can be split. The structures on the medial side which needs to be identified and preserved are the basal vein of Rosenthal, internal cerebral vein, vein of Galen, the trochlear nerve, and the posterior choroidal arteries (Fig. 5.11).

5.6.1 Transsylvian–Transinsular Approach

Tumors presenting a close relationship with the insula can be reached with a pterional transsylvian–transinsular approach. Especially, the ventral posterior thalamic region lesions are good candidates for this approach. Yasargil has described this approach for the resection of AVMs, cavernomas, and gliomas of the insular or striocapsular regions [56]. Özek and Türe modified it for thalamic low-grade tumors [1]. The patient is positioned in supine with the head rotated opposite to the lesion

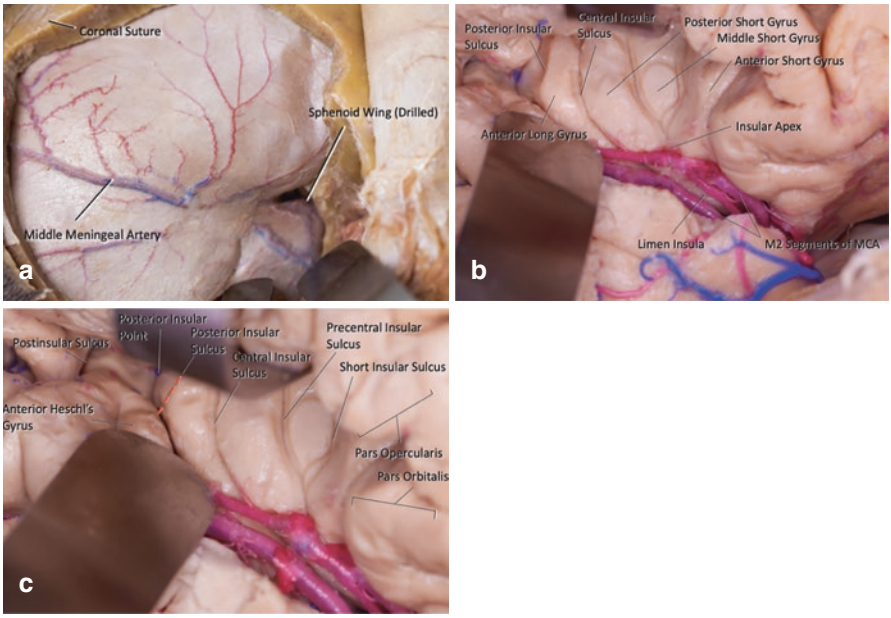

Fig. 5.12 Transsylvian–transinsular approach. (**a**) The pterional or posteriorly extended pterional craniotomy is performed. (**b**) Insular cortex and MCA M2 segments are identified by sylvian dissection. (**c**) Small incision has been made in the mid-portion of the postcentral sulcus of the insula (red line)

location. A wide pterional craniotomy is performed to allow wide dissection of the sylvian sulcus. Dura is opened in a C-shape and folded over the sphenoid side. For adequate visualization of the insula, the sylvian fissure should be opened along its entire length (Fig. 5.12). Care should be given to protect the sylvian veins as well as the branches of the middle cerebral artery.

The M2 segment of the middle cerebral artery appears over the insular cortex. The short and long gyri are identified. The posterior portion of the insular region is visualized, and it indicates the direction of exploration, which should follow the posterior limit of the posterior limb of the internal capsule. A short corticotomy at the mid-portion of the postcentral sulcus of the insula is performed and immediately, the tumor can be identified beneath the insular cortex. The lesion is then removed using routine microsurgical techniques. Precise knowledge of the topographical and vascular anatomy of the insular region allows us to use this surgical approach.

The use of this technique in patients with thalamic tumors is comparable to Kelly's and Villarejo et al. technique for treating ventral posterior lesions [8, 55]. Compared with a cortical incision in the inferior temporo-occipital region and a transcortical transtemporal approach between T1 and T2, the transsylvian–transinsular approach is less invasive [15] (Fig. 5.13). The main criticism of this approach is that it apparently traverses the retrolenticular portion of the internal capsule.

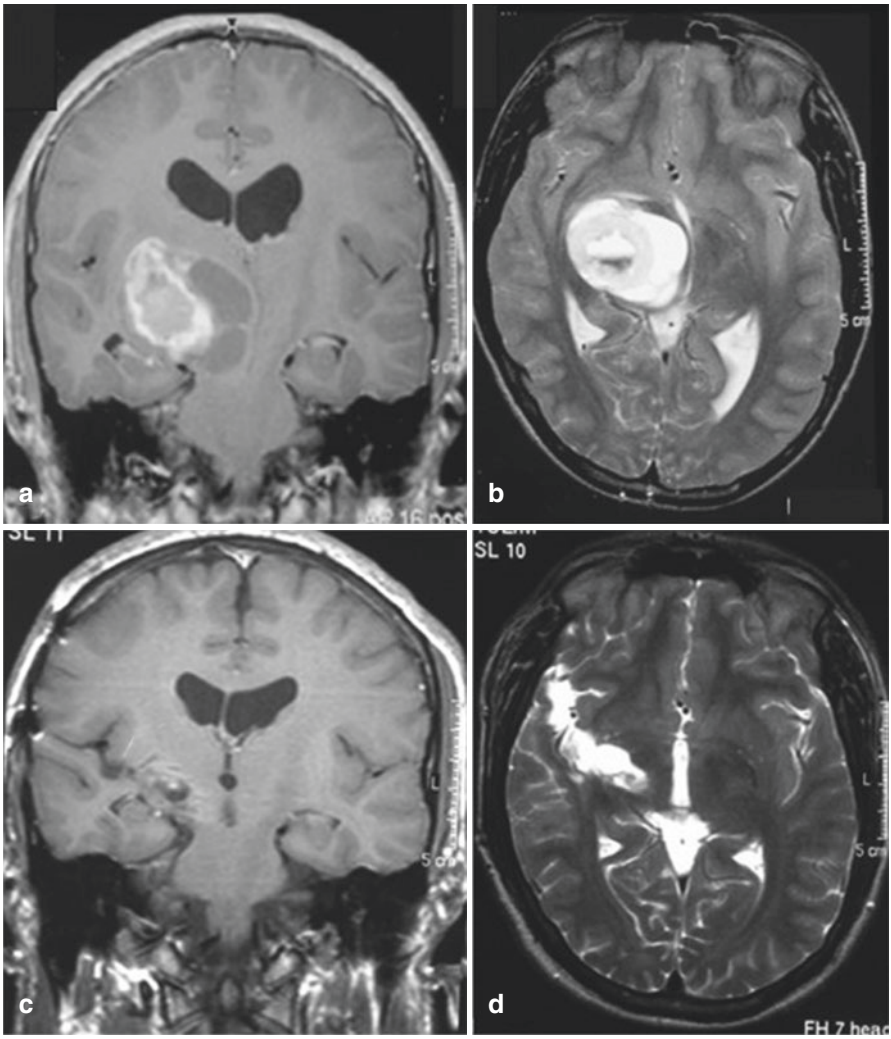

Fig. 5.13 A 16-year-old patient presented with headache and left-sided hemiparesis. (**a**, **b**) T2-weighted axial and T1-weighted contrast images demonstrate well demarcated heterogeneous mass lesion in the inferior portion of the right thalamic region. Note the close relationship between the mass lesion and the insular cortex. A right-sided pterional-transsylvian approach was performed. The patient's left-sided hemiparesis was totally resolved within 3 months. (**c**, **d**) Axial and coronal MR images performed 6 months after surgery demonstrate the radical resection of the tumor. Histology: pilocytic astrocytoma

However, it is the experience of some authors that the white matter tracts are separated and splayed by the expanding tumor and can be safely preserved by confining the surgical dissection to the lesion [1, 15].

5.7 Conclusion

Thalamic tumors can be resected with low mortality and morbidity. Different surgical approaches are available depending on location of the tumor within the thalamus and its extension. Resection of these lesions needs specific anatomical knowledge, especially the vascular anatomy of the region and the white matter tracts of the thalamus.

References

1. Özek MM, Türe U. Surgical approach to thalamic tumors. Childs Nerv Syst. 2002;18:450–6.
2. Puget S, Crimmins DW, Garnett MR, Grill J, Oliveira R, Boddaert N, Sainte-Rose C. Thalamic tumors in children: a reappraisal. J Neurosurg. 2007;106(5 Suppl):354–62.
3. Steinbok P, Gopalakrishnan CV, Hengel AR, Vitali AM, Poskitt K, Hawkins C, Drake J, Pasculli M, Ajani O, Hader W, Mehta V, McNeely PD, McDonald PJ, Ranger A, Vassilyadi M, Atkinson J, Ryall S, Eisenstat DD, Hukin J. Pediatric thalamic tumors in the MRI era: a Canadian perspective. Childs Nerv Syst. 2016;32:269–80.
4. Baroncini M, Vinchon M, Mineo JF, Pichon F, Francke JP, Dhellemmes P. Surgical resection of thalamic tumors in children: approaches and clinical results. Childs Nerv Syst. 2007;23:753–60.
5. Cinalli G, Aguirre DT, Mirone G, Ruggiero C, Cascone D, Quaglietta L, Aliberti F, Santi S, Buonoccore MC, Nastro A, Spennato P. Surgical treatment of thalamic tumors in children. J Neurosurg Pediatr. 2018;21:247–57.
6. Souweidane MM, Hoffman HJ. Current treatment of thalamic gliomas in children. J Neurooncol. 1996;28:157–66.
7. Cuccia V, Monges J. Thalamic tumors in children. Childs Nerv Syst. 1997;13:514–21.
8. Kelly PJ. Stereotactic biopsy and resection of thalamic astrocytomas. Neurosurgery. 1989;25:185–95.
9. Prakash B. Surgical approach to large thalamic gliomas. Acta Neurochir. 1985;74:100–4.
10. Baran O, Baydin S, Güngör A, Balak N, Middlebrooks E, Saygı T, Aydın İ, Tanrıöver N. Surgical approaches to the thalamus in relation to the white matter tracts of the cerebrum. World Neurosurg. 2019;128:1048–86.
11. Serra C, Türe H, Yaltırık CK, Harput MV, Türe U. Microneurosurgical removal of thalamic lesions: surgical results and considerations from a large, single-surgeon consecutive series. J Neurosurg. 2020;2:1–11.
12. Serra C, Türe U, Krayenbühl N, Şengül G, Yaşargil DC, Yaşargil MG. Topographic classification of the thalamus surfaces related to microneurosurgery: a white matter fiber microdissection study. World Neurosurg. 2017;97:438–52.
13. Steiger HJ, Gotz C, Schmid-Elsaesser R, Stummer W. Thalamic astrocytomas: surgical anatomy and results of a pilot series using maximum microsurgical removal. Acta Neurochir. 2000;142:1327–37.
14. Yaşargil MG. Microneurosurgery, vol. 4B. Stuttgart: Thieme; 1996. p. 29–91.

15. Mishra S, Mishra RC. The transsylvian trans-insular approach to lateral thalamic lesions. Neurol India. 2012;60:385–9.
16. Bordes S, Werner C, Mathkour M, McCormack E, Iwanaga J, Loukas M, Lammle M, Dumont AS, Tubbs RS. Arterial supply of the thalamus: a comprehensive review. World Neurosurg. 2020;137:310–8.
17. Schmahmann JD. Vascular syndromes of the thalamus. Stroke. 2003;34:2264–78.
18. Bogousslavsky JU, Regli FR, Assal G. The syndrome of unilateral tuberothalamic artery territory infarction. Stroke. 1986;17:434–41.
19. Khanni JL, Casale JA, Koek AY, Del Pozo PH, Espinosa PS. Artery of Percheron infarct: an acute diagnostic challenge with a spectrum of clinical presentations. Cureus. 2018;10:9.
20. Bogousslavsky J, Regli F, Uske A. Thalamic infarcts: clinical syndromes, etiology, and prognosis. Neurology. 1988;38:837.
21. Graff-Radford NR, Damasio H, Yamada T, Eslinger PJ, Damasio AR. Nonhaemorrhagic thalamic infarction: clinical, neuropsychological and electrophysiological findings in four anatomical groups defined by computerized tomography. Brain. 1985;108:485–516.
22. Lisovoski F, Koskas P, Dubard T, Dessarts I, Dehen H, Cambier J. Left tuberothalamic artery territory infarction: neuropsychological and MRI features. Eur Neurol. 1993;33:181–4.
23. Percheron G. The anatomy of the arterial supply of the human thalamus and its use for the interpretation of the thalamic vascular pathology. Z Neurol. 1973;205:1–13.
24. Carrera E, Michel P, Bogousslavsky J. Anteromedian, central, and posterolateral infarcts of the thalamus: three variant types. Stroke. 2004;35:2826–31.
25. Tatu L, Moulin T, Bogousslavsky J, Duvernoy H. Arterial territories of the human brain: cerebral hemispheres. Neurology. 1998;50:1699–708.
26. Dejerine J, Roussy G. Le syndrome thalamique. Rev Neurol (Paris). 1906;14:521–32.
27. Takahashi S, Goto K, Fukasawa H, Kawata Y, Uemura K, Yaguchi K. Computed tomography of cerebral infarction along the distribution of the basal perforating arteries. Part II: Thalamic arterial group. Radiology. 2014;155:119–30.
28. Segarra JM. Cerebral vascular disease and behavior: the syndrome of the mesencephalic artery (basilar artery bifurcation). Arch Neurol. 1970;22:408–18.
29. Caruso P, Manganotti P, Moretti R. Complex neurological symptoms in bilateral thalamic stroke due to Percheron artery occlusion. Vasc Health Risk Manag. 2017;13:11.
30. Castaigne P, Lhermitte F, Buge A, Escourolle R, Hauw JJ, Lyon-Caen O. Paramedian thalamic and midbrain infarcts: clinical and neuropathological study. Ann Neurol. 1981;2:127–48.
31. Fujii K, Lenkey C, Rhoton AL. Microsurgical anatomy of the choroidal arteries: lateral and third ventricles. J Neurosurg. 1980;52:165–88.
32. Neau JP, Bogousslavsky J. The syndrome of posterior choroidal artery territory infarction. Ann Neurol. 1996;39:779–88.
33. Li S, Kumar Y, Gupta N, Abdelbaki A, Sahwney H, Kumar A, Mangla M, Mangla R. Clinical and neuroimaging findings in thalamic territory infarctions: a review. J Neuroimaging. 2018;28:343–9.
34. Ono M, Rhoton AL Jr, Peace D, Rodriguez RJ. Microsurgical anatomy of the deep venous system of the brain. Neurosurgery. 1984;15:621–57.
35. Bozkurt B, Yağmurlu K, Belykh E, Meybodi AT, Staren MS, Aklinski JL, Preul MC, Grande AW, Nakaji P, Lawton MT. Quantitative anatomic analysis of the transcallosal–transchoroidal approach and the transcallosal-subchoroidal approach to the floor of the third ventricle: an anatomic study. World Neurosurg. 2018;118:219–29.
36. Nieuwenhuys R, Voogd J, Van Huijzen C. The human central nervous system. 4th ed. Berlin: Springer Science & Business Media; 2007. p. 253–5.
37. Schmahmann JD, Pandya D. Fiber pathways of the brain. New York: OUP; 2009. p. 527–33.
38. Wakana S, Jiang H, Nagae-Poetscher LM, Van Zijl PC, Mori S. Fiber tract-based atlas of human white matter anatomy. Radiology. 2004;230:77–87.
39. Sussmann JE, Lymer GK, McKirdy J, Moorhead TW, Maniega SM, Job D, Hall J, Bastin ME, Johnstone EC, Lawrie SM, McIntosh AM. White matter abnormalities in bipolar disorder and

schizophrenia detected using diffusion tensor magnetic resonance imaging. Bipolar Disord. 2009;11:11–8.
40. Aralasmak A, Ulmer JL, Kocak M, Salvan CV, Hillis AE, Yousem DM. Association, commissural, and projection pathways and their functional deficit reported in literature. J Comput Assist Tomogr. 2006;30:695–715.
41. Tamraz JC, Comair YG, Tamraz JC. Atlas of regional anatomy of the brain using MRI. Cham: Springer; 2004.
42. Frieling H, Fischer J, Wilhelm J, Engelhorn T, Bleich S, Hillemacher T, Dörfler A, Kornhuber J, de Zwaan M, Peschel T. Microstructural abnormalities of the posterior thalamic radiation and the mediodorsal thalamic nuclei in females with anorexia nervosa—a voxel-based diffusion tensor imaging (DTI) study. J Psychiatr Res. 2012;46:1237–42.
43. Cremers LG, de Groot M, Hofman A, Krestin GP, van der Lugt A, Niessen WJ, Vernooij MW, Ikram MA. Altered tract-specific white matter microstructure is related to poorer cognitive performance: the Rotterdam study. Neurobiol Aging. 2016;39:108–17.
44. Milner B. Effects of different brain lesions on card sorting: the role of the frontal lobes. Arch Neurol. 1963;9:90–100.
45. Moore TL, Schettler SP, Killiany RJ, Rosene DL, Moss MB. Effects on executive function following damage to the prefrontal cortex in the rhesus monkey (*Macaca mulatta*). Behav Neurosci. 2009;123:231.
46. Mamah D, Conturo TE, Harms MP, Akbudak E, Wang L, McMichael AR, Gado MH, Barch DM, Csernansky JG. Anterior thalamic radiation integrity in schizophrenia: a diffusion-tensor imaging study. Psychiatry Res Neuroimaging. 2010;183:144–50.
47. Klingler J, Gloor P. The connections of the amygdala and of the anterior temporal cortex in the human brain. J Comp Neurol. 1960;115:333–69.
48. Whitlock DG, Nauta WJ. Subcortical projections from the temporal neocortex in *Macaca mulatta*. J Comp Neurol. 1956;106:183–212.
49. Velasco F, Velasco M, Jiménez F, Velasco AL, Salin-Pascual R. Neurobiological background for performing surgical intervention in the inferior thalamic peduncle for treatment of major depression disorders. Neurosurgery. 2005;57:439–48.
50. Velasco M, Velasco F, Jiménez F, Carrillo-Ruiz JD, Velasco AL, Salín-Pascual R. Electrocortical and behavioral responses elicited by acute electrical stimulation of inferior thalamic peduncle and nucleus reticularis thalami in a patient with major depression disorder. Clin Neurophysiol. 2006;117:320–7.
51. Hauptman JS, DeSalles AA, Espinoza R, Sedrak M, Ishida W. Potential surgical targets for deep brain stimulation in treatment-resistant depression. Neurosurg Focus. 2008;25:E3.
52. Jiménez F, Velasco F, Salin-Pascual R, Hernández JA, Velasco M, Criales JL, Nicolini H. A patient with a resistant major depression disorder treated with deep brain stimulation in the inferior thalamic peduncle. Neurosurgery. 2005;57:585–93.
53. Lee DJ, Dallapiazza RF, De Vloo P, Elias GJ, Fomenko A, Boutet A, Giacobbe P, Lozano AM. Inferior thalamic peduncle deep brain stimulation for treatment-refractory obsessive–compulsive disorder: a phase 1 pilot trial. Brain Stimul. 2019;12:344–52.
54. Senova S, Clair AH, Palfi S, Yelnik J, Domenech P, Mallet L. Deep brain stimulation for refractory obsessive–compulsive disorder: towards an individualized approach. Front Psych. 2019;10:905.
55. Villarejo F, Amaya C, Perez Diaz C, Pascual A, Alvarez Sastre C, Goyenechea F. Radical surgery of thalamic tumors in children. Childs Nerv Syst. 1994;10:111–4.
56. Yasargil MG. Microneurosurgery, vol. 3B. Stuttgart: Thieme; 1988. p. 137–49.

Chapter 6
Convection-Enhanced Delivery in Children: Techniques and Applications

K. Aquilina, A. Chakrapani, L. Carr, M. A. Kurian, and D. Hargrave

6.1 Introduction

Since it was first described in 1994, convection-enhanced delivery (CED) has undergone extensive pre-clinical and clinical investigations [1]. Although predominantly rooted in oncology, CED has been also used extensively in other fields in both adults and children, including neurodegenerative, metabolic, and neurotransmitter disorders. The unique ability of CED to reliably deliver macromolecules, nanoparticles, and viruses directly to their site of action in the brain, bypassing the blood brain barrier, continues to hold promise. In this article, we review the principles of CED and describe its techniques and applications in children.

K. Aquilina (✉)
Department of Neurosurgery, Great Ormond Street Hospital, London, UK
e-mail: Kristian.aquilina@gosh.nhs.uk

A. Chakrapani
Department of Metabolic Medicine, Great Ormond Street Hospital, London, UK
e-mail: Anupam.chakrapani@gosh.nhs.uk

L. Carr
Department of Neurology and Neurodisability, Great Ormond Street Hospital, London, UK
e-mail: Lucinda.carr@gosh.nhs.uk

M. A. Kurian
Department of Neurology and Neurodisability, Great Ormond Street Hospital, London, UK

Neurogenetics Group, Developmental Neurosciences, Zayed Centre for Research into Rare Disease in Children, UCL-Great Ormond Street Institute of Child Health, London, UK
e-mail: Manju.kurian@ucl.ac.uk

D. Hargrave
Cancer Group, UCL-Great Ormond Street Institute of Child Health, London, UK
e-mail: d.hargrave@ucl.ac.uk

C. Di Rocco (ed.), *Advances and Technical Standards in Neurosurgery*, Advances and Technical Standards in Neurosurgery 45,
https://doi.org/10.1007/978-3-030-99166-1_6

6.2 The Blood Brain Barrier and Interstitial Fluid

The blood brain barrier (BBB) is the interface between the brain parenchyma and the vascular system. Its primary function is to maintain brain homeostasis by regulating transport into and out of brain cells. The architecture and development of the brain microvasculature is highly conserved across species. Early growth of brain capillaries has been extensively described in the zebrafish, where the development of BBB properties parallels early angiogenesis and is strikingly similar to the mammalian brain [2]. The human brain contains an extensive network of capillaries, with an average diameter of 7 μm, and an estimated surface area of 15–25 m^2. The vascular system of the brain is arranged such that each neuron is no further than 10–20 μm from the nearest capillary [3].

The BBB, at the level of the vascular endothelium, maintains homoeostasis for water, ions, amino acids, hormones, neurotransmitters, and immune cells as well as provides a barrier for toxic or infectious agents. In this way, it protects the brain against disruption of controlled neuronal signalling, inflammation, cerebral oedema, and exposure to pathogens. The neurovascular unit represents a structural and functional interaction between vascular cells (endothelial cells, pericytes), the basement membrane, and glial cells (microglia, astrocytes, and oligodendroglia). Endothelial cells are held together by interactions between the extracellular domains of transmembrane proteins, which are anchored on their intracellular side to the cytoskeleton. These prevent paracellular transport of molecules, enforcing the need for transcellular active transport. This is a dynamic interaction, such that increased shear stress due to blood flow upregulates genes associated with junctional proteins and transporters. Endothelial cells lack fenestrations and allow only low rates of transcytosis [4]. In the post-capillary venules, endothelial cells also have low expression of leucocyte adhesion molecules, allowing higher control of white cell recruitment to the perivascular spaces, limiting inflammation and oedema.

Brain capillaries are almost completely surrounded by astrocytic end feet. An astrocyte may support multiple endothelial cells. Astrocytes have a role in regulating blood flow in response to increased local neuronal activity, probably by changing calcium ion concentration in their end feet. The pericytes wrap around capillaries and are aligned with the direction of blood flow. They are separated from the endothelial cells by a thin 100 nm basement membrane. One pericyte typically supports three endothelial cells [5]. Pericytes are contractile, as they have actin fibres spread throughout their body; they can regulate capillary diameter and blood flow. They are recruited to nascent capillaries during development.

The extracellular space in the brain occupies 15–30% of the brain volume. It surrounds the neurons and glia in the brain and consists of a hyaluronan-based matrix and a fluid phase that contains lower protein, K^+, and Ca^{2+} concentrations than plasma but higher Mg^{2+} levels. Its fraction of total brain volume has been estimated at 0.15–0.30 [6]. The fluid phase represents a reservoir of ions and neurotransmitters and allows movement of solutes and nutrients between the most peripheral capillaries and the brain cells. It originates at the BBB, as the sodium–potassium pump

generates a net inflow of filtered plasma into the fluid phase [7]. CSF flow in the glymphatic system also mixes within the interstitial fluid, as it flows along the Virchow Robin spaces [8]. The geometry of the extracellular space has been described as an interconnected network of pores, up to 100 nm in diameter, running between adjacent cell membranes [6].

The BBB is a key obstacle in the treatment of several conditions that affect the CNS; only depression, schizophrenia, chronic pain, some of the white matter, neurotransmitter and autoimmune disorders, and epilepsy are currently treatable with orally administered small molecule drug therapy [3]. The BBB represents an important component of the gap between in vitro pharmacological success and patient outcomes in clinical trials. While small (<500 Da) lipophilic molecules can diffuse across the luminal and abluminal membranes of the endothelial cells, small polar molecules such as amino acids and nucleosides require carrier-mediated transport through the endothelial cells. Larger molecules such as proteins require endocytic transport, mediated by receptors or adsorption [3]. Efflux pumps actively return unwanted molecules back into the circulation. Ninety eight percent of all small molecules do not cross the BBB.

6.3 Convection-Enhanced Delivery: General Principles

6.3.1 Volume of Distribution

CED involves the bulk movement of a solute or drug along a pressure differential into the interstitial compartment, gradually replacing the extracellular fluid with infusate. The first injection studies, using blunt stainless steel 23G cannulae, were carried out in the corona radiata of anaesthetized cats, using a large (transferrin) and a small (sucrose) molecule [1]. These initial studies showed that 'microinfusion' could effectively raise the concentration of a substance within the brain parenchyma to several orders of magnitude of that in the systemic circulation. Early CED trials using diphtheria toxin for recurrent malignant gliomas demonstrated local tumour responses without systemic adverse effects [9].

CED was confirmed to be five to tenfold more effective than diffusion in delivering a substance [10]. Whereas diffusion is driven by a concentration gradient, CED can continue despite equal concentrations of the substance throughout the tissue. Distribution achieved by diffusion alone is limited to a maximum of 1–2 mm and is dependent on the size of the molecule. Diffusion is less effective for large molecules. There is a steep drop-off at the peripheral margin of the distribution, by about 250–1000-fold. In addition, the concentration of molecule at the point of dispersal must be very high, and therefore potentially toxic to brain tissue, at least at that point.

In contrast, CED, driven by a pressure differential, is able to distribute a molecule homogeneously throughout a high volume of interstitial brain tissue. Molecular size is not a limiting factor, as the interstitial fluid is displaced by bulk flow of the

solute containing the drug. Its eventual distribution is limited by the total volume infused, the metabolism of the drug, the degree to which it is bound to or taken up by the local cells, and whether it is transported back into the microvasculature. Distribution by CED is best for high molecular weight (>400 Da) hydrophilic molecules, which are therefore not easily cleared out of the interstitial fluid by absorption into the systemic circulation through the local capillaries. Large, hydrophilic molecules are more likely to remain in the interstitial fluid rather than diffuse back into the circulation [11]. Long infusion times allow a longer opportunity for metabolism and clearance at the periphery of the distribution cloud, leading to reduction in distribution volume [12]. As a continuous pressure differential is required, it is essential that the materials used to inject the drug into the brain, including the syringes, tubing, and implanted catheters, are made of stiff non-compliant materials.

Several variables affect delivery of the drug into the brain parenchyma. These include anatomy of the target site, infusion rate, infusion frequency, drug type and concentration, as well as catheter design and placement [11]. Delivery is defined by the ratio of the volume of brain permeated (V_d) by the volume infused (V_i). This varies by the permeability of the target brain tissue; a higher ratio implies superior delivery. Brain grey matter (cortex) has a lower interstitial fraction than white matter and has a typical distribution ratio of 4:1. White matter is more permeable and typically has a distribution ratio of 7:1. The high density of the white matter tracts in the brainstem gives it a typical ratio of up to 10:1. In addition, the anatomy of the target region defines the shape of permeation. In the cortex, flow is typically not constrained in any one direction (anisotropic) and fluid distribution is therefore spherical. In white matter, the direction of the tracts determines permeability, leading to isotropic distribution that is higher along the tracts.

The volume of distribution is also limited by ependymal and pial surfaces. Once the infused volume reaches these boundaries, the solute will then be lost to CSF. One study monitored the volume of distribution of gadoteridol-loaded liposomes infused by CED into non-human primates and canines [13]. This demonstrated that once leakage into the ventricles or sulci began, further distribution into the brain ceased or underwent marked attenuation. However, high molecular weight compounds may be contained by the pia and prevented from leaking into the subarachnoid space, if the pial surface itself is not punctured [14].

Particular issues related to the interstitial fluid and volume of distribution apply to CED in brain tumours. Brain tumours, especially higher-grade ones, disrupt the intercellular space and the physiological fluid flow within it. Neovascularization, increased permeability of immature blood vessels, sequestration of protein, and increased cellular components all raise fluid volume within the space and increase interstitial pressure [15]. The interstitial pressure in normal brain tissue is 0.8 mmHg, while within a tumour it has been measured at 7 mmHg [16]. Bulk flow of interstitial fluid from inside to outside the tumour may reduce the efficacy of CED. Cystic tumour components create their own local effects on the surrounding tumour tissue and brain parenchyma, depending on their content, fullness, and permeability, and the pressure within them may be different from that in the ventricles or subarachnoid space [17]. While in adult GBMs CED is usually administered after resection

of the tumour, this is not the case for diffuse intrinsic pontine glioma (DIPG) in children, where it is usually administered after radiotherapy. However, radiotherapy is known to degrade extracellular matrix, increasing its permeability [18]. Necrotic areas may act as sinks, reducing further forward flow of infusate. This is an important factor considering that in most current trials CED is administered after other treatment modalities have failed.

DIPGs can contain cystic regions; precise positioning of a catheter tip at least 10 mm from the cyst has been shown to preserve infusate volume, with avoidance of leakage into the cyst [19]. Regions of tumour necrosis lack interstitial architecture and may lead to pooling of the infusate, and highly vascular regions in malignant tumours can lead to infusate leaking into the systemic circulation [13]. The presence of a rich network of lenticulostriate vessels around the putamen may draw interstitial fluid and CED infusate into perivascular channels in a dorsoventral direction along a preferential extracellular flow pathway; a putaminal infusion approaching from a dorsal direction exploits this natural flow [20].

The volume of distribution is also influenced by viscosity and surface properties of the infused solute [21]. Monodispersed maghemite nanoparticles distributed better when their viscosity was increased by coating with dextran or when the infusate also contained sucrose or polyethylene glycol [22]. In a study evaluating delivery of viral particles, surface characteristics were found to be critical for their distribution [23]. Similarly, in another study evaluating spread of liposomes infused by CED, liposomes shielded by polyethylene glycol distributed further than unshielded liposomes [24]. Positively charged liposomes were also more effectively bound to cells, reducing their spread in comparison to neutral or negatively charged ones [24].

6.3.2 Infusate Backflow

High variability in flow rate and infusion patterns has made it harder to evaluate the impact of CED across clinical trials; infusion rates, for example, have ranged from 0.5 to 66 μL/min, and volumes infused from 2 to 108 mLs [11]. Infusions are usually commenced at a low rate, starting from 0.1 to 5 μL/min. The rate is slowly increased over subsequent hours. Effective infusion rates are specific to the catheter used and the target tissue. Historically, infusion rates have increased to enable sufficient drug delivery within a reasonable time. Although an increase in flow rate theoretically increases the volume of distribution, in practice this also leads to an increase in backflow along the cannula back towards the surface of the brain.

Backflow, or reflux, reduces pressure at the point of injection, limiting wide solute distribution. Once an annular gap around the catheter is formed, backflow is established, offering a path of least resistance and leading to loss of large volumes of fluid [25]. The needle tract effectively forms a pressure sink with lower hydraulic resistance than brain parenchyma [26]. Rotational movement during insertion may compromise the parenchymal seal around the cannula and increase reflux [27]. Conversely, rapid needle insertion may reduce parenchymal injury and reduce reflux

[28]. Reflux is more extensive, both in volume lost and distance travelled, when cannulas with large diameter are used [26]. When catheters similar to shunt catheters were used, either with a single opening at the end or with multiple side openings, distribution was poor; sealing of the burr holes, or use of a very low flow rate, was required to reduce large reflux [29, 30]. When multi-port hydrocephalus shunts were used, 80% of the fluid escaped through the three proximal holes, severely limiting any forward solute delivery [31]. The position of the catheter tip with regard to the tumour and peri-tumoural region, as well as distance from the ventricle, the cortical surface, and major sulcal boundaries, also influences the extent of backflow and success of solute delivery [14].

Backflow is also influenced by hydraulic resistance in the region of the ventricles. In computational three-dimensional models designed specifically to evaluate backflow and using realistic non-linear brain geometry, backflow varied with infusion flow rates, catheter distance from the ventricles, and intraventricular pressure [32]. Catheters implanted close to low-pressure ventricles were shown to lose more fluid to ventricular CSF, whereas catheters close to high-pressure ventricles had high backflow. The authors recognize that more accurate flow modeling must be patient-specific and needs to take into account heterogeneities of brain tissue, particularly in the vicinity of a tumour, and the changes in the mechanical properties of the parenchyma occurring as a result of cannula insertion and progressive infusion [32]. A recent study in adult rat brains has demonstrated the efficacy of electrokinetic CED of charged molecules along a current between two implanted electrodes; in this way, the infusion pressure, essential for CED, and the cause of backflow, is replaced by the electrophoretic mobility of the solute [33]. This technique also provides definitive directionality of distribution. Further pre-clinical studies are required to explore this concept further.

6.3.3 Catheters for CED

Catheters in current use are up to about 32G in diameter. Mechanical disruption and trauma of brain tissue around the catheter caused during insertion, as well as the presence of air bubbles, intermittent blockage, pressure spikes during infusion, large catheter diameter, and catheter hardness, all increase the volume and extent of backflow [34, 35]. Delaying the first injection to allow a longer tissue sealing time between the catheter and the brain has not been shown to effectively reduce backflow, probably because the healing time required is longer than the permissible waiting time. Insertion of a small soft catheter over a stylet increases the risk of introducing air bubbles. To limit this, catheters often have an outer coat that is more rigid, obviating the need for an internal stylet.

Five categories of catheter design have been described. These include the end-port cannula, stepped profile catheters, multi-port catheters, porous-tipped catheters, and balloon-tipped catheters [21]. Most have been evaluated in agarose gel phantoms, considered similar to brain tissue, although understandably more

homogenous and validated against the porcine brain model [36]. The microporous-tipped cannula is characterized by a ceramic tip containing a large number of small holes, up to 0.45 μm in diameter, arranged around the circumference of the catheter. As the holes are so small, pressure within the core distal to the proximal holes is maintained, allowing for a more even flow from the whole tip.

Porous catheters, with high porosity over a 13 mm segment, starting 4 mm from the tip, have been evaluated for infusion of large volumes of fluid over a wide distribution, such as an entire hemisphere [37]. When compared to the SmartFlow™ cannula, a step end-port catheter, used in vivo in porcine brain, larger distribution volumes were obtained with the porous catheter, as fluid emanated radially and uniformly from the entire porous length. Balloon-tipped catheters have been used only experimentally; these allow a small balloon at the top to be inflated within the post-resection tumour cavity, allowing the drug to be delivered into the periphery where tumour recurrence is most likely, without the risk of pooling or sequestration into the cavity [38]. The infusate was delivered effectively into the brain parenchyma around the balloon in a canine model to a depth of 25 mm, which would be expected to cover the region of recurrence in a glioblastoma [39]. In another study, the balloon did not have an exit port; it was filled with ^{125}I radiation source to deliver brachytherapy instead [40].

Stepped catheters have been used extensively for experimental and clinical CED and several designs have been developed. A step, fashioned close to the tip of the cannula, reduces reflux up the catheter, increases perfusion and interstitial pressure around the tip, and improves distribution (Fig. 6.1). The first stepped catheter was composed of a 0.2 mm needle with a glued-in silica tubing, 0.168 mm in external diameter, that extended beyond the tip of the needle by 5–10 mm [41]. Rigid cannulas, which contain ceramic or steel tubing with fused silica liners, are preferable for acute injection, as they minimize macro-motion during implantation and

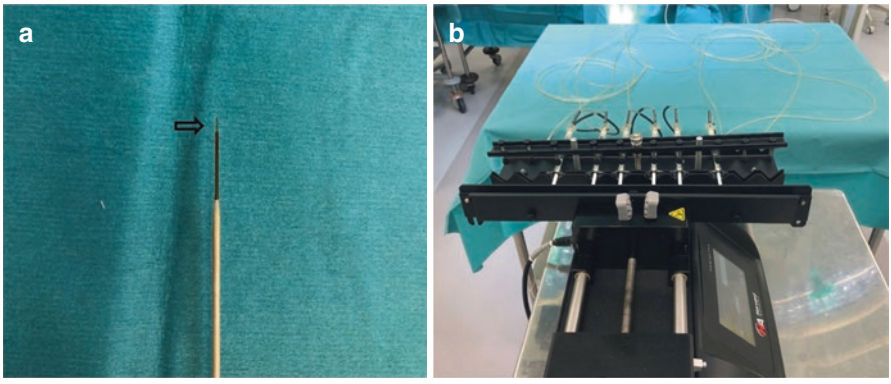

Fig. 6.1 (**a**) Tip of the Smartflow TM CED cannula. The block arrow points to the step proximal to the tip of the cannula, designed to prevent reflux. The body of the cannula is made of rigid ceramic. (**b**) Intraoperative infusion of AAV2 gene therapy for San Filippo syndrome, with six simultaneous infusions connected to the same Harvard syringe pump

injection [36]. For long-term implantation, however, the relative movement between the rigid cannula and the brain may promote reflux. A flexible cannula can move harmlessly with the frequent brain movements related to day-to-day activities. Subsequent developments included flexible cannulas with a rigid distal infusion tip, inserted over a removable rigid core. One of the first flexible catheter assemblies that was suitable for long-term implantation was used in a glial cell-line-derived neurotrophic factor (GDNF) study in Parkinson's disease [42].

Renishaw PLC have subsequently developed a recessed sub-millimetre diameter catheter in which two guide tubes, an inner and a longer outer one, form a step 1.5 mm long just proximal (3–18 mm) to the catheter tip; the inner guide tube is shorter than the outer one, thereby forming a recess which, on insertion, is plugged with tissue and therefore limits further reflux [25, 38]. The developers argue that this cannula does not act as a point source of distribution, but rather as a controlled reflux device [25]. A higher recess (or longer step length) led to a longer and narrower ellipsoid distribution; higher infusion flow rates led to reduced distribution. This applied to both in vitro and porcine grey matter evaluation (thalamic and putaminal) [25]. The authors argue that the distribution can be designed as spherical or ellipsoid by using catheters with shorter or longer recess length, aiming to match their target more completely. A step length between 3 and 6 mm causes a length to width ratio of 1:1–1:1.5 (spherical), whereas a step length over 12 mm increases the ratio to 2:1 or 3:1 (ellipsoid). Except for infusion at high pressures, the step limited further backflow around the cannula. Infusate rose to the step and then stabilized and distributed laterally. The highest reflux was seen with the shortest step lengths and the highest infusion rates. This study also showed that large backflow rates could be reduced by lowering infusion rates, but in vivo this would necessitate MR imaging during infusion [25]. These catheters are able to connect to a delivery system incorporating a transcutaneous port at the skull surface.

Another cannula involves a valve-tip device, where a solid rod is inserted into the core of the cannula, and on insertion, is withdrawn 3–5 mm. The design of the core is such that this allows infusate to flow around the rod, reducing the dead volume of the cannula [43].

Specialist pumps that are able to maintain such low flow rates are clearly required.

6.3.4 Catheter Insertion Techniques

Various aspects of catheter insertion procedures have been described in the recent literature. Implantation of the Renishaw stepped catheter utilizes image guidance and stereotactic robot assistance, based on the NeuroInspire software [25, 44]. Each component of the cannula is delivered over guide rods. The outer guide tube is delivered over a tungsten carbide delivery rod, just short of the implantation position. The inner guide tube is then passed over an inner steel rod under continuous aspiration to minimize entry of air into the tract. Finally, a 0.6 mm rod is advanced

beyond the inner guide tube to the injection point, creating a pre-formed track for the unsupported flexible cannula [25].

One of the principal difficulties in CED is the ability to visualize the distribution of the drug, ideally in real time, so that appropriate corrective action can be taken, if necessary, during the infusion to ensure complete coverage of the target. One technique to achieve real-time CED uses intraoperative MRI [45]. The ClearPoint navigation platform (MRI Interventions, Irvine, CA, USA) was developed to improve safety and accuracy of electrode implantation in deep brain stimulation and was subsequently modified to allow accurate drug delivery and real-time visualization in an intraoperative MRI setting [45, 46]. The SmartGrid, a localizing adhesive grid, is positioned over the expected entry site before MR volumetric scanning and informs the positioning of the SmartFrame, a scalp or skull-mounted frame which contains the infusion cannula guide. The ClearPoint software generates the trajectory and provides depth as well as co-ordinates on the XY axis. In addition, adjustments using hand controllers that extend beyond the bore of the magnet can be made by the neurosurgeon, allowing the expected error at the target to lie below 0.5 mm. A burr hole is then drilled through the mounted frame along the appropriate trajectory, and the SmartFlow cannula, after priming, is inserted to the required depth. Co-infusion with gadolinium allows real-time visualization of the injection; fast multiplanar T1 images are acquired every 5 min during the infusion. Once the infused fluid is seen in the target, the flow is increased as required by the protocol [45]. Bilaterally mounted SmartFrames allow simultaneous infusions in both hemispheres.

The aforementioned authors have used this system widely, including for the delivery of adeno-associated virus serotype 2 (AAV2), carrying a gene for amino acid decarboxylase (AADC), into the putamen of patients with medically refractory Parkinson's disease. The primary benefit of the technique is that the volume infused may be varied depending on the coverage of the putamen, as it is visualized in real time [45]. The system has also been used in early phase trials for recurrent glioblastoma, delivering nanoliposomal irinotecan and a retroviral replicating vector containing the gene for cytosine deaminase, an enzyme that converts the prodrug flucytosine to 5-fluoruracil in tumour cells. An implantable reservoir is currently being developed, opening the possibility of continuous long-term infusions.

A further development that has been trialled in non-human primate studies involves a frameless skull-mounted ball-joint guide array (BJGA) [27]. This device, made of PEEK and therefore MRI compatible, fixes to the skull through three screws; it rotates through 360° and has a maximum angulation of 16° to the vertical. Its centre contains three 2 mm holes, each allowing cannulas, electrodes, or biopsy needles up to 16 gauge to be inserted through. The device also contains fiducials filled with gadolinium that allows registration using T1-weighted MRI scans. The software allows the trajectory of the cannula to be matched to the pre-planned route. In a non-human primate study evaluating delivery along the long axis of the putamen, the mean Euclidean error at the target was 1.18 ± 0.60 mm. This is similar to the frame-based ClearPoint system, as evaluated in a small series of patients undergoing CED for DIPG or Parkinson's disease [47]; a significant contribution to this

error comes from non-linearities in the MR field. As in the ClearPoint system, real-time visualization of the infusion is also possible [27]. The small size of the device is particularly suited for paediatric use and allows multiple burr holes to be used simultaneously, either bilaterally or unilaterally with multiple directions to the same target. The three close parallel tracts allow real-time optimization of trajectory by switching to an adjacent port as a 'rescue infusion'. Real-time adjustment in the MRI scanner also allows compensation for brain shift, related to loss of CSF or entry of air [27].

Matching distribution of infusate to the target remains a challenge, particularly when the target is elongated or irregular and therefore difficult to cover with multiple spherical infusion points. The 'infuse-as-you-go' technique has been described in a study that infused AAV solution to the putamen of non-human primates through an occipital trajectory [20]. The catheters were advanced in 2–4 mm increments during the infusion, under real-time MR guidance. Coverage of the putamen was superior to the standard transfrontal approach and could be achieved with a single trajectory. No reflux along the infusion cannula was noted [20].

6.3.5 Long-Term and Intermittent Infusions

Delivery of chemotherapy to brain tumours using CED is unlikely to be effective if only carried out once, or if general anaesthesia and insertion of a new catheter are required for every injection episode. Maintenance of a stable volume of chemotherapeutic agent within the parenchyma allows the drug to target tumour cells over various phases of the cell cycle. Prolonged use of external catheters connected to intracranial CED cannulas is difficult due to the inherent infection risk. The typical scenario in adults occurs after resection of the contrast-enhancing components of a glioblastoma multiforme (GBM). Tumour cells are still likely to be present within 2–3 cm of the margins of the resection cavity. These cells, despite adjuvant therapy with radiotherapy and temozolamide, are almost always the source of tumour recurrence. The ability to effectively infuse chemotherapeutic agents in this area, for a prolonged period or at regular intervals, in a way that maintains a high dose throughout the entire volume is required if CED is to be successful at prolonging survival. In one phase 1b study, continuous 100 h infusions of topotecan, to a total infused volume of 40 mLs, in 16 patients, in and around recurrent GBMs, using an external catheter, demonstrated tumour regression in 69% of patients [48, 49]. GBM patients in the cohort had a 20% 2 year survival, and one remains alive at submission of a subsequent report in 2020 [50].

The proof of principle for prolonged CED was established in a study on adult pigs [51]. A single catheter was implanted into the anterior limb of the right internal capsule and connected to a Synchromed II pump (model 8637-20, Medtronic) implanted subcutaneously. Topotecan was co-infused with gadolinium for 3 or 10 days. Maximum enhancement volume was reached by day 3 and remained stable in those pigs that underwent 10 days of infusion [51]. The longer infusion period led

to a sustained volume of distribution beyond that achieved by the shorter 3-day infusion. Long-term topotecan infusion was well-tolerated in all animals.

A longer study by the same group has been published recently and describes important aspects of the effects of chronic infusions [12]. This involved infusion of topotecan in adult pig brains over periods ranging between 4 and 32 days. Infusions were carried out in the posterior centrum semiovale and were well-tolerated. A fully implantable system using a SmartFlow Flex ventricular catheter, 0.5 mm internal diameter (MRI Intervention Inc.), connected via a silastic lumbar catheter to a Synchromed II pump was used. The infusion pumps were emptied and refilled every 4–5 days. Typical infused volumes varied between 2 and 4 mLs per day. Priming the target tissue with a slow infusion for 1 or 2 days prior to increasing to a maximal dose reduced extravasation into the ventricles at the higher infusion rate. Drug distribution was measured by co-infusion with gadolinium. The distributed volume reached its peak early during the infusion and demonstrated a slight reduction as the steady state was reached [12]. Placement of the catheter tip within the sub-cortical white matter led to a distribution volume of 37.5% of the ipsilateral hemispheric volume; this was not significantly different between the short and long-term infusions, with most of the incremental gains in distribution occurring in the first 48 h, suggesting that a steady state equilibrium between infusion and clearance develops within 4 days of continuous infusion. This balance is dependent on local anatomy, and in this study, was significantly lower in the hippocampus. The maximal volume of distribution was achieved prior to the development of a steady state, suggesting that intermittent short-term dosing may still achieve the same levels of distribution. Despite the long-term infusion, none of the animals developed adverse effects, and no topotecan was detectable systemically.

The authors also conducted an in vitro study to demonstrate that the presence of gadolinium does not affect the cytotoxicity of topotecan on U87 human glioma cells. In addition, multiple biopsies taken prior to sacrifice demonstrated a significant positive correlation between gadolinium intensity and topotecan concentration. Histological analysis showed reactive astrocytes, microglia, and macrophages extending a few hundred microns from the catheter tip; this may be relevant to reducing backflow in long-term catheter implantation [12].

Another device that allows chronic or intermittent CED infusions has been developed by Renishaw PLC and has been used for recurrent glioblastoma, DIPG, and Parkinson's disease to infuse carboplatin, valproate, and GDNF [52–54]. The device consists of implantable catheters connected to a transcutaneous bone-anchored port [52]. In the first report on its use, a patient with recurrent glioblastoma underwent stereotactic implantation of four carbothane microcatheters, with an outside diameter of 0.6 mm, targeting the tumour enhancement and the peritumoural penumbra. The bone-anchored port was implanted using the skin-flap dermatome technique pioneered in bone-anchored hearing aid surgery. A dermatome was used to elevate a small flap of skin on an inferior pedicle, typically 25 mm in diameter; the underlying subcutaneous tissue was excised. The port was anchored to a burr hole in the skull bone at this site, the flap replaced, and the port then brought out through an opening in the skin flap. Infusions were begun on the third day, with

attachment of a needle administration device to the bone-anchored port. Hyperintensity on the T2-weighted MR sequence was used as a surrogate for volume distribution [52]. 12-h infusions were administered on three consecutive days, delivering a total volume of 27.9 mLs per day. Imaging showed a maximal distribution volume of 97.6 mLs, with a distribution to infusion ratio of around 3. Infusions were repeated using higher carboplatin concentrations at 4 weeks. Imaging at 8 weeks demonstrated an almost 50% reduction in the volume of contrast enhancement. Unfortunately, however, clear tumour progression was evident on further imaging 8 weeks later, outside the volumes of T2 signal change seen during the infusions. The patient subsequently died 8 months after implantation of the drug delivery system, and 33 months from diagnosis of her GBM [52]. All infusions were well-tolerated, with the exception of a single seizure on the third day of the first infusion set.

The ability to safely administer drugs by CED intermittently over long periods of time raises additional questions and opportunities. These include the development of infusion regimes to ensure satisfactory and efficient volume distribution, limit accumulation and toxicity, and allow periods of drug washout. Long-term scarring around catheter tips may modulate infusion volumes and require further development of catheter design and materials. For devices that use implanted pumps with an integral drug reservoir, the stability of the drug at body temperature needs to be addressed, as well as safe and easy ways of emptying and refilling the drug. The effects of long-term infusions on serial imaging also need further study.

6.4 Applications of CED in Paediatric Neuro-Oncology

Diffuse intrinsic pontine glioma (DIPG) remains the main tumour for which CED has been evaluated in children. DIPG carries the worst prognosis of all paediatric brain tumours. It typically presents between the ages of 5 and 10 years, with a classic triad of long tract signs, cranial neuropathies, and cerebellar signs [55]. Hydrocephalus, due to occlusion of the fourth ventricle related to tumour growth and infiltration in the fourth ventricular floor, is rare at presentation. Latency between symptom onset and diagnosis is almost always under 3 months [56]. Median survival following radiotherapy is around 10 months, with overall survival of 30% at 1 year, 10% at 2 years, and 1% at 5 years [57]. These statistics have not been improved for decades. Diagnosis is traditionally based on MR imaging, with a mass lesion that causes expansion of the pons, has poorly defined boundaries, occupies more than 50% of its axial diameter, remains clearly above the ponto-medullary junction, and often encircles the basilar artery. The lesion is hypointense on T1 and hyper-intense on T2-weighted imaging and may demonstrate variable enhancement with gadolinium. Contrast enhancement is an indicator of poor prognosis [58] (Fig. 6.2).

Stereotactic biopsy has been demonstrated to be safe, with diagnostic success of up to 96% and permanent morbidity of only 0.6% [59–61]. Biopsy has become

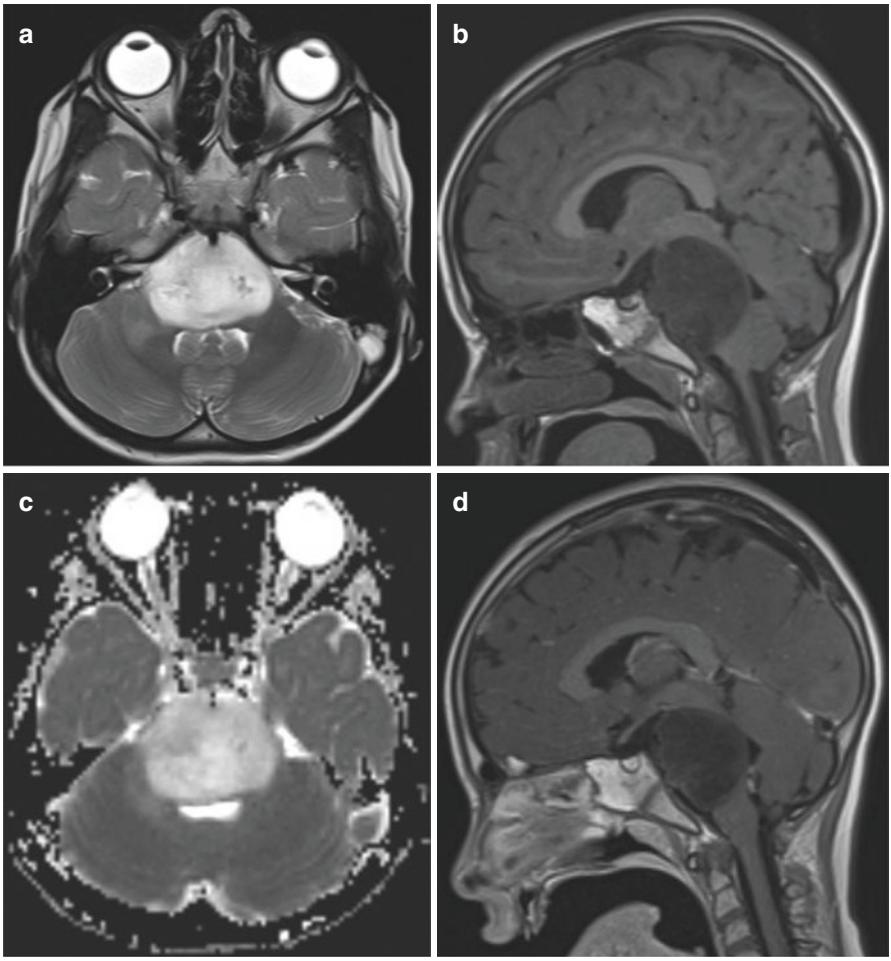

Fig. 6.2 Typical MR characteristics of DIPG, with large pontine mass, hyper-intense on T2-weighted axial image, encircling the basilar artery ventrally (**a**), and clearly delineated by the ponto-medullary junction on sagittal T1 sequence (**b**). The tumour does not restrict on diffusion-weighted imaging (**c**) and does not enhance on gadolinium administration (**d**)

more frequent as commitment to understanding the biology of DIPG and attempts to develop targeted therapy have intensified. Although routine biopsy has been advocated in several publications, a recent survey of European paediatric neurosurgeons suggested that most surgeons would only consider biopsy within the governance of a clinical trial [62, 63]. Biopsy specimens have consistently demonstrated the H3K27M mutation, and this has led to a revision of DIPG nomenclature in the WHO classification of CNS tumours as 'midline glioma, H3K27M mutant' [64]. Beyond these histone changes, several additional genomic aberrations emphasize the molecular diversity of this tumour [65].

In view of its infiltrative nature within the pons, cytoreductive surgery is not possible. Standard treatment involves focal, wide field radiation therapy to the pons, aiming to deliver up to 59.4 Gy in 30–33 fractions of 1.8 Gy daily [56]. Unfortunately, this is not curative, and the tumour recurs within months. Various chemotherapy regimens have been unsuccessful in improving the survival advantage conferred by radiotherapy alone. In particular, the use of concurrent temozolamide, effective in adult GBM, has had no impact on DIPG [66, 67]. Similarly, the addition of radiosensitizing agents such as topotecan, or raising the radiation dose to 78 Gy, has also had no impact on survival [68, 69]. The BIOMEDE trial offered targeted therapy with everolimus, erlotinib, or dasatinib based on biopsy findings; no statistical improvement in survival could be documented.

CED is a potentially promising drug delivery technique for DIPG. Unlike other high-grade tumours, which are usually associated with some degree of BBB compromise, DIPG appears to be protected by a relatively intact barrier, hence the frequent failure to enhance on MR imaging. Dosing of chemotherapeutic agents administered systemically is limited by toxicity. From a CED perspective, the factors for and against CED in DIPG have been clearly summarized by Tosi et al. [70]. The tumour is located within an anatomically defined region, and lack of previous surgery ensures that it has remained as homogeneous a tissue as possible prior to CED. Distant dissemination is not commonly seen on MRI early in DIPG. In addition, the uniformly poor prognosis, despite extensive research over at least two decades, may reduce the regulatory burden of new investigative techniques. On the other hand, the diseased brainstem in a young child is potentially vulnerable to stress and pressure, and the infusion of relatively large volumes of toxic substances may worsen its ability to function, with potentially dire neurological consequence [70].

Several pre-clinical and clinical studies have reported on the infusion of a number of drugs by CED into DIPG, including the radiolabelled monoclonal antibody Omburtamab, interleukin 13 pseudomonas toxin, panobinostat, small molecule kinase inhibitors, topotecan, and a combination of carboplatin and sodium valproate [30, 71–74] (Table 6.1). Panobinostat, a pan-histone deacetylase inhibitor, previously shown to have pre-clinical efficacy against DIPG, was evaluated in rat and porcine CED models and demonstrated satisfactory distribution without brainstem toxicity [73]. This is particularly encouraging considering that its ability to cross the blood brain barrier when administered intravenously is poor.

The highly complex nature of the brainstem, with its compact arrangement of long tracts and cranial nerve nuclei, may have been expected to preclude the infusion of high volumes of drug by CED. However, several studies have demonstrated relative safety of single, prolonged, and even multiple infusions [30, 71, 72, 75]. In the first reported CED of an agent into a DIPG, IL13-pseudomonas toxin, a chimeric fusion protein, was administered to a 4-year-old girl at recurrence [76]. The infusion was carried out through a single frontal catheter, using a co-infusion with gadolinium-DTPA, under direct MR imaging. A maximal infusion volume of 1.4 mLs was reached. A deterioration in the patient's sixth nerve palsy improved after 5 days of corticosteroid therapy. Although tumour progression was arrested by

Table 6.1 Clinical CED studies in DIPG in children, published to date

First author (Refs)	Publication date	Study	Number of patients	Agent	Trajectory	Catheter	Catheter placement	Duration and number of infusions
Lonser et al. [76]	2007	Single patient	1	IL-13 pseudomonas toxin	Frontal	Single, external	Stereotactic frame, MRI guidance	Single, continued to tumour coverage on iMRI
Anderson et al. [30]	2013	Pilot feasibility study	2	Topotecan	Cerebellar peduncles	Two, external	Stereotactic frame	100 h; single
Souweidane et al. [71]	2018	Dose escalation phase I	28	^{124}I-Omburtamab	Frontal	One, external	ClearPoint	1.18–15.53 h; single
Heiss et al. [72]	2019	Dose escalation phase I	5	IL-13 pseudomonas exotoxin	Frontal	One, external	Navigus Medtronic; ClearPoint	Up to 13 hours; one or two
Bander et al. [78]	2020	Dose escalation phase I	7	^{124}I-Omburtamab	Frontal	One, external	ClearPoint	One or two additional infusions (same as in ref)
Szychot et al. [75]	2021	Retrospective, compassionate use	13	Carboplatin and valproate	Frontal, cerebellar peduncles	Two, implanted	Renishaw, Neuroinspire	1–7 cycles, 3–6 weekly

4 weeks, the child died 4 months after treatment [76]. In another of the earlier studies, and the first to use the transcerebellar peduncle route, topotecan was delivered by CED through two catheters in two children with DIPG, following a tumour biopsy in the same procedure [30]. CED was continued for 100 h, but did not prolong survival in these two patients, and although low infusion rates were well-tolerated, high infusion rates up to 2.8 mLs/h resulted in new neurological deficits and deterioration in the KPS scores.

IL13-Psuedomonas toxin was also administered by CED to five children with DIPG through a single catheter in a single-institution phase 1 study [72]. Most glioma cell lines are known to overexpress IL13 receptors. In this study, it was hypothesized that Pseudomonas exotoxin is internalized by cells expressing IL13 receptors, which will lead to inhibition of protein synthesis and apoptotic cell death [77]. Complete tumour coverage was not obtained in any of the five patients. Two patients demonstrated short-term radiological benefit, with temporary arrest of disease progression. Two patients reported transient cranial nerve deficits and lethargy. Progression was radiologically evident by 12 weeks after infusion [72].

Outcomes of a first single centre phase 1 dose-escalation trial using CED of the radiolabelled monoclonal antibody Omburtamab were reported in 2018 [71]. This antibody was radiolabelled with ^{124}I; it targets the membrane-bound protein CD276 (B7-H3), which is overexpressed in DIPG and other paediatric brain tumours. Eligible patients were 3–21 years of age and had completed radiotherapy between 4 and 14 weeks before enrolment. In this way, changes in the tumour evaluated over a 30-day follow-up period were unlikely to be confounded by ongoing disease progression. Seven dose-escalation cohorts were planned, with the primary end point being the maximum tolerated dose. A semi-flexible catheter was inserted using the ClearPoint system, and ^{124}I—Omburtamab was infused in an intensive care environment. The prescribed dose ranged from 0.25 to 4.00 mCi, using an infused volume of 240–4540 μL at a rate of up to 7.5 μL/min [71]. The half-life of ^{124}I is 4.2 days, and therefore, as a true theranostic agent, is able to delineate drug distribution for several days, both in the brain and systemically, on PET imaging.

Twenty eight children were enrolled in this trial. No dose-related toxicity was observed, precluding the identification of the maximal tolerated dose. Only one patient developed treatment-related temporary hemiparesis. Estimated volumes of distribution were measured using MR and PET imaging and ranged from 1.5 to 20.1 cm^3, with a V_d to V_i ratio of 3.4. The distributions as measured on T2-weighted MRI and PET were not identical; distribution lasted for a longer period of time, up to a week, on PET imaging, and the V_d measured on PET was lower. The lesion to whole body ratio for the absorbed dose of radiation was higher than 1200. Although the authors emphasize that the purpose of the study was not to evaluate impact on survival, the median overall survival rate was 17.5 months, with 58.5% survival at 1 year and three patients surviving for more than 3 years [70, 71]. It is also important to note that at 30-day follow-up, 71% of the patients had performance indices identical to those at recruitment. In subsequent work, the authors have infused up to 8000 μL, obtaining volumes of distribution up to 35 mLs [70].

Seven of these children, who did not develop any evidence of tumour progression or toxicity within 30 days, went on to have further infusions of the same agent [78]. Six underwent a second infusion, and a seventh underwent a second and a third. Different entry sites and catheter trajectories were used. The distribution volume was not compromised on sequential infusions; in three patients where the new catheter tip was within 15 mm of the trajectory of a previous catheter, leakage of some of the infusate into an earlier track or injection site was noted. No significant adverse events were recorded.

A recent study has reported on a series of children who underwent CED with carboplatin and valproate for DIPG using a drug delivery system that allowed repeated infusion along four catheters [75]. All patients were treated on compassionate grounds after DIPG recurrence. Thirteen children were treated between 2017 and 2020. With the exception of two patients who developed persistent sixth nerve palsy, requiring reduction of drug concentration, all other adverse effects were transient. The four catheters, two frontal and two transcerebellar, were inserted stereotactically and positioned to optimize coverage of the pontine tumour, centrally and laterally. Infusion rates were started at 0.03 mL/h and increased incrementally to 0.3 mL/h. The side effect profile of each catheter was determined on the first infusion; the group developed the Pontine Infusion Neurological Evaluation (PIINE) score which defined the potential adverse effects of each catheter depending on its anatomical location [54]. Typically, infusions along the catheters were continued until the expected side effects occurred, at which point the infusion was discontinued. In this way, the maximal tolerated volume was infused every time. Infusions were repeated every 4–6 weeks. Infusion was commenced within 72 h of implantation. Infusions through three or four catheters simultaneously at rates of up to 3–5 μL/min were better tolerated than infusion through one or two catheters at higher flow rates. The estimated distribution was up to 30 cm^3 per day. Children were typically discharged within 24 h of finishing the infusion [75].

Baseline performance status was maintained in all patients up to the time of tumour progression. The median progression free survival was 13 months. The median overall survival was 15.3 months, with three out of the 13 patients alive and independently ambulant at the time of reporting. The last five patients received what the investigators considered as the optimal combination in terms of drug dosage and delivery; their median overall survival was 17.9 months at report [75]. This case series shows interesting preliminary activity which needs confirmation in a prospective clinical trial.

Several issues with regards to CED in DIPG are still unclear. None of the trials to date have advocated a biopsy in addition to CED. There is concern that a biopsy needle track may divert drug infused by CED and compromise optimal coverage of the tumour [79]. Frontal catheters are considered essential to ensure satisfactory tumour distribution and are positioned along a trajectory towards the long axis of a DIPG; they are therefore likely to interrupt the corticospinal tract. A study evaluating catheter position with corticospinal tractography, however, showed that catheter transgression of the tract and its incorporation in the volume of distribution only rarely resulted in a neurological deficit [80].

As DIPGs, like other infiltrative brain tumours, are already hyper-intense on T2-weighted MR imaging, the extent of tumour coverage during CED is difficult to determine. One case is described where ICOVIR-5, an oncolytic virus, was confused with Gd-DTPA [81]. This showed a satisfactory volume of distribution of the combined solute, which was completely washed out by 30 h. The authors emphasize that the duration of distribution is unrelated to the duration of the tumour's exposure to the virus, or indeed of any other drug, which is determined by the agent's specific cellular affinity, rather than by the continued association of the drug with Gd-DTPA [81]. In addition, as it is a relatively small molecule, Gd-DTPA may overestimate the distribution of a therapeutic agent [19].

The deformational changes in the brainstem caused by infusion of fluid into DIPG have been investigated [82]. This is particularly concerning, as the volume of distribution within the pons is greater than the volume of fluid infused, and any increase in pontine swelling can potentially worsen obstructive hydrocephalus or increase pressure on tracts and cranial nerve nuclei. Twenty three children with DIPG underwent volumetric evaluation of the pons and lateral ventricles pre-, 1 day post-, and 30 days post-infusion of a single dose of radioimmunotherapy. With a mean volume of infusion of 3.9 mLs, pontine volume increased by a mean of 2.5 mLs on day 1 post-infusion and tended to return to baseline by day 30. Lateral ventricle volume remained a mean of 5 mLs higher at 30 days compared to pre-infusion. None of the patients required a shunt within 90 days. The infusion volume had a weak positive correlation with the volume change in the pons and lateral ventricles, but changes in pontine volume did not relate to neurological deficits [82]. This study also suggests that an increase in pontine volume in the first month after CED is expected and not representative of tumour progression.

Oncological applications of CED in children are likely to extend beyond DIPG. Other tumours, such as thalamic, hypothalamic, and other midline high-grade gliomas (HGGs), as well as cortical ones, are sometimes not completely resectable. CED applied to unresectable components, either at recurrence or even at their primary presentation, may become a realistic option. Safety concerns and drug toxicity related to the eloquence of the brainstem may be less significant for tumours in these locations and therapeutic windows for supratentorial tumours may be wider. For example, pre-clinical evaluation of doxorubicin in mouse models of brainstem and thalamic HGG demonstrated that the maximum tolerated dose when infused to the thalamus was ten times that in the brainstem, allowing an effective dose to be reached in the thalamus but not in the brainstem [83].

CED has been evaluated extensively for adult HGGs and it is likely that some of these findings are translatable to some paediatric tumours. Glioblastoma multiforme (GBM) represents the commonest brain tumour in adults. Although there has been some progress over the last 10 years, its prognosis remains poor, with a median survival of up to 2 years [84]. Jahangiri et al. and Ung et al. have recently summarized some of the most relevant clinical and pre-clinical studies related to CED for GBM [49, 85]. Cytotoxins such as pseudomonas exotoxin targeted towards cell surface receptors that are overexpressed in glioma cells, such as the TGF-alpha, CD155, and IL4 receptors, have been used in phase I and II trials [86]. Topotecan,

gemcitabine, and carboplatin administered by CED to animal models showed better survival than controls [87, 88]. Bevacizumab administered by CED increased survival in an animal model over intravenous bevacizumab [89]. Fourteen clinical trials undertaken between 1997 and 2010 used conjugated toxins specifically taken up by glioma cells or chemotherapy agents that do not cross the BBB [85].

A notable improvement in a recent study was the inclusion of MRI-localized biopsies to allow study of the effects of drug infusion, in this case topotecan, on tumour cells and their microenvironment [50]. In addition, the importance of measuring neurocognitive function and quality of life after CED in recurrent HGG was underlined in a study on 16 patients who underwent single dose topotecan CED; most patients demonstrated stability on the Cognitive Stability Index and SF-36 over a 4 month follow-up period [90].

6.4.1 Reflections on CED Trial Failures in Oncology

CED should in theory be very effective treatment, yet the impact of CED in clinical trials has not been clear. Although these trials demonstrated the safety of CED, and many also showed some therapeutic efficacy, such as significant regression of recurrent GBM, overall success has been limited [48]. The translational model from animal to clinical studies, progressing from single to multiple to prolonged infusions, is well-illustrated by the long-term infusions of topotecan described above [49, 50].

One of the key issues related to trial failures in CED is catheter target accuracy and predictability of drug distribution, as shown in the phase III PRECISE trial, where IL 13-Pseudomonas exotoxin was delivered for recurrent GBM [91, 92, 93]. In this trial, fewer than half of the catheters had been optimally implanted, and although more accurate catheter placement correlated with a larger volume of distribution of agent, the coverage of the tumour was still low [92].

Another source of error, seen first in pre-clinical studies of gene therapy for Parkinson's disease, is the presence of perivascular spaces in the basal ganglia that divert the infusate away from the target [94]. Delivery platforms that allow real-time imaging, or the ability to change volumes in subsequent infusions, should mitigate against this problem.

Particularly in the context of chronic multiple infusions, it is essential that catheters are also placed in the periphery of a tumour, or where tumour recurrence may be expected. Attention to detail is required across a range of variables that also include the molecule, solute, and the histo-architecture of the target not just in the acute phase, but also in the longer term healing phase. This suggests that optimization of distribution needs to be tailored to the patient and to the catheter, as well as to the time from implantation, and the stage of the disease process. It is unlikely that a standard infusion regime will ever lead to an optimal distribution in all patients. For example, in a resection cavity, it has been shown that the catheter tips should be positioned 2 cm from the margin, in the direction of anticipated tumour progression [95]. Multiple catheters should be at least 2–4 cm apart and should avoid proximity

to the ventricle, subarachnoid space, and areas of necrosis or cystic degeneration [48].

The optimization of CED is a long translational process, which combines first principles and empirical pre-clinical, in vivo, and clinical evidence. Use of tracers is essential to allow optimization of coverage, and newer techniques using MR spectroscopy or PET imaging may be helpful.

Some mathematical models have been successful at predicting infusate distribution and coverage. These MRI-based models first identify fluid-filled cavities and surfaces, and using infusion volume, rate and catheter diameter calculate the extent of backflow and distribution with particular catheter positions [95]. The addition of diffusion tensor imaging has been useful [96]. More complex models have evaluated additional variables, including protein binding, cell uptake, and drug metabolism, as well as tissue permeability and drug diffusivity in different directions [97]. It is likely that a more refined understanding of the nature of interstitial fluid flow and bulk flow within the brain parenchyma, including that in the perivascular and perineuronal spaces, along white matter tracts, into the g lymphatics and along the meningeal layers is essential for optimization of CED [11].

Validation of the extent of drug distribution, at the correct dose, throughout the whole target volume is essential for a reliable assessment of outcome. Failure to cover the entire tumour leads to resistance and recurrence. In the study on CED of iodine-labelled omburtamab for DIPG, even in a small number of patients, the variance in tumour coverage was between 25 and 96% [71]. In addition, dosimetry considerations are site-specific. Pre-clinical studies have shown that agents such as doxorubicin are more likely to cause adverse effects when injected into the brainstem in DIPG animal models, rather than into the thalamus in similar HGG models; the dose tolerated in the thalamus was ten times higher [98].

The choice of drug is also relevant. A CED study using paclitaxel delivery to GBM was limited by toxicity [99]. Paclitaxel targets tubulin, stabilizing the microtubule polymer, in this way preventing cells from undergoing metaphase during mitosis. As microtubules are also required for nutrient transport in all cell types of the brain, paclitaxel delivered by CED also damages non-tumour cells. In contrast, topotecan, by binding to the DNA—topoisomerase complex, only affects dividing cells and is therefore expected to be safe and tumour-specific in the low replicative environment of the brain. Topotecan use for GBM has historically been limited by its poor BBB penetration and severe systemic side effects. Similarly, carboplatin, also used in CED, binds to DNA and inhibits successful replication.

The use of combined systemic treatment for tumours that may spread early beyond their local confines in the brain or brainstem is an important consideration. At the time of autopsy, up to a third of DIPG patients had leptomeningeal disease and a fourth had disease outside the brainstem [100]. However, this does not mean that local therapy such as CED is not useful. Focal radiotherapy has been the mainstay of treatment for DIPG for decades and is the only treatment modality that has improved survival. Focal surgical control, whenever possible, remains the first treatment to most brain tumours in adults and children. This suggests that the combination of a local with a systemic or CSF-delivered approach will need to be explored for DIPG.

6.4.2 New Trends and Opportunities in Neuro-Oncology

The combination of drugs with nanoparticle vehicles provides novel opportunities. Nanoparticles are typically 60–180 nm in size and have been investigated mostly in the context of GBM [101]. A size of about 70 nm appears to be ideal for delivery within the tumour interstitium [102]. Nanoparticles may promote drug retention in tissues, enhance accumulation of drug in specific regions, shield drugs from degradation processes, improve long-term and controlled release, and reduce toxicity to healthy tissue. Drugs that were previously deemed too toxic, insoluble, or chemically unstable may potentially be re-explored in combination with nanoparticles [101]. Successful delivery with nanoparticles may reduce the need for repeated or prolonged infusions. Liposomes, micelles, and polymeric nanoparticles have all been used in combination with CED [103].

Poly(lactic-*co*-glycolic acid) (PLGA) nanoparticles have been approved by the US Federal Drug Agency (FDA) and were used in a study evaluating its combination with carboplatin in rat and porcine CED models, as well as in glioma cell lines [104]. PLGA is biodegradable and breaks down into its natural metabolites lactic acid and glycolic acid. The study demonstrated that the combined drug provided greater tumour cytotoxicity and increased the tissue half-life of carboplatin. Similarly, PLGA combined with camptothecin and delivered by CED into rat models of high-grade glioma led to improved animal survival [105]. Camptothecin was present in tissues harvested 53 days after infusion, suggesting that this long tissue half-life may maintain exposure to the drug and potentially reduce the need for repeated dosing [105]. Nanoparticles may also support tumour imaging. 10 nm iron oxide nanoparticles conjugated to an antibody specific to the mutant epidermal growth factor receptor found on human GBM cells not only showed good efficacy against the tumour cells in vitro and in mouse models, but also allowed tumour cell and agent tracking by MRI [106].

Peptide-based nanofibres represent a new type of vehicle which are amenable to bind drugs and be infused by CED [102]. These carriers can be synthesized homogenously in various sizes, have a hydrophilic pegylated surface, and are, in addition, negatively charged, supporting more widespread parenchymal distribution. In a detailed evaluation, NFP-400 demonstrated the ideal size for wide convection, with a V_d to V_i ratio of 2.47, and reliably formed a sphere around the tip of the cannula; in terms of its clearance from the infused parenchyma, its half-life was calculated at 25 h. The larger NFP-1000 had a longer half-life, up to 42 h, but its large size meant that its distribution was poor, with a V_d to V_i ratio of 1.07. The smaller NFP-100 had a shorter half-life of about 18 h, but distributed effectively along white matter tracts, potentially making it the vehicle of choice for tumours infiltrating white matter such as DIPG [102].

Genetically modified T cells that express chimeric antigen receptors, CAR T cells, are now considered an important component of cancer immunotherapy and have shown remarkable success in the treatment of haematological malignancies. Radiological regression and increased survival have been demonstrated with CAR

T cells in GBM, and a number of trials are currently underway [107, 108]. In one reported case involving a patient with diffuse recurrent GBM where the radiological and clinical response persisted for 7.5 months after initiation of therapy, CAR T cells were administered by direct intracavitary and intraventricular infusion using separate catheters [107]. CAR T cells have also shown efficacy in mouse orthotopic xenograft models of H3-K27M mutant paediatric diffuse midline gliomas [109]. In an animal model of xenograft atypical teratoid rhabdoid tumour (ATRT), CAR T cells delivered directly into the tumour and CSF showed significant benefits over cells delivered intravenously, with higher potency at the tumour and lower levels of peripheral inflammation [110]. However, the delivery of T cells by CED is challenging. Long delivery times inherent to CED lead to sedimentation of the T cells in their saline medium. The use of a low viscosity hyaluronic acid-based hydrogel carrier prevents sedimentation and allows homogenous delivery of T cells that remain viable and active on deposition [111].

6.5 CED for Neurotransmitter Deficiency and Metabolic Disease

CED also provides an opportunity to deliver gene therapy to targeted cells within the brain. Currently, gene delivery to the brain requires packaging of the DNA or RNA within an AAV vector. This is a small non-replicative non-pathogenic virus that lacks an envelope and adheres to the target cell membrane through heparin sulphate proteoglycan receptors. It then undergoes endocytosis, with transport to and release of the genetic material at the host nucleus. There it forms an extrachromosomal episome and enables the host cell to translate its nucleic acid on a long-term basis. It can also integrate within the host genome at specific sites, as in human chromosome 19. The absence of most viral proteins prevents an inflammatory response to the virus. Although small, the 20 nm AAV does not penetrate the BBB when administered intravenously. Pre-existing humoral immunity, thought to be present in 32% of the population, may also prevent the virus from surviving in the circulation [112]. When given through the CSF, it is unable to penetrate the ependymal barrier. CED is therefore an effective way of transporting it to the brain parenchyma [113].

Different viral capsids allow anterograde or retrograde transport along interconnected circuits in a serotype-specific manner [113]. Transport to diffuse cortical regions after CED to the thalamus in non-human primates has been explored [114]. Barua et al. were subsequently able to demonstrate in their swine model that CED of AAV vectors into the white matter leads to specific and effective distribution into the overlying cortex [115].

A number of trials using AAV vectors are currently underway and include studies on Parkinson's disease, mucopolysaccharidoses, AADC deficiency, and Alzheimer's disease. In children, AAV2–AADC has been administered to

AADC-deficient patients. AADC is essential for the production of dopamine and serotonin from levodopa and 5-hydroxytryptophan, respectively. Children with AADC deficiency typically have a life expectancy of up to 7 years and present with movement disorders (hypotonia, hypokinesia, and dystonia), recurrent oculogyric crises, and autonomic dysfunction [116]. An early study involved infusion of AAV2–AADC into the putamen in ten children [117]. Although this did lead to an improvement in motor scores, the poor retrograde transport of AAV2 from the putamen to the substantia nigra and ventral tegmental pathways, where most of the dopamine is produced, compromised the benefits of this approach. A current trial is exploring the benefit of direct injection into the substania nigra and ventral tegmental areas and hopes to replicate the high AADC expression in the nigrostriatal and mesolimbic pathways which has been shown in non-human primate studies [118].

The mucopolysaccharidoses (MPS) are a group of rare monogenetic lysosomal storage disorders, caused by mutations in genes encoding proteins necessary for the breakdown of glycosaminoglycans. As a result, partially metabolized substrates accumulate in tissues, leading to widespread pathological effects that, in some, also include the central nervous system. MPS I (Hurler), II (Hunter) and IIIA and IIIB (San Filippo) involve the brain and are associated with progressive cognitive decline [119]. Bone marrow transplantation is effective at reducing only the systemic effects of MPS. Intravenous enzyme replacement does not cross the BBB and also has minimal effect on disease progression in the brain.

One of the earliest trials of CED in MPS was in Gaucher disease, due to glucocerebrosidase deficiency, where intravenous replacement of the enzyme had no effect on the neurological component of the disease [120]. CED into the frontal white matter in rats and subsequently in primates showed satisfactory activity of the enzyme in neurons throughout the infused frontal lobe and pons. This was subsequently replicated safely in a patient [121].

The MPS are considered ideal for gene therapy, as only one, known, gene is involved in a metabolic process that is well-understood and has been replicated in animal models. Lysosomal enzymes also transport well along axons and across synapses [122].

The injection of AAV vectors by CED has been investigated in MPS IIIA. In one trial, four MPS IIIA symptomatic patients, aged between 32 months and 6 years, underwent bilateral CED with an AAVrh10-based vector, using three hemispheric white matter trajectories on each side [123]. One-year data confirmed that the procedure and the vector were well-tolerated, with stabilization of brain atrophy on MRI in some patients. A larger phase II/III trial is currently underway.

6.6 Conclusion

The potential to deliver large molecules directly to target areas in the brain has developed enormously over the last 20 years. This has required collaboration across multiple disciplines, with most successful CED projects progressing through a

common pathway starting with identification of a promising agent, pre-clinical testing in small and large animals, and finally the multiple phases of a clinical trial to establish dosimetry, safety, and efficacy. Neurosurgeons have a unique practical understanding of the physiology and tolerance of the brain and have been intimately involved in this journey.

Further refinement of this process is necessary if clinical trials in CED are to become more successful, with continuous optimization of technology as well as prediction and visualization of volumes of distribution. A clear and well-defined roadmap, which could allow agents to be evaluated through a trusted delivery system, could accelerate the regulatory processes and ensure that successful agents can be made available to patients in a timely manner, particularly for diseases where no treatment currently exists, such as DIPG.

References

1. Bobo RH, Laske DW, Akbasak A, Morrison PF, Dedrick RL, Oldfield EH. Convection-enhanced delivery of macromolecules in the brain. Proc Natl Acad Sci U S A. 1994;91(6):2076–80.
2. Quiñonez-Silvero C, Hübner K, Herzog W. Development of the brain vasculature and the blood–brain barrier in zebrafish. Dev Biol. 2020;457(2):181–90.
3. Wong AD, Ye M, Levy AF, Rothstein JD, Bergles DE, Searson PC. The blood–brain barrier: an engineering perspective. Front Neuroeng. 2013;30(6):7.
4. Obermeier B, Daneman R, Ransohoff RM. Development, maintenance and disruption of the blood–brain barrier. Nat Med. 2013;19(12):1584–96.
5. Shepro D, Morel NM. Pericyte physiology. FASEB J. 1993;7(11):1031–8.
6. Syková E, Nicholson C. Diffusion in brain extracellular space. Physiol Rev. 2008;88(4):1277–340.
7. Abbott NJ. Evidence for bulk flow of brain interstitial fluid: significance for physiology and pathology. Neurochem Int. 2004;45(4):545–52.
8. Abbott NJ, Pizzo ME, Preston JE, Janigro D, Thorne RG. The role of brain barriers in fluid movement in the CNS: is there a “glymphatic” system? Acta Neuropathol. 2018;135(3):387–407.
9. Laske DW, Youle RJ, Oldfield EH. Tumor regression with regional distribution of the targeted toxin TF-CRM107 in patients with malignant brain tumors. Nat Med. 1997;3(12):1362–8.
10. Morrison PF, Laske DW, Bobo H, Oldfield EH, Dedrick RL. High-flow microinfusion: tissue penetration and pharmacodynamics. Am J Physiol. 1994;266(1 Pt 2):R292–305.
11. Stine CA, Munson JM. Convection-enhanced delivery: connection to and impact of interstitial fluid flow. Front Oncol. 2019;9:966.
12. D'Amico RS, Neira JA, Yun J, Alexiades NG, Banu M, Englander ZK, et al. Validation of an effective implantable pump-infusion system for chronic convection-enhanced delivery of intracerebral topotecan in a large animal model. J Neurosurg. 2019;133:1–10.
13. Varenika V, Dickinson P, Bringas J, LeCouteur R, Higgins R, Park J, et al. Detection of infusate leakage in the brain using real-time imaging of convection-enhanced delivery. J Neurosurg. 2008;109(5):874–80.
14. Sampson JH, Brady ML, Petry NA, Croteau D, Friedman AH, Friedman HS, et al. Intracerebral infusate distribution by convection-enhanced delivery in humans with malignant gliomas: descriptive effects of target anatomy and catheter positioning. Neurosurgery. 2007;60(2 Suppl 1):ONS89–98. discussion ONS98–9.

15. Soltani M, Chen P. Numerical modeling of interstitial fluid flow coupled with blood flow through a remodeled solid tumor microvascular network. PLoS One. 2013;8(6):e67025.
16. Boucher Y, Salehi H, Witwer B, Harsh GR, Jain RK. Interstitial fluid pressure in intracranial tumours in patients and in rodents. Br J Cancer. 1997;75(6):829–36.
17. Ali MJ, Navalitloha Y, Vavra MW, Kang EW-Y, Itskovich AC, Molnar P, et al. Isolation of drug delivery from drug effect: problems of optimizing drug delivery parameters. Neuro Oncol. 2006;8(2):109–18.
18. Leroi N, Lallemand F, Coucke P, Noel A, Martinive P. Impacts of ionizing radiation on the different compartments of the tumor microenvironment. Front Pharmacol. 2016;7:78.
19. Ivasyk I, Morgenstern PF, Wembacher-Schroeder E, Souweidane MM. Influence of an intratumoral cyst on drug distribution by convection-enhanced delivery: case report. J Neurosurg Pediatr. 2017;20(3):256–60.
20. Sudhakar V, Naidoo J, Samaranch L, Bringas JR, Lonser RR, Fiandaca MS, et al. Infuse-as-you-go convective delivery to enhance coverage of elongated brain targets: technical note. J Neurosurg. 2019;133:1–8.
21. Debinski W, Tatter SB. Convection-enhanced delivery for the treatment of brain tumors. Expert Rev Neurother. 2009;9(10):1519–27.
22. Perlstein B, Ram Z, Daniels D, Ocherashvilli A, Roth Y, Margel S, et al. Convection-enhanced delivery of maghemite nanoparticles: increased efficacy and MRI monitoring. Neuro Oncol. 2008;10(2):153–61.
23. Chen MY, Hoffer A, Morrison PF, Hamilton JF, Hughes J, Schlageter KS, et al. Surface properties, more than size, limiting convective distribution of virus-sized particles and viruses in the central nervous system. J Neurosurg. 2005;103(2):311–9.
24. MacKay JA, Deen DF, Szoka FC. Distribution in brain of liposomes after convection enhanced delivery; modulation by particle charge, particle diameter, and presence of steric coating. Brain Res. 2005;1035(2):139–53.
25. Lewis O, Woolley M, Johnson DE, Fletcher J, Fenech J, Pietrzyk MW, et al. Maximising coverage of brain structures using controlled reflux, convection-enhanced delivery and the recessed step catheter. J Neurosci Methods. 2018;1(308):337–45.
26. Chen MY, Lonser RR, Morrison PF, Governale LS, Oldfield EH. Variables affecting convection-enhanced delivery to the striatum: a systematic examination of rate of infusion, cannula size, infusate concentration, and tissue-cannula sealing time. J Neurosurg. 1999;90(2):315–20.
27. Sudhakar V, Mahmoodi A, Bringas JR, Naidoo J, Kells A, Samaranch L, et al. Development of a novel frameless skull-mounted ball-joint guide array for use in image-guided neurosurgery. J Neurosurg. 2019;132(2):595–604.
28. Casanova F, Carney PR, Sarntinoranont M. Influence of needle insertion speed on backflow for convection-enhanced delivery. J Biomech Eng. 2012;134(4):041006.
29. Tanner PG, Holtmannspötter M, Tonn J-C, Goldbrunner R. Effects of drug efflux on convection-enhanced paclitaxel delivery to malignant gliomas: technical note. Neurosurgery. 2007;61(4):E880–2. discussion E882.
30. Anderson RCE, Kennedy B, Yanes CL, Garvin J, Needle M, Canoll P, et al. Convection-enhanced delivery of Topotecan into diffuse intrinsic brainstem tumors in children. J Neurosurg Pediatr. 2013;11(3):289–95.
31. Lin J, Morris M, Olivero W, Boop F, Sanford RA. Computational and experimental study of proximal flow in ventricular catheters: technical note. J Neurosurg. 2003;99(2):426–31.
32. Orozco GA, Smith JH, García JJ. Three-dimensional nonlinear finite element model to estimate backflow during flow-controlled infusions into the brain. Proc Inst Mech Eng H. 2020;234(9):1018–28.
33. Faraji AH, Jaquins-Gerstl AS, Valenta AC, Ou Y, Weber SG. Electrokinetic convection-enhanced delivery of solutes to the brain. ACS Chem Nerosci. 2020;11(14):2085–93.
34. Mehta AM, Sonabend AM, Bruce JN. Convection-enhanced delivery. Neurotherapeutics. 2017;14(2):358–71.

35. White E, Bienemann A, Malone J, Megraw L, Bunnun C, Wyatt M, et al. An evaluation of the relationships between catheter design and tissue mechanics in achieving high-flow convection-enhanced delivery. J Neurosci Methods. 2011;199(1):87–97.
36. Chen Z-J, Gillies GT, Broaddus WC, Prabhu SS, Fillmore H, Mitchell RM, et al. A realistic brain tissue phantom for intraparenchymal infusion studies. J Neurosurg. 2004;101(2):314–22.
37. Brady ML, Raghavan R, Mata J, Wilson M, Wilson S, Odland RM, et al. Large-volume infusions into the brain: a comparative study of catheter designs. Stereotact Funct Neurosurg. 2018;96(3):135–41.
38. Lewis O, Woolley M, Johnson D, Rosser A, Barua NU, Bienemann AS, et al. Chronic, intermittent convection-enhanced delivery devices. J Neurosci Methods. 2015;259:47–56.
39. Olson JJ, Zhang Z, Dillehay D, Stubbs J. Assessment of a balloon-tipped catheter modified for intracerebral convection-enhanced delivery. J Neurooncol. 2008;89(2):159–68.
40. Tatter SB, Shaw EG, Rosenblum ML, Karvelis KC, Kleinberg L, Weingart J, et al. An inflatable balloon catheter and liquid ^{125}I radiation source (GliaSite radiation therapy system) for treatment of recurrent malignant glioma: multicenter safety and feasibility trial. J Neurosurg. 2003;99(2):297–303.
41. Fiandaca MS, Forsayeth JR, Dickinson PJ, Bankiewicz KS. Image-guided convection-enhanced delivery platform in the treatment of neurological diseases. Neurotherapeutics. 2008;5(1):123–7.
42. Gill SS, Patel NK, Hotton GR, O'Sullivan K, McCarter R, Bunnage M, et al. Direct brain infusion of glial cell line-derived neurotrophic factor in Parkinson disease. Nat Med. 2003;9(5):589–95.
43. Sillay K, Schomberg D, Hinchman A, Kumbier L, Ross C, Kubota K, et al. Benchmarking the ERG valve tip and MRI interventions smart flow neurocatheter convection-enhanced delivery system's performance in a gel model of the brain: employing infusion protocols proposed for gene therapy for Parkinson's disease. J Neural Eng. 2012;9(2):026009.
44. Barua NU, Lowis SP, Woolley M, O'Sullivan S, Harrison R, Gill SS. Robot-guided convection-enhanced delivery of carboplatin for advanced brainstem glioma. Acta Neurochir. 2013;155(8):1459–65.
45. Han SJ, Bankiewicz K, Butowski NA, Larson PS, Aghi MK. Interventional MRI-guided catheter placement and real time drug delivery to the central nervous system. Expert Rev Neurother. 2016;16(6):635–9.
46. Richardson RM, Kells AP, Martin AJ, Larson PS, Starr PA, Piferi PG, et al. Novel platform for MRI-guided convection-enhanced delivery of therapeutics: preclinical validation in non-human primate brain. Stereotact Funct Neurosurg. 2011;89(3):141–51.
47. Chittiboina P, Heiss JD, Lonser RR. Accuracy of direct magnetic resonance imaging-guided placement of drug infusion cannulae. J Neurosurg. 2015;122(5):1173–9.
48. Bruce JN, Fine RL, Canoll P, Yun J, Kennedy BC, Rosenfeld SS, et al. Regression of recurrent malignant gliomas with convection-enhanced delivery of topotecan. Neurosurgery. 2011;69(6):1272–9. discussion 1279–80.
49. Ung TH, Malone H, Canoll P, Bruce JN. Convection-enhanced delivery for glioblastoma: targeted delivery of antitumor therapeutics. CNS Oncol. 2015;4(4):225–34.
50. Upadhyayula PS, Spinazzi EF, Argenziano MG, Canoll P, Bruce JN. Convection enhanced delivery of topotecan for gliomas: a single-center experience. Pharmaceutics. 2020;13(1):39.
51. Sonabend AM, Stuart RM, Yun J, Yanagihara T, Mohajed H, Dashnaw S, et al. Prolonged intracerebral convection-enhanced delivery of topotecan with a subcutaneously implantable infusion pump. Neuro Oncol. 2011;13(8):886–93.
52. Barua NU, Hopkins K, Woolley M, O'Sullivan S, Harrison R, Edwards RJ, et al. A novel implantable catheter system with transcutaneous port for intermittent convection-enhanced delivery of carboplatin for recurrent glioblastoma. Drug Deliv. 2014;23(1):167–73.
53. Whone AL, Boca M, Luz M, Woolley M, Mooney L, Dharia S, et al. Extended treatment with glial cell line-derived neurotrophic factor in Parkinson's disease. J Parkinsons Dis. 2019;9(2):301–13.

54. Hollingworth MA, Zacharoulis S. Development of a clinical scale for assessment of patients with diffuse intrinsic pontine glioma (DIPG) receiving experimental therapy: the PONScore. J Neurooncol. 2020;149(2):263–72.
55. Hargrave D. Pediatric diffuse intrinsic pontine glioma: can optimism replace pessimism? CNS Oncol. 2012;1(2):137–48.
56. Clymer J, Kieran MW. The integration of biology into the treatment of diffuse intrinsic pontine glioma: a review of the North American clinical trial perspective. Front Oncol. 2018;8:169.
57. Grasso CS, Tang Y, Truffaux N, Berlow NE, Liu L, Debily M-A, et al. Functionally defined therapeutic targets in diffuse intrinsic pontine glioma. Nat Med. 2015;21(7):827.
58. Poussaint TY, Kocak M, Vajapeyam S, Packer RI, Robertson RL, Geyer R, et al. MRI as a central component of clinical trials analysis in brainstem glioma: a report from the pediatric brain tumor consortium (PBTC). Neuro Oncol. 2011;13(4):417–27.
59. Hamisch C, Kickingereder P, Fischer M, Simon T, Ruge MI. Update on the diagnostic value and safety of stereotactic biopsy for pediatric brainstem tumors: a systematic review and meta-analysis of 735 cases. J Neurosurg Pediatr. 2017;20(3):261–8.
60. Puget S, Beccaria K, Blauwblomme T, Roujeau T, James S, Grill J, et al. Biopsy in a series of 130 pediatric diffuse intrinsic pontine gliomas. Childs Nerv Syst. 2015;31(10):1773–80.
61. Grasso CS, Tang Y, Truffaux N, Berlow NE, Liu L, Debily M-A, et al. Functionally defined therapeutic targets in diffuse intrinsic pontine glioma. Nat Med. 2015;21(6):555–9.
62. Williams JR, Young CC, Vitanza NA, McGrath M, Feroze AH, Browd SR, et al. Progress in diffuse intrinsic pontine glioma: advocating for stereotactic biopsy in the standard of care. Neurosurg Focus. 2020;48(1):E4.
63. Tejada S, Aquilina K, Goodden J, Pettorini B, Mallucci C, van Veelen ML, et al. Biopsy in diffuse pontine gliomas: expert neurosurgeon opinion—a survey from the SIOPE brain tumor group. Childs Nerv Syst. 2020;36(4):705–11.
64. Louis DN, Perry A, Reifenberger G, Deimling von A, Figarella-Branger D, Cavenee WK, et al. The 2016 World Health Organization classification of tumors of the central nervous system: a summary. Acta Neuropathol. 2016;131(6):803–20.
65. Mackay A, Burford A, Carvalho D, Izquierdo E, Fazal-Salom J, Taylor KR, et al. Integrated molecular meta-analysis of 1000 pediatric high-grade and diffuse intrinsic pontine glioma. Cancer Cell. 2017;32(4):520–5.
66. Cohen KJ, Heideman RL, Zhou T, Holmes EJ, Lavey RS, Bouffet E, et al. Temozolomide in the treatment of children with newly diagnosed diffuse intrinsic pontine gliomas: a report from the Children's Oncology Group. Neuro Oncol. 2011;13(4):410–6.
67. Bailey S, Howman A, Wheatley K, Wherton D, Boota N, Pizer B, et al. Diffuse intrinsic pontine glioma treated with prolonged temozolomide and radiotherapy—results of a United Kingdom phase II trial (CNS 2007 04). Eur J Cancer. 2013;49(18):3856–62.
68. Packer RJ, Boyett JM, Zimmerman RA, Albright AL, Kaplan AM, Rorke LB, et al. Outcome of children with brain stem gliomas after treatment with 7800 cGy of hyperfractionated radiotherapy. A childrens cancer group phase I/II trial. Cancer. 1994;74(6):1827–34.
69. Chastagner VB, Grill J, Doz F, Bracard S. Topotecan as a radiosensitizer in the treatment of children with malignant diffuse brainstem gliomas. Cancer. 2005;104(12):2792–7.
70. Tosi U, Souweidane M. Convection enhanced delivery for diffuse intrinsic pontine glioma: review of a single institution experience. Pharmaceutics. 2020;12(7):660.
71. Souweidane MM, Kramer K, Pandit-Taskar N, Zhou Z, Haque S, Zanzonico P, et al. Convection-enhanced delivery for diffuse intrinsic pontine glioma: a single-centre, dose-escalation, phase 1 trial. Lancet Oncol. 2018;19(8):1040–50.
72. Heiss JD, Jamshidi A, Shah S, Martin S, Wolters PL, Argersinger DP, et al. Phase I trial of convection-enhanced delivery of IL13-pseudomonas toxin in children with diffuse intrinsic pontine glioma. J Neurosurg Pediatr. 2018;23(3):333–42.

73. Singleton WGB, Bienemann AS, Woolley M, Johnson D, Lewis O, Wyatt MJ, et al. The distribution, clearance, and brainstem toxicity of panobinostat administered by convection-enhanced delivery. J Neurosurg Pediatr. 2018;22(3):288–96.
74. Zhou Z, Ho SL, Singh R, Pisapia DJ, Souweidane MM. Toxicity evaluation of convection-enhanced delivery of small-molecule kinase inhibitors in naïve mouse brainstem. Childs Nerv Syst. 2015;31(4):557–62.
75. Szychot E, Walker D, Collins P, Hyare H, Shankar A, Bienemann A, et al. Clinical experience of convection-enhanced delivery (CED) of carboplatin and sodium valproate into the pons for the treatment of diffuse intrinsic pontine glioma (DIPG) in children and young adults after radiotherapy. Int J Clin Oncol. 2021;26(4):647–58.
76. Lonser RR, Warren KE, Butman JA, Quezado Z, Robison RA, Walbridge S, et al. Real-time image-guided direct convective perfusion of intrinsic brainstem lesions. J Neurosurg. 2007;107(1):190–7.
77. Kawakami M, Kawakami K, Puri RK. Interleukin-4-pseudomonas exotoxin chimeric fusion protein for malignant glioma therapy. J Neurooncol. 2003;65(1):15–25.
78. Bander ED, Ramos AD, Wembacher-Schroeder E, Ivasyk I, Thomson R, Morgenstern PF, et al. Repeat convection-enhanced delivery for diffuse intrinsic pontine glioma. J Neurosurg Pediatr. 2020;26(6):661–6.
79. Chittiboina P, Heiss JD, Warren KE, Lonser RR. Magnetic resonance imaging properties of convective delivery in diffuse intrinsic pontine gliomas. J Neurosurg Pediatr. 2014;13(3):276–82.
80. Morgenstern PF, Zhou Z, Wembacher-Schröder E, Cina V, Tsiouris AJ, Souweidane MM. Clinical tolerance of corticospinal tracts in convection-enhanced delivery to the brainstem. J Neurosurg. 2018;131(6):1812–8.
81. Tosi U, Souweidane MM. Longitudinal monitoring of Gd-DTPA following convection enhanced delivery in the brainstem. World Neurosurg. 2020;137:38–42.
82. Bander ED, Tizi K, Wembacher-Schroeder E, Thomson R, Donzelli M, Vasconcellos E, et al. Deformational changes after convection-enhanced delivery in the pediatric brainstem. Neurosurg Focus. 2020;48(1):E3.
83. Sewing ACP, Caretti V, Lagerweij T, Schellen P, Jansen MHA, van Vuurden DG, et al. Convection enhanced delivery of carmustine to the murine brainstem: a feasibility study. J Neurosci Methods. 2014;238:88–94.
84. Clark AJ, Lamborn KR, Butowski NA, Chang SM, Prados MD, Clarke JL, et al. Neurosurgical management and prognosis of patients with glioblastoma that progresses during bevacizumab treatment. Neurosurgery. 2012;70(2):361–70.
85. Jahangiri A, Chin AT, Flanigan PM, Chen R, Bankiewicz K, Aghi MK. Convection-enhanced delivery in glioblastoma: a review of preclinical and clinical studies. J Neurosurg. 2017;126(1):191–200.
86. Rand RW, Kreitman RJ, Patronas N, Varricchio F, Pastan I, Puri RK. Intratumoral administration of recombinant circularly permuted interleukin-4-pseudomonas exotoxin in patients with high-grade glioma. Clin Cancer Res. 2000;6(6):2157–65.
87. Degen JW, Walbridge S, Vortmeyer AO, Oldfield EH, Lonser RR. Safety and efficacy of convection-enhanced delivery of gemcitabine or carboplatin in a malignant glioma model in rats. J Neurosurg. 2003;99(5):893–8.
88. Kaiser MG, Parsa AT, Fine RL, Hall JS, Chakrabarti I, Bruce JN. Tissue distribution and antitumor activity of topotecan delivered by intracerebral clysis in a rat glioma model. Neurosurgery. 2000;47(6):1391–8. discussion 1398–9.
89. Wang W, Sivakumar W, Torres S, Jhaveri N, Vaikari VP, Gong A, et al. Effects of convection-enhanced delivery of bevacizumab on survival of glioma-bearing animals. Neurosurg Focus. 2015;38(3):E8.
90. Oberg JA, Dave AN, Bruce JN, Sands SA. Neurocognitive functioning and quality of life in patients with recurrent malignant gliomas treated on a phase Ib trial evaluating topotecan by convection-enhanced delivery. Neurooncol Pract. 2014;1(3):94–100.

91. Kunwar S, Chang S, Westphal M, Vogelbaum M, Sampson J, Barnett G, et al. Phase III randomized trial of CED of IL13-PE38QQR vs Gliadel wafers for recurrent glioblastoma. Neuro Oncol. 2010;12(8):871–81.
92. Mueller S, Polley M-Y, Lee B, Kunwar S, Pedain C, Wembacher-Schröder E, et al. Effect of imaging and catheter characteristics on clinical outcome for patients in the PRECISE study. J Neurooncol. 2011;101(2):267–77.
93. Sampson JH, Archer G, Pedain C, Wembacher-Schröder E, Westphal M, Kunwar S, et al. Poor drug distribution as a possible explanation for the results of the PRECISE trial. J Neurosurg. 2010;113(2):301–9.
94. Krauze MT, Saito R, Noble C, Bringas J, Forsayeth J, Mcknight TR, et al. Effects of the perivascular space on convection-enhanced delivery of liposomes in primate putamen. Exp Neurol. 2005;196(1):104–11.
95. Sampson JH, Raghavan R, Brady ML, Provenzale JM, Herndon JE, Croteau D, et al. Clinical utility of a patient-specific algorithm for simulating intracerebral drug infusions. Neuro Oncol. 2007;9(3):343–53.
96. Rosenbluth KH, Eschermann JF, Mittermeyer G, Thomson R, Mittermeyer S, Bankiewicz KS. Analysis of a simulation algorithm for direct brain drug delivery. Neuroimage. 2012;59(3):2423–9.
97. Zhan W, Rodriguez Y BF, Dini D. Effect of tissue permeability and drug diffusion anisotropy on convection-enhanced delivery. Drug Deliv. 2019;26(1):773–81.
98. Sewing ACP, Lagerweij T, van Vuurden DG, Meel MH, Veringa SJE, Carcaboso AM, et al. Preclinical evaluation of convection-enhanced delivery of liposomal doxorubicin to treat pediatric diffuse intrinsic pontine glioma and thalamic high-grade glioma. J Neurosurg Pediatr. 2017;19(5):518–30.
99. Lidar Z, Mardor Y, Jonas T, Pfeffer R, Faibel M, Nass D, et al. Convection-enhanced delivery of paclitaxel for the treatment of recurrent malignant glioma: a phase I/II clinical study. J Neurosurg. 2004;100(3):472–9.
100. Buczkowicz P, Bartels U, Bouffet E, Becher O, Hawkins C. Histopathological spectrum of paediatric diffuse intrinsic pontine glioma: diagnostic and therapeutic implications. Acta Neuropathol. 2014;128(4):573–81.
101. McCrorie P, Vasey CE, Smith SJ, Marlow M, Alexander C, Rahman R. Biomedical engineering approaches to enhance therapeutic delivery for malignant glioma. J Control Release. 2020;10(328):917–31.
102. Singh R, Bellat V, Wang M, Schweitzer ME, Wu YL, Tung C-H, et al. Volume of distribution and clearance of peptide-based nanofiber after convection-enhanced delivery. J Neurosurg. 2018;129(1):10–8.
103. Seo Y-E, Bu T, Saltzman WM. Nanomaterials for convection-enhanced delivery of agents to treat brain tumors. Curr Opin Biomed Eng. 2017;4:1–12.
104. Arshad A, Yang B, Bienemann AS, Barua NU, Wyatt MJ, Woolley M, et al. Convection-enhanced delivery of carboplatin PLGA nanoparticles for the treatment of glioblastoma. PLoS One. 2015;10(7):e0132266.
105. Sawyer AJ, Saucier-Sawyer JK, Booth CJ, Liu J, Patel T, Piepmeier JM, et al. Convection-enhanced delivery of camptothecin-loaded polymer nanoparticles for treatment of intracranial tumors. Drug Deliv Transl Res. 2011;1(1):34–42.
106. Hadjipanayis CG, Machaidze R, Kaluzova M, Wang L, Schuette AJ, Chen H, et al. EGFRvIII antibody-conjugated iron oxide nanoparticles for magnetic resonance imaging-guided convection-enhanced delivery and targeted therapy of glioblastoma. Cancer Res. 2010;70(15):6303–12.
107. Brown CE, Alizadeh D, Starr R, Weng L, Wagner JR, Naranjo A, et al. Regression of glioblastoma after chimeric antigen receptor T-cell therapy. N Engl J Med. 2016;375(26):2561–9.
108. Salinas RD, Durgin JS, O'Rourke DM. Potential of glioblastoma-targeted chimeric antigen receptor (CAR) T-cell therapy. CNS Drugs. 2020;34(2):127–45.

109. Mount CW, Majzner RG, Sundaresh S, Arnold EP, Kadapakkam M, Haile S, et al. Potent antitumor efficacy of anti-GD2 CAR T cells in H3-K27M+ diffuse midline gliomas. Nat Med. 2018;24(5):572–9.
110. Theruvath J, Sotillo E, Mount CW, Graef CM, Delaidelli A, Heitzeneder S, et al. Locoregionally administered B7-H3-targeted CAR T cells for treatment of atypical teratoid/rhabdoid tumors. Nat Med. 2020;26(5):712–9.
111. Atik AF, Suryadevara CM, Schweller RM, West JL, Healy P, Herndon Ii JE, et al. Hyaluronic acid based low viscosity hydrogel as a novel carrier for convection enhanced delivery of CAR T cells. J Clin Neurosci. 2018;56:163–8.
112. Chirmule N, Propert K, Magosin S, Qian Y, Qian R, Wilson J. Immune responses to adenovirus and adeno-associated virus in humans. Gene Ther. 1999;6(9):1574–83.
113. Lonser RR, Akhter AS, Zabek M, Elder JB, Bankiewicz KS. Direct convective delivery of adeno-associated virus gene therapy for treatment of neurological disorders. J Neurosurg. 2020;134(6):1751–63.
114. Kells AP, Hadaczek P, Yin D, Bringas J, Varenika V, Forsayeth J, et al. Efficient gene therapy-based method for the delivery of therapeutics to primate cortex. Proc Natl Acad Sci U S A. 2009;106(7):2407–11.
115. Barua NU, Woolley M, Bienemann AS, Johnson D, Wyatt MJ, Irving C, et al. Convection-enhanced delivery of AAV2 in white matter—a novel method for gene delivery to cerebral cortex. J Neurosci Methods. 2013;220(1):1–8.
116. Brun L, Ngu LH, Keng WT, Ch'ng GS, Choy YS, Hwu WL, et al. Clinical and biochemical features of aromatic L-amino acid decarboxylase deficiency. Neurology. 2010;75(1):64–71.
117. Chien Y-H, Lee N-C, Tseng S-H, Tai C-H, Muramatsu S-I, Byrne BJ, et al. Efficacy and safety of AAV2 gene therapy in children with aromatic L-amino acid decarboxylase deficiency: an open-label, phase 1/2 trial. Lancet Child Adolesc Health. 2017;1(4):265–73.
118. San Sebastian W, Richardson RM, Kells AP, Lamarre C, Bringas J, Pivirotto P, et al. Safety and tolerability of magnetic resonance imaging-guided convection-enhanced delivery of AAV2-hAADC with a novel delivery platform in nonhuman primate striatum. Hum Gene Ther. 2012;23(2):210–7.
119. Hopwood JJ, Morris CP. The mucopolysaccharidoses. Diagnosis, molecular genetics and treatment. Mol Biol Med. 1990;7(5):381–404.
120. Lonser RR, Walbridge S, Murray GJ, Aizenberg MR, Vortmeyer AO, Aerts JMFG, et al. Convection perfusion of glucocerebrosidase for neuronopathic Gaucher's disease. Ann Neurol. 2005;57(4):542–8.
121. Lonser RR, Schiffman R, Robison RA, Butman JA, Quezado Z, Walker ML, et al. Image-guided, direct convective delivery of glucocerebrosidase for neuronopathic Gaucher disease. Neurology. 2007;68(4):254–61.
122. Lau AA, Hemsley KM. Adeno-associated viral gene therapy for mucopolysaccharidoses exhibiting neurodegeneration. J Mol Med. 2017;95(10):1043–52.
123. Tardieu M, Zerah M, Husson B, de Bournonville S, Deiva K, Adamsbaum C, et al. Intracerebral administration of adeno-associated viral vector serotype rh.10 carrying human SGSH and SUMF1 cDNAs in children with mucopolysaccharidosis type IIIA disease: results of a phase I/II trial. Hum Gene Ther. 2014;25(6):506–16.

Chapter 7
Cortical Spreading Depolarizations in Aneurysmal Subarachnoid Hemorrhage: An Overview of Current Knowledge and Future Perspectives

Moncef Berhouma, Omer Faruk Eker, Frederic Dailler, Sylvain Rheims, and Baptiste Balanca

M. Berhouma (✉)
Department of Neurosurgical Oncology and Vascular Neurosurgery, Pierre Wertheimer Neurological and Neurosurgical Hospital, Hospices Civils de Lyon (Lyon University Hospital), Lyon, France

Creatis Lab, CNRS UMR 5220, INSERM U1206, Lyon 1 University, INSA Lyon, Lyon, France

O. F. Eker
Creatis Lab, CNRS UMR 5220, INSERM U1206, Lyon 1 University, INSA Lyon, Lyon, France

Department of Interventional Neuroradiology, Pierre Wertheimer Neurological and Neurosurgical Hospital, Hospices Civils de Lyon (Lyon University Hospital), Lyon, France
e-mail: omer.eker@chu-lyon.fr

F. Dailler
Department of Neuro-Anesthesia and Neuro-Critical Care, Pierre Wertheimer Neurological and Neurosurgical Hospital, Hospices Civils de Lyon (Lyon University Hospital), Lyon, France
e-mail: frederic.dailler@chu-lyon.fr

S. Rheims
Department of Functional Neurology and Epileptology, Pierre Wertheimer Neurological and Neurosurgical Hospital, Hospices Civils de Lyon (Lyon University Hospital), Lyon, France

Lyon's Neurosciences Research Center, INSERM U1028/CNRS, UMR 5292, University of Lyon, Lyon, France
e-mail: sylvain.rheims@chu-lyon.fr

B. Balanca
Department of Neuro-Anesthesia and Neuro-Critical Care, Pierre Wertheimer Neurological and Neurosurgical Hospital, Hospices Civils de Lyon (Lyon University Hospital), Lyon, France

Lyon's Neurosciences Research Center, INSERM U1028/CNRS, UMR 5292, University of Lyon, Lyon, France
e-mail: baptiste.balanca@chu-lyon.fr

C. Di Rocco (ed.), *Advances and Technical Standards in Neurosurgery*, Advances and Technical Standards in Neurosurgery 45,
https://doi.org/10.1007/978-3-030-99166-1_7

7.1 Introduction

Aneurysmal subarachnoid hemorrhage (SAH) is a devastating condition that may lead to poor functional outcome and death. The outcome results from both early and delayed brain injuries that may occur during the intensive care unit (ICU) stay. Delayed cerebral ischemia (DCI) represents the most feared potentially preventable complication of SAH [1–3]. Hence, prevention, timely detection, and specific active management of DCI are crucial. Historically, DCI was thought to result from cerebral arterial vasospasm appearing usually around the tenth posthemorrhagic day. Nevertheless, a direct link between arterial vasospasm, DCI, and poor neurological outcome is still debated [2, 4]. Recently, several studies have confirmed the role of spreading depolarizations (SDs) in DCI and worse functional outcome during SAH [5, 6]. SDs are defined as self-propagating front of depolarization waves involving all central nervous system cell types located in the cortical matter. These can occur in a variety of acute brain injuries including SAH in which they can lead to vasoconstriction, decreased cerebral blood flow (CBF), anomalies of the blood–brain barrier, and cytokine release, all resulting in secondary brain injury [7–9]. This review will emphasize on the current experimental and clinical knowledge concerning the pathogenesis of SD occurrence in SAH. Furthermore, key therapeutic perspectives are discussed.

7.2 Pathogenesis of Cortical Spreading Depolarizations (SD)

In the context of his doctorate in Harvard University in 1944, Aristides A. Leão was studying the propagation of epileptic activity in the cerebral cortex. He approached the problem by applying electrical stimulation to the frontal convexity cortex of anesthetized rabbits and recording from an array of corticography electrodes posterior to this. Instead of seeing propagating epileptic activity, he observed a period of electrical silence, which was first seen adjacent to the stimulating electrodes, and did propagate from the site of stimulation backwards along the cerebral hemisphere at a rate of around 3 mm/min. The phenomenon resolved spontaneously after 5–15 min, with apparently full resumption of cortical electrical activity. He reported his findings in a landmark paper entitled “Spreading depression of activity in the cerebral cortex” [10]. A few years later, he described the large depolarization associated with these depressions of cortical activity and found that they looked like the slow DC shifts he observed after prolonged cerebral ischemia (during carotid artery occlusion). Triggering SDs in different conditions, he already suggested that their development and characteristics were not determined by the stimuli, but depended on the local characteristics and conditions of the affected regions [11].

The mechanism underlying SDs onset is still debated and experimentally SD can be triggered by a wide range of cortical aggression such as potassium (K+) or

glutamate injection as well as ischemic, mechanical, or electrical stimulation. Following acute brain injuries, primary affected regions exhibit cell destructions with membrane rupture and massive ion spillage and glutamate release. For instance, extracellular K+ has been found to increase when cerebral blood flow (CBF) drops below 10 mL 100/g/min [12] or during hypoglycemia. SDs can also be triggered in penumbra area with higher CBF levels by worsening the supply-demand mismatch with cortical activation such as during tactile stimulation [13]. The infusion of fresh autologous blood in the subarachnoid space of normally perfused tissue is also able to trigger SDs which are even more frequent when there is the formation of a clot in a sulcus [14]. The subsequent acute hemolysis causes a marked K+ increase in the extracellular space, thereby leading to neuronal and glial depolarization that will spread from the site of injury to neighboring cortical areas at a rate of 2–6 mm/min [15]. During normal brain activity, the low extracellular K+ increase is normally recaptured by neurons with the NA+/K+ ATPase; the remaining K+ is recaptured by astrocytes and diffuse through their network via gap junctions [16]. When the ion regulation capacity is exceeded or impaired such as during cerebral edema with astrocytic swelling, the subsequent K+ accumulation may start SD that will last longer than in healthy cortical tissue [17]. The exact mechanisms that promote the cellular membrane depolarization are still to be elucidated as well as the nature of the ions channels that prolong this state. Neurons and their proximal dendrites are the main active players of spreading depolarization. The near complete breakdown of ions gradients that takes place leads to an initial explosive opening of conductance along pyramidal neuron with transmembrane potential reaching almost zero and followed by a wave-like centripetal closure towards the apical dendrites [18, 19]. Potassium release with sodium, chlorine, and calcium inward current overcomes the pumps' capacity and leads to a near complete loss of electrochemical energy with a passive ion distribution across the membrane [20]. Intracellular hyperosmolality due to charged proteins will lead to cellular swelling, distortion of dendritic spine, and fragmentation of intracellular organelles such as mitochondria. However, in healthy well-perfused cortex, sodium ATPase pumps induce a rapid recovery of this ionic breakdown and restore cell morphology within minutes. Conversely, clusters of peri-infarct depolarizations induce sustain dendritic beading, suggesting that energy needs for recovery exceeded energy supply of compromised blood flow [21, 22]. The slow propagation of SDs across the cortical matter does not involve synaptic transmission, but is rather a multifactorial process that remains a matter of debate. It involves the release of glutamate into the extracellular medium propagating the depolarization from near to near, notably via the NMDA receptors; as well as transcellular ion diffusion through gap junction in astrocytes and neurons [18, 23–25].

From an energetic point of view, life and subsequently brain homoeostasis is a nonequilibrium steady state. The amount of energy being consumed at any moment in time for the signaling and maintenance of the resting potential and ion gradients is small in relation to the total electrochemical energy that is already stored up in the system in the form of physiological ion gradients. This implies that much more energy is required to reboot the system after a breakdown than to maintain the

system [20]. Two pathological states can challenge this steady state: ictal epileptic activity and spreading depolarization. However, the loss of ion gradients across the membrane is much larger after SD. The energy that is needed to recover from an SD leads to a massive increase in glucose and oxygen consumption, leading to a drop in oxygen and glucose with a release in lactate in the extracellular space; a state also known as hyperglycolysis that characterizes a normal response to an aggression [26]. In the healthy brain, cortical tissue recovers within 45 min; however, repeated SDs in a cluster may lead to a prolonged drop in cerebral glucose and oxygen [27].

The restoration of the ionic gradients after SD is extremely energetically demanding, and in the normal brain, the rise in metabolism is matched by a huge increase in CBF. In 1944, Leão already described a very conspicuous dilatation of the pial arteries that occurred as the electrical activity becomes progressively more and more depressed. This hyperemic response was occasionally followed by a long period of a relatively much slighter reduction of vessel's caliber. The hyperemic vasomotor spread was strictly analogous to that of the depression of the electrical activity [28]. From now on, this pattern has been extensively reproduced and is now considered as a specific feature, so that some authors use it as a surrogate to electrophysiologic recordings for SD detection [29]. This CBF increase can be altered by systemic cerebral aggressions such as hypoxia and/or hypotension with an initial dip, a lower CBF increase, and a long-lasting hypoperfusion [30]. In patients with acute brain injuries, SD consequences on microvascularization range from a classic hyperemic response to a flat one or even an ischemic response [8]. When an SD spread across differentially perfused cortical area, such as after an ischemic stroke, it will have different vasomotor consequences: a classic hyperemic pattern in normally perfused cortex (remote from the ischemic core), whereas in the ischemic core an inverse ischemic response occurs [31, 32]. In the penumbra area, a range of multiphasic patterns can be observed: the lower the pre-SD CBF, the more pronounced the decrease in CBF induced by SD [31–33]. In the well-perfused cortex, SD can also lead to a sustain oligemic or ischemic response when neurovascular coupling-needed compound concentrations are modified. For example, in conditions that mimic a subarachnoid hemorrhage [i.e., high extracellular K+ and nitric oxide (NO) scavenging with Hb or decreasing its release with NO synthase inhibitors], SD will trigger an ischemic vascular response [34, 35].

7.3 Experimental Models

Various animal models exist depending upon the SAH induction mechanism used: Endovascular perforation, blood injection into subarachnoid space, or cortical vessel perforation. Different techniques have been experienced to detect SDs: The gold standard remains local field potential recordings with a DC amplifier and a glass micropipette to record the negative DC shift (i.e., the depolarization); however, several authors used indirect measurement of SD consequences such as magnetic resonance imaging, nicotinamide adenine dinucleotide (NAD(H)) fluorescence, intrinsic

optical signal changes, extracellular potassium recording, and cerebral blood flow monitoring. One of the most detailed model studying SD mechanism in an SAH-like condition was developed by the team of Jens Dreier [34, 35]. Using cortical infusion of artificial cerebrospinal fluid (CSF) with purified hemoglobin (Hb) and elevated levels of K+ that mimic the hemolysis that follows SAH, they were able to demonstrate that the combination of NO scavenging by Hb and the blockage of the Na+/K+ ATPase by high extracellular K+ turns the SD-induced hyperemic CBF response into a CBF decrease also termed spreading ischemia. They were also able to demonstrate the impact of nimodipine that mitigates the spreading ischemia and restores the CBF-expected increase and clearly showed the tissue necrosis resulting from spreading ischemia [35]. The same group, among others, showed the inhibiting effect of elevated potassium on *N*-methyl-D-aspartate (NMDA) receptor antagonist, that is known to restrain SDs [36].

These experimental models not only served to produce studies aiming at demonstrating the occurrence of SDs in SAH models and better understanding the pathogenesis of SDs following SAH, but also helped to test different therapeutic hypotheses. Among these, Dreier et al. confirmed the inhibiting effect of nimodipine associated with moderate volume expansion and hemodilution on spreading ischemia probably through an effect on cortical microcirculation [37]. More recently, Sugimoto et al. studied the effect of a phosphodiesterase-3 inhibitor (Cilostazol) on SDs in a prospective clinical trial and experimental study (rats): In their clinical series of 50 patients with aneurysmal SAH, there was a nonstatistically significant trend toward less DCI in the cilostazol group. However, in their experimental work on rats, cilostazol significantly reduced the duration of spreading ischemia [38]. The effect of valproate on SDs has also been investigated by Hamming et al. on SAH rat model (carotid endovascular puncture and potassium application for the induction of SDs): the authors found that valproate significantly reduced the lesion growth in the rat group that has received topical cortical potassium [39].

7.4 Patterns of CSD in Patients with Acute Brain Injury

Cortical recordings in animal models and in patients with acute brain injuries (i.e., SAH, severe traumatic brain injury, intracerebral hematoma, or malignant hemispheric stroke) evidenced that SDs propagate in the gyrencephalic brain at a speed of 1.7–9.2 mm/min [40]. Most SDs evolve with a radial propagation from the injured site on the surface of the gyrus, while some display spiral patterns or reverberation on anatomical structure; some sulci and pial vessels may also block the propagation of SD wavefront [41]. The spread of the depolarization, recorded on cortical electrodes, from one electrode to another is a characteristic feature of SDs; but the direction of the spread between electrodes may vary from one SD to the other if their propagation pattern is different [7, 41]. The terms and characteristics of SD-related event that can be observed on cortical recordings have been harmonized in a recent review from the cooperative study on brain injury depolarization

(COSBID) group [7]. The Table 7.1 reports the current definition of each elements that constitute SDs: the negative DC shift (i.e., the depolarization) that spreads across the cortical surface will lead to a depression of the background activity, if present; ictal epileptic event that may be superimposed to SDs; the patterns that are clearly associated with ongoing cerebral damage (Fig. 7.1).

Although the occurrence of SDs is associated with a worse outcome, the pathogenicity of isolated SDs remains controversial. Isolated SDs can be observed in patient with an improving neurological examination, in whom invasive monitoring removal would be considered, but they may also reflect ongoing injury in non-eloquent brain areas remote from the recording site [42]. On the contrary, there is now a consensus on the deleterious nature of certain patterns. Flowing the first SD at the onset of a new brain damage further SD may develop in a cluster pattern defined as at least 3 SDs occurring within 3 or less consecutive hours. SD clusters can be recorded remotely from the injured site, although the DC shifts are shorter as the depolarization spread in healthy cortical tissue [7]. Furthermore, cluster of SD may produce new brain lesions with persistent cellular edema and depression of brain activity [7, 21, 22]. In patient with an SAH, clusters of SD are associated with

Table 7.1 Definitions of spreading depolarization features observed on cortical recordings

Cortical recording features of spreading depolarization (SD)	
Negative DC shift	Abrupt negative shift of the slow potential recorded with a DC amplifier; the longer the duration of the DC shift, the more the metabolic burden imposed to the tissue. If the shift is recorded with a near-DC amplifier (frequency above 0.01 Hz), the shape is distorted with multiphasic slow potential changes The DC shift spread from one recording electrode to another at ~1.5–9.5 mm/min. Non-spreading DC changes on all electrodes with unchanged background activity are considered as noise
Spreading depression of activity	SD-induced reduction of neuronal activity that is recorded by a cortical electrode. The duration of the depression outlasts that of the depolarization and may be persistent in case of repetitive SDs or if a cortical infarct occurs
Spreading convulsion	SD with a superimposed epileptic event, usually on the tail of the DC shift
Biomarker of cortical lesion	
Cluster of SDs	At least three SDs occurring within three or fewer consecutive recording hours
Isoelectric SD	SD that occurs in electrically inactive tissue (no spreading depression is possible) For example, a cluster of SD may lead to a persistent depression of background activity and evolve toward isoelectric SDs
Non-spreading depression of activity	Simultaneous arrest of spontaneous activity in neighboring electrodes before the occurrence of SDs +/− NUP, as a consequence of a drop in cerebral energy supply such as during an ischemic stroke, a cardiac arrest, or a severe hemodynamic shock Short-lasting non-spreading depression of brain activity may be observed due to sedation or arousal changes, but does not fulfill the current definition
Negative ultraslow potential (NUP)	A very long-lasting, shallow negativity of the DC potential with superimposed SDs. The NUP is the electrophysiological correlates of the development of a cortical infarct with the inability of neurons to repolarize

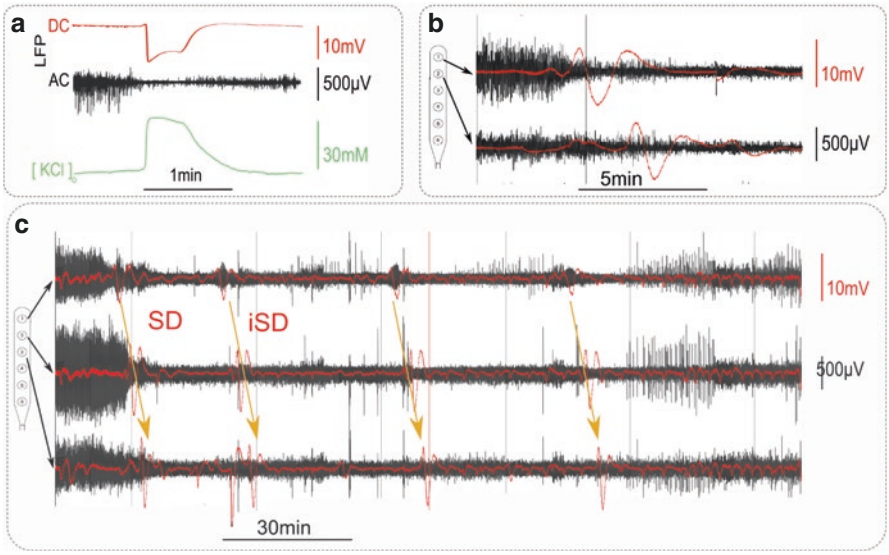

Fig. 7.1 (**a**) Local field potential (LFP) intracortical recording of a spreading depolarization (SD) with a glass micropipette (DC signal in red, AC signal in black) and a potassium selective electrode (green). (**b**) Cortical recording of an SD with a platinum/iridium subdural strip (DC signal in red, AC signal in black). (**c**) Cluster of SDs recording with a platinum/iridium subdural strip (DC signal in red, AC signal in black); note that the second SD is an isoelectric SD (iSD)

the occurrence of a delayed neurological deficit that may evolve to a cortical infarct [43]. If cortical electrodes are located in area undergoing new cortical ischemia, the drop of CBF under 15–23 ml/100 g/min will trigger a non-spreading depression of neuronal activity followed by the onset of a SDs on an isoelectric background (i.e., isoelectric SD) [44]. If the CBF is not restored, neurons will not be able to repolarize and a negative ultraslow potential (NUP) can be observed. The recording of a NUP reflects the onset of a cortical infarct under the recording site [7, 45].

7.5 CSD in the Clinical Setting of SAH

Several clinical studies, mostly prospective, have established an association between SDs' occurrence and functional outcome in SAH [6]. In 2006, Dreier et al. performed a multicenter prospective study recording SDs using a subdural electrode strip placed on the cortical surface in patients with SAH requiring aneurysm surgery. The authors noted the occurrence of SDs in 72% of their patients with high-grade SAH and confirmed a clear association between repeated SDs with prolonged depression periods and delayed ischemic brain lesions [43]. Prolonged depressions were also associated to late epilepsy occurrence in patients with SAH [46]. Additionally to the deleterious effect of prolonged depression, the duration of SDs

itself has also been shown to be correlated to DCI [47]. Furthermore, Woitzik et al. found a high incidence of SDs and DCI in patients with aneurysmal SAH even in the absence of angiographic vasospasm, reshuffling the cards in the common knowledge concerning the pathogenesis of DCI and vasospasm in SAH [48]. Additional studies aimed at better understanding the mechanisms underlying the association between SDs and DCI in patients with SAH. Variation of CBF is one of main parameters involved in this association. In contrast with the normal brains where the occurrence of SDs leads to hyperemia, SDs in acute brain injury including SAH provoke an inverse decreased blood flow response that may lead to ischemia [8, 15]. In 2016, Sugimoto et al. used simultaneous electrocorticography and monitoring of the pressure reactivity index to show a possible association between impaired cerebrovascular autoregulation and increased duration of spreading depressions related to SDs in a patient with aneurysmal SAH [49]. In addition to the effect on cerebral blood flow, SDs may interfere with oxygen availability by increasing the consumption required for the correction of ionic transmembrane gradients, particularly in the case of clusters of SDs [50–52]. The role of metabolic anomalies involving lactates and glucose concentrations has also been questioned, but still remains unanswered [52, 53].

7.6 Monitoring of CSD

In 1996, Mayevsky et al. were the first to record cortical SDs in the human cortex after traumatic brain injury (one out of 14 patients) using a multiparametric device with depth electrodes [54]. In 2002, Strong et al. set up a linear subdural strip, made of 6 platinum electrodes, placed on the cortex after a craniotomy in order to record both the depolarization and its spread [55]. This subdural strip of electrodes had become the standard recording technique in the human brain. From now on, an international group of investigators built the “Cooperative Studies on Brain Injury Depolarization” (COSBID) to discuss ways to advance these findings and further investigate their implications.

Unlike conventional EEG, the recording of SDs requires the acquisition of the full frequency electrophysiological signal: The DC band from 0 to 0.5 Hz, and the AC band over 0.5 Hz. The DC signal is usually deleted with a high pass filter to avoid artefacts and large baseline drift. The spreading negative DC shift that defines SD therefore requires amplifier devoid of analog high pass filters to acquire DC signal (>0 Hz) or near-DC signal (>0.01 Hz). Indeed, the slow potential change of spreading depolarization seems to be invisible in scalp EEG recordings, whereas the tenfold smaller discharges of epileptic seizures are easily identified. This paradox results from the potent capacitive resistance of the dura and skull, which filters slow voltage changes but allows high-frequency epileptic activity to pass through. On scalp EEG, slow potential changes with a depression of background activity may be observed when cluster of SDs occurs as evidenced on cortical subdural electrodes [56]. Yet it is not currently possible to rely solely on EEG data to detect SDs as a

clear spreading DC shift with or without spreading depression of activity cannot be identified [57]. Epidural electrodes were also recently tried to record SDs without opening the dura. They are also able to record SDs with similar characteristics compared to subdural electrodes; however, some SDs may not be detected by epidural electrodes [58, 59]. Therefore, to date the gold standard in patients remains the platinum–iridium subdural strips placed on the surface of a gyrus in areas at risk of developing new lesions [7]. Although those electrodes are able to record SDs, the shape of the DC shift is altered compared to that recorded in animals with intracortical glass micropipettes (Fig. 7.1), and the use of other cortical devices such as graphene micro-transistors may overcome this drawback [60].

In the clinical setting, recording of SDs may be obtained either with a 6-contact subdural cortical electrode strip (Fig. 7.2) or an intraparenchymal electrode array (Spencer depth electrode) (Fig. 7.3), all made of an alloy of platinum and iridium. The cortical strip electrode usually has 6 contacts and may be placed on the cortical surface of the brain during surgery (aneurysm clipping for example). Care must be taken to place the shiny side with exposed contacts toward the cortex. The contacts should be placed as close as possible from the lesion, but should avoid any infarcted cortex. Ideally, the strip should be positioned on the "penumbra" zone and extend to the healthy cortex, lying, if possible, in the same gyrus to avoid crossing major sulci and fissures. Attention is required to leave sufficient dural opening and a bone burr hole around the probe for an easy removal at the patient's bed. The skin exit of the probe should also be enlarged with a forcep to 7–8 mm of width to allow the strip

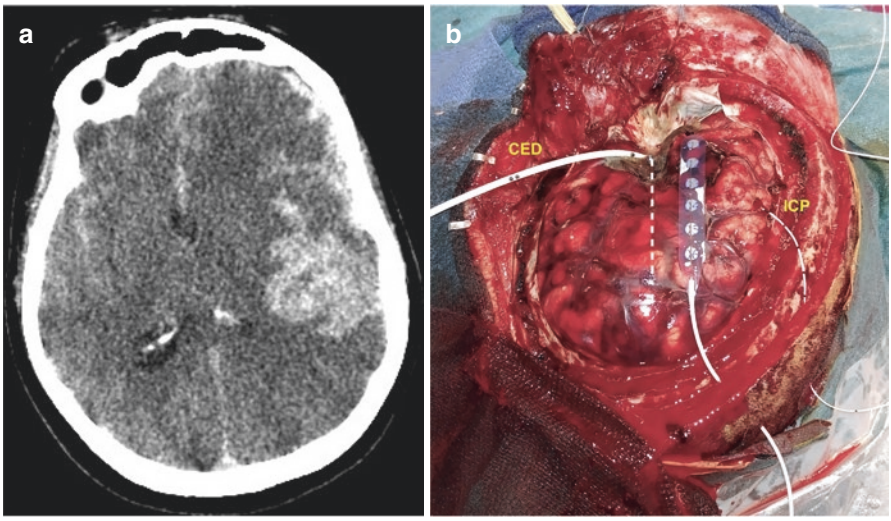

Fig. 7.2 (**a**) CT-scan showing a severe SAH with large sylvian cisternal hematoma. (**b**) Large decompressive left hemicraniectomy after middle cerebral artery aneurysm clipping and sylvian cisternal hematoma removal. The strip electrode is positioned on the inferior frontal gyrus parallel to the sylvian fissure (dotted line). *ICP* intraparenchymal intracranial pressure electrode, *CED* cisternal external drainage

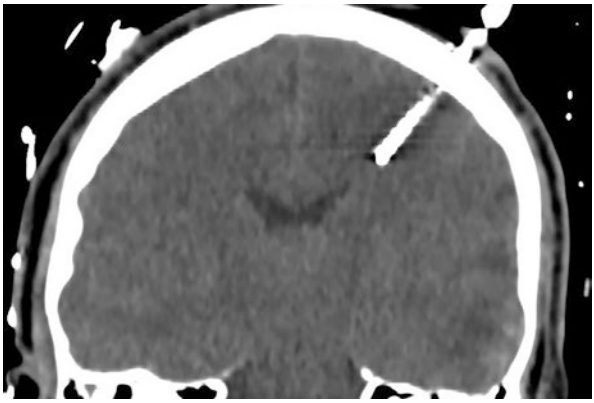

Fig. 7.3 Depth SD electrode positioning

removal and should finally be sutured once the probe has been removed to avoid any CSF leak. The depth electrode can be tunneled or placed through an intracranial access bolt with other monitoring devices (microdialysis and/or ICP monitoring for example). It can also be positioned during an external ventricular drainage. In this case, data recording will be possible only for the most superficial contacts located in the cortical matter, while deeper contacts in the white matter could be used as reference electrodes. In parallel to SD recording, other simultaneous intracranial monitoring are feasible (e.g., $PbtO_2$ or CBF probes or cerebral microdialysis) to implement in the ICU similar information that are used at the bench using laser speckle, laser Doppler, or videomicroscopy and better understand the correlation between SD occurrence and CBF and/or metabolic changes [61, 62].

7.7 Therapeutic Perspectives

The course of SAH follows a biphasic course. The first brain insult resulting from the initial bleeding is grouped together and termed early brain injuries (EBI) with up to 30% of patient remaining uncurious for several days during the next period at risk of DCI [63, 64]. DCI is defined as the occurrence of a new focal neurological deficit or decrease of the level of consciousness lasting more than 1 h, in the absence of other neuro-worsening cause [65]. Frequent neurological assessment is therefore critical and monitored in the ICU with the modified Glasgow Coma Scale (mGCS, i.e., using the worse motor score) or the abbreviated National Institute of Health Stroke Scale (aNIHSS, i.e., rating 7 items including the level of consciousness, left and right arm motor movement, left and right leg motor movement, speech fluency, and speech clarity). A 2-point mGCS decrease or a NIHSS increase and/or a new focal neurological deficit in patients with a reliable clinical examination must evoke a DCI in the absence of other differential diagnosis [66]. In patients with poor grade SAH who remain unconscious (because of early brain injuries or due to ongoing sedation), the detection of DCI is more challenging before irreversible ischemic

lesions are present. Daily wake-up trials in brain-injured sedated patients should be performed with extreme caution as it can raise intracranial pressure and reduce brain oxygenation [67]. Multimodal neuromonitoring is thus advocated looking for proximal vasospasm, cerebral energetic mismatch, or abnormal neurological activities. Any changes that would suggest a proximal vasospasm or a new cerebral injury would trigger a brain imaging (i.e., CT or MRI with vascular and perfusion information) to confirm the presence of perfusion deficits with or without a proximal vasospasm. The monitoring of SDs could therefore be implemented in this multimodal approach, as SDs are both a mechanism of DCI pathophysiology and a biomarker of new cortical injury even if the electrodes are distant from the injured area [7, 43, 68–70]. The current management of patients who develop a DCI is based on a tiered approach. The first tier when a DCI occurs includes controlled hypertension with the optimization of cerebral perfusion pressure as well as cerebral metabolic supply such as blood glucose and oxygen concentrations. If a symptomatic vasospasm is evidenced, the next tiers include a cerebral angiography with intra-arterial calcium channels blockers and/or mechanical angioplasty [68, 71]. The escalation and de-escalation are based on the changes in clinical examination and multimodal monitoring. Electrocorticography (ECoG) monitoring that seeks SD occurrence can therefore be implemented in this multimodal monitoring both to optimize a cerebral metabolic supply and to detect DCI occurrence to trigger cerebral imaging.

The SD pattern that should be used as a biomarker to trigger therapeutic interventions is still debated; however it is now accepted that SDs are a marker of ongoing cortical injury. When new SDs occur, the first tier would be to use SD as a biomarker of cerebral aggression and to look for systemic cerebral injury and correct systemic physiological parameters such as hypotension, hypoxemia, hypoglycemia, or hyperthermia. If those parameters are in a normal ranges, the presence of SDs (particularly if associated with other multimodal monitoring changes such as a decrease in $PbtO_2$, CBF, or cerebral glucose) should lead to targeting more aggressive ranges with permissive and controlled hypertension or hypercapnia [42, 71]. Nevertheless, it has been reported that SDs could also be recorded in patients with an improving clinical examination in whom invasive neuromonitoring would be withdrawn. In this situation, the appropriate response is debated; some argue for a withdrawal of monitoring, while others are in favor of a more aggressive management to block the occurrence of SDs [42]. There are clear patterns described in the Table 7.1 that reveal clearly a new and severe cortical injury and are associated with a worse outcome. For instance, the occurrence of clusters of SDs with or without isoelectric SDs for at least 3–4 h indicates the presence of a severe and continuous cerebral aggression and produces persistent cellular edema that can be evidenced as diffusion abnormalities on an MRI [42]. The most effective agents that have proved to reduce the propagation and occurrence of SDs both in experimental models and in patients are the NMDA receptor blockers [72, 73]. The subsequent tier to reduce the burden of SD would therefore be to start ketamine infusion at a rate of 1–2 mg/kg/h in addition to ongoing sedation (e.g., midazolam and sufentanyl); lower doses below 0.55 mg/kg/h having no effect on SDs [72]. There is a dose-dependent effect of ketamine; therefore if clusters of SDs are still present, a stepwise increase up to

4 mg/kg/h could be performed with close monitoring of side effects such as hepatotoxicity [74, 75]. The feasibility of ketamine infusion to reduce SDs has been tested in one prospective trial that included 10 patients admitted for aneurysm clipping in SAH or hemicraniectomy in TBI, in the University hospital of New Mexico, Albuquerque [75]. However, the impact of such strategy on patient's outcome or CBF and metabolism has not yet been evaluated in a prospective trial. During the last meeting of the COSBID group, it has been advocated that the first step should be to conduct a feasibility trial of a management algorithm based on ECoG monitoring with a tier approach and its effect on SD burden [42]. Several elements that would compose this algorithm are not defined and may vary depending on each center organization since it requires a close collaboration between physicians trained in SD detection and interpretation and the ICU staff in charge of the patient. The frequency of ECoG interpretation and thereby the stepwise escalation or de-escalation in the protocol steps should perhaps depend on patients' condition and SD occurrence. We would argue for a more frequent reevaluation in patient with ongoing vasospasm, DCI, and/or SDs compared to stable patients. Moreover, a frequent ECoG evaluation requires the availability of dedicated physicians able to interpret SD signals on a 24/7 basis.

7.8 Conclusion

An increasing number of experimental and clinical studies have produced clear evidence of the association between SDs and DCI in aneurysmal SAH, even if the pathogenesis still remains debated. Further clinical trials will certainly help to identify interesting therapeutic targets to prevent the occurrence of DCI. Despite the fact that the monitoring of SDs in the clinical practice still remains invasive, SDs may be considered as a useful biomarker of brain injury during the evolution of aneurysmal SAH.

References

1. Francoeur CL, Mayer SA. Management of delayed cerebral ischemia after subarachnoid hemorrhage. Crit Care. 2016;20:277.
2. Geraghty JR, Testai FD. Delayed cerebral ischemia after subarachnoid hemorrhage: beyond vasospasm and towards a multifactorial pathophysiology. Curr Atheroscler Rep. 2017;19:50.
3. Serrone JC, Maekawa H, Tjahjadi M, Hernesniemi J. Aneurysmal subarachnoid hemorrhage: pathobiology, current treatment and future directions. Expert Rev Neurother. 2015;15:367–80.
4. James RF, Kramer DR, Aljuboori ZS, Parikh G, Adams SW, Eaton JC, Abou Al-Shaar H, Badjatia N, Mack WJ, Simard JM. Novel treatments in neuroprotection for aneurysmal subarachnoid hemorrhage. Curr Treat Options Neurol. 2016;18:38.
5. Chung DY, Sugimoto K, Fischer P, et al. Real-time non-invasive in vivo visible light detection of cortical spreading depolarizations in mice. J Neurosci Methods. 2018;309:143–6.

6. Sugimoto K, Chung DY. Spreading depolarizations and subarachnoid Hemorrhage. Neurotherapeutics. 2020;17:497–510.
7. Dreier JP, Fabricius M, Ayata C, et al. Recording, analysis, and interpretation of spreading depolarizations in neurointensive care: review and recommendations of the COSBID research group. J Cereb Blood Flow Metab. 2017;37:1595–625.
8. Dreier JP, Major S, Manning A, et al. Cortical spreading ischaemia is a novel process involved in ischaemic damage in patients with aneurysmal subarachnoid haemorrhage. Brain. 2009;132:1866–81.
9. Shuttleworth CW, Andrew RD, Akbari Y, et al. Which spreading depolarizations are deleterious to brain tissue? Neurocrit Care. 2020;32:317–22.
10. Leao AAP. Spreading depression of activity in the cerebral cortex. J Neurophysiol. 1944;7:359–90.
11. Leo AA. Further observations on the spreading depression of activity in the cerebral cortex. J Neurophysiol. 1947;10:409–14.
12. Harris RJ, Symon L, Branston NM, Bayhan M. Changes in extracellular calcium activity in cerebral ischaemia. J Cereb Blood Flow Metab. 1981;1:203–9.
13. Hansen AJ. The extracellular potassium concentration in brain cortex following ischemia in hypo- and hyperglycemic rats. Acta Physiol Scand. 1978;102:324–9.
14. Hartings JA, Li C, Hinzman JM, Shuttleworth CW, Ernst GL, Dreier JP, Wilson JA, Andaluz N, Foreman B, Carlson AP. Direct current electrocorticography for clinical neuromonitoring of spreading depolarizations. J Cereb Blood Flow Metab. 2017;37:1857–70.
15. Dreier JP. The role of spreading depression, spreading depolarization and spreading ischemia in neurological disease. Nat Med. 2011;17:439–47.
16. Somjen GG. Ions in the brain: normal function, seizures, and stroke. New York: OUP USA; 2004.
17. Menyhárt Á, Frank R, Farkas AE, et al. Malignant astrocyte swelling and impaired glutamate clearance drive the expansion of injurious spreading depolarization foci. J Cereb Blood Flow Metab. 2020;42(4):584–99.
18. Herreras O, Makarova J. Mechanisms of the negative potential associated with Leão's spreading depolarization: a history of brain electrogenesis. J Cereb Blood Flow Metab. 2020;40:1934–52.
19. Makarova J, Gómez-Galán M, Herreras O. Variations in tissue resistivity and in the extension of activated neuron domains shape the voltage signal during spreading depression in the CA1 in vivo. Eur J Neurosci. 2008;27:444–56.
20. Dreier JP, Isele T, Reiffurth C, Offenhauser N, Kirov SA, Dahlem MA, Herreras O. Is spreading depolarization characterized by an abrupt, massive release of Gibbs free energy from the human brain cortex? Neuroscientist. 2013;19:25–42.
21. Kirov SA, Fomitcheva IV, Sword J. Rapid neuronal ultrastructure disruption and recovery during spreading depolarization-induced cytotoxic edema. Cereb Cortex. 2020;30:5517–31.
22. Risher WC, Ard D, Yuan J, Kirov SA. Recurrent spontaneous spreading depolarizations facilitate acute dendritic injury in the ischemic penumbra. J Neurosci. 2010;30:9859–68.
23. Van Harreveld A. Compounds in brain extracts causing spreading depression of cerebral cortical activity and contraction of crustacean muscle. J Neurochem. 1959;3:300–15.
24. Rogers ML, Feuerstein D, Leong CL, Takagaki M, Niu X, Graf R, Boutelle MG. Continuous online microdialysis using microfluidic sensors: dynamic neurometabolic changes during spreading depolarization. ACS Chem Neurosci. 2013;4:799–807.
25. Hinzman JM, DiNapoli VA, Mahoney EJ, Gerhardt GA, Hartings JA. Spreading depolarizations mediate excitotoxicity in the development of acute cortical lesions. Exp Neurol. 2015;267:243–53.
26. Cesarini KG, Enblad P, Ronne-Engström E, Marklund N, Salci K, Nilsson P, Hårdemark H-G, Hillered L, Persson L. Early cerebral hyperglycolysis after subarachnoid haemorrhage correlates with favourable outcome. Acta Neurochir. 2002;144:1121–31.

27. Balança B, Meiller A, Bezin L, Dreier JP, Marinesco S, Lieutaud T. Altered hypermetabolic response to cortical spreading depolarizations after traumatic brain injury in rats. J Cereb Blood Flow Metab. 2017;37:1670–86.
28. Leo AAP. Pial circulation and spreading depression of activity in the cerebral cortex. J Neurophysiol. 1944;7:391–6.
29. Kao Y-CJ, Li W, Lai H-Y, Oyarzabal EA, Lin W, Shih Y-YI. Dynamic perfusion and diffusion MRI of cortical spreading depolarization in photothrombotic ischemia. Neurobiol Dis. 2014;71:131–9.
30. Sukhotinsky I, Dilekoz E, Moskowitz MA, Ayata C. Hypoxia and hypotension transform the blood flow response to cortical spreading depression from hyperemia into hypoperfusion in the rat. J Cereb Blood Flow Metab. 2008;28:1369–76.
31. Shin HK, Dunn AK, Jones PB, Boas DA, Moskowitz MA, Ayata C. Vasoconstrictive neurovascular coupling during focal ischemic depolarizations. J Cereb Blood Flow Metab. 2006;26:1018–30.
32. Feuerstein D, Takagaki M, Gramer M, Manning A, Endepols H, Vollmar S, Yoshimine T, Strong AJ, Graf R, Backes H. Detecting tissue deterioration after brain injury: regional blood flow level versus capacity to raise blood flow. J Cereb Blood Flow Metab. 2014;34:1117–27.
33. Bere Z, Obrenovitch TP, Kozák G, Bari F, Farkas E. Imaging reveals the focal area of spreading depolarizations and a variety of hemodynamic responses in a rat microembolic stroke model. J Cereb Blood Flow Metab. 2014;34:1695–705.
34. Dreier JP, Körner K, Ebert N, et al. Nitric oxide scavenging by hemoglobin or nitric oxide synthase inhibition by *N*-nitro-L-arginine induces cortical spreading ischemia when K+ is increased in the subarachnoid space. J Cereb Blood Flow Metab. 1998;18:978–90.
35. Dreier JP, Ebert N, Priller J, et al. Products of hemolysis in the subarachnoid space inducing spreading ischemia in the cortex and focal necrosis in rats: a model for delayed ischemic neurological deficits after subarachnoid hemorrhage? J Neurosurg. 2000;93:658–66.
36. Petzold GC, Windmüller O, Haack S, et al. Increased extracellular K+ concentration reduces the efficacy of *N*-methyl-D-aspartate receptor antagonists to block spreading depression-like depolarizations and spreading ischemia. Stroke. 2005;36:1270–7.
37. Dreier JP, Windmüller O, Petzold G, Lindauer U, Einhäupl KM, Dirnagl U. Ischemia triggered by red blood cell products in the subarachnoid space is inhibited by nimodipine administration or moderate volume expansion/hemodilution in rats. Neurosurgery. 2002;51:1457–65. discussion 1465–1467
38. Sugimoto K, Nomura S, Shirao S, et al. Cilostazol decreases duration of spreading depolarization and spreading ischemia after aneurysmal subarachnoid hemorrhage. Ann Neurol. 2018;84:873–85.
39. Hamming AM, van der Toorn A, Rudrapatna US, et al. Valproate reduces delayed brain injury in a rat model of subarachnoid hemorrhage. Stroke. 2017;48:452–8.
40. Woitzik J, Hecht N, Pinczolits A, et al. Propagation of cortical spreading depolarization in the human cortex after malignant stroke. Neurology. 2013;80:1095–102.
41. Santos E, Schöll M, Sánchez-Porras R, Dahlem MA, Silos H, Unterberg A, Dickhaus H, Sakowitz OW. Radial, spiral and reverberating waves of spreading depolarization occur in the gyrencephalic brain. Neuroimage. 2014;99:244–55.
42. Helbok R, Hartings JA, Schiefecker A, et al. What should a clinician do when spreading depolarizations are observed in a patient? Neurocrit Care. 2020;32:306–10.
43. Dreier JP, Woitzik J, Fabricius M, et al. Delayed ischaemic neurological deficits after subarachnoid haemorrhage are associated with clusters of spreading depolarizations. Brain. 2006;129:3224–37.
44. Hossmann KA. Viability thresholds and the penumbra of focal ischemia. Ann Neurol. 1994;36:557–65.
45. Lückl J, Lemale CL, Kola V, et al. The negative ultraslow potential, electrophysiological correlate of infarction in the human cortex. Brain. 2018;141:1734–52.

46. Dreier JP, Major S, Pannek H-W, et al. Spreading convulsions, spreading depolarization and epileptogenesis in human cerebral cortex. Brain. 2012;135:259–75.
47. Hartings JA, Wilson JA, Look AC, Vagal A, Shutter LA, Dreier JP, Ringer A, Zuccarello M. Full-band electrocorticography of spreading depolarizations in patients with aneurysmal subarachnoid hemorrhage. Acta Neurochir Suppl. 2013;115:131–41.
48. Woitzik J, Dreier JP, Hecht N, et al. Delayed cerebral ischemia and spreading depolarization in absence of angiographic vasospasm after subarachnoid hemorrhage. J Cereb Blood Flow Metab. 2012;32:203–12.
49. Sugimoto K, Shirao S, Koizumi H, et al. Continuous monitoring of spreading depolarization and cerebrovascular autoregulation after aneurysmal subarachnoid hemorrhage. J Stroke Cerebrovasc Dis. 2016;25:e171–7.
50. von Bornstädt D, Houben T, Seidel JL, et al. Supply-demand mismatch transients in susceptible peri-infarct hot zones explain the origins of spreading injury depolarizations. Neuron. 2015;85:1117–31.
51. Bosche B, Graf R, Ernestus R-I, Dohmen C, Reithmeier T, Brinker G, Strong AJ, Dreier JP, Woitzik J, Members of the Cooperative Study of Brain Injury Depolarizations (COSBID). Recurrent spreading depolarizations after subarachnoid hemorrhage decreases oxygen availability in human cerebral cortex. Ann Neurol. 2010;67:607–17.
52. Seule M, Keller E, Unterberg A, Sakowitz O. The hemodynamic response of spreading depolarization observed by near infrared spectroscopy after aneurysmal subarachnoid hemorrhage. Neurocrit Care. 2015;23:108–12.
53. Sarrafzadeh A, Santos E, Wiesenthal D, Martus P, Vajkoczy P, Oehmchen M, Unterberg A, Dreier JP, Sakowitz O. Cerebral glucose and spreading depolarization in patients with aneurysmal subarachnoid hemorrhage. Acta Neurochir Suppl. 2013;115:143–7.
54. Mayevsky A, Doron A, Manor T, Meilin S, Zarchin N, Ouaknine GE. Cortical spreading depression recorded from the human brain using a multiparametric monitoring system. Brain Res. 1996;740:268–74.
55. Strong AJ, Fabricius M, Boutelle MG, Hibbins SJ, Hopwood SE, Jones R, Parkin MC, Lauritzen M. Spreading and synchronous depressions of cortical activity in acutely injured human brain. Stroke. 2002;33:2738–43.
56. Drenckhahn C, Winkler MKL, Major S, et al. Correlates of spreading depolarization in human scalp electroencephalography. Brain. 2012;135:853–68.
57. Hofmeijer J, van Kaam CR, van de Werff B, Vermeer SE, Tjepkema-Cloostermans MC, van Putten MJAM. Detecting cortical spreading depolarization with full band scalp electroencephalography: an illusion? Front Neurol. 2018;9:17.
58. Dreier JP, Major S, Lemale CL, Kola V, Reiffurth C, Schoknecht K, Hecht N, Hartings JA, Woitzik J. Correlates of spreading depolarization, spreading depression, and negative ultraslow potential in epidural versus subdural electrocorticography. Front Neurosci. 2019;13:373.
59. Lehmenkühler A, Richter F. Cortical spreading depolarization (CSD) recorded from intact skin, from surface of dura mater or cortex: comparison with intracortical recordings in the neocortex of adult rats. Neurochem Res. 2020;45:34–41.
60. Masvidal-Codina E, Illa X, Dasilva M, et al. High-resolution mapping of infraslow cortical brain activity enabled by graphene microtransistors. Nat Mater. 2019;18:280–8.
61. Berhouma M, Picart T, Dumot C, et al. Alterations of cerebral microcirculation in peritumoral edema: feasibility of in vivo sidestream dark-field imaging in intracranial meningiomas. Neurooncol Adv. 2020;2:vdaa108.
62. Lal C, Leahy MJ. An updated review of methods and advancements in microvascular blood flow imaging. Microcirculation. 2016;23:345–63.
63. Balança B, Ritzenthaler T, Gobert F, Richet C, Bodonian C, Carrillon R, Terrier A, Desmurs L, Perret-Liaudet A, Dailler F. Significance and diagnostic accuracy of early S100B serum concentration after aneurysmal subarachnoid hemorrhage. J Clin Med. 2020;9:1746. https://doi.org/10.3390/jcm9061746.

64. Rass V, Helbok R. Early brain injury after poor-grade subarachnoid hemorrhage. Curr Neurol Neurosci Rep. 2019;19:78.
65. Vergouwen MDI, Vermeulen M, van Gijn J, et al. Definition of delayed cerebral ischemia after aneurysmal subarachnoid hemorrhage as an outcome event in clinical trials and observational studies: proposal of a multidisciplinary research group. Stroke. 2010;41:2391–5.
66. Macdonald RL, Higashida RT, Keller E, et al. Clazosentan, an endothelin receptor antagonist, in patients with aneurysmal subarachnoid haemorrhage undergoing surgical clipping: a randomised, double-blind, placebo-controlled phase 3 trial (CONSCIOUS-2). Lancet Neurol. 2011;10:618–25.
67. Helbok R, Kurtz P, Schmidt MJ, et al. Effects of the neurological wake-up test on clinical examination, intracranial pressure, brain metabolism and brain tissue oxygenation in severely brain-injured patients. Crit Care. 2012;16:R226.
68. Diringer MN, Bleck TP, Claude Hemphill J, et al. Critical care management of patients following aneurysmal subarachnoid hemorrhage: recommendations from the Neurocritical Care Society's Multidisciplinary Consensus Conference. Neurocrit Care. 2011;15:211–40.
69. Gathier CS, van den Bergh WM, van der Jagt M, Verweij BH, Dankbaar JW, Müller MC, Oldenbeuving AW, GJE R, AJC S, HIMALAIA Study Group. Induced hypertension for delayed cerebral ischemia after aneurysmal subarachnoid hemorrhage: a randomized clinical trial. Stroke. 2018;49:76–83.
70. Engquist H, Lewén A, Hillered L, Ronne-Engström E, Nilsson P, Enblad P, Rostami E. CBF changes and cerebral energy metabolism during hypervolemia, hemodilution, and hypertension therapy in patients with poor-grade subarachnoid hemorrhage. J Neurosurg. 2020;134:1–10.
71. Rass V, Helbok R. How to diagnose delayed cerebral ischaemia and symptomatic vasospasm and prevent cerebral infarction in patients with subarachnoid haemorrhage. Curr Opin Crit Care. 2021;27:103–14.
72. Sánchez-Porras R, Santos E, Schöll M, Kunzmann K, Stock C, Silos H, Unterberg AW, Sakowitz OW. Ketamine modulation of the haemodynamic response to spreading depolarization in the gyrencephalic swine brain. J Cereb Blood Flow Metab. 2017;37:1720–34.
73. Hertle DN, Dreier JP, Woitzik J, et al. Effect of analgesics and sedatives on the occurrence of spreading depolarizations accompanying acute brain injury. Brain. 2012;135:2390–8.
74. Carlson AP, Alchbli A, Hänggi D, Macdonald RL, Shuttleworth CW. Effect of locally delivered nimodipine microparticles on spreading depolarization in aneurysmal subarachnoid hemorrhage. Neurocrit Care. 2020;34(1):345–9. https://doi.org/10.1007/s12028-020-00935-1.
75. Golub D, Yanai A, Darzi K, Papadopoulos J, Kaufman B. Potential consequences of high-dose infusion of ketamine for refractory status epilepticus: case reports and systematic literature review. Anaesth Intensive Care. 2018;46:516–28.

Chapter 8
State of the Art and Advances in Peripheral Nerve Surgery

Javier Robla-Costales, Carlos Rodríguez-Aceves, Fernando Martínez-Benia, and Mariano Socolovsky

Abbreviations

BNB	Blood nerve barrier
CN	Compressive neuropathies
CT	Connective tissue
EDS	Electrodiagnostic studies
EMG	Electromyography
MRI	Magnetic resonance imaging
NCS	Nerve conduction studies
PN	Peripheral nerve
US	Ultrasonogram

J. Robla-Costales
Department of Neurosurgery, Hospital de León, León, Spain

C. Rodríguez-Aceves
Neurological Center, The American British Cowdray Medical Center campus Santa Fe, Mexico City, Mexico

F. Martínez-Benia
Department of Neurosurgery, Hospital de Clínicas, Universidad de la República, Montevideo, Uruguay

M. Socolovsky (✉)
Department of Neurosurgery, Hospital de Clínicas, Universidad de Buenos Aires, Buenos Aires, Argentina

C. Di Rocco (ed.), *Advances and Technical Standards in Neurosurgery*, Advances and Technical Standards in Neurosurgery 45,
https://doi.org/10.1007/978-3-030-99166-1_8

8.1 Part I: Traumatic Lesions

8.1.1 Introduction

Traumatic peripheral nerves injury is a complication that affects around 3–10% of patients who suffer a polytrauma [1–3]. These traumatic injuries primarily affect young adults and they are a major cause of physical and occupational disability.

In some cases, the injured nerves regain their function spontaneously, but in others surgery is the only option that allows their functional recovery or the relief of neuropathic pain secondary to the injury. Proper management of these injuries can, in many cases, restore the lost function of the injured nerve.

The indication for a surgical treatment in patients with a peripheral nerve injury depends on several variables, including the mechanism and severity of the injury, the findings in the clinical examination, the intensity of the neuropathic pain, and the interval between injury and treatment [1–4]. This last variable, also known as the surgical timing, is one of the most important factors that influences obtaining a good result after the surgical repair [5–7]. Knowing the right moment for performing a nerve repair surgery will allow us to avoid unnecessary surgeries in cases in which a spontaneous recovery can be expected and, in other cases, to avoid a delay in the treatment, which could reduce the chances of success due to long-lasting muscular atrophy [8, 9].

8.1.2 Classification of Peripheral Nerve Injuries

Peripheral nerves can suffer different degrees of injury that has been classically divided by Seddon's classification into three types: neurapraxia, axonotmesis, and neurotmesis [4].

This classification, described by Herbert Seddon in 1943 [10, 11], is still the most widely used since it allows us to, based on the pathophysiology of a nerve injury, establish a possible prognosis and an appropriate management [12] (Fig. 8.1).

Neurapraxia represents according to this classification the mildest type of peripheral nerve injury, defined as a local nerve conduction block without axonal involvement and, therefore, without distal Wallerian degeneration. It occurs due to a mild segmental demyelination of the nerve. Larger nerve fibers in the nerve are affected in a greater degree than small fibers, leading to a greater motor function involvement and to some degree of fine tactile hypoesthesia while thermo-analgesic sensibility is usually preserved. The prognosis of these lesions is excellent since distal axonal degeneration does not occur. The function of the injured nerve recovers quickly, usually in the first 2 weeks. The nerve transmission blockage disappears through the remyelination of the nerve [4]. Since there is no direct axonal injury, there will be no axonal regeneration and, therefore, no Tinel's sign advancing distally through the nerve path will be observed [13]. This type of injury is common in

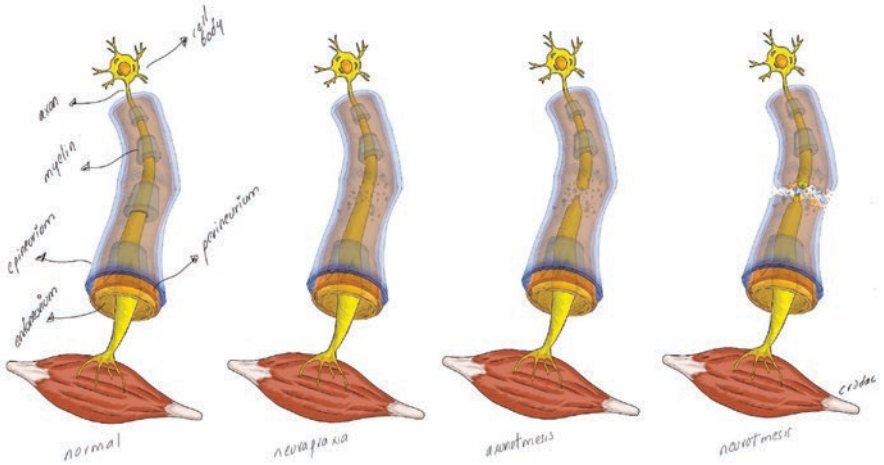

Fig. 8.1 Types of nerve injuries according to Seddon. (Illustration by Crodac (Rodríguez-Aceves CA))

nerve palsies associated to tourniquet nerve compressions or other acute focal compressions (e.g., radial nerve palsy called "Saturday night palsy").

Axonotmesis, the second degree of injury, occurs when the trauma produces a loss of axonal continuity, but the nerve structure remains preserved, including the endoneurium that surrounds each axon [14]. So, axonotmesis is a specific lesion of the axon, always associated with Wallerian degeneration distal to the injury site. The preservation of the connective tissue covers (epineurium, perineurium, and endoneurium) guarantees the correct guidance of the regenerating axons from the point of injury to the end of the nerve fibers. The axon growth rate is around 1–1.5 mm/day [10, 13, 15]. Although the damage is of a greater degree than in neurapraxia, spontaneous recovery is also possible, yet requires a longer period of time than in neurapraxia. This period of time varies from several weeks to months (up to 6). When there is axonal regeneration in this type of injury, we can assess the nerve regeneration over time with the progress of a Tinel's sign along the path of the nerve [13].

In neurotmesis, in addition to the loss of axonal continuity and the internal nerve connective tissue structure, there is a rupture of the epineurium and therefore a loss of macroscopic continuity of the nerves, which prevents spontaneous regeneration. Neurotmesis represents the maximum nerve injury degree, associated to a complete section of the nerve, with loss of its function and the absence of any type of spontaneous recovery. The correct identification of this type of injury is the main objective since it requires prompt surgical treatment in all cases [4]. Neurotmesis is characteristic of penetrating injuries with sharp objects, although it is also associated to severe traction injuries in which nerve avulsion occurs.

Both in axonotmesis and in neurotmesis, Wallerian degeneration of the axon occurs in the segment of the nerve distal to the injury site. Shortly after injury to the

nerve and secondary denervation of the muscle, the degeneration of the muscle fibers begins; 18–24 months after the nerve injury, muscle fibers are replaced by connective tissue and fat, which makes the muscle progressively refractory to reinnervation if it occurs [4]. As mentioned above, this fact emphasizes that nerve surgery, when correctly indicated, must be performed as soon as possible [9].

Later, in 1951, Sunderland expanded the classification system by adding two more degrees of injury to the three described by Seddon [16]. The third and fourth degrees of Sunderland's classification are subtypes of the original Seddon's axonotmesis and neurotmesis. The third degree of Sunderland classification is a mixed injury of the axon and the endoneurium, which carries a recovery similar to an axonotmetic injury (Sunderland grade 2), but it is not complete in this case, since some axons are not able to cross the site of the injury. So, if in the time of evolution necessary to recover the nerve function ad integrum in an axonotmesis-type lesion (1–1.5 mm/day) we observe an incomplete recovery, we will classify the injury as Sunderland grade 3 [13]. A progressive advancement of Tinel's sign along the nerve will be seen, but not a complete recovery of the nerve function.

The fourth degree is similar to neurotmesis, but the appearance of the nerve in this case is in continuity, since both severed ends of the nerve are joined by scarred connective tissue. So, even if the nerve is in anatomical continuity, axonal regeneration through the injury site will definitely not occur and thus nerve function will not spontaneously recover, similar to what happens in a Sunderland grade 5 lesion (neurotmesis) [13]. A positive Tinel sign at the level of the nerve injury site will be present, but we will not observe its progress through the path of the nerve in periodic reviews since axonal regeneration will be blocked at the functional section site by scar tissue. This type of injury is frequently observed in severe nerve injuries due to traction and crush, in thermal injuries by cauterization, and in iatrogenic injuries due to injection of chemical substances [13].

In clinical practice, differentiate between second and third Sunderland degrees is difficult before the sixth month (i.e., complete recovery does not always occur before that time) and the differentiation between fourth and fifth degrees is frequently made during surgical exploration, which is actually of little value from the point of view of managing the injury. The use of ultrasound and MRI neurography might help differentiate grades 4 and 5, but in practical terms, both needs surgical repair. In other words, although the Sunderland classification is more precise than Seddon classification, in the clinical practice it is less used because it adds complexity without practical utility in the management of traumatic nerve injuries.

In 1988, Mackinnon and Dellon established a sixth degree of injury, which was defined as a mixed nerve injury, in which several or all five degrees of Sunderland nerve injury coexist variably within the same nerve injury [17]. We will observe a complete recovery of the fascicles function with a Sunderland grade 1 and 2 injury, a partial recovery in fascicles with a grade 3 injury, and we will not observe any type of recovery of the fascicles with grade 4 and 5 injury (Table 8.1). These types of injuries will benefit performing an internal neurolysis of the nerve and reconstructing the fascicles affected by a Sunderland's grade 4 and 5 injury. Again, this grade

Table 8.1 Classification of the types of nerve injury according to Seddon and Sunderland

Seddon	Sunderland	Grade of recovery	Time of recovery	Surgery
Neurapraxia	I	Complete	Few days to 3 months	–
Axonotmesis	II	Complete	1–1.5 mm/day (few weeks to 6 months)	–
	III	Partial	1–1.5 mm/day (few weeks to 6 months)	+/–
Neurotmesis	IV (neuroma in continuity)	None	–	+
	V	None	–	+

Recovery prognosis and surgical management

of injury added by Mackinnon and Dellon broadens the Seddon and Sunderland classifications, but does not imply a different attitude in the clinical management of traumatic peripheral nerve injuries. The three degrees classification described by Seddon allows justifying an initial expectant management in most of the closed nerve injuries, awaiting the characteristic spontaneous recovery of neurapraxia and axonotmesis [18]. In the event that spontaneous recovery does not occur, the injury is interpreted as neurotmesis, and exploration and surgical reconstruction is indicated. Of course, these types of generalizations are dangerous: a case-by-case management warrants a better diagnosis of the type of injury, and therefore, upon performing a correct management, we can obtain the best possible result in each case.

An additional tool that we have when determining the type of nerve injury is electromyography (EMG). The neurophysiological study should always be carried out from the third or fourth week before the trauma, because the axonal degeneration occurs up to 2–3 weeks after the nerve injury. Conducting neurophysiological studies before this time can lead to false results, confusing the management of the lesion [1, 9].

Fibrillation potentials, as a consequence of spontaneous muscle fibers contraction, are characteristic when the continuity between the motor axon and the muscle fiber has been interrupted. Therefore, usually starting the third week after the injury, in the EMG at muscular rest, a fibrillation tracing in all the degrees of nerve injury except in grade I or neurapraxia is detected. Even more important in determining the type of nerve injury are the motor unit potentials (MUP), which consist of the sum of different action potentials of muscle fiber groups that are contracting almost synchronously. These potentials are obtained by weakly contracting the scanned muscle. The appearance of motor unit potentials from the 10th to 12th week after a nerve injury is a sign of reinnervation, and it will help differentiating injuries with potential for spontaneous recovery (axonotmesis, Sunderland grade 2 and 3) and those that will not have spontaneous recovery (neurotmesis, Sunderland grade 4 and 5). MUPs are a very important tool to evaluate reinnervation since their presence indicates reinnervation even before voluntary movement is appreciated (Table 8.2).

Table 8.2 Injured nerve structures in each grade of the Sunderland classification

	Nerve injury					EMG			
Grade	Myelin	Axon	Endon	Perin	Epin	FIB	MUP	Tinel	Tinel progress
I	+/−					−	N	−	−
II	+	+				+	+	+	+
III	+	+	+			+	+	+	+
IV	+	+	+	+		+	−	+	−
V	+	+	+	+	+	+	−	+	−
VI						+/−	+/−	+	+/−

Findings in electromyography. Tinel's sign and progress of tinel's sign along the path of the injured nerve
ENDON endoneurium, *PERIN* perineurium, *EPIN* epineurium, *EMG* electromyography, *FIB* fibrillations, *MUP* motor unit potentials

8.1.3 Management of Open and Closed Injuries

Traumatic peripheral nerve injuries can be classified as open or closed, depending on whether the skin integrity has been disrupted or not during the original trauma. This concept is essential in traumatic nerve injuries, as it determines the management (Fig. 8.2).

Closed injuries are more frequently associated with lesions in continuity, in which the nerve is not sectioned and neurapraxia and axonotmesis are the main types of injury [19]. Therefore, spontaneous recovery is possible in these injuries and surgery will be indicated in general if no improvement is observed 3 months after the trauma. This waiting period until deciding whether to perform surgery or not is determined based on axonal growth (1–3 mm/day) and on the findings that can suggest reinnervation in the clinical, neurophysiological, and imagenological examination [1].

Conversely, open lesions in relation to the course of a nerve are more frequently associated with neurotmesis-type nerve lesions, in which the capacity for spontaneous recovery is nil. This type of injuries requires an early exploration and nerve reparation [20]. But: how early the surgery should be indicated?

8.1.4 Open Injuries: Clean Section Versus Blunt Nerve Ends

The anatomical type of nerve lesion determines the intraoperative election of a determined surgical reconstruction strategy (Fig. 8.3). As mentioned before, an open wound in an extremity with an impaired peripheral nerve function should prompt us to do an acute nerve exploration and repair before closing the wound [21]. But there are a number of factors that will determine the suitability of performing a primary repair or wait to do a secondary repair. We must assess the type of nerve injury, the type of wound, and if there is an adequate vascularization in the

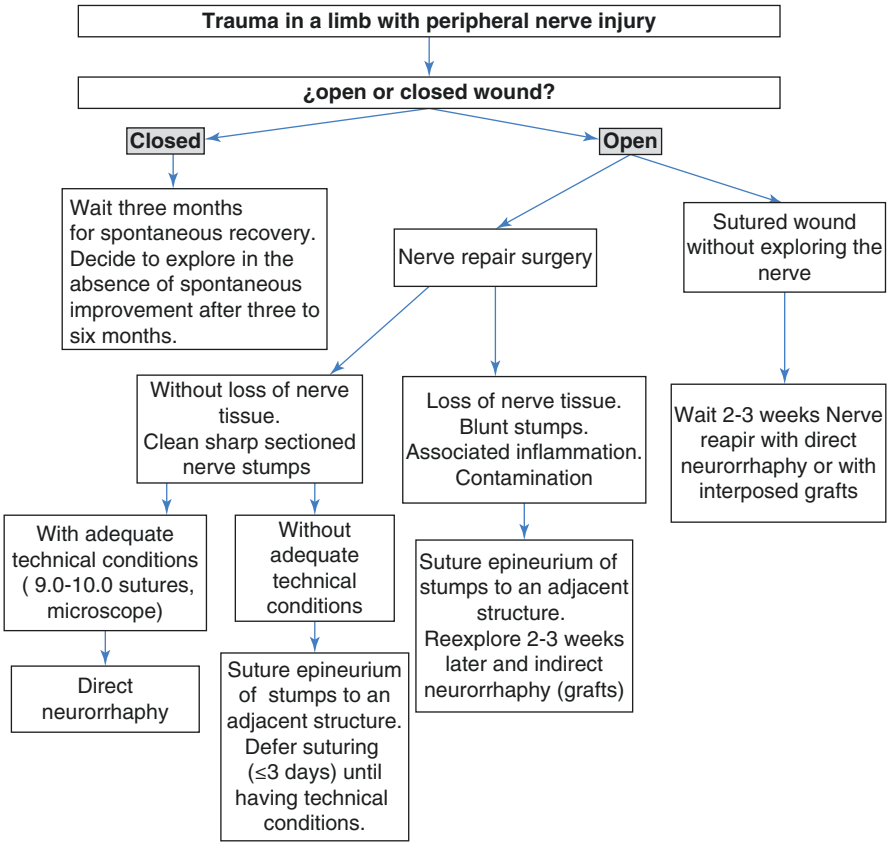

Fig. 8.2 Management of traumatic peripheral nerve injuries

surgical area. The appearance of the nerve stumps during the exploration of an open injury is the main factor in the decision to perform an acute primary repair or a secondary repair [19, 20]. We can differentiate between two different scenarios: sharp sectioned nerve stumps without associated inflammation or contused blunt stumps with an inhomogeneous appearance and significant inflammation.

8.1.4.1 Clean Section

If the nerve injury is a clean section from a sharp object, immediate repair should be performed by direct end-to-end neurorrhaphy. The clean section of a nerve allows for a correct coaptation of the stumps and a suture without tension [20]. The repair should be performed by a surgeon adequately trained in peripheral nerve surgery, using microsurgical technique [22, 23]. When lacking the appropriate ecquipment [24] (microsurgical instruments, 9.0 or 10.0 suture, and microscope), or training,

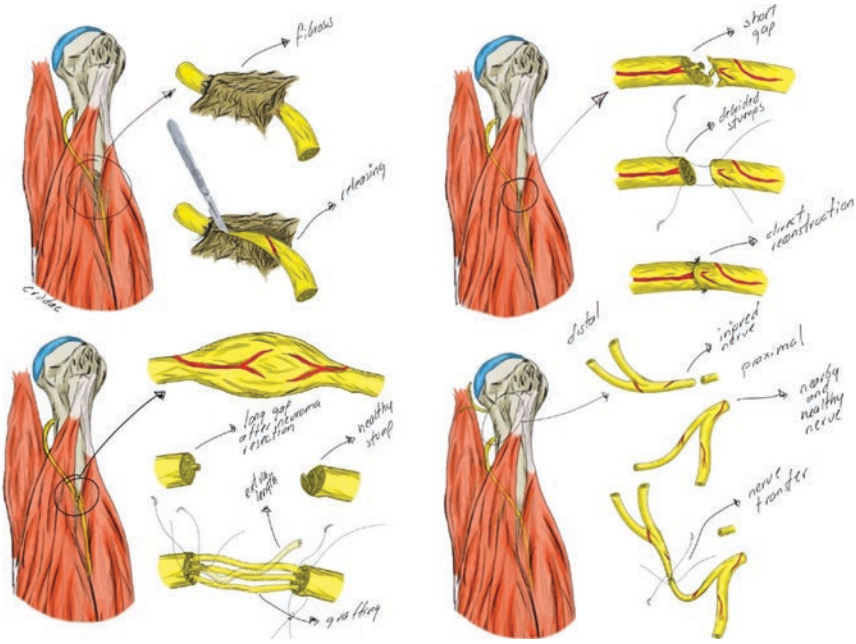

Fig. 8.3 Different strategies of nerve reconstruction. (Illustration by Crodac (Rodríguez-Aceves CA))

the repair should be deferred: any attempt to perform a nerve suture that is not performed correctly will lead to unnecessary trauma to the nerve ends, increasing the fibrosis at the suture site, and therefore worsening the long-term results [25]. In these cases, in which a direct neurorrhaphy can't be performed adequately, it is preferable to wait and carry out a good repair than to do it in poor conditions at the acute moment.

The term primary nerve repair is applied when the surgery is performed within the first week after the section. Undoubtedly, the optimal repair is the one performed just after the traumatic section, but it has been reported that nerve repair by direct neurorrhaphy between 5–7 days after section (delayed primary repair) has functional results equivalent to a primary repair in the acute phase [21, 26].

A repeated situation in clinical practice is the outpatient evaluation of a patient who has undergone a nerve repair in the emergency service without the correct microsurgical technique-or perhaps with a doubtful reparation-, who has no signs of recovery of strength or sensibility after 6 or 8 months. At this point, it prevails the doubt whether the elapsed time from repair since repair is not enough, or the failure is due to an unsuccessful suture itself. This doubt will often result in delaying the reexploration of the nerve, which leads to a greater muscle atrophy and worse final results. Alternatively, an imagenological study with MRI-neurography or ultrasound can help the treating physician to decide whether to explore or wait for spontaneous recovery.

As we have mentioned previously, it is important to consider not only if the nerve section is clean, as other important factors need to be considered. The wound should be acceptably clean, without excessive contamination (especially organic), and the adjacent tissues should not be severely damaged. If these features are present, a primary repair is not recommended. In these cases, it is better to suture the epineurium of each nerve stump to an adjacent structure (tendon, fascia, etc.) to avoid excessive retraction of the nerve ends and facilitate their identification at the time of a secondary repair [1, 22]. At 3 weeks after section, as we will discuss later, or when the wound allows it, the nerve will be reexplored and repaired using the adequate technique (direct neurorrhaphy or graft, according to what is indicated) [21].

8.1.4.2 Blunt Nerve Ends

If during a nerve exploration blunt and contused nerve ends are noticed, a primary repair should not be done, since the inflammatory process that occurs at the nerve ends may last up to 3 weeks [19]. Therefore, we must wait at least 3 weeks to carry out the secondary repair. If the nerve repair is carried out before this period of time, there is a risk that fibrosis normally occurring during the nerve stump healing process will prevent the passage of the regenerating axons [7, 19]. At 3 weeks-at the secondary repair-successive cuts in both nerves ends have to be done to remove the inflammatory tissue and the fibrosis that has been developed until healthy fascicles are identified. This differentiation between tissues is easy at that step, as fibrosis is whitish, hard, and has scarce bleeding [7, 25].

8.1.5 Towards a Consensus in the Management of Open Injuries

In the usual practice in many centers, deep wounds at the extremities are managed by just cleaning and closing the planes of the wound, without exploring the nerves neither repairing them. The patient usually comes to the consultation with a deficit established without any type of improvement and with a completely healed cutting wound of weeks or months of evolution. There is currently a consensus in the literature in the sense of not excessively deferring exploration and reconstruction nerve surgery in open wounds, since most of them are associated with a section of the nerve (neurotmesis).

The ideal time for the repair of this type of open lesions, already closed and healed, is around 1 month after the trauma, long enough to be sure that the proximal and distal stumps are not inflamed and it is possible to perform an end-to-end or interposed graft repair, according to what's indicated [25].

In conclusion, with regard to open wounds with nerve involvement, we can establish that the best management is an early exploration and direct repair with

adequate microsurgical technique in cases where the circumstances previously described allow this strategy. If there is loss of nerve substance, blunt ends or any of the conditions that contraindicate a primary repair (contaminated wound, heavily damaged tissues), repair with, or without graft will be deferred for 3 weeks. Likewise, if the wound was not explored in acute, or if the adequate elements to repair the nerve were not available at that time, we should also perform the surgery 3 weeks after the trauma, or as soon as possible in case this interval of time cannot be accomplished.

8.1.6 Exceptions in the Treatment of Open Injuries

Wounds from a firearm projectile, although they are penetrating, will be considered closed since there is no opening and tissue exposure, and the injury they generate is usually thermal due to the high kinetic energy of the projectile. This type of injury usually spontaneously recovers in many cases, at least partially. This occurs because the projectile generally does not pass through the nerve, but indirectly heats or traumatizes it. The continuity of the nerve will be preserved, causing neurapraxia or more frequently axonotmesis [27–29]. Therefore, nerve surgery for gunshot wounds should be performed when necessary, starting at the third or fourth month after the injury [29].

8.1.7 Closed Injuries

As we have previously mentioned, closed lesions are more frequently associated with nerve injuries in continuity, in which the nerve is not sectioned and neurapraxia or axonotmesis are the fundamental types of lesion. Therefore, a delayed management is the general rule in closed nerve injuries: there is practically no indication for acute primary examination (some exceptions will be mentioned later). The observation period is usually 3 months, time during which the patient and his deficit must be closely monitored through serial clinical examination and electromyograms. Starting 3 weeks after the injury, and according to the clinical evolution, the EMG may be repeated every 1 or 2 months. Three months after the injury, if no sensory or motor improvement is proved, surgery will be indicated.

As mentioned before, when this type of lesions is explored, in many cases a neuroma in continuity is observed. In these cases, neurophysiological intraoperative monitoring with Nerve Action Potentials (NAPs) acquires important relevance [30], since they allow to determine if there is a block of conduction across the site of the nerve injury and therefore the injured portion should be removed and replaced by a graft. On the other side, if a nerve action potential can be elicited through the lesion, it will be enough to perform an external-plus more rarely an internal-neurolysis [1, 31, 32].

If the nerve function improvement occurs spontaneously after 3 months, but it is not sustained over time or if it is partial at 6 months, the nerve should also be explored. In these cases, in which there is partial recovery of function, neurolysis is usually sufficient as surgical treatment, and NAPs are not as important as mentioned above in determining the intraoperative procedure; in these cases, the necessity of cutting the nerve and replacing it with a graft is practically ruled out because, at least partially, the impulse is conducted through the site of the injury, which explains the clinical improvement of the patient before surgery. Likewise, the possibility of just a partial lesion, and an internal neurolysis under the microscope, with a graft repair of just the most severely injured part of the nerve should be done.

8.1.8 Exceptions in the Treatment of Closed Injuries

As it was mentioned in the precedent part, there are certain situations in which closed nerve injuries are explored before the 3–6 months waiting period has elapsed, and early surgical exploration is warranted. Actually, three different clinical situations meet the requirements.

The first one is when an injured nerve is in the same area where surgery will be performed for another cause. An example is when urgent vascular surgery has to be done in order to repair an artery or vein adjacent to a nerve [33]. Another frequent case is when traumatology must perform an open bone reduction, for example placing a plate in the humerus exposing the radial nerve during the approach [34, 35]. Although the nerve injuries associated with long bone fractures are generally of the neurapraxia or axonotmesis type, in some cases the nerve may be sectioned. In both cases, a surgeon experienced in nerve injuries should be present at the time of the surgery, which will avoid undergoing a second later surgery to repair the severed or compressed nerve.

The second situation in which a delayed exploration of a closed nerve lesion should not be done is when the affected nerve is in a noncompliant compartment of a limb and may be affected by the compression associated to edema. For example, a median nerve acutely trapped in the anterior compartment of the forearm or a peroneal nerve at the head of the fibula is a rare situation that requires a careful diagnosis of the cause of compression and an acute decompressive surgery can be indicated.

The third situation when a prolonged conservative strategy is not recommended is in the case of a patient suffering from severe neuropathic pain that does not respond to maximal doses of antineuritic medication (Gabapentin, Amitriptyline, etc.). The typical injury-but not the only one-associated to this clinical picture are bullet wounds affecting the nerves. A good neurolysis is generally enough to solve the pain, yet in some serious injuries a neurorrhaphy is needed.

Outside of these three situations described before, one must wait at least 3–6 months to explore a closed traumatic injury of a peripheral nerve.

8.1.9 Conclusions of Part I

Peripheral nerve injuries suppose a functional deficit of the affected limb that can be treated and recovered appropriately. The moment in which the surgery is performed and the employed microsurgical reconstruction technique are the most important factors in the final result. Open lesions with associated nerve injury should be managed with an early exploration carried out before 7 days. Closed injuries are usually deferred, with few exceptions, from 3 to 6 months after the trauma.

A frequently observed fact in the clinical practice is the late evaluation of nerve injuries, which leads to worse surgical and functional results than they could have and to permanent sequelae. The management of a traumatic injured nerve should be referred quickly to those who are accustomed to treat this type of injuries. This will result in better functional results.

8.2 Part 2: Compressive Neuropathies

8.2.1 Introduction

Compressive neuropathies (CN) refer to a group of pathological conditions that are characterized by a chronic nerve injury resulting from different degrees of "sustained and segmental pressure-induced" neuropathy that manifests with pain and sensory or motor disturbances in the cutaneous distribution or muscles innervated by the affected nerve; even when nerves carry mixed fibers, autonomic dysfunction is uncommon [36, 37].

We must distinguish chronic compressions from acute compressions, the latter being a prolonged period of pressure resulting from a single traumatic episode, as in crush injuries. In contrast, CN are neurodegenerative changes that occur over time [38, 39].

Entrapments of upper and lower limbs are frequent in primary care or specialized consultation, with an estimated prevalence of 3.3%, being the compression of median nerve at carpal tunnel, the most common in the human being, followed by entrapment of ulnar nerve and common peroneal nerve at the elbow and knee, respectively [39–43]. However, several entrapment neuropathies exist currently, including nerves of the head, trunk and extremities, named according to the involved nerve, the anatomical region, the motion producing the compression, or the name of the describing authors [37]. In fact, CN are the most common entity in Peripheral Nerve Surgery's daily practice.

Although the development of this condition relates to narrow anatomical spaces, the etiology is wide, and therefore, any people may be affected. Nevertheless, associations with external and internal factors should be considered, which relay on general health status, comorbidities, family history, traumatisms, anatomical variations, and repetitive activities, as in sports or occupations. For this reason, we

observe that some syndromes occur more frequently in women than in men, and inversely.

Clinical manifestations can range from diffuse pain to well-established sensory or motor deficits in a specific nerve distribution, thus misdiagnosis is not uncommon and frequently confused with polyneuropathies, other pain syndromes, musculoskeletal, spine and brain disorders, and also interpreted as psychiatric illness. For that reason, a complete patient history, physical examination, and complementary electrodiagnostic studies (EDS) or imaging studies, if are necessary, should be part of the physician armamentarium for diagnosis. Namely, a proper diagnosis and a timely treatment will reduce the possibilities of irreversible damage to the affected nerve, evading devastating clinical consequences.

8.2.2 Microanatomical and Physiological Considerations

The classic descriptions of peripheral nerve (PN) anatomy focus on a characterization of the arrangement of connective tissue (CT) and the nervous components. Understanding the pathophysiology of PN chronic compression requires a more detailed knowledge of the whole PN as a system, described less frequently.

Four very different layers of CT constitute a peripheral nerve: (1) the *endoneurium*, which surrounds individually each axon/Schwann cell (in unmyelinated fibers) and axon/myelin (in myelinated fibers); (2), the *perineurium* that surrounds a fascicle that is a group of axons; (3) the epineurium that forms the nerve trunk itself, and (4) the *mesoneurium* which is the outermost layer composed by loose areolar tissue located between the nerve trunk and the neighboring tissues [13, 44–48]. The first three CT coverages play a fundamental role in normal PN, functioning as scaffold, and providing strength, elasticity, nutrition, maintenance of internal environment, and serving as a diffusion barrier. By contrast, the mesoneurium acts as a gliding tissue during limbs' movements. Besides, a repetitive pattern arrangement in the perineurium and endoneurium forming transverse and oblique bands along the peripheral nerve bands called *spiral bands of Fontana* gives to the nerve trunk the ability to stretch and recover its normal length when it is subjected to stress without suffering damage. Thus, mesoneurium and the spiral bands of Fontana enable nerve trunk excursion or gliding [49–51]. Besides these properties, CT/neural tissue ratio changes along the path of all PN. When a nerve lies superficially, passes near a joint or within areas of greater tension, the number of fascicles increases and CT layers thicken, providing protection against stretching or compression forces [45, 49].

An external and internal vascular system characterized by a dense branching anastomotic network of vessels in all layers of CT, and also by a system of larger endoneurial capillaries, delivers blood supply to the PN [45, 46]. These features allow the PN to tolerate episodes of ischemia for an unusual time, in comparison with the rest of the neurological tissue. However, this peculiarity does not protect PN to external chronic pressure [46, 49, 52, 53].

The association between perineurial myofibroblasts and tight junctions of endoneurial capillaries (endothelial cells) forms the blood-nerve barrier (BNB), which maintains the endoneurial microenvironment isolated from the rest of the nerve, serving as a semipermeable diffusion barrier and protecting the fascicles. When BNB disrupts, it loses its gate function, and in the absence of true endoneurial lymphatic vessels, endoneurial milieu is compromised by edema and endoneurial microcirculation impairment [45, 52–58].

The continuous supply of oxygen provided by the efficient vascular system and the integrity of BNB enables the proper neuronal functioning for normal impulse transmission and the energy-dependent axonal transport of necessary elements. There are identified two types of axonal transport: (1) anterograde transport for supplying distal axon with neurotransmitters, structural proteins, and lipids to maintain presynaptic activity, and (2) retrograde transport to maintain homeostasis by degradation and recycling of elements, and neurotrophic signaling. In fact, compression on nerve fiber affects the normal axonal transport [52, 59, 60].

8.2.3 Pathophysiology

As we described before, acute and chronic nerve compressions should be distinguished. The former shows axonal damage and pathologic changes that spread to neuromuscular junction and target organs [38]. By contrast, chronic nerve compression is independent of axonal damage, although in later stages, axonal degeneration and degeneration of distal targets are present. Proliferation of Schwann cells and demyelination and re-myelination are the leading findings in this type of nerve injury [38]. In any case, PN structural changes in chronic compression settle slowly and relate directly with the degree and duration of the compression: thus, these histopathologic changes correlate with the clinical evolution, physical examination, and electrodiagnostic and imaging findings during patient evaluation.

Initial stages after applying a sustained compression are characterized by a reduced epineurial venular blood flow and an inhibition of the axonal transport, followed by cessation of intraneural blood flow. Besides these changes, with a more prolonged compression, disruption of BNB is present, developing edema, followed by proliferation of inflammatory cells that leads to fibrosis and scar formation in all nerve compartments, increasing the pressure in the endoneurial compartment in late stages. If the compression persists, local and then diffuse demyelination may develop with subsequent conduction block. At a final stage, Wallerian degeneration appears. Associated thickening of connective tissue layers and loss of spiral bands of Fontana decrease the gliding capacity of the nerve trunk, increasing the tension on nerve fibers during excursion and worsening the nerve function with repetitive movements setting up a vicious circle, as exposed by Lundborg [13, 38, 49, 52–55, 61–64].

In summary, mechanical and ischemic factors both contribute to peripheral nerve injury in chronic compression syndromes by microstructural changes and reduction

of flexibility and mobility, injuring first the peripheral and larger nerve fibers, which are more vulnerable to the effects of compression, mediated by an increased mechanosensitivity induced by inhibition of axonal transport [65–69]. If a parallel to nerve trauma is traced, normally nerve compressions categorize either as grade I (neurapraxia) or grade II (axonotmesis), yet very severe injuries might behave like as a grade V (neurotmesis) injury.

8.2.4 Etiology

Even though the main predisposing factor for nerve compression is the passage of the affected nerve through a well-identified narrow anatomical region, several internal and external causes, which can work separately or in concert, contribute to the development of injury. We must understand this condition as the result of an interaction of static and dynamic processes [37, 68]. Several generic names have been given to these anatomical narrow spaces. For the purposes of this review, they will be referred as "tunnels".

Apart from occupational factors (related to work, sports, activities, etc.), the external and internal factors may be categorized as follows: (1) external factors that increase the volume within the tunnel on either side of the nerve (e.g., obesity); (2) intrinsic factors that increase the volume within the tunnel (e.g., tumors); (3) extrinsic factors that alter the contour of the tunnel (e.g., fractures); and (4) intrinsic neuropathic factors (e.g., diabetes) [70] (Table 8.3).

Table 8.3 Etiologies of peripheral nerve entrapments

Category	Agent
Idiopathic	Apparent spontaneous origin or unknown origin
External and internal factors	
Acquired	Postural, occupational, repetitive trauma, footwear, tight clothes, edema, heart failure, renal failure, musculoskeletal conditions, etc.
Degenerative	Connective tissue disease, osteophyte, etc.
Congenital	Accessory ribs, muscles, fibrous bands, narrow shapes, hypermobility, deformity, etc.
Trauma	Fracture, dislocation, sprain, hematoma, direct injury
Vascular	Aneurysm, arterio-venous malformation
Inflammatory	Viral infection, bacterial infection, vasculitis, etc.
Autoimmune	Arthritis, osteoarthritis, rheumatoid arthritis, other rheumatic disease
Metabolic	Diabetes, hypothyroidism, drugs, intoxications, etc.
Iatrogenic	Surgery, casting, manipulation, anesthetic position
Tumor	Extrinsic tumors (soft tissue tumor, hematologic neoplasm, lymphoproliferative, cyst, neighboring tumors of any lineage), intrinsic tumors (schwannoma, hemangioma, etc.)
Hormonal	Pregnancy, acromegaly, etc.

Static process relates with the anatomical shape of osteofibrous, fibro-muscular, or muscular-tendinous passages which act as a tunnel with null or reduced capacity to expand its boundaries due to the rigidity of its components. As expected, a drastic change in space to alter function is unnecessary (Fig. 8.4). In opposition, dynamic processes are related to friction, stretching, or constriction of the nerve during joint mobility, muscular contraction, or even nerve mobility itself in the presence of fibrosis with reduced excursion (Fig. 8.5) [37, 68].

Considering these concepts, it will be easier to understand the trigger factors in the development of certain nerve compression syndromes. For instance, in Pronator Teres syndrome (compression of the proximal median nerve in the forearm), there is a dynamic muscular compression as the main cause of the compression. By distinction, in a nerve compression due to a metabolic disease like mucopolysaccharidosis, surgical decompression probably will not relieve the symptoms. Thus, having

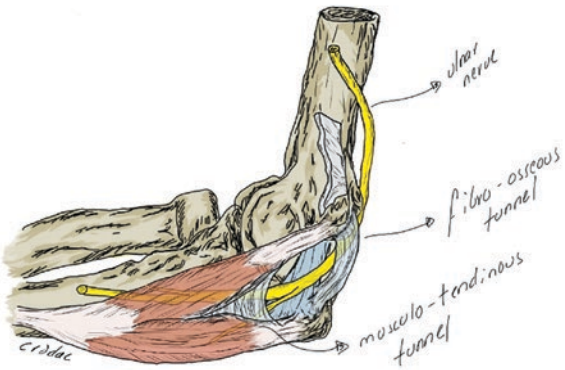

Fig. 8.4 Static representation of a nerve compression. (Illustration by Crodac (Rodríguez-Aceves CA))

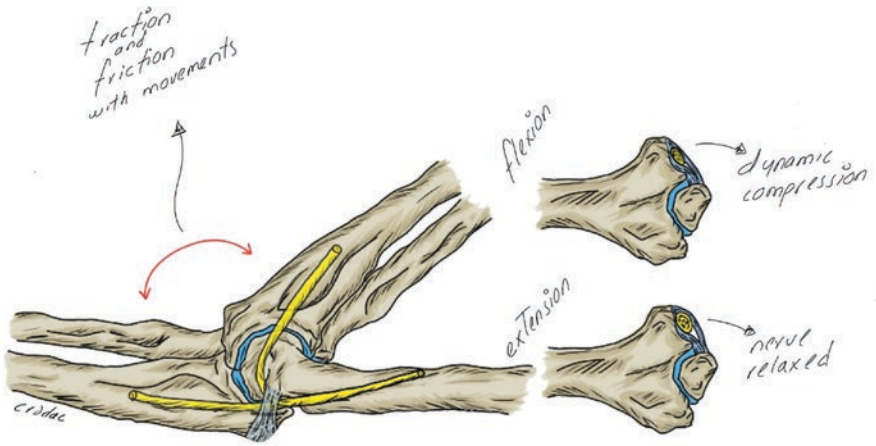

Fig. 8.5 Dynamic representation of a nerve compression. (Illustration by Crodac (Rodríguez-Aceves CA))

a clear identification of the precipitating or responsible factor is imperative for a proper management in NC syndromes.

8.2.5 Diagnosis

Chronic nerve compression may cause insidiously and slowly progressive symptoms, ranging from mild discomfort to localized pain over the site of entrapment, or diffused pain with proximal and distal radiation, alone or in association with sensory and motor disturbances in the distribution of the affected nerve. These clinical manifestations are related with the pathophysiological underlying process and physical examination findings, so that it is possible to stage clinically the severity of illness as shown in Table 8.4 [52, 53, 68, 71, 72].

8.2.5.1 Clinical Assessment

The primary tools for a correct diagnosis are a detailed clinical history and physical examination. EDS, an imaging study, can be helpful additional tools to confirm the diagnosis. It is essential to distinguish peripheral nerve entrapments from other neurologic entities such as plexopathy, radiculopathy, myelopathy, other central and peripheral nervous system, and musculoskeletal disorders. A perfect knowledge of anatomy and function of each nerve is imperative. Moreover, different predictable constellations of specific symptoms and signs exist even in compressions within the same nerve because of its different and variable branching patterns [39]. Table 8.5 resumes some common and uncommon nerves entrapments found in practice [73–76].

Table 8.4 Clinical staging of compressive neuropathies

	Features		
Stage	Symptoms	Signs	Structural
I (early and mild)	Pain at rest, transient positive sensory symptoms (e.g., paresthesia, tingling), night worsening	Positive provocative tests	Blood flow impairment, blood–nerve barrier disruption
II (subacute and moderate)	Pain worsening, constant positive sensory symptoms, incipient negative sensory symptoms (hypoesthesia), subjective occasional weakness	Threshold tests, paresia, positive tinel's sign	Edema, connective tissue thickening, local and diffuse demyelination
III (late and severe)	Constant pain, anesthesia, pronounced weakness, and autonomic dysfunction*	Abnormal two-point discrimination and sensory evaluation, paralysis and atrophy	Wallerian degeneration

*Autonomic dysfunction is less easy to identify unless severe nerve injury is present

Table 8.5 Common and uncommon nerve entrapments

Nerve	Site	Symptoms
Head and neck		
Greater, lesser and third occipital nerves	Between suboccipital muscles	Chronic headaches in occipital region
Supraorbital and supratrochlear	Frontal paramedian region and supraorbital notch	Chronic headaches in frontal and supraorbital region
Upper limbs		
Median nerve	Carpal tunnel	Pain and paresthesias in 1°–3° digits and radial half of 4°, worst at night. Abductor pollicis brevis weakness and thenar atrophy
	Ligament of struthers Bicipital aponeurosis Pronator teres muscle Sublimis arch	Pain in volar forearm increased with prono-supination. Paresthesias and hypoesthesias in median sensory distribution. Weakness in anterior interosseous nerve supplied muscles
Ulnar nerve	Arcade of struthers Intermuscular septum Cubital tunnel Medial epicondyle Arcade of osborne	Pain and paresthesias in 4°–5° digits, pain or discomfort at medial elbow Blunder and weakness grip Atrophy in first dorsal interosseous and abductor digiti minimi
	Guyon's canal	Pain and paresthesias in 4°–5° digits Clawing and blunder in 4°–5° digits Atrophy in first dorsal interosseous and abductor digiti minimi
Radial nerve	Radial tunnel	Pain in dorsal forearm, worst with elbow extension and prono-supination Weakness in posterior interosseous nerve supplied muscles
Brachial plexus	Thoracic outlet	Pain in shoulder, scapula Numbness and paresthesias in distal distribution of C8-T1, worst with arm elevation
Superficial sensory branch of radial nerve	Between brachioradialis and extensor carpi radialis longus in forearm	Paresthesias in dorsolateral hand, worst with ulnar flexion of wrist and gripping
Intercostal nerves	Vertebral foramen Any site in the course of the nerve	Pain in a part of the corresponding dermatome
Axillary nerve	Quadrangular space	Pain in posterior shoulder Weakness in shoulder abduction Numbness in lateral arm
Suprascapular nerve	Suprascapular notch	Pain in suprascapular area, posterior and lateral shoulder Weakness and atrophy in supraspinatus and infraspinatus
Lower limbs		
Common peroneal nerve	Peroneal tunnel at ankle	Pain and paresthesias in anterolateral leg and dorsal foot Weakness in dorsiflexion, eversion and toes extension

Table 8.5 (continued)

Nerve	Site	Symptoms
Tibial nerve	Tarsal tunnel	Pain and paresthesias in medial ankle, heel, sole and toes Weakness and atrophy in intrinsic muscles
Lateral femoral cutaneous nerve	Inguinal ligament Anterosuperior iliac spine	Pain and paresthesias in anterolateral thigh, worst with activity
Plantar nerves	Metatarsal heads	Pain and paresthesias in involved webspace, worst with activity and relieved with rest
Sciatic nerve	Piriformis muscle	Pain and paresthesias in buttocks and posterior thigh
Femoral nerve	Inguinal ligament Iliacus fascia	Paresthesias in anteromedial thigh and medial leg Weakness in hip flexion and knee extension Atrophy in femoral nerve supplied muscles
Superficial peroneal nerve	Distal third of leg	Pain and paresthesias in lateral leg and foot
Deep peroneal nerve	Anterior tarsal tunnel	Pain and paresthesias in foot, ankle and first web space
Inguinal complex of nerves	Inguinal region Hypogastrium Iliac region	Pain and paresthesias in inguinal region, pubis, proximal anterior and medial thigh and external genitalia
Obturator nerve	Obturator canal at medial thigh	Pain and paresthesias in medial thigh Weakness in thigh adduction and internal rotation
Pudendal nerve	Alcock's canal	Pain and discomfort in perineum, perianal region and genitalia

History and physical exploration require a careful, systematic, and routine approach, usually oriented by the main patient's complaint. The present complex of symptoms, its onset, quality, frequency, distribution, progression, association with certain movements, positions or activities, relief factors, previous treatments for present illness, occupation, dominant hand, recreational activities, past medical history, medications, and family history need questioning [77–80].

A positive Tinel's sign, yet unspecific, involves an abnormal mechanosensitivity of the regenerating nerves, produced by light percussion over a nerve, and it is described as a tingling sensation in a specific anatomic distribution. It is a pure sensory sign, without any value for motor function evaluation [81, 82].

Physical examination should be completed with the evaluation of provocative tests, whose goal is to reproduce the sensory symptoms by two mechanisms: increasing tension on the nerve with stretching, or increasing pressure on the nerve with additional mechanical compression over an enclosed space. Many provocative tests have been described for different sites of entrapment [36, 37, 67, 68, 83, 84]. Like for Tinel's sign, its presence is owing to an abnormal mechanosensitivity and is not specific sign, but forms an integral part of clinical examination [85].

8.2.5.2 Complementary Studies

EDS and imaging studies may help in the diagnostic workup; however, if history and physical examination provide enough information for supporting the diagnosis, no further investigation is needed [76]. That said, electrical and radiologic investigations should never replace the clinical assessment, and on the contrary, should serve as a complementary tool to confirm diagnosis.

EDS comprise of nerve conduction studies (NCS) and electromyography (EMG): both are helpful to establish the localization, severity, timing, and extent of injury in neural elements; hence, they are also helpful to differentiate entrapment neuropathies from other conditions that can mimic their clinical picture.

NCS tests sensory and motor pathways by assessing parameters such as latency, conduction velocity, and amplitude of the generated potentials (sensory nerve action potentials for sensory conduction, and compound motor action potentials for motor conduction). Initial stages of entrapment neuropathies exhibit delayed distal latencies along with slowing in conduction velocity. Also, a conduction block may be present in severe cases due to demyelination. When axonal damage is present, decreased amplitudes or prolonged or absent potentials are observed.

EMG assesses electrical activity within skeletal muscles. The examination uses a single concentric needle electrode introduced into the muscle, where it records four phases of muscular activity (insertion, resting, mild contraction, and maximal contraction) and tests the motor unit potential features. Characteristic neurogenic pattern in CN is only present in severe cases, showing signs of denervation (hyperexcitability, spontaneous activity at resting phase, abnormal motor unit potentials, and decreased interference pattern) [86–89].

While the different techniques included in EDS play an important role in the evaluation of entrapment neuropathies, limitations, pitfalls, and disadvantages exist. For instance: its sensibility and specificity are limited by the clinical setting and nerve location, normal values don't exclude nerve compression, and abnormal values could be misinterpreted as nerve compression in the absence of a thorough clinical evaluation. The EMG is uncomfortable for patients, as well as it is contraindicated in certain circumstances (e.g., coagulopathy, pacemakers, etc.). Finally, EDS studies are operator-dependent.

Radiological assessment may include simple radiographies, computed tomography, magnetic resonance imaging (MRI) neurography, or ultrasonogram (US). The first two techniques may help in visualizing bone or joint abnormalities or demonstrate osseous causes of compression. MRI neurography and US are useful to evaluate peripheral nerve anatomy, nearby tissues, and local pathology with an excellent resolution that allows for the identification of etiologic agents.

Nerves appear in US as oval or rounded shape structures with hypo-echoic signal in fascicles, and hyper-echoic signal in CT, giving the aspect of a "honeycomb" in the transverse axis. Peripheral nerve entrapments may produce changes in shape (flattening in the site of entrapment) or deviation of the involved nerves with fusiform enlargement in the cross-sectional area of nerve trunk proximal to the site of compression, changes in echotexture (hypo-echoic) inside and outside the nerve, increased vascularity and decreased mobility for edema, and perineurial/

endoneurial thickening [90–94]. US evaluation also is a dynamic technique, which enables the evaluation of nerves during motion in real-time, as in ulnar nerve subluxation. From its first description for the evaluation of peripheral nerves in 1988 [95], continuous and fast evolution of technical advances has developed high-resolution transducers with superior capacity to contrast nerve from surrounding tissues and for nerves' inner anatomy identification. It is a low-cost, portable, moderately fast, and versatile modality, but requires a learning curve for an optimal use [96, 97].

MRI scanners with a field strength of 1.5–3 Tesla enable the evaluation of peripheral nerves with multi-sequential and multi-planar and selective and nonselective reconstructions, regardless the anatomical location [92]. The involved site will determine the precise technique and necessary coil. Subtle signal alterations in nerves owing to its high soft tissue contrast can be detected, which also allows a high-resolution evaluation of nearby normal and abnormal tissues. MRI is very sensitive to show collateral damage as denervation changes in muscles. More recently, the acquisition of images based on diffusion-weighted imaging and diffusion tensor imaging techniques enables the evaluation of nerves, not only from a morphological-qualitative aspect, but also from a functional-quantitative point of view [97–100].

The aforementioned advantages are overshadowed by its high cost, time consumption, inability to evaluate multiple sites at once, the magnetic effects on metallic devices, the produced artifacts by some osteosynthesis materials, and the claustrophobic effect that generates in some patients.

The general protocol for morphological MRI includes T1-weighted spin echo and T2-weighted fat-suppression sequences in the axial plane and isovoxel 3D T2-weighted fat-suppression sequence reconstructed in different planes. Axial plane defines better the course of nerve, and T1-weighted sequence delineates with high resolution its internal structure. Normal nerves appear as oval/rounded isointense structures with well-delineated intra-fascicular pattern, surrounded by a rim of hyperintense fat, within muscles' interfacial plane. On T2-weighted fat-suppression sequences, the nerve is isointense or slightly hyperintense in relation with surrounding muscles. Compression may produce enlargement, distortion of fascicular pattern, and increased signal in T2-weighted sequences [99–102].

8.2.6 Treatment

The proper management strategy in CN relay on staging, meaning that, either conservative or surgical, the goal is to ease symptoms by identifying the cause of entrapment and releasing the underlying compression.

8.2.6.1 Conservative Treatment

During the initial steps of a CN, the patient can be managed conservatively, especially if just sensitive symptoms are present. Conservative treatment measures include, among others: (1) treatment, when present, of the systemic conditions

causing compression (e.g., hypothyroidism, diabetes, etc.), (2) reeducation measures, directed to reduce or remove occupational or recreational activities that produce vicious postures, repetitive trauma, or frequent deleterious mobility affecting the involved region, (3) rest and splinting, if the involved nerve crosses a joint and dynamic compression is a major issue; however, in the presence of additional static factors such as intra-tunnel masses or spurs, these measures are inefficient, (4) tailored physical and occupational therapy: it is necessary to adjust the program to the patient's needs and characteristics (e.g., age, associated conditions, access to therapy, etc.) and ideally should be conducted by a specialist in rehabilitation medicine with experience in the field (stretching therapy, strengthening therapy, massages, pulsatile ultrasound, transcutaneous electrical stimulation, laser therapy, hydrotherapy, cold and heat application, and sensory stimulation have demonstrated to be the most useful techniques), (5) oral nonsteroidal anti-inflammatory drugs, analgesics, and in certain cases, presenting incoercible neuropathic pain, anticonvulsants-antineuritic agents and tricyclic antidepressants, (6) PN blocks with corticosteroid plus local anesthetics-guided or not with ultrasound, fluoroscopy, computed tomography, and electric nerve stimulation-into the tunnel or over the entrapped nerve course allowed as the last option before surgery if symptoms worsen, to confirm diagnosis or for opening aggressive management of pain in refractory cases, (7) in carefully selected cases with chronic intractable pain, chemoneurolysis, termofrequency lesioning, cryoneuroablation, and neuromodulation of injured nerve [37, 68, 85, 103–111].

Broadly, conservative management is recommended for at least 3–4 months, and during this time, close monitoring is necessary to follow up patient's evolution. Thereafter, when symptoms get worse, don't improve despite conservative management, or if at first consultation the patient complaints of severe symptoms (stage II), or motor symptoms like muscle atrophy are consigned (stage III), surgical treatment is necessary [65].

8.2.6.2 Surgical Treatment Considerations

In virtue of CN physiopathology, its basic surgical management consists in releasing the nerve with decompression. This goal can be achieved either by open surgery or employing minimally invasive endoscopic-assisted techniques. However, additional surgical strategies may be necessary in selected cases, such as nerve transposition (e.g., ulnar nerve at the elbow), neurectomy in certain syndromes with recurrence of symptoms after primary decompressive surgery or even as primary procedure (e.g., Morton's neuroma, Meralgia Parestetica), tissue interposition flaps also in recurrence and revision surgery (e.g., median nerve at carpal tunnel), and the recently described and still controversial "supercharge end-to-side nerve transfer", designed to improve axonal regeneration in severe compressions (e.g., distal median to ulnar nerve in ulnar tunnel syndrome) [36, 111–116].

The chosen surgical strategy depends on the type of nerve compression syndrome, compression degree, the nerves and structures affected, and the existence of

previous surgeries. While outcomes after surgery are globally good, the success in each case depends on a constellation of factors, including the time of evolution, the severity of symptoms, and other underlying health conditions.

The planned surgical incision must be oriented out of sites of tension or pressure to avoid wound complications and to allow enough exposure to identify the nerve, its branches, the tunnel limits, and the structures to be sectioned or resected. Whenever possible, cutaneous branches should be respected. The surgeon must be sure to perform a complete release through the entire site of compression. Internal neurolysis has been described before, but its use is controversial, and in general is not recommended due to the risk of iatrogenic injury and intraneural fibrosis [117–123].

Regarding the endoscopic-assisted or the pure endoscopic decompression, many authors have described its use in different entrapment sites and its advantages in aesthetical wound appearance and shorter hospitalization time. Nevertheless, long-term outcomes comparing open versus endoscopic release are similar [112, 124].

Since incomplete decompressions, wrong diagnosis, and mismanagement of medical underlying associated conditions are the main causes of surgical failure [125], all these factors should be avoided.

Whichever decompression technique we use, complications' avoidance is of paramount importance: consequently, a correct diagnosis and an adequate surgical technique should be always warranted to each patient.

8.2.7 Conclusions of Part II

CN are common conditions that have a profound impact in patient's quality of life. Some important facts should be remembered in CN: any nerve can be subject of compression, pain and sensory symptomatology over a well-defined nerve distribution in association with predisposing factors could be a sign of compression, motor dysfunction and atrophy should be surgically treated immediately, the diagnosis of nerve compressions is clinical, and a delayed diagnosis and incorrect management may cause irreversible nerve damage.

Appropriate management in early stages often results in symptoms improvement. Surgical interventions, when are necessary, carry favorable outcomes. In recent years, peripheral nerve surgeons have introduced minimally invasive techniques for nerve entrapment surgery, and even when its use by now is limited to certain syndromes, reduced surgical morbidity and improved postoperative recovery times are possible. Radiological studies have evolved significantly in the procurement of high-resolution images that make possible both structural and functional evaluation of the nerves. New insights concerning nerve compressions are focused on the association with chronic headaches and the possibility of successful outcomes after nerve decompression [126, 127].

8.3 Part III: Peripheral Nerve Tumors

8.3.1 Introduction

Peripheral nerve tumors are rare lesions that can originate in any nerve and any region of the body. Consequently, the list of differential diagnoses is often very long.

Peripheral nerves can be affected by various types of tumor. They can originate outside the nerve and compress it or start in one of the types of cell that the nerve itself contains, like unmyelinated and myelinic axons, Schwann cells, fibroblasts, comb cells, smooth muscle cells, and endothelium (in the vasa nervorum). Only those tumors that originate in one of the above-mentioned cell types should be considered peripheral nerve tumors, among which they can exhibit a broad range of biological behaviors: from benign (e.g., schwannomas, neurofibromas, and perineuriomas) to highly malignant, like malignant tumors of the peripheral nerve sheath (MTPNS) [128–137] (Fig. 8.6).

In general, given the relative quantities of each tissue type in peripheral nerves, most tumors are benign and originate in Schwann cells (schwannomas).

With a detailed clinical examination and neuroimaging studies, a fairly reliable preoperatory diagnosis can usually be made, which will ultimately always depend on histological confirmation. This diagnostic exercise is a crucial step in the management of peripheral nerve tumors, as surgical treatment varies widely, depending on whether a tumor is suspected to be benign or malignant.

8.3.2 Clinical Characteristics

Peripheral nerve tumors obviously originate within a nerve, and this clearly influences how they present and is the main clue to their diagnosis.

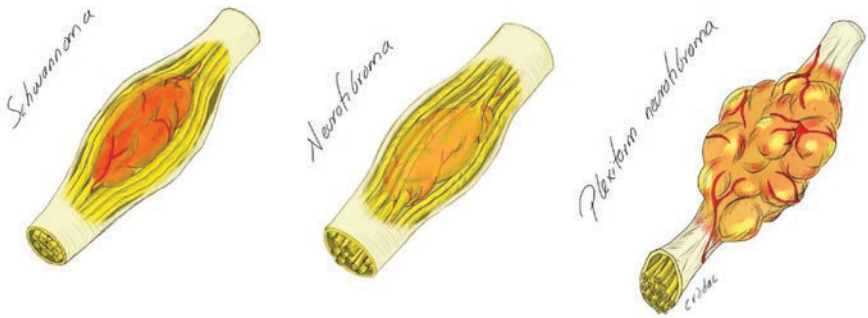

Fig. 8.6 Different types of benign nerve tumors. (Illustration by Crodac (Rodríguez-Aceves CA))

Benign tumors generally exhibit slow growth and, because of this, may be associated with very subtle symptoms, if symptomatic at all when first diagnosed (some may present as a painless mass).

When such tumors begin to generate symptoms, the symptoms are most commonly sensory, such as paresthesia or pain in the territory of that nerve. It is quite typical for percussion of nerve tumors to generate a positive Tinel's sign. In later stages, even benign nerve tumors can produce motor symptoms. However, if motor deficits appear early and/or progress quickly, or if they appear in locations other than at entrapment points (carpal tunnel, retro-epitrochlear canal, fibular tunnel, etc.), malignancy should be suspected [134].

In terms of semiology, in general, benign nerve tumors are tapered, moving easily along the transverse axis of the nerve, but not longitudinally. They also are generally soft upon palpation.

Conversely, malignancy should be suspected when a tumor is larger than 5 cm, grows rapidly, is very painful, presents with early motor signs, adheres to surrounding tissue planes, and/or is firm on palpation.

8.3.3 Common Types of Benign Nerve Tumor

Schwannomas are the most common benign tumors of the peripheral nervous system (PNS) and they can arise anywhere.

Macroscopically, they are firm but elastic, tapered or rounded in shape, and smooth.

Voluminous tumors present as irregular lobulations or even as cysts, secondary to bleeding that occurs during their growth.

These tumors are composed of Schwann cells, with normal nerve fibers displaced towards the periphery of the nerve. They are located anywhere along a nerve's course.

They can present as single or multiple tumors, the latter characteristic of conditions like neurofibromatosis and schwannomatosis.

Percussion or palpation of the tumor usually generates paresthesia or pain in the sensory territory of the affected nerve (Tinel's sign), but generally not motor deficits. This is quite characteristic that pain and sensory symptoms clearly predominate over motor deficits.

From a microscopic point of view, schwannomas contain, as an almost exclusive element, a single cell type; that is, Schwann cells. The tumor is surrounded by a fibrous capsule composed of epineurium and residual nerve fibers. On histological study, the most distinctive characteristic of these tumors is the configuration of cells forming Antoni A or B patterns. They also form clusters called "Verocay bodies", which initially were described by the Uruguayan pathologist José Verocay.

Some schwannomas test positive for gliofibrillar acid protein (GFAP), while others contain keratin and antibodies that react to various keratins [pankeratins,

keratin cocktail (CK) (AE1/AE3)]. These two markers highlight the cellular areas of Antoni A, especially those adjacent to the capsule, in myxoid or degenerative areas, and in perivascular zones. In recent studies assessing large numbers of retroperitoneal schwannomas, 84% of the tumors were positive for AE1/AE3 and GFAP.

Immunohistochemical staining using anti-S-100 protein antibodies reveals uniform and intense staining of the tumor's Schwann cells. This technique is an important tool for diagnosis; in poor differentiated schwannomas, S-100 protein staining is helpful for confirming the diagnosis.

Neurofibromas lack the thick collagen capsule that characterizes schwannomas, instead surrounded by perineurium or epineurium of varying thickness. They also do not exhibit Antoni A or B areas or Verocay bodies, again characteristic of schwannomas. One distinctive feature of neurofibromas is that immunoreactivity to the S-100 protein is observed only in a portion of their cells, as opposed to the uniform reactivity exhibited by schwannomas.

Neurofibromas become suspected based on clinical findings, but are confirmed by imaging studies like ultrasound and magnetic resonance imaging (MRI), followed by microscopic evaluation. On MRI, these tumors usually form a mass within the nerve, are spindle-shaped, capture contrast intensely, and demonstrate sharp edges that delineate the tumor from surrounding tissues [138].

8.3.4 Treatment

There is no pharmacological therapy for either of the above-described tumors, rendering surgery the cornerstone of treatment. In general, resection of these tumors is safe, if done under magnification and employing neurostimulation, which permits the separation and preservation of motor fibers.

As a basic principle, the entire tumor must be exposed, the capsule 360° stimulated to identify passing motor nerve fibers, and incised in such a way that either fibers are not seen, or a motor response is elicited. Then the surgeon must look for the plane that distinguishes the nerve from the tumor. Subsequently, the tumor should be dissected both proximally and distally, locating the fascicles of the nerve's origin, which must be sacrificed. It is the current authors' practice to resect a 'safety margin', ensuring at least 0.5 cm of "healthy" nerve-referring to the fascicles from which the nerve arises—to reduce the risk of tumor recurrence. Obviously, only the tumor's bundle of origin is sacrificed.

Normally, if dissection is performed meticulously and a good tissue plane is maintained, there will be complete preservation of motor function, though small areas of transient hypoesthesia may become evident postoperatively. With good surgical technique, motor and sensory preservation can be achieved in 95% of patients [139, 140].

8.3.5 Peripheral Nerve Tumors in Neurofibromatosis (NF) Types I and II

Neurofibromatosis (NF) is a serious genetic disorder that affects roughly one in 3000–4000 individuals and has variable penetrance. It is a generalized and progressive process that involves both the central and peripheral nervous systems. It also is multisystemic and is associated with cutaneous, neurological, and orthopedic manifestations. Its implications for SNP tumors will be discussed briefly.

Individuals with NF I or II warrant special consideration. This is because, over the course of their life, they tend to develop multiple tumors in different peripheral nerves, which may vary widely in their need for and approach to treatment. Neurofibromas are the characteristic tumor, but NF patients also may develop other tumor types, like schwannomas, atypical tumors of uncertain evolutionary potential (ATUEP), and malignant peripheral nerve sheath tumors (MPNST). Epidemiological data show that people with neurofibromatosis have a 100-fold increased likelihood of developing a MPNST than the rate observed in the general population [141–145].

There is no curative treatment. Management consists of monitoring patients to identify tumors that might require resection and, otherwise, supportive treatment. In addition to the markedly increased risk of MPNST, NF patients may experience malignant transformation of previously benign tumors, like schwannomas or neurofibromas.

8.3.6 Genetic Aspects

The NF-1 gene is located on chromosome 17 and produces a protein called neurofibromin. Its main action is to regulate cell division within the nervous system. In essence, it serves as a kind of brake that prevents excessive cell multiplication.

The gene for NF-2, located on chromosome 22, has also been identified. As with NF-1, the gene product for NF-2 is an onco-suppressor protein (called schwannomin).

8.3.6.1 NF-1

NF-1 is a progressive disease, in which tumors develop in the peripheral nerves. Moreover, preexisting tumors can continue to grow at the same time that new lesions appear.

The prototype lesion seen in NF-1 is a neurofibroma, a benign tumor that originates from a medium-sized or large nerve. Neurofibromas usually contain elongated spindle cells and pleomorphic pseudo-fibroblastic cells. From a clinical and surgical points of view, neurofibromas are benign tumors that grow in the connective tissue of nerves and, as such, cannot always be completely resected without sacrificing nerve function.

Occasionally, neurofibromas—typically, plexiform neurofibromas that are bulky, deep, or located in the brachial or lumbar plexus—undergo malignant degeneration and transform into ATUEPs or MPNSTs. Unlike benign neurofibromas, MPNST are typically hypercellular and contain giant cells, a greater number of mitoses, and more vascular proliferation.

From the perspective of their natural clinical history, four types of neurofibromas are distinguished:

(a) *Cutaneous neurofibromas* form within the dermis and epidermis, making it possible to move them along with the skin.
(b) *Subcutaneous neurofibromas* are located deep within the dermis, such that the skin moves over them.
(c) *Plexiform neurofibromas* can be either nodular or diffuse. Diffuse plexiform neurofibromas contain some elements typical of schwannomas or cutaneous or subcutaneous neurofibromas. They develop several fingerlike extensions that invade normal tissues extensively, so they typically cannot be completely excised. They can affect both superficial and deep tissues.
(d) *Nerve neurofibromas* grow exhibiting a pseudo-infiltrative pattern, since they may invade more than one nerve bundle. Therefore, complete resection often entails sacrificing the nerve. For this reason, in neurofibromatosis patients, incomplete resection is an option that sometimes must be considered.

8.3.6.2 NF-2

Neurofibromatosis type 2 is also called central NF, since those affected have a relative scarcity of cutaneous manifestations, but a high incidence of tumors involving the central nervous system (meningiomas, gliomas of the optic nerve or tectal plate) and neurinomas within the VIII cranial nerve (usually bilateral).

NF-1 has a better prognosis than NF-2, since it has a lower incidence of CNS tumors. However, morbidity and mortality from NF-1 are not insignificant, largely depending on the number and location of the tumors that develop [141].

8.3.6.3 Considerations Regarding Surgical Treatment in Patients with NF

Given that, in NF, there will be sequential development of tumors that can affect virtually any nerve, the main therapeutic objective is to treat symptomatic tumors, those that are deemed to endanger either life or important functions, and in some patients, tumors that are aesthetically disfiguring.

Symptomatic peripheral nerve sheath tumors that are located in the brachial or lumbosacral plexuses become indications for surgery when they cause motor deficits or severe, intractable pain. This said, the risk of postsurgical neurological

dysfunction is high; consequently, the decision to operate often requires careful consideration and extensive discussion with patients +/− their families to select the treatment best suited to them.

When a tumor invades the nervous tissue of a single nerve, resecting the nerve and restoring function with a nerve graft may be indicated, in rare instances. However, it is essential to consider the specific regenerative capacity of each nerve. Potential benefits should always be weighed against the index of suspicion for a malignant tumor and the potential for long-term neurological sequelae.

Plexiform neurofibromas often recur after resection, because residual clumps of tumor cells remain in deep soft tissues. Resection of these lesions also can cause copious bleeding, given their high vascularity and extensive spread.

With spinal tumors, it may be necessary to operate for minor symptoms to prevent progression to spinal cord compression, even if the resection is incomplete.

Determining prognosis largely depends on the severity of disease. Most people with NF-1 have normal lifespans, but life expectancy can be shortened by up to 15 years or even more with aggressive forms. In addition to reduced survival. Patients with aggressive forms of NF also tend to have a reduced quality of life [145, 146].

8.3.6.4 Neurofibromatosis Type 3

Neurofibromatosis type 3 was first described in 1973 and is a diagnosis reserved for patients who fail to meet the criteria for NF-1, but have schwannomas in several peripheral nerves, except for the acoustic nerve [147].

8.3.6.5 Segmental Neurofibromatosis (SN)

Segmental neurofibromatosis is a disease characterized by the presence of manifestations of NF-1 limited to one area of the body. Symptoms may include *café-au-lait* spots, neurofibromas, freckles in the axillary or groin crease, and Lisch's nodules, which are more frequent than either brown spots or neurofibromas. The reported incidence of SN is roughly one in 36,000–40,000 individuals in the general population, making it 10–20 times less frequent than NF-1. SN may result from postzygotic mutation within the NF-1 gene, which leads to somatic mosaicism. This has been documented in patients with segmental neurofibromatosis, in whom microdeletion of the NF-1 gene was reported in 18% of fibroblasts cultured from a café au lait patch, but was absent in fibroblasts from normal skin and blood lymphocytes. Its segmental distribution and the absence of any family history allow us to suggest that NS is a form of somatic mosaicism in the NF-1 gene located on chromosome 17.

8.3.7 Malignant Tumors of the Peripheral Nerve Sheath (MPNST)

Luckily, MPNST are much rarer than most benign peripheral nerve tumors. By definition, they are malignant lesions that arise within a peripheral nerve or its nerve sheath, excluding tumors that originate in the epineurium or vasculature of peripheral nerves. Given that they invade perineural structures during their growth, for years they were mistaken as soft tissue sarcomas exhibiting neural invasion. Due to their low incidence, experience in the management of these lesions is limited, and it is difficult to propose "standard" treatments.

The macroscopic appearance of MPNST is that of a pseudo-encapsulated spindle-shaped or globoid lesion of firm-to-hard consistency that usually is several centimeters in diameter at the time of diagnosis. These tumors form within nerve bundles, but usually invade adjacent soft tissues through the epineurium. Therefore, the approach to treatment must be multidisciplinary and customized to each patient [128, 134, 146].

Microscopically, they are highly cellular tumors that usually have fascicular characteristics, spindle-shaped nuclei, scant cytoplasm, and frequent mitoses.

As a first step, it is essential to obtain a complete history and look for signs of neurofibromatosis, since up to two thirds of MPNSTs arise from a plexiform neurofibroma. The risk of a non-NF-1 plexiform neurofibroma becoming a MPNST is somewhat lower, estimated to be less than 1%.

Because these tumors are rare and have a very broad differential diagnosis, MPNST patients are often referred first to other surgical specialists and then to a peripheral nerve unit after the tumor is biopsied. It is recommended that patients with clinical signs considered suspicious for a malignant peripheral nerve tumor or having an initial biopsy confirming the diagnosis are referred to a multidisciplinary peripheral nerve unit for optimized treatment.

One debated point is whether or not a biopsy should be undertaken, since a needle biopsy can spread the tumor to superficial planes. On the other hand, definitive treatment of a MPNST is resection with cancer-free margins, which implies sacrificing the nerve and other structures within the same tissue compartment. It is clear that, to propose such radical treatment, it is necessary to have a very high index of suspicion for malignancy and, if possible, pathological confirmation.

For this reason, some authors recommend exposing the tumor at the start of surgery as would be required for a very wide resection, then taking an open biopsy after isolating the tumor from all surrounding tissues (to avoid seeding it). If malignancy is confirmed, the surgeon then can proceed to maximum resection.

Four specific MRI features have been proposed for use distinguishing MPNST from neurofibromas, with sensitivity and specificity rates of 61 and 90%, respectively. Malignancy is highly suspected when two or more of the following features are observed: large size, peripheral enhancement pattern, perilesional edema, and intra-tumoral cystic changes.

However, it is not possible to accurately characterize features delineating benign from malignant peripheral nerve tumors based on imaging findings alone, since schwannomas (particularly bulky ones), neurofibromas, and atypical nonmalignant schwannomas can also exhibit zones of varying signal intensity. Recent studies suggest that PET is more specific for diagnosing malignancy, by assessing a lesion's uptake of 2-fluoro-2-deoxy-D-glucose (FDG).

Making a presumptive diagnosis of a MPNST or of secondary involvement of a nerve by tumor originating from an occult primary neoplasm (e.g., Pancoast tumor) is supported by obtaining the patient's history, performing a general physical examination, and obtaining complementary studies.

If it is the site where MPNSTs' most frequently metastasize is the lung, computed tomography (CT) examination of the chest is warranted if the index of suspicion for malignancy is high. If the lung contains a suspicious lesion, a biopsy is necessary to confirm or rule out the presence of metastatic spread, one of the main determinants of whether treatment of the primary tumor should be radical or more conservative. The presence of metastases has an obviously negative effect on a patient's prognosis and generally spurs the early initiation of adjuvant radiation therapy and chemotherapy.

MPNSTs have high metastatic potential. Surgical resection can be performed by plastic surgeons, orthopedics, and neurosurgeons, depending on the practitioner's training; but, ideally, treatment should be multidisciplinary. Because MPNSTs are infrequent, the treatment of these tumors usually corresponds to whatever therapeutic protocol is deemed indicated for a soft tissue sarcoma. It is not yet clear whether such an extrapolation of therapeutic plans is appropriate; but the low incidence of these tumors prevents single centers from gaining sufficient experience or performing adequately sized studies to determine which treatment approaches are best.

The currently recommended diagnostic workup for MPNST involves local staging by CT or MRI, performing an open biopsy at a specialized center, determining the tumor's pathological grade, and confirming or ruling out the presence of metastases. Thereafter, each case should proceed to multidisciplinary management, the first objective of which is usually to establish local control. For this purpose, wide resection to achieve tumor-free margins is usually indicated, which in the past often included amputation/disarticulation of any affected limb. Today, however, most centers and surgeons prefer to perform wide oncological resections that encompass the tumor, as well as the adjacent fascial and muscular planes, followed by chemotherapy and/or adjuvant or neoadjuvant radiation therapy to spare the limb. Even in instances where tumor-free margins appear to have been achieved, adjuvant radiotherapy is often administered, because tumor cells spread extensively within fascial planes, resulting in high rates of recurrence.

Most patients do not have evidence of metastases at the time of initial diagnosis, but the risk of future metastasis is high. For this reason, routine follow-up should be done with short intervals between assessments, using clinical evaluations and radiological studies to detect both local recurrence and distant metastases.

The role of 18FDG PET/CT in the diagnosis of peripheral nerve tumors has been emphasized in recent years, as a way to permit practitioners to more accurately

determine what type of tumor they are treating. Given what has been discussed above, with peripheral nerve tumors, preoperatively determining whether a given tumor is benign or malignant is essential to surgical planning. Therefore, any test that might aid in obtaining an accurate diagnosis must be considered: MRI, PET/CT, biopsy, etc. The diagnostic acumen of PET scanning stems from its capacity to assess a tumor's metabolic activity, taking into account that tumor cells generally overexpress transporters due to increased glucose metabolism. The greater the poor differentiation, the greater the metabolism and, therefore, the greater the expression of glucose transporters.

One of the parameters used during PET scanning is the so-called SUV max, since it measures metabolism and has been shown to exhibit high sensitivity and specificity for a variety of tumors. In peripheral nerve tumors, an SUV max greater than 3.5 has been shown to be 97% sensitive and 87% specific for malignancy. The 18F-FDG PET/CT has certain advantages over other imaging approaches for the diagnosis and monitoring of peripheral nerve sheath tumors, especially those in which malignancy is suspected. It is superior to resonance imaging in its ability to determine cell behavior and is, therefore, ideal for guiding biopsies (which should be in areas characterized by higher-level metabolism). It is also very useful during patient follow-up, as it evaluates a tumor's response to treatment, detects metastases, and assesses the biological behavior of tumor remnants (in cases of incomplete resection) [148–152].

8.3.8 Conclusions to Part III

How peripheral nerve tumors are treated depends entirely on their specific pathology. A thorough preoperative evaluation is, hence, crucial. Benign tumors (mostly schwannomas and neurofibromas) can usually be safely and completely resected without sacrificing the nerve of origin. When there is some suspicion of malignancy, whether associated with neurofibromatosis or not, confirmatory biopsy, together with modern diagnostic techniques, has been recommended by several specialized centers, though whether biopsies are indeed appropriate remains controversial. When malignancy is confirmed, extensive resection to optimize patient survival is the main objective, potentially at the expense of neurological function. This may then be followed by adjuvant radiation and/or chemotherapy, depending on the nature of the tumor and the completeness of resection attained.

References

1. Martins RS, Bastos D, Siqueira MG, Heise CO, Teixeira MJ. Traumatic injuries of peripheral nerves: a review with emphasis on surgical indication. Arq Neuropsiquiatr. 2013;71(10):811–4.
2. Hudson AR, Hunter D. Timing of peripheral nerve repair: important local neuropathological factors. Clin Neurosurg. 1977;24:391–405.

3. Noble J, Munro CA, Prasad VS, Midha R. Analysis of upper and lower extremity peripheral nerve injuries in a population of patients with multiple injuries. J Trauma. 1998;45(1):116–22.
4. Campbell WW. Evaluation and management of peripheral nerve injury. Clin Neurophysiol. 2008;119(9):1951–65.
5. Hubbard JH. The quality of nerve regeneration. Factors independent of the most skillful repair. Surg Clin N Am. 1972;52(5):1099–108.
6. Brown PW. The time factor in surgery of upper-extremity peripheral nerve injury. Clin Orthop. 1970;68:14–21.
7. Kline DG. Physiological and clinical factors contributing to the timing of nerve repair. Clin Neurosurg. 1977;24:425–55.
8. Sunderland S, Ray LJ. Denervation changes in mammalian striated muscle. J Neurol Neurosurg Psychiatry. 1950;13(3):159–77.
9. Robinson LR. Traumatic injury to peripheral nerves. Muscle Nerve. 2000;23(6):863–73.
10. Seddon HJ, Medawar PB, Smith H. Rate of regeneration of peripheral nerves in man. J Physiol. 1943;102(2):191–215.
11. Seddon HJ. A classification of nerve injuries. Br Med J. 1942;2(4260):237–9.
12. Seddon HJ. The surgery of nerve injuries. Practitioner. 1960;184:181–7.
13. Maggi SP, Lowe JB, Mackinnon SE. Pathophysiology of nerve injury. Clin Plast Surg. 2003;30(2):109–26.
14. Grant GA, Goodkin R, Kliot M. Evaluation and surgical management of peripheral nerve problems. Neurosurgery. 1999;44(4):825–39.
15. Sunderland S. Rate of regeneration of sensory nerve fibers. Arch Neurol Psychiatry. 1947;58(1):1–6.
16. Sunderland S. A classification of peripheral nerve injuries producing loss of function. Brain J Neurol. 1951;74(4):491–516.
17. Mackinnon SE. New directions in peripheral nerve surgery. Ann Plast Surg. 1989;22(3):257–73.
18. Millesi H, Terzis JK. Nomenclature in peripheral nerve surgery. Committee report of the International Society of Reconstructive Microsurgery. Clin Plast Surg. 1984;11(1):3–8.
19. Spinner RJ, Kline DG. Surgery for peripheral nerve and brachial plexus injuries or other nerve lesions. Muscle Nerve. 2000;23(5):680–95.
20. Weber RV, Mackinnon SE. Bridging the neural gap. Clin Plast Surg. 2005;32(4):605–16.
21. Dvali L, Mackinnon S. Nerve repair, grafting, and nerve transfers. Clin Plast Surg. 2003;30(2):203–21.
22. Harris ME, Tindall SC. Techniques of peripheral nerve repair. Neurosurg Clin N Am. 1991;2(1):93–104.
23. Millesi H. Reappraisal of nerve repair. Surg Clin N Am. 1981;61(2):321–40.
24. Sunderland S. The anatomic foundation of peripheral nerve repair techniques. Orthop Clin N Am. 1981;12(2):245–66.
25. Lee MS, Dellon A. Surgery of the peripheral nerve. New York: Thieme Medical; 1988.
26. Birch R, Raji AR. Repair of median and ulnar nerves. Primary suture is best. J Bone Jt Surg Br. 1991;73(1):154–7.
27. Deitch EA, Grimes WR. Experience with 112 shotgun wounds of the extremities. J Trauma. 1984;24(7):600–3.
28. Grossman MD, Reilly P, McMahan D, Kauder D, Schwab CW. Gunshot wounds below the popliteal fossa: a contemporary review. Am Surg. 1999;65(4):360–5.
29. Katzman BM, Bozentka DJ. Peripheral nerve injuries secondary to missiles. Hand Clin. 1999;15(2):233–44.
30. Sulaiman WAR, Kline DG. Nerve surgery: a review and insights about its future. Clin Neurosurg. 2006;53:38–47.
31. Kline DG, Hudson A, Kim D. Atlas of peripheral nerve surgery. Philadelphia: WB Saunders Company; 2001.
32. Kline DG, Hudson AS. Nerve injuries: operative results for major nerve injuries, entrapment and tumors. Philadelphia: WB Saunders Company; 1995.

33. Manord JD, Garrard CL, Kline DG, Sternbergh WC, Money SR. Management of severe proximal vascular and neural injury of the upper extremity. J Vasc Surg. 1998;27(1):43–7.
34. Thomsen NOB, Dahlin LB. Injury to the radial nerve caused by fracture of the humeral shaft: timing and neurobiological aspects related to treatment and diagnosis. Scand J Plast Reconstr Surg Hand. 2007;41(4):153–7.
35. Amillo S, Barrios RH, Martínez-Peric R, Losada JI. Surgical treatment of the radial nerve lesions associated with fractures of the humerus. J Orthop Trauma. 1993;7(3):211–5.
36. Trescot AM. Peripheral nerve entrapments: clinical diagnosis and management. Cham: Springer; 2016.
37. Pecina MM, Markiewitz AD, Krmpotic-Nemanic J. Tunnel syndromes: peripheral nerve compression syndromes. 3rd ed. Boca Raton: CRC Press; 2001.
38. Tapadia M, Mozaffar T, Gupta R. Compressive neuropathies of the upper extremity: update on pathophysiology, classification, and electrodiagnostic findings. J Hand Surg Am. 2010;35(4):668–77.
39. Khedr EM, Fawi G, Allah Abbas MA, El-Fetoh NA, Zaki AF, Gamea A. Prevalence of common types of compression neuropathies in Qena Governorate/Egypt: a population-based survey. Neuroepidemiology. 2016;46(4):253–60.
40. Martyn CN, Hughes RA. Epidemiology of peripheral neuropathy. J Neurol Neurosurg Psychiatry. 1997;64(4):310–8.
41. Papanicolau GD, McGabe SJ, Firrell J. The prevalence and characteristics of nerve compression symptoms in the general population. J Hand Surg Am. 2001;26(3):460–6.
42. Latinovic R, Gulliford MC, Hughes RAC. Incidence of common compressive neuropathies in primary care. J Neurol Neurosurg Psychiatry. 2006;77(2):263–5.
43. Kandil MR, Darwish ES, Khedr EM, Sabry MM, Abdulah MA. A community-based epidemiological study of peripheral neuropathies in Assiut, Egypt. Neurol Res. 2012;34(10):960–6.
44. Sunderland S. Anatomical features of nerve trunks in relation to nerve injury and nerve repair. Clin Neurosurg. 1970;17:38–62.
45. Reina MA, López A, Villanueva MC, de Andrés JA, León GI. Morfología de los nervios periféricos, de sus cubiertas y de su vascularización. Rev Esp Anestesiol Reanim. 2000;47:464–75.
46. Smith BE. Anatomy and histology of peripheral nerve. In: Kimura J, editor. Peripheral nerve diseases. Handbook of clinical neurophysiology. Amsterdam: Elsevier; 2006. p. 3–22.
47. Rigoard P, Buffenoir K, Wager S, Bauche J, Giot P, Robert F, et al. Organisation anatomique et physiologique du nerf périphérique. Neurochirurgie. 2009;55(Suppl 1):S3–12.
48. Menorca RMG, Fussell TS, Elfar JC. Nerve physiology: mechanisms of injury and recovery. Hand Clin. 2013;29(3):317–30.
49. Mackinnon SE. Pathophysiology of nerve compression. Hand Clin. 2002;18(2):231–41.
50. Zachary LS, Dellon ES, Nicholas EM, Dellon AL. The structural basis of Felice Fontana's spiral bands and their relationship to nerve injury. J Reconstr Microsurg. 1993;9(2):131–8.
51. Merolli A, Mingarelli L, Rocchi L. A more detailed mechanism to explain the "bands of Fontana" in peripheral nerves. Muscle Nerve. 2012;46(4):540–7.
52. Rempel D, Dahlin L, Lundborg G. Pathophysiology of nerve compression syndromes: response of peripheral nerves to loading. J Bone Jt Surg Am. 1999;81(11):1600–10.
53. Lundborg G, Dahlin LB. Anatomy, function, and pathophysiology of peripheral nerves and nerve compression. Hand Clin. 1996;12(2):185–93.
54. Lundborg G, Dahlin LB. The pathophysiology of nerve compression. Hand Clin. 1992;8(2):215–27.
55. Dahlin LB. Aspects on pathophysiology of nerve entrapments and nerve compression injuries. Neurosurg Clin N Am. 1991;2(1):21–9.
56. Reina MA, López A, Villanueva MC, de Andrés JA, Machés F. La barrera hemato-nerviosa en los nervios periféricos. Rev Esp Anestesiol Reanim. 2003;50:80–6.
57. Ubogu EE. The molecular and biophysical characterization of the human blood–nerve barrier: current concepts. J Vasc Res. 2013;50(4):289–303.

58. Ubogu EE. Biology of the human blood–nerve barrier in health and disease. Exp Neurol. 2020;328:113272.
59. Maday S, Twelvetrees AE, Moughamian AJ, Holzbaur EL. Axonal transport: cargo-specific mechanisms of motility and regulation. Neuron. 2014;84(2):292–309.
60. Sleigh JN, Rossor AM, Fellows AD, Tosolini AP, Schiavo G. Axonal transport and neurological disease. Nat Rev Neurol. 2019;15(12):691–703.
61. Dellon AL, Mackinnon SE. Chronic nerve compression model for the double crush hypothesis. Ann Plast Surg. 1991;26(3):259–64.
62. Gupta R, Steward O. Chronic nerve compression induces concurrent apoptosis and proliferation of Schwann cells. J Comp Neurol. 2003;461:174–86.
63. Rempel DM, Diao E. Entrapment neuropathies: pathophysiology and pathogenesis. J Electromuogr Kinesiol. 2004;14:71–5.
64. Gupta R, Rummler L, Steward O. Understanding the biology of compressive neuropathies. Clin Orthop Relat Res. 2005;436:151–60.
65. Spinner M, Spencer PS. Nerve compression lesions of the upper extremity. A clinical and experimental review. Clin Orthop Relat Res. 1974;104:46–67.
66. Dahlin LB, Sjöstrand J, McLean WG. Graded inhibition of retrograde axonal transport by compression of rabbit vagus nerve. J Neurol Sci. 1986;76(2–3):221–30.
67. Siqueira MG, Martins RS. Síndromes compressivas de nervos periféricos: diagnóstico e tratamento. Rio de Janeiro: Di Livros; 2009.
68. Allieu Y, Mackinnon SE. Nerve compression syndromes of the upper limb. Boca Raton: CRC; 2002.
69. Dilley A, Bove GM. Disruption of axoplasmic transport induces mechanical sensitivity in intact rat C-fiber nociceptor axons. J Physiol. 2008;586:593–604.
70. Genova A, Dix O, Saefan A, Thakur M, Hassan A. Carpal tunnel syndrome: a review of literature. Cureus. 2020;12(3):e7333.
71. Hirose CB, McGarvey WC. Peripheral nerve entrapments. Foot Ankle Clin. 2004;9(2):225–69.
72. Wahab KW, Sanya EO, Adebayo PB, Babalola MO, Ibraheem HG. Carpal tunnel syndrome and other entrapment neuropathies. Oman Med. 2017;32(6):449–54.
73. Toussaint CP, Perry EC 3rd, Pisansky MT, Anderson DE. What's new in the diagnosis and treatment of peripheral nerve entrapment neuropathies. Neurol Clin. 2010;28(4):979–1004.
74. Jacobson L, Dengler J, Moore AM. Nerve entrapments. Clin Plast Surg. 2020;47(2):267–78.
75. Zylicz Z. Entrapment neuropathies. Adv Pall Med. 2010;9(3):103–8.
76. Fuller G. Focal peripheral neuropathies. J Neurol Neurosurg Psychiatry. 2003;74(Suppl 2):220–4.
77. Fustinoni O. Semiología del Sistema nervioso. Buenos Aires: El Ateneo; 2014.
78. Campbell WW. DeJong's the neurologic examination. 8th ed. New York: Lippincott Williams & Wilkins; 2019.
79. O'Brien M. Aids to the examination of the peripheral nervous system. 5th ed. Philadelphia: W. B. Saunders; 2010.
80. Russell S. Examination of peripheral nerve injuries: an anatomical approach. 2nd ed. New York: Thieme; 2015.
81. Montagna P. Motor tinel sign. A new localizing sign in entrapment neuropathy. Muscle Nerve. 1994;17:1493–4.
82. Montagna P, Liguori R. The motor tinel sign: a useful sign in entrapment neuropathy? Muscle Nerve. 2000;23(6):976–8.
83. Novak CB, Lee GW, Mackinnon SE, Lay L. Provocative testing for cubital tunnel syndrome. J Hand Surg Am. 1994;19(5):817–20.
84. Zhang D, Chruscielski CM, Blazar P, Earp BE. Accuracy of provocative test for carpal tunnel syndrome. J Hand Surg Glob. 2020;2(3):121–5.
85. Schmid AB, Fundaun J, Tampin B. Entrapment neuropathies: a contemporary approach to pathophysiology, clinical assessment, and management. Pain Rep. 2020;5(4):e829.

86. Neal S, Fields KB. Peripheral nerve entrapment and injury in the upper extremity. Am Fam Physician. 2010;81(2):147–55.
87. Bromberg MB. An electrodiagnostic approach to the evaluation of peripheral neuropathies. Phys Med Rehabil Clin N Am. 2013;24(1):153–68.
88. Rodríguez-Aceves CA, Domínguez-Páez M, Fernández Sánchez VE. Electrodiagnostic pre-, intra-, and postoperative evaluations. In: Socolovsky M, Rasulic L, Midha R, Garozzo E, editors. Manual or peripheral nerve surgery: from the basics to complex procedures. New York: Thieme; 2018. p. 48–57.
89. Pugdahl K, Tankisi H, Fuglsang-Frederiksen A. Electrodiagnostic testing of entrapment neuropathies: a review of existing guidelines. J Clin Neurophysiol. 2020;37(4):209–305.
90. Spratt JD, Stanley AJ, Graigner AJ, Hide IG, Campbell RS. The role of diagnostic radiology in compressive and entrapment neuropathies. Eur Radiol. 2002;12(9):2352–64.
91. Linda DD, Harish S, Stewart BG, Finlay K, Parasau N, Rebello RP. Multimodality imaging of peripheral neuropathies of the upper limb and brachial plexus. Radiographics. 2010;30(5):1373–400.
92. Peer S, Gruber H. Atlas of peripheral nerve ultrasound: with anatomic and MRI correlation. Cham: Springer; 2013.
93. Cartwright MS, Walker FO. Neuromuscular ultrasound in common entrapment neuropathies. Muscle Nerve. 2013;48(5):696–704.
94. Fornage BD. Peripheral nerves of the extremities: imaging with US. Radiology. 1988;167:179–82.
95. Schminke U. Ultrasonography of peripheral nerves—clinical significance. Pers Med. 2012;1:422–6.
96. Kerasnoudis A, Tsiygoulis G. Nerve ultrasound in peripheral neuropathies: a review. J Neuroimaging. 2015;25(4):528–38.
97. Hochman MG, Zilberfarb JL. Nerves in a pinch: imaging of nerve compression syndromes. Radiol Clin North Am. 2004;42(1):221–45.
98. Hof JJ, Kliot M, Slimp J, Haynor DR. What's new in MRI of peripheral nerve entrapment? Neurosurg Clin N Am. 2008;19(4):583–95.
99. Aggarwal A, Jana M, Srivastava DN, Sharma R, Gamanagatti S, Kumar A, et al. Magnetic resonance neurography and ultrasonogram findings in upper limb peripheral neuropathies. Neurol India. 2019;67(Supplement):S125–34.
100. Martín Noguerol T, Barousse R. Update in the evaluation of peripheral nerves by MRI, from morphological to functional neurography. Radiologia. 2020;62(2):90–101.
101. Dong Q, Jacobson JA, Jamadar DA, Gandikota G, Brandon C, Morag Y, et al. Entrapment neuropathies in the upper and lower limbs: anatomy and MRI features. Radiol Res Pract. 2012;2012:230679.
102. Schmid AB, Hailey L, Tampin B. Entrapment neuropathies: challenging common beliefs with novel evidence. J Orthop Sport Phys Ther. 2018;48(2):58–62.
103. Wilson JK, Sevier TL. A review of treatment for carpal tunnel syndrome. Disabil Rehabil. 2003;25(3):113–9.
104. Coppieters M. Extrapolation of neuroscience research to the non-surgical management of compressive neuropathies. Phys Ther Rev. 2010;15(2):113–4.
105. Roghani RS, Rayegani SM. Basics of peripheral nerve injury rehabilitation. In: Rayegani SM, editor. Basic principles of peripheral nerve disorders. London: InTech; 2012.
106. Eker HE, Cok OY, Aribogan A, Arslan G. Management of neuropathic pain with methylprednisolone at the site of nerve injury. Pain Med. 2012;13(3):443–51.
107. Schmid AB, Nee RJ, Coppieters MW. Reappraising entrapment neuropathies—mechanisms, diagnosis and management. Man Ther. 2013;18(6):449–57.
108. Suszyński K, Marcol W, Górka D. Physiotherapeutic techniques used in the management of patients with peripheral nerve injuries. Neural Regen Res. 2015;10(11):1770–2.
109. Nwawka OK, Miller TT. Ultrasound-guided peripheral nerve injection techniques. AJR Am J Roentgenol. 2016;207(3):507–16.

110. Bani Hani DA, Alawneh KZ, Aleshawi AJ, Ahmad AI, Raffee LA, Alhowary AAA, et al. Successful and complete recovery of the ulnar nerve after eight years of chronic injury through local steroid injections: a case report. Pain Ther. 2020;9(1):327–32.
111. Hirasawa Y. Treatment of nerve injury and entrapment neuropathy. Cham: Springer; 2005.
112. Krishnan KG, Pinzer T, Schackert G. A novel endoscopic technique in treating single nerve entrapment syndromes with special attention to ulnar nerve transposition and tarsal tunnel release: clinical application. Neurosurgery. 2006;59(1 Suppl 1):ONS89–100.
113. Şahin O, Haberal B, Şahin MŞ, Demirörs H, Kuru İ, Tuncay İC. Is simple decompression enough for the treatment of idiopathic cubital tunnel syndrome: a prospective comparative study analyzing the outcomes of simple decompression versus partial medial epicondylectomy. Jt Dis Relat Surg. 2020;31(3):523–31.
114. Fernández-Gibello A, Moroni S, Camuñas G, Montes R, Zwierzina M, Tasch C, Starke V, Sañudo J, Vazquez T, Konschake M. Ultrasound-guided decompression surgery of the tarsal tunnel: a novel technique for the proximal tarsal tunnel syndrome-part II. Surg Radiol Anat. 2019;41(1):43–51.
115. Jarvie G, Hupin-Debeurme M, Glaris Z, Daneshvar P. Supercharge end-to-side anterior interosseous nerve to ulnar motor nerve transfer for severe ulnar neuropathy: two cases suggesting recovery secondary to nerve transfer. J Orthop Case Rep. 2018;8(5):25–8.
116. Lu VM, Puffer RC, Everson MC, et al. Treating Morton's neuroma by injection, neurolysis, or neurectomy: a systematic review and meta-analysis of pain and satisfaction outcomes. Acta Neurochir. 2020;163(2):531–43.
117. Thatte MR, Mansukhani KA. Compressive neuropathy in the upper limb. Indian J Plast Surg. 2001;44(2):283–97.
118. Spinner RJ, Amadio PC. Compressive neuropathies of the upper extremity. Clin Plast Surg. 2003;30(2):155–73.
119. Thoma A, Levis C. Compression neuropathies of the lower extremity. Clin Plast Surg. 2003;30(2):189–201.
120. Helfenstein JM. Uncommon compressive neuropathies of upper limbs. Best Pract Res Clin Rheumatol. 2020;34(3):101516.
121. Doughty CT, Bowley MP. Entrapment neuropathies of the upper extremity. Med Clin N Am. 2019;103(2):357–70.
122. Bowley MP, Doughty CT. Entrapment neuropathies of the lower extremity. Med Clin N Am. 2019;103(2):371–82.
123. Shapiro BE, Preston DC. Entrapment and compressive neuropathies. Med Clin N Am. 2009;93(2):285–315.
124. Leclère FMP, Bignion D, Franz T, et al. Endoscopically assisted nerve decompression of rare nerve compression syndromes at the upper extremity. Arch Orthop Trauma Surg. 2013;133:575–82.
125. Russell SM, Kline DG. Complication avoidance in peripheral nerve surgery: injuries, entrapments, and tumors of the extremities—part 2. Neurosurgery. 2006;59(4 Suppl 2):ONS449–56.
126. de Ru JA, Filipovic B, Lans J, van der Veen EL, Lohuis PJFM. Entrapment neuropathy: a concept for pathogenesis and treatment of headaches—a narrative review. Clin Med Insights Ear Nose Throat. 2019;12:1179550619834949.
127. Blake P, Burstein R. Emerging evidence of occipital nerve compression in unremitting head and neck pain. J Headache Pain. 2019;20:76.
128. Angelov L, Davis A, O'Sullivan B, Bell R, Guha A. Neurogenic sarcomas: experience at the University of Toronto. Neurosurgery. 1998;43:56–64.
129. Antman K, Corson JM, Eberlein TJ, Singer S. Prognostic factors predictive of survival and local recurrence for extremity soft tissue sarcoma. Arch Surg. 1992;127(5):548–54.
130. Cerofolini E, Landi A, DeSantis G, Maiorana A, Canossi G, Romagnoli R. MR of benign peripheral nerve sheath tumors. J Comput Assist Tomogr. 1991;15:593–7.

131. Feldkamp MM, Lau N, Provias JP, Gutmann DH, Guha A. Acute presentation of a neurogenic sarcoma in a patient with neurofibromatosis type 1: a pathological and molecular explanation: case report. J Neurosurg. 1996;84:867–73.
132. Ferner RE, Golding JF, Smith M, Calonje E, Jan W, Sanjayanathan V, et al. [18F]2-fluoro-2-deoxy-D-glucose positron emission tomography (FDG PET) as a diagnostic tool for neurofibromatosis 1 (NF1) associated malignant peripheral nerve sheath tumours (MPNSTs): a long-term clinical study. Ann Oncol. 2008;19:390–4.
133. Alexandre A. Bening tumor of peripheral nerves. In: Basso A, Carrizo G, Mezzadri JJ, Goland J, Socolovsky M, editors. Neurocirugía. Aspectos clínicos y quirúrgicos. Buenos Aires: Corpus; 2010. p. 1058–67.
134. Midha R. Malignant peripheral nerves tumors. In: Basso A, Carrizo G, Mezzadri JJ, Goland J, Socolovsky M, editors. Neurocirugía. Aspectos clínicos y quirúrgicos. Buenos Aires: Corpus; 2010. p. 1088–75.
135. Halliday AL, Sobel RA, Martuza RL. Benign spinal nerve sheath tumors: their occurrence sporadically and in neurofibromatosis types 1 and 2. J Neurosurg. 1991;74(2):248–53.
136. Mautner VF, Tatagiba M, Guthoff R. Neurofibromatosis 2 in the pediatric age group. Neurosurgery. 1993;33(1):92–6.
137. Martínez F, Pinazzo S, Armand Ugón G, Diamant M, Gonzalez F. Multidisciplinary approach to lumbar plexus tumors. Report of two cases. Rev Latinoamer Neurocirugía/Neurocirurgia. 2016;25(1):69–75.
138. León Cejas L, Binaghi D, Socolovsky M, Dubrovsky A, Pirra L, Marchesoni C, et al. Intraneural perineuromas: diagnostic value of magnetic resonance neurography. J Peripher Nerv Syst. 2018;23(1):23–8.
139. Siqueira MG, Socolovsky M, Martins RS, Robla-Costales J, Di Masi G, Heise CO, et al. Surgical treatment of typical peripheral schwannomas: the risk of new postoperative deficits. Acta Neurochir. 2013;155(9):1745–9.
140. Martínez F, Dominguez Paez M, Cuadros Romero M, Moragues R, Segura-Fernandez Noguera M, Casales N, et al. Tumors of peripheral nerves: a retrospective study about 66 cases. Neurocirugia (Astur). 2020;31:105–11.
141. Fisher MJ, Belzberg AJ, de Blank P, De Raedt T, Elefteriou F, Ferner RE, et al. 2016 Children's tumor foundation conference on neurofibromatosis type 1, neurofibromatosis type 2, and schwannomatosis. Am J Med Genet A. 2018;176(5):1258–69.
142. Ahlawant S, Blakeley J, Montgnomery A, Subramaniam RM, Belzberg A, Fayad LM. Schwannoma in neurofibromatosis type 1: a pitfall for detecting malignancy by metabolic imaging. Skeletal Radiol. 2013;42(9):1317–22.
143. Nitsch L, Kurzwelly D, Kornblum C, Pieper C, Clusmann H, Müller M. High-resolution ultrasound as a powerful diagnostic tool in peripheral nerve lesions: detection of an intraneural ganglion cyst in a patient with painful subacute peroneal nerve palsy. Ultraschall Med. 2020;41(1):77–9.
144. Ogose A, Hott T, Morita T, Yamamura S, Hosaka N, Kobayashi H, Hirata T. Tumors of peripheral nerves: correlation of symptoms, clinical signs, imaging features, and histologic diagnosis. Skeletal Radiol. 1999;28(4):183–8.
145. Rhodes SD, He Y, Smiths A, Jiang L, Lu Q, Mund J, et al. Cdkn2a (Arf) loss drives NF1-associated atypical neurofibroma and malignant transformation. Hum Mol Genet. 2019;28(16):2752–62.
146. Bhat DI, Socolovsky M, Singh V. Surgical dilemmas in the management of peripheral nerve tumors in neurofibtomatosis 1. Neurol India. 2019;67(Supplement):S45–6.
147. Albas Sorrosa S, Modesto Dos Santos J, Leturia Delfrade I, Leon Rosique M, Rojo Alvaro J, Perez Ricarte S, Oliván Ballariga A, Rubio VT. Neurofibromatosis type 3 or schwannomatosis. Rev Clin Esp. 2016;216(Espec Congr):46.
148. Ladrón De Guevara D, Catalán P, Hernández C, Zhindon JP. Value of semicuantitative PET/CT (SUV max) on the sturdy of lung tumors. Rev Chil Enfer Respir. 2019;35(2):116–23.

149. Vidal M, López JE, Alvarado AM, Velez A. The value of 18F-FDG PET/TC in the assessment of peripheral nerve sheath tumors. Rev Colomb Radiol. 2018;29(4):5039–43.
150. Hall S. Nerve repair: a neurobiologist's view. J Hand Surg Edinb Scotl. 2001;26(2):129–36.
151. Spinner RJ. Outcomes for peripheral nerve entrapment syndromes. Clin Neurosurg. 2006;53:285–94.
152. Rosas M, Cerisola A, Martinez F, Gontade C, Medici C, Gonzalez G. Segmental neurofibromatosis segmentaria: a underdiagnosed entity. Rev Urug Med Int. 2016;3:110–7.

Chapter 9
Disorders of Secondary Neurulation: Suggestion of a New Classification According to Pathoembryogenesis

Jeyul Yang, Ji Yeoun Lee, Kyung Hyun Kim, Hee Jin Yang, and Kyu-Chang Wang

Abbreviations

CCM	Caudal cell mass
CDS	Congenital dermal sinus
CDupS	Caudal duplication syndrome
HH	Hamburger and Hamilton
IONM	Intraoperative neurophysiological monitoring
JNTD	Junctional neural tube defect

J. Yang · K.-C. Wang (✉)
Neuro-Oncology Clinic, Center for Rare Cancers, National Cancer Center, Goyang, Kyounggi-do, South Korea
e-mail: kcwang@snu.ac.kr

J. Y. Lee
Division of Pediatric Neurosurgery, Seoul National University Children's Hospital, Seoul, South Korea

Department of Anatomy and Cell Biology, Seoul National University College of Medicine, Seoul, South Korea
e-mail: ddang1@snu.ac.kr

K. H. Kim
Division of Pediatric Neurosurgery, Seoul National University Children's Hospital, Seoul, South Korea

H. J. Yang
Department of Neurosurgery, SMG-SNU Boramae Medical Center, Seoul, South Korea

C. Di Rocco (ed.), *Advances and Technical Standards in Neurosurgery*, Advances and Technical Standards in Neurosurgery 45,
https://doi.org/10.1007/978-3-030-99166-1_9

LDM	Limited dorsal myeloschisis
LLM	Lumbosacral lipomatous malformation
MRI	Magnetic resonance imaging
ONTD	Open neural tube defect
RMC	Retained medullary cord
SSD	Segmental spinal dysgenesis
TMC	Terminal myelocele
TMCC	Terminal myelocystocele

9.1 Introduction

Over the last two decades, the number of patients with spinal open neural tube defects (ONTDs) has rapidly decreased in developed countries because of improved nutrition and sanitation, genetic counseling, prenatal prophylaxis and diagnosis, and termination of pregnancy. Instead, due to increased levels of clinical suspicion and advanced diagnostic tools, the number of patients with occult spinal dysraphism is rapidly increasing. Simultaneously, secondary neurulation became the central topic of research in this field.

Based on the advanced knowledge on secondary neurulation and new technologies in management including intraoperative neurophysiological monitoring (IONM), pioneers in the field have enabled dramatic changes in the understanding of pathoembryogenesis and management strategies in occult spinal dysraphism [1].

In this chapter, we briefly described the normal process of secondary neurulation and its various anomalous entities, mainly focusing on pathoembryogenesis (Table 9.1). This chapter includes summaries of our recent publication [2].

Some ideas proposed in this chapter were extrapolated from the data of chick embryos. In terms of secondary neurulation, human embryos are known to be more similar to chick embryos than to rodent embryos. Although the findings in chick embryos may not be the same as those in human embryos, they are still a good alternative model. Some of our speculations are conjectural, controversial, and contradictory to the previous understanding. However, we hope they motivate further research to obtain deeper insights in this field.

Table 9.1 Disorders of secondary neurulation and the results

Failed junction with the primary neural tube
Junctional neural tube defect
With the stenosis of the surrounding bony structures: segmental spinal dysgenesis
Hypoplasia or arrest of secondary neurulation associated with disturbed activity of caudal mesenchymal tissue
Hypoplasia of the notochord: vertebral bone defect
Failed formation of the spinal cord: hypoplasia of the distal spinal cord with blunt conus
Failed regression of the spinal cord: failed regression spectrum of medullary cord
Hypoplasia of the caudal mesenchymal tissue: anorectal, genitourinary, and abdominal wall anomalies
Remote effects of an unknown mechanism
Duplication of the caudal cell mass associated with disturbed activity of caudal mesenchymal tissue
Duplicated caudal cell mass: focal double vertebral columns and spinal cords
Hyperplasia of the midline caudal mesenchymal tissue: septum formation in hindgut (including cloaca)
Hypoplasia of the lateral caudal mesenchymal tissue: anorectal, genitourinary, and abdominal wall anomalies as shown in caudal agenesis
Remote effects of an unknown mechanism: as shown in caudal agenesis
Failed ingression of the primitive streak to the caudal cell mass
Associated with wide attachment between the primitive streak and the caudal cell mass: transitional myelomeningocele
Failed ingression of the distal medullary cord from the ruptured terminal balloon: caudal (terminal) myelomeningocele
Focal limited dorsal neuro-cutaneous nondisjunction
Pulling of the medullary cord to the surface ectoderm side: limited dorsal myeloschisis
Pulling of the surface ectoderm to the medullary cord side: congenital dermal sinus
Neuro-mesenchymal adhesion
Adhesion between the cranial part and the distal end of the medullary cord: lumbosacral lipomatous malformation (LLM) of transitional type
Adhesion at the distal tip of the medullary cord with a pulling of the attachment site to the neural side without regression of the medullary cord: LLM of the caudal type
Adhesion at the distal tip of the medullary cord with a pulling of the attachment site to the neural side associated with regression of the medullary cord: LLM of the filar type
Failed regression spectrum of medullary cord
Incomplete regression of the medullary cord to the filum: thick filum
Delayed luminal collapse of the last part of the medullary cord: filar cyst
Failed regression at the stage of the medullary cord attached to the cul-de-sac with or without persistent luminal dilatation: ‘typical’ retained medullary cord, cystic or non-cystic type
Failed regression at the stage of the medullary cord detached from the cul-de-sac: retained medullary cord with ‘low-lying conus’
Failed regression at the stage of the medullary cord attached to the collapsed terminal balloon: terminal myelocele
Failed regression at the stage of the medullary cord attached to the persistent terminal balloon: terminal myelocystocele

Reprinted from Yang et al. [2] with permission from the Korean Neurosurgical Society

9.2 Brief Summary of Normal Secondary Neurulation

Secondary neurulation is associated with various anomalies of the distal spinal cord. Therefore, knowledge on steps in secondary neurulation is essential for understanding pathoembryogenesis of the congenital anomalies in this area.

The processes of secondary neurulation have been studied extensively in chick embryos and mouse embryos. Various types of research were plausible with little difficulty in chick embryos. Moreover, the processes of secondary neurulation in human embryos are more similar to those in chick embryos than in mouse embryos. Here, the morphological and cytokinetic features during secondary neurulation in the chick embryo are briefly described.

In chick embryos, at the time when the posterior neuropore closes, the secondary neural tube is formed by aggregation of cells in the caudal cell mass (CCM). The CCM is separated from the surface-located primitive streak and it forms the caudal mesenchymal tissue as well. The multipotent cells of CCM at the node-streak border [3] ('rhomboidal area' [4]) arrange into a cord-like mass (medullary cord) which is continuous with the primary neural tube like a wedge-shaped ventral insertion from the caudal side (Figs. 9.1 and 9.2). The caudal end of the notochord at the area

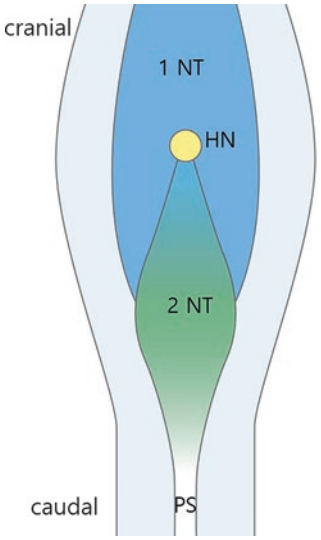

Fig. 9.1 A schematic drawing of Hensen's node area in a chick embryo of Hamburger and Hamilton stage 8. The area immediately caudal to the Hensen's node in the midline is the starting point of medullary cord formation. To the bilateral side of the area, neural plates at the caudal end of the primary neural tube are located. If the area immediately caudal to Hensen's node (cranial part of the node-streak border) is adhered to mesenchymal tissue, the laterally located neural plates of the primary neural tube may not neurulate properly. Then the fat may be attached to the dorsal midline of the spinal cord up beyond the normal dorsocaudal end of the primary neural tube which is known as the junction of S1–2 spinal cord segments. 1 *NT* primary neural tube, 2 *NT* secondary neural tube, *HN* Hensen's node, *PS* primitive streak. (Reprinted from Yang et al. [2] with permission from the Korean Neurosurgical Society)

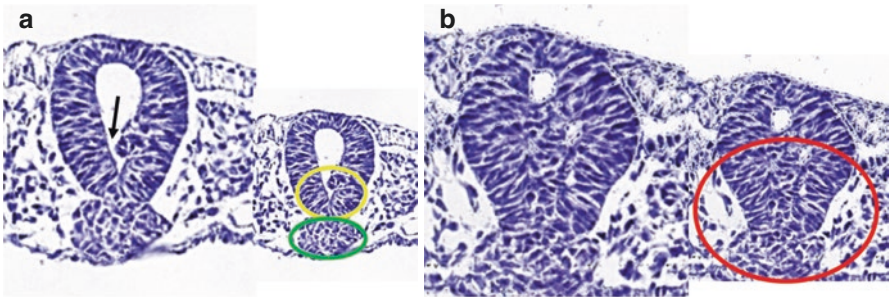

Fig. 9.2 Axial sections of the junctional zone between the primary and secondary neural tubes in a chick embryo of Hamburger and Hamilton stage 16. (**a**) At the cranial part of the newly formed medullary cord (yellow circle), the lumen of the ventrally located medullary cord is continuous to the lumen of the dorsally located primary neural tube (arrow). The notochord (green circle) is in close contact with the medullary cord. (**b**) At a more caudal section, the size of the medullary cord compared with the primary neural tube is increased. There are tiny lumens in the medullary cord. The notochord merged with the ventral aspect of the medullary cord (red circle). H&E, ×400

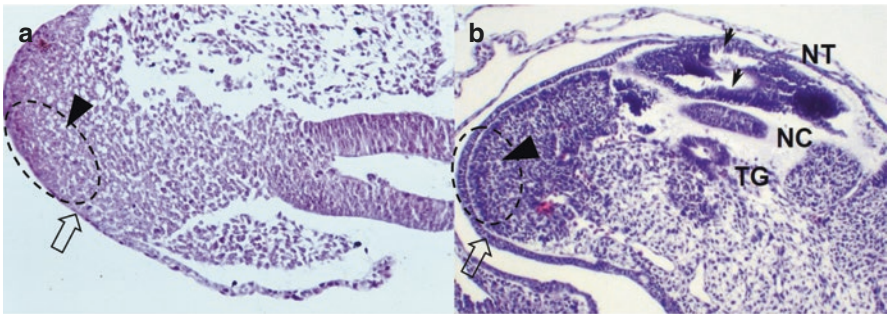

Fig. 9.3 (**a**) The caudal cell mass (arrowhead) and the surface ectoderm (open arrow) are continuous in a Hamburger and Hamilton (HH) stage 16 chick embryo. (**b**) At HH stage 20, the two layers are clearly separated. *Arrows* multiple cavities in the medullary cord, *NC* notochord, *NT* neural tube, *TG* tail gut. (Reprinted from Kim et al. [46] with permission from the Congress of Neurological Surgeons)

of the primary neural tube is continuous and merges with the cranial wedge of the medullary cord (chordo-neural hinge) and the cord-notochord demarcation in the axial section is no longer present distally. The overlapping of the caudal end of the primary neural tube and the cranial end of the secondary neural tube is called 'junctional neurulation' [3]. Normally the junctional process does not involve anatomical separation of the two structures. The wedge-shaped ends of the primary and the secondary neural tubes face and contact each other. Multiple small cavities are formed in the medullary cord, and these cavities coalesce with the lumen of the primary neural tube (Figs. 9.2 and 9.3b). The medullary cord elongates to the caudal direction and the process of coalescence of cavities is completed by Hamburger and Hamilton (HH) stage 35 and the whole neural tube is transformed into one tube with a single continuous lumen. At this stage, the terminal portion of the medullary tube is dilated dorsally and contacts the surface ectoderm ('terminal balloon') (Fig. 9.4).

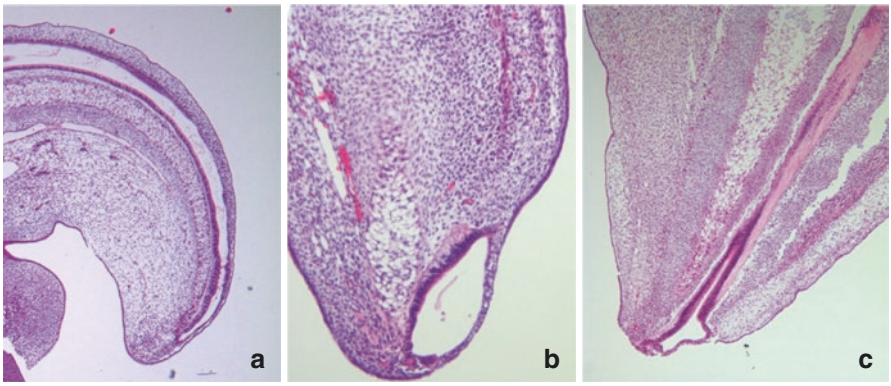

Fig. 9.4 Serial images of chick embryos showing a 'terminal balloon'. (**a**) The central canal of the medullary cord is shown in Hamburger and Hamilton (HH) stage 28. (**b**) At HH stage 32, a terminal balloon is seen as a focal dilatation of the distal end of the central canal which contacts the surface ectoderm. (**c**) At HH stage 36, the balloon shows partial deflation. (Modified from Lee et al. [41] with permission from Springer-Nature)

Thereafter, the balloon collapses, the caudal portion of the neural tube regresses, and the proximal portion develops into the normal spinal cord [5].

There have been some debates on whether the morphological changes in secondary neurulation in human embryos are more similar to those of chick embryos or mouse embryos [6–8]. It is now generally accepted that cavitation and coalescence of these cavities take place in chick embryos in a similar pattern to human embryos [9, 10].

Secondary neurulation does not involve the process of folding and fusion of the ectoderm as shown in primary neurulation. It made a belief that secondary neurulation disorders do not make skin defects. However, we no longer support this belief as stated below in a separate section.

It is not easy to compare the steps of secondary neurulation of chick embryos to those in human embryos directly, because stages of development are classified by different scales: HH stages for chick embryos and Carnegie stages for human embryos. Nonetheless, considering the important milestones of development, Carnegie stage 18 of human embryos seems to be comparable to HH stage 35 of chick embryos, when the formation of the medullary cord is completed to the tip of the caudal end of the embryo with multiple cavities inside (Fig. 9.5a–c). The terminal balloon is also found at this stage (Fig. 9.5d). After this stage, the caudal portion of the medullary cord reveals findings suggestive of involution [10] as in chick embryos [5].

During embryonal development, there are dynamic changes in the activities of cell proliferation and apoptosis concomitantly with the morphological changes. In the early stages of secondary neurulation of chick embryos, considerable activities of cell division are seen in the CCM. By HH stage 22, the rate of cell division begins to decline and apoptotic cells appear, especially in the central region. Thereafter, cell division is overtaken by apoptosis and stays the same until the CCM disappears [11]. The notochord itself did not show any proliferative activity which suggests that it is

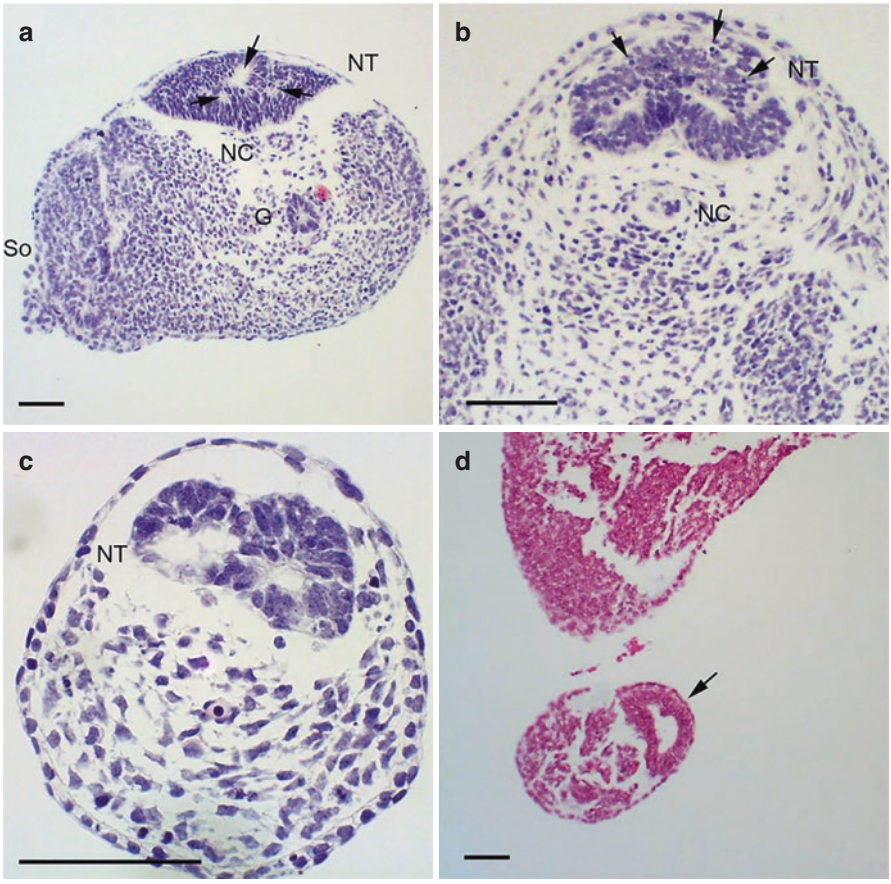

Fig. 9.5 Human medullary cords at Carnegie stage 17 (**a**) and stage 18 (**b**–**d**). (**a**) At Carnegie stage 17, multiple cavities in the secondary neural tube (NT, arrows), notochord (NC), tail gut (G), and somites (So) are seen. (**b**) The tail gut is invisible at stage 18. There are multiple nuclear pyknoses at the secondary neural tube (arrows). (**c**) At a more caudal level at stage 18, the notochord is invisible. (**d**) In another embryo of stage 18, the caudal neural tube shows terminal dilatation of the lumen which contacts the surface ectoderm (arrow). H&E, bar 100 μm, (**a**–**c**) reprinted from Yang et al. [10] with permission from Springer-Nature, (**d**) reprinted from Pang et al. [72] with permission from Congress of Neurological Surgeons

formed from terminally differentiated cells that have already passed the stage of proliferation. The apoptotic cells in the CCM adjacent to the surface-located primitive streak at HH stages 16 and 18 are also notable [12–14]. This supports the idea that the separation of the CCM from the surface-located primitive streak may be the result of cell death [11] (Fig. 9.6a). Such a role of cell death may further be applied to a similar process in the later stages of terminal balloon formation. The peak proliferative activity in the medullary cord corresponds to HH stage 40, whereas during primary neurulation, the peak of proliferation occurs at HH stages 26 and 28, which reflects the time delay in the secondary neurulation compared to the primary neurulation [11, 15, 16]. The ventral portion of the tail shows fan-shaped distribution of

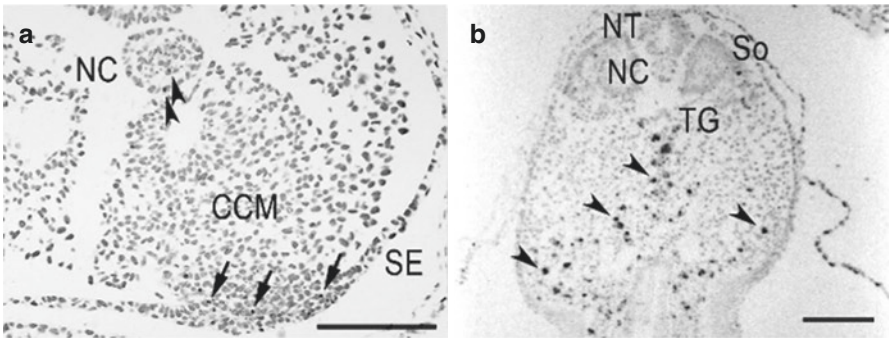

Fig. 9.6 TUNEL assays in chick embryos of Hamburger and Hamilton stages 16 (**a**) and 20 (**b**). The lower side of each photograph corresponds to the ventral side of the embryo. (**a**) TUNEL-positive cells are found in the caudal cell mass (CCM) adjacent to the surface epithelium (SE) (arrows). There are also a few positive cells in the notochord (NC) (arrowheads). (**b**) There are many labeled cells in the ventral and ventrolateral regions of the tail (arrowheads). There are no labeled cells in the secondary neural tube (NT), notochord (NC), and somites (So). *TG* tail gut. (Reprinted from Yang et al. [11], with permission from Springer-Nature, H&E, bar 100 μm)

apoptotic cells in HH stage 20. It gives an impression that cells that are not destined to differentiate into structures such as medullary cord, notochord, and somites degenerate as early as HH stage 20, while the medullary cord still shows active proliferation [11] (Fig. 9.6b). It is also notable that there is no remarkable dorsoventral differences in proliferative activity in the medullary cord probably due to the different mode of neural tube formation compared with the primary neural tube. The small multiple cavities detected at HH stages 40 and 45 at the tip of the tail may be the evidence of regression, supported by cytokinetic study [5, 11].

In human embryos, nuclear pyknosis at the medullary cord is observed at Carnegie stages 17 and 18, which suggests regression comparable to the morphological and cytokinetic findings observed in chick embryos [5, 11]. It is noteworthy that the apoptotic cells in the CCM adjacent to the surface epithelium are observed at the equivalent stages of not only chick and human embryos, but also mouse embryos. This suggests that the separation of CCM from the surface-located primitive streak is a highly conserved event in secondary neurulation [10, 17, 18].

In summary, there are several characteristics in secondary neurulation compared with primary neurulation. First of all, secondary neurulation occurs later in time than primary neurulation. A step of separation of the CCM from the surface-located primitive streak is present. There is a transitional or junctional area between the primary and secondary neural tubes and the secondary neural tube needs functional connection with the primary neural tube. Both of the medullary cord and the caudal mesenchymal tissue are derived from the CCM and the disturbed activities of the caudal mesenchyme may be associated with caudal spinal cord malformations. Secondary neurulation progresses in the caudal direction from the node-streak border. The ventrodorsal difference, prominent in primary neurulation, is not so evident in secondary neurulation. There is a regressive phase in secondary neurulation [19].

9.3 Failed Junction with the Primary Neural Tube

Peculiar cases in which the upper primary spinal cord is functionally disconnected from the lower secondary spinal cord and the two structures are connected via a thin fibrous band have been reported (Fig. 9.7) [20]. The entity was named 'junctional neural tube defect (JNTD)'. Lesions were found in the thoracolumbar junction or upper lumbar region, and the lower spinal cord usually looked similar to a normal conus. Direct electrical stimulation elicited some electromyographic responses in the ankle and/or sphincter muscles. Some of the reported cases had elaborate anomalies of the spinal bone with severe narrowing of the spinal canal at the level of the nonfunctional band. The lesions are very similar to the older entity of segmental spinal dysgenesis (SSD) which has been defined and described based on bony anomalies [21]. Although the 'neural' structures have not received much attention in SSD, a review of cases with available information showed that most of the SSD cases also had typical disconnected cords and were found in regions similar to JNTD [22]. Hence, SSD seems to describe cases of JNTD with varying degrees of bony anomalies, originating from the same pathoembryogenesis which is the error that occurs during junctional neurulation.

Junctional neurulation, or the process of the connection of the primary and secondary neural tubes, has been elucidated in basic research [4, 23]. Most recently, Dady et al. [3] used chick embryos to map the fate of the cells contributing to

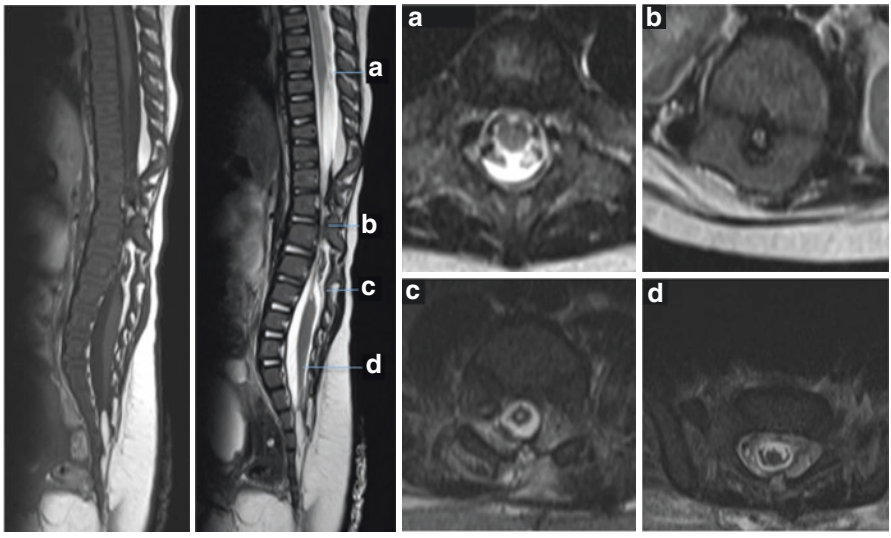

Fig. 9.7 T2 sagittal and axial MRI images of a patient with segmental spinal dysgenesis which seems to be a kind of junctional neural tube defect. (**a**) The normal upper spinal cord is seen at the mid-thoracic level which tapers to a thin band below. (**b**) Severe bony stenosis is noted at the thoracolumbar junction. (**c**, **d**) The band widened to form a relatively normal looking spinal cord and conus below L2. (Modified from Wang et al. [22] with permission from Springer-Nature)

secondary neural tube formation during junctional neurulation. They suggested that the junctional zone seems to extend from the lower thoracic to the upper sacral spinal cord in humans providing an important clue to explain how various secondary neurulation anomalies including caudal agenesis, caudal duplication syndrome (CDupS), SSD, and lumbosacral lipomatous malformation (LLM) of the transitional type are placed in higher regions than previously expected (below the junction between S1 and S2 segments of the spinal cord).

9.4 Hypoplasia or Arrest of Secondary Neurulation Associated with Disturbed Activity of Caudal Mesenchymal Tissue

Caudal agenesis is a disease entity with the common features of 'agenesis of the lower sacral and coccygeal spine' involving a wide variety of anomalies of the spinal cord and the other organs (urogenital and gastrointestinal organs) of the 'caudal' region. It is frequently seen in complex syndromes including VACTERL (vertebral anomaly, anal atresia, cardiac anomaly, tracheoesophageal fistula, renal anomaly, limb anomaly), OEIS (omphalocele, cloacal exstrophy, imperforate anus, spinal defects), and the Currarino triad (caudal agenesis, presacral mass, anorectal anomaly). The location of the disease obviously points to the CCM and secondary neurulation as the main players of its pathoembryogenesis explaining the wide spectrum of the clinical phenotypes [24–26].

As secondary neurulation begins with the formation of the medullary cord and is eventually completed by its regression, the anomaly of the spinal cord in caudal agenesis involves either the 'failure of formation' or the 'failure of regression' of the medullary cord (Fig. 9.8). If a developmental error occurs during the early period, the medullary cord is not completely formed resulting in a 'blunt-ended' conus frequently seen in the thoracolumbar junction [27]. The thoracolumbar region is more cephalad to the area in which the spinal cord is formed by secondary neurulation only, implying that the junctional zone of the primary and secondary neurulation may be involved in the development of caudal agenesis. Errors during the late phase of secondary neurulation will cause the 'failure of regression' of the medullary cord and the patient will have a conus at the normal or lower level with tethering lesions. The 'failure of formation' type usually will not benefit from neurosurgical intervention and the 'failure of regression' type may have tethered cord syndrome which needs untethering.

In the developmental process of the urogenital and distal gastrointestinal tracts, the mechanical role of the caudal mesenchyme originating from the CCM is known to be important. The association of the various anomalies of these organs may be explained by the problem in the formation of the caudal mesenchyme from the CCM. Hypothetically, an insufficient supply of the caudal mesenchyme will cause defective caudal–ventral push of the caudal mesoderm resulting in the various faults in formation of the urorectal septum and closure of the cloacal membrane [27, 28]. This will in turn generate anorectal anomalies such as imperforate anus or

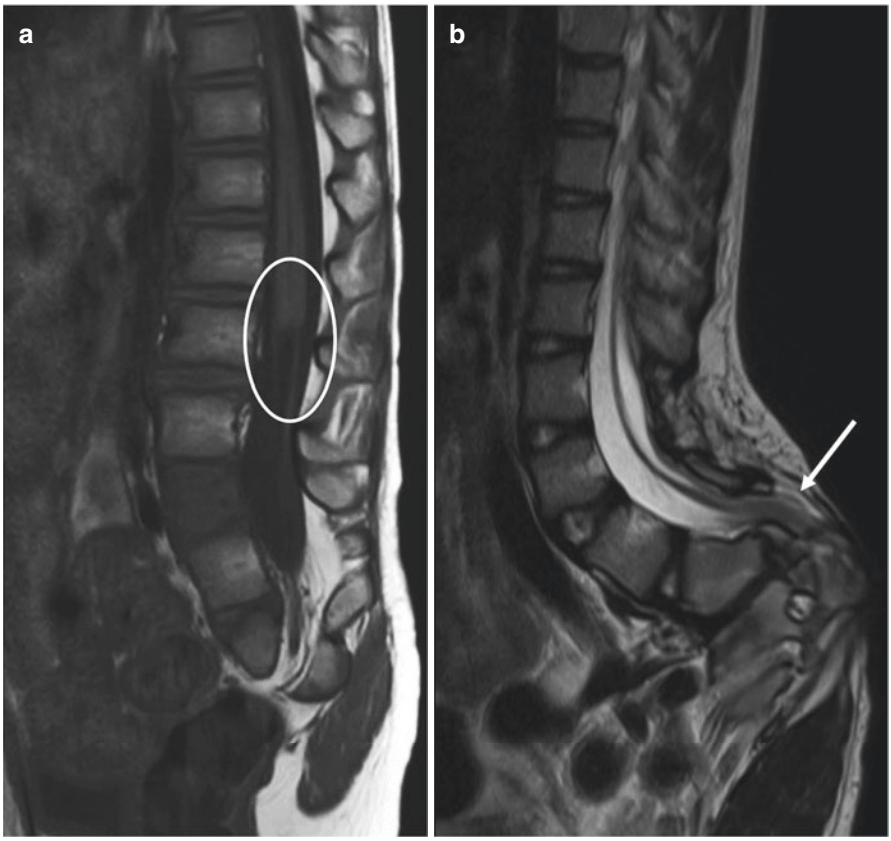

Fig. 9.8 MRI images of patients with caudal agenesis and 'failure of formation' (**a**) and 'failure of regression' (**b**) of the spinal cord. (**a**) A T1 sagittal MRI image shows a blunt-ended conus at L1 level (circle). (**b**) A T2 sagittal MRI image demonstrates a fatty filum with a low-lying conus (arrow). (Reprinted from Yang et al. [2] with permission from the Korean Neurosurgical Society)

genitourinary anomalies such as bladder exstrophy and hypospadia. An imperforate anus will be formed if the urorectal septum is deviated to an abnormally posterior location and the outflow of the anorectal canal is narrowed or occluded (Fig. 9.9). The failed fusion of the urethral folds may cause hypospadia, also due to the lack of the caudal–ventral push of the caudal mesenchyme (Fig. 9.10) [28].

9.5 Duplication of the CCM Associated With Disturbed Activity of Caudal Mesenchymal Tissue

CDupS is a complex anomaly involving the distal end of the trunk: a combination of gastrointestinal, genitourinary, spinal cord, and vertebral anomalies [29]. Due to its rare incidence, pathoembryogenesis of CDupS is still unknown, and hypotheses

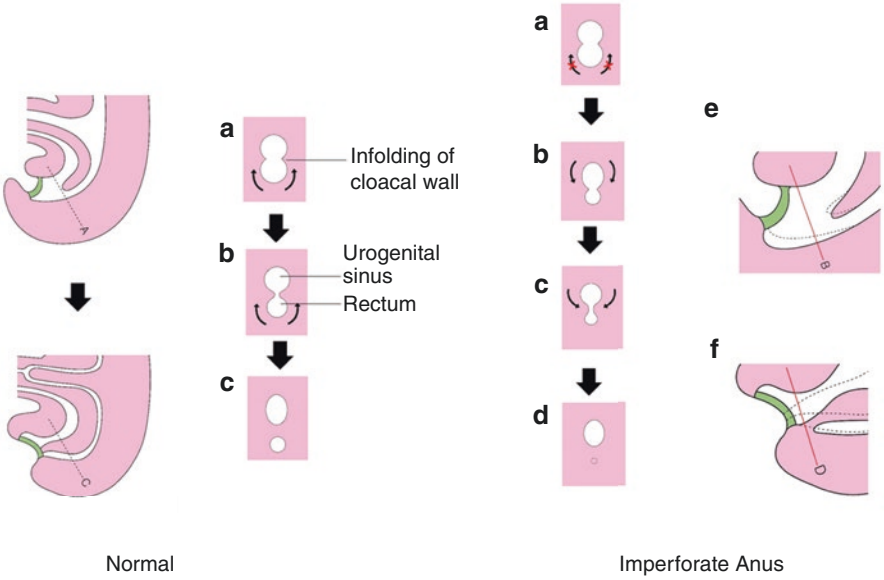

Fig. 9.9 Speculative drawings showing division of the cloaca into the anteriorly located urogenital sinus and the posteriorly located anorectal canal (left) and formation of an imperforate anus by a posteriorly deviated urorectal septum (right). The caudal–ventral push of the caudal mesenchyme (curved arrows in left **a** and **b**) is crucial. When the ventral push of the caudal mesenchyme is ineffective (curved arrows with red Xs in right **a**), the urorectal septum is displaced posteriorly resulting in an imperforate anus. (Reprinted from Lee et al. [28] with permission from Springer-Nature)

have been made based on fragmentary case reports. This led to the need for a systematic review of the cases and a logical deduction of pathoembryogenesis according to common clinical manifestations [30]. Moreover, recent advances in molecular biology have inspired new pathoembryogenetic theories that are more evidence-based.

9.5.1 Clinical Characteristics

Despite the diverse clinical manifestations of CDupS, common characteristics could be found. Regarding gastrointestinal anomalies, the mid-transverse colon was the most common originating point of duplication. Duplicated colons were not doubled into two different sets, but shared a common wall, or a septum, which made two colons (Fig. 9.11). Consequently, the duplicated colons ran in parallel. An anus was formed for each of duplicated rectums. From where the duplication started, triplication may occasionally occur, such as a triple sigmoid colon or triple ani. Other features among gastrointestinal anomalies were anterior body wall defects such as

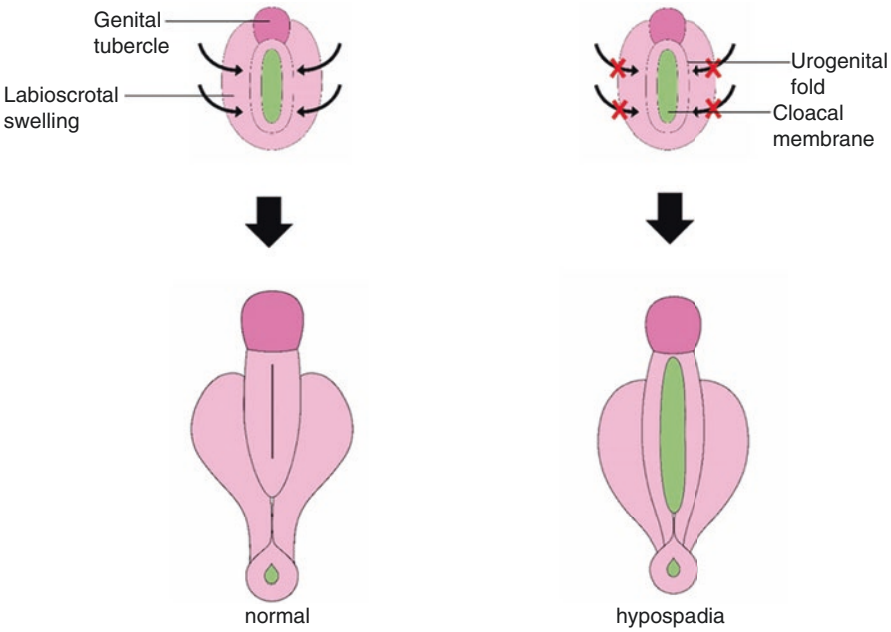

Fig. 9.10 A speculative drawing showing formation of a normal penis (left) and a hypospadia (right). Normally, the urogenital fold is fused in the midline by the bilateral caudal–ventral push of the caudal mesenchyme (curved arrows in left), resulting in the elongation of the genital tubercle to form a penis. The weak ventral push of the caudal mesenchyme results in failed closure of the urogenital folds in the ventral midline, leading to a hypospadia. (Reprinted from Lee et al. [28] with permission from Springer-Nature)

omphalocele, gastroschisis, or intestinal mesentery defects [29, 31, 32]. Imperforate ani were also reported [33].

Anomalies involving genitourinary organs resembled those of gastrointestinal organs. Duplicated bladders or uteri were separated by a septum. More distal structures were formed from corresponding proximal structures as normal, such as the urethras or vaginas from each of double bladders or double uteri. Anterior body wall defects such as exstrophy of bladder may also be associated. Renal anomalies including malrotation or agenesis may be combined [29, 30, 34].

Whole-set duplication of the spinal cord and vertebral column commonly started from the lower thoracic level to the distal end. The duplication branched off from one normal spine, resembling an inverted 'Y' shape. There was no case of CDupS in which duplicated segments merged again to form one spine below the level of duplication. Myelomeningocele, lumbosacral lipoma, or lipomeningomyelocele were frequently accompanied [29, 33, 35].

Developmental milestones were appropriate to age. Symptoms varied according to the duplicated organs. Constipation, recurrent urinary tract infection, urinary incontinence, or symptoms related to tethered spinal cord were reported. Symptomatic treatments such as staged correction of the colon with colostomy or

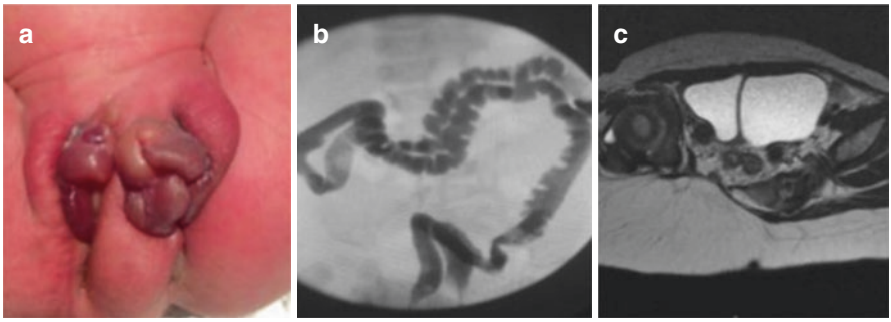

Fig. 9.11 Common patterns of caudal duplication syndrome. Proximal duplicated organs are separated by a septum, whereas the distal duplicated organs are formed from each of the proximal organ independently. (**a**) The patient has two urethral, vaginal and anal orifices. (**b**) In contrast to (**a**), duplicated colons are separated by a septum and run parallel. (**c**) Similar to (**b**), duplicated bladders share a septum in the midline. (Reprinted from Harris et al. [73] with permission from Sage publications, Inc.)

bladder augmentation were mostly successful. Aesthetic surgery was performed for duplicated external genitalia for those who desired, although the function was usually normal. Except for those with severe heart anomalies [33], patients lived an ordinary life, such that female patients had no problems in giving birth.

9.5.2 Pathoembryogenesis

Common features provide clues to pathoembryogenesis. Regions of whole-set duplication (spinal cord and vertebra) correspond to the area of the CCM, where secondary neurulation takes place. Therefore, our speculation is that it suggests duplication of the CCM.

At the late gastrulation phase, the area of the primitive streak is referred to as the CCM or caudal eminence. After the primary neural tube closes, secondary neurulation progresses through the processes of condensation, vacuolization, and canalization [8]. On the other hand, the hindgut, which is the premordium of the duplicated organ of CDupS, is not formed from the CCM but from the primordial gut [36]. However, caudal mesenchymal cells around the cloaca which were derived from the CCM normally migrate in from both lateral sides and separate the cloaca into the anorectal canal and the urogenital sinus (Fig. 9.12). Regarding septum formation of the proximal portion of duplicated organs, we inferred that invasion of mesenchymal cells between the duplicated medullary cords (located in the posterior midline) into the cloaca may make the septum. Furthermore, the leakage of growth power of caudal mesenchymal tissue into the space between the two medullary cords (and midline of the cloaca) may reduce the normal migrating power of mesenchymal cells along the lateral and caudal aspects of the medullary cord. It may result in imperforate anus or abdominal wall defect such as gastroschisis or bladder

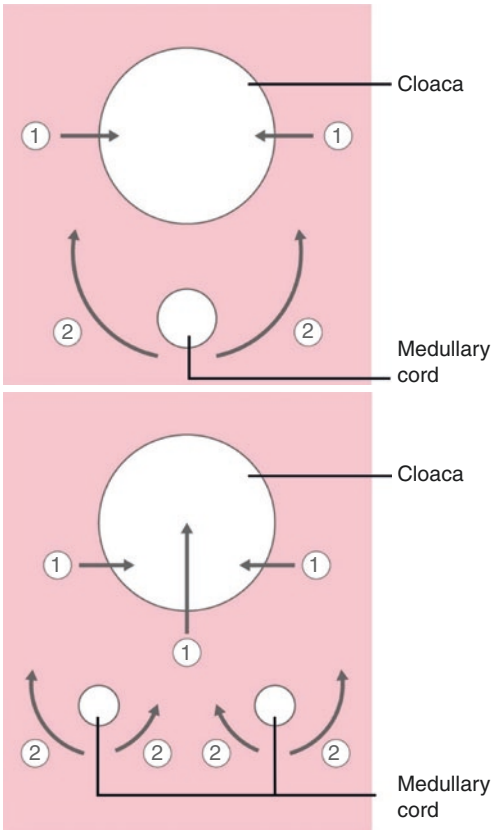

Fig. 9.12 A schematic drawing of the hindgut (including cloaca) and medullary cord during the anteroposterior division of the cloaca into the urogenital sinus and anorectal canal in the normal state (**a**) and in caudal duplication syndrome (CDupS) (**b**). The upper large circle indicates the cloaca, and the lower small circle(s) indicates the medullary cord. The arrow shows the movement of mesenchymal cells, whereas the length of the arrow indicates the power of the movement. Arrows numbered ① means the formation of the septum (normally urorectal septum, additional midline septum in CDupS) in the cloaca by the mesenchymal push from both lateral walls in normal development and from the posterior wall as well in CDupS. Arrows numbered ② indicate the ventral push of the caudal mesenchyme. Duplicated medullary cords give rise to an aberrant insertion of mesenchymal tissue between the two medullary cords at the midline (**b**), which causes abnormal midline septation of the cloaca (or hindgut). Note that the ventral push of the mesenchyme around the lateral sides of the medullary cords in CDupS (**b**) is weaker than that in the normal state (**a**) due to a leakage of mesenchymal growth power through the midline. Weak ventral push along the lateral sides of the cloaca makes the urorectal septum located more posteriorly than in the normal position, as in caudal agenesis, which may later result in an imperforate anus. (Reprinted from Yang et al. [30] with permission from Springer-Nature)

exstrophy which are also shown in caudal agenesis [27, 28] (Fig. 9.12). It is intriguing that CDupS shares common features with caudal agenesis in the case reports. This may implicate developmental errors at similar stages.

Experimental molecular studies have demonstrated the duplication or formation of ectopic primitive streaks in animals. In chick embryos, ectopic primitive streaks with embryonic delivery of the *Gata2* gene have been shown [37]. Chordin misexpression also led to an ectopic primitive streak [38]. *CYP26* gene was involved in duplication of the primitive streak [39].

In summary, duplication of the CCM that results from insult by molecular interaction at the late gastrulation phase may be a pathoembryogenetic mechanism. The leakage of caudal mesenchymal cells through the midline between the duplicated medullary cords may later form septa between the duplicated organs, whereas the deficient lateral and caudal mesenchymal movement caused by the mesenchymal leakage into the space between the two medullary cords may cause the anomalies shown in caudal agenesis including imperforate anus and ventral body wall defects.

9.6 Failed Ingression of the Primitive Streak to the CCM

Although ONTD has long been known as an anomaly resulting from the failure of primary neural tube closure, cases of myelomeningocele are found in the region of secondary neurulation, which is below the S1–S2 junction of the spinal cord. The typical morphology of the open type of skin is seen. Compared to 'classic' myelomeningocele, the rate of association with hydrocephalus or Chiari malformation is lower but the chance of retethering is known to be higher [40]. The elongated cord may have a cranial turn, to be attached to the skin defect as the neural placode (Fig. 9.13) or extend down through the sacral hiatus (Fig. 9.14). The former is similar to the morphology of the transitional type of LLM and the latter resembles the caudal type of LLM.

Although not as intuitive as the incomplete neurulation hypothesis during primary neurulation, various potential errors during secondary neurulation may bring about the ONTD. First, the formation of CCM from ingressed cells of the primitive streak may be considered. After the completion of ingression, the surface and the underlying CCM are disconnected. However, incomplete ingression may result in 'remnant' adhesion between the surface and the medullary cord (Fig. 9.3). Second, during the late phase of secondary neurulation, a structure called the 'terminal balloon' can be seen [41] (Fig. 9.4). If it does not degenerate and rupture, this may also result in ONTD. It should be noted that such 'rupture' of the terminal balloon with subsequent healing as a normal process has been described in chick embryos in the literature [42]. Arrest at this ruptured state may cause ONTD.

Interestingly, a recent study on junctional neurulation in chick embryos revealed that knockdown of a key gene, *Prickle*-1, resulted in the formation of an ONTD in the junctional region [3]. This study provides a clue that ONTD may be related to junctional neurulation.

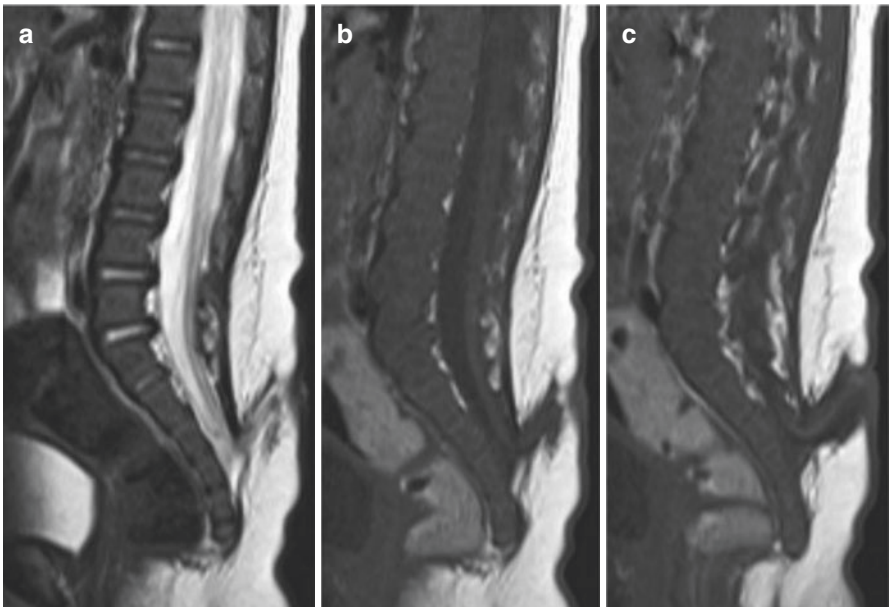

Fig. 9.13 A 2-month-old girl with a sacral myelomeningocele (MMC) who underwent a delayed operation. T2 (**a**) and T1 (**b**, **c**) MRI sagittal sections reveal a typical feature of an MMC at the level below S3. The distal spinal cord turns to the cranial side. (Reprinted from Yang et al. [2] with permission from the Korean Neurosurgical Society)

9.7 Focal Limited Dorsal Neuro-Cutaneous Nondisjunction

Congenital dermal sinus (CDS), a continuation of the surface squamous epithelium into the deeper layers of the body, is a well-known entity. Its potential catastrophic presentations have garnered the attention of clinicians, namely, neurologic deficits caused by intraspinal infection/inflammation or inclusion tumors. CDS is regarded as a result of failed normal disjunction between the primary neural tube and the cutaneous ectoderm during the process of primary neurulation, drawing the squamous epithelium-lined skin tissue to the neural side. Dermoid or epidermoid cysts may be formed at the stalk.

It was not rare to encounter patients who show stalks similar to CDS on magnetic resonance imaging (MRI), but have different types of skin lesions, frequently ‘closed’ flat cigarette-burn scars. Histological examination revealed fibroneural components and no squamous epithelial components in the stalk. In 2010, Pang et al. [43] introduced the term ‘limited dorsal myeloschisis (LDM)’ to these lesions and explained the pathoembryogenesis: failed normal disjunction between the primary neural tube and the cutaneous ectoderm like in CDS but pulling the neural tissue to the skin side, the direction opposite to that in CDS (Fig. 9.15). They classified LDMs into flat (noncystic) and cystic types.

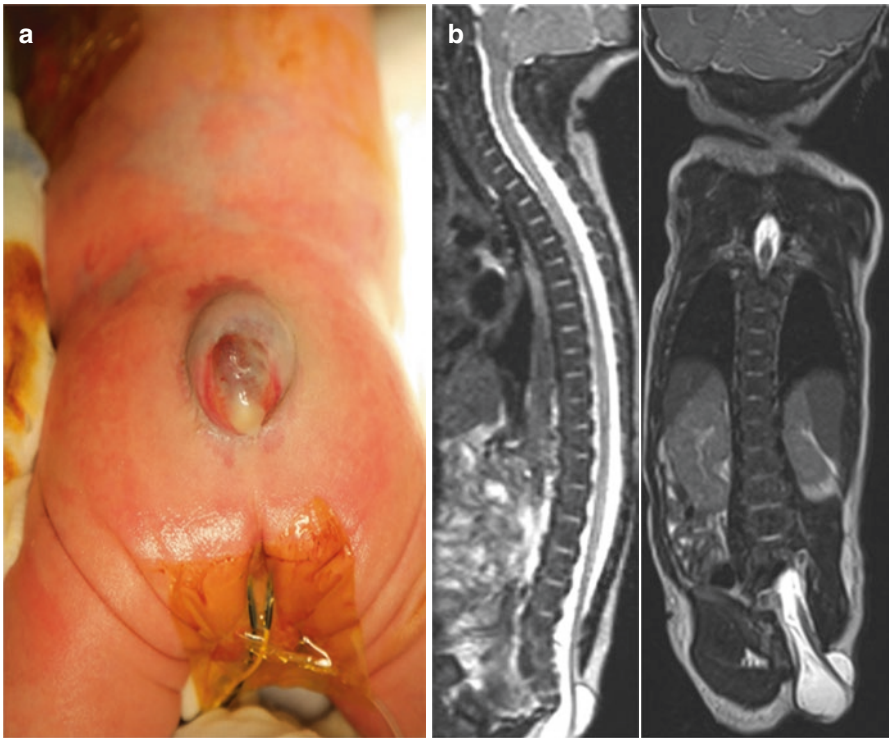

Fig. 9.14 A one-day-old girl with a low sacrococcygeal myelomeningocele. (**a**) A gross photo shows a cystic sac with a skin defect at the sacrococcygeal level. (**b**) T2 sagittal and coronal MRI sections demonstrate the low-lying cord protruding through the sacral hiatus going straight to the caudal skin defect area. (Reprinted from Yang et al. [2] with permission from the Korean Neurosurgical Society)

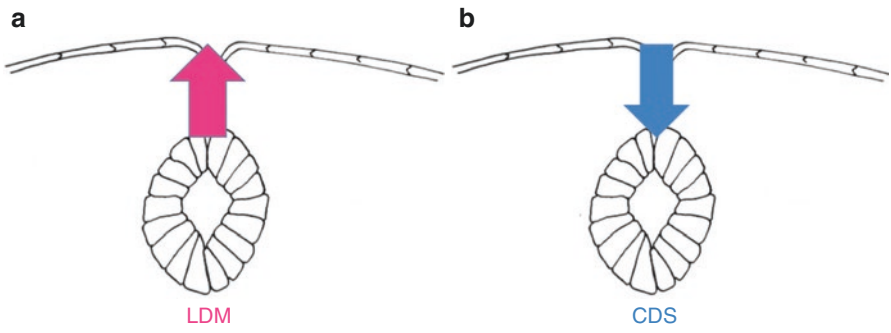

Fig. 9.15 A schematic drawing showing pathoembryogenesis of limited dorsal myeloschisis (LDM) versus congenital dermal sinus (CDS). The common basic error is the failed normal neurocutaneous disjunction during primary neurulation. If the neural tissue is pulled up to the skin side, it results in LDM (**a**), whereas if the cutaneous tissue is pulled down to the neural side, it leads to CDS (**b**). (Reprinted from Yang et al. [2] with permission from the Korean Neurosurgical Society)

Considering the common pathoembryogenesis of CDS and LDM, it is not surprising that there are cases showing both CDS and LDM, in serial or in parallel fashion [44] and they are collectively categorized within a spectrum as 'focal limited dorsal spinal neuro-cutaneous nondisjunction disorder' [45].

According to the pathoembryogenesis suggested by Pang et al. [43], LDM is believed to be an anomaly occurring during the process of primary neurulation only. However, we experienced cases of low-lying LDM as well as those in the area of the primary neural tube. Pang et al. [43] counted the level of LDM by the level of the vertebral body where the LDM stalk was attached to the dorsal spinal cord. We thought that this method of identifying the level of the lesion is not reasonable. We paid attention to the fact that the lumbosacral spinal nerve roots traverse a significant distance to exit from the spinal canal or enter into the spinal cord through the corresponding intervertebral foramen. The level of spinal roots is determined by the level of the intervertebral foramen, not by the level of the vertebral body where the roots contact the spinal cord. Likewise, we determined the level of LDM by the level of the interspinous ligament through which the LDM stalk passes.

It has been reported that the spinal cord below the S1–2 junction is formed by secondary neurulation only [8]. Therefore, LDM stalks passing through the interspinous ligament below S1–2 level can be assumed to attach to the spinal cord derived from the secondary neural tube.

In 2020, through the methods mentioned above, our team reported that approximately 40% (11/28) of all our LDMs were attached to the area of secondary neural tube [46] (Fig. 9.16). We could explain the pathoembryogenesis of the low level LDM by the continuity of CCM with the surface-located primitive streak in the early phase of CCM formation (Fig. 9.3). The abnormal persistence of the connection may cause LDM and CDS at the area of secondary neurulation. They are frequently associated with low-lying cords or tethering spinal lesions.

9.8 Neuro-Mesenchymal Adhesion

In 1982, LLMs of the conus were classified by Chapman [47] into three types (dorsal, transitional, and caudal). There were minor modifications: filar type, lipomyelomeningoceles (an extraspinal extension of the LLM with extraspinal herniation of the subarachnoid space), and chaotic type (involving a placode and roots) [48, 49].

Regarding the pathoembryogenesis of dorsal-type LLM, McLone and Naidich [50] proposed the 'premature disjunction theory' in 1985 that the unilateral premature focal separation of the neural fold into the future neuroectoderm and the future cutaneous ectoderm provides a chance for underlying mesenchymal tissue to enter into the developing primary neural tube. It was widely accepted and experimentally supported [51].

Although the pathoembryogenesis of dorsal-type LLM has been well-described, less attention has been given to the transitional, caudal, or filar type. For these types, we suggest 'neuro-mesenchymal adhesion' during secondary neurulation as the

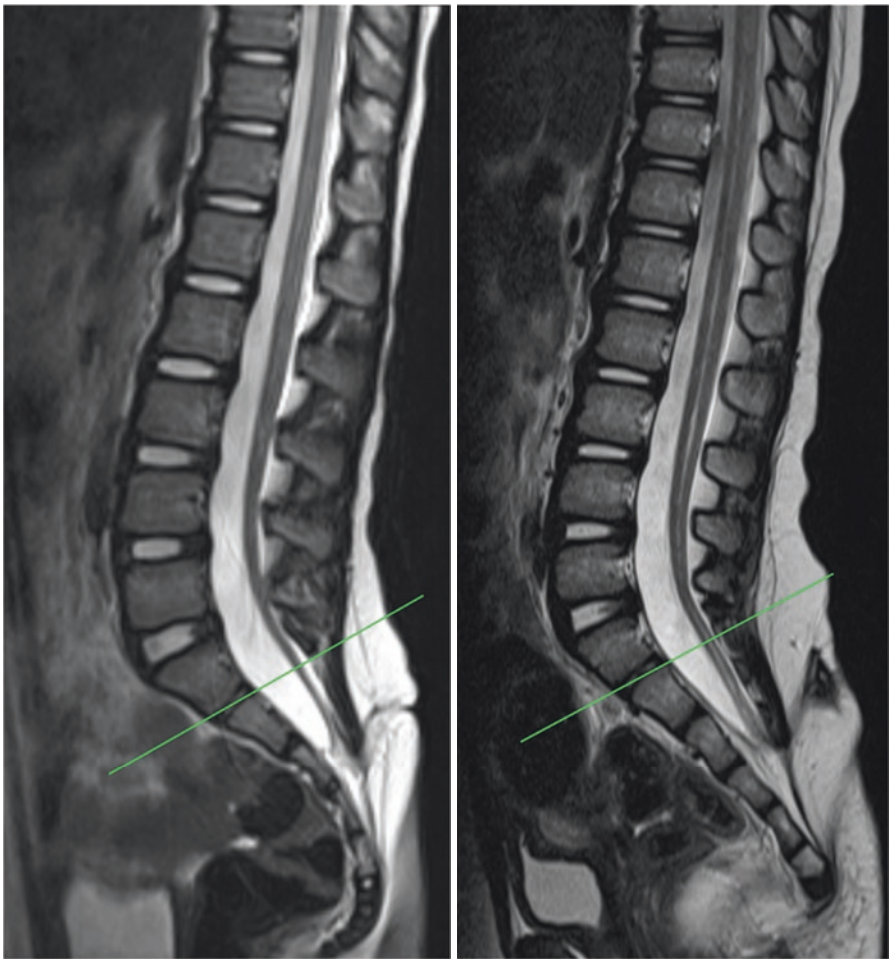

Fig. 9.16 Cases with a low-lying limited dorsal myeloschisis (LDM). The LDM stalks pass through the S3–4 interspinous ligament and are attached to the low-lying coni. The level of the stalks is counted as S3. (Reprinted from Yang et al. [2] with permission from the Korean Neurosurgical Society)

pathoembryogenetic mechanism. The fact that the main fat masses in LLMs are directly connected to subcutaneous fat in the majority of LLMs (except for pure intradural lipomas which are rare and prevalent at locations other than the lumbosacral area, and some filar-type LLMs) supports our speculation. Occasionally, isolated small satellite fat masses are found, but they are closely located to the main fat masses and seem to fall off from them. The subcutaneous fat extends into the spinal canal through the lamina defect (in dorsal and transitional types) or sacral hiatus (caudal type and some of filar type). These findings suggest neuro-mesenchymal adhesion rather than the aberrant differentiation of hidden CCM cell clusters in the

medullary cord into fat tissue as the pathoembryogenetic mechanism. If the multipotent cells of the CCM remain hidden in the medullary cord and differentiate into fat later, the continuity to the subcutaneous fat in almost all cases of transitional and caudal types cannot be explained.

Some minor modifications may be present. (1) If the spinal cord and subarachnoid space are herniated through the lamina defect, a lipomyelomeningocele (an extraspinal extension type) is formed. In some cases, only the spinal cord is herniated out (lipomyelocele). (2) The medullary cord and adhered mesenchymal tissue may pull each other. More frequently, the mesenchymal tissue is pulled into the neural side, but occasionally, the spinal cord can be pulled out to the subcutaneous fat, especially in the extraspinal extension type where the traction force is increased by the protruding dome of the skin. (3) Frequently, the adhesion site is off the midline, and the developing laminae from both sides push the adhesion site to the midline rotating the spinal cord. On the other hand, enlargement of the fat mass, especially in early infancy, may push and rotate the cord to the opposite direction. (4) Small fragments may chip off, especially when the connection between the medullary cord and mesenchymal tissue is thin, as shown in the filar type.We do not know why the neuro-mesenchymal adhesion occurs. As described above, abnormal continuity between the CCM and the surface-located primitive streak may bring about nondisjunctional anomalies such as ONTD, LDM, or CDS. We may imagine that the medullary cord may abnormally adhere to the mesenchymal tissue through focal defects in the basement membrane, although the CCM have normally been separated from the surface-located primitive streak. However, we do not have experimental supports yet.

9.8.1 Transitional Type

The transitional type may be the result of adhesion between the dorsal surface of the medullary cord and the surrounding mesenchymal tissue. Because the mesenchymal tissue of the early phase may include multipotent cells of the CCM, it is not surprising that fat tissue may have various mesenchymal components such as muscle, cartilage, bone, blood vessels, and even renal tissue [52, 53] as well as peripheral nerve twigs from the adjacent neural crest.

In the early phase of secondary neurulation, the secondary neural tube is formed at the midline just distal to Hensen's node and occupies the space between the bilaterally located neural plates of the primary neural tube. Then, it elongates to the caudal direction [3, 4] (Fig. 9.1). When neuro-mesenchymal adhesion occurs at this place of early secondary neurulation (immediate caudal part of Hensen's node), the closure of the caudal neural placodes of the primary neural tube is disturbed. Consequently, the dorsal neuro-adipose connection may extend up along the midline between the laterally located neural plates beyond the normal caudodorsal end of the primary neural tube (the junction of S1 and S2 spinal cord segments).

Dorsal adhesion to mesenchymal tissue in transitional-type LLMs may extend down to the caudal end of the fully formed (before beginning regression) medullary cord. A wide contact area between the medullary cord and the mesenchymal tissue increases the chance of multiple fat masses as previously reported [54].

9.8.2 Caudal Type

If most of the medullary cord is well-formed and only the caudal end of the medullary cord is attached to the caudal mesenchymal tissue pulling the abnormal neuromesenchymal adhesion site to the neural side through the sacral hiatus without formation of the normal filum, a caudal-type LLM is formed (Fig. 9.17).

9.8.3 Filar Type

If the neuro-mesenchymal connection in the caudal type is thin and the regression of the distal medullary cord progresses well (or close to normal), the product may be the filar-type LLM. When the fat tissue is slender, parts of the fat tissue may easily fall off from the main fat mass, forming satellite lesions.

Because the filar-type LLM is formed at the late phase of secondary neurulation, the dorsal part of the medullary cord is normally formed. Therefore, only the distal end of the medullary cord is involved. The small focal fat masses in the filum never have connections to the dorsal subcutaneous fat tissue through the laminar defect or interspinous ligament.

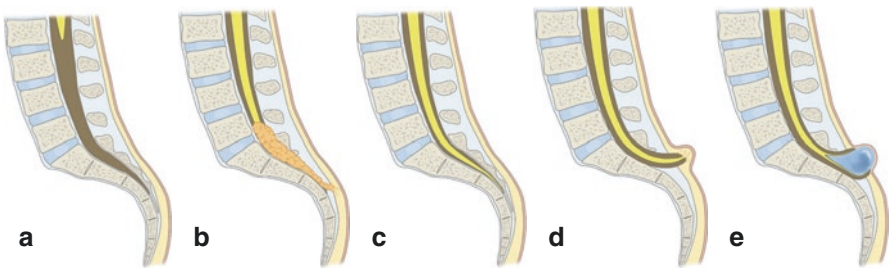

Fig. 9.17 A schematic drawing demonstrating relationship among the caudal-type lumbosacral lipomatous malformation (LLM), retained medullary cord (RMC), terminal myelocele (TMC), and terminal myelocystocele (TMCC). (**a**) A normal caudal spinal cord. (**b**) If the site of neuromesenchymal adhesion at the caudal end of the medullary cord is pulled into the spinal canal through the sacral hiatus, it results in LMM of the caudal type. (**c**) When abnormal neuromesenchymal adhesion occurs but there is no traction of adhesion site into the neural side, it may cause typical RMC. (**d**, **e**) If the spinal cord is pulled out to the extraspinal side, a TMC (if the terminal balloon collapses, **d**) or a TMCC (if the terminal balloon persists, **e**) is formed. (Reprinted from Yang et al. [2] with permission from the Korean Neurosurgical Society)

9.9 Regression Failure Spectrum of the Medullary Cord

'Failure of formation' and 'failure of regression' are two types of mechanisms in spinal cord anomalies caused by defects in secondary neurulation. Based on the timing during each phase, different entities are assumed to emerge. Every disease entity described here appears during the regression phase, which occurs later in secondary neurulation.

9.9.1 Filar Lesion

The normal filum is a strand of thin elastic tissue continuous from the tip of the conus medullaris to the coccyx. If fat or fibrous tissue replaces glial tissue in the filum, it may form a fatty filum or thickened filum terminale. The pathological filum can lose its elasticity, causing the spinal cord to become abnormally tethered. Ion channel dysfunction is closely related to neuronal membrane deformity, and spinal cord traction can induce disrupted microcirculation and oxidative metabolism of neural tissue [55–57]. Gait disturbances, pain, sensory deficits, urological dysfunction, scoliosis, and foot deformities are all possible symptoms. Filar lesions are found by chance in 0.24–6% of the general population [58–60]. Surgery is recommended if symptoms occur, and prophylactic surgery can be performed before symptoms arise. Symptoms are reduced or stabilized in 88% of patients after surgery, and retethering may occur in up to 5% of patients [61, 62].

Filar cysts are generally asymptomatic and do not pose any harm (Fig. 9.18). On follow-up, filar cysts can remain unchanged, diminish, or even vanish, indicating arrested or delayed regression as the pathoembryogenesis. An isolated filar cyst is a benign condition that does not require surgery [63].

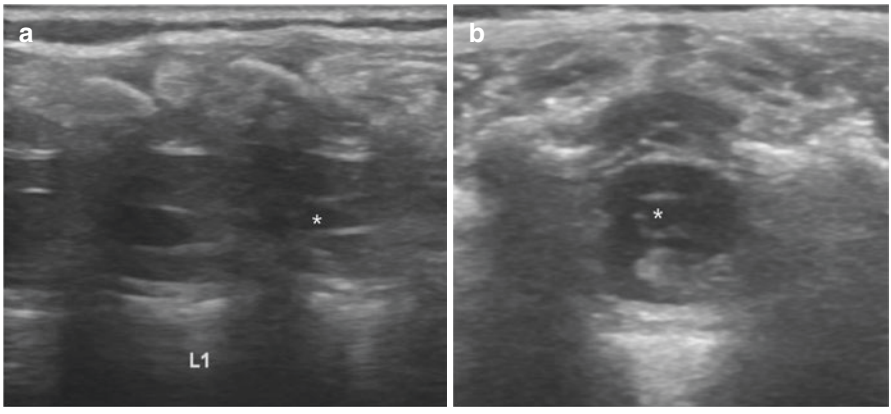

Fig. 9.18 Sagittal (**a**) and axial (**b**) sonographic images of a 6-month old boy show a filar cyst immediately below the conus medullaris as a hypoechoic cyst (asterisk). (Reprinted from Yang et al. [2] with permission from the Korean Neurosurgical Society)

9.9.2 *Retained Medullary Cord (RMC)*

Pang et al. [64] coined the word 'RMC' to describe a spinal cord with a functionless part that runs all the way down to the cul-de-sac. The RMC is thought to be a medullary cord that has remained in place as a result of regression failure in secondary neurulation.

In RMC, MRI can detect the descent of the conus medullaris from its normal location. However, IONM testing for the existence of a caudal nonfunctional segment is needed to verify the diagnosis.

An RMC was originally described as a spinal cord that continues to the cul-de-sac without development of the thin filum terminale. On the other hand, Kim et al. [65] proposed that if there is a part of a nonfunctional distal cord, it may be an RMC even when the tip of the conus is not attached to the cul-de-sac. An RMC is a spinal cord with a nonfunctional portion in the distal conus, according to their definition no matter where the end of the conus is located (Fig. 9.19).

Many of the patients previously diagnosed with a low-lying conus are considered to have nonfunctional parts as well as cysts or fat masses. They could be considered

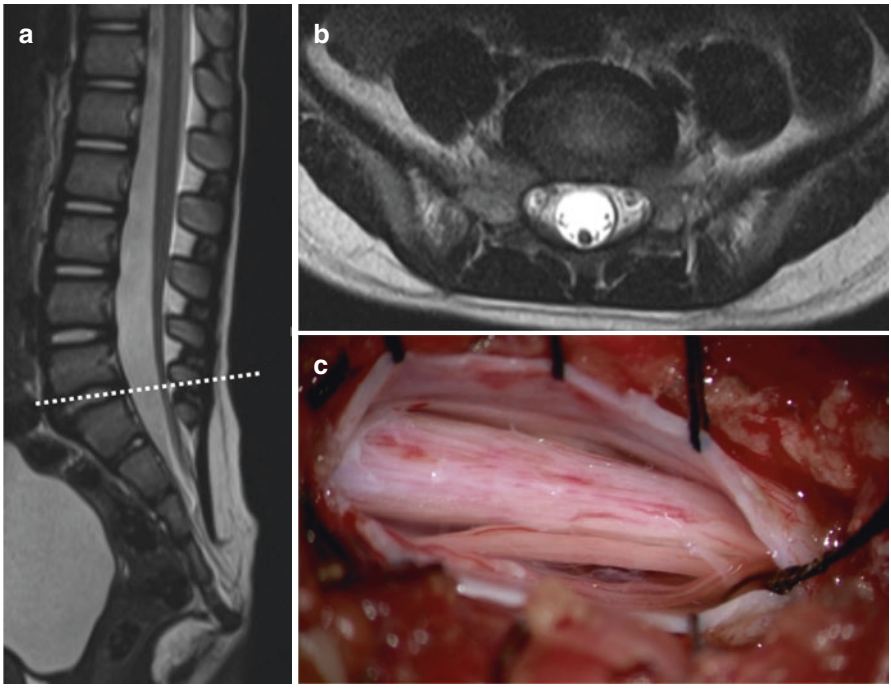

Fig. 9.19 MRI images and an intraoperative photograph in a patient with retained medullary cord (RMC). (**a**) In a T2 sagittal image, a cord-like structure was extended to the sacral area. (**b**) T2 axial images at L5–S1 level (dotted line in **a**) show a tapering spinal cord or a thick filum. (**c**) Left L5 partial hemilaminectomy reveals an RMC passing through. (Reprinted from Kim et al. [65] by permission from the Korean Neurosurgical Society)

as ‘probable RMC’ if the area of interest (distal conus) was not explored by IONM [65].

An RMC is thought to be triggered by a halt in regression during the secondary neurulation process. However, there is no straightforward reason why this arrest occurs. Many animal studies have indicated that apoptosis is the mechanism of medullary cord regression. As a result, if ‘apoptosis’ does not occur when it should, it can result in the formation of an RMC [7, 14, 66].

The clinical symptoms may include motor deficits, foot deformities, neurogenic bladder and bowel, frequent urinary tract infection, dysesthesia, leg pain, and coccydynia. Surgery is required if the patient has symptoms. In some cases, even if the patient does not have symptoms, surgery may be performed to prevent neurological events. IONM must be combined during surgery for definite diagnosis. RMC seems to have a favorable prognosis when safe and complete untethering is accomplished with IONM [67, 68].

9.9.3 Terminal Myelocele (TMC)

TMC is a skin-covered spinal dysraphism in which the spinal cord herniates along laminar and fascial defects, similar to terminal myelocystocele (TMCC). However, there is no trumpet-like flaring, which is a terminal syringomyelic dilatation seen in TMCC. Only an expanded subarachnoid space and a herniated spinal cord and roots are responsible for the cystic contents (Fig. 9.20 left). Except for the collapse of terminal balloons, this entity has the same pathoembryogenetic background as TMCC. TMC may be considered one of the extraspinal forms of LLM because the spinal cord is attached to the subcutaneous fat tissue.

9.9.4 Terminal Myelocystocele (TMCC)

The syringomyelic distal spinal cord and the enlarged subarachnoid space are herniated through the posterior laminar and fascial defects and covered by the skin in TMCC, a rare case of spinal dysraphism.

There are essential and nonessential features in TMCC. The caudal spinal cord, which extends out of the spinal canal, is an essential feature. The end of the spinal cord is adhered to the subcutaneous fat and is flared like a trumpet [69]. If the distal spinal cord lacks a syringomyelic cavity but has the other characteristics mentioned above, it is a TMC.

The pathoembryogenesis of TMCC is also regarded as a defect of secondary neurulation. Using chick embryos, Lee et al. [41] showed the embryological background. Normally, a ‘terminal balloon’ develops at the caudal tip of the medullary cord during secondary neurulation. The distal end (dome) of the balloon is adhered to the skin of the chick embryo. It had the same appearance as TMCC (Figs. 9.4 and

9.20 right). The terminal balloon then collapses and detaches from the skin as time passes. Schumacher [42] characterized the rupture and healing of the terminal balloon in chick embryos as a normal process. TMCC is thought to be the result of regression arrest when the terminal balloon is attached to the skin.

Anomalies that may be associated with TMCC include imperforate anus, ambiguous genitalia, omphalocele, bladder exstrophy, and sacral bony abnormalities. These abnormalities come as no surprise when TMC and TMCC are regarded as

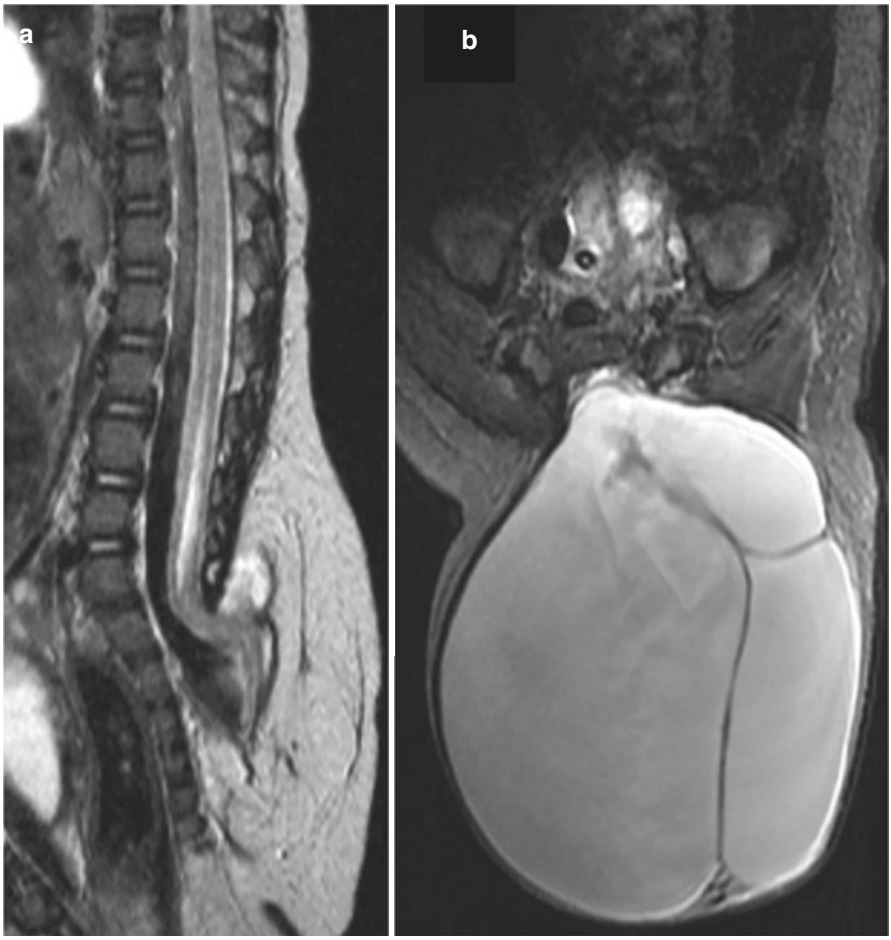

Fig. 9.20 MRI images of terminal myelocele (TMC) (**a**) and terminal myelocystocele (TMCC) (**b**). (**a**) A T2 sagittal MRI image of a case with TMC shows extraspinal herniation of the spinal cord through the laminar and fascial defects. Trumpet-like flaring is not seen. (**b**) A T2 axial MRI image demonstrates a terminal dilatation of the central canal as the trumpet-like flaring. The shape is similar to the 'terminal balloon' shown in Fig. 9.4b. (**a**) Reprinted from Lee et al. [41] with permission from Springer-Nature, (**b**) reprinted from Yang et al. [2] with permission from the Korean Neurosurgical Society

extraspinal variations of caudal-type LLM (type III by Morota et al. [54]) in which anorectal and urogenital anomalies may be associated. TMC or TMCC may be an associated spinal cord lesion of 'failure of regression' type in caudal agenesis. Hydrocephalus can also be combined.

A tethered cord is clearly made by a TMCC. However, the signs and symptoms can go unnoticed at first. Neurological deterioration can occur gradually, but if the cyst grows exponentially, neurological deterioration can occur unimaginably quickly due to the end of the spinal cord that is connected to the cyst dome being pulled away. Therefore, early repair with resection is advised. The cyst enlargement tends to occur in younger patients. Caution is needed for patients in infancy [70, 71]. IONM is needed for maximum elimination of the nonfunctioning cord during surgery for successful untethering and prevention of retethering.

A schematic drawing showing a spectrum of caudal-type LLM, RMC, TMC, and TMCC is shown in Fig. 9.17.

9.10 Conclusion

Secondary neurulation has its own characteristics, differing from primary neurulation: such as the need for a functional junction with the primary neural tube, a relatively absent neural-inductive role of the notochord, relation to the skin and caudal mesenchyme or the caudal endoderm and the presence of a regressive phase. Disordered secondary neurulation at each phase may cause various corresponding lesions, such as (1) failed junction with the primary neural tube (JNTD and SSD), (2) dysgenesis or duplication of the CCM associated with disturbed activity of caudal mesenchymal tissue (caudal agenesis and CDupS), (3) abnormal continuity of the medullary cord to the surrounding layers, namely, failed ingression of the primitive streak to the CCM (myelomeningocele), focal limited dorsal neuro-cutaneous nondisjunction (LDM and CDS), and neuro-mesenchymal adhesion (LLM), and (4) regression failure spectrum of the medullary cord (thickened filum and filar cyst, RMC and low-lying conus, TMC and TMCC). We found that almost every anomalous entity of primary neurulation can occur at the area of secondary neurulation even though the pathoembryogenetic mechanisms are different. Furthermore, the close association of CCM with the activity of caudal mesenchymal tissue involves a wider range of surrounding structures than in primary neurulation. However, we do not exclude the possibility that multiple anomalies are caused by some molecular events or other primary events rather than by interactions among the structures involved as we suggested in this chapter.

Advanced knowledge of secondary neurulation and its application to the interpretation of the morphological features in patients have led to updates in the classification of anomalous lesions in this area. Further revision of the classification in spinal dysraphism is expected in the near future.

References

1. Wang K-C. Spinal dysraphism in the last two decades: what I have seen during the era of dynamic advancement. J Korean Neurosurg Soc. 2020;63(3):272–8.
2. Yang J, Lee JY, Kim KH, Wang K-C. Disorders of secondary neurulation: mainly focused on pathoembryogenesis. J Korean Neurosurg Soc. 2021;64(3):386–405.
3. Dady A, Havis E, Escriou V, Catala M, Duband J-L. Junctional neurulation: a unique developmental program shaping a discrete region of the spinal cord highly susceptible to neural tube defects. J Neurosci. 2014;34(39):13208–21.
4. Shimokita E, Takahashi Y. Secondary neurulation: fate-mapping and gene manipulation of the neural tube in tail bud. Dev Growth Differ. 2011;53(3):401–10.
5. Yang H-J, Wang K-C, Chi JG, Lee M-S, Lee Y-J, Kim S-K, et al. Neural differentiation of caudal cell mass (secondary neurulation) in chick embryos: Hamburger and Hamilton stages 16–45. Dev Brain Res. 2003;142(1):31–6.
6. Lemire RJ. Variations in development of the caudal neural tube in human embryos (horizons XIV–XXI). Teratology. 1969;2(4):361–9.
7. Hughes A, Freeman R. Comparative remarks on the development of the tail cord among higher vertebrates. Development. 1974;32(2):355–63.
8. Müller F, O'Rahilly R. The development of the human brain, the closure of the caudal neuropore, and the beginning of secondary neurulation at stage 12. Anat Embryol. 1987;176(4):413–30.
9. Saitsu H, Yamada S, Uwabe C, Ishibashi M, Shiota K. Development of the posterior neural tube in human embryos. Anat Embryol. 2004;209(2):107–17.
10. Yang H-J, Lee D-H, Lee Y-J, Chi JG, Lee JY, Phi JH, et al. Secondary neurulation of human embryos: morphological changes and the expression of neuronal antigens. Childs Nerv Syst. 2014;30(1):73–82.
11. Yang H-J, Wang K-C, Chi JG, Lee M-S, Lee Y-J, Kim S-K, et al. Cytokinetics of secondary neurulation in chick embryos: Hamburger and Hamilton stages 16–45. Childs Nerv Syst. 2006;22(6):567–71.
12. Schoenwolf GC. Histological and ultrastructural observations of tail bud formation in the chick embryo. Anat Rec. 1979;193(1):131–47.
13. Schoenwolf GC. Morphogenetic processes involved in the remodeling of the tail region of the chick embryo. Anat Embryol. 1981;162(2):183–97.
14. Mills C, Bellairs R. Mitosis and cell death in the tail of the chick embryo. Anat Embryol. 1989;180(3):301–8.
15. Hamburger V. The mitotic patterns in the spinal cord of the chick embryo and their relation to histogenetic processes. J Comp Neurol. 1948;88(2):221–83.
16. Wang K-C, Park I-S, Chi JG, Lee M-S, Lee Y-J, Cho B-K. Cytokinetic pattern in the thoracic spinal cord of chick embryos (incubation day 5–13) using PCNA staining and TUNEL method. J Korean Med Sci. 1998;13:405–13.
17. Grüneberg H. The pathology of development: a study of inherited disorders in animals. Oxford: Blackwell; 1963.
18. Fallon JF, Simandl BK. Evidence of a role for cell death in the disappearance of the embryonic human tail. Am J Anat. 1978;152(1):111–29.
19. Wang K-C. Perspectives: the role of clinicians in understanding secondary neurulation. J Korean Neurosurg Soc. 2021;64(3):414–7.
20. Eibach S, Moes G, Hou YJ, Zovickian J, Pang D. Unjoined primary and secondary neural tubes: junctional neural tube defect, a new form of spinal dysraphism caused by disturbance of junctional neurulation. Childs Nerv Syst. 2017;33(10):1633–47.
21. Scott RM, Wolpert SM, Bartoshesky LE, Zimbler S, Karlin L. Segmental spinal dysgenesis. Neurosurgery. 1988;22(4):739–44.
22. Wang K-C, Lee JS, Kim K, Im YJ, Park K, Kim KH, et al. Do junctional neural tube defect and segmental spinal dysgenesis have the same pathoembryological background? Childs Nerv Syst. 2020;36(2):241–50.

23. Criley BB. Analysis of the embryonic sources and mechanisms of development of posterior levels of chick neural tubes. J Morphol. 1969;128(4):465–501.
24. Balioğlu MB, Akman YE, Ucpunar H, Albayrak A, Kargın D, Atıcı Y, et al. Sacral agenesis: evaluation of accompanying pathologies in 38 cases, with analysis of long-term outcomes. Childs Nerv Syst. 2016;32(9):1693–702.
25. Denton JR. The association of congenital spinal anomalies with imperforate anus. Clin Orthop Relat Res. 1982;162:91–8.
26. Nour S, Kumar D, Dickson J. Anorectal malformations with sacral bony abnormalities. Arch Dis Child. 1989;64(11):1618–20.
27. Pang D. Sacral agenesis and caudal spinal cord malformations. Neurosurgery. 1993;32(5):755–79.
28. Lee JY, Pang D, Wang K-C. Caudal agenesis and associated spinal cord malformations. In: Di Rocco C, Pang D, Rutka JT, editors. Textbook of pediatric neurosurgery. Cham: Springer International; 2020. p. 2557–75.
29. Dominguez R, Rott J, Castillo M, Pittaluga RR, Corriere JN. Caudal duplication syndrome. Am J Dis Child. 1993;147(10):1048–52.
30. Yang J, Kim KH, Lee JY, Wang K-C. Caudal duplication syndrome: a literature review and reappraisal of its pathoembryogenesis. Childs Nerv Syst. 2021;37(8):2577–87. https://doi.org/10.1007/s00381-021-05166-z.
31. Acer T, Ötgün İ, Akıllı MS, Gürbüz EE, Güney LH, Hiçsönmez A. A newborn with caudal duplication and duplex imperforate anus. J Pediatr Surg. 2013;48(5):e37–43.
32. Al Alayet YF, Samujh R, Lyngdoh TS, Mansoor K, Al Kasim F, Al-Mustafa AA. An extremely rare case of classic complete caudal duplication: dipygus. J Indian Assoc Pediatr Surg. 2014;19(3):169–71.
33. Bannykh SI, Bannykh GI, Mannino FL, Jones KL, Hansen L, Benirschke K, et al. Partial caudal duplication in a newborn associated with meningomyelocele and complex heart anomaly. Teratology. 2001;63(2):94–9.
34. Sur A, Sardar SK, Paria A. Caudal duplication syndrome. J Clin Neonatol. 2013;2(2):101–2.
35. Bansal G, Ghosh D, George U, Bhatti W. Unusual coexistence of caudal duplication and caudal regression syndromes. J Pediatr Surg. 2011;46(1):256–8.
36. Moore KL, Persaud TVN, Torchia MG. The developing human-e-book: clinically oriented embryology. Amsterdam: Elsevier Health Sciences; 2018.
37. Bertocchini F, Stern CD. Gata2 provides an early anterior bias and uncovers a global positioning system for polarity in the amniote embryo. Development. 2012;139(22):4232–8.
38. Streit A, Lee KJ, Woo I, Roberts C, Jessell TM, Stern CD. Chordin regulates primitive streak development and the stability of induced neural cells, but is not sufficient for neural induction in the chick embryo. Development. 1998;125(3):507–19.
39. Uehara M, Yashiro K, Takaoka K, Yamamoto M, Hamada H. Removal of maternal retinoic acid by embryonic CYP26 is required for correct nodal expression during early embryonic patterning. Genes Dev. 2009;23(14):1689–98.
40. Lee JY, Kim KH, Park K, Wang K-C. Retethering: a neurosurgical viewpoint. J Korean Neurosurg Soc. 2020;63(3):346–57.
41. Lee JY, Kim SP, Kim SW, Park S-H, Choi JW, Phi JH, et al. Pathoembryogenesis of terminal myelocystocele: terminal balloon in secondary neurulation of the chick embryo. Childs Nerv Syst. 2013;29(9):1683–8.
42. Schumacher S. Über Bildungs-und Rückbildungsvorgänge am Schwanzende des Medullarrohres bei älteren Hühnerembryonen mit besonderer Berücksichtigung des Auftretens eines sekundären hinteren Neuroporus. Z Mikrosk Anat Forsch. 1928;13:269–327.
43. Pang D, Zovickian J, Oviedo A, Moes GS. Limited dorsal myeloschisis: a distinctive clinicopathological entity. Neurosurgery. 2010;67(6):1555–80.
44. Lee JY, Park S-H, Chong S, Phi JH, Kim S-K, Cho B-K, et al. Congenital dermal sinus and limited dorsal myeloschisis: “spectrum disorders” of incomplete dysjunction between cutaneous and neural ectoderms. Neurosurgery. 2019;84(2):428–34.

45. Wong ST, Kan A, Pang D. Limited dorsal spinal nondisjunctional disorders: limited dorsal myeloschisis, congenital spinal dermal sinus tract, and mixed lesions. In: Di Rocco C, Pang D, Rutka JT, editors. Textbook of pediatric neurosurgery. Cham: Springer International; 2020. p. 2365–422.
46. Kim JW, Wang K-C, Chong S, Kim S-K, Lee JY. Limited dorsal myeloschisis: reconsideration of its embryological origin. Neurosurgery. 2020;86(1):93–100.
47. Chapman PH. Congenital intraspinal lipomas. Pediatr Neurosurg. 1982;9(1):37–47.
48. Arai H, Sato K, Okuda O, Miyajima M, Hishii M, Nakanishi H, et al. Surgical experience of 120 patients with lumbosacral lipomas. Acta Neurochir. 2001;143(9):857–64.
49. Pang D, Zovickian J, Oviedo A. Long-term outcome of total and near-total resection of spinal cord lipomas and radical reconstruction of the neural placode: part I—surgical technique. Neurosurgery. 2009;65(3):511–29.
50. McLone DG, Naidich TP. Spinal dysraphism: experimental and clinical. The tethered spinal cord. New York: Thieme-Stratton; 1985. p. 14–28.
51. Li YC, Shin S-H, Cho B-K, Lee M-S, Lee Y-J, Hong S-K, et al. Pathogenesis of lumbosacral lipoma: a test of the 'premature dysjunction' theory. Pediatr Neurosurg. 2001;34(3):124–30.
52. Griffith C, Sanders EJ. Effects of extracellular matrix components on the differentiation of chick embryo tail bud mesenchyme in culture. Differentiation. 1991;47(2):61–8.
53. Griffith C, Wiley M. Direct effects of retinoic acid on the development of the tail bud in chick embryos. Teratology. 1989;39(3):261–75.
54. Morota N, Ihara S, Ogiwara H. New classification of spinal lipomas based on embryonic stage. J Neurosurg Pediatr. 2017;19(4):428–39.
55. Yamada S, Won DJ, Pezeshkpour G, Yamada BS, Yamada SM, Siddiqi J, et al. Pathophysiology of tethered cord syndrome and similar complex disorders. Neurosurg Focus. 2007;23(2):1–10.
56. Yamada S, Won DJ, Yamada SM. Pathophysiology of tethered cord syndrome: correlation with symptomatology. Neurosurg Focus. 2004;16(2):1–5.
57. Yamada S, Zinke DE, Sanders D. Pathophysiology of "tethered cord syndrome". J Neurosurg. 1981;54(4):494–503.
58. Al-Omari MH, Eloqayli HM, Qudseih HM, Al-Shinag MK. Isolated lipoma of filum terminale in adults: MRI findings and clinical correlation. J Med Imaging Radiat Oncol. 2011;55(3):286–90.
59. Brown E, Matthes JC, Bazan C III, Jinkins JR. Prevalence of incidental intraspinal lipoma of the lumbosacral spine as determined by MRI. Spine. 1994;19(7):833–6.
60. Emery JL, Lendon R. Lipomas of the cauda equina and other fatty tumours related to neurospinal dysraphism. Dev Med Child Neurol. 1969;20:62–70.
61. Finger T, Schaumann A, Grillet F, Schulz M, Thomale U-W. Retethering after transection of a tight filum terminale, postoperative MRI may help to identify patients at risk. Childs Nerv Syst. 2020;36(7):1499–506.
62. Ostling LR, Bierbrauer KS, Kuntz C IV. Outcome, reoperation, and complications in 99 consecutive children operated for tight or fatty filum. World Neurosurg. 2012;77(1):187–91.
63. Irani N, Goud AR, Lowe LH. Isolated filar cyst on lumbar spine sonography in infants: a case-control study. Pediatr Radiol. 2006;36(12):1283–8.
64. Pang D, Zovickian J, Moes GS. Retained medullary cord in humans: late arrest of secondary neurulation. Neurosurgery. 2011;68(6):1500–19.
65. Kim KH, Lee JY, Wang K-C. Secondary neurulation defects-1: retained medullary cord. J Korean Neurosurg Soc. 2020;63(3):314–20.
66. Griffith CM, Wiley M, Sanders EJ. The vertebrate tail bud: three germ layers from one tissue. Anat Embryol. 1992;185(2):101–13.
67. Pang D, Chong S, Wang K-C. Secondary neurulation defects-1: thickened filum terminale, retained medullary cord. In: Di Rocco C, Pang D, Rutka JT, editors. Textbook of pediatric neurosurgery. Cham: Springer International; 2020.
68. Sala F, Barone G, Tramontano V, Gallo P, Ghimenton C. Retained medullary cord confirmed by intraoperative neurophysiological mapping. Childs Nerv Syst. 2014;30(7):1287–91.

69. Pang D, Zovickian J, Lee JY, Moes GS, Wang K-C. Terminal myelocystocele: surgical observations and theory of embryogenesis. Neurosurgery. 2012;70(6):1383–405.
70. Kim KH, Wang K-C, Lee JY. Enlargement of extraspinal cysts in spinal dysraphism: a reason for early untethering. J Korean Neurosurg Soc. 2020;63(3):342–5.
71. Lee JY, Phi JH, Kim S-K, Cho B-K, Wang K-C. Urgent surgery is needed when cyst enlarges in terminal myelocystoceles. Childs Nerv Syst. 2011;27(12):2149–53.
72. Pang D, Wang K-C. Terminal myelocystocele reply. Neurosurgery. 2013;72(4):E698–700.
73. Harris J, Blackwood B, Pillai S, Kanard R. Caudal duplication: management of a rare congenital condition. Am Surg. 2016;82(9):E227–9.

Chapter 10
The Management of Idiopathic and Refractory Syringomyelia

Pasquale Gallo and Chandrasekaran Kaliaperumal

10.1 Introduction

Tsz-Lu asked to the Master: "As the prince of Wei, sir, has been waiting for you to act for him in his government, what is it your intention to take in hand first?", and the master answered: "One thing of necessity, the rectification of terms" [1]. This sentence from the Analects of Confucius seems perfect to introduce this very controversial topic.

Syringomyelia is a term used to describe a fluid-filled cavity within the spinal cord. This disorder does not usually constitute a disease in its own right, but it is rather a sign of another underlying condition which typically involves an obstruction of the cerebrospinal fluid (CSF) pathways caused by pathologies such as Chiari 1 malformation (CM1), a cranio-cervical junction (CCJ) anomaly, a spinal cord tumor, a spinal degenerative pathology, a posttraumatic, posthemorrhagic or postinfective arachnoiditis, a spinal tethered cord, or a craniosynostosis [2–19].

However, not every fluid-filled cavity in the spinal cord deserves the diagnosis of syringomyelia. For example, cystic spinal cord tumors, glioependymal cysts, myelomalacias, and central cord cavitation (sometimes called hydromyelia) should be distinguished from the syringomyelia [7, 9].

P. Gallo (✉)
Department of Paediatric Neurosurgery, Birmingham Women's and Children's NHS Foundation Trust, Birmingham, UK
e-mail: pasquale.gallo@nhs.net

C. Kaliaperumal
Department of Clinical Neurosciences, Edinburgh BioQuarter, Royal Infirmary Edinburgh, Edinburgh, UK
e-mail: chandrasekaran.kaliaperumal@nhslothian.scot.nhs.uk

C. Di Rocco (ed.), *Advances and Technical Standards in Neurosurgery*, Advances and Technical Standards in Neurosurgery 45,
https://doi.org/10.1007/978-3-030-99166-1_10

When the cause of the syringomyelia is identified and correctly treated, the syringomyelia usually regresses and the symptoms improve or do not deteriorate. If the underlying condition is unknown, the syringomyelia is classified as idiopathic.

Until the recent introduction of the magnetic resonance imaging (MRI) as routine diagnostic tool, syringomyelia was diagnosed as idiopathic in the majority of the cases [20]. Nowadays, employing high resolution MRI and a specific sequence such as the cardiac-gated cine-MRI to study spinal CSF flow, areas of flow obstruction, and turbulence which may correspond to circumscribed arachnoid pathologies can be identified [21].

Nonetheless, in clinical practice, nearly 40% of patients presenting with syringomyelia will be still diagnosed as having an idiopathic syringomyelia (IS) [21]. In the pediatric population, about 50% of children diagnosed with IS present with a concomitant scoliosis [22]. Some authors have reported cases of IS with neurological symptoms and signs consistent with CM-1 [6], but without cerebellar tonsillar descent where the foramen magnum decompression improved patients' clinical symptoms and syringomyelia radiological appearance; hence they suggested to define the condition as Chiari 0 malformation [10, 22].

The topic is controversial, vast, and confused. This is mainly due to the heterogeneity of the underlying conditions, the interchanged terminology of syringomyelia with hydromyelia often used in the publications, the different methods employed to determine when the condition is idiopathic, the treatment options proposed, and the outcome measures.

Even when the syringomyelia has a defined cause and the main condition is treated, like in patients with CM-1, the syringomyelia may fail to resolve, can deteriorate or recur after an initial shrinkage in up to 66% of the cases [20, 23, 24]. We define such syringomyelia as refractory syringomyelia.

This chapter will first try to clarify when a syringomyelia can be truly defined as idiopathic and subsequently it will focus on the management of syringomyelia refractory to previous surgery, proposing an algorithm of treatment for both these challenging clinic-radiological conditions. In the final part, a description of the neurosurgical armamentarium available to manage the idiopathic and refractory syringomyelia is described.

10.2 Idiopathic Syringomyelia

Considerable debate exists in the literature regarding the terms utilized to define this condition.

Holly and Batzdorf argued that a slit-like syrinx is not a true syringomyelia and is also different from a pre-syrinx state [25]. However, in the literature, there is no uniformity regarding this opinion. For example, Roser et al. consider hydromyelia only a dilated central canal and affirm that IS presents with different clinical and radiological signs [12]. The 34 patients with hydromyelia in their study had no neurological deficits and presented with pain that could be radicular, burning, or

musculoskeletal. They further distinguish hydromyelia as a congenital condition and differentiated it from IS [26].

Batzdorf makes a clear distinction between syringomyelia and a persistent central canal. The latter is characterized by linear or fusiform appearance on sagittal MRI scans, is between 2 and 4 mm in maximal width, and almost perfectly round, centrally placed in the cord on axial MRI scans obtained through these areas [27].

Analyzing the available literature, it is really challenging to differentiate between slit-like syringomyelia, hydromyelia, and IS and understand if they are different entities or simply a continuum on a spectrum. A deep pathophysiological review is beyond the scope of this chapter, and it would be enough to mention scenarios such as the case of a patient who had undergone shock wave lithotripsy for renal calculi and developed arachnoid scarring 7 years later near the level of the affected kidney [21], or the cases of a slit-like syringomyelia which represent the late phase of a spontaneous resolution of a preexistent bigger syrinx [15] to demonstrate the complexity of this condition.

A particularly important first distinction which should and is possible to be made is between a central canal dilation and a syringomyelia (Fig. 10.1a, b).

We have found six useful criteria to distinguish between a central canal dilatation and a syringomyelia which can assist the clinician in distinguishing between these two entities.

The central canal dilatation usually presents the following features: (1) lower cervical and/or mid-thoracic cord location, (2) no space-occupying effect, (3) no change or regression on follow-up MRIs, (4) spindle or slit like shape suggestive of lower intracavitary pressure, (5) no flow signal inside the dilatation and no obstruction of the CSF flow around it on the cine-MRI, (6) no correlation between location of the cord dilatation and patient's clinical symptoms [25, 26, 28]. The management

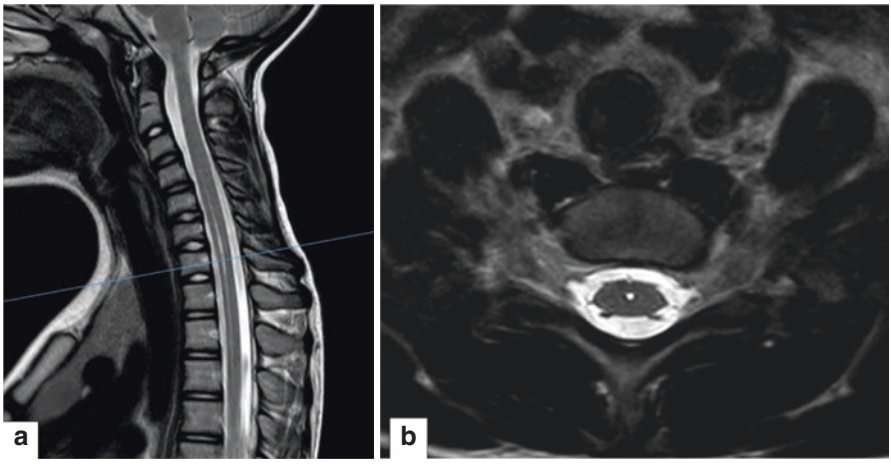

Fig. 10.1 MRI sagittal (**a**) and axial (**b**) T2 sequences of a typical central canal dilation

of central cord dilatation is nonsurgical; patients should be reassured about the diagnosis and ensure that a "label" of syringomyelia is not attached to their notes.

Once this first distinction has been made, in order to succeed in the treatment of a patient with a "true" syringomyelia it is essential to try our best efforts to disclose the underlying causative mechanism. This can be done in our opinion in the majority of cases where there are enough health care resources.

In a patient presenting with a syringomyelia, the following diagnostic algorithm should be followed

1. MRI of the head and the entire spine, including gadolinium enhancement.
2. Cardiac-gated phase-contrast CSF flow studies of the cranio-cervical junction and the cervical, thoracic, and lumbar spine in the median sagittal plane for the visualization of craniocaudal CSF flow. Cardiac-gated phase-contrast CSF flow studies are also known as fast imaging employing steady state acquisition (FIESTA), a technique in which the MRI signal acquisition is synchronized to the cardiac and/or respiratory cycle. This is a noninvasive investigation which has been proved to be more reliable compared to the invasive conventional myelography [21].
3. Serum and CSF samples' analysis to rule out the presence of demyelinating diseases, immunological disorders, vasculitis, infection, and vitamin deficits.

Once the available technology and laboratory tests have been employed without disclosing the cause of the syringomyelia, this can be defined as IS and managed according to the algorithm proposed (Fig. 10.2). In these cases of IS, usually the commonest cause remains a thoracic arachnopathy [7–9, 29, 30].

At this point, it is crucial to distinguish between asymptomatic and symptomatic IS patients. The former should be always managed conservatively and followed up clinically with or without radiological investigations in selected cases. For instance, in case of an oval-shaped three-level cervical syringomyelia, previous reports of isolated cervical IS hiding low-grade tumors (especially ependymomas non-enhancing after contrast MRI) which then progressed into a high-grade lesion should always serve as lesson, and long-term clinical and MRI follow-up are recommended for these syringes [31]. Nonspecific and manageable pain, sensory impairment, and a relatively stable small syrinx are often managed conservatively [21]. There is evidence to prove that children with IS remain asymptomatic, stable, or improve in over 90% of cases and, radiologically, the majority of their syringes (87.5%) remain stable or shrank over time, with no clear correlation between changes in size and changes in symptoms [32]. These patients should be managed nonsurgically with parental reassurance about the condition.

The situation becomes a challenge when these patients become symptomatic or present with neurological deterioration. In these cases, the severity and the progression of the symptoms should guide the treatment. Surgical exploration is recommended in patients with IS and progressive neurological deficits [12].

Several procedures have been proposed to treat the IS ranging from the insertion of shunt into the cavity to drain it into the subarachnoid space, pleura, or peritoneum till the direct arachnidolysis and duroplasty [33].

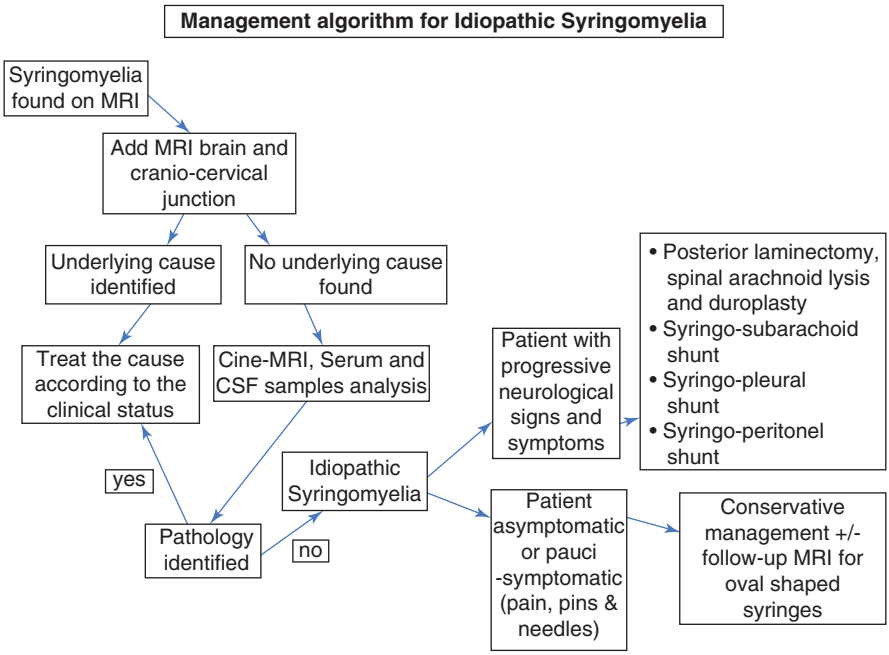

Fig. 10.2 Management algorithm in patients with idiopathic syringomyelia (IS)

Reaffirming that syringomyelia is always an epiphenomenon of an underlying pathology, any surgical intervention should always be directed to resolve the underlying causative mechanism. In presence of a true IS, after a rigorous workup, this usually means unblocking CSF pathway obstruction in the thoracic spinal canal, reserving shunting techniques to nonresponsive cases.

In the authors' experience, when the radiological workout hasn't been helpful in disclosing a precise location of the CSF obstruction, a "rule of thumb" is to perform a posterior decompression and arachnoidolysis at the spinal level (usually thoracic) where a turbulence inside the syringomyelia is visible on the MRI T2 sagittal sequences. An example of this scenario is depicted in Fig. 10.3a, b.

Posterior arachnolysis and duroplasty have shown better long-term outcomes compared to syrinx-shunting procedures in the treatment of an arachnoid pathology which as we have explained above is the cause of the IS in the majority of cases [7].

10.3 Refractory Syringomyelia

We define refractory a syringomyelia that remains persistent on the postoperative follow-up MRI scans despite surgical treatment or recurs after an initial response to the surgical management.

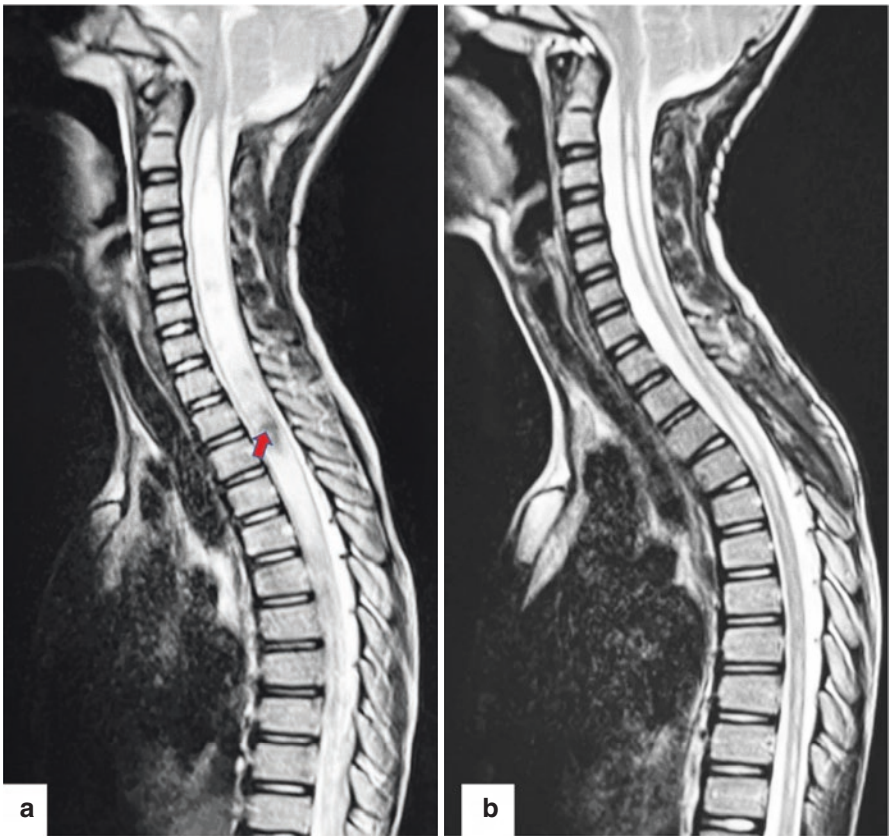

Fig. 10.3 10 years old boy with IS where a full laboratory and radiological workout failed to disclose the underlying cause of the syringomyelia or a precise location of the CSF obstruction. The patient was initially followed up, but after 1 year he experienced a clinical and radiological progression of the syrinx; hence a posterior decompression and arachnoidolysis was performed at the spinal level T3 where a turbulence on the MRI was visible inside the syringomyelia. (**a**) Preoperative MRI sagittal-T2 sequence showing the holocord syrinx and the turbulence inside it (red arrow); (**b**) postoperative MRI sagittal-T2 sequence showing the syrinx decompression 3 months after the T3–4 laminectomy and posterior arachnoidolysis

The reasons for persistent syringomyelia are dependent on various factors. The primary etiology that contributes to the syringomyelia falls into one of these: i.e., Chiari Malformation 1 (CM1), cranio-cervical junction (CCJ) anomalies, spinal dysraphisms, spinal tumor, spinal degenerative diseases, posttraumatic, posthemorrhagic, and postinfective arachnoiditis, hydrocephalus, and craniosynostosis. Depending on the initial causative mechanism of the syringomyelia, the initial surgical technique employed, and the clinical symptomatology of the patient when the refractory syringomyelia is diagnosed, the management will vary.

10.3.1 Chiari 1 Malformation (CM-1)

In CM-1 patients, improvement of syringomyelia post-foramen magnum decompression (FMD) usually occurs within 3 months and continues thereafter, with most patients experiencing syrinx reduction in the first postoperative year [16]. Nonetheless, persistent, progressive, or recurrent syringomyelia following FMD for CM1 is described in up to 66% of the cases in long-term follow-ups [7, 8].

In case of FMD for CM1, the CSF flow through foramen magnum is hindered by intrinsic and extrinsic factors. Intrinsic factors are usually secondary to the obstruction of the foramen of Magendie due to tonsils overlying the foramen of Magendie or posterior inferior cerebellar artery (PICA) and/or arachnoid veils obstructing it [34]. On the other hand, the extrinsic factors include pseudomeningocele formation with adhesions in the foramen magnum and inter-tonsillar adhesions, primary insufficient decompression of the foramen magnum resulting in persistent tonsillar herniation impacting the foramen magnum or causing brainstem compression, bone regrowth at the edges of the previous craniectomy or complete reclosure of the craniectomy (e.g., in infants or young children), and scar formation (and arachnoiditis) after a sufficient suboccipital decompression [35]. According to Tosi et al. in case of small or incomplete decompression or reclosure of the craniectomy, an enlargement of the previous decompression reduced the syrinx size in 15 of 16 patients [16].

In case of refractory syringomyelia post CM-1 where a satisfactory decompression has been performed, the first thing to consider is if any arachnoid veil has been possibly left behind or if a postsurgical scar has formed and is now the causative mechanism sustaining the syringomyelia. The latter is usually the case when the syringomyelia recurs after an initial shrinkage. In these circumstances, a reexploration of the previous cranio-cervical decompression with arachnoid lysis and enlarged duroplasty is recommended [13, 36, 37]. If an enlarged watertight duroplasty was not performed during the first operation, we strongly recommend, in case of RS, to reexplore the previous decompression and perform it. In the authors' experience, this is an effective remedy to resolve the syringomyelia [38, 39]. An example of a similar scenarios is shown in Fig. 10.4a–f. We have previously described our surgical technique regarding performing an enlarged watertight duroplasty [38].

If the cranio-cervical decompression seems appropriate on post-op MRI and cine-MRI study and/or the cranio-cervical junction has already been reexplored with no success and the patient is symptomatic or with progressive neurological symptoms, a direct exploration of the arachnoid surrounding the syrinx, a syrinx fenestration, and/or syringo-shunting technique can be considered.

Posterior arachnolysis and duroplasty, in general, have a better long-term outcome compared to syrinx-shunting procedures in the treatment of a localized arachnoid pathology [7–9, 30]. Nevertheless, it should be acknowledged that it is not often possible to predict the level of CSF blockage on the basis of the site, size, and shape of syringomyelia [21].

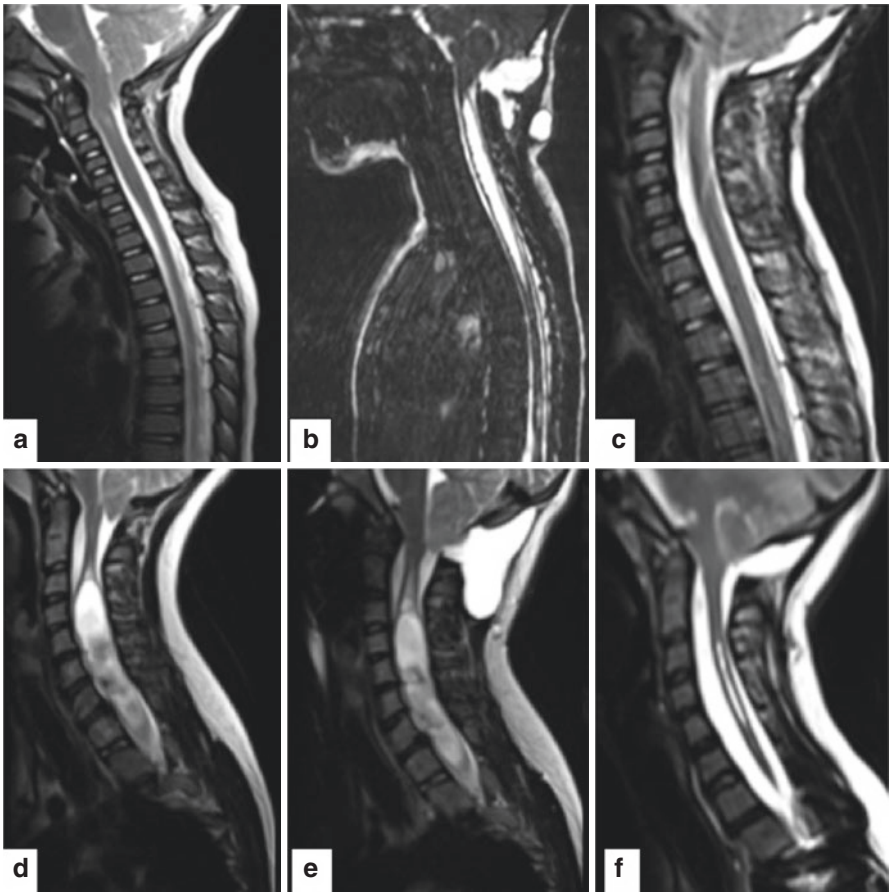

Fig. 10.4 (**a**) Preoperative MRI sagittal T2 sequence of a patient with CM-1 undergone foramen magnum decompression and durotomy without duroplasty; (**b**) postoperative MRI sagittal T2 2 months after the initial operation showing a large pseudomeningocele and a de-novo syringomyelia; (**c**) MRI sagittal T2 sequence of the same patient 3 months after reexploration of the FMD, arachnoidolysis, and enlarged watertight duroplasty showing a complete resolution of the syringomyelia; (**d**) preoperative MRI sagittal T2 sequence of another patient with CM-1 and preoperative cervico-thoracic syringomylia undergone foramen magnum decompression and durotomy without duroplasty; (**e**) postoperative MRI sagittal T2 3 months after the initial operation showing a large pseudomeningocele and a further upward enlargement of the previous syringomyelia; (**f**) MRI sagittal T2 sequence of the same patient 6 months after reexploration of the FMD, arachnoidolysis, and enlarged watertight duroplasty showing a remarkable improvement of the syringomyelia

In terms of shunting options, such as syringo-subarachnoid shunt (SSS), syringo-pleural shunt, and syringo-peritoneal shunt [11, 33, 36–42], Soleman et al. have shown that SSS has a favorable clinical and radiological outcome [43] and in our opinion should be preferred to the other shunting techniques.

10.3.2 Cranio-Cervical Junction (CVJ) Anomalies

The pathophysiology of syringomyelia combined with CVJ anomalies is only partially understood and its treatment is still a matter of debate [18, 44–46]. The most common form of cranio-cervical pathology associated to syringomyelia is foramen magnum arachnoiditis [8] which can usually be treated successfully with posterior fossa decompression, arachnoidolysis, and expansile duroplasty. The second most common cause is basilar invagination/atlanto-axial dislocation (BA/AAD). In this case, several theories have been proposed to explain the pathogenesis of syringomyelia [5] which remains still unclear.

The main factors thought to be responsible are (1) ventral compression by dislocated odontoid process, (2) dorsal compression due to a small posterior fossa, and (3) concomitant Klippel–Feil syndrome and occipitalization of atlas [47, 48].

Several surgical techniques have been proposed to treat BA/AAD [44, 46], but still disagreement exists on what represents the best way to manage the condition [46]. In the last 20 years, there has been a shift toward posterior approaches (including direct posterior reduction and fixation—C0–C2, C0–C3 or C1–C2—plus or less decompression), leaving the ventral transoral odentoidectomy (which nowadays can be also performed endoscopically) only to cases of unsolved ventral compressions without clinical improvement [45].

Untreated CVJ anomalies are usually one of the causes of persistent syringomyelia in patients who previously underwent foramen magnum decompression (FMD) for CM-1 and the CVJ pathology was missed or left untreated. Addressing the cranio-cervical instability is of paramount importance to manage the syringomyelia in these patients.

10.3.3 Spinal Dysraphisms

Syringomyelia is reported in the various types of spinal dysraphism ranging from 21 to 67% of the patients [6, 49]; myelomeningocele and split cord malformation are the most common disorders associated with syringomyelia [50]. Several hypotheses exist regarding the pathophysiology of this syringomyelia.

Greiz has speculated that tensile radial stress on the spinal cord may cause syrinx in spinal dysraphisms, as the transient lower pressure of the cord parenchyma may draw in interstitial fluid causing enlargement of the syrinx [5]. Lee et al. showed how producing epidural compression using kaolin material in a rat model caused a syrinx cranially to the compression in the animals, speculating that compression of the cord related to spinal dysraphism with cord tethering is sufficient to cause the syringomyelia [50].

The presence of syrinx in an asymptomatic patient with spinal dysraphism does not represent a reason per se to recommend a surgical intervention, especially if the size of the syrinx is not extensive [51].

An increase in size of the syringomyelia, instead, could represent a progression of the cord tethering and usually warrants a surgical untethering [52]. The syrinx status is also an important factor to know during the postoperative follow-up. Although an improvement of the syrinx in the postoperative period is a sign that untethering was successful, an unchanged syrinx does not represent a failure of the treatment as several reports have shown that symptomatic improvement is frequently seen in patients in whom the syrinx was unchanged [51].

On the other hand, a syrinx deterioration is an important radiological sign of retethering (Fig. 10.5a–d) and sometimes can be useful to anticipate symptomatic deterioration in the patient [50].

There has been debate in the past regarding whether direct drainage of the syrinx was needed in these cases [53]; however, the recent evidence suggests that the best strategy is, as in all cases of syringomyelia, to treat the main cause and hence perform a spinal cord re-untethering under intraoperative neuromonitoring (IOM) [14, 54].

Finally, worthy of note is a worsening syringomyelia in a patient with myelomeningocele and a ventricular shunt due to hydrocephalus. Shunt malfunction should always be ruled out as it is the commonest cause of the increase in size of the syringomyelia (Fig. 10.6a–d).

10.3.4 Spinal Tumors

Intradural extramedullary tumors (such as meningiomas, schwannomas), intradural arachnoid cysts, or most commonly, intramedullary tumors can present with syringomyelia [55–57]. This association is known at least since 1875 [58], and in a postmortem study of 209 patients with an intramedullary tumor, a syringomyelia cavity was found in 31% of the cases [57]. Ependymomas, angioblastomas, and astrocytomas are the commonest to show an association with syringomyelia [8].

However, the pathogenesis of this kind of syringomyelia is still debated; several theories have been proposed which can be summarized in five main groups: (1) the syringomyelia cavity is part of the tumor, (2) the syrinx arises from the stasis of tissue fluid resulting from occlusion of the normal drainage pathways, (3) spread of edema and spontaneous autolysis of the tumor itself or hemorrhage from the tumor into the cord, (4) altered perimedullary CSF pathway from the extrinsic compression of the tumor resulting in the intramedullary cavity, and (5) exudation caused by disruption of the blood–brain barrier [59]. In the majority of cases, a combination of the above mechanisms is likely the driver for the syringomyelia formation, according to the location and the etiology of the tumor. For instance, intramedullary ependymomas present with syringomyelia in half of the cases [60].

Surgical excision of the tumor usually improves or resolves the syringomyelia and a residual syringomyelia after tumor resection does not usually require any additional surgical treatment. Occasionally, the syringomyelia can deteriorate, in case of incomplete tumor resection and regrowth, following adjuvant treatment,

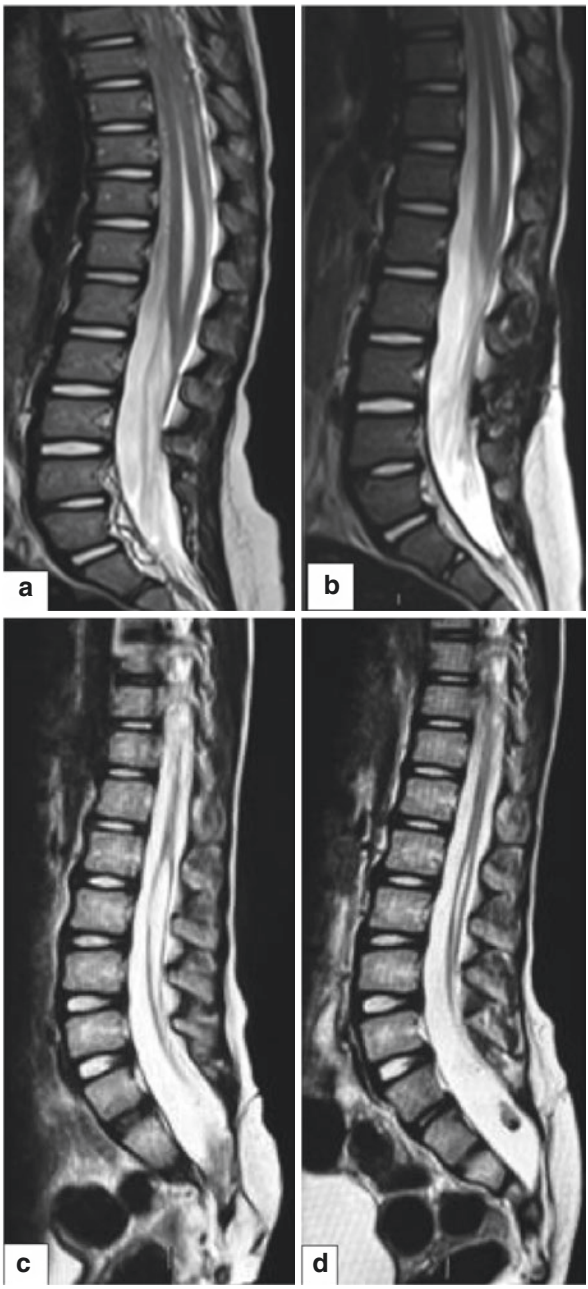

Fig. 10.5 (**a**) MRI sagittal T2 sequence showing a re-tethering of a previously (7 years before) untethered fatty filum with syringomyelia; (**b**) MRI sagittal T2 sequence of the same patient 6 months after re-untethering of the spinal cord showing improvement of the syringomyelia; (**c**) MRI sagittal T2 sequence of a 5-year-old girl with spinal lipoma previously partially untethered (4 years before) showing a de novo syringomyelia onset as first sign of cord re-tethering; (**d**) MRI sagittal T2 sequence 6 months after re-untethering and lipoma resection under IOM showing remarkable improvement of the syringomyelia

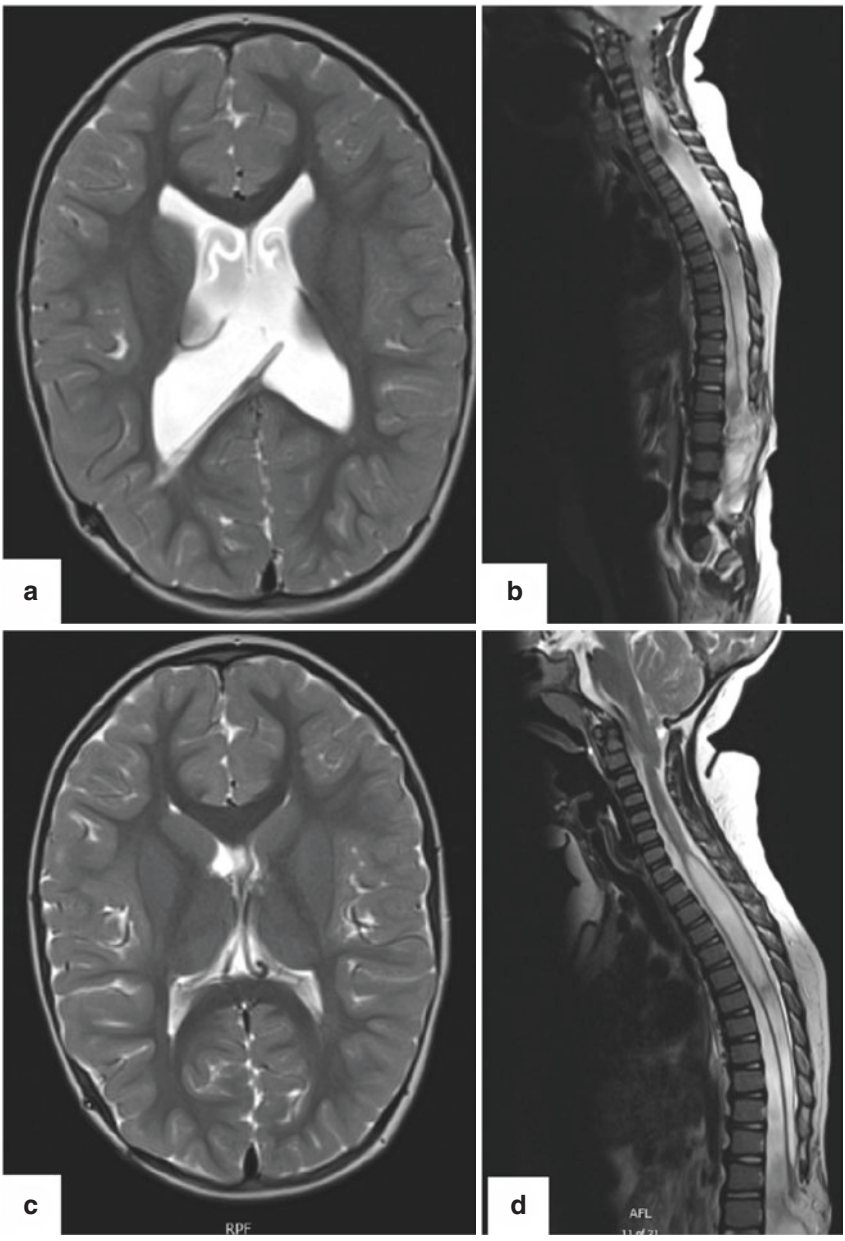

Fig. 10.6 (**a**) MRI head axial T2 sequence of a patient with spina bifida, Chiari 2 malformation, and ventricular enlargement secondary to VP shunt malfunction; (**b**) MRI whole spine sagittal T2 sequence of the same patient showing a holocord syringomyelia at the time of the VP shunt malfunction; (**c**) MRI head axial T2 sequence 3 weeks after shunt revision showing reduced ventricles size; and (**d**) MRI spine sagittal T2 sequence showing reduction in size of the previous holocord syringomyelia

including chemotherapy and radiotherapy, or when there is a disseminated spinal tumor (tumoral leptomeningitis) not amenable of surgical treatment. In these cases, if the syringomyelia is the cause of a severe progressive neurological deterioration, and according to the oncological prognosis, direct fenestration of the syrinx or shunting of the syrinx is recommended.

The management is purely on a case-by-case basis and preferably performed in centers that have the appropriate expertise with facility for long-term oncological follow-up.

10.3.5 Trauma/Hemorrhage/Infection

We have complied this in one group as the etiology of RS in this cohort is primarily due to arachnoidal adhesions. The adhesions may sometimes be very extensive posing a challenge in management.

Phase-contrast cine MRI may accurately localize subarachnoid space obstruction and demonstrate normalization of CSF flow after surgery, and it may also be used to confirm spinal cord tethering and communication of spinal cord cysts with the subarachnoid space [4]. Surgical intervention should be considered only in patients with progressive debilitating neurological deficits. A number of surgical strategies have been suggested in the literature including cyst aspiration, fenestration and shunt placement, and intradural exploration and duraplasty. Many recommend intradural exploration, lysis of subarachnoid adhesions, and duraplasty as the preferred primary treatment options for this kind of syringomyelia in case of neurological deterioration. The goal of this intervention is to create a channel for CSF circulation extrinsic to the spinal cord itself. By creating this pathway, CSF is no longer forced into the parenchyma of the cord, thereby allowing the syrinx to collapse. In cases where this technique is not possible or it has failed, shunting of the syrinx may be considered. Syringo-subarachnoid, syringo-peritoneal, and syringopleural shunts have been described. In all cases, septations in the syrinx need to be lysed to allow an optimal decompression. Syrinx shunts, however, have a propensity to fail, which can limit their usefulness. Cyst aspiration alone is a palliative procedure, and as such, has limited usefulness in this patient population [3].

In posttraumatic syringomyelia, reconstruction of the subarachnoid space by arachnoidolysis and untethering the cord usually allows to improve or stabilize the vast majority of patients [2].

The adhesions can be quite diffuse in case of infection and the primary aim should be based on management of infection as initial step followed by surgery. SSS can be resorted to if arachnoidolysis fails. There can be associated hydrocephalus post-initial surgery and this may contribute to CSF malabsorption. In such cases, endoscopic third ventriculostomy or ventriculoperitoneal shunt can be utilized to manage the hydrocephalus and this may help the resolution of the syringomyelia.

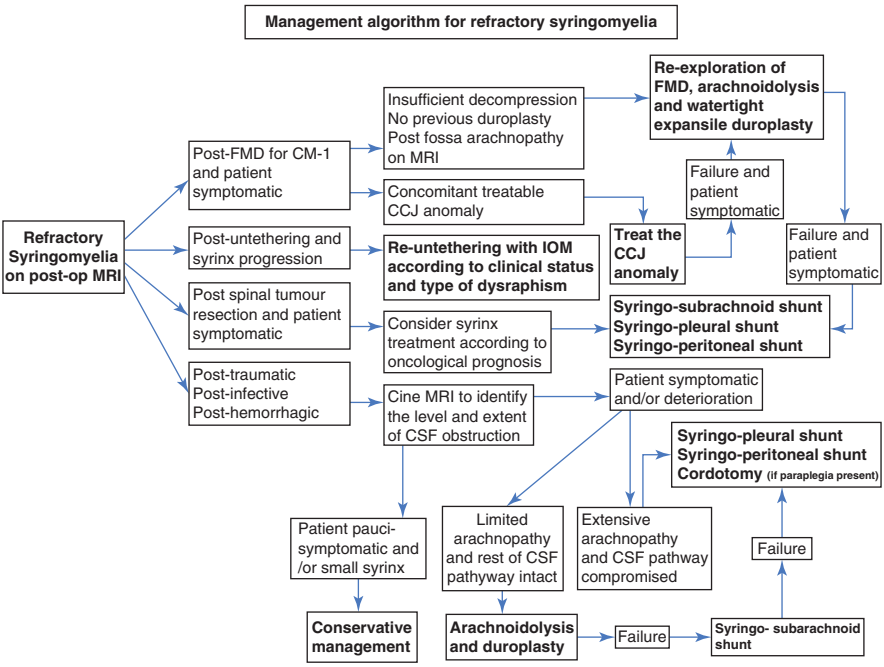

Fig. 10.7 Management algorithm in patients with refractory syringomyelia (IS)

Arachnoidolysis, untethering, and duroplasty provide good long-term results for focal arachnopathies. Nonetheless, for extensive pathologies with a history of subarachnoid hemorrhage or meningitis, treatment remains a major challenge [8].

Shunt placement should be reserved to these cases of diffuse arachnoiditis or with recurrences on the basis of their short-term effect and the possibility to reoperate in case of failure [29, 30]. Overall, improvement after shunt placement, regardless of modality and circumstances (syringo-subarachnoid, syringo-peritoneal or syringo-pleural shunts, primary operation or recurrence), accounts for 60% of cases with a recurrence rate of 50% [30].

Patients with a complete spinal cord lesion can be treated with cordectomy which has proved to be a very effective form of treatment for syringomyelia [9]. However, accepting this kind of operation is not easy for patients and the psychological burden should be considered when proposing such option.

An algorithm for the management of recurrent syringomyelia is outlined in Fig. 10.7.

10.4 Surgical Techniques

We describe below the neurosurgical armamentarium employed in patients with IS and RS. The most common surgical procedures are described below:

10.4.1 Reexploration of Posterior Fossa, Arachnoidolysis, and Enlarged Duroplasty

Under general anesthesia, the patient is positioned prone on Mayfield 3 pins headrest. Previous midline scar is explored under microscopic guidance to carefully dissect the soft tissue layers and reach the dura. Subsequently, the dura is carefully opened to inspect the foramen magnum and to explore for patency of the foramen of Magendie to ensure the presence of CSF egress. Tonsillar coagulation may be necessary to accomplish this during the primary procedure. In case of adhesions, careful arachnoidolysis is performed. As previously discussed, careful consideration should be given to possible obstruction of the Foramen of Magendie due to tonsils overlying the Foramen of Magendie, posterior inferior cerebellar artery (PICA) obstructing the foramen of Magendie, veil obstructing the Foramen of Magendie, and pseudomeningocele formation with adhesions [34, 61]. Expansile duroplasty should be performed following reexploration due to high chance of adhesions due to bleeding and by the procedure per se. McGirt et al. showed in their series that by performing duraplasty during posterior fossa decompression decreased the likelihood of reoperation; 72% of their patients underwent duraplasty and 70% had improvement in their syrinx [62]. We have successfully used Duraguard (bovine pericardium dura) in these cases to perform an enlarged watertight duroplasty with running prolene 5/0 or 6/0 [38, 39].

10.4.2 Spinal Laminectomy, Arachnoidolysis, and Duroplasty

Decompression procedures of the spinal subarachnoid space may have beneficial effects unless the patient shows longitudinally extensive arachnoiditis (such as in case of meningitis).

Under general anesthesia and with the use of intraoperative neuromonitoring (IOM) [54], the patient is placed prone and a laminectomy is performed at the levels involved with arachnoid scarring (previously visualized on FIESTA MRI). We suggest the use of intraoperative ultrasound to identify the ideal place where to start the dura opening under the microscope; this helps in avoiding direct injury to the spinal cord which in some cases can be directly adherent to the overlying dura. Once the dura is opened and separated from the arachnoid, the arachnoid and the scar are dissected away from the pial surface of the cord using sharp dissection in order to untether the spinal cord and reestablish free CSF flow.

Following these manoeuvres, the normal pulsations of the spinal cord, which are usually attenuated or absent at the level of the scar, reappear and occasionally the syrinx visibly collapses [29, 30]. With extensive arachnoid scarring, the arachnoid appears thicker, denser, and whiter and, occasionally vascularized obscuring the underlying spinal cord. In these cases, to prevent any spinal cord injury, the arachnoid dissection should be limited to the dorsal surface of the spinal cord. The

duroplasty can be performed either with autologous fascia lata or lyophilized dura [8, 9]. The authors have successfully used bovine pericardium dura (Duraguard) in these cases.

10.4.3 Syringo-Subarachnoid Shunt (SSS)

Among the shunting technique, SSS is usually the first choice when there is normal CSF flow in the subarachnoid space; it should not be used in cases of severe arachnoiditis.

Under general anesthesia, the patient is positioned prone. IOM is recommended for this procedure as this can alert the surgeon to potential intraoperative threats to the functional integrity of the spinal cord [23, 54]. After skin disinfection and draping, a midline skin incision is completed over the previously identified spinal levels. The muscle fascia is opened, and the muscles are dissected exposing the desired spinal processes and laminae. A standard laminectomy of one or two laminae is performed. Under microscopic magnification, the dura is incised in the midline and suspended on each side. We recommend the use of a fine ultrasound probe prior to opening the arachnoid and performing the myelotomy to confirm the most dilated location of the syrinx [14] and decide where to define the subarachnoid pocket (rostral or caudal in line with the syrinx). An appropriate length of patent subarachnoid space is needed to allow the inline placement of the catheter. The arachnoid is opened and a 5–6 cm lumboperitoneal shunt (Medtronic, Minneapolis, MN, USA) is inserted into the caudal or cranial subarachnoid space for 3–4 cm distally, while the proximal side of the shunt catheter is put between the dural retraction sutures in the meantime the myelotomy is performed [24, 63].

It is crucial to ensure that the tip is actually subarachnoid (and not just subdural), otherwise it will not function. A midline myelotomy is usually performed. Sometimes it might be difficult to define the midline (posterior median sulcus), especially if the cord is rotated, or if significantly compressed by the syrinx. In these cases, the small pial arteries folding medially towards the central canal should be sought and recognized, since they point out towards the posterior median sulcus. Another tip to identify the midline is to expose the nerve roots bilaterally and the posterior midline sulcus is situated equidistant from both nerve roots. Alternatively, if the syringomyelia is bulging laterally, the myelotomy can be safely performed in the dorsal entry zone (DREZ) between the lateral and posterior columns because this is the thinnest part especially when there is already an upper extremity proprioceptive deficit caused from the syrinx [33].

If the midline is defined, the superficial pial vessels are cauterized and the pia is incised using a diamond knife. With the help of a non-tooth forceps, the cord is split until the syrinx is reached. When the cord is under high pressure, the opening of the syrinx is completed before inserting the tip of the shunt into the subarachnoid space, to avoid a possible injury to the cord tissue [63]. Following syrinx decompression,

the proximal tip of the shunt is inserted into the syrinx cavity for 2–3 cm cranially or caudally. A 6–0 prolene suture is used to fix the shunt to the arachnoid to avoid dislocation. The dura is closed in a watertight fashion using a running suture 5–0 prolene. In case of laminoplasty, the laminae are fixed using plates and screws. The wound is closed in layers.

10.4.4 Syringo-Pleural Shunt (SPS)

Syringo-pleural shunting is safe and a straightforward technique with good results both clinically and radiologically. The result is to be expected within the first few weeks and may be long lasting [64]. Under general anesthesia, the patient is positioned prone. A laminectomy or a laminotomy of 1–2 laminae is performed, preferably below the T1 level. The best level of shunt insertion remains controversial: the advantage to place it under the T1 level is the avoidance of neurological injury of the upper extremities; however, it should be considered that the dorsal columns of the thoracic cord are extremely fragile, and the "non-gentle" manipulation may have a higher chance of causing neurological symptoms of the lower extremities [64, 65].

Different types of shunt can be used such as the 1-piece Spetzler lumboperitoneal shunt (Integra Neurosciences, Plainsboro, NJ), with a 0.7-mm inner diameter, 1.5-mm outer diameter, and 31.5-inch length; the lumbar end of this catheter, with multiple perforations, is placed inside the syrinx, and the opposite end is positioned in the pleural space; lumboperitoneal shunt catheter (Medtronic, Minneapolis, MN, USA) or a T- or Y-shaped catheter or antibiotic impregnated catheter can also be utilized for the SPS [42, 64–66]. A distal slit valve to avoid over drainage of the syrinx into the pleural cavity should be considered.

The patient is placed in the prone position and after radiographic confirmation, a midline mid-thoracic incision is made. A single-level laminectomy followed by durotomy is performed. Syrinx location and spinal cord thickness are verified with the help of intraoperative ultrasound. A standard dorsal midline or dorsal root entry zone (DREZ) myelotomy is performed, and the catheter is inserted, under microscopic magnification, and directed superiorly for approximately 4–5 cm through a small midline myelotomy. The use of IOM is recommended to perform this surgery. Somatosensory potential (SSEPs) is often lost during a midline myelotomy; if motor-evoked potentials (MEPs) drop significantly or disappear and/or do not recover after a short period of time, the catheter should be repositioned [54]. The catheter is sutured to the dura and tunnelled toward the separate paramedian incision, previously made at the level of the fifth intercostal space 5 on the right side. This incision is taken down to the superior margin of the sixth rib, and the parietal pleura is entered via a stab incision just over the superior margin of the rib. The distal end of the catheter is inserted into the pleural space. Two anchoring sutures are placed to the paraspinal and intercostal muscles to prevent catheter migration [34].

10.4.5 Syringo-Peritoneal Shunt (SPRS)

The syringo-peritoneal shunt has undergone several modifications over the past five decades [41, 67]. The skin over the spine, neck, chest, and abdomen is draped as for a ventriculoperitoneal shunt. Under general anesthesia, the patient is placed in a lateral position with the head in a Mayfield 3 pins headrest. A single-level laminectomy and a midline durotomy are performed. The operating microscope is used to perform a small myelotomy into the thinnest portion of the spinal cord, usually the dorsal root entry zone. The use of IOM is recommended also for this operation and the considerations about IOM features and catheter repositioning are the same as described above for the SPS.

The flexible T-tube arms shunt with multiple drainage holes is used as this can be cut to the desired length and inserted into the syrinx. The shunt is brought out through the spinal cord and dura at a right angle and is secured with the suture tab. A metal step-up connector is used to adapt the SPRS to a standard peritoneal shunt tubing. Standard techniques are used to insert a low-pressure peritoneal catheter into the abdominal cavity. Similar to the SPS, adding a distal slit valve is beneficial to prevent over drainage. The shunt is then inserted into the peritoneum through a mini-laparotomy, with a peritoneal trocar, or laparoscopically assisted [10, 41].

10.5 Conclusions

The most important step in treating a syringomyelia is to differentiate it from other clinico-radiological conditions that should not be termed as syringomyelia.

In presence of a syringomyelia, it is of paramount importance to utilize appropriate diagnostic facilities available to identify the underlying cause, considering that this entity represents always an epiphenomenon of another pathology. If our best efforts to identify the cause have failed, then such syringomyelia should be deemed “idiopathic”. Most patients with this condition can be managed conservatively with clinical and radiological follow-up if asymptomatic or pauci-symptomatic. Rarely patients can present with deteriorating neurological signs and symptoms; in these circumstances, surgery should be warranted. Several techniques can be offered; however, the favored first line option is either a posterior thoracic laminectomy and arachnoidolysis or a syringo-subarachnoid shunt.

Refractory syringomyelia is a multifactorial condition, and understanding the pathophysiology of the persistent, progressing, or recurrent syrinx is crucial in order to offer the patient the right treatment [68].

In patients with refractory syringomyelia secondary to CM-1 treated in the first instance with foramen magnum decompression, reexploration of the foramen should be considered the initial option and enlarged watertight duroplasty should be performed if not performed during the first operation. A cranio-cervical instability should also be treated when present.

RS secondary to arachnoidal adhesions (posttraumatic, postinfective, or post-hemorrhagic arachnopathies) is the most difficult etiology to successfully treat. However, the best option is always to try to resolve the arachnopathy with arachnoidolysis, marsupialization of the subarachnoid space, and duroplasty before offering any kind of shunting diversion. If the above fails, among the different shunting techniques, SSS should be preferred over other shunting options when feasible.

Finally, it is worth stressing how a multidisciplinary approach is indicated in patients with refractory syringomyelia as there are several aspects of their care that need to be considered including pain management, neuropathic bladder and/or bowel, orthopedic issues, psychological support, and neurorehabilitation along with physiotherapy and occupational therapy.

References

1. Confucius C, Lin Y, Sima Q, Gu H, Wong J. The wisdom of Confucius. Book 13. New York: Illustrated Modern Library; 1943.
2. Aghakhani N, Baussart B, David P, Lacroix C, Benoudiba F, Tadie M, Parker F. Surgical treatment of posttraumatic syringomyelia. Neurosurgery. 2010;66(6):1120–7; discussion 1127. https://doi.org/10.1227/01.NEU.0000369609.30695.AB.
3. Ajit AK, Bhalla T. Posttraumatic and idiopathic syringomyelia. Benzel's spine surgery ebook: techniques, complication avoidance and management. Amsterdam: Elsevier; 2016. p. 1572–4.
4. Brodbelt AR, Stoodley MA. Post-traumatic syringomyelia: a review. J Clin Neurosci. 2003;10(4):401–8. https://doi.org/10.1016/s0967-5868(02)00326-0.
5. Greitz D. Unraveling the riddle of syringomyelia. Neurosurg Rev. 2006;29(4):251–63; discussion 264; Epub 2006 May 31. https://doi.org/10.1007/s10143-006-0029-5.
6. Iskandar BJ, Oakes WJ, McLaughlin C, Osumi AK, Tien RD. Terminal syringohydromyelia and occult spinal dysraphism. J Neurosurg. 1994;81(4):513–9. https://doi.org/10.3171/jns.1994.81.4.0513.
7. Klekamp J. How should syringomyelia be defined and diagnosed? World Neurosurg. 2018;111:e729–45. Epub 2018 Jan 6. https://doi.org/10.1016/j.wneu.2017.12.156.
8. Klekamp J. Treatment of syringomyelia related to nontraumatic arachnoid pathologies of the spinal canal. Neurosurgery. 2013;72(3):376–89; discussion 389. https://doi.org/10.1227/NEU.0b013e31827fcc8f.
9. Klekamp J. Syringomyelia 2017. Book chapter. Syringomyelia—diagnosis and treatment. Heidelberg: Springer; 2001.
10. Kyoshima K, Kuroyanagi T, Oya F, Kamijo Y, El-Noamany H, Kobayashi S. Syringomyelia without hindbrain herniation: tight cisterna magna. Report of four cases and a review of the literature. Neurosurgery. 2002;96:239–49.
11. Lu VM, Phan K, Crowley SP, Daniels DJ. The addition of duraplasty to posterior fossa decompression in the surgical treatment of pediatric Chiari malformation type I: a systematic review and meta-analysis of surgical and performance outcomes (Erratum in: J Neurosurg Pediatr. 2018 Feb;21(2):197). J Neurosurg Pediatr. 2017;20(5):439–49. https://doi.org/10.3171/2017.6.PEDS16367.
12. Roy AK, Slimack NP, Ganju A. Idiopathic syringomyelia: retrospective case series, comprehensive review, and update on management. Neurosurg Focus. 2011;31(6):E15. https://doi.org/10.3171/2011.9.FOCUS11198.
13. Sacco D, Scott RM. Reoperation for Chiari malformations. Pediatr Neurosurg. 2003;39(4):171–8. https://doi.org/10.1159/000072467.

14. Sgouros S. Chapter 28: Syringomyelia principles of neurological surgery. 3rd ed. Amsterdam: Elsevier; 2015. https://doi.org/10.1016/B978-1-4377-0701-4.00028-2.
15. Shetty J, Kandasamy J, Sokol D, Gallo P. Clinical deterioration despite syringomyelia resolution after successful foramen magnum decompression for Chiari malformation: case series. Eur J Paediatr Neurol. 2019;23(2):333–7. https://doi.org/10.1016/j.ejpn.2019.01.003.
16. Tosi U, Lara-Reyna J, Chae J, Sepanj R, Souweidane MM, Greenfield JP. Persistent syringomyelia after posterior fossa decompression for Chiari malformation. World Neurosurg. 2020;136:454–61. https://doi.org/10.1016/j.wneu.2020.01.148.
17. Tsitouras V, Sgouros S. Syringomyelia and tethered cord in children. Childs Nerv Syst. 2013;29(9):1625–34. https://doi.org/10.1007/s00381-013-2180-y.
18. Tubbs RS, Elton S, Grabb P, Dockery SE, Bartolucci AA, Oakes WJ. Analysis of the posterior fossa in children with the Chiari 0 malformation. Neurosurgery. 2001;48(5):1050–4; discussion 1054-5. https://doi.org/10.1097/00006123-200105000-00016.
19. Tubbs RS, Webb DB, Oakes WJ. Persistent syringomyelia following pediatric Chiari I decompression: radiological and surgical findings. J Neurosurg. 2004;100(5 Suppl Pediatrics):460–4. https://doi.org/10.3171/ped.2004.100.5.0460.
20. Struck AF, Haughton VM. Idiopathic syringomyelia: phase-contrast MR of cerebrospinal fluid flow dynamics at level of foramen magnum. Radiology. 2009;253(1):184–90. https://doi.org/10.1148/radiol.2531082135.
21. Mauer UM, Freude G, Danz B, Kunz U. Cardiac-gated phase-contrast magnetic resonance imaging of cerebrospinal fluid flow in the diagnosis of idiopathic syringomyelia. Neurosurgery. 2008;63(6):1139–44; discussion 1144. https://doi.org/10.1227/01.NEU.0000334411.93870.45.
22. Rodriguez A, Kuhn EN, Somasundaram A, Couture DE. Management of idiopathic pediatric syringohydromyelia. J Neurosurg Pediatr. 2015;16(4):452–7. https://doi.org/10.3171/2015.3.PEDS14433.
23. Soleman J, Roth J, Bartoli A, Rosenthal D, Korn A, Constantini S. Syringo-subarachnoid shunt for the treatment of persistent syringomyelia following decompression for Chiari type I malformation: surgical results. World Neurosurg. 2017;108:836–43. https://doi.org/10.1016/j.wneu.2017.08.002.
24. Soleman J, Roth J, Constantini S. Direct syrinx drainage in patients with Chiari I malformation. Childs Nerv Syst. 2019;35(10):1863–8. https://doi.org/10.1007/s00381-019-04228-7.
25. Holly LT, Batzdorf U. Slitlike syrinx cavities: a persistent central canal. J Neurosurg. 2002;97(2 Suppl):161–5. https://doi.org/10.3171/spi.2002.97.2.0161.
26. Roser F, Ebner FH, Sixt C, Hagen JM, Tatagiba MS. Defining the line between hydromyelia and syringomyelia. A differentiation is possible based on electrophysiological and magnetic resonance imaging studies. Acta Neurochir. 2010;152(2):213–9; discussion 219; Epub 2009 Jun 16. https://doi.org/10.1007/s00701-009-0427-x.
27. Batzdorf U. Primary spinal syringomyelia. Invited submission from the joint section meeting on disorders of the spine and peripheral nerves. J Neurosurg Spine. 2005;3:429–35.
28. Magge SN, Smyth MD, Governale LS, Goumnerova L, Madsen J, Munro B, Nalbach SV, Proctor MR, Scott RM, Smith ER. Idiopathic syrinx in the pediatric population: a combined center experience. J Neurosurg Pediatr. 2011;7(1):30–6. https://doi.org/10.3171/2010.10.PEDS1057.
29. Klekamp J, Batzdorf U, Samii M, Bothe HW. Treatment of syringomyelia associated with arachnoid scarring caused by arachnoiditis or trauma. J Neurosurg. 1997;86(2):233–40. https://doi.org/10.3171/jns.1997.86.2.0233.
30. Klekamp J, Samii M. Syringomyelia—diagnosis and treatment. Heidelberg: Springer; 2001. ISBN 978-3-642-56023-1.
31. Ng S, Aghakhani N, Bauchet L. Clinical image of a spinal ependymoma discovered 8 years after initial misdiagnosis as an idiopathic syringomyelia. World Neurosurg. 2021;145:338–9. https://doi.org/10.1016/j.wneu.2020.09.162.

32. Fu KM, Smith JS, Polly DW, Ames CP, Berven SH, Perra JH, Glassman SD, McCarthy RE, Knapp DR, Shaffrey CI, Scoliosis Research Society Morbidity and Mortality Committee. Morbidity and mortality associated with spinal surgery in children: a review of the Scoliosis Research Society morbidity and mortality database. J Neurosurg Pediatr. 2011;7(1):37–41. https://doi.org/10.3171/2010.10.PEDS10212.
33. Schmidek HH, Sweet WH, editors. Operative neurosurgical techniques. 1st ed. New York: Grune and Stratton; 1982. p. 1317.
34. Williams B. Syringomyelia. Neurosurg Clin N Am. 1990;1(3):653–85.
35. Aoki N, Oikawa A, Sakai T. Spontaneous regeneration of the foramen magnum after decompressive suboccipital craniectomy in Chiari malformation: case report. Neurosurgery. 1995;37:340–2.
36. Attenello FJ, McGirt MJ, Gathinji M, Datoo G, Atiba A, Weingart J, Carson B, Jallo GI. Outcome of Chiari-associated syringomyelia after hindbrain decompression in children: analysis of 49 consecutive cases. Neurosurgery. 2008;62(6):1307–13; discussion 1313. https://doi.org/10.1227/01.neu.0000333302.72307.3b.
37. Schuster JM, Zhang F, Norvell DC, Hermsmeyer JT. Persistent/recurrent syringomyelia after Chiari decompression-natural history and management strategies: a systematic review. Evid Based Spine Care J. 2013;4(2):116–25. https://doi.org/10.1055/s-0033-1357362.
38. Gallo P, Copley PC, McAllister S, Kaliaperumal C. The impact of neurosurgical technique on the short- and long-term outcomes of adult patients with Chiari I malformation. Clin Neurol Neurosurg. 2021;200:106380. Epub 2020 Nov 28. https://doi.org/10.1016/j.clineuro.2020.106380.
39. Gallo P, Sokol D, Kaliaperumal C, Kandasamy J. Comparison of three different cranio-cervical decompression procedures in children with Chiari malformation type I: does the surgical technique matter? Pediatr Neurosurg. 2017;52(5):289–97. https://doi.org/10.1159/000479327.
40. Gil Z, Rao S, Constantini S. Expansion of Chiari I-associated syringomyelia after posterior-fossa decompression. Childs Nerv Syst. 2000;16(9):555–8. https://doi.org/10.1007/s003810000329.
41. Suzuki M, Davis C, Symon L, Gentili F. Syringoperitoneal shunt for treatment of cord cavitation. J Neurol Neurosurg Psychiatry. 1985;48(7):620–7. https://doi.org/10.1136/jnnp.48.7.620.
42. Williams B, Page N. Surgical treatment of syringomyelia with syringopleural shunting. Br J Neurosurg. 1987;1(1):63–80. https://doi.org/10.3109/02688698709034342.
43. Soleman J, Bartoli A, Korn A, Constantini S, Roth J. Treatment failure of syringomyelia associated with Chiari I malformation following foramen magnum decompression: how should we proceed? Neurosurg Rev. 2019;42(3):705–14. https://doi.org/10.1007/s10143-018-01066-0. Epub 2018 Dec 15
44. Jian FZ, Chen Z, Wrede KH, Samii M, Ling F. Direct posterior reduction and fixation for the treatment of basilar invagination with atlantoaxial dislocation. Neurosurgery. 2010;66(4):678–87; discussion 687. https://doi.org/10.1227/01.NEU.0000367632.45384.5A.
45. Joaquim AF, Osorio JA, Riew KD. Transoral and endoscopic endonasal odontoidectomies—surgical techniques, indications, and complications. Neurospine. 2019;16(3):462–9. https://doi.org/10.14245/ns.1938248.124.
46. Kim LJ, Rekate HL, Klopfenstein JD, Sonntag VK. Treatment of basilar invagination associated with Chiari I malformations in the pediatric population: cervical reduction and posterior occipitocervical fusion. J Neurosurg. 2004;101(2 Suppl):189–95. https://doi.org/10.3171/ped.2004.101.2.0189.
47. Goel A, Bhatjiwale M, Desai K. Basilar invagination: a study based on 190 surgically treated patients. J Neurosurg. 1998;88(6):962–8. https://doi.org/10.3171/jns.1998.88.6.0962.
48. Goel A. Treatment of basilar invagination by atlantoaxial joint distraction and direct lateral mass fixation. J Neurosurg Spine. 2004;1(3):281–6. https://doi.org/10.3171/spi.2004.1.3.0281.
49. Ikenouchi J, Uwabe C, Nakatsu T, Hirose M, Shiota K. Embryonic hydromyelia: cystic dilatation of the lumbosacral neural tube in human embryos. Acta Neuropathol. 2002;103(3):248–54. https://doi.org/10.1007/s00401-001-0465-9.

50. Lee JY, Kim KH, Wang KC. Syringomyelia in the tethered spinal cords. J Korean Neurosurg Soc. 2020;63(3):338–41. https://doi.org/10.3340/jkns.2020.0097.
51. Kashlan ON, Wilkinson DA, Morgenstern H, Khalsa SS, Maher CO. Predictors of surgical treatment in children with tethered fibrofatty filum terminale. J Neurosurg Pediatr. 2019;1:1–8. https://doi.org/10.3171/2019.8.PEDS19292.
52. Beaumont A, Muszynski CA, Kaufman BA. Clinical significance of terminal syringomyelia in association with pediatric tethered cord syndrome. Pediatr Neurosurg. 2007;43(3):216–21. https://doi.org/10.1159/000098834.
53. Bruzek AK, Starr J, Garton HJL, Muraszko KM, Maher CO, Strahle JM. Syringomyelia in children with closed spinal dysraphism: long-term outcomes after surgical intervention. J Neurosurg Pediatr. 2019;13:1–7. https://doi.org/10.3171/2019.9.PEDS1944.
54. Pencovich N, Korn A, Constantini S. Intraoperative neurophysiologic monitoring during syringomyelia surgery: lessons from a series of 13 patients. Acta Neurochir. 2013;155:785–91. https://doi.org/10.1007/s00701-013-1648-6.
55. Barnett, H.J.M. (1973) Syringomyelia and tumours of the nervous system. In: Bamett, H.J.M., Foster, J.B. and Hudgson, P. (Eds.), Syringomyelia, Saunders, London, pp. 245L12-245301.
56. Nishiura I, et al. An extramedullary spinal cord tumor associated with syringomyelia: a case report. No Shinkei Geka. 1989;17(2):181–5.
57. Poser CM. The relationship between syringomyelia and neoplasm. Springfield: Charles C Thomas; 1956.
58. Simon T. Beitrtige zur pathologie und pathologischen anatomie des zentralnervensystems. Arch Psychiat. 1875;5:108.
59. Lohle PN, Wurzer HA, Hoogland PH, Seelen PJ, Go KG. The pathogenesis of syringomyelia in spinal cord ependymoma. Clin Neurol Neurosurg. 1994;96(4):323–6. https://doi.org/10.1016/0303-8467(94)90123-6.
60. Slooff JL, Kemohan J, MacCarthy CS. Primary intramedullary tumors of the spinal cord and filum terminale. Philadelphia: W. B. Saunders; 1964.
61. Yuan C, Guan J, Du Y, Zhang C, Ma L, Yao Q, Cheng L, Liu Z, Wang K, Duan W, Wang X, Wu H, Chen Z, Jian F. Repeat craniocervical decompression in patients with a persistent or worsening syrinx: a preliminary report and early results. World Neurosurg. 2020;138:e95–e105. https://doi.org/10.1016/j.wneu.2020.02.015.
62. McGirt MJ, Garces-Ambrossi GL, Parker S, Liauw J, Bydon M, Jallo GI, et al. Primary and revision suboccipital decompression for adult Chiari I malformation: analysis of long-term outcomes in 393 patients. Neurosurgery. 2009;65:924.
63. Soleman J, Roth J, Constantini S. Syringo-subarachnoid shunt: how I do it. Acta Neurochir. 2019;161:367–70. https://doi.org/10.1007/s00701-019-03810-x.
64. Fan T, Zhao X, Zhao H, Liang C, Wang Y, Gai Q, Zhang F. Treatment of selected syringomyelias with syringo-pleural shunt: the experience with a consecutive 26 cases. Clin Neurol Neurosurg. 2015;137:50–6. https://doi.org/10.1016/j.clineuro.2015.06.012.
65. Cacciola F, Capozza M, Perrini P, Benedetto N, Di Lorenzo N. Syringopleural shunt as a rescue procedure in patients with syringomyelia refractory to restoration of cerebrospinal fluid flow. Neurosurgery. 2009;65(3):471–6; discussion 476. https://doi.org/10.1227/01.NEU.0000350871.47574.DE.
66. McComb JG. Techniques for CSF diversion. In: Scott RM, editor. Hydrocephalus. Baltimore: Williams and Wilkins; 1990. p. 47–65.
67. Barbaro NM, Wilson CB, Gutin PH, Edwards MS. Surgical treatment of syringomyelia. Favorable results with syringoperitoneal shunting. J Neurosurg. 1984;61(3):531–8. https://doi.org/10.3171/jns.1984.61.3.0531.
68. Prince A, Mullin JP, Benzel EC. Syringomyelia. In: van de Kelft E, editor. Surgery of the spine and spinal cord. Cham: Springer; 2016. https://doi.org/10.1007/978-3-319-27613-7_13.

Chapter 11
Evolution of Complex Spine Surgery in Neurosurgery: From Big to Minimally Invasive Surgery for the Treatment of Spinal Deformity

Mohamed Macki and Frank La Marca

11.1 Introduction

Spinal instrumentation for adult spinal deformity dates back to the surgical correction of secondary complications from infectious processes, such as Pott's disease and poliomyelitis [1]. With the population aging at a longer life expectancy today, advanced degenerative spinal diseases and idiopathic scoliosis supersede as the most common causes of adult spinal deformity. Correction of the thoracolumbar malignment, specifically, has rapidly evolved with the burgeoning success of spinal instrumentation. The objective of this chapter is to review the metamorphosis of operative principles for adult thoracolumbar deformity, from aggressive osteotomies in the posterior bony elements to minimally invasive surgery (MIS) at the intervertebral disc space.

11.2 History

Advances for spinal reconstructive surgery have rapidly evolved to meet the growing prevalence of adult spinal deformity over the past century [1]. Initial attempts to correct spinal malalignment focused on nonoperative strategies, including external braces, traction, and casts. In the late nineteenth century, surgical approaches were entertained when Berthold Ernest Hadra first described wiring of the spinous process for Potts disease [2]. After the turn of the century, Fritz Lange wrote of an "artificial spinal column of steel" with thick wires along each side of the spinous

M. Macki · F. La Marca (✉)
Department of Neurosurgery, Henry Ford Allegiance Hospital, Jackson, MI, USA
e-mail: flamarc1@hfhs.org

C. Di Rocco (ed.), *Advances and Technical Standards in Neurosurgery*, Advances and Technical Standards in Neurosurgery 45,
https://doi.org/10.1007/978-3-030-99166-1_11

process for the stabilization of a progressive kyphotic deformity in patients with a history of spondylitic diseases [3]. After another surge in poliomyelitis in 1940s, focus shifted to the debilitating spinal deformities secondary to truncal muscle atrophy. Paul R. Harrington developed laminar hooks fastened to large rods for polio-related scoliosis [4, 5]. Through several iterations of this technique, including the placement of bone graft, the Harrington rods were eventually adopted for idiopathic scoliosis in the 1970s, when, for the first time, the goal of surgery shifted from spinal stabilization to deformity correction. At this same time, Dwyer et al. described anterior thoracolumbar instrumentation on the convexity of a coronal deformity [6]. Vertebral body screw heads threaded through titanium cables were progressively approximated to straighten a scoliotic spine. The Kaneda system was constructed by *two* anterior screws connected to two separate rods for greater corrective forces for adult spinal deformity [7]. In the 1980s, posterior transpedicular screws connected to separate rods were introduced with the biomechanical promise of superior pull-out strength and load-bearing capacity as compared to hooks and sublaminar wires [8]. Finally, the 1990s introduced the polyaxial screw head that facilitated rod placement for misaligned pedicles secondary to spinal curvature [9]. These advancements in instrumentation laid the groundwork for innovations in the correction of adult spinal deformity. This chapter will review how operative techniques improved with continued developments in spine technology.

11.3 Spinal Alignment

Spinal alignment assesses the normal spinal curvature in the coronal and sagittal plane (Fig. 11.1). Coronal deformities from asymmetrical disc degeneration in the aging spine, bony anomalies from focal versus systemic pathologies, congenital failure of bony formation, or segmentation cause scoliosis. A more important clinical indicator, the sagittal deformity, reflects the shape of the spine with little muscle effort, or the sum of the vertebral and disc shapes. The sagittal alignment indicates the condition of the lumbar lordosis (LL) and thoracic kyphosis. Sagittal balance has been demonstrated as an independent predictor of patient-reported outcomes after surgery for not only larger operations in adult scoliosis [10] and spinal deformity [11], but also routine surgeries for degenerative disc disease and spondylolisthesis [12, 13]. Spinopelvic parameters were derived to quantify the alignment of the axial skeleton [14–16]:

- Sagittal vertical axis (SVA): the distance from the S1 posterior superior endplate to the C7 plumb line—the vertical line from the midpoint of the C7 vertebral body. A SVA >6 cm defines a global kyphotic deformity or sagittal imbalance: lumbar kyphosis with normal to increased thoracic kyphosis.
- Sacral slope (SS): the angle subtended by the horizontal reference line and the S1 superior endplate.

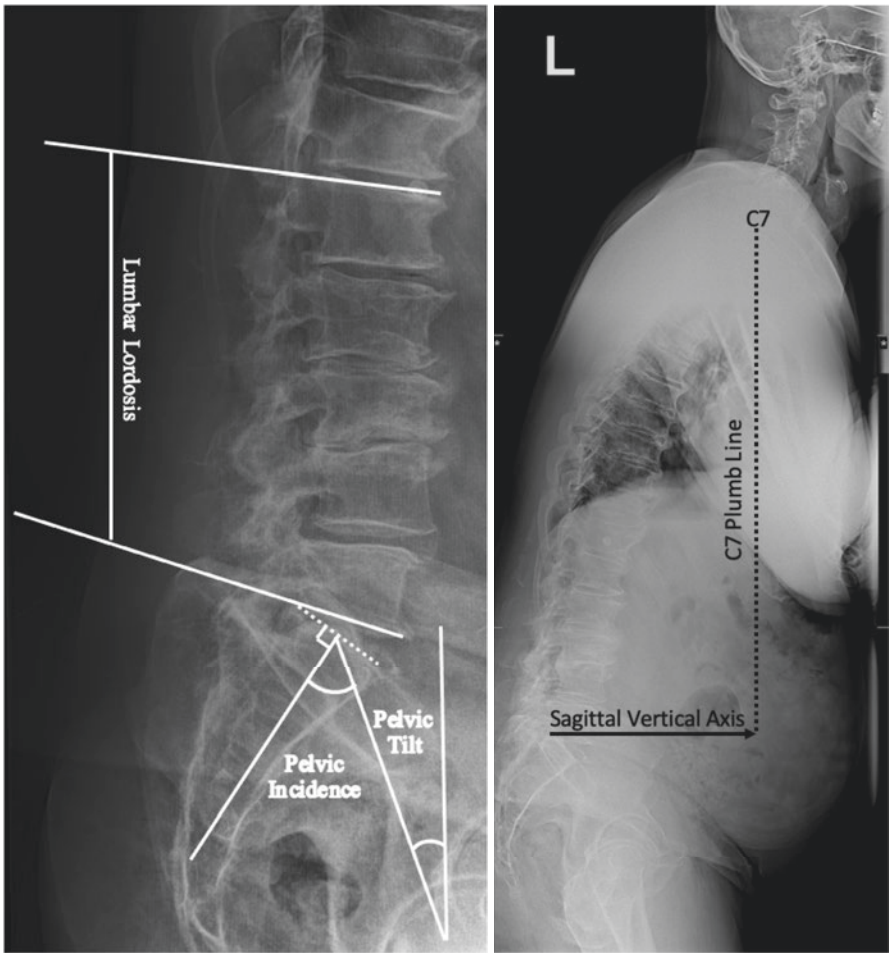

Fig. 11.1 36-in. standing X-ray demonstrating measurements of spinopelvic parameters

- Pelvic tilt (PT): the angle subtended by the vertical reference line and the line from the head to the midpoint of the S1 superior endplate. PT > 25 cm reflects pelvic compensation for an underlying sagittal imbalance.
- Pelvic incidence (PI): the angle subtended by the line from the femoral head to the line perpendicular to the midpoint of the S1 superior endplate. The PI equals the sum of SS and PT. A fixed parameter, the PI refers to the orientation of the pelvis in space.
- PI–LL mismatch: a difference between PI and LL > 10° indicates lumbar flat flatback from loss of LL.
- Cobb angle: the angle subtended by the lines along the endplates of the vertebrae at the top and bottom of a coronal curvature; that is, the two vertebra most tilted towards each other. Cobb angle >10° defines scoliosis.

All spinal parameters are calculated from 36-in. film standing scoliosis films from the base of the occiput to the mid-femur (Fig. 11.1). Images should be obtained prior to surgery as well as on outpatient follow-up. The parameters are intended to guide operative planning for thoracolumbar fusion, even in patients with very mild deformity. Prudent for spine surgeons to understand that any fusion operation is a deformity correction, so the armamentarium of operative methods must be well-understood. Herein, we discuss a breadth of surgeries from osteotomies of the posterior bony elements to interbody fusion of the intervertebral disc space.

11.4 Osteotomy

Spinal malalignment in the sagittal and coronal planes carries a well-recognized impact on pain and disability, especially in adult scoliosis, flat back syndrome, iatrogenic fixed sagittal imbalance, and kyphotic decompensation syndrome [17]. Modern correction of spinopelvic parameters began with bony resections, known as osteotomies. Although multiple spinal osteotomy techniques have been described in the literature, interchangeable terms and substantial surgical variations render the discussion challenging. This chapter will utilize the Spinal Osteotomy Classification described by Schwab et al. [17] who proposed 6 grades of resection (Fig. 11.2):

- Grade 1: Partial Facet Joint Resection is ideally suited for surgeons unfamiliar with more aggressive osteotomies. Resection of the inferior facet and joint capsule allows for de-articulation that unroofs a cancellous surface for bony fusion. Described for previously fused segments most commonly at L1, L2, and L3, the Smith–Peterson osteotomy includes resection of the bilateral facet joints, part of the lamina, and posterior ligaments at the osteotomy site [18]. Terms such as Chevron osteotomy and extension osteotomy were described for unfused facets. Regardless of the history of spinal fusion, Grade 1 osteotomies require a mobile anterior column (disc space) for compression at the transpedicular screw heads; previous interbody arthrodesis is a contraindication to the osteotomy at that level. Approximately one degree of correction per millimeter of bone resected yields 5°–10° of sagittal improvement at each level [19]. Thus, the grade 1 osteotomy should be reserved for minor kyphotic deformities <30° or a C7 plumbline 6–8 cm positive. More experienced surgeons whose aggressive osteotomies distract the anterior disc space >10 m in height may opt for subsequent disc space grafting. Potential complications from lengthening of the anterior column and shortening the posterior column include cauda equina compression and abdominal vessel stretch injury [18]. Nerve roots may kink from decreased neural foraminal height. The procedure at thoracolumbar junction may compromise the cord from sagittal translation (coronal decompensation) of the column. Intraoperative neuromonitoring should evaluate both the spinal cord (somatosensory-evoked potentials and/or motor-evoked potentials) and nerve roots (electromyography).

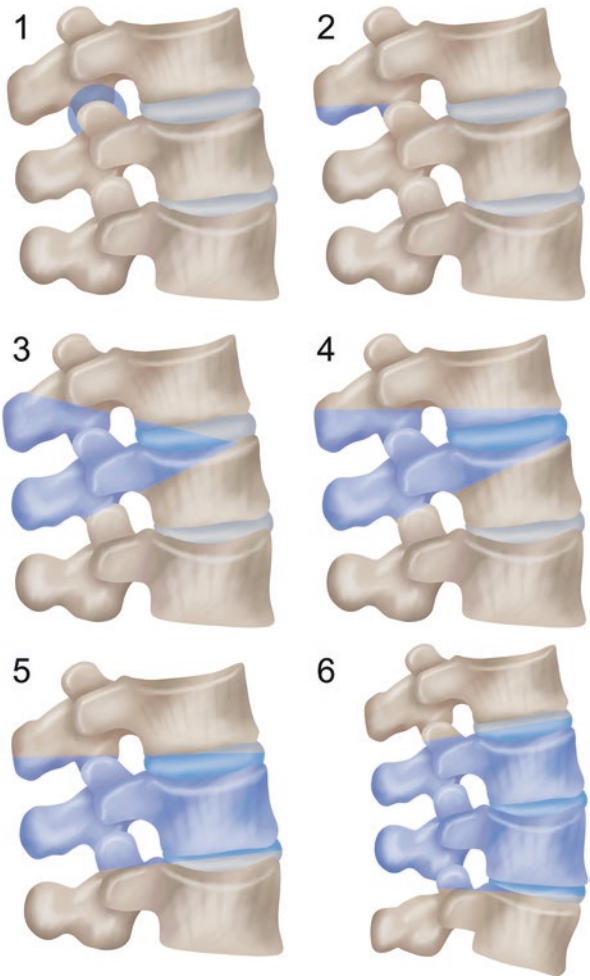

Fig. 11.2 Spinal Osteotomy Classification described by Schwab et al. [17] who proposed 6 grades of resection

- Grade 2: Complete Facet Joint Resection removes the entire superior and inferior facet joint. Resections may extend to more of the medial lamina, spinous process, and underlying ligaments (supraspinous ligament, infraspinous ligament, and ligamentum flavum). Approximately, 10° of sagittal alignment may be restored at each level for up to 40°–50° of global correction. The Ponte osteotomy, specifically, refers to the removal of multiple facets and spinous processes for a larger deformity correction [20]. The operation is intended for multiple levels particularly in the thoracic spine, such as Scheuermann's kyphosis and adolescent idiopathic scoliosis [21]. Like Grade 1 osteotomy, Grade 2 also requires a flexible disc space. However, because Grade 2 osteotomies are often performed at multiple levels, even bony resection at each level is unlikely. Some levels will completely fuse across the contact surface, while a small gap will persist at other levels, increasing the risk for pseudoarthrosis [22]. To facilitate

posterior closure, the operation may be combined with anterior longitudinal ligament (ALL) release (discussed below). Global kyphotic deformity of the thoracic spine ventrally displaces the spinal cord, decreasing the risk of spinal cord injury during posterior column shortening. However, the osteotomy at the thoracolumbar junction, when kyphosis transitions to lordosis, carries the highest risk of neurological injury and dural tear [22].

- Grade 3: Pedicle and Partial Body Resection entails removing all of the posterior elements including the spinous process, lamina, transverse processes, and the facet joint above and below. The bottom of the superior spinous process and the top of the inferior spinous process are also removed. A triangular wedge through the pedicle, via a de-cancellation technique or an osteotome, is removed. The posterior spine is shortened by closing the osteotomy, using the anterior cortex as a hinge [19]. A specialized operating table with flexion–extension capabilities facilitates the closure of the osteotomy. The most commonly described technique is the pedicle subtraction osteotomy (also known as the closing wedge osteotomy or the transpedicular wedge osteotomy) (Fig. 11.3). Between 25° and 35° of correction could be obtained at any given level. The operation is ideally suited for patients with flat back syndrome (PI–LL mismatch >30°) after prior 360° spinal fusion because the osteotomy does not require a mobile disc space; that is, prior interbody arthrodesis does not obviate the procedure. Patients with significant kyphosis between 30° and 40° with a sharp, angular deformity may require a significant hinge at the apex of the curvature, as patients with SVA > 12 cm are ideally corrected with a grade 3 osteotomy. To that end, a unilateral PSO can correct a severe coronal imbalance. A significant amount of stress is placed above and below the osteotomy level, so interspace grafting of an unfused disc space immediately rostral and caudal is advisable. If the disc space is already fused with an interbody, then short-segment satellite rods may be considered. Otherwise, pseudoarthrosis may reach upwards of 30% [19]. The operation does not lengthen the anterior column, circumventing the complications described in Grade 1 and 2 osteotomies. On the other hand, disadvantages of Grade 3 osteotomies include significant blood loss during the operation; meticulous hemostasis is of utmost importance. Up to 20% of cases reported transient neurological deficits, including radiculopathy, transient single nerve root weakness, and cauda equina syndrome. Neuromonitoring is mandatory during these procedures [19]. The highly destabilizing operation may cause vertebral translation; a temporary rod may be necessary to prevent cord injury.
- Grade 4: Pedicle, Partial Body, and Disc Resection is similar to a Grade 3 osteotomy, except that the vertebral body resection extends through adjacent intervertebral disc. The rib must be resected in the thoracic spine. Next, the wedge-shaped osteotomy is closed to decrease the risk of pseudoarthrosis, although a cage may be placed to obtain anterior column lengthening [19]. After posterior approximation, the proximity of the pedicle screws above and below the osteotomy site is thought to improve arthrodesis rates with a stronger fusion construct. Removal of the disc space also decreases the rate of pseudoarthrosis as compared to Grade 3 osteotomies [23, 24]. Sometimes referred to as

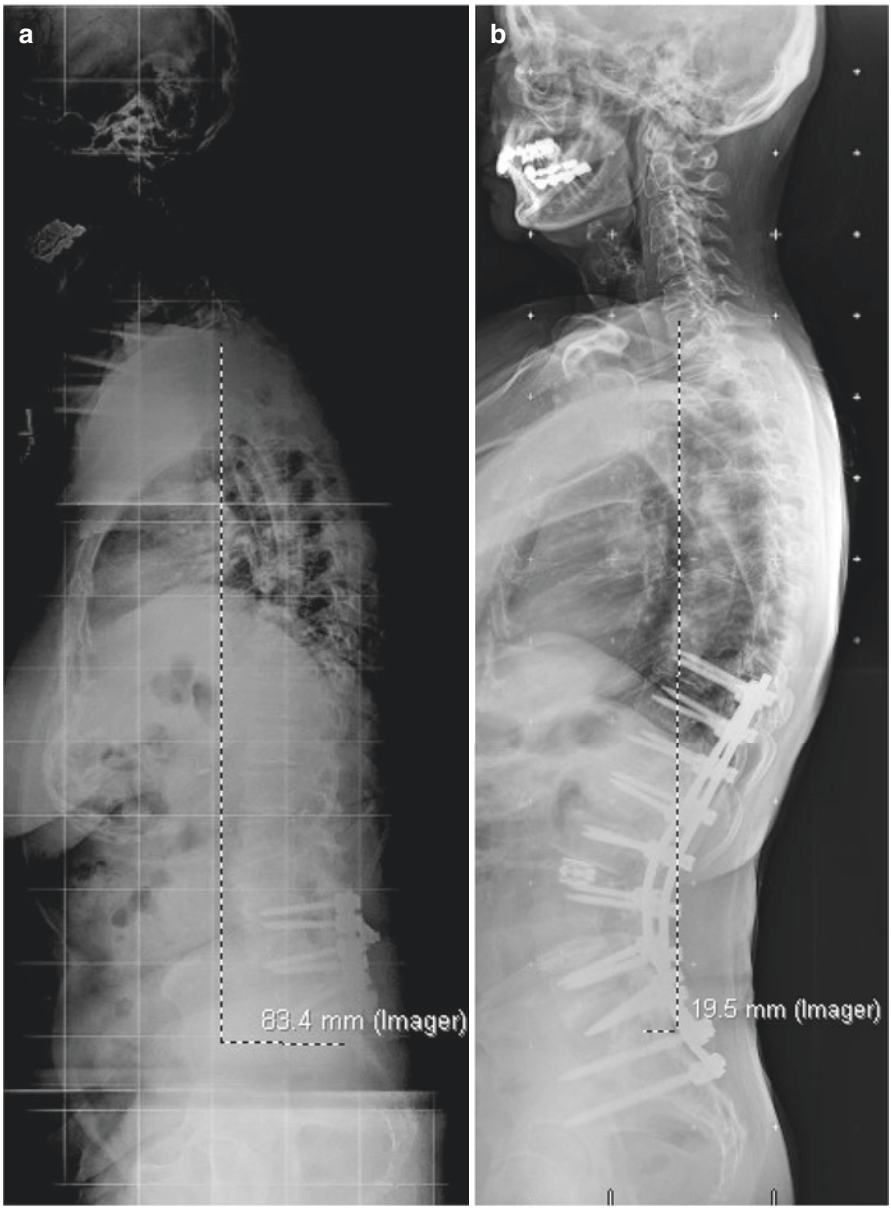

Fig. 11.3 36-in. standing X-ray. (**a**) Preoperative sagittal vertical axis. (**b**) Improvement in the sagittal vertical axis after a pedicle subtraction osteotomy

bone-disc-bone osteotomy, the procedure ideally corrects a deformity with the disc space at its apex. Ankylosing spondylitis with a calcified anterior anulus is a poor indication for Grade 4 osteotomy. Risks of neurovascular injury and blood loss with Grade 3 osteotomies apply here as well.

- Grade 5: Complete Vertebra and Discs Resection is associated with removal of the entire vertebra as well as the rostral and caudal intervertebral disc space. As with Grade 4, the rib must be resected in the thoracic spine. Although posterior-only approaches have been described, the operation usually entails both a posterior and anterior approach to the spine, which poses significant anatomical challenges in the upper thoracic spine given the great vessels, heart, and lungs [25, 26]. All the vertebral body bone must be resected to prevent buckling of the posterior longitudinal ligament into the spinal cord. If shortening of the entire spinal column is desired, a cage smaller in height may be placed anteriorly. Over-shortening may cause buckling of the spinal cord, so intraoperative neuromonitoring is imperative. Neurological deficits after correction most commonly occur by subluxation of the spinal column, dural buckling, and cord compression by residual bone or soft tissue. A temporary rod is typically required.
- Commonly known as a vertebral column resection, the procedure has been described for sharp angulated deformities or multi-planar deformities [19]. The most common surgical indication for deformity is a fixed coronal imbalance after prior operation for idiopathic scoliosis, although congenital scoliosis may have fixed deformities as well. Vertebral resections are not needed if the shoulder alignment remains leveled despite a severe coronal deformity. Otherwise, spinal tumors requiring en bloc resection is a popular indication for the Grade 5 osteotomies, but spondyloptosis, hemivertebrae, and posttraumatic deformities may also fall into this category. Grade 5 resections are rarely performed because of the high morbidity, including significant blood loss and neurological deficits [27].
- Grade 6: Multiple Adjacent Vertebrae and Discs Resection are similar to Grade 5 osteotomy, except more than one vertebra is involved. The operation is intended for children and adolescents undergoing three-dimensional corrections of spinal deformities. Similar surgical principles and risks apply in single-level vertebral resections.

Despite the aforementioned indications, aggressive osteotomies have fallen out of favor. The significant morbidity associated with higher-grade osteotomies needed for larger correction of adult spinal deformities with grossly imbalanced spinopelvic parameters compounded with advances in minimally invasive technologies contributed to a shift in the spine surgery paradigm from resection of the bony elements to surgery at the disc space. The so-called disc-space surgery lends itself to the MIS principles that have changed the landscape of complex spine, inasmuch as osteotomies have now been conserved for just a selected few conditions. According to a decision tree in adult spinal deformity set forth by the International Spine Study Group [15], the Minimally Invasive Spinal Deformity Revision 2 (MISDEF2) algorithm reserved osteotomies to only Class III—mini-open surgery and Class IV—open surgery. Class III patients had an SVA > 6 cm, PT > 25°, LL–PI mismatch >30°, and/or thoracic kyphosis >60°. Class IV patients had a fused or rigid spine.

Even if younger generation surgeons were still uncomfortable with bony resections in adult spinal deformity with Class III parameters, the MISDEF-2 guidelines ushered in an alternative or supplementary to osteotomies: the anterior column release (ACR). The procedure marks a critical turning point in the evolution of complex spine surgery in that MIS could finally address grossly imbalanced spinopelvic parameters. Moreover, in patients who did not require an ACR for larger spinal deformities, minimally invasive techniques still allowed for reasonable correction as the design of intervertebral spacers has improved in lumbar interbody fusions. In the next section, various MIS strategies in adult patients without fixed or rigid spinal deformity are discussed.

11.5 Minimally Invasive Surgery

Minimally invasive methods in spine surgery have gained widespread notoriety after the initial description in 2002 [28]. Benefits of microsurgical approaches include decreased length of stay, intraoperative blood loss, wound infections, and narcotic use. Because the muscle and soft tissues are not dissected off of the posterior elements, arthrodesis after minimally invasive spine surgery does not occur over the pedicle screw construct, but rather across the interbody in the intervertebral space. The appropriate spacer, therefore, becomes of utmost importance. The spacer also indirectly decompresses the neural elements. In addition to the anterior column support, the insert that increases the height of the intervertebral space restores foraminal height for the exiting nerve root. And, the greater tension of the posterior longitudinal ligament across the heightened intervertebral space will reduce soft-tissue redundancy or bulging into the spinal canal—a phenomenon known as ligamentotaxis—that will ameliorate spinal stenosis [29]. Initial spacers included iliac crest graft, which was associated with significant donor site pain at the hip. Common practice today includes artificial cages, which include a diversity of materials from polyetheretherketone (PEEK) to titanium cages. These cages provide an interface for arthrodesis in MIS. Fusion rarely occurs within the lateral gutters at the transpedicular screw-rod construct because the muscles are not dissected off the facet joints to allow ossification across the posterior elements.

As interbody implants have been perfected to optimize fusion, the role of minimally invasive spine surgery is becoming more commonplace in complex thoracolumbar reconstructions. Owing to the technical demands of larger osteotomies that carry an unfavorable safety profile, MISDEF-2 now recommends minimally invasive interbody fusion for LL–PI mismatch <30°, thoracic kyphosis <60°, thoracolumbar kyphosis <10°, and/or coronal Cobb angle >20° [15]. According to a retrospective review of a multicenter database for adult spinal deformity, three column osteotomies decreased from 36% in 2011 to 16.7% in 2016 [30]. While minimally invasive interbody fusions have flourished, the surgical approach of the interbody must be carefully selected based on the surgical goals, patient pathology, unique anatomy, and spinal level (Table 11.1) [31]. Preferences for interbody approach are also

Table 11.1 A comparison of transforaminal lumbar interbody fusion (TLIF) to lateral lumbar interbody fusion (LLIF)

	Transforaminal lumbar interbody fusion (TLIF)	Lateral lumbar interbody fusion (LLIF)	
		Trans-psoas	Anterior-to-psoas
Decompression	Optimal if direct decompression of the spinal canal necessary – Extension of the facetectomy medially to include a hemilaminotomy which provides access to remove the ligamentum flavum hypertrophy – Resection of the facet joint will address a synovial cyst that compresses the neural elements	Difficult to reach the spinal canal; primarily used for indirect decompression only	
Revision surgery	Excess scar tissue from prior posterior decompression and/or fusion will limit the surgical corridors to place the interbody cage; higher risk of durotomy	Optimal for access through virgin tissue in patients with prior surgery or prior infection posteriorly; decreased risk for durotomy	
Neurological deficit	Potential injury of the exiting nerve root at the level above (hypotenuse of Kambin's triangle) or the descending nerve root of the level below (medial border of Kambin's triangle)	Potential injury to the lumbosacral plexus, including transient paresthesia (ilioinguinal, iliohypogastric, and genitofemoral nerves) and/or femoral nerve weakness	Potential injury to the sympathetic chain
Musculature	Paraspinal muscle dissection necessary between the multifidus and longissimus muscles	The "rising psoas" will carry the lumbosacral plexus anteriorly, increasing the risk of nerve injury. Approach should be limited to psoas anatomically positioned lateral to the vertebral column	An anteriorly positioned psoas will limit the working corridor between the artery and muscle
Vasculature	Bleeding from the facetal artery is well-tolerated without significant blood loss	Injury to the segmental vessels	Entry limited to only the left side because injury to the aorta/iliac artery is more easily repaired than injury to the vena cava/iliac vein
		[a]An understanding of the renal artery position is necessary in the upper lumbar spine	

Table 11.1 (continued)

	Transforaminal lumbar interbody fusion (TLIF)	Lateral lumbar interbody fusion (LLIF)	
		Trans-psoas	Anterior-to-psoas
Peritoneum	Low risk	Higher risk for intestinal perforation. Injury to the liver is more common from a right-sided approach	
Anterior column realignment	Anterior longitudinal ligament difficult to reach	Necessary approach for anterior longitudinal ligament release	
Positioning	Single-position prone surgery	Single-position lateral, single-position prone, or interbody in the lateral position and transpedicular fusion in the prone position	Single-position lateral, or interbody in the lateral position and transpedicular fusion in the prone position. Single-position prone not possible
Duration of surgery	Increased retraction time on the paraspinal muscles increases postoperative pain	Dilation through the psoas muscle >30 min will risk hip flexion injury or damage to the lumbosacral plexus	Not time-limited
Lumbar level	Amenable at all lumbar levels	Iliac crest prevents access to L5–S1 and, occasionally, L4–L5	Amenable to all lumbar levels – L5–S1 usually requires an access surgeon for the oblique, retroperitoneal approach
		[a]Working around free-floating ribs at T12–L1 and L1–L2 is required	

Lateral approach may be accessed either trans-psoas or anterior-to-psoas
[a]At the upper lumbar spine, the psoas muscle tapers such that the trans-psoas and anterior-to-psoas difference no longer applies

influenced by the dynamic landscape in implant technology. Lateral lumbar interbody fusion (LLIF) increased from 6.4 to 24.1%, anterior lumbar interbody fusion (ALIF) decreased from 22.9 to 16.7%, and transforaminal lumbar interbody fusion (TLIF)/posterior lumbar interbody fusion utilization remained similar. The role of ALIF will be discussed later in the chapter. The decision between TLIF and LLIF depends on not only surgeon preference, but also the pathology addressed.

11.6 Anterior Column Realignment

The competence of the ALL prevents the interbody cage from dislodgement as well as provides a tension for grafting. However, with sagittal imbalance, the ALL limits lengthening of the anterior column, which, in and of itself, represents a fundamental

Fig. 11.4 36-in. standing X-ray. (**a**) Preoperative sagittal vertical axis. (**b**) Improvement in the sagittal vertical axis after an anterior column realignment

goal of surgery for focal kyphotic deformity correction. Herein lies the value of ACR, which releases the ALL and the annulus to allow for placement of a hyperlordotic cage for a focal kyphotic deformity correction (Fig. 11.4) [32].

11.7 Surgical Anatomy

11.7.1 Anterior Longitudinal Ligament

The ALL is composed of a strong band of fibers that attaches loosely to the anterior periosteum of the vertebral body, but the interval widening/thinning at each disc space affords a tight bind to the annulus fibrosus and the hyaline cartilage vertebral

end plates. This renders dissection of ALL at the intervertebral disc space difficult [32].

The ALL spans the entire length of the spinal column, ending at the ventral face of the sacrum. At the anterior arch of C1, the tough tension band continues rostrally to assimilate into the anterior atlantooccipital membrane. The ALL widens caudally into the lumbar spine, where the ligament becomes thickest with three layers: the deep and short intersegmental fibers, the intermediate fibers that span two to three vertebrae, and the superficial layer that spans three to four vertebrae [33].

11.7.2 Lumbar Plexus and Sympathetic Plexus

The sympathetic plexus runs along the lateral boarder of the ALL and therefore becomes at high risk for injury during the release procedure. As with all lateral approaches, the lumbar plexus travels intimately with the psoas muscle. The genitofemoral nerve (L1–L2) is especially at risk during its posterior-to-anterior course over the L2–L3 and L3–L4 disc spaces. At the inferior L4 endplate, the genitofemoral nerve travels anteriorly along with the sympathetic plexus. Here, both nerve structures are at risk for injury during the ALL release [32, 34].

11.7.3 Great Vessels

The aorta courses left paracentric to the lumbar spine. The aorta gives off four paired segmental lumbar arteries that travel along the vertebral body, avoiding the disc space. At approximately 18 mm above the L4–L5 disc space, the aorta bifurcates into the left and right common iliac arteries. The vena cava, on the other hand, forms from the left and right common iliac veins approximately 2 mm above the L4–L5 disc space, and the large vessel sits right paracentric to the lumbar spine. A thin layer of adipose tissue creates a surgical plane between the great vessels and the vertebral body. While the great vessels are at risk for injury during an ALL release, the fatty tissue serves as a safe zone of dissection [35, 36].

11.8 ACR Surgical Techniques

After computed tomography (CT) and magnetic resonance imaging analysis to assess ability to mobilize the disc space of interest, the patient was offered the ACR procedure (Fig. 11.4). The patient was positioned in a lateral position on a Jackson table and secured with cloth tape, then prepped and draped. Once level was assessed with fluoroscopy, a small incision was made in the flank and a minimally invasive approach to the spinal column was carried out. The disc was entered with a knife

from an anterior to the psoas access, and when not possible entirely, a small section of the ventral psoas was split bluntly. The disc space was prepared in the usual fashion with special attention not to disrupt the endplates. Spacer trials were used to distract the disc minimally until the adequate height was attained to allow for the interbody spacer to be placed. Bicortical disruption of the annulus was attained prior to placing the final implant. An ELSA expandable interbody lateral cage from Globus Medical, Inc. was used. Once the implant was placed and secured to the rostral and caudal vertebra with cortical screws through the appropriate tabs, a fourth dissector blade was used to gain access ventral to the ALL and dorsal to the greater vessels. By expanding the spacer progressively, the ALL would be placed under tension and sequentially dissected with a rongeur and/or knife. Once the ALL was completely dissected, the cage would be completely expanded without resistance.

Once the flank wound was closed and dressed, the patient was positioned onto a Jackson frame and prepped and draped. An iliac reference arch for the Excelsius Surgical Robot from Globus Medical, Inc. was gently impacted into the iliac crest and intraoperative CT imaging was obtained. The screws and posterior release osteotomy locations were planned. Attention was made to assure correct alignment of the screws. A midline incision to the fascia when possible was made to allow for the transmuscular placement of the screws using the robotic guide. Through small tubular exposures along the screw trajectories, the facets and caudal portion of the lamina were exposed and drilled away, thus allowing for a Smith Peterson type osteotomy to be completed. Bone was packed into the facet spaces. A rod was placed bilaterally and compression of the screws to close the osteotomies was carried out before locking the screws down to the rods. Final scoliosis imaging was obtained to assure adequate deformity correction prior to wound closure.

11.8.1 Anterior Column Realignment

Release of the ALL carries the highest rate of successful lengthening of the anterior spinal column (Fig. 11.4) [37]. However, surgeons must be comfortable with a variety of surgical approaches to the ALL and anterior disc space in order to address focal kyphotic deformities at the different spinal levels. While the iliac crest limits access to the L5–S1—and sometimes the L4–L5—segment in the lateral approaches, traditional ALIF are best suited at these interspaces situated between the bifurcation of the iliac vessels [38]. More minimally invasive techniques to L4–L5 and L5–S1 include an oblique lumbar interbody fusion that allows for less dissection of the retroperitoneal space in a minimally invasive fashion [39]. Above L4, the aorta and vena cava that straddle along the sides of the ALL render an anterior retroperitoneal approach challenging. At those higher lumbar interspaces, strict adherence to the surgical techniques in lateral or oblique lumbar interbody fusions is imperative to minimize the risk of complications [37]. Because both of these minimally invasive approaches have narrow operative corridors, visualization of the ALL and annulus

cannot be overemphasized for protection of the neurovascular structures seated anterior to the ligament [37]. Patients with aberrant vascular anatomy or extensively calcified aorta as well as prior retroperitoneal infections or operations may not be ideal candidates for ACR. Fixed deformities at the disk space, such as calcified bony bridges or prior interbody fusion, may require more extensive operations than release of the ALL. A high risk of vascular injury has been reported while removing anterior implants [40]. Similarly, posterior arthrodesis across the disc space would thwart any distraction from an ACR procedure; such revision cases are more amenable to posterior osteotomies [37].

The anterior column transmits 80% of the axial load applied to the spine [41]. Thus, placement of an interbody at the anterior disc space requires meticulous endplate preparation with a large footprint spacer. A wide interface between the implant and endplate will decrease the risk of subsidence [42]. With adequate surgical technique, the average single motion segment of correction for focal kyphosis with ACR has been reported between 24° and 34°, which are comparable to the average 30°–40° afforded by PSO [37, 43–45]. The advent of hyperlordotic cages has narrowed the gap between ACR and 3-column osteotomies. However, overambitious distraction with these cages may reduce the neuroforaminal area. Both the anterior *and* posterior height of the interbody must be measured for sufficient nerve root space [46]. A favorable anterior correction with ACR is a highly destabilizing procedure, and posterior fixation is required.

11.8.2 Navigated Posterior Fixation

Posterior transpedicular screws afford the strongest fusion construct. Traditionally, posterior supplementation was performed as a staged procedure on a different operative day. As minimally invasive techniques have facilitated ACR [47] single-stage surgery has become more commonplace. In fact, according to the MISDEF2, strictly open operations are now reserved for fused or rigid spine with >5 level fusion including L5–S1 or >10 levels [15]. In such cases, PSO over ALL release is warranted for sagittal imbalance; thus, an open operation is necessary for the entire procedure.

Regardless of minimally invasive versus open, the value of navigated screw placement cannot be overstated. Navigation options include an intraoperative CT scanner. Navigation facilitates the screw trajectory in the oftentimes distorted anatomy seen with adult spinal deformity. In a randomized trial comparing fluoroscopic versus navigated screws in deformity surgery, the latter decreased screw breaches, surgical time, and radiation exposure [48]. A meta-analysis comparing computer-navigation versus freehand insertion reported that the non-navigated group incurred higher rates of complications, including neurological deficits, dura mater violations, wound infection, cerebrospinal fluid leak, pleural injury, and injections [49]. These results underscore the value of navigation, especially in the thoracic vertebrae where the dimensions of the pedicles vary widely at each spinal level. To exacerbate

matters, in adult spinal deformity, the orientation of the pedicle between the left versus right side of the primary coronal curvature at each level varies considerably [48]. Malpositioning of the screws is less forgiving in the thoracic spine. A decreased canal-cord ratio carries a higher risk of damage to the neural elements [48]. Spinal cord injury in the thoracic spine may have more of a detrimental effect as compared to nerve root injuries in the lumbar spine, albeit damage to the lumbar nerve roots should not be understated. Because ACR in conjunction with hyperlordotic cages changes the direction of the pedicles in the lumbar spine, intraoperative imaging after placement of the interbody permits a greater appreciation of the shifting anatomy of the bony elements.

The sweeping success of computer-navigated screw placement in adult spinal deformity pushed the demand for technology with even greater accuracy [50]. An increasing interest in improved consistency, complication reduction, and decreased length of hospitalization saw the rise of robot-navigation. Within the field of deformity surgery, robot-assisted operations were popularized in the placement of the S2-alar-iliac screw, which arguably confers one of the strongest points of fixation for long-segment fusion in patients with sagittal imbalance [51]. But, robot-assisted spine surgery has many applications in transpedicular fusion. As compared to conventional freehand, a meta-analysis of nine randomized controlled trials with the robot-assisted technique found fewer proximal facet violations, which affects the incidence of proximal junctional kyphosis in larger constructs for deformity correction [52]. Because the robot assistance accounts for the three-dimensional anatomy, surgeons usually select a more lateral starting point that avoids the facet joint. With pre-instrumentation robotic planning in complex spinal fusions, the vertebral bodies can accommodate both a pedicle screw and lateral cortical screw that allow for a four-rod construct with more points of fixation points that decrease the rate of pseudoarthrosis and hardware failure for realignment surgery [53]. More specific to ACR that usually includes lateral approaches to the disc and ALL, robots allow for single-position surgery with pedicle screw placement in the lateral position, which has profound implications on length of surgery [54]. Herein, robotics have found the solution to improve surgical ergonomics and enhance surgical dexterity. These benefits of the robot, however, must be weighed against its limitations, which are most commonly cited as (1) soft-tissue pressures on the robotic arm that can cause deviations and (2) slipping of the guide down the slope of the facet [55].

11.9 Conclusion

Most spinal operations can be addressed with minimally invasive approaches. The choice of interbody approach as well as cage technology becomes imperative for successfully addressing spinopelvic imbalance. Osteotomies are mostly reserved for fixed deformities, whose correction goals will adjudicate the type of bony resection. In summary, complex spine surgeons must be comfortable with a wide range

of surgical techniques from larger open osteotomies to smaller minimally invasive corridors to provide optimal treatment for their patients.

References

1. Mohan AL, Das K. History of surgery for the correction of spinal deformity. Neurosurg Focus. 2003;14(1):e1.
2. Hadra BE. The classic: Wiring of the vertebrae as a means of immobilization in fracture and Potts' disease. Berthold E. Hadra. Med Times and Register, Vol 22, May 23, 1891. Clin Orthop Relat Res. 1975;112:4–8.
3. Lange F, Peltier LF. The classic. Support for the spondylitic spine by means of buried steel bars, attached to the vertebrae. By Fritz Lange. 1910. Clin Orthop Relat Res. 1986;203:3–6.
4. Harrington PR. Treatment of scoliosis. Correction and internal fixation by spine instrumentation. J Bone Jt Surg Am. 1962;44-A:591–610.
5. Harrington PR. The history and development of Harrington instrumentation. By Paul R. Harrington, 1973. Clin Orthop Relat Res. 1988;227:3–5.
6. Dwyer AF, Newton NC, Sherwood AA. An anterior approach to scoliosis. A preliminary report. Clin Orthop Relat Res. 1969;62:192–202.
7. Kaneda K, Shono Y, Satoh S, Abumi K. New anterior instrumentation for the management of thoracolumbar and lumbar scoliosis: application of the Kaneda two-rod system. Spine (Phila Pa 1976). 1996;21(10):1250–61; discussion 61–2.
8. Cotrel Y, Dubousset J. A new technic for segmental spinal osteosynthesis using the posterior approach. Rev Chir Orthop Reparatrice Appar Mot. 1984;70(6):489–94.
9. Sullivan M. AO ASIF principles in spine surgery. Spinal Cord. 1998;36(9):665.
10. Mac-Thiong JM, Transfeldt EE, Mehbod AA, Perra JH, Denis F, Garvey TA, et al. Can c7 plumbline and gravity line predict health related quality of life in adult scoliosis? Spine (Phila Pa 1976). 2009;34(15):E519–27.
11. Glassman SD, Berven S, Bridwell K, Horton W, Dimar JR. Correlation of radiographic parameters and clinical symptoms in adult scoliosis. Spine (Phila Pa 1976). 2005;30(6):682–8.
12. Videbaek TS, Bunger CE, Henriksen M, Neils E, Christensen FB. Sagittal spinal balance after lumbar spinal fusion: the impact of anterior column support results from a randomized clinical trial with an eight- to thirteen-year radiographic follow-up. Spine (Phila Pa 1976). 2011;36(3):183–91.
13. Kim MK, Lee SH, Kim ES, Eoh W, Chung SS, Lee CS. The impact of sagittal balance on clinical results after posterior interbody fusion for patients with degenerative spondylolisthesis: a pilot study. BMC Musculoskelet Disord. 2011;12:69.
14. Schwab FJ, Blondel B, Bess S, Hostin R, Shaffrey CI, Smith JS, et al. Radiographical spinopelvic parameters and disability in the setting of adult spinal deformity: a prospective multicenter analysis. Spine (Phila Pa 1976). 2013;38(13):E803–12.
15. Mummaneni PV, Park P, Shaffrey CI, Wang MY, Uribe JS, Fessler RG, et al. The MISDEF2 algorithm: an updated algorithm for patient selection in minimally invasive deformity surgery. J Neurosurg Spine. 2019;32(2):221–8.
16. Lamartina C, Berjano P. Classification of sagittal imbalance based on spinal alignment and compensatory mechanisms. Eur Spine J. 2014;23(6):1177–89.
17. Schwab F, Blondel B, Chay E, Demakakos J, Lenke L, Tropiano P, et al. The comprehensive anatomical spinal osteotomy classification. Neurosurgery. 2014;74(1):112–20. discussion 20
18. Hu WH, Wang Y. Osteotomy techniques for spinal deformity. Chin Med J (Engl). 2016;129(21):2639–41.
19. Kose KC, Bozduman O, Yenigul AE, Igrek S. Spinal osteotomies: indications, limits and pitfalls. EFORT Open Rev. 2017;2(3):73–82.

20. Ponte A, Orlando G, Siccardi GL. The true Ponte osteotomy: by the one who developed it. Spine Deform. 2018;6(1):2–11.
21. Pizones J, Sanchez-Mariscal F, Zuniga L, Izquierdo E. Ponte osteotomies to treat major thoracic adolescent idiopathic scoliosis curves allow more effective corrective maneuvers. Eur Spine J. 2015;24(7):1540–6.
22. Perez-Grueso FS, Cecchinato R, Berjano P. Ponte osteotomies in thoracic deformities. Eur Spine J. 2015;24(Suppl 1):S38–41.
23. Enercan M, Ozturk C, Kahraman S, Sarier M, Hamzaoglu A, Alanay A. Osteotomies/spinal column resections in adult deformity. Eur Spine J. 2013;22(Suppl 2):S254–64.
24. Ozturk C, Alanay A, Ganiyusufoglu K, Karadereler S, Ulusoy L, Hamzaoglu A. Short-term X-ray results of posterior vertebral column resection in severe congenital kyphosis, scoliosis, and kyphoscoliosis. Spine (Phila Pa 1976). 2012;37(12):1054–7.
25. Suk SI, Kim JH, Kim WJ, Lee SM, Chung ER, Nah KH. Posterior vertebral column resection for severe spinal deformities. Spine (Phila Pa 1976). 2002;27(21):2374–82.
26. Bradford D. Vertebral column resection. Printed abstract from the association of bone and joint surgeons annual meeting. Orthop Trans. 1987;11:502.
27. Bradford DS, Tribus CB. Vertebral column resection for the treatment of rigid coronal decompensation. Spine (Phila Pa 1976). 1997;22(14):1590–9.
28. Calvachi-Prieto P, McAvoy MB, Cerecedo-Lopez CD, Lu Y, Chi JH, Aglio LS, et al. Expandable versus static cages in minimally invasive lumbar interbody fusion: a systematic review and meta-analysis. World Neurosurg. 2021;151:e607–14.
29. Yoshihara H. Indirect decompression in spinal surgery. J Clin Neurosci. 2017;44:63–8.
30. Daniels AH, Reid DB, Tran SN, Hart RA, Klineberg EO, Bess S, et al. Evolution in surgical approach, complications, and outcomes in an adult spinal deformity surgery multicenter study group patient population. Spine Deform. 2019;7(3):481–8.
31. Barbagallo GM, Albanese V, Raich AL, Dettori JR, Sherry N, Balsano M. Lumbar lateral interbody fusion (LLIF): comparative effectiveness and safety versus PLIF/TLIF and predictive factors affecting LLIF outcome. Evid Based Spine Care J. 2014;5(1):28–37.
32. Cheung ZB, Chen DH, White SJW, Kim JS, Cho SK. Anterior column realignment in adult spinal deformity: a case report and review of the literature. World Neurosurg. 2019;123:e379–e86.
33. Bogduk N. Clinical and radiological anatomy of the lumbar spine. Amsterdam: Elsevier Health Sciences; 2012.
34. Ozgur BM, Aryan HE, Pimenta L, Taylor WR. Extreme lateral interbody fusion (XLIF): a novel surgical technique for anterior lumbar interbody fusion. Spine J. 2006;6(4):435–43.
35. Deukmedjian AR, Le TV, Dakwar E, Martinez CR, Uribe JS. Movement of abdominal structures on magnetic resonance imaging during positioning changes related to lateral lumbar spine surgery: a morphometric study: clinical article. J Neurosurg Spine. 2012;16(6):615–23.
36. Arslan M, Comert A, Acar HI, Ozdemir M, Elhan A, Tekdemir I, et al. Surgical view of the lumbar arteries and their branches: an anatomical study. Neurosurgery. 2011;68(1 Suppl):16–22.
37. Akbarnia BA, Mundis GM Jr, Moazzaz P, Kabirian N, Bagheri R, Eastlack RK, et al. Anterior column realignment (ACR) for focal kyphotic spinal deformity using a lateral transpsoas approach and ALL release. J Spinal Disord Tech. 2014;27(1):29–39.
38. Hosseini P, Mundis GM Jr, Eastlack RK, Bagheri R, Vargas E, Tran S, et al. Preliminary results of anterior lumbar interbody fusion, anterior column realignment for the treatment of sagittal malalignment. Neurosurg Focus. 2017;43(6):E6.
39. Phan K, Maharaj M, Assem Y, Mobbs RJ. Review of early clinical results and complications associated with oblique lumbar interbody fusion (OLIF). J Clin Neurosci. 2016;31:23–9.
40. Nguyen HV, Akbarnia BA, van Dam BE, Raiszadeh K, Bagheri R, Canale S, et al. Anterior exposure of the spine for removal of lumbar interbody devices and implants. Spine (Phila Pa 1976). 2006;31(21):2449–53.
41. Dvorak MF, Kwon BK, Fisher CG, Eiserloh HL 3rd, Boyd M, Wing PC. Effectiveness of titanium mesh cylindrical cages in anterior column reconstruction after thoracic and lumbar vertebral body resection. Spine (Phila Pa 1976). 2003;28(9):902–8.

42. Macki M, Anand SK, Surapaneni A, Park P, Chang V. Subsidence rates after lateral lumbar interbody fusion: a systematic review. World Neurosurg. 2019;122:599–606.
43. Bridwell KH, Lewis SJ, Lenke LG, Baldus C, Blanke K. Pedicle subtraction osteotomy for the treatment of fixed sagittal imbalance. J Bone Jt Surg Am. 2003;85(3):454–63.
44. Lafage V, Schwab F, Vira S, Hart R, Burton D, Smith JS, et al. Does vertebral level of pedicle subtraction osteotomy correlate with degree of spinopelvic parameter correction? J Neurosurg Spine. 2011;14(2):184–91.
45. Kim KT, Suk KS, Cho YJ, Hong GP, Park BJ. Clinical outcome results of pedicle subtraction osteotomy in ankylosing spondylitis with kyphotic deformity. Spine (Phila Pa 1976). 2002;27(6):612–8.
46. Saigal R, Mundis GM Jr, Eastlack R, Uribe JS, Phillips FM, Akbarnia BA. Anterior column realignment (ACR) in adult sagittal deformity correction: technique and review of the literature. Spine (Phila Pa 1976). 2016;41(Suppl 8):S66–73.
47. Smith ZA, Fessler RG. Paradigm changes in spine surgery: evolution of minimally invasive techniques. Nat Rev Neurol. 2012;8(8):443–50.
48. Rajasekaran S, Vidyadhara S, Ramesh P, Shetty AP. Randomized clinical study to compare the accuracy of navigated and non-navigated thoracic pedicle screws in deformity correction surgeries. Spine (Phila Pa 1976). 2007;32(2):E56–64.
49. Shin BJ, James AR, Njoku IU, Hartl R. Pedicle screw navigation: a systematic review and meta-analysis of perforation risk for computer-navigated versus freehand insertion. J Neurosurg Spine. 2012;17(2):113–22.
50. Ghasem A, Sharma A, Greif DN, Alam M, Maaieh MA. The arrival of robotics in spine surgery: a review of the literature. Spine (Phila Pa 1976). 2018;43(23):1670–7.
51. Bederman SS, Hahn P, Colin V, Kiester PD, Bhatia NN. Robotic guidance for S2-alar-iliac screws in spinal deformity correction. Clin Spine Surg. 2017;30(1):E49–53.
52. Li HM, Zhang RJ, Shen CL. Accuracy of pedicle screw placement and clinical outcomes of robot-assisted technique versus conventional freehand technique in spine surgery from nine randomized controlled trials: a meta-analysis. Spine (Phila Pa 1976). 2020;45(2):E111–E9.
53. Patel R. Use of robotic assistance in complex spine cases. Spine. 2018;43(7S):S26–S7.
54. Huntsman KT, Riggleman JR, Ahrendtsen LA, Ledonio CG. Navigated robot-guided pedicle screws placed successfully in single-position lateral lumbar interbody fusion. J Robot Surg. 2020;14(4):643–7.
55. Joseph JR, Smith BW, Liu X, Park P. Current applications of robotics in spine surgery: a systematic review of the literature. Neurosurg Focus. 2017;42(5):E2.

Chapter 12
Thoracoscopic Microdiscectomy with Preservation of Rib and Costovertebral Joint

E. M. J. Cornips and E. A. M. Beuls

Abbreviations

CT	Computed tomography
CTJ	Costotransverse joint
CVJ	Costovertebral joint
HD	High-definition
TDH	Thoracic disc herniation
TMD	Thoracoscopic microdiscectomy
TMD-R	Thoracoscopic microdiscectomy with preservation of rib and costovertebral joint

12.1 Introduction

The clinical and radiological spectrum of thoracic disc herniations (TDHs) is surprisingly divers. While the incidence of symptomatic TDHs is often claimed at 1 per 1×10^6, their true incidence is likely underestimated due to their diverse and often misleading presentation unfamiliar to most clinicians with little experience with these lesions [1, 2]. Many of them are to a variable degree calcified and may have

E. M. J. Cornips (✉)
Department of Neurosurgery, Ziekenhuis Oost-Limburg, Genk, Belgium
e-mail: Erwin.Cornips@zol.be

E. A. M. Beuls
Centrum voor Gerechtelijke Geneeskunde, Antwerp University, Antwerp, Belgium

C. Di Rocco (ed.), *Advances and Technical Standards in Neurosurgery*, Advances and Technical Standards in Neurosurgery 45,
https://doi.org/10.1007/978-3-030-99166-1_12

been present for a long time before producing symptoms and eventually being diagnosed [3, 4]. This observation, their potential to become very large (so-called giant [5] or massive [6] TDHs), as well as their frequent association with morbus Scheuermann (kyphosis juvenalis dorsalis) suggest a completely different pathogenesis (part of a growth disorder of the thoracic or thoracolumbar spine) as compared to their cervical and lumbar counterparts (part of a degenerative process) [2]. While different techniques have been reported over the years to address these challenging lesions [7–14], some of the largest series published to date are thoracoscopic microdiscectomy (TMD) series [6, 8, 15–17] as this technique has proven to be safe and efficient for the entire spectrum of symptomatic TDHs, regardless of size [6], laterality, consistency, and multiplicity.

Clearly, every technique has its drawbacks and limitations. The TMD technique requires significant material investment including a dedicated instrument set (e.g., Miaspas TL®, Aesculap), a long drill attachment (e.g., long straight attachment, Midas Rex Legend®, Medtronic), a high-quality endoscope and video tower, etc. Moreover, it requires significant personal investment to master the learning curve. The upper limit for a standard TMD is T4–T5, as above that level the angle becomes too steep to safely decompress the spinal cord anteriorly. However, the T3–T4 level may be approached through a single right-sided axillary incision (fixed position of the aortic arch on the left side) through which scope and instruments are advanced while applying essentially the same technique. The rarely affected T2–T3 level may require a sternotomy. The lower limit for a standard TMD (with some experience) should be T11–T12 in all patients provided they are carefully positioned and well-curarized (diaphragm relaxation). A fan retractor (e.g., Endo Retract II®, Tyco Auto Suture) may be necessary to keep diaphragm and/or lung away from the affected level especially on the left side. Pleural adhesions can usually be dealt with endoscopically. Obesity obscures surface anatomy including segmental vessels that may retract when injured. Morbid obesity (BMI $\geq$ 40) is a contraindication for single-lung ventilation in lateral decubitus as excessive weight on top of the dependent (ventilated) lung would necessitate very high ventilatory pressures.

One specific drawback never thoroughly discussed in the literature is the problem of postoperative band-like pain on the ipsilateral side of the thorax. Acute ipsilateral costal pain can be minimized with optimal patient positioning and flexible plastic trocars (e.g., Flexipath® 15 mm trocar, Ethicon Endo-Surgery) to keep intercostal spaces open while minimizing periosteal trauma (Fig. 12.1) [18]. Moreover, intercostal nerve blocks can be administered either at the beginning (provided the procedure doesn't take too long) or at the end of surgery. Chronic ipsilateral band-like pain, however, is a more complex problem of variable intensity and duration. If after 4–6 weeks and certainly after 3 months the pain is still prominent, it will likely become a chronic pain and, in some cases, a truly incapacitating pain that is very difficult to treat. On the other hand, we were reluctant not to offer patients suffering severe pain (Anand grade 1–3B) [15] as well as a substantial part of patients presenting with a myelopathy (Anand grade 4 and 5) [15], a potentially life-altering operation only because they might develop another type of pain related to the

Fig. 12.1 Patient positioning on a vacuum mattress (left-sided approach, right lateral decubitus), the OR table bent underneath the thorax in order to open up ipsilateral intercostal spaces allowing easy access in between the ribs. Possible pressure points (including ulnar and peroneal nerve) are carefully padded

procedure itself. After all, as most of our cervical and lumbar disc herniation operations are related to pain, why should TDH patients (often suffering refractory pain for many years) be treated any differently? In this regard, we strongly believe that the issue of indicating surgical decompression in case of a TDH causing refractory pain urgently deserves more attention in the literature.

In this paper, we present a novel TMD-R technique—and the rationale behind it—that significantly reduces acute and chronic postoperative pain by preserving the rib and the costovertebral joint (CVJ) at the involved level.

12.2 Material and Methods

After the introduction of the TMD technique in 2000, many patients were sent to us mainly from Belgium and The Netherlands. In June 2013, two young otherwise healthy patients with TDH-related refractory pain were scheduled for single level TMD (case # 376 and 377 in our consecutive series). As part of an informed consent, they had been thoroughly informed with regard to possible complications and drawbacks related to the procedure, including postoperative band-like pain that we had come to believe might be related to destruction of the costovertebral joint (CVJ). The option of trying to preserve the CVJ was discussed and both agreed. As it turned out to be rather straightforward in both cases, this novel technique was applied to all subsequent patients and further refined over the past 6 years.

12.2.1 Original TMD Technique (Rosenthal, 1994) (Fig. 12.2)

The TMD technique was originally described by Rosenthal in 1994 [7]. In a subsequent paper, Rosenthal and Dickman describe the following steps to expose and decompress the dura (Fig. 12.2):

> *Remove the proximal 2 cm (including the head) of the rib and pedicle to expose the spinal canal and visualize the lateral surface of the dura. Detach the neurovascular bundle, intercostal muscles, costotransverse and costovertebral ligaments from the rib, then transect the rib. Identify the pedicle caudal to the disc space, cut the foraminal ligaments from its superior edge, and remove the pedicle using a Kerrison rongeur to expose the epidural space. Early identification of the dura allows to visualize the anterolateral border of the spinal canal and enables constant visual orientation to the position of the spinal cord during any subsequent dissection. Proper orientation and creation of a sufficiently large cavity in dorsal disc space and adjacent vertebral bodies are critical to safe decompression. The cavity should provide enough room to pull the TDH away from the epidural space into the cavity while minimizing the entry of tools into the compressed epidural space. The cavity should be wide enough so that it extends cephalad and caudal to the TDH allowing the surgeon to visualize normal dura above and below the pathological level. The cavity should be deep enough to expose the entire ventral surface of the dura across the spinal canal to the medial border of the contralateral pedicle. For the treatment of small or moderate-sized TDHs, the working cavity is shaped like a pyramid. To expose large, ossified, or intradural TDHs, much more room (a corpectomy) is needed.* [8].

The TMD technique was introduced in our center (at the time the MUMC+, Maastricht, The Netherlands) in 2000 and modified over the years as technology evolved and experience accumulated. The low-speed irrigated drill and oscillating saw used to cut the rib (Miaspas TL®, Aesculap) were substituted by a high-speed irrigated drill (Midas Rex Legend®, Medtronic) that allowed faster yet more delicate

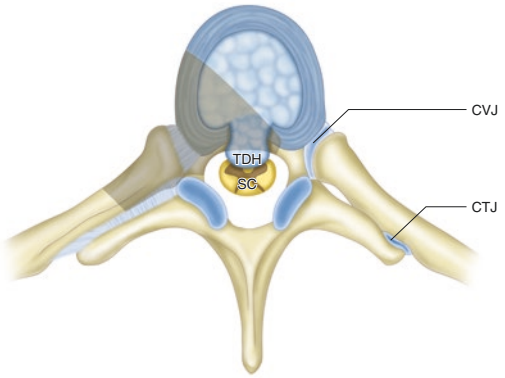

Fig. 12.2 Original TMD technique with typical bone removal (shaded area, right-sided approach). The proximal 2 cm of the rib is removed destroying the costovertebral joint. *CVJ* costovertebral joint, *CTJ* costotransverse joint, *SC* spinal cord, *TDH* thoracic disc herniation

bone removal. The low-resolution video tower was substituted by a high-definition (HD), and more recently, a 3D HD video tower (IMAGE 1 S™ 3D, Storz). Also, for a long time, we had been wondering whether it was really necessary to remove the proximal 2 cm of the rib and pedicle as this had several (theoretical) disadvantages. First, as the epidural venous plexus is essentially situated lateral to the thecal sac, opening the spinal canal laterally (as in the cervical and lumbar spine) often causes brisk venous bleeding difficult to control especially as long as the dura is not adequately decompressed. Second, destroying the complex articulation of the rib with the vertebral bodies (costovertebral joint, CVJ) and (when going a little more posterior) the transverse process (costotransverse joint, CTJ) may contribute to the little understood and difficult to treat problem of postoperative band-like pain we had observed in too many patients and we believed was likely caused by anomalous and asynchronous movements of the involved rib. Finally, in anterior cervical discectomy, we also go straight to the offending disc herniation which is then gently pulled away from the dura while avoiding manipulation close to the epidural venous plexus and vertebral artery situated laterally.

Thus, after 375 consecutive TMD procedures performed by the first author (EC), we decided to try decompress the dura without removing the proximal 2 cm of the rib and pedicle. As the first two cases were an immediate success, we subsequently applied this novel technique (so-called TMD-R) in another 179 consecutive cases in between June 2013 and October 2019.

12.2.2 Novel TMD-R Technique (**n = *142***) (Figs. 12.3, 12.4 and 12.5)

Patient positioning and initial exposure are identical to the original TMD technique (Fig. 12.1) [7, 8]. The parietal pleura covering vertebral bodies and proximal 2 cm of the rib at the involved level is opened and the posterior part of the intervertebral disc up to the anterior border of the head of the rib (Y-shape) is incised using monopolar coagulation. We do not use intraoperative imaging or navigation techniques as we localize the level preoperatively [19], count the ribs (top-down) intraoperatively, and during actual drilling rely on our anatomical knowledge of the thoracic spine and most importantly of the unique situation in any given patient at any specific level. Actually, it turns out that by preserving the head of the rib, the working area is reduced and the risk of drilling too posteriorly (into pedicle or even facet joint) is virtually eliminated. Of note, it is of paramount importance to have relevant neuroimaging files clearly visible to the attending surgeon, including axial and sagittal CT or CT myelography images, as all important landmarks are bony and no other examination comes close in depicting the exact relationship between them [6–8, 19]. With experience, every little (bony) detail may become a relevant landmark.

We agree with Rosenthal that creation of a sufficiently large cavity in dorsal disc space and adjacent vertebral bodies is critical to safe decompression [8]. However,

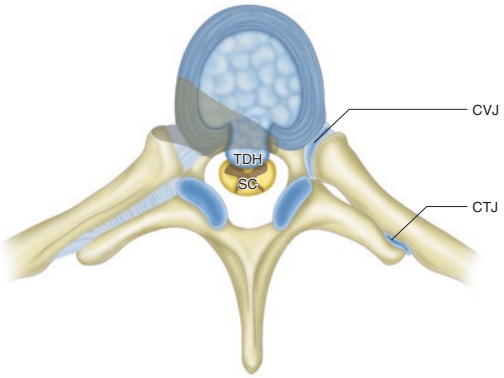

Fig. 12.3 TMD-R technique with typical bone removal (shaded area, right-sided approach). A few mm of the head of the rib is shaved while costovertebral joint and pedicle are preserved. *CVJ* costovertebral joint, *CTJ* costotransverse joint, *SC* spinal cord, *TDH* thoracic disc herniation

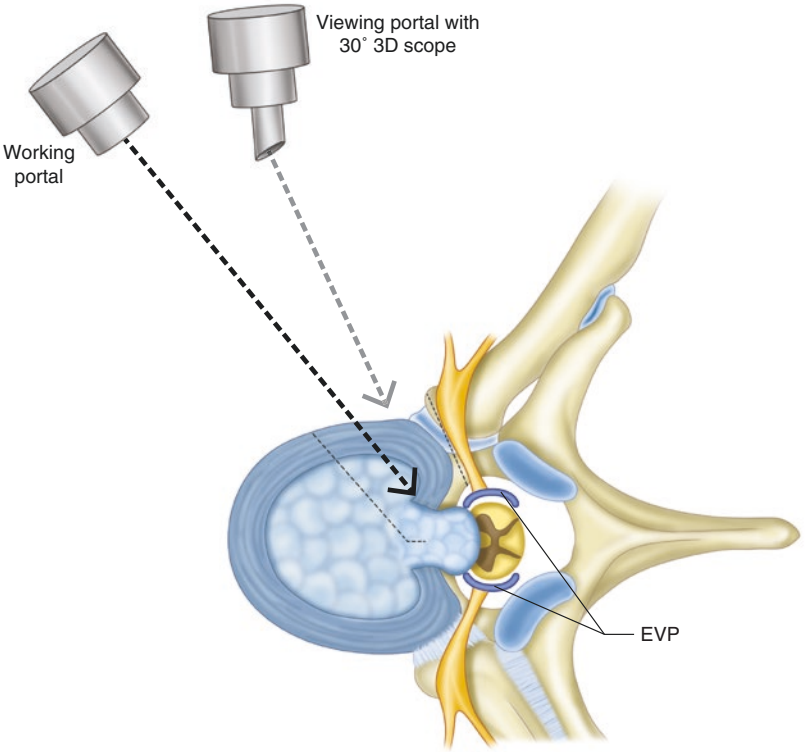

Fig. 12.4 TMD-R technique, surgeon's perspective. A few mm of the head of the rib is shaved in order to gain access and an unobstructed line of sight into the spinal canal ipsilaterally. The pedicle and epidural venous plexus underneath are untouched thus minimizing epidural venous oozing. *EVP* epidural venous plexus, situated lateral to the thecal sac

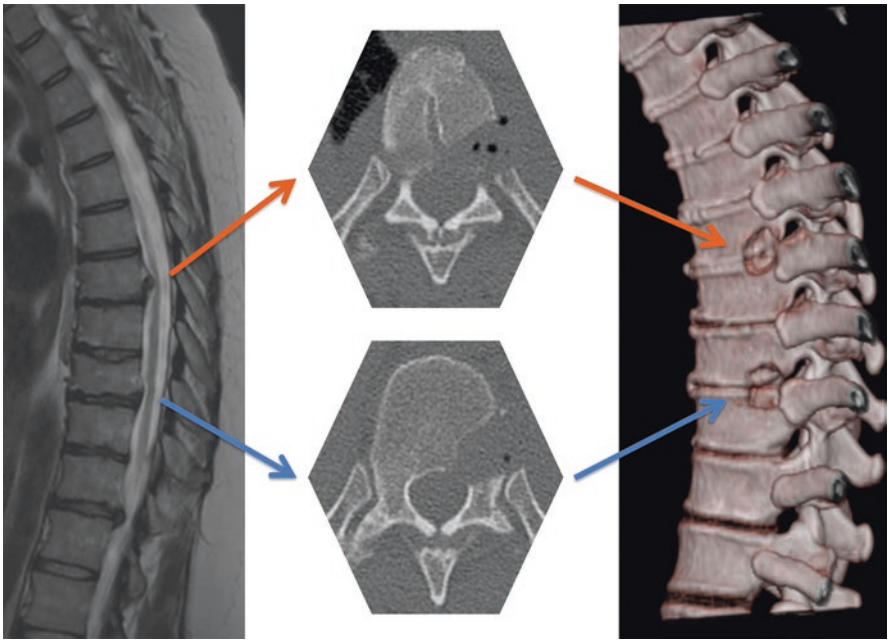

Fig. 12.5 Two-level symptomatic TDHs with postoperative 3D-reconstructed CT image demonstrating adequate decompression with preservation of both ribs and costovertebral joints

in order to accomplish this, we start drilling immediately anterior to the head of the rib in the adjacent vertebrae and resect the ipsilateral part of the intervertebral disc using grasping forceps on our way down (Fig. 12.3). As a rule of thumb, the drill angle is about 30°–45° aimed posteriorly (while the patient's spine is perpendicular to the table) starting immediately anterior (and usually no further than 1–1.5 cm anterior) to the head of the rib (Fig. 12.4). This entry point is connected to a point at the contralateral margin of the TDH at the level of the intervertebral disc bordering the anterior spinal canal on the relevant axial CT or CT myelography image (Figs. 12.3 and 12.4). This line marks the triangular posterior part of vertebral bodies and intervertebral disc in between to be removed and gives an indication how deep one has to drill (usually in between 2.5 and 3.5 cm). As mentioned, in case of small or medium-sized TDHs (and even beyond), we do not drill any further than 1–1.5 cm anterior to the head of the rib. We do, however, shave a few mm of the head of the rib using the 6 mm fine diamond drill in order to gain access and an unobstructed line of sight into the spinal canal ipsilaterally (Figs. 12.3, 12.4 and 12.5). This is a small yet important step that helps to find the right drill angle and to avoid going too much anteriorly, while it will not affect the CVJ and CTJ thus preserving physiological motion of the rib [20]. We shave off just enough to have an unobstructed line of sight and drill all the way down to the posterior wall which once identified is freed from ipsilateral to as far contralateral we need to go depending on size and laterality of the TDH (tailored size of the resection cavity).

We keep the surgical field clean using an irrigated drill and continuous suction, while avoiding early opening of the spinal canal (at which point venous oozing will start). In these conditions, state-of-the-art HD video screens will clearly show the bone changing color and texture from slightly purple porous spongious bone to more ivory solid cortical bone when approaching the posterior vertebral wall corresponding to the anterior border of the spinal canal. With some experience, it is safe to drill up to this level and even to open the posterior wall very gently at which point some venous oozing will invariably occur. This is a sign we are entering the spinal canal which we do not open any further (a small breach can easily be sealed with some gelatin sponge) until we have reached the posterior wall cranial, caudal, and contralateral to the TDH as measured using depth markings on the instruments. The remaining almost transparent shell of cortical bone and (at thoracic level quite variable) posterior longitudinal ligament can now be opened using drill or 2 mm up and down-biting Kerrison punch. The TDH can subsequently be delivered into the resection cavity in pieces (as in anterior cervical discectomy) or as a single (calcified) fragment using delicate instruments (short or medium length exploration hook, curved dissector, 2 mm up and down-biting Kerrison punch).

We explore the cleavage plane between TDH and dura cranial, caudal, but first of all ipsilateral to the TDH where the transition between ventral dura (perpendicular to the table and covered by the TDH) and lateral dura (in line with the table and covered by the epidural venous plexus and caudal pedicle) is observed. By gently lifting or even retracting the epidural venous plexus 1 or 2 mm using a short exploration hook, the lateral dura lying underneath may be observed. The ipsilateral cleavage plane between TDH and dura is identified, while the apex of the TDH may still be pushing the ventral dura backward even though resection of the posterior wall and base of the TDH have already created some initial decompression into the vertebral resection cavity. Of note, in our experience at thoracic levels, the posterior longitudinal ligament has a variable thickness ranging from virtually nonexistent to a few mm thick. Occasionally, the TDH seems to be incorporated into the ligament, and as in anterior cervical discectomy, leaving the ligament may then result in inadequate decompression. One can only be sure the TDH is completely resected when the dura (more bluish than the ligament) is exposed and the long exploration hook can move freely in the epidural compartment in every direction. Of note, transdural extension of very large TDHs may be less frequent than previously thought as most CSF leaks may in fact be iatrogenic [5, 21].

Manipulating the TDH will activate epidural venous oozing that will diminish once the dura has been adequately decompressed. It is then easily controlled using small cubes of gelatin sponge and irrigation. The trick to minimize venous oozing, as mentioned before, is to enter the canal only when drilling has completely freed the TDH from its surroundings including resection of its large base. This creates some initial decompression (as residual TDH and underlying dura move forward into the resection cavity) and substantially shortens the time frame in which epidural venous oozing may occur [6]. After TDH resection, the surgical field is irrigated, dura and epidural venous plexus are covered with small cubes of gelatin sponge (Spongostan™ Dental, Ethicon), and the resection cavity is gently filled but

not overfilled with larger pieces of gelatin sponge. Finally, the thoracic cavity is gently irrigated and inspected to remove bone dust and other debris, and the incisions are closed using staples after reinsufflation of the lung.

12.2.3 Novel TMD-R Technique Applied to Giant and Massive TDHs (n = 39) (Figs. 12.3, 12.4 and 12.6)

Giant TDHs (occupying >40% of the antero-posterior diameter of the spinal canal) [5] and massive TDHs (both antero-posterior and transverse diameters >10 mm) [6] are among the most challenging lesions in spinal surgery. They may be very large and extend deep into the spinal canal, disorienting the surgeon. They may be adherent to or even perforate the dura. They may be largely calcified or even ossified in

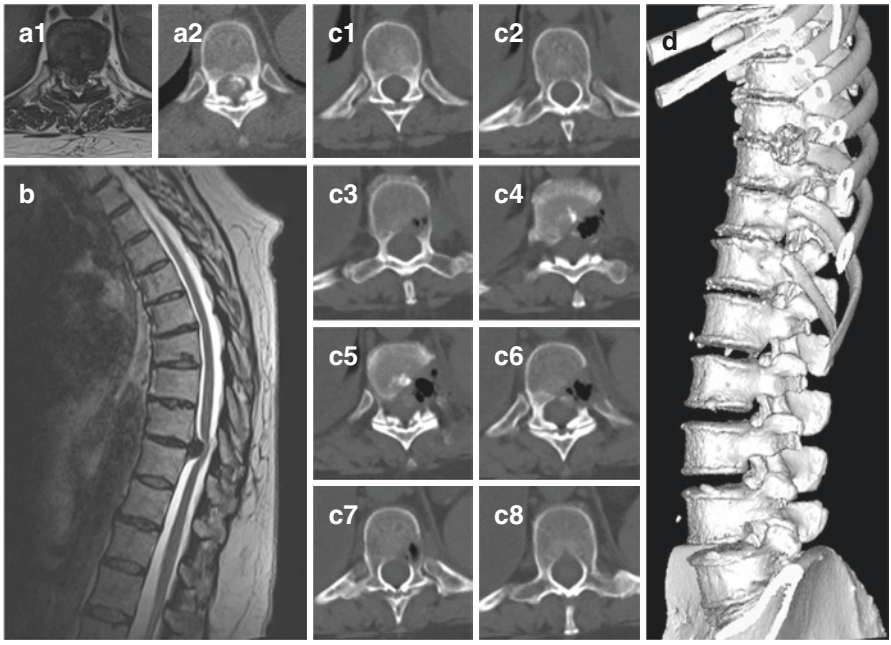

Fig. 12.6 Massive partially calcified T9–T10 TDH almost completely filling the spinal canal causing major spinal cord compression (residual anteroposterior spinal cord diameter 2 mm) and right dorsolateral displacement (**A1** and **B**, axial and sagittal T2-weighted MRI; **A2**, axial CT). Postoperative axial CT images (cranio-caudal sequence from T9 to T10) demonstrating T9 corpus, rib, and pedicle (**C1**–**C2**), T9–T10 resection cavity with small TDH residual strongly adherent to the dura (**C3**–**C6**), resection of a few mm of the head of the tenth rib with preservation of the CVJ (**C5**–**C7**), and resection of the upper border of the T10 pedicle anteriorly in order to gain better access ipsilaterally (**C6**–**C8**). A 3D-reconstructed CT image confirms a very targeted resection cavity that preserves the CVJ as well as segmental stability, thus obviating the need for segmental stabilization despite the hernia's massive dimensions (**D**)

contrast to the underlying chronically compressed, flattened, fragile spinal cord. We have previously published a series of high-risk TDHs operated using intraoperative motor-evoked potential (MEP) monitoring, demonstrating that in experienced hands such lesions can be dealt with safely using strict endoscopic technique [6]. The technique is essentially the same as the basic TMD-R technique described above, including preservation of rib and CVJ, yet some points deserve extra attention. It is even more important to drill all around the TDH, i.e., far enough ipsilateral, contralateral, cranial, and caudal. For ipsilateral exposure (especially when the TDH extends underneath the pedicle), a few mm more of the head of the rib can be drilled away. Again, care should be taken not to open the spinal canal too early, which is of paramount importance when dealing with massive TDHs that completely fill the canal causing massive engorgement of the epidural venous plexus.

Giant calcified TDHs tend to be strongly attached to intervertebral disc, endplates, and adjacent vertebral bodies. As long as they have not been completely freed from these structures (at which point what is left of them suddenly becomes mobile), we can safely reduce their volume with gentle use of a high-speed 6 mm diamond drill until only the deeper part (of variable size and sometimes merely a cortical shell) remains [6]. As such, we stay inside the TDH as long as it is still attached, and until its bulk has been resected and dura and epidural venous plexus have been partially decompressed. At this point, the cleavage plane between dura and residual TDH (often a large ossified fragment with the exception of transdural fragments that tend to be more porous) is carefully developed using delicate instruments (short or medium length exploration hook and curved dissector (Miaspas TL®, Aesculap)), while strictly avoiding leverage against the spinal cord [5, 6]. In case of transdural extension, at some point CSF will suddenly enter the surgical field [6, 21]. As we have now access into the thecal sac containing the spinal cord, exploration for any residual intradural fragments should be done with extreme care, and the defect reconstructed meticulously using a previously reported multilayer technique [21]. Of note, we can drill all the way to the contralateral margin of the spinal canal without compromising stability in the vast majority of cases, as long as the anterior 2/3 of vertebral bodies, pedicle, and posterior structures are preserved (Fig. 12.6).

12.3 Results

Between November 2000 and June 2013, 375 patients were operated consecutively in the MUMC+ (Maastricht, The Netherlands) by the first author (EC) for a maximum of three symptomatic TDHs using either a TMD or a mini-thoracotomy approach. The latter approach was used in the early series in patients previously operated at another institution through a posterior approach that did not achieve adequate cord decompression or in patients with giant or massive TDHs [5, 6], as both were offered decompression and immediate anterior stabilization. With increasing experience, however, we were able to safely remove even giant TDHs

using the endoscopic TMD technique [6]. As such, between June 2013 and October 2019, 181 patients were operated consecutively by the first author (EC) for a maximum of three symptomatic TDHs using a strictly endoscopic TMD-R technique. After the first two cases were successfully operated on in June 2013, we immediately abandoned standard TMD technique as the novel TMD-R technique turned out to be quite straightforward and much better tolerated.

12.3.1 Surgical Procedure

Some procedures were classified as high-risk considering relevant patient and TDH characteristics as defined in a previous paper [6]. These patients ($n = 39$) were operated with intraoperative MEP monitoring at one ($n = 29$), two ($n = 9$), or three ($n = 1$) levels. The other patients ($n = 142$) were operated without MEP monitoring at a maximum of three levels. MEP signals in the lower limbs were absent in five, unreliably low in two, and stable throughout the procedure in 18 (including one patient operated abroad). We noted a temporary signal drop in four, a fluctuating pattern in two, and a sudden bilateral loss of signal in one during intradural exploration which did not result in neurological deterioration. One case of a calcified T8–T9 TDH and severe clinical and radiological myelopathy (barely able to walk a few meters with a rollator) was particularly complicated as he had previous left-sided lobectomy for lung cancer. He was operated from the left side again because he would likely not tolerate single-lung ventilation on his single remaining left lobe while being operated from the right side. As expected, the procedure despite support of a thoracic surgeon was very difficult and took 360′ as frequent saturation and tension drops necessitated intermittent breaks with ventilation of both lungs. At some point during surgery, MEP signals (absent on the right and marginal on the left from the beginning) completely disappeared. Unfortunately, he suffered complete paralysis, with MRI suggesting anterior spinal cord infarction (despite adequate decompression) likely due to the ventilatory and circulatory problems encountered.

Mean operation time in high-risk cases ($n = 39$) was an acceptable 162′ including (or 155′ excluding) the 360′ case described above. In all other cases ($n = 142$) 15 took less than 60′, 49 between 60 and 90′, 48 between 90 and 120′, and 20 > 120′ with a maximum of 210′ for a maximum of three affected levels. For ten cases, the exact operation time was unknown. Over the years, we have learned that investing more time in preparation (positioning patient, double-lumen tube, and trocars, as well as preparing all surgical tools) pays off with an improved workflow during the actual procedure. Blood loss was minimal in the vast majority of procedures. In two procedures it was <50 mL, in 74 it was in between 50–100 mL, in 48 in between 100–250 mL, in 18 in between 250–500 mL, in 14 in between 500–1000 mL in 14 in between 1000–2000 mL (including one hemothorax from an intercostal vessel injured during the localization procedure) [19], and in 2 > 2000 mL (max 4000 mL). In nine cases, the exact blood loss was not registered. Of note, mean blood loss in the high-risk group ($n = 39$) was a very acceptable 537 mL, and besides an

occasional intercostal vessel bleeding (either paraspinal or at one of the trocars), most blood as in other spinal procedures came from the epidural venous plexus. Dural defects were infrequent (5%) as we observed five minor leaks and four major leaks including three transdural TDHs (two of which actually presented with symptoms and signs of intracranial hypotension and a spinal extradural CSF collection) [22]. All defects were successfully repaired using a meticulous multilayer dura reconstruction technique [6, 21, 22].

12.3.2 Postoperative Neurological Deficit

Two patients suffered an increased neurological deficit postoperatively (1.1%). The first patient (a 61-year-old man who survived both prostate cancer and lung cancer) was considered a high-risk case and had a lengthy procedure (360′) as discussed above. Despite every possible precaution, periprocedural ventilatory and circulatory problems (unrelated to merely 450 mL blood loss) caused an anterior infarction in his already compromised spinal cord with partially preserved sensation in both legs. The second patient (a healthy 50-year-old woman) suffered pain in her back and left leg and sensory problems in both legs caused by two large, partially calcified TDHs and myelomalacia at T10–T11–T12. After an uneventful operation (duration 130′, blood loss 400 mL), she woke up with flaccid paralysis and partially preserved sensation in both legs which improved to a grade 3 paresis on the left leg within a few days. Her MRI scan demonstrated a small contusion in the right anterior horn at T10–T11.

12.3.3 Incomplete Decompression

Except for one patient who had wrong level surgery as another TDH with almost identical configuration at an incorrect level had been mistakenly localized preoperatively, we achieved adequate cord decompression in all patients (no clinically significant TDH residual).

12.3.4 Other Complications

Three patients had a fever for several days postoperatively that subsided without any action. One patient developed an aspiration pneumonia after vomiting in the wake-up room. Four patients developed dyspnea with some consolidation in the ipsilateral lung likely due to atelectasis rather than true infection and treated with painkillers, physiotherapy, and a short course of antibiotics. One patient developed dyspnea due

to pulmonary embolism on the first postoperative day despite prophylaxis, most likely because he had been bedridden for over a week at another institution before referral. One patient lost approximately 1500 mL blood in her drain and another 500 mL in her thorax likely related to clopidrogel administered at another institution and discontinued merely 2 days before the operation. One patient developed a pleural hematoma treated conservatively. One patient developed a pseudoaneurysm after extensive coagulation on a sclerotic T10 segmental artery that retracted in abundant subpleural fat. He was successfully treated endovascularly. Two patients (1.1%) developed a vertebral insufficiency fracture despite limited bone resection (one of them had been previously operated for another TDH at an adjacent level) and were treated conservatively. Of note, in the entire series ($n = 556$) we did not observe a correlation with the amount of vertebral bone resection, as insufficiency fractures may occur sporadically in cases with limited bone resection depending on local and overall quality of the bone. One patient suddenly developed severe pain in her thorax while leaving bed for a postoperative CT scan. The pain was apparently myogenic and treated accordingly.

12.3.5 Acute Postoperative Pain

We will never forget observing one of the first few patients we operated using our TMD-R technique lifting a suitcase above his shoulders on top of a closet without any hesitation on the second postoperative day. As compared to classic TMD, TMD-R patients clearly use less analgesics, mobilize faster, and leave hospital in better shape on average 4–5 days postoperatively. Of note, our primary goal has never been to discharge them much sooner, but rather to discharge them in better shape after a comprehensive package including physiotherapy-supervised mobilization and slowly tapering their pain medication. We want our patients to be ready and well-instructed when they return home. Interestingly, at their first check-up 6 weeks postoperatively, several TMD-R patients reported a vague discomfort inside at the exact spinal level they were operated, something we had never heard before. It seems that band-like pain in patients operated using the original TMD technique (early series) used to be so prominent it completely overshadowed this minor discomfort inside.

12.3.6 Chronic Postoperative Pain

In 2005, Oskouian et al. stated “in spinal surgery there is probably no pathological entity more difficult to quantify than outcome after thoracic disc surgery” and “the optimal surgical approach to herniated thoracic discs remains unclear and the literature testifying to the efficacy, indications, or limitations of thoracoscopic disc

surgery has not been established" [18]. Unfortunately, not much has changed, as the prevalence of (symptomatic) TDHs is still underestimated, and essential outcome studies are still missing. In this regard, we must admit we have yet to establish outcome in a standardized prospective way including neurological, pain, and quality-of-life scores, as well as a cost-effectiveness analysis. Still, we have seen very promising results with this novel TMD-R technique both in the acute and late postoperative phase, including a dramatic drop in chronic band-like pain from approximately 10–15% to <3%.

12.3.7 Clinical Result (Pain, Quality-of-Life, Cost-Effectiveness)

This study presents the TMD-R technique as an evolution of the original TMD technique able to preserve both rib and CVJ. The concept of the painful rib explains why this novel technique significantly reduces acute and most importantly chronic band-like pain. The study is a feasibility study that does not include any pain and quality-of-life scores evaluated by a blinded researcher, nor a much-anticipated cost-effectiveness analysis as compared to conservative therapies for symptomatic TDHs. We will start collecting such data in a prospective way in the near future.

12.4 Discussion

In 1950, Love and Kiefer [23] recognized that TDHs had received little recognition. In 1971, Carson et al. [24] postulated a very low incidence of symptomatic TDHs ($1/1 \times 10^6$). Although this incidence was based on a simple estimate in the pre-CT/MRI era, it has been repeated all over the literature until this day. In 1995, however, Wood et al. [1] demonstrated a staggering incidence of 37% on MRI in asymptomatic individuals, which makes TDHs no less frequent than their cervical or lumbar counterparts. Although exact epidemiological studies are lacking largely because of their diverse clinical presentation, the actual incidence of symptomatic TDHs must be significantly higher than $1/1 \times 10^6$. Undoubtedly, these patients are out there, receiving little recognition, often having to wait a long time for a correct diagnosis and even longer for symptomatic relief which may be impossible to achieve without surgery in a relatively large proportion. While different surgical techniques published over the years [7–18] testify to their omnipresence, results are difficult to compare as they are very diverse lesions with (single or multi-level) small, soft, paramedian or lateral TDHs, on the one end, and giant [5] or massive [6] calcified TDHs on the other end causing myelopathy or sometimes merely refractory pain.

12.4.1 What Is Wrong with the Original TMD Technique?

There is no doubt the original TMD technique (published in 1994) [7] has revolutionized surgical treatment of TDHs as the technique using specifically designed instruments was safe, efficient, and suited for a wide range of TDHs including central calcified ones (Fig. 12.2). Major drawbacks from the surgeon's perspective were the initial investment, unfamiliarity with endoscopic and especially thoracoscopic techniques, the learning curve, and last but not the least the fear for complications including paraparesis and paraplegia especially in ambulatory patients with merely (albeit very disabling) pain. Nevertheless, no other technique seems to have reached the same level of acceptance as the TMD technique [3, 6–8, 15–18, 21].

There is, however, another drawback that needs to be mentioned, namely, the problem of chronic band-like pain on the operated side that occurs in a significant proportion of patients (approximately 10–15%) after TMD and may have discouraged some colleagues who just started applying the technique. This pain can be disabling, resist medication and even invasive pain treatment, and as such completely overshadow an otherwise successful operation. When dealing with patients who present with symptoms and signs of a myelopathy (Anand grade 4 and 5, still a large proportion of patients treated to date as those with merely pain are often advised against surgery) [3, 15], such postoperative pain may be more readily accepted as collateral damage. It is therefore likely underreported, even though these patients may suffer substantially. When dealing with patients who present with axial and/or band-like pain whether or not irradiating to the legs (Anand grade 1–3B) [15], such postoperative pain may turn an otherwise successful operation (that has effectively cured the patient from his or her preoperative pain) into a nightmare. While this pain is often attributed to an intercostal neuralgia [18], it tends not to be as sharply demarcated, and it tends to resist intercostal nerve blocks as well as radiofrequency rhizotomies. We believe it must have a different cause as we will now discuss.

12.4.2 Importance of Preserving the CVJ

The original TMD technique, as briefly presented in Sect. 12.2, involves detaching the costotransverse and costovertebral ligaments and removing the pedicle to expose the ipsilateral epidural space (Fig. 12.2) [7, 8]. At some point, we realized we had never encountered chronic band-like postoperative pain in patients operated at the T11–T12 level, the only level the rib actually articulates slightly caudal to the intervertebral disc, and the head of the rib does not have to be resected to gain access to the caudal pedicle and ipsilateral dura mater. This prompted our hypothesis that chronic band-like pain (as opposed to acute wound pain) after TMD may not be related to trocars damaging rib periosteum and intercostal nerves (intercostal neuralgia) [18], but rather to damaging the CVJ, a very strong joint that (together with

the CTJ) allows complex 3D movements in harmony with adjacent ribs and the entire rib cage. Indeed, while acute pain was clearly incision-related, chronic pain could be exacerbated by pressing anywhere on the disarticulated rib, either a few fingers from the dorsal midline, over the CTJ, in the flank, or more anteriorly at the transition with the costal cartilage.

The movements of the ribs individually and as a whole (thoracic cage) are complex. The axis of rotation of the rib changes progressively down the thoracic cage [25]. The upper ribs have a pump-handle movement, with the anterior end swinging upward and outward. The lower ribs have a bucket-handle movement, with the ribs moving laterally and upward. The lowest ribs have a caliper movement, with the entire rib swinging laterally. These combinations of movements lift the rib cage as well as expand it in anteroposterior and lateral direction to increase its volume [25]. It appears these harmonious movements can be disrupted by destroying a single CVJ. Moreover, innervation of the CVJ suggests that pain in this joint can be referred to the anterior chest [20]. As such, dysfunction of the CVJ may cause localized pain approximately 3–4 cm from the dorsal midline, referred pain ranging from the dorsal midline to the lateral chest wall, as well as anterior chest pain, and any movement of the involved rib may provoke pain at the CVJ and/or reproduce such referred pain [20]. It is therefore of paramount importance to keep the CVJ intact at all times while not compromising on the safety and efficacy of any given procedure.

12.4.3 Advantages of the TMD-R Technique (Figs. 12.3 and 12.4)

As mentioned, we have witnessed a big difference with regard to acute and chronic postoperative pain comparing 375 original TMD procedures (except for those at T11–T12) with 181 subsequent TMD-R procedures in which rib and CVJ were preserved without compromising on safety and efficacy of the technique with regard to TDHs of different size, level, and laterality. With correct technique and experience, even very large TDHs can be safely removed using this novel technique [6]. The difference is that obvious we feel it would be unethical to do a randomized controlled trial comparing both techniques, and even more so as the TMD-R technique seems to have other advantages as well. First, the technique is truly minimally invasive (instead of being merely minimally incisional) as we go straight to target while preserving important structures such as pedicle, head of the rib, and CVJ (Fig. 12.3). Second, limited vertebral bone resection obviates the need for additional stabilization in the vast majority of cases (notwithstanding an occasional vertebral insufficiency fracture) (Figs. 12.3, 12.5 and 12.6). Third, less tissue destruction promotes faster healing (including an eventual dural defect). Fourth, less surgical steps mean a faster procedure (many procedures <90′, and many high-risk TDHs <180′ of course with ample experience). As mentioned, investing more time in preparation pays off with an improved workflow during the actual procedure. Fifth, venous

oozing is minimal because we do not open the spinal canal laterally where the epidural venous plexus is situated, drill all around the TDH and take out its base before opening the spinal canal (Fig. 12.4). This creates some initial decompression (as residual TDH and underlying dura move anteriorly into the resection cavity) and substantially reduces intensity and duration of epidural venous oozing [blood loss was <100 mL in 76 patients and <250 mL in another 48 patients, while mean blood loss was an acceptable 537 mL even in the high-risk group (n = 39)]. All in all, patients make a faster recovery, including early postoperative mobilization, tapering their pain medication, and probably (though unproven) eventual return to work.

12.4.4 Study Limitations and Future Directions

We present a novel TMD-R technique that preserves rib and CVJ as well as the rationale behind it. We describe our technique in detail and identify possible advantages, including a significant reduction in acute and chronic postoperative pain as well as in epidural venous oozing.

Oskouian et al. [18] stated "in spinal surgery there is probably no pathological entity more difficult to quantify than outcome after thoracic disc surgery" while identifying two reasons [18]. First, the natural history of the disease is not clearly understood, which makes it hard to determine which patients will benefit from surgery. As mentioned, more research has to be done to clarify this important issue. Second, the incidence of TDHs is extremely low (an estimated incidence of 1% of all herniated discs). As mentioned, we believe that TDHs are an underestimated disease even to date. We would like to add two additional reasons. Third, the clinical presentation of TDHs is very diverse (different types of pain and/or myelopathy, compressive lumbar myelopathy, abdominal wall bulge, spontaneous spinal CSF leak, etc.) [3, 4, 15–17, 22, 23, 26] and as such, outcome after surgery has many different aspects. Fourth, TDHs are often multiple which may explain residual or recurrent complaints attributable to another level.

Oskouian et al. [18] also stated "the optimal surgical approach to herniated thoracic discs remains unclear and the literature testifying to the efficacy, indications, or limitations of thoracoscopic disc surgery has not been established" [18]. Unfortunately, not much has changed, as the prevalence of symptomatic TDHs is still underestimated, and essential outcome studies are still missing. In this regard, we too must admit we have yet to establish outcome in a standardized prospective way including neurological pain and quality-of-life scores as well as a (comparative) cost-effectiveness analysis. Still, we have seen very promising results with this novel technique, including a dramatic drop in chronic band-like pain on the operated side often resisting even invasive pain therapy. As many TDH patients suffer intractable pain for years or even longer that resists conservative treatment (inducing chronic use of morphine derivatives), we anticipate an excellent cost-effectiveness provided surgery is applied to the right patient at the right level(s)

while being safe, efficient, and at low risk of inducing another pain as an unwanted side effect.

In a broader perspective, measuring quality in spine surgery is still in its infancy [27]. This certainly holds true for the surgical treatment of TDHs which are intriguing lesions that receive relatively little attention in the literature as compared to their cervical and lumbar counterparts. We need to understand why so many are asymptomatic, while other similar TDHs are clearly symptomatic, why small TDHs may occasionally cause a myelopathy while much larger TDHs may cause merely pain, etc. It seems their pathogenesis (part of a growth disorder of the thoracic or thoracolumbar spine rather than degenerative) [2] and pathophysiology (compression of the cord, congestion of the veins, irritation of the dura, and inflammation [28]) are unique, and studying them will likely learn us a lot about spinal cord pathophysiology as well. For example, we hope one day to be able to compare segmental spinal cord perfusion in asymptomatic and symptomatic TDH patients before and after decompression. We need to study TDHs in order to better understand them, which will likely involve an update of the Anand classification [15] and the development of validated outcome scores specifically for TDHs.

12.5 Conclusion

We present a novel TMD-R technique that preserves rib and CVJ without compromising on safety and efficacy with regard to TDHs of different size, level, and laterality. Possible advantages include less bone resection, less epidural venous oozing, improved orientation, shorter OR time, significant reduction in acute and chronic postoperative pain, and an overall faster recovery and return-to-work. We hope this novel technique supported by the latest high-speed drill and 3D HD camera systems will find a broader acceptance among a new generation of spine surgeons who already feel comfortable using an endoscope, to the benefit of patients suffering myelopathy and/or intractable pain who may still face reluctance among surgeons to offer surgery. Last but not the least, recognizing TDHs as an important health issue should prompt more research on their unique pathogenesis, pathophysiology, natural history, and outcome after surgery using validated neurological, pain, and quality-of-life outcome scores.

Acknowledgements The authors wish to express their gratitude to the neuro OR nurses, the neuroradiologists, and most importantly to all patients who entrusted them with their problem.

Funding This research did not receive any specific grant from funding agencies in the public, commercial, or not-for-profit sectors.

Compliance with Ethical Standards The present paper does not contain any experimental work. It merely describes our surgical technique as it evolved into a rib and costovertebral joint sparing

technique after many years of experience with thoracoscopic surgery for thoracic disc herniations.

The authors declare that they have no conflict of interest.

For this type of retrospective study formal consent is not required.

References

1. Wood KB, Garvey TA, Gundry C, Heithoff KB. Magnetic resonance imaging of the thoracic spine. Evaluation of asymptomatic individuals. J Bone Jt Surg Am. 1995;77:1631–8.
2. Overvliet GM, Beuls EAM, ter Laak-Poort M, EMJ C. Two brothers with a symptomatic thoracic disc herniation at T11–T12: clinical report. Acta Neurochir. 2009;151(4):393–6.
3. Cornips EMJ, Janssen MLF, Beuls EAM. Thoracic disc herniation and acute myelopathy: clinical presentation, neuroimaging findings, surgical considerations, and outcome. J Neurosurg Spine. 2011;14:520–8.
4. Cornips EMJ. Crippling upper back pain after whiplash and other motor vehicle collisions caused by thoracic disc herniations. Spine. 2014;39(12):988–95.
5. Hott JS, Feiz-Erfan I, Kenny K, Dickman CA. Surgical management of giant herniated thoracic discs: analysis of 20 cases. J Neurosurg Spine. 2005;3:191–7.
6. Cornips E, Habets J, van Kranen-Mastenbroek V, Bos H, Bergs P, Postma A. Anterior transthoracic surgery with motor evoked potential monitoring for high-risk thoracic disc herniations: technique and results. World Neurosurg. 2017;105:441–55. https://doi.org/10.1016/j.wneu.2017.05.173.
7. Rosenthal D, Rosenthal R, de Simone A. Removal of a protruded thoracic disc using microsurgical endoscopy. A new technique. Spine. 1994;19(9):1087–91.
8. Rosenthal D, Dickman CA. Thoracoscopic microsurgical excision of herniated thoracic discs. J Neurosurg. 1998;89(2):224–35.
9. Chi JH, Dhali SS, Kanter AS, Mummaneni PV. The mini-open transpedicular thoracic discectomy: surgical technique and assessment. Neurosurg Focus. 2008;25(2):E5.
10. Choi KY, Eun SS, Lee SH, Lee HY. Percutaneous endoscopic thoracic discectomy; transforaminal approach. Minim Invasive Neurosurg. 2010;53:25–8.
11. Khoo LT, Smith ZA, Asgarzadie F, Barlas Y, Armin SS, Tashjian V, Zarate B. Minimally invasive extracavitary approach for thoracic discectomy and interbody fusion: 1-year clinical and radiographic outcomes in 13 patients compared with a cohort of traditional anterior transthoracic approaches. J Neurosurg Spine. 2011;14:250–60.
12. Lidar Z, Lifshutz J, Bhattacharjee S, Kurpad SN, Maiman DJ. Minimally invasive, extracavitary approach for thoracic disc herniation: technical report and preliminary results. Spine J. 2006;6:157–63. https://doi.org/10.1016/j.spinee.2005.05.377.
13. Sheikh H, Samartzis D, Perez-Cruet MJ. Techniques for the operative management of thoracic disc herniation: minimally invasive thoracic microdiscectomy. Orthop Clin N Am. 2007;38:351–61. https://doi.org/10.1016/j.ocl.2007.04.004.
14. Yanni DS, Connery C, Perin NI. Video-assisted thoracoscopic surgery combined with a tubular retractor system for minimally invasive thoracic discectomy. Oper Neurosurg. 2011;68(3):138–43.
15. Anand N, Regan JJ. Video-assisted thoracoscopic surgery for thoracic disc disease. Classification and outcome study of 100 consecutive cases with a 2-year minimum follow-up period. Spine. 2002;27(8):871–9.
16. Stillerman CB, Chen TC, Couldwell WT, Zhang W, Weiss MH. Experience in the surgical management of 82 symptomatic herniated thoracic discs and review of the literature. J Neurosurg. 1998;88:623–33.

17. Quint U, Bordon G, Preissl I, Sanner C, Rosenthal D. Thoracoscopic treatment for single level symptomatic thoracic disc herniation: a prospective cohort study in a group of 167 consecutive cases. Eur Spine J. 2012;21:637–45. https://doi.org/10.1007/s00586-011-2103-0.
18. Oskouian RJ, Johnson P. Endoscopic thoracic microdiscectomy. J Neurosurg Spine. 2005;3:459–64.
19. Cornips E, Beuls E, Geskes G, Janssens M, van Aalst J, Hofman P. Preoperative localization of herniated thoracic discs using myelo-CT guided transpleural puncture: technical note. Childs Nerv Syst. 2007;23:21–6. https://doi.org/10.1007/s00381-006-0223-3.
20. Winzenberg T, Jones G, Callisaya M. Musculoskeletal chest wall pain. Aust Fam Physician. 2015;44(8):540–4.
21. Cornips E. Multilayer dura reconstruction after thoracoscopic microdiscectomy: technique and results. World Neurosurg. 2017;109:1–8. https://doi.org/10.1016/j.wneu.2017.10.056.
22. Cornips E, Grouls M, Bekelaar K. Transdural thoracic disk herniation with longitudinal slitlike dural defect causing intracranial hypotension: report of 2 cases. World Neurosurg. 2020;140:E311–9. https://doi.org/10.1016/j.wneu.2020.05.077.
23. Love JG, Kiefer EJ. Root pain and paraplegia due to protrusions of thoracic intervertebral disks. J Neurosurg. 1950;7(1):62–9. https://doi.org/10.3171/jns.1950.7.1.0062.
24. Carson J, Gumpert J, Jefferson A. Diagnosis and treatment of thoracic intervertebral disc protrusions. J Neurol Neurosurg Psychiatry. 1971;34:68–77.
25. Sly PD, Collins RA. Applied clinical respiratory physiology. In: Taussig LM, Landau LI, editors. Pediatric respiratory medicine. 2nd ed. Amsterdam: Elsevier; 2008. p. 73–88.
26. Kleopa KA, Zamba-Papanicolaou E, Kyriakides T. Compressive lumbar myelopathy presenting as segmental motor neuron disease. Muscle Nerve. 2003;28(1):69–73.
27. Graves C, Meyer S, Knightly J, Glassman S. Quality in spine surgery. Neurosurgery. 2018;82(2):136–41. https://doi.org/10.1093/neuros/nyx476.
28. Andrade P, Cornips EMJ, Sommer C, Daemen MA, Visser-Vandewalle V, Hoogland G. Elevated inflammatory cytokine expression in CSF from patients with symptomatic thoracic disc herniations correlates with increased pain scores. Spine J. 2018;18(12):2316–22. https://doi.org/10.1016/j.spinee.2018.07.023.

Chapter 13
Efficacy of Selective Dorsal Rhizotomy and Intrathecal Baclofen Pump in the Management of Spasticity

Pramath Kakodkar, Hidy Girgis, Perla Nabhan, Sharini Sam Chee, and Albert Tu

13.1 Background

Spasticity is a motor disorder that is defined by its velocity-dependent increase in muscle tone. Clinically, spasticity can be identified by its 'clasp-knife' feature during evaluation of passive limb mobility [1, 2]. Unmanaged spasticity leads to musculoskeletal remodeling and deformity including contractures, muscle shortening, long bone torsion, and joint destruction [1–6]. Spasticity is a common consequence of multiple conditions including cerebral palsy (CP), multiple sclerosis (MS), traumatic brain injury (TBI), and spinal cord injury (SCI) [1, 3, 4, 6–11]. Unmanaged, these patients experience significant limitation in their movement, functional ambulation, and quality of life. While a variety of treatments exist, neurosurgical intervention is largely centered on the provision of two keystone therapies—selective dorsal rhizotomy (SDR) and intrathecal baclofen pump (ITB) [12–20]. Determining

P. Kakodkar
School of Medicine, National University of Ireland Galway, Galway, Republic of Ireland
e-mail: pramath.kakodkar@usask.ca

H. Girgis
Division of Neurosurgery, University of Ottawa, Ottawa, ON, Canada
e-mail: higirgis@toh.ca

P. Nabhan
Faculty of Science, University of Ottawa, Ottawa, Canada

S. S. Chee
Schulich School of Medicine and Dentistry, Western University, London, ON, Canada

A. Tu (✉)
Division of Pediatric Neurosurgery, Children's Hospital of Eastern Ontario, Ottawa, ON, Canada
e-mail: atu@cheo.on.ca

C. Di Rocco (ed.), *Advances and Technical Standards in Neurosurgery*, Advances and Technical Standards in Neurosurgery 45,
https://doi.org/10.1007/978-3-030-99166-1_13

which of these interventions is most appropriate for individual patients is dependent on a myriad of variables [14, 21–33]. Given that the predilection of spasticity varies drastically in adult and pediatric patients, it would be of interest to evaluate the outcomes of unique patient cohorts to determine whether specific etiologies may favor ITB or SDR [24, 33–38]. Therefore, this systematic review is conducted across a large scope of patients that encompasses the adults and pediatrics populations undergoing ITB or SDR for management of spasticity.

13.2 Methods

A systematic literature review was conducted during January 2021 by authors PK, SSC, PN, and HG in accordance with PRISMA (2015) guidelines as shown in Fig. 13.1 [39]. The review was restricted to publications between January

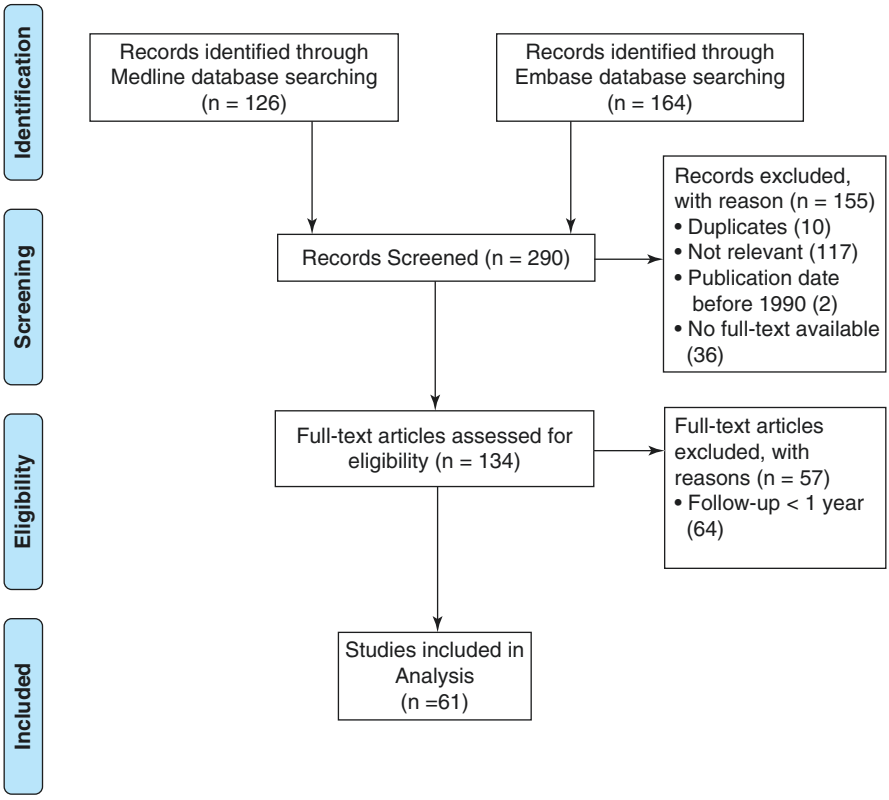

Fig. 13.1 Systematic review process

1990 to January 2021. Combinations of search terms 'Selective Dorsal Rhizotomy', 'Selective Posterior Rhizotomy', 'functional posterior rhizotomy', 'intrathecal baclofen pump', and 'spasticity' were queried on Medline and Embase databases. All studies that were not published in English language, inaccessible via digital or local repository, or reviews without any original data were excluded. Additionally, only studies with at least 1 year of follow-up duration were included in the analysis. Publications were evaluated for patient gender, etiology of spasticity, surgical parameters, operating parameters of ITB, need for postprocedural intervention, and pre- and postprocedural clinical status (i.e., spasticity, tone, ambulatory status, complications). Additional interventions for spasticity (i.e., oral antispasmodic medications, botulinum A toxin injections, etc.) as well as orthopedic procedures (i.e., tendon lengthening, osteotomies, etc.) were also documented when available. Complications related to treatment (i.e., metabolic derangement, spinal deformity, etc.) were analyzed when reported. Outcomes were evaluated quantitatively when possible and described qualitatively when not.

13.3 Results

13.3.1 Search Results

Our search criteria yielded a total of 290 potential publications. Thirty six were unavailable on digital or local repository. One hundred and seventeen described studies did not include data irrelevant to SDR or ITB. Furthermore, 64 publications were eliminated as their follow-up duration was shorter than 12 months. The remaining 61 publications described the use and outcomes of SDR and ITB in 1291 adult patients and 2263 pediatric patients (Fig. 13.1).

13.3.2 Demographics

In the adult cohort (patients 18 years of age or older) (n = 1291), the mean age at time of intervention was 39.1 ± 14.6 years with a slight predilection for male gender (M:F = 1.4:1). The mean follow-up duration for this cohort is 71.8 ± 62.0 months. 76.1% of the patients underwent ITB (n = 983) and 23.9% underwent SDR (n = 308). Conversely, the pediatric cohort (age under 18 years of age) (n = 2263) had a mean age at intervention of 7.9 ± 3.5 years with a slight predilection for female gender (M:F = 1:1.3). The mean follow-up duration for this cohort was 24.6 ± 48.6 months. 24.6% of the patients underwent ITB (n = 557) and 75.4% underwent SDR (n = 1706).

13.3.3 Etiology of Spasticity in All Patients

The adult cohort data are derived from 27 publications [9, 15, 19, 20, 26, 28, 34, 40–53]. The most common etiologies of spasticity in these patients were multiple sclerosis (35.4%, $n = 457$), cerebral palsy (21.9%, $n = 283$), and traumatic brain injury (14.7%, $n = 190$). The remainder of the adult data is summarized in Tables 13.1 and 13.2. The pediatric cohort data are derived from 35 publications [12, 14,

Table 13.1 Study demographics and proportion of spasticity management in adult patients ($n = 1291$)

Spasticity etiology	*n*	Mean age (SD) years	Mean FU (SD) month	Proportion of overall undergoing SDR% (*n*)	Proportion of overall undergoing ITB % (*n*)
ALS	9	34.1 (10.2)	39.4 (27.7)	33% (3)	66% (6)
CP	283	31.1 (5.7)	54.8 (46.1)	42.4% (120)	57.6% (163)
CVA	43	45.9 (7.07)	65.2 (28.4)	0	100% (43)
HBI	40	39.1 (2.9)	38.1 (16.3)	0	100% (40)
ICH	6	39 (0)	42 (0)	0	100% (6)
Inflammatory/ infectious	17	42.6 (1.5)	87.5 (18.3)	0	100% (17)
MS	457	43.6 (10.1)	102.3 (82.9)	22.8% (104)	77.2% (353)
Neurodegenerative	23	36.9 (0.58)	104.6 (32.1)	30.4% (7)	69.6% (16)
Spinocerebellar degenerative disease	12	37.7 (7.5)	40.7 (20.7)	33.3% (4)	66.7% (8)
SAH	3	39 (0)	42 (0)	0	100% (3)
SCI	135	42.0 (10.8)	35.6 (18.5)	22.2% (30)	77.8% (105)
TBI	190	35.2 (6.4)	67.9 (35.4)	21.1% (40)	78.9% (150)
CRPS	7	55.3 (0)	36 (0)	0	100% (7)
Other cerebral pathology[a]	35	36.9 (4.3)	41.5 (10.4)	0	100% (35)
Other spinal pathology[b]	28	48.8 (9.6)	51.6 (15.0)	0	100% (28)
Other PNS pathology[c]	3	44.3 (5.5)	20.5 (18.7)	0	100% (3)

[a]Holoprosencephaly ($n = 1$), idiopathic torsion dystonia ($n = 2$), thrombosis ($n = 1$), transverse myelitis ($n = 2$)

[b]Brainstem tumor ($n = 1$), transverse myelitis ($n = 1$), meningomyelocele ($n = 1$), neuromyelitis opyica ($n = 1$), leigh syndrome ($n = 1$)

[c]Glutaric aciduria ($n = 1$), Hallervorden–Spatz disease ($n = 7$), Huntington's disease ($n = 1$), mitochondrial disease ($n = 1$), Wilson's disease ($n = 1$), glutaric aciduria type 1 ($n = 2$), hereditary spastic paraplegia ($n = 2$)

Table 13.2 Extent of rootlet resection and ITB dosing by etiology of spasticity in adult patients ($n = 1291$)

Spasticity etiology	*n*	Rootlets sectioned during SDR	ITB baclofen mean dose μg/day (SD)	ITB baclofen max dose μg/day (SD)
ALS	9	Bilateral L1–S2 (50–67%) + unilateral S2	NA	500 (0)
CP	283	Bilateral L1–S2 (50–67%) + unilateral S2	244.3 (61.6)	419.1 (93.7)
CVA	43	–	251.7 (12.2)	422.5(32.5)
HBI	40	–	314.1 (174.0)	681.6 (607.6)
ICH	6	–	200 (0)	320 (0)
Inflammatory/infectious	17	–	273.4 (93.8)	459.4 (128.3)
MS	457	Bilateral L1–S2 (50–67%) + unilateral S2	193.4 (90.6)	355.0 (257.0)
Neurodegenerative	23	Bilateral L1–S2 (50–67%) + unilateral S2	230 (0)	400 (0)
Spinocerebellar degenerative disease	12	Bilateral L1–S2 (50–67%) + unilateral S2	NA	500 (0)
SAH	3	–	200 (0)	320 (0)
SCI	135	Bilateral L1–S2 (50–67%) + unilateral S2	337.3 (136.8)	507.8 (183.4)
TBI	190	Bilateral L1–S2 (50–67%) + unilateral S2	271.9 (141.2)	533.5 (405.4)
CRPS	7	–	NA	NA
Other cerebral pathology[a]	35	–	200 (0)	460 (74.8)
Other spinal pathology[b]	28		325.1 (167.0)	692.8 (153.1)
Other PNS pathology[c]	3		203.7 (3.7)	305 (15.1)

[a]Holoprosencephaly ($n = 1$), idiopathic torsion dystonia ($n = 2$), thrombosis ($n = 1$), transverse myelitis ($n = 2$)

[b]Brainstem tumor ($n = 1$), transverse myelitis ($n = 1$), meningomyelocele ($n = 1$), neuromyelitis opyica ($n = 1$), Leigh syndrome ($n = 1$)

[c]Glutaric aciduria ($n = 1$), Hallervorden–Spatz disease ($n = 7$), Huntington's disease ($n = 1$), mitochondrial disease ($n = 1$), Wilson's disease ($n = 1$), glutaric aciduria type 1 ($n = 2$), hereditary spastic paraplegia ($n = 2$)

15, 30, 34, 40, 54–82]. The most common etiologies of spasticity in these patients were cerebral palsy (92.8%, $n = 2100$), brain or spinal cord injury (4.9%, $n = 110$), and hypoxic brain injury (HBI) (0.75%, $n = 17$). The remainder of the pediatric data are summarized in Tables 13.3 and 13.4.

Table 13.3 Study demographics and proportion of spasticity management in pediatric patients ($n = 2263$)

Spasticity etiology	*n*	Mean age (SD) years	Mean FU (SD) month	Proportion of overall undergoing SDR % (*n*)	Proportion of overall undergoing ITB % (*n*)
CP (unclassified)	1162	7.1 (3)	40.1 (56.8)	75.9% (882)	24.1% (280)
CP (dyskinetic)	25	10.9 (0)	18.1 (0)	80% (20)	20% (5)
CP (severe dystonia)	3	10.6 (3.3)	59 (35.3)	100% (3)	0%
CP (spastic diplegic/ quadriplegic)	159	5.4 (8.7)	44.4 (68.7)	100% (159)	0%
CP (spastic diplegic)	404	7.9 (3.7)	42.4 (39.9)	94.1% (380)	5.9% (24)
CP (spastic quadriplegic)	347	8.4 (2.5)	18.2 (21.5)	67.4% (234)	32.6% (113)
HBI	17	12.4 (2.7)	28 (2.6)	0%	100% (17)
Inflammatory/ infectious[a]	6	13.4 (1.3)	30.7 (2.3)	16.7 (1)%	83.3% (5)
Other cerebral pathology[a]	4	12.5 (1.5)	26.2 (2.8)	0%	100% (4)
Other spinal pathology[b]	5	12.3 (0.5)	15.9 (2.8)	60% (3)	40% (2)
Other genetic pathology[c]	15	13.5 (0)	29.4 (0)	40% (6)	60% (9)
Trauma (SCI/TBI)	110	14.8 (3.1)	38.4 (6.3)	12.7% (14)	87.3% (96)
MS/degenerative	3	13 (0.9)	24.8 (32.4)	33.3% (1)	66.7% (2)
Other	3	12.3	19	100% (3)	–

SD standard deviation, *FU* follow-up, *SDR* selective dorsal rhizotomy, *ITB* intrathecal baclofen pump, *μg* micrograms, *SLL* single level laminectomy, *NA* not available, – not applicable, *ALS* amyotrophic lateral sclerosis, *CP* cerebral palsy, *CVA* cerebrovascular accident, *HBI* hypoxic brain injury, *ICH* intracerebral hemorrhage, *MS* multiple sclerosis, *SAH* subarachnoid hemorrhage, *SCI* spinal cord injury, *TBI* traumatic brain injury, *BTX-A* botulinum toxin A

[a]Holoprosencephaly ($n = 1$), idiopathic torsion dystonia ($n = 2$), thrombosis ($n = 1$), transverse myelitis ($n = 2$)

[b]Brainstem tumor ($n = 1$), transverse myelitis ($n = 1$), meningomyelocele ($n = 1$), neuromyelitis opyica ($n = 1$), Leigh syndrome ($n = 1$)

[c]Glutaric aciduria ($n = 1$), Hallervorden–Spatz disease ($n = 7$), Huntington's disease ($n = 1$), mitochondrial disease ($n = 1$), Wilson's disease ($n = 1$), glutaric aciduria type 1 ($n = 2$), hereditary spastic paraplegia ($n = 2$)

13.3.4 Technical Details

13.3.4.1 ITB in Adult Patients

ITB was most often utilized in patients with MS (35.9%, $n = 353$ out of 983), CP (16.6%, $n = 163$ out of 983), and TBI (15.3%, $n = 150$ out of 983). Patients with SCI ($n = 44$), other spinal pathologies ($n = 9$), and HBI ($n = 23$) had the highest mean

Table 13.4 Extent of rootlet resection and ITB dosing by etiology of spasticity in pediatric patients ($n = 2263$)

Spasticity etiology	*n*	Rootlets sectioned during SDR	ITB baclofen mean dose (SD) μg/day	ITB baclofen max dose (SD) μg/day
CP (unclassified)	1162	[L1–S2, 65%] (15.1%, *n* = 133) [L2–S2, 50%] (1.4%, *n* = 12) [L1–L2] (14.9%, *n* = 131) [L2–S2] (3.2%, *n* = 28) [L2–S1] (4.6%, *n* = 41) [L4–S1] (3.6%, *n* = 32)	275.8 (135.1)	1145.3 (71.6)
CP (dyskinetic)	25	NA	NA	NA
CP (severe dystonia)	3	NA	–	–
CP (spastic diplegic/ quadriplegic)	159	MLL [L3–L4] (0.6%, *n* = 1) MLL [L4–S1] (17, *n* = 27)	–	–
CP (spastic diplegic)	404	[L2–S1] (7.6%, *n* = 29) MLL [L3–L4] (7.1%, *n* = 27) MLL [L4–S1] (7.1%, *n* = 27)	1100 (535)	NA
CP (spastic quadriplegic)	347	[L2–S2] (10.7%, *n* = 25) [L3–L4] (10.3%, *n* = 24)	485	2000
HBI	17	–	423.9	2000
Inflammatory/infectious[a]	6	NA	419.4	2000
Other cerebral pathology[a]	4	–	485	2000
Other spinal pathology[b]	5	[L1–S2, 14–50%] (100%, *n* = 3)	627.9 (0)	NA
Other genetic pathology[c]	15	[L1–S2, 14–50%] (100%, *n* = 4)	474.8 (0)	2000
Trauma (SCI/TBI)	110	[L1–S2, 14–50%] (100%, *n* = 14)	450 (294.7)	NA
MS/degenerative	3	NA	627.9	NA
Other	3	NA	–	–

SD standard deviation, *FU* follow-up, *SDR* selective dorsal rhizotomy, *ITB* intrathecal baclofen pump, *μg* micrograms, *SLL* single level laminectomy, *NA* not available, – not applicable, *ALS* amyotrophic lateral sclerosis, *CP* cerebral palsy, *CVA* cerebrovascular accident, *HBI* hypoxic brain injury, *ICH* intracerebral hemorrhage, *MS* multiple sclerosis, *SAH* subarachnoid hemorrhage, *SCI* spinal cord injury, *TBI* traumatic brain injury, *BTX-A* botulinum toxin A

[a]Holoprosencephaly ($n = 1$), idiopathic torsion dystonia ($n = 2$), thrombosis ($n = 1$), transverse myelitis ($n = 2$)

[b]Brainstem tumor ($n = 1$), transverse myelitis ($n = 1$), meningomyelocele ($n = 1$), neuromyelitis opyica ($n = 1$), Leigh syndrome ($n = 1$)

[c]Glutaric aciduria ($n = 1$), Hallervorden–Spatz disease ($n = 7$), Huntington's disease ($n = 1$), mitochondrial disease ($n = 1$), Wilson's disease ($n = 1$), glutaric aciduria type 1 ($n = 2$), hereditary spastic paraplegia ($n = 2$)

Table 13.5 Preprocedural medications in adult patients ($n = 16$) undergoing ITB

Medication class	Agent (n)
Anti-spasticity	Baclofen (16)
	Tizanidine (2)
β-Blocker	Propranolol (11)
Opioid	Morphine (2)
	Buprenorphine (2)
	Hydromorphone (1)
	Fentanyl (1)
Benzodiazepine	Lorazepam (3)
	Clonazepam (1)
	Diazepam (1)
Anticonvulsant/barbiturate	Phenobarbital (1)

All patients from single study of TBI patients

doses of baclofen documented at 337.3 ± 136.8 μg/day, 325.1 ± 167 μg/day, and 314.1 ± 174 μg/day, respectively. The remainder of patients with varied etiologies of spasticity are summarized in Table 13.5. One study documented the preprocedural pharmacologic therapies used in TBI patients; the most common were baclofen (100%, $n = 16$ out of 16) and Propranolol (68.7%, $n = 11$ out of 16) [40].

13.3.4.2 ITB in Pediatric Patients

In this cohort, ITB was most frequently provided to patients with CP (75.8%, $n = 422$ out of 557), trauma (pooled TBI and SCI) (17.2%, $n = 96$ out of 557), and HBI (3.0%, $n = 17$ out of 557). Patients with spastic diplegic CP ($n = 404$) had the highest mean dosage of 1100 ± 535 μg/day of baclofen. Both neurodegenerative disease ($n = 3$) and other spinal pathologies ($n = 5$) had a mean dosage of 627.9 μg/day. The remainder of these patients with varied causes of spasticity are summarized in Table 13.6. Three studies documented the preprocedural medications in patients with spasticity of varied etiology; the most common medication was oral baclofen (40.1%, $n = 168$ out of 419). A comprehensive list of these medications is provided in Table 13.6.

13.3.4.3 SDR in Adult Patients

The most common etiologies of spasticity in adult patients undergoing SDR were CP (39.0%, $n = 120$ *out of* 308), MS (33.8%, $n = 104$ *out of* 308), and TBI (13.0%, $n = 40$ *out of* 308). The remainder of patients with varied spasticity who underwent SDR are summarized in Tables 13.1 and 13.2. All adult patients described that underwent SDR ($n = 308$) had a single-level laminectomy at L1 and in some

Table 13.6 Preprocedural medications in pediatric patients ($n = 419$) undergoing ITB

Medication class	Agent
Antispasticity agent	Oral baclofen (168)
	ITB via external pump (86)
	Dantrolene sodium (80)
	Trihexyphenidyl (1)
Benzodiazepine	Clonazepam (2)
	Clorazepate (80)
Psychiatry medication	Trazodone (1)
	Tetrabenazine (1)

instances, extended to L2. Patients underwent bilateral rhizotomy with a range of 50–67% of the L1–S2 rootlets being sectioned; in patients with a spastic bladder, unilateral S2 rhizotomy was also described (Tables 13.1 and 13.2). Electrophysiological monitoring was utilized intraoperatively in all depictions.

13.3.4.4 SDR in the Pediatric Patients

Patients with CP made up the majority of pediatric individuals undergoing SDR (98%, $n = 1678$ *out of* 1706); a smaller number of patients with trauma (composite of TBI and SCI) comprised the second most common etiology for spasticity (0.82%, $n = 14$ *out of* 1706). The remainder of patients with other pathologies are summarized in Tables 13.3 and 13.4. Multilevel laminectomy (83.6%, $n = 556$) was the predominant choice in the pediatric patients who underwent SDR ($n = 665$). Exposure most commonly extended from L1 to L5 (27.2%, $n = 181$), although other starting and ending levels were also described. Single-level laminectomy, when described, occurred most commonly at L1 (6.2%, $n = 41$). A complete breakdown of extent of surgery is shown in Table 13.7. Only 166 patients who underwent bilateral rhizotomy had documented rootlet resection percentages. In these patients, extent of rootlet division ranged from 14 to 65% at each level. Only posterior rootlet division was described. Distribution of starting and ending rootlets is shown in Tables 13.3 and 13.4. Electrophysiological monitoring was utilized intraoperatively in all procedures.

13.3.5 Measured Outcomes

13.3.5.1 Efficacy of ITB on Tone

In adult patients with quantitative tone measurement, all patients ($n = 211$) undergoing ITB had improved Mean Ashworth Score (MAS) at the time of their follow-up relative to their baseline [15, 20, 40]. TBI ($n = 47$) patients improved by a mean

Table 13.7 Levels of laminectomy for SDR in pediatric patients ($n = 665$)

Laminectomy type	Level	% Involvement (n)
Single level laminectomy (11.1%, $n = 74$)	L1	6.2% (41)
	Not documented	5.0% (33)
Posterior laminectomy (4.8%, $n = 32$)	L2–L5	1.8% (12)
	S2	3.0% (20)
Multilevel laminectomy (83.6%, $n = 556$)	T12–S2	5.9% (39)
	L1–L5	27.2% (181)
	L1–S1	6.6% (44)
	L1–L2	3.6% (24)
	L2–L5	13.4% (89)
	L2–S1	12.1% (81)
	L5–S1	14.7% (98)

of 1.8 grades in their MAS from baseline. The remainder of patients including those with CP ($n = 20$), MS ($n = 37$), SCI ($n = 42$), and other diagnoses ($n = 65$) improved by 2 grades on average from baseline. In contrast, 95% of pediatric patients with reported quantitative measures ($n = 99$ patients) improved their MAS from baseline, whereas 5% deteriorated post-ITB by the time of their final follow-up [54, 56, 57, 60, 71, 83]. Patients with CP ($n = 81$) improved by an average of 1.7 grades measured by MAS from baseline. In the remainder of the patients with TBI ($n = 10$), SCI ($n = 1$), and other diagnoses ($n = 7$), an average improvement of 2 grades was seen. Of significance, substantial decrease in dystonia was qualitatively reported in the pediatric patients diagnosed with CP ($n = 25$) after ITB placement.

13.3.5.2 Efficacy of SDR on Tone

All adult patients undergoing SDR with reported post intervention quantitative outcomes ($n = 100$) had an improved MAS at the time of their final follow-up relative to baseline. Patients with CP ($n = 60$), MS ($n = 29$), and TBI ($n = 5$) improved on MAS by an average of 3, 2, and 1 grade, respectively. The remaining patients ($n = 6$) improved by a mean of 1.5 grades. Conversely, pediatric patients who underwent SDR primarily consisted of those with CP ($n = 20$). These patients had a mean improvement of 0.9 on scores after surgery by final follow-up.

13.3.5.3 Efficacy of SDR and ITB on ROM

Only one study compared the lower extremity passive ROM in adult patients who underwent SDR ($n = 71$) to those undergoing ITB ($n = 71$) [44]. A composite score was calculated from the scoring of the Passive Range of Motion (PROM) in hip abduction, knee flexion, and ankle dorsiflexion. The SDR cohort had a statistically significant improvement in lower extremity PROM when compared to the ITB

cohort (−0.77 vs. −0.33, $p = 0.0138$). Another study found that of the 152 patients who underwent SDR, 80% ($n = 122$) had improved lower extremity ROM while the 20% ($n = 30$) remained unchanged [15].

In pediatric patients, PROM quantitative data were analyzed from 43 patients [84]. There was significant improvement in the ankle dorsiflexion in patients who underwent SDR (Table 13.8). Active Range of Motion (AROM) was quantitatively analyzed from 5 publications [50, 59, 65, 69, 85]. There was significant bilateral improvement in the AROM in hip abduction and popliteal angle in pediatric patients who underwent SDR. Only hip extension and flexion was not observed to improve to a statistically significant degree after SDR (Table 13.9). No studies in this review were found to describe AROM or PROM in pediatric patients who underwent ITB

13.3.5.4 Efficacy of SDR and ITB on Ambulation in Adult Patients

Overall, all adult patients undergoing SDR remained stable or had significant improvement in their functional ambulation when measured by Gross Motor Functional Classification Scale (GMFCS) after an average of 12 months of follow-up (Table 13.10). Etiologies for spasticity were most commonly CP ($n = 60$), MS ($n = 52$), and trauma (including TBI and SCI) ($n = 35$). Rare etiologies included

Table 13.8 Change in the PROM after SDR in pediatric patients compared to baseline

Passive ROM	Preoperative	Postoperative	Difference	*p* value [95% CI]
Ankle DF ($n = 43$)	− 5 ± 10.7	0.46 ± 9.14	**5.45**	0.0128 [1.19–9.73]
Knee flexion/extension ($n = 43$)	19.5 ± 13.8	18.4 ± 12.1	−1.10	0.6953 [−6.67 to 4.67]
Hip flexion/extension ($n = 12$)	− 15.0 ± 10.2	− 7.5 ± 9.9	7.5	0.0812 [−1.01 to 16.01]

Table 13.9 Change in AROM after SDR in pediatric patients compared to baseline

Active ROM	Preoperative	Postoperative	Difference	*p* value [95% CI]
Ankle DF ($n = 43$)	3.6 ± 10.8	9.8 ± 7.2	**6.16**	0.0024 [2.26–10.14]
Left ankle DF ($n = 88$)	− 6.2 ± 8.1	4.2 ± 7.1	**10.4**	0.0001 [8.13–12.67]
Right ankle DF ($n = 88$)	− 4.6 ± 7.5	4.4 ± 7.3	9.1	0.0001 [6.80–11.20]
Knee flexion/extension ($n = 43$)	24.3 ± 14.6	34.3 ± 13.7	**10.1**	0.0015 [3.93–16.07]
Hip flexion/extension ($n = 43$)	24.7 ± 12.1	27.5 ± 11.0	2.8	0.2647 [− 2.16 to 7.76]
Left Thompson Test ($n = 75$)	− 7.4 ± 6.9	− 1.1 ± 2.6	**6.3**	0.0001 [4.62–7.98]
Right Thompson Test ($n = 75$)	− 6.8 ± 6.1	0.2 ± 1.9	**7.0**	0.0001 [5.54–8.46]
Left hip abduction ($n = 75$)	24.9 ± 7.7	35.5 ± 7.7	**10.5**	0.0001 [8.12–13.09]
Right hip abduction ($n = 75$)	22.8 ± 6.5	33.3 ± 10.0	**10.6**	0.0001 [7.78–13.22]
Left popliteal angle ($n = 88$)	40.8 ± 8.0	50.0 ± 11.6	**9.1**	0.0001 [6.24–12.17]
Right popliteal angle ($n = 88$)	38.2 ± 8.2	48.9 ± 11.6	**10.7**	0.0001 [7.71–13.69]

Table 13.10 Change in GMFCS of adult patients after SDR compared to baseline

	Post-SDR at mean follow-up duration of 12 months		
Baseline GMFCS	Improvement % (*n*)	Stable % (*n*)	Deterioration % (*n*)
GMFCS I (*n* = 18)	NA	100% (18)	–
GMFCS II (*n* = 31)	100% (31)	–	–
GMFCS III (*n* = 13)	100% (13)	–	–
GMFCS IV (*n* = 67)	26.9% (18)	73.1% (49)	–
GMFCS V (*n* = 26)	–	100% (26)	–
Subtotal (*n* = 155)	**40% (62)**	**60% (93)**	**–**

spinocerebellar degenerative disease (*n* = 5) and amytrophic lateral sclerosis (ALS) (*n* = 3) (Table 13.11). While patients with MS and CP saw potential for improvement in their postintervention functional classification, patients with spasticity secondary to trauma or degenerative disease remained unchanged in ambulatory status. It should be noted that all patients with CP who underwent SDR had a GMFCS I–III, whereas all patients with trauma or degenerative disease were already GMFCS IV or V. In comparison, the etiologies for spasticity in the majority of patients undergoing placement of ITB were CP (*n* = 20), MS (*n* = 27), and trauma (*n* = 15) (Table 13.14). An additional number of patients were diagnosed with hypoxic brain injury (HBI) (*n* = 5), ALS (*n* = 2), and a mix of other pathologies (including spastic paralysis NYD, posterior lateral sclerosis, myelitis, and cerebrovascular accident) (*n* = 5).

Outcomes in patients receiving ITB were much more varied (Table 13.12). A significant number of patients, even those with a pre-intervention GMFCS of I or II, experienced a functional deterioration to worse than baseline by time of final follow-up. The exception to this observation were patients with spasticity related to trauma—these all remained stable (i.e., no better or worse functional classification) by the time of final follow-up. Of note, however, patients undergoing SDR had much shorter mean reported follow-up than those undergoing placement of ITB (12 months vs. 47.5 months). When reviewing publications that describe ambulatory outcomes on a qualitative basis, approximately 66% of adult patients who are ambulatory at baseline experienced an improvement after SDR, while the remaining 34% remained unchanged. In comparison, only 19.6% of nonambulatory patients improved after SDR, while the remainder remained stable after intervention. Of patients undergoing placement of ITB, 82.8% of ambulatory patients improved in comparison to only 0.9% of nonambulatory patients gaining function.

13.3.5.5 Efficacy of SDR and ITB on Ambulation in Pediatric Patients

In pediatric patients undergoing SDR (*n* = 131), improvement or stabilization of function was observed in 25.3% (*n* = 55) and 71% (*n* = 154) of patients, respectively (Tables 13.13 and 13.14) [73]. Deterioration in ambulation occurred in 3.7% (*n* = 8) patients after a mean follow-up duration of 132.6 months. No patients who

Table 13.11 Change in GMFCS of adult patients after SDR compared to baseline, stratified by etiology of spasticity

Etiologies of spasticity	Baseline GMFCS	Post-SDR changes in GMFCS			
		Improvement % (*n*)	Stable % (*n*)	Deterioration % (*n*)	Mean follow-up (months)
CP (*n* = 60)	GMFCS I (*n* = 18)	NA	100% (18)	–	12
	GMFCS II (*n* = 30)	100% (30)	–	–	
	GMFCS III (*n* = 12)	100% (12)	–	–	
	Subtotal (*n* = 60)	**70% (42)**	**30% (18)**	**–**	
MS (*n* = 52)	GMFCS II (*n* = 1)	100% (1)	–	–	12
	GMFCS III (*n* = 1)	100% (1)	–	–	
	GMFCS IV (*n* = 41)	43.9% (18)	56.1% (23)	–	
	GMFCS V (*n* = 9)	–	100% (9)	NA	
	Subtotal (*n* = 52)	**38.5% (20)**	**61.5% (32)**	**–**	
Trauma: SCI + TBI (*n* = 35)	GMFCS IV (*n* = 26)	–	100% (26)	–	12
	GMFCS V (*n* = 9)	–	100% (9)	NA	
	Subtotal (*n* = 35)	**–**	**100% (35)**	**–**	
Spinocerebellar degenerative disease (*n* = 5)	GMFCS V (*n* = 5)	–	100% (5)	NA	12
	Subtotal (*n* = 5)	**–**	**100% (5)**	**NA**	
ALS (*n* = 3)	GMFCS V (*n* = 3)	–	100% (3)	–	12
	Subtotal (*n* = 3)	**–**	**100% (3)**	**–**	

were GMFCS I deteriorated by the end of follow-up, whereas 4.1% (*n* = 2), 6.4% (*n* = 5), and 1.5% (*n* = 1) of GMFCS II, III, and IV, respectively, underwent measureable decline in function by the end of their follow-up in comparison to baseline. GMFM data were also available for 93 patients. In the entire population, the mean baseline GMFM% was approximately 69.6 ± 14.4 and post SDR, GMFM rose to a mean of 76.8 ± 12.6 by follow-up period of 51.1 ± 46.5 months [59, 76, 81, 84]. An unpaired *t* test indicates statistically significant improvement of 7.2 on the GMFM (95% CI 3.28–11.12, $p = 0.0004$). No reports fitting inclusion criteria described pediatric patients undergoing ITB with documented pre- and postprocedure GMFCS.

Table 13.12 Change in GMFCS of adult patients after ITB compared to baseline

Baseline GMFCS	Post ITB at mean follow-up duration of 35.75 months		
	Improvement % (*n*)	Stable % (*n*)	Deterioration % (*n*)
GMFCS I (*n* = 13)	NA	61.5% (8)	31.5% (5)
GMFCS II (*n* = 28)	14.3% (4)	75% (21)	10.7% (3)
GMFCS III (*n* = 41)	19.5% (8)	70.7% (29)	9.8% (4)
GMFCS IV (*n* = 33)	30.3% (10)	69.7% (23)	–
GMFCS V (*n* = 0)	–	–	–
Subtotal (*n* = 115)	**19.1% (22)**	**70.4% (81)**	**10.4% (12)**

Table 13.13 Change in GMFCS of adult patients after ITB compared to baseline, stratified by etiology of spasticity

Etiologies of spasticity	Baseline GMFCS	Post ITB changes in GMFCS			
		Improvement % (*n*)	Stable % (*n*)	Deterioration % (*n*)	Mean follow-up (months)
CP (*n* = 20)	GMFCS I (*n* = 4)	NA	50% (2)	50% (2)	47.5 ± 35.9
	GMFCS III (*n* = 4)	–	75% (3)	25% (1)	
	GMFCS IV (*n* = 12)	50% (6)	50% (6)	–	
	Subtotal (*n* = 20)	**30% (6)**	**55% (11)**	**15% (3)**	
MS (*n* = 27)	GMFCS I (*n* = 1)	NA	100% (1)	–	47.5 ± 35.9
	GMFCS II (*n* = 6)	16.7% (1)	50% (3)	33.3% (2)	
	GMFCS III (*n* = 19)	21% (4)	68.4% (13)	10.5% (2)	
	GMFCS IV (*n* = 1)	100% (1)	–	–	
	Subtotal (*n* = 27)	**22.2% (6)**	**63% (32)**	**14.8% (4)**	
Trauma: SCI + TBI (*n* = 15)	GMFCS III (*n* = 2)	100% (2)	–	–	47.5 ± 35.9
	GMFCS IV (*n* = 13)	15.4% (2)	84.6% (11)	–	
	Subtotal (*n* = 15)	**26.7% (4)**	**73.3% (11)**	**–**	
HBI (*n* = 5)	GMFCS IV (*n* = 5)	20% (1)	80% (4)	–	47.5 ± 35.9
	Subtotal (*n* = 5)	**20% (1)**	**80% (4)**	**–**	
ALS (*n* = 2)	GMFCS III (*n* = 2)	–	50% (1)	50% (1)	47.5 ± 35.9
	Subtotal (*n* = 2)	**–**	**50% (1)**	**50% (1)**	
Other pathologies[a] (*n* = 5)	GMFCS I (*n* = 1)	NA	100% (1)	–	47.5 ± 35.9
	GMFCS II (*n* = 3)	33.3% (1)	33.3% (1)	33.3% (1)	
	GMFCS III (*n* = 1)	100% (1)	–	–	
	Subtotal (*n* = 5)	**40% (2)**	**40% (2)**	**20% (1)**	

[a]Spastic paralysis of unknown etiology (*n* = 2), posterior lateral sclerosis (*n* = 1), myelitis (*n* = 1), CVA (*n* = 1)

Table 13.14 Change in GMFCS of pediatric patients after SDR compared to baseline

Etiology of spasticity	Baseline GMFCS	Post SDR changes in GMFCS at mean follow-up of 132.6 ± 35.6 months		
		Improvement % (*n*)	Stable % (*n*)	Deterioration % (*n*)
CP (*n* = 217)	GMFCS I (*n* = 14)	NA	100% (14)	–
	GMFCS II (*n* = 49)	38.8% (19)	57.1% (28)	4.1% (2)
	GMFCS III (*n* = 78)	28.2% (22)	65.4% (51)	6.4% (5)
	GMFCS IV (*n* = 67)	20.9% (14)	77.6% (52)	1.5% (1)
	GMFCS V (*n* = 9)	–	100% (9)	NA
	Total (*n* = 217)	**25.3% (55)**	**71.0% (154)**	**3.7% (8)**

13.3.5.6 Efficacy of SDR and ITB on Pain

Pain improved after SDR in 100% of descriptions of adult patients who underwent SDR that measured for pain (*n* = 27 out of 27). There were no data available regarding pain outcomes in adult patients undergoing ITB. Pain improved in 60% and 91% of pediatric patients who underwent ITB (*n* = 9 out of 15) and SDR (*n* = 48 out of 54), respectively.

13.3.5.7 Adjunct Interventions After SDR and ITB

The need for adjunct interventions related to spasticity after initial surgical intervention was also available in 217 patients undergoing ITB (41 adult and 176 pediatric) as well as in 416 patients undergoing SDR (259 adult and 157 pediatric) (Table 13.15). Overall, adult patients underwent fewer adjunct interventions in comparison to their pediatric counterparts after spasticity surgery. In adults receiving ITB, 4.8% of reported patients required further hard or soft tissue (i.e., osteotomy, tendon transfer, etc.). Forty two percent of pediatric patients receiving ITB, in contrast, underwent further hard or soft tissue surgery. In patients undergoing SDR, 13.5% of adults and 79.0% of pediatric patients received further limb deformity correction after their initial intervention. The need for surgical correction of spinal deformity was only reported in pediatric patients. 14.7% of those undergoing ITB went on for further spinal surgery in comparison to 1.3% of those undergoing SDR. The use of DREZ was further only reported in adult patients. Of this cohort, 2.4% of patients receiving ITB underwent further DREZ in contrast to 5.0% of those undergoing SDR.

Table 13.15 Summary of adjunct surgical interventions post SDR and ITB

	FU = 24 months	FU = 96 +/− 84 months	FU = 33/9 +/− 13.9 months	FU = 97.9 +/− 64.7 months
	Adult ITB % (*n*) (*N* = 41)	Pediatric ITB % (*n*) (*N* = 176)	Adult SDR % (*n*) (*N* = 259)	Pediatric SDR % (*n*) (*N* = 157)
Pooled hard tissue and soft tissue surgery	4.8 (2)	42.0 (74)	13.5 (35)	79.0 (124)
Surgical correction for scoliosis	0	14.7 (26)	0	1.3 (2)
Anterior rhizotomy	0	0	3.1 (8)	0
Other neurosurgical intervention (i.e., DREZ)	2.4 (1)	0	5.0 (13)	0

13.3.5.8 Adverse Events After SDR and ITB

Complications post-SDR and ITB was also available in 620 adult and 841 pediatric patients [86]. Overall, events were described in 59.4% and 59.0% of adult and pediatric patients undergoing ITB, respectively, whereas events were described in 46.8% and 22.8% of adult and pediatric patients undergoing SDR, respectively (Table 13.16). The most common complication in adult patients receiving ITB was some sort of hardware problem (i.e., catheter disconnect, pump rotation, etc.); these were seen in 20.2% of patients. CSF leaks were also seen in 8.6% of patients. 'Other symptoms' were seen in an additional 8.6% of patients; this category included events such as pneumonia or infections not directly related to the surgery or surgical wound itself. In pediatric patients receiving ITB, the most common complication, in contrast, was CSF leak that was present in 17.8% of patients. Hardware problems were also commonly identified (11.2%), while 'other symptoms' were also slightly more common in this group (11.3%). Very few patients in adult or pediatric cohorts had perioperative medication-related complications (overdose or withdrawal), although a small number (2.4% and 1.6% in adult and pediatric patients, respectively) did experience cardiorespiratory dysfunction. This was most frequently reported as shortness of breath or dyspnea post-ITB insertion. In patients undergoing SDR, the only event reported in adult patients was bladder dysfunction which occurred in 46.7%. In pediatric patients, the incidence of bladder dysfunction was much lower (2.4%). The most common complications in pediatric patients included development of new sensory dysfunction (9.1%) as well as new bony deformity (4.0%). A small number of patients (2.4%) also experienced new psychiatric changes after SDR; further elucidation of the exact diagnoses or events was not possible. Patients undergoing SDR had no incidence of medication overdose or withdrawal. No patients in either group received both SDR and ITB.

Table 13.16 Summary of complications post SDR and ITB at time of final follow-up (FU)

	FU = 82.9 ± 23.0 months	FU = 12 months	FU = 30.3 ± 11.6 months	FU = 75.4 ± 46.7 months
	Adult (ITB) % (*n*) (*N* = 466)	Adult (SDR) % (*n*) (*N* = 154)	Pediatric (ITB) % (*n*) (*N* = 512)	Pediatric (SDR) % (*n*) (*N* = 329)
Technical/surgical	0	0	0.78% (4)	0.9% (3)
New bladder dysfunction	1.1% (5)	46.7% (72)	3.3% (17)	2.4% (8)
New GI/bowel dysfunction	2.8% (13)	0	0.2% (1)	0
Drug overdose/ withdrawal	0.2% (1)	NA	0.4% (2)	NA
Psychiatric	1.3% (6)	0	0.1% (5)	2.1% (7)
New seizures	0.6% (3)	0	0	0
Vertigo/fatigue	4.1% (19)	0	0.8% (4)	0.6% (2)
Cranial nerve dysfunction	1.5% (7)	0	0	0
Cardiorespiratory dysfunction	2.4% (11)	0	1.2% (6)	0
New motor symptoms	6.0% (28)	0	0.6% (3)	2.1% (7)
New sensory symptoms	0.2% (1)	0	1.2% (6)	9.1 (30)
Wound dehiscence	0.9% (4)	0	5.3% (27)	0
CSF leak	8.6% (40)	0	17.8% (91)	0
Hardware problem	20.2% (94)	0	11.2% (59)	0
Infection	1.1% (5)	0	0.2% (1)	0
Mortality	0	0	0	0
Further spasticity surgery	0	0	0	0
Pressure ulcers	0	0	2.7% (14)	0.6% (2)
Other symptoms	8.6% (40)	0	11.3% (58)	0.9% (3)
Bony deformity	0	0	0.78% (4)	4.0% (13)
Overall	59.4 (277)	46.8 (72)	59 (302)	22.8 (329)

13.4 Discussion

The role for neurosurgical intervention in spasticity management is multifaceted and often depends on availability of resources and expertise as much as the patients themselves [2, 12, 14, 21–23, 28, 56, 57, 70, 87]. While both ITB and SDR overlap in their ability to manage spasticity, the specific advantages and disadvantages of each approach vary significantly. ITB involves the implantation of a mechanical pump and reservoir that allows the programmed dispensation of a pharmacologic

agent to a target site (i.e., the thecal sac). This intervention is nondestructive in the sense that should patients not acquire benefit from the device, it may be removed while reversing any changes that occurred postimplantation. Furthermore, ITB allows for fine-tuning throughout the day as well as progressive titration of tone reduction over time. Patients may increase their drug dosing overnight when they desire to have maximal tone reduction allowing for comfort while resting; during the daytime, pumps may be programmed to reduce drug delivery to avoid potential side effects or if desiring an increase in tone to help maintain posture (i.e., while sitting). ITB, furthermore, is typically considered the intervention of choice in patients with mixed tone disorders, given baclofen's therapeutic benefit for dystonia as well as spasticity [21, 26, 28, 60, 70].

In comparison, SDR is generally reserved for patients with pure tone disorders given the generally held belief that traditional posterior rhizotomy alone does very little to affect dystonic posturing and movement [88, 89]. Unlike ITB, SDR is a destructive technique that relies on interruption of under-inhibited reflex arcs thought to be contributing to dysfunctional movement [2, 3]. While there are several different approaches to carry out SDR, most involve a limited lumbar laminectomy and lesioning of the posterior nerve rootlets with either electrophysiologic guidance or direct anatomical selection [22, 25, 32, 87, 90]. The procedure is irreversible and the degree of intraoperative titration possible is controversial. This procedure, however, does offer several distinct advantages over ITB including the lack of implantable hardware. While ITB inherently commits patients to routine pump refills (approximately every 3–6 months depending on use) in addition to pump replacements (reported to be 2–10 years), SDR is largely a onetime procedure. Furthermore, the lack of persistent medication infusion avoids any potential pharmacologic complications including drug overdose or withdrawal, both of which may lead to major morbidity or mortality [23, 34].

The use of SDR in pediatric populations is heavily skewed towards patients with established diagnoses of cerebral palsy [91–93]. The use of SDR for other etiologies of spasticity in pediatric patients has not been well-assessed in the literature given limited follow-up and less defined natural history of other etiologies of spasticity (i.e., hereditary spastic paraparesis, etc.) [94]. Anecdotally, the authors of this paper and presumably those in other centers have typically managed these patients with ITB or interventions other than SDR. While some centers have proposed combined anterior and posterior rhizotomy for patients with mixed tone disorders, this approach has not yet gained widespread adoption [88, 89]. Given our observations from this study, however, and the efficacy of tradition SDR in adult patients for a variety of non-CP conditions, further consideration should be made for pediatric patients with potential corollary conditions. A key aspect of the pediatric patient with CP that favors good response to SDR is the inherent stability of the neurologic injury [95–97]. While the natural history of patients with CP is of progressive functional decline, this outcome is often a consequence of unmanaged spasticity causing aberrations in musculoskeletal growth and anatomical development as opposed to progressive deterioration in neurologic function [14, 25, 98]. Thus, selected pediatric patients with similarly stable neurologic injury or disease (i.e., TBI, SCI, or

treated MS) may stand to potentially benefit from SDR as opposed to being triaged to ITB or other interventions.

The comparison of SDR to ITB in terms of efficacy for tone management is exceptionally challenging given the typically disparate populations that each treatment is offered to. While both strategies are able to achieve tone reduction, patient comorbidities and specific pattern of tone dysfunction are likely larger determinants for which intervention may be best suited for specific patients. In rare cases where true clinical equipoise exists, consideration must be given to the risk profile of each intervention as well as the long-term implications of device implantation in comparison to relative lack of treatability of SDR. It is in the author's practice that ITB is further only offered to patients who are able to reliably access healthcare services. Given the relative frequency of mechanical failure and implications of an acute pump failure leading to medication withdrawal, the authors do advocate to pursue SDR or non-implanted device intervention in those patients who are in remote settings or would be otherwise unreliable in routinely accessing healthcare.

When reviewing currently available data, adult patients with CP and MS appear to experience greater improvements in ambulation after SDR in comparison to ITB, when accounting for baseline GMFCS and etiology of spasticity. Other pathologies have much more unpredictable responses making identification of a singular approach difficult to ascertain. This dataset, however, is retrospective and is prone to bias. High volume spasticity programs identifying patients for SDR include in their selection criteria the inherent potential to gain functional improvement after intervention. In comparison, the placement of ITB does not inherently presume that patients will obtain a measurable gain in locomotion. Any potential advantage of SDR in these populations, however, must also be weighed against the very significantly higher incidence of bladder dysfunction (2.8% vs. 46.7%). Whether this finding represents a technical issue, i.e., extent of rhizotomy, or a reporting bias (i.e., adult patient able to report urinary dysfunction more easily) is unknown. Furthermore, the follow-up duration in ITB patients is much longer and any literature reported differences in outcome may be reflective of the natural history of deterioration that many patients experience over time regardless of the intervention they may receive. Older reports that were not part of the primary data collection in this study have found that adult patients with MS actually have worse response to SDR compared to patients with other etiologies of spasticity [99, 100]. Given that this finding was not seen in more recent studies with similar follow-up durations, one possible explanation may be the advent of more efficacious or durable MS treatments that have limited the progressive deterioration that many patients previously experienced, thus improving the durability of spasticity treatment.

Other significant limitations of the currently available literature are the sheer multitude of measures for outcome that currently exist. While spasticity is a fairly common end result of a variety of neurologic insults and diseases, many measures of outcome are reported in disparate fashions and not immediately translatable or allowing for a straightforward comparison. In addition, there have been only limited attempts to truly quantify outcome as a comparison to the natural history of the etiology of spasticity. Given the often evolving nature of many neurologic

conditions over time, long-term outcomes of any intervention measured against a single baseline may fail to capture the true effect of treatment [14]. Moreover, there is a genuine paucity of patient-level reported outcomes that exist in the literature (i.e., quality of life, patient satisfaction) [101, 102]. These outcome measures provide valuable insight into the benefit and utility of the interventions offered while allowing care providers to better provide patient-centered standards of care [103, 104]. Future prospective studies should utilize standardized measures as well as patient-level outcomes to assist in better personalizing interventions for individuals [20, 33, 38, 101, 105].

13.5 Conclusion

SDR and ITB are both very effective interventions in the management of spasticity of a variety of etiologies in both adult and pediatric patients. The durability of these interventions is sustained over time in a majority of patients. Patterns of complications vary depending on the intervention; ITB is associated with a significant risk for hardware and wound-related problems including CSF leak, whereas SDR is associated with a higher risk for new bladder or sensory dysfunction. While the application of each intervention is determined by a variety of nonmodifiable patient factors, in cases of true clinical equipoise, there may be an opportunity to consider SDR in nontraditional populations (i.e., pediatric patients without CP diagnosis) given the increasing experience reported. There is an overall need in the literature to expand reporting of patient-perceived outcomes such as quality of life given the relative paucity and significant value of currently reported measures.

Disclosure The authors have no personal, financial, or institutional interest in any of the drugs, materials, or devices described in this article.

References

1. Baagøe SK, Kofoed-Hansen M, Poulsen I, Riberholt CG. Development of muscle contractures and spasticity during subacute rehabilitation after severe acquired brain injury: a prospective cohort study. Brain Inj. 2019;33(11):1460–6.
2. Goldstein M. The treatment of cerebral palsy: what we know, what we don't know. J Pediatr. 2004;145(2 Suppl):S42–6.
3. Bose P, Hou J, Thompson FJ. Traumatic brain injury (TBI)-induced spasticity: neurobiology, treatment, and rehabilitation. In: Kobeissy FH, editor. Brain neurotrauma: molecular, neuropsychological, and rehabilitation aspects. Frontiers in neuroengineering. Boca Raton: CRC; 2015.
4. Calancie B, Molano MR, Broton JG. Interlimb reflexes and synaptic plasticity become evident months after human spinal cord injury. Brain. 2002;125(Pt 5):1150–61.
5. Clowry GJ. The dependence of spinal cord development on corticospinal input and its significance in understanding and treating spastic cerebral palsy. Neurosci Biobehav Rev. 2007;31(8):1114–24.

6. Foran JR, Steinman S, Barash I, Chambers HG, Lieber RL. Structural and mechanical alterations in spastic skeletal muscle. Dev Med Child Neurol. 2005;47(10):713–7.
7. Pidgeon TS, Ramirez JM, Schiller JR. Orthopaedic management of spasticity. RI Med J. 2015;98(12):26–31.
8. Ravindra VM, Christensen MT, Onwuzulike K, Smith JT, Halvorson K, Brockmeyer DL, et al. Risk factors for progressive neuromuscular scoliosis requiring posterior spinal fusion after selective dorsal rhizotomy. J Neurosurg Pediatr. 2017;20(5):456–63.
9. Mazarakis NK, Vloeberghs MH. Spasticity secondary to Leigh syndrome managed with selective dorsal rhizotomy: a case report. Childs Nerv Syst. 2016;32(9):1745–8.
10. Shahani BT, Young RR. Human flexor reflexes. J Neurol Neurosurg Psychiatry. 1971;34(5):616–27.
11. Westbom L, Lundkvist Josenby A, Wagner P, Nordmark E. Growth in children with cerebral palsy during five years after selective dorsal rhizotomy: a practice-based study. BMC Neurol. 2010;10:57.
12. Ailon T, Beauchamp R, Miller S, Mortenson P, Kerr JM, Hengel AR, et al. Long-term outcome after selective dorsal rhizotomy in children with spastic cerebral palsy. Childs Nerv Syst. 2015;31(3):415–23.
13. Daunter AK, Kratz AL, Hurvitz EA. Long-term impact of childhood selective dorsal rhizotomy on pain, fatigue, and function: a case-control study. Dev Med Child Neurol. 2017;59(10):1089–95.
14. Dudley RW, Parolin M, Gagnon B, Saluja R, Yap R, Montpetit K, et al. Long-term functional benefits of selective dorsal rhizotomy for spastic cerebral palsy. J Neurosurg Pediatr. 2013;12(2):142–50.
15. Salame K, Ouaknine G, Rochkind S, Constantini S, Razon N. Surgical treatment of spasticity by selective posterior rhizotomy: 30 years experience. Isr Med Assoc J. 2003;5(8):543–6.
16. Shilt JS, Lai LP, Cabrera MN, Frino J, Smith BP. The impact of intrathecal baclofen on the natural history of scoliosis in cerebral palsy. J Pediatr Orthop. 2008;28(6):684–7.
17. Tedroff K, Lowing K, Jacobson DN, Astrom E. Does loss of spasticity matter? A 10-year follow-up after selective dorsal rhizotomy in cerebral palsy. Dev Med Child Neurol. 2011;53(8):724–9.
18. Tu A, Steinbok P. Long term outcome of Selective Dorsal Rhizotomy for the management of childhood spasticity-functional improvement and complications. Childs Nerv Syst. 2020;36(9):1985–94.
19. Yoon YK, Lee KC, Cho HE, Chae M, Chang JW, Chang WS, et al. Outcomes of intrathecal baclofen therapy in patients with cerebral palsy and acquired brain injury. Medicine. 2017;96(34):e7472.
20. Zahavi A, Geertzen JH, Middel B, Staal M, Rietman JS. Long term effect (more than five years) of intrathecal baclofen on impairment, disability, and quality of life in patients with severe spasticity of spinal origin. J Neurol Neurosurg Psychiatry. 2004;75(11):1553–7.
21. Albright AL, Turner M, Pattisapu JV. Best-practice surgical techniques for intrathecal baclofen therapy. J Neurosurg. 2006;104(4 Suppl):233–9.
22. Aquilina K, Graham D, Wimalasundera N. Selective dorsal rhizotomy: an old treatment re-emerging. Arch Dis Child. 2015;100(8):798–802.
23. Awaad Y, Rizk T, Siddiqui I, Roosen N, McIntosh K, Waines GM. Complications of intrathecal baclofen pump: prevention and cure. ISRN Neurol. 2012;2012:575168.
24. Chicoine MR, Park TS, Kaufman BA. Selective dorsal rhizotomy and rates of orthopedic surgery in children with spastic cerebral palsy. J Neurosurg. 1997;86(1):34–9.
25. Farmer J-P, Sabbagh AJ. Selective dorsal rhizotomies in the treatment of spasticity related to cerebral palsy. Childs Nerv Syst. 2007;23(9):991–1002.
26. Francisco GE, Hu MM, Boake C, Ivanhoe CB. Efficacy of early use of intrathecal baclofen therapy for treating spastic hypertonia due to acquired brain injury. Brain Inj. 2005;19(5):359–64.
27. Gigante P, McDowell MM, Bruce SS, Chirelstein G, Chiriboga CA, Dutkowsky J, et al. Reduction in upper-extremity tone after lumbar selective dorsal rhizotomy in children with spastic cerebral palsy. J Neurosurg Pediatr. 2013;12(6):588–94.

28. Gray N, Morton RE, Brimlow K, Keetley R, Vloeberghs M. Goals and outcomes for non ambulant children receiving continuous infusion of intrathecal baclofen. Eur J Paediatr Neurol. 2012;16(5):443–8.
29. Hurvitz EA, Marciniak CM, Daunter AK, Haapala HJ, Stibb SM, McCormick SF, et al. Functional outcomes of childhood dorsal rhizotomy in adults and adolescents with cerebral palsy. J Neurosurg Pediatr. 2013;11(4):380–8.
30. Mathur SN, Chu SK, McCormick Z, Chang Chien GC, Marciniak CM. Long-term intrathecal baclofen: outcomes after more than 10 years of treatment. PM&R. 2014;6(6):506–13.e1.
31. Mittal S, Farmer JP, Al-Atassi B, Montpetit K, Gervais N, Poulin C, et al. Impact of selective posterior rhizotomy on fine motor skills. Long-term results using a validated evaluative measure. Pediatr Neurosurg. 2002;36(3):133–41.
32. Ou C, Kent S, Miller S, Steinbok P. Selective dorsal rhizotomy in children: comparison of outcomes after single-level versus multi-level laminectomy technique. Can J Neurosci Nurs. 2010;32(3):17–24.
33. Park TS, Edwards C, Liu JL, Walter DM, Dobbs MB. Beneficial effects of childhood selective dorsal rhizotomy in adulthood. Cureus. 2017;9(3):e1077.
34. Natale M, Mirone G, Rotondo M, Moraci A. Intrathecal baclofen therapy for severe spasticity: analysis on a series of 112 consecutive patients and future prospectives. Clin Neurol Neurosurg. 2012;114(4):321–5.
35. Nordmark E, Josenby AL, Lagergren J, Andersson G, Strömblad L-G, Westbom L. Long-term outcomes five years after selective dorsal rhizotomy. BMC Pediatr. 2008;8:54.
36. Park TS, Liu JL, Edwards C, Walter DM, Dobbs MB. Functional outcomes of childhood selective dorsal rhizotomy 20–28 years later. Cureus. 2017;9(5):e1256.
37. Peter JC, Arens LJ. Selective posterior lumbosacral rhizotomy for the management of cerebral palsy spasticity. A 10-year experience. S Afr Med J. 1993;83(10):745–7.
38. Reynolds MR, Ray WZ, Strom RG, Blackburn SL, Lee A, Park TS. Clinical outcomes after selective dorsal rhizotomy in an adult population. World Neurosurg. 2011;75(1):138–44.
39. Moher D, Shamseer L, Clarke M, Ghersi D, Liberati A, Petticrew M, et al. Preferred reporting items for systematic review and meta-analysis protocols (PRISMA-P) 2015 statement. Syst Rev. 2015;4:1.
40. Pucks-Faes E, Hitzenberger G, Matzak H, Verrienti G, Schauer R, Saltuari L. Intrathecal baclofen in paroxysmal sympathetic hyperactivity: impact on oral treatment. Brain Behav. 2018;8(11):e01124.
41. Reis PV, Vieira CR, Midões AC, Rebelo V, Barbosa P, Gomes A. Intrathecal baclofen infusion pumps in the treatment of spasticity: a retrospective cohort study in a Portuguese Centre. Acta Med Port. 2019;32(12):754–9.
42. Pucks-Faes E, Hitzenberger G, Matzak H, Fava E, Verrienti G, Laimer I, et al. Eleven years' experience with intrathecal baclofen—complications, risk factors. Brain Behav. 2018;8(5):e00965.
43. McCarty SF, Gaebler-Spira D, Harvey RL. Improvement of sleep apnea in a patient with cerebral palsy. Am J Phys Med Rehabil. 2001;80(7):540–2.
44. Kan P, Gooch J, Amini A, Ploeger D, Grams B, Oberg W, et al. Surgical treatment of spasticity in children: comparison of selective dorsal rhizotomy and intrathecal baclofen pump implantation. Childs Nerv Syst. 2008;24(2):239–43.
45. Sammaraiee Y, Yardley M, Keenan L, Buchanan K, Stevenson V, Farrell R. Intrathecal baclofen for multiple sclerosis related spasticity: a twenty year experience. Mult Scler Relat Disord. 2019;27:95–100.
46. Sammaraiee Y, Stevenson VL, Keenan E, Buchanan K, Lee H, Padilla H, et al. Evaluation of the impact of intrathecal baclofen on the walking ability of people with multiple sclerosis related spasticity. Mult Scler Relat Disord. 2020;46:102503.
47. Meythaler JM, Guin-Renfroe S, Grabb P, Hadley MN. Long-term continuously infused intrathecal baclofen for spastic-dystonic hypertonia in traumatic brain injury: 1-year experience. Arch Phys Med Rehabil. 1999;80(1):13–9.

48. Buizer AI, van Schie PEM, Bolster EAM, van Ouwerkerk WJ, Strijers RL, van de Pol LA, et al. Effect of selective dorsal rhizotomy on daily care and comfort in non-walking children and adolescents with severe spasticity. Eur J Paediatr Neurol. 2017;21(2):350–7.
49. Buckon CE, Sienko Thomas S, Aiona MD, Piatt JH. Assessment of upper-extremity function in children with spastic diplegia before and after selective dorsal rhizotomy. Dev Med Child Neurol. 1996;38(11):967–75.
50. Engsberg JR, Ross SA, Wagner JM, Park TS. Changes in hip spasticity and strength following selective dorsal rhizotomy and physical therapy for spastic cerebral palsy. Dev Med Child Neurol. 2002;44(4):220–6.
51. Meythaler JM, Guin-Renfroe S, Law C, Grabb P, Hadley MN. Continuously infused intrathecal baclofen over 12 months for spastic hypertonia in adolescents and adults with cerebral palsy. Arch Phys Med Rehabil. 2001;82(2):155–61.
52. Natale M, D'Oria S, Nero VV, Squillante E, Gentile M, Rotondo M. Long-term effects of intrathecal baclofen in multiple sclerosis. Clin Neurol Neurosurg. 2016;143:121–5.
53. Gerszten PC, Albright AL, Barry MJ. Effect on ambulation of continuous intrathecal baclofen infusion. Pediatr Neurosurg. 1997;27(1):40–4.
54. Mazarakis NK, Ughratdar I, Vloeberghs MH. Excellent functional outcome following selective dorsal rhizotomy in a child with spasticity secondary to transverse myelitis. Childs Nerv Syst. 2015;31(11):2189–91.
55. Walter M, Altermatt S, Furrer C, Meyer-Heim A. Intrathecal baclofen therapy in children with severe spasticity: outcome and complications. Dev Neurorehabil. 2014;17(6):368–74.
56. Gooch JL, Oberg WA, Grams B, Ward LA, Walker ML. Care provider assessment of intrathecal baclofen in children. Dev Med Child Neurol. 2004;46(8):548–52.
57. Campbell WM, Ferrel A, McLaughlin JF, Grant GA, Loeser JD, Graubert C, et al. Long-term safety and efficacy of continuous intrathecal baclofen. Dev Med Child Neurol. 2002;44(10):660–5.
58. Van Campenhout A, Huenaerts C, Poulussen L, Prinsen SD, Desloovere K. Role of femoral derotation on gait after selective dorsal rhizotomy in children with spastic cerebral palsy. Dev Med Child Neurol. 2019;61(10):1196–201.
59. Wright FV, Sheil EM, Drake JM, Wedge JH, Naumann S. Evaluation of selective dorsal rhizotomy for the reduction of spasticity in cerebral palsy: a randomized controlled trial. Dev Med Child Neurol. 1998;40(4):239–47.
60. Eek MN, Olsson K, Lindh K, Askljung B, Påhlman M, Corneliusson O, et al. Intrathecal baclofen in dyskinetic cerebral palsy: effects on function and activity. Dev Med Child Neurol. 2018;60(1):94–9.
61. Tedroff K, Hägglund G, Miller F. Long-term effects of selective dorsal rhizotomy in children with cerebral palsy: a systematic review. Dev Med Child Neurol. 2020;62(5):554–62.
62. Josenby AL, Wagner P, Jarnlo GB, Westbom L, Nordmark E. Motor function after selective dorsal rhizotomy: a 10-year practice-based follow-up study. Dev Med Child Neurol. 2012;54(5):429–35.
63. Bolster EA, van Schie PE, Becher JG, van Ouwerkerk WJ, Strijers RL, Vermeulen RJ. Long-term effect of selective dorsal rhizotomy on gross motor function in ambulant children with spastic bilateral cerebral palsy, compared with reference centiles. Dev Med Child Neurol. 2013;55(7):610–6.
64. Bloom KK, Nazar GB. Functional assessment following selective posterior rhizotomy in spastic cerebral palsy. Childs Nerv Syst. 1994;10(2):84–6.
65. Staudt LA, Nuwer MR, Peacock WJ. Intraoperative monitoring during selective posterior rhizotomy: technique and patient outcome. Electroencephalogr Clin Neurophysiol. 1995;97(6):296–309.
66. Ruggiero C, Meccariello G, Spennato P, Mirone G, Graziano S, Gilone M, et al. Early intraventricular baclofen therapy (IVB) for children with dystonic and dysautonomic storm. Childs Nerv Syst. 2019;35(1):15–8.

67. Peter JC, Hoffman EB, Arens LJ, Peacock WJ. Incidence of spinal deformity in children after multiple level laminectomy for selective posterior rhizotomy. Childs Nerv Syst. 1990;6(1):30–2.
68. Rushton PRP, Nasto LA, Aujla RK, Ammar A, Grevitt MP, Vloeberghs MH. Intrathecal baclofen pumps do not accelerate progression of scoliosis in quadriplegic spastic cerebral palsy. Eur Spine J. 2017;26(6):1652–7.
69. Peacock WJ, Staudt LA. Functional outcomes following selective posterior rhizotomy in children with cerebral palsy. J Neurosurg. 1991;74(3):380–5.
70. Albright AL, Barry MJ, Shafton DH, Ferson SS. Intrathecal baclofen for generalized dystonia. Dev Med Child Neurol. 2001;43(10):652–7.
71. McLaughlin JF, Bjornson KF, Astley SJ, Graubert C, Hays RM, Roberts TS, et al. Selective dorsal rhizotomy: efficacy and safety in an investigator-masked randomized clinical trial. Dev Med Child Neurol. 1998;40(4):220–32.
72. Carraro E, Zeme S, Ticcinelli V, Massaroni C, Santin M, Peretta P, et al. Multidimensional outcome measure of selective dorsal rhizotomy in spastic cerebral palsy. Eur J Paediatr Neurol. 2014;18(6):704–13.
73. Josenby AL, Wagner P, Jarnlo GB, Westbom L, Nordmark E. Functional performance in self-care and mobility after selective dorsal rhizotomy: a 10-year practice-based follow-up study. Dev Med Child Neurol. 2015;57(3):286–93.
74. Silva S, Nowicki P, Caird MS, Hurvitz EA, Ayyangar RN, Farley FA, et al. A comparison of hip dislocation rates and hip containment procedures after selective dorsal rhizotomy versus intrathecal baclofen pump insertion in nonambulatory cerebral palsy patients. J Pediatr Orthop. 2012;32(8):853–6.
75. Morota N, Ihara S, Ogiwara H. Neurosurgical management of childhood spasticity: functional posterior rhizotomy and intrathecal baclofen infusion therapy. Neurol Med Chir. 2015;55(8):624–39.
76. Steinbok P, Gustavsson B, Kestle JR, Reiner A, Cochrane DD. Relationship of intraoperative electrophysiological criteria to outcome after selective functional posterior rhizotomy. J Neurosurg. 1995;83(1):18–26.
77. Peacock WJ, Staudt LA. Spasticity in cerebral palsy and the selective posterior rhizotomy procedure. J Child Neurol. 1990;5(3):179–85.
78. Zhan Q, Yu X, Jiang W, Shen M, Jiang S, Mei R, et al. Whether the newly modified rhizotomy protocol is applicable to guide single-level approach SDR to treat spastic quadriplegia and diplegia in pediatric patients with cerebral palsy? Childs Nerv Syst. 2020;36(9):1935–43.
79. Krach LE, Kriel RL, Gilmartin RC, Swift DM, Storrs BB, Abbott R, et al. GMFM 1 year after continuous intrathecal baclofen infusion. Pediatr Rehabil. 2005;8(3):207–13.
80. Zaino NL, Steele KM, Donelan JM, Schwartz MH. Energy consumption does not change after selective dorsal rhizotomy in children with spastic cerebral palsy. Dev Med Child Neurol. 2020;62(9):1047–53.
81. Kim DS, Choi JU, Yang KH, Park CI, Park ES. Selective posterior rhizotomy for lower extremity spasticity: how much and which of the posterior rootlets should be cut? Surg Neurol. 2002;57(2):87–93.
82. Lazareff JA, Garcia-Mendez MA, De Rosa R, Olmstead C. Limited (L4–S1, L5–S1) selective dorsal rhizotomy for reducing spasticity in cerebral palsy. Acta Neurochir. 1999;141(7):743–51. discussion 51–2
83. Middel B, Kuipers-Upmeijer H, Bouma J, Staal M, Oenema D, Postma T, et al. Effect of intrathecal baclofen delivered by an implanted programmable pump on health related quality of life in patients with severe spasticity. J Neurol Neurosurg Psychiatry. 1997;63(2):204–9.
84. Engsberg JR, Ross SA, Collins DR, Park TS. Effect of selective dorsal rhizotomy in the treatment of children with cerebral palsy. J Neurosurg. 2006;105(1 Suppl):8–15.
85. Munger ME, Aldahondo N, Krach LE, Novacheck TF, Schwartz MH. Long-term outcomes after selective dorsal rhizotomy: a retrospective matched cohort study. Dev Med Child Neurol. 2017;59(11):1196–203.

86. Albright AL, Richard G, Dale S, Linda EK, Cindy BI, John FM. Long-term intrathecal baclofen therapy for severe spasticity of cerebral origin. J Neurosurg. 2003;98(2):291–5.
87. Children L. Surgical techniques of selective dorsal rhizotomy for spastic cerebral palsy. Neurosurg Focus. 2006;21(2):e7.
88. Abdel Ghany WA, Nada M, Mahran MA, Aboud A, Mahran MG, Nasef MA, et al. Combined anterior and posterior lumbar rhizotomy for treatment of mixed dystonia and spasticity in children with cerebral palsy. Neurosurgery. 2016;79(3):336–44.
89. Albright AL, Tyler-Kabara EC. Combined ventral and dorsal rhizotomies for dystonic and spastic extremities: report of six cases. J Neurosurg. 2007;107(4 Suppl):324–7.
90. Park TS, Johnston JM. Surgical techniques of selective dorsal rhizotomy for spastic cerebral palsy. Neurosurg Focus. 2006;21(2):e7.
91. Hurvitz EA, et al. Functional outcomes of childhood dorsal rhizotomy in adults and adolescents with cerebral palsy. J Neurosurg Pediatr. 2019;11(4):380–8.
92. Kim DS, Choi JU, Yang KH, Park CI. Selective posterior rhizotomy in children with cerebral palsy: a 10-year experience. Childs Nerv Syst. 2001;17(9):556–62.
93. Langerak NG, Tam N, Vaughan CL, Fieggen AG, Schwartz MH. Gait status 17–26 years after selective dorsal rhizotomy. Gait Posture. 2012;35(2):244–9.
94. Sharma J, Bonfield C, Steinbok P. Selective dorsal rhizotomy for hereditary spastic paraparesis in children. Childs Nerv Syst. 2016;32(8):1489–94.
95. Aisen ML, Kerkovich D, Mast J, Mulroy S, Wren TA, Kay RM, et al. Cerebral palsy: clinical care and neurological rehabilitation. Lancet Neurol. 2011;10(9):844–52.
96. Allievi AG, Arichi T, Tusor N, Kimpton J, Arulkumaran S, Counsell SJ, et al. Maturation of sensori-motor functional responses in the preterm brain. Cereb Cortex. 2016;26(1):402–13.
97. Andrew MJ, Sullivan PB. Growth in cerebral palsy. Nutr Clin Pract. 2010;25(4):357–61.
98. Mittal S, Farmer JP, Al-Atassi B, Gibis J, Kennedy E, Galli C, et al. Long-term functional outcome after selective posterior rhizotomy. J Neurosurg. 2002;97(2):315–25.
99. Sindou M, Millet MF, Mortamais J, Eyssette M. Results of selective posterior rhizotomy in the treatment of painful and spastic paraplegia secondary to multiple sclerosis. Appl Neurophysiol. 1982;45(3):335–40.
100. Laitinen LV, Nilsson S, Fugl-Meyer AR. Selective posterior rhizotomy for treatment of spasticity. J Neurosurg. 1983;58(6):895–9.
101. Park TS, Dobbs MB, Cho J. Evidence supporting selective dorsal rhizotomy for treatment of spastic cerebral palsy. Cureus. 2018;10(10):e3466.
102. Park SK, Yang DJ, Heo JW, Kim JH, Park SH, Uhm YH. Study on the quality of life of children with cerebral palsy. J Phys Ther Sci. 2016;28(11):3145–8.
103. Ronen GM, Rosenbaum MP, Streiner DL. Outcome measures in pediatric neurology: why do we need them? J Child Neurol. 2000;15(12):775–80.
104. Varni JW, Seid M, Rode CA. The PedsQL: measurement model for the pediatric quality of life inventory. Med Care. 1999;37(2):126–39.
105. Tedroff K, Lowing K, Astrom E. A prospective cohort study investigating gross motor function, pain, and health-related quality of life 17 years after selective dorsal rhizotomy in cerebral palsy. Dev Med Child Neurol. 2015;57(5):484–90.